

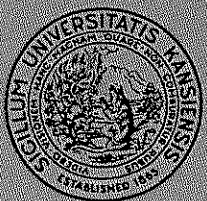
BOND STRENGTH OF HIGH RELATIVE RIB AREA REINFORCING BARS

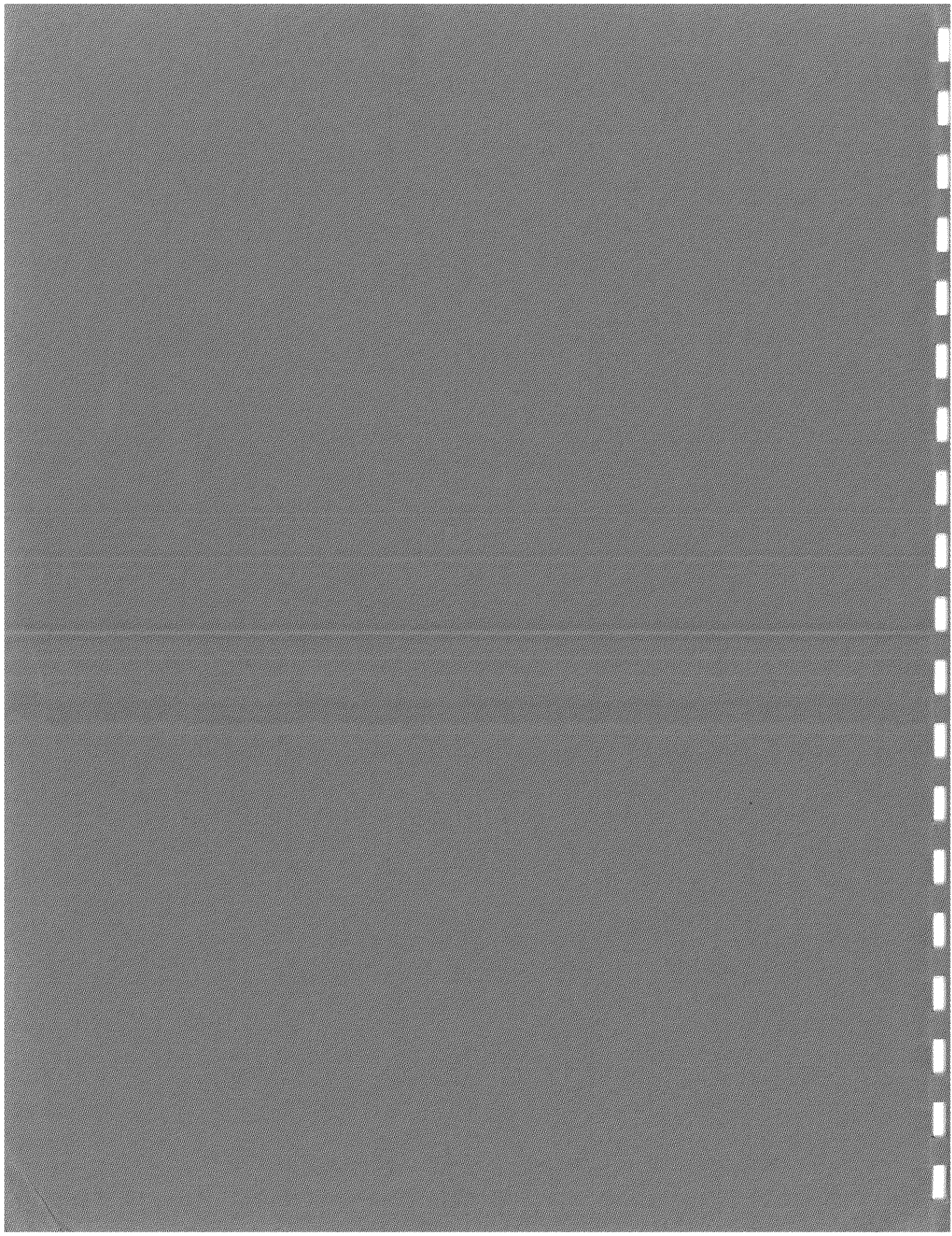
By
Jun Zuo
David Darwin

A Report on Research Sponsored by
THE NATIONAL SCIENCE FOUNDATION
Research Grants No. MSS-9021066 and CMS-9402563
THE U.S. DEPARTMENT OF TRANSPORTATION
FEDERAL HIGHWAY ADMINISTRATION
THE CIVIL ENGINEERING RESEARCH FOUNDATION
Contract No. 91-N6002

Structural Engineering and Engineering Materials
SM Report No. 46
January 1998

THE UNIVERSITY OF KANSAS CENTER FOR RESEARCH, INC.
2291 Irving Hill Drive - Campus West, Lawrence, Kansas 66045





**BOND STRENGTH OF
HIGH RELATIVE RIB AREA REINFORCING BARS**

**By
Jun Zuo
David Darwin**

A Report on Research Sponsored by

**THE NATIONAL SCIENCE FOUNDATION
Research Grants No. MSS-9021066 and CMS-9402563**

**THE U.S. DEPARTMENT OF TRANSPORTATION
FEDERAL HIGHWAY ADMINISTRATION**

**THE CIVIL ENGINEERING RESEARCH FOUNDATION
Contract No. 91-N6002**

**Structural Engineering and Engineering Materials
SM Report No. 46**

**UNIVERSITY OF KANSAS CENTER FOR RESEARCH, INC.
LAWRENCE, KANSAS
January 1998**

ABSTRACT

The bond strengths of uncoated and epoxy-coated high relative rib area (R_r) and conventional reinforcing bars are studied. Equations for evaluating development/splice strength and design criteria for development/splice lengths are developed based on the test results from this study and a large data base. The bond behavior of reinforcing bars under reversed cyclic loading is also investigated.

One hundred and forty beam-splice specimens are tested to study the effects of bar placement, concrete properties, bar size and deformation pattern, transverse reinforcement, and epoxy coating on splice strength. The test results are combined with the previous results for analysis. The combined results include tests for No. 5, No. 8, and No. 11 bars with R_r ranging from 0.065 to 0.141. The results confirm the observations of previous studies that splice strength is unaffected by R_r for bars not confined by transverse reinforcement, and that splice strength increases with an increase in bar size and R_r for bars confined by transverse reinforcement.

The results show that the top-bar behavior of high R_r bars is similar to that of conventional bars. The average clear spacing between splices should be used in design, whether the splices are arranged symmetrically or unsymmetrically.

The test results indicate that concrete containing stronger coarse aggregate provides higher splice strength. For specimens with bars confined by transverse reinforcement in the splice region, concrete with a higher coarse aggregate content produces higher splice strength. For bars not confined by transverse reinforcement, the 1/4 power of concrete compressive strength better characterizes the effect of concrete strength on splice strength than the traditionally used 1/2 power. For bars confined by transverse reinforcement, the 3/4 power of concrete compressive strength

better characterizes the effect of concrete strength on the contribution of transverse reinforcement to splice strength than the 1/2 power.

The results of 62 matched pairs of uncoated and epoxy-coated splice specimens show that epoxy coating is less detrimental to the splice strength of high R_r bars than to the splice strength of conventional bars. The relative splice strength of epoxy-coated high R_r bars is higher in normal-strength concrete than in high-strength concrete.

The development/splice strength design criteria developed in this study accurately represent the effects of bar size, relative rib area, transverse reinforcement, and concrete strength. The new design criteria, which incorporate a reliability-based strength reduction factor, are more economical and have a higher safety margin than the design criteria in ACI 318-95.

Under reversed cyclic loading, high R_r bars exhibit lower slip and less deterioration of bond than conventional bars.

Keywords: bond (concrete to reinforcement); building codes; deformed reinforcement; development; epoxy coating; high-strength concrete; lap connections; reliability; relative rib area; reversed cyclic loading; splicing; structural engineering

ACKNOWLEDGEMENTS

This report is based on a thesis submitted by Jun Zuo in partial fulfillment of the requirements of the Ph.D. degree. Support for this research was provided by the National Science Foundation under NSF Grants No. MSS-9021066 and CMS-9402563, the U.S. Department of Transportation – Federal Highway Administration, the Civil Engineering Research Foundation under CERF Contract No. 91-N6002, the Lester T. Sunderland Foundation, ABC Coating, Inc., AmeriSteel (formerly Florida Steel Corporation), Birmingham Steel Corporation, Chaparral Steel, Fletcher Coating Company, Herberts-O'Brien Inc., North Star Steel Company, and 3M Corporation. Epoxy coating was applied to the C bars by ABC Coating, Inc., to the F bars by AmeriSteel, and to the N bars by Simcote, Inc. The basalt coarse aggregate was supplied by Geiger Ready-Mix and Iron Mountain Trap Rock Company. Form release agent, curing compound, and mounting hardware were supplied by Richmond Screw Anchor Company.

TABLE OF CONTENTS

	<u>Page</u>
ABSTRACT	i
ACKNOWLEDGMENTS	iii
LIST OF SYMBOLS	vii
LIST OF TABLES	xii
LIST OF FIGURES	xvi
CHAPTER 1: INTRODUCTION	1
1.1 General	1
1.2 Previous Work	2
1.3 Discussion	21
1.4 Objective and Scope	22
CHAPTER 2: BEAM SPLICE TESTS	24
2.1 General	24
2.2 Test Specimens	24
2.3 Materials	26
2.4 Specimen Manufacture	29
2.5 Test Procedure	31
2.6 Results and Observations	32
CHAPTER 3: EFFECTS OF SPLICE PLACEMENT AND ARRANGEMENT ON SPLICE STRENGTH	37
3.1 General	37
3.2 Top-cast High Relative Rib Area Reinforcing Bars	39
3.3 Unsymmetrical Arrangement of Splices	40
3.4 Multiple Splice layers	42
3.5 Effect of Shear Force on Splice Strength	44

CHAPTER 4: EFFECTS OF CONCRETE AND REINFORCING BAR PROPERTIES.....	47
4.1 General	47
4.2 Effects of Concrete Properties	49
4.3 Effects of Reinforcing Bars	54
CHAPTER 5: DEVELOPMENT LENGTH CRITERIA	60
5.1 General	60
5.2 Bars Not Confined by Transverse Reinforcement	61
5.3 Bars with Confining Transverse Reinforcement	68
5.4 Effect of Bar Stress on Development/Splice Strength	83
5.5 Design Expression for Development/Splice Length	84
5.6 Comparison to ACI 318-95 Criteria	92
CHAPTER 6: SPLICE STRENGTH OF EPOXY-COATED HIGH RELATIVERIB AREA BARS	101
6.1 General	101
6.2 Splice Strength Ratio, C/U	103
6.3 Effect of Concrete Properties	105
6.4 Effect of Relative Rib Area	106
6.5 Flexural Cracking	107
6.6 Development Length Modification Factor for High R _r Bars	108
CHAPTER 7: REVERSED CYCLIC LOADING TESTS	110
7.1 General	110
7.2 Test Specimens	111
7.3 Materials	111
7.4 Concrete Placement and Curing	112
7.5 Test Procedures	112

7.6 Results and Evaluation	113
CHAPTER 8: SUMMARY AND CONCLUSIONS	117
8.1 Summary	117
8.2 Observations and Conclusions	118
8.3 Suggestion for Further Studies	122
REFERENCES	124
TABLES	133
FIGURES	220
APPENDIX A: CALCULATION OF FLEXURAL STRESS OF DEVELOPED AND SPLICED BARS	312
APPENDIX B: DATA FOR DEVELOPING DEVELOPMENT/SPLICE LENGTH CRITERIA IN CHAPTER 5	335
APPENDIX C: DATA OF FLEXURAL CRACK AND DENSITY FOR THE MATCHED PAIRS OF SPECIMENS CONTAINING EPOXY-COATED AND UNCOATED BARS	346

LIST OF SYMBOLS

A_b	= bar area, in in. ²
A_s	= total steel area, in in. ²
b	= beam width, in in.
c	= $c_{\min} + 0.5 d_b$, in in.
	= distance from the extreme concrete compressive fiber to the neutral axis of beams – used to calculate bar stress, in in.
C_i	= coefficients used to derive Eq. 3.3 (i = 1 to 6)
c_{si}	= one-half clear spacing between bars, in in.
c_{so}	= side cover in same plane as c_{so} , in in.
c_b	= cover perpendicular to c_{si} and c_{so} , in in.
c_{\min}	= minimum value of c_s or c_b , in in.
c_{\max}	= maximum value of c_s or c_b , in in.
c_s	= minimum value of c_{so} and $c_{si} + 0.25$ in., or c_{so} and c_{si} , in in.
COV	= coefficient of variation
C/U	= relative bond strength of epoxy-coated bar to uncoated bar
d	= beam effective depth, in in.
d_b	= nominal bar diameter, in in.
d_s	= nominal stirrup diameter, in in.
E_c	= modulus of elasticity of concrete, in ksi
E_s	= modulus of elasticity of steel, in ksi
E_{sh}	= modulus of elasticity of steel for strain hardening, in ksi
f'_c	= concrete compressive strength, in psi
f'_c^p	= concrete compressive strength to the power p (p = 1/4, 1/2, 3/4, and 1.0), in psi
f_y	= bar yield strength, in psi

f_{yt}	= yield strength of transverse reinforcement, in psi
f_s	= bar stress at failure, in psi
f_{sc}	= bar stress calculated using the moment-curvature method, in ksi
f_{sw}	= bar stress calculated using the working stress method, in ksi
f_{su}	= bar stress calculated using the ultimate strength method, in ksi
HHB	= high strength concrete containing a "high" quantity of basalt coarse aggregate
HHL	= high strength concrete containing a "high" quantity of limestone coarse aggregate
HNL	= high strength concrete containing a "normal" quantity of limestone coarse aggregate
HSC	= high strength concrete [$f'_c \geq 8000$ psi (55.2 MPa)]
h	= beam height, in in.
K_i	= constant in Eq. 5.3 or Eq. 5.12 ($i = 1$ to 4)
K_{tr}	<p>= term representing the effect of transverse reinforcement on bond strength. The value depends on the stage of the analysis and the design expression in which it is used. $K_{tr} = (0.518 t_r t_d A_{tr}/sn) f'_c^{1/2}$ based on initial analysis; $K_{tr} = (0.52 t_r t_d A_{tr}/sn) f'_c^{1/2}$ based on final analysis</p> <p>= $35.3 t_r t_d A_{tr}/sn$ in the expressions developed by Darwin et al. (1995b, 1996b)</p> <p>= $A_{tr} f_{yt}/(1500 sn)$ in the expression for ACI 318-95</p>
l	= beam length, in ft
l_c	= length of constant moment region, in ft
l_s	= splice length, in in.
l_d	= development length, in in.
M	= slope of the modified relationship in Eq. 5.7
$M_{R_r = 0.075}$	= value of M at $R_r = 0.075$
M_u	= moment at splice or development failure, in kip-in.
m	= slope of the best-fit lines relating T_s/f'_c^P with NA_{tr}/n

N	= number of transverse reinforcing bars (stirrups or ties) along splice or development length
n	= number of spliced or developed bars
NHL	= normal strength concrete containing a "high" quantity of limestone coarse aggregate
NNB	= normal strength concrete containing a "normal" quantity of basalt coarse aggregate
NNL	= normal strength concrete containing a "normal" quantity of limestone coarse aggregate
NSC	= normal strength concrete [$f'_c < 8000 \text{ psi (55.2 Mpa)}$]
P	= total applied load at splice failure, in kips
Q_D	= random variable representing dead load effects
Q_{Dn}	= nominal dead load
Q_L	= random variable representing live load effects
Q_{Ln}	= nominal live load
$(Q_L/Q_D)_n$	= nominal ratio of live to dead load
q	= loading random variable
R	= random variable for resistance
R_n	= nominal resistance
R_p	= predicted capacity random variable
R_r	= relative rib area of bar (ratio of projected rib area normal to bar axis to the product of the nominal bar perimeter and the center-to-center rib spacing)
r	= resistance random variable = $R/R_n = X(1)R_p/R_n$
s	= spacing of transverse reinforcement, in in.
S_r	= rib center-to-center spacing, in in.
T_b	= total force in a bar at splice failure, in lb
T_c	= concrete contribution to total force in a bar at splice failure, in lb

T_s	= steel contribution to total force in a bar at splice failure, in lb
t_d	= term representing the effect of bar size on T_s . The value depends on the power of f'_c used in the analysis and the design expression in which it is used. In the final analysis, $t_d = 0.78 d_b + 0.22$ for $p = 3/4$. In the initial analysis, $t_d = 0.78 d_b + 0.13$ for $p = 1/4$, $t_d = 0.83 d_b + 0.17$ for $p = 1/2$, and $t_d = 0.73 d_b + 0.27$ for $p = 1.0$
	= $0.72 d_b + 0.28$ used in the design expressions developed by Darwin et al. (1995a, 1995b)
t_r	= term representing the effect of relative rib area on T_s . The value depends on the power of f'_c used in the analysis and the design expression in which it is used. In the final analysis, $t_r = 9.6 R_r + 0.28$ for $p = 3/4$. In the initial analysis, $t_r = 7.9 R_r + 0.41$ for $p = 1/4$, $t_r = 8.8 R_r + 0.34$ for $p = 1/2$, and $t_r = 10.3 R_r + 0.23$ for $p = 1.0$
	= $9.6 R_r + 0.28$ used in the design expressions developed by Darwin et al. (1995a, 1996a)
V_Q	= coefficient of variation for random variable for total load
V_m	= coefficient of variation associated with the predictive equation (or model) itself
V_{Q_D}	= coefficient of variation of random variable representing dead load effects
V_{Q_L}	= coefficient of variation of random variable representing live load effects
V_{R_r}	= coefficient of variation of relative rib area
V_r	= coefficient of variation of resistance random variable r
V_{TP}	= coefficient of variation of test/prediction ratio
V_{ts}	= coefficient of variation of the predictive equation caused by uncertainties in the measured loads and differences in the actual material and geometric properties of the specimens from values used to calculate the predicted strength
$V_{X(i)}$	= coefficient of variation of random variable $X(i)$
$V_{\phi q}$	= coefficient of variation of loading random variable q
W_r	= rib width (measured at 1/2 or 3/4 rib height), in in.
$X(1)$	= test-to-predicted load capacity random variable
$X(2)$	= actual-to-nominal dead load random variable

X(3)	= actual-to-nominal live load random variable
β	= reliability index
β_1	= ratio of the average concrete compressive stress to the maximum concrete stress used to calculate bar stress
ϵ_o	= concrete strain at maximum concrete stress
ϵ_{ct}	= strain at the extreme concrete compressive fiber of a beam at failure
ϵ_{sh}	= steel strain at the initiation of strain hardening
ϕ	= strength reduction factor for the main loading
ϕ_b	= overall strength reduction factor against bond failure
ϕ_d	= ϕ_b/ϕ , effective strength reduction factor for use in calculating development/splice length
γ_D	= load factor for dead loads
γ_L	= load factor for live loads

LIST OF TABLES

<u>Table</u>	<u>Page</u>
2.1 Splice specimen properties and test results	133
2.2 Properties of reinforcing bars	139
2.3 Concrete mix proportions (lb/yd ³) and properties	140
2.4a Number of cracks and crack widths at a bar stress of 20 ksi	142
2.4b Number of cracks and crack widths at a bar stress of 30 ksi	144
2.4c Number of cracks and crack widths at a bar stress of 40 ksi	146
3.1 Comparison of bottom-cast and top-cast splice specimens	148
3.2 Comparison of symmetrical and unsymmetrical splice specimens	149
3.3 Comparison of splice strength between one spliced layer and two spliced layers	150
3.4 Effect of shear force on splice strength	151
4.1 Splice specimen properties and test results from Darwin et al. (1995a, 1996a)	152
4.2 Splice specimen properties and test results from Hester et al. (1991, 1993)	156
4.3 Splice specimen properties and test results from Choi et al. (1990, 1991)	158
4.4 Effect of concrete properties on splice strength of the splices not confined by transverse reinforcement	159
4.5 Effect of deformation pattern on splice strength of the splices not confined by transverse reinforcement	159
4.6 Measurements of bar rib widths and rib width/spacing ratios	160
4.7 Effect of rib width/spacing ratio on splice strength of the splices not confined by stirrups	160
4.8 Comparison of flexural crack density and flexural crack width at a bar stress of 40 ksi between high relative rib area and conventional bars in matched pairs of specimens	161

4.9	Comparison of flexural crack density and flexural crack width at a bar stress of 20 ksi between high relative rib area and conventional bars in matched pairs of specimens	162
4.10	Comparison of flexural crack density and flexural crack width at a bar stress of 30 ksi between high relative rib area and conventional bars in matched pairs of specimens	163
5.1	Coefficients obtained in the derivation of Eq. 5.4 ($p = 1/4$)	164
5.2	Coefficients obtained in the derivation of Eq. 5.5 ($p = 1/2$)	165
5.3	Summary of test/prediction ratios using Eq. 5.3 for different powers of f'_c^p and definitions of effective value of c_{si}	166
5.4	Results of dummy variable analysis for $A_b f_s / f'_c^p$ versus the right side of Eq. 5.3 based on concrete strength	168
5.5	Data and test/prediction ratios for developed and spliced bars without confining reinforcement	169
5.6	Comparisons of the coefficients of determination for the best-fit lines of $T_s / f'_c^{1/4}$ versus NA_{tr}/n for bars in normal-strength concrete using c_{si} , $c_{si} + 0.25$ in., and $1.6c_{si}$ as the effective value of c_{si}	172
5.7	Comparisons of the coefficients of determination for the best-fit lines of T_s / f'_c^p versus NA_{tr}/n for high relative rib area and conventional bars	173
5.8	Results of best-fit lines for T_s / f'_c^p versus NA_{tr}/n (T_s in lb, f'_c^p in psi, and A_{tr} in in. ²)	173
5.9	Analysis of effects of relative rib area, R_r , and bar diameter, d_b , on increase in splice strength, represented by $T_s / f'_c^{3/4}$, provided by transverse reinforcement, represented by NA_{tr}/n (T_s in lb, $f'_c^{3/4}$ in psi, and A_{tr} in in. ²)	174
5.10	Summary of the expressions for t_r and t_d terms using different p values	174
5.11	Data and test/prediction ratios for developed and spliced bars with confining reinforcement	175
5.12	Results of dummy variable analyses, based on study and bar size, of increase in bond force due to transverse reinforcement, T_s , normalized with respect to f'_c^p versus $t_r t_d NA_{tr}/n$ for 163 beams (T_s in lb, f'_c^p in, psi and A_{tr} in in. ²)	180

5.13	Results of dummy variable analyses, based on study, for test/prediction ratio versus f'_c ^p using Eqs. 5.13a - 5.13d for 163 beams	181
5.14	Test/predicted splice strength ratios, using Eqs. 5.13a - 5.13d, for specimens tested by Kadoriku (1994)	182
5.15	Results of dummy variable analyses, based on study and bar size, of increase in bond force due to transverse reinforcement, T_s , normalized with respect to $f'_c^{3/4}$ versus $t_r t_d N A_{tr}/n$ for 196 beams (T_s in lb, $f'_c^{3/4}$ in. psi and A_{tr} in. ²)	183
5.16	Results of dummy variable analyses, based on study and bar size, of increase in bond force due to transverse reinforcement, T_s , normalized with respect to $f'_c^{3/4}$ versus $t_r t_d N A_{tr}/n$ for 191 beams with $(c + K_{tr})/d_b \leq 4$ [$K_{tr} = (0.518 t_r t_d A_{tr}/sn) f'_c^{1/2}$] (T_s in lb, $f'_c^{3/4}$ in psi and A_{tr} in. ²)	184
5.17a	Data for hypothetical beams without confining transverse reinforcement	185
5.17b	Data for hypothetical beams with confining transverse reinforcement	186
5.18	Strength reduction (ϕ) factor for bond	190
5.19	Data, development and splice lengths for hypothetical beams without confining transverse reinforcement	191
5.20	Test/prediction ratios for developed and spliced bars without confining transverse reinforcement using Eq. 5.33 and the ACI 318-95 criteria	193
5.21	Data, development and splice lengths for hypothetical beams with confining transverse reinforcement	196
5.22	Test/prediction ratios for developed and spliced bars with confining transverse reinforcement using Eq. 5.33 and the ACI 318-95 criteria	202
6.1	Effect of epoxy coating on splice strength for high relative rib area bars	206
6.2	Effect of epoxy coating on splice strength for conventional bars	208
6.3	Comparison of C/U ratio for using different types of coarse aggregate in concrete	210
6.4	Comparison of flexural crack density and flexural crack width at a bar stress of 40 ksi between beams containing coated and uncoated bars in matched pairs of specimens	211

7.1	Properties of reinforcing bars	213
7.2	Concrete mix proportions (lb/yd^3) and properties	213
7.3	Maximum slips under reversed cyclic loading at peak load	214
7.4	Comparison of average maximum slips under reversed cyclic loading at peak load for high R_t and conventional bars: (a) loaded end slips, (b) unloaded end slips	219
A.1	Data and bar stress for specimens containing developed and spliced bars	318
B.1	Coefficients obtained in the derivation of Eq. 5.3 for different powers of f'_c , p , and different effective values of c_{si}	336
B.2	Test/prediction ratios using Eq. 5.3 for different powers of f'_c and definitions of effective value c_{si}	338
B.3	Test/prediction strength ratios, using Eqs. 5.13a - 5.13d, for 163 beams	341
C.1	Comparison of flexural crack density and flexural crack width at a bar stress of 20 ksi between beams containing coated and uncoated bars in matched pairs of specimens	347
C.2	Comparison of flexural crack density and flexural crack width at a bar stress of 30 ksi between beams containing coated and uncoated bars in matched pairs of specimens	349

4.6	Increase in bond force, T_s , normalized with respect to $f'_c^{1/4}$ versus NA_{tr}/n for No. 8 (8N0) conventional bars in high-strength concrete as affected by type of coarse aggregate	248
4.7	Increase in bond force, T_s , normalized with respect to $f'_c^{1/4}$, versus NA_{tr}/n for No. 8 conventional bars and the 8N3 and 11F3 high R _r bars as affected by concrete strength	249
4.8	Increase in bond force, T_s , normalized with respect to $f'_c^{1/4}$, versus NA_{tr}/n for bars in NNL concrete as affected by bar size and relative rib area	250
4.9	Increase in bond force, T_s , normalized with respect to $f'_c^{1/4}$, versus NA_{tr}/n for No. 8 bars in NNB concrete as affected by relative rib area	251
4.10	Comparison of increase in bond force, T_s , normalized with respect to $f'_c^{1/4}$, for No. 8 high R _r bars as affected by bar rib width/spacing ratio	252
5.1	Bond cracks: (a) $c_{si} > c_b$, (b) $c_{si} < c_b$ (Darwin et al. 1995a, 1996a)	253
5.2	Experimental bond force, $T_c = A_b f_s$, normalized with respect to $f'_c^{1/2}$, versus predicted bond strength determined using Eq. 5.5 as a function of concrete strength for bars without confining transverse reinforcement	254
5.3	Range of relative intercept obtained from dummy variable analyses for experimental bond force, normalized with respect to f'_c^p versus predicted bond strength determined using Eq. 5.3 and $c_{si} + 0.25$ in. as the effective value of c_{si} as a function of the power of f'_c for bars without confining transverse reinforcement	255
5.4	Experimental bond force, $T_c = A_b f_s$, normalized with respect to $f'_c^{1/4}$, versus predicted bond strength determined using Eq. 5.4 as a function of concrete strength for bars without confining transverse reinforcement	256
5.5a	Test/prediction ratio determined using Eq. 5.4 versus concrete compressive strength, f'_c , for bars without confining transverse reinforcement	257
5.5b	Test/prediction ratio determined using Eq. 5.5 versus concrete compressive strength, f'_c , for bars without confining transverse reinforcement	258
5.6	Increase in bond force due to transverse reinforcement, T_s , normalized with respect to f'_c^p versus NA_{tr}/n for the 8N3 bars, (a) $p = 3/4$, (b) $p = 1/4$	259

LIST OF FIGURES

<u>Figure</u>		<u>Page</u>
2.1 Typical bottom-cast beam splice specimens	220	
2.2 Typical top-cast beam splice specimens	221	
2.3 Beam splice specimens in test group 22	222	
2.4 Beam splice specimens 23b.5 and 23b.6	223	
2.5 Beam splice specimens with two layers of bars	224	
2.6 Schematic of splice test setup	225	
2.7a Load-deflection curves for splice specimens in group 19	226	
2.7b Load-deflection curves for splice specimens in group 20	226	
2.7c Load-deflection curves for splice specimens in group 21	227	
2.7d Load-deflection curves for splice specimens in group 22	227	
2.7e Load-deflection curves for splice specimens in group 23a	228	
2.7f Load-deflection curves for splice specimens in group 23b	228	
2.7g Load-deflection curves for splice specimens in group 24	229	
2.7h Load-deflection curves for splice specimens in group 25	229	
2.7i Load-deflection curves for splice specimens in group 26	230	
2.7j Load-deflection curves for splice specimens in group 27	230	
2.7k Load-deflection curves for splice specimens in group 28	231	
2.7l Load-deflection curves for splice specimens in group 29	231	
2.7m Load-deflection curves for splice specimens in group 30	232	
2.7n Load-deflection curves for splice specimens in group 31	232	
2.7o Load-deflection curves for splice specimens in group 32	233	
2.7p Load-deflection curves for splice specimens in group 33	233	
2.7q Load-deflection curves for splice specimens in group 34	234	
2.7r Load-deflection curves for splice specimens in group 35	234	

2.7s	Load-deflection curves for splice specimens in group 36	235
2.7t	Load-deflection curves for splice specimens in group 37	235
2.7u	Load-deflection curves for splice specimens in group 38	236
2.7v	Load-deflection curves for splice specimens in group 39	236
2.7w	Load-deflection curves for splice specimens in group 40	237
2.7x	Load-deflection curves for splice specimens in group 41	237
2.7y	Load-deflection curves for splice specimens in group 42	238
2.7z	Load-deflection curves for splice specimens in group 43	238
2.8	Cracked splice specimen cast with normal-strength concrete after failure: (a) without stirrups, (b) with stirrups	239
2.9	Cracked splice specimens cast with high-strength concrete after failure: (a) without stirrups, (b) with stirrups	240
2.10	Flexural crack distribution on west side of splice region: (a) uncoated bars, (b) epoxy-coated bars	241
2.11	Cracked splice specimens with two-layer bars after failure: (a) one spliced layer and one continuous layer, (b) two spliced layers	242
4.1	Test/prediction ratio versus concrete compressive strength, f'_c , for splices not confined by transverse reinforcement in concrete containing basalt and limestone coarse aggregates	243
4.2	Test/prediction ratio versus concrete compressive strength, f'_c , for splices not confined by transverse reinforcement in concrete containing basalt and limestone coarse aggregates, using dummy variable analysis based on type of coarse aggregate	244
4.3	Increase in bond force, T_s , normalized with respect to $f'_c^{1/4}$, versus $t_r N A_{tr} / n$ for No. 8 conventional bars in NNL, NHL, HNL, and HHL concretes, showing contributions to splice strength as a function of concrete strength and quantity of coarse aggregate	245
4.4	Increase in bond force, T_s , normalized with respect to, $f'_c^{1/4}$ versus $N A_{tr} / n$ for the 8N3 bars in NNL, HNL, and HHL concrete, showing contributions to splice strength as a function of concrete strength and quantity of coarse aggregate	246
4.5	Increase in bond force, T_s , normalized with respect to, $f'_c^{1/4}$ versus $N A_{tr} / n$ for No. 8 bars in normal-strength concrete as affected by type of coarse aggregate and relative rib area	247

5.7	Increase in bond force due to transverse reinforcement, T_s , normalized with respect to $f'_c P$ versus NA_{tr}/n for the 11F3 bars, (a) $p = 3/4$, (b) $p = 1/4$	260
5.8	Increase in bond force due to transverse reinforcement, T_s , normalized with respect to $f'_c P$ versus NA_{tr}/n for No. 8 conventional bars, (a) $p = 1.0$, (b) $p = 1/4$	261
5.9	Increase in bond force due to transverse reinforcement, T_s , normalized with respect to $f'_c^{3/4}$, versus NA_{tr}/n for bars in concrete containing limestone coarse aggregate	262
5.10	Increase in bond force due to transverse reinforcement, T_s , normalized with respect to $f'_c^{3/4}$, versus NA_{tr}/n for bars in concrete containing basalt coarse aggregate	263
5.11	Mean slope from Eq. 5.7, M, for $p = 3/4$ versus relative rib area, R_r , for No. 5, No. 8, and No. 11 bars cast in concrete containing limestone coarse aggregate and No. 8 bars cast in concrete containing basalt coarse aggregate	264
5.12	Factor representing effect of relative rib area on increase in bond strength due to transverse reinforcement, $M/M_{Rr} = 0.075$, versus relative rib area, R_r	265
5.13	Mean slope from Eq. 5.7, M, normalized with respect to $t_r = 9.6 R_r + 0.28$, versus nominal bar diameter, d_b	266
5.14a	Increase in bond force due to transverse reinforcement, T_s , normalized with respect to $f'_c^{1/4}$, versus $(t_r t_d NA_{tr}/n)_{p=1/4}$ for 163 specimens with $l_d/d_b \geq 16$ and $(c + K_{tr})/d_b \leq 4$, [in this case, $K_{tr} = 35.3 t_r t_d N A_{tr}/n$, $t_r = 9.6 R_r + 0.28$, and $t_d = 0.72 d_b + 0.28$, as developed by Darwin et al. (1995b, 1996b)]	267
5.14b	Increase in bond force due to transverse reinforcement, T_s , normalized with respect to $f'_c^{1/2}$, versus $(t_r t_d NA_{tr}/n)_{p=1/2}$ for 163 specimens with $l_d/d_b \geq 16$ and $(c + K_{tr})/d_b \geq 4$, [in this case, $K_{tr} = 35.3 t_r t_d N A_{tr}/n$, $t_r = 9.6 R_r + 0.28$, and $t_d = 0.72 d_b + 0.28$, as developed by Darwin et al. (1995b, 1996b)]	268
5.14c	Increase in bond force due to transverse reinforcement, T_s , normalized with respect to $f'_c^{3/4}$, versus $(t_r t_d NA_{tr}/n)_{p=3/4}$ for 163 specimens with $l_d/d_b \geq 16$ and $(c + K_{tr})/d_b \leq 4$, [in this case, $K_{tr} = 35.3 t_r t_d N A_{tr}/n$, $t_r = 9.6 R_r + 0.28$, and $t_d = 0.72 d_b + 0.28$, as developed by Darwin et al. (1995b, 1996b)]	269

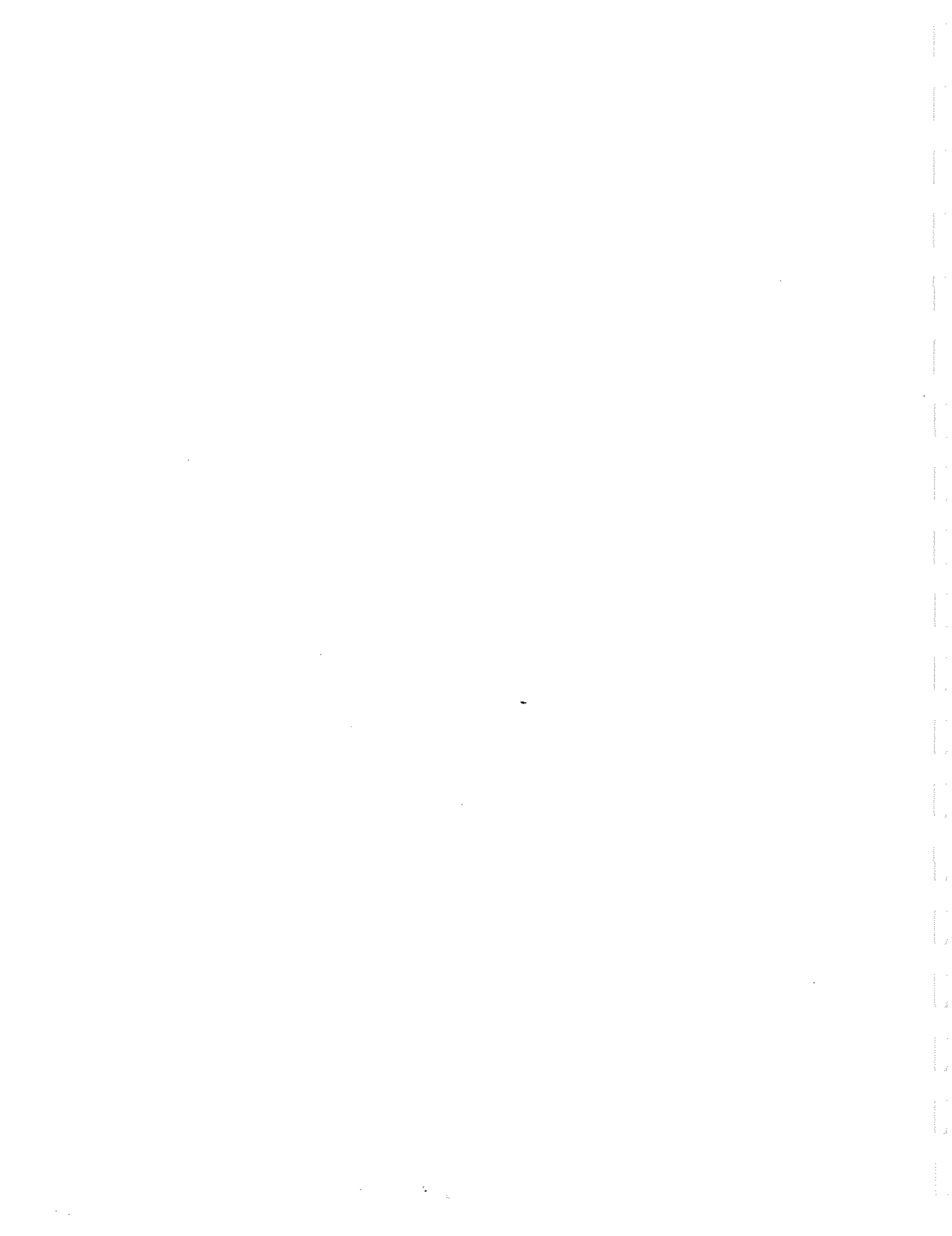
5.14d	Increase in bond force due to transverse reinforcement, T_s , normalized with respect to f'_c , versus $(t_r t_d N A_{tr}/n)_{p=1.0}$ for 163 specimens with $l_d/d_b \geq 16$ and $(c + K_{tr})/d_b \leq 4$, [in this case, $K_{tr} = 35.3 t_r t_d N A_{tr}/n$, $t_r = 9.6 R_r + 0.28$, and $t_d = 0.72 d_b + 0.28$, as developed by Darwin et al. (1995b, 1996b)]	270
5.15	Test/prediction ratios determined using Eqs. 5.13a - 5.13d corresponding to the powers of f'_c , $p = 1/4, 1/2, 3/4$, and 1.0, respectively, versus concrete compressive strength, f'_c , for 163 specimens	271
5.16	Test/prediction ratios determined using Eqs. 5.13a - 5.13d corresponding to the powers of f'_c , $p = 1/4, 1/2, 3/4$, and 1.0, respectively, versus concrete compressive strength, f'_c , for specimens tested by Kadoriku (1994)	272
5.17	Increase in bond force due to transverse reinforcement, T_s , normalized with respect to $f'_c^{3/4}$, versus $(t_r t_d N A_{tr}/n)_{p=3/4}$ for 196 specimens with $l_d/d_b \geq 16$ and $(c + K_{tr})/d_b \leq 4$, [in this case, $K_{tr} = 35.3 t_r t_d N A_{tr}/n$, $t_r = 9.6 R_r + 0.28$, and $t_d = 0.72 d_b + 0.28$ as developed by Darwin et al. (1995b, 1996b)]	273
5.18	Test/prediction ratio versus $(c + K_{tr})/d_b$ for 196 specimens [$K_{tr} = (0.518 t_r t_d A_{tr}/sn) f'_c^{1/2}$, $t_r = 9.6 R_r + 0.28$, $t_d = 0.78 d_b + 0.22$]	274
5.19	Increase in bond force due to transverse reinforcement, T_s , normalized with respect to $f'_c^{3/4}$, versus $t_r t_d N A_{tr}/n$ for 191 specimens with $l_d/d_b \geq 16$ and $(c + K_{tr})/d_b \leq 4$, [in this case, $K_{tr} = (0.52 t_r t_d A_{tr}/n) f'_c^{1/2}$, $t_r = 9.6 R_r + 0.28$, and $t_d = 0.78 d_b + 0.22$]	275
5.20	Test/prediction ratio using Eq. 5.18 versus $(c + K_{tr})/d_b$ for 213 specimens with $l_d/d_b \geq 16$ [$K_{tr} = (0.52 t_r t_d A_{tr}/sn) f'_c^{1/2}$, $t_r = 9.6 R_r + 0.28$, $t_d = 0.78 d_b + 0.22$]	276
5.21	Test/prediction ratio using Eq. 5.18 versus $(c + K_{tr})/d_b$ for 191 specimens with $l_d/d_b \geq 16$ and $(c + K_{tr})/d_b \leq 4$ [$K_{tr} = (0.52 t_r t_d A_{tr}/sn) f'_c^{1/2}$, $t_r = 9.6 R_r + 0.28$, $t_d = 0.78 d_b + 0.22$]	277
5.22	Test/prediction ratio using Eq. 5.20 versus $(c + K_{tr})/d_b$ for 213 specimens with $l_d/d_b \geq 16$ and setting $(c + K_{tr})/d_b \leq 4$ [$K_{tr} = (0.52 t_r t_d A_{tr}/sn) f'_c^{1/2}$, $t_r = 9.6 R_r + 0.28$, $t_d = 0.78 d_b + 0.22$]	278
5.23	Experimental bond force, $T_b = A_b f_s$, normalized with respect to $f'_c^{1/4}$ versus predicted bond strength determined using Eq. 5.18 for 191 specimens containing bars confined by transverse reinforcement with $l_d/d_b \geq 16$ and $(c + K_{tr})/d_b \leq 4$ [$K_{tr} = (0.52 t_r t_d A_{tr}/sn) f'_c^{1/2}$, $t_r = 9.6 R_r + 0.28$, $t_d = 0.78 d_b + 0.22$]	279

5.24	Comparison of test/prediction ratio distribution using Eq. 5.33 and ACI 318-95 for specimens containing bars without confining Transverse reinforcement	280
5.25	Comparison of test/prediction ratio distribution using Eq. 5.33 and ACI 318-95 for specimens containing No. 7 and larger bars without confining transverse reinforcement	281
5.26	Comparison of test/prediction ratio distribution using Eq. 5.33 and ACI 318-95 for specimens containing No. 6 and smaller bars without confining transverse reinforcement	282
5.27	Comparison of test/prediction ratio distribution using Eq. 5.33 and ACI 318-95 for specimens containing bars with confining Transverse reinforcement	283
5.28	Comparison of test/prediction ratio distribution using Eq. 5.33 and ACI 318-95 for specimens containing No. 7 and larger bars with confining transverse reinforcement	284
5.29	Comparison of test/prediction ratio distribution using Eq. 5.33 and ACI 318-95 for specimens containing No. 6 and smaller bars with confining transverse reinforcement	285
6.1	Normalized relative splice strength ratio, C/U, versus concrete compressive strength, f'_c , for matched pairs of specimens containing epoxy-coated and uncoated No. 8 conventional bars and No. 8 and No. 11 high relative rib area bars	286
6.2	Normalized relative splice strength ratio, C/U, versus concrete compressive strength, f'_c , for 62 matched pairs of specimens containing epoxy-coated and uncoated bars	287
6.3	Normalized relative splice strength ratio, C/U, versus relative rib area, R_r , for matched pairs of specimens cast with normal-strength concrete containing epoxy-coated and uncoated bars	288
6.4	Normalized relative splice strength ratio, C/U, versus relative rib area, R_r , for matched pairs of specimens cast with high-strength concrete containing epoxy-coated and uncoated bars	289
7.1	Schematic of reversed cyclic loading specimen	290
7.2	Schematic of reversed cyclic loading test setup	291
7.3a	Load versus loaded end and unloaded end slips for bar 8C0A-3 on the left side of the specimen	292
7.3b	Load versus loaded end and unloaded end slips for bar 8C0A-3 on the right side of the specimen	293

7.3c	Load versus loaded end and unloaded end slips for bar 8C0A-5 on the left side of the specimen	294
7.3d	Load versus loaded end and unloaded end slips for bar 8C0A-5 on the right side of the specimen	295
7.3e	Load versus loaded end and unloaded end slips for bar 8C0A-7 on the left side of the specimen	296
7.3f	Load versus loaded end and unloaded end slips for bar 8C0A-7 on the right side of the specimen	297
7.3g	Load versus loaded end and unloaded end slips for bar 8C0A-9 on the left side of the specimen	298
7.3h	Load versus loaded end and unloaded end slips for bar 8C0A-9 on the right side of the specimen	299
7.3i	Load versus loaded end and unloaded end slips for bar 8C0A-11 on the left side of the specimen	300
7.3j	Load versus loaded end and unloaded end slips for bar 8C0A-11 on the right side of the specimen	301
7.3k	Load versus loaded end and unloaded end slips for bar 8N3-4 on the left side of the specimen	302
7.3l	Load versus loaded end and unloaded end slips for bar 8N3-4 on the right side of the specimen	303
7.3m	Load versus loaded end and unloaded end slips for bar 8N3-6 on the left side of the specimen	304
7.3n	Load versus loaded end and unloaded end slips for bar 8N3-6 on the right side of the specimen	305
7.3o	Load versus loaded end and unloaded end slips for bar 8N3-8 on the left side of the specimen	306
7.3p	Load versus loaded end and unloaded end slips for bar 8N3-8 on the right side of the specimen	307
7.3q	Load versus loaded end and unloaded end slips for bar 8N3-10 on the left side of the specimen	308
7.3r	Load versus loaded end and unloaded end slips for bar 8N3-10 on the right side of the specimen	309
7.4	Average slips of conventional bars 3, 5, 7, 9, and 11 and high relative rib area bars 4, 6, 8, and 10 at peak loads versus number of loading cycles for left side loading	310

7.5	Average slips of conventional bars 3, 5, 7, 9, and 11 and high relative rib area bars 4, 6, 8, and 10 at peak loads versus number of loading cycles for right side loading	311
A.1	Typical compressive stress-strain curves for normal density Concrete (Nilson 1997)	325
A.2	Concrete compressive strain at maximum compressive stress, ε_0 , versus concrete compressive strength, f'_c , for normal density concrete used in the current study	325
A.3	Typical stress-strain curves for reinforcing bars (Nilson 1997)	326
A.4	Ideal stress-strain curves for reinforcing bars used in the current Study	326
A.5	Ratio of bar stress calculated using the working stress method, f_{sw} , to bar stress calculated using the moment-curvature method, f_{sc} , versus ratio of concrete strain at extreme compressive fiber to concrete strain at maximum stress from concrete stress-strain curve for bars with $f_{sc} < f_y$	327
A.6	Ratio of bar stress calculated using the working stress method, f_{sw} , to bar stress calculated using the moment-curvature method, f_{sc} , versus concrete compressive strength, f'_c , for bars with $f_{sc} < f_y$	328
A.7	Ratio of bar stress calculated using the ultimate strength method, f_{su} , to bar stress calculated using the moment-curvature method, f_{sc} , versus ratio of concrete strain at extreme compressive fiber to concrete strain at maximum stress from concrete stress-strain curve for bars with $f_{sc} < f_y$	329
A.8	Ratio of bar stress calculated using the ultimate strength method, f_{su} , to bar stress calculated using the moment-curvature method, f_{sc} , versus concrete compressive strength, f'_c , for bars with $f_{sc} < f_y$	330
A.9	Ratio of bar stress calculated using the working stress method, f_{sw} , to bar stress calculated using the moment-curvature method, f_{sc} , versus ratio of concrete strain at extreme compressive fiber to concrete strain at maximum stress from concrete stress-strain curve for bars with $f_{sc} \geq f_y$	331
A.10	Ratio of bar stress calculated using the working stress method, f_{sw} , to bar stress calculated using the moment-curvature method, f_{sc} , versus concrete compressive strength, f'_c , for bars with $f_{sc} \geq f_y$	332

A.11	Ratio of bar stress calculated using the ultimate strength method, f_{su} , to bar stress calculated using the moment-curvature method, f_{sc} , versus ratio of concrete strain at extreme compressive fiber to concrete strain at maximum stress from concrete stress-strain curve for bars with $f_{sc} \geq f_y$	333
A.12	Ratio of bar stress calculated using the working stress method, f_{sw} , to bar stress calculated using the moment-curvature method, f_{sc} , versus concrete compressive strength, f'_c , for bars with $f_{sc} \geq f_y$	334



CHAPTER 1: INTRODUCTION

1.1 General

Reinforced concrete consists of reinforcing steel bars embedded in concrete. Concrete is strong in compression but weak in tension. Steel is strong in both compression and tension. By combining the advantages of the two materials, reinforced concrete has become widely used as a structural material.

In reinforced concrete structures, adequate bond must be developed to ensure that reinforcing bars and concrete work together and that stress is transferred between the two materials. The bond between reinforcing bars and concrete is provided by chemical adhesion, friction, and mechanical interlock. For smooth bars, bond strength is provided by chemical adhesion and friction. For deformed bars, bond strength is higher than for smooth bars due to the mechanical interlock provided by bearing of ribs on the bars against the surrounding concrete. Inadequate bond may cause a reinforced concrete structure to fail.

In reinforced concrete structural design, reinforcing bars must be developed or spliced where the bars are discontinued or cut off. Development and splice strength is dependent on the bond characteristics of both reinforcing bars and concrete. It has been demonstrated that the deformation properties of reinforcing bars, such as rib height and rib spacing, as well as rib face angle, significantly affect bond strength. Concrete strength also plays an important role in bond. Other parameters that affect bond strength include bar size and spacing, placement of bars, coating of bars, concrete cover, and confinement by transverse reinforcement. An accurate representation for predicting development and splice strength should consider all of these parameters.

This study is an extension of previous work at the University of Kansas to improve the development characteristics of steel reinforcing bars. The previous studies have shown that modified deformation patterns can improve the development and splice strength of steel reinforcement. The current study includes experiments and analyses focusing on the effects of high strength concrete, deformation properties of reinforcing bars, placement of bars, and epoxy coating. The test results from this study, along with results of previous studies, are used to establish accurate design equations to predict the development/splice strength. A reliability analysis is used to obtain the resistance factors for use with design equations.

1.2 Previous Studies

1.2.1 Effect of bar deformations

The earliest study on bond resistance of smooth and deformed reinforcing bars was done by Abrams (1913). Both pullout and beam specimens were tested. The test results showed that deformed bars produced higher bond resistance than smooth bars. Abrams found that, in pullout tests of smooth bars, bond resistance reached its maximum value at a loaded end slip of about 0.01 in. (0.25 mm). For deformed bars, the load-slip performance was the same as for smooth bars until a slip corresponding to the maximum bond resistance of the smooth bars. As slip continued, the projections (ribs) on deformed bars provided a further increase in bond resistance by direct bearing of the projections on the adjacent concrete. Abrams observed that the ratio of the bearing area of the projections (projected area measured perpendicular to the bar axis) to the superficial area (entire surface area) of the bar in the same length could be used as criterion for evaluating the bond resistance of deformed bars. To improve bond resistance, he recommended that the ratio not be less than 0.2, resulting

in closer spacings of the projections than were used in commercial deformed bars at that time.

Over thirty years later, Clark (1946, 1949) investigated 17 commercial deformation patterns using pullout and beam tests. The bond performance for each pattern was evaluated based on the bond stress developed at predetermined values of slip. Based on Clark's investigations, standard deformation requirements were introduced for the first time in the Tentative Specification ASTM A 305-47T (1947) that was later modified to ASTM A 305-49 (1949). The requirements included a maximum average spacing of deformations equal to 70 percent of the nominal diameter of the bar and a minimum height of deformations equal to 4.5 percent of the nominal diameter for bars with a nominal diameter of 5/8 in. or smaller and 5 percent for larger bars. Forty seven years later, these requirements remain unchanged in the current ASTM specifications for reinforcing bars (ASTM A 615/A 615M-95b, ASTM A 616/A 616M-95b, ASTM A 617/A 617M-95b, ASTM A 706/A 706M-95b, ASTM A 722-90).

In addition to the specification criteria, Clark found that bond performance was improved for bars with lower ratios of shearing area (bar perimeter times center to center distance between ribs) to bearing area (projected rib area normal to the bar axis). The inverse of this ratio, the relative rib area, R_r , is used most often today to describe deformation geometry. Clark recommended that the ratio of shearing area to bearing area be limited to a maximum of 10 and, if possible, 5 or 6, which, in turn, become a minimum value of R_r equal to 0.1 with desirable values of 0.2 or 0.17 [not so different from Abrams (1913) recommendations]. These later recommendations were not incorporated in ASTM requirements, so that typical values of relative rib

area of the bars currently used in U. S. range between 0.057 and 0.087 (Choi, Hadje-Ghaffari, Darwin, and McCabe 1990a).

Rehm (1957, 1961) reported that one of two failure modes, splitting or pullout, can occur when a reinforcing bar moves with respect to concrete. If the ratio of rib spacing to rib height is greater than 10 and the rib face angle (the angle between the face of the rib and the longitudinal axis of the bar) is greater than 40° , the concrete in front of concrete crushes, forming wedges and then inducing tensile stress perpendicular to the bar axis, which results in transverse cracking and splitting of surrounding concrete. If the ribs have a spacing to height ratio less than 7, with a rib face angle greater than 40° , the concrete in front of ribs gradually crushes, causing a pullout failure.

Lutz, Gergely and Winter (1966) and Lutz and Gergely (1967) found that for a deformed bar with a rib face angle greater than 40° , slip occurs by progressively crushing concrete in front of the ribs, producing a region of crushed concrete with a face angle of 30° to 40° , which acts as a wedge. Lutz et al. also showed that no crushing of concrete occurs if the rib face angle is less than 30° . These observations were supported by Skorobogatov and Edwards (1979). Based on tests using bars with face angles of 48.5° and 57.8° , Skorobogatov and Edwards showed that these differences in face angle do not affect bond strength because the high face angle is flattened by crushed concrete in front of the ribs.

Losberg and Olsson (1979) tested three commercial deformation patterns used in Sweden, as well as some machined bars with different values of rib spacing and rib height. They found that the bond forces produced by the three patterns were obviously different in a pullout test in which a pullout failure governed. However, if splitting failure governed, as in beam end and "ring pull out" tests, there was little

difference in the bond forces obtained using the three patterns. Losberg and Olsson concluded that pullout tests are not suitable to study bond performance, since the state of stress in a pullout test resulting from the additional confinement provided to the concrete does not represent the state of stress in actual structures. In most structural applications, a splitting failure is more common, while in pullout tests, a splitting failure normally does not occur. Their test results also showed that the splitting force is not sensitive to rib spacing and that transverse ribs (ribs oriented perpendicular to the longitudinal axis of the bar) give slightly higher splitting force than inclined ribs.

Soretz and Holzenbein (1979) studied the effect of pattern parameters, including rib height and spacing, rib inclination, and the cross sectional shape of ribs. Three bars were machined with different rib heights and spacings, but the same rib bearing area per unit length. Soretz and Holzenbein found that, for the three patterns, the bond forces showed no significant differences up to 1 mm of slip. However, when the slip was greater than 1 mm, the bond force for the bar with the lowest rib height was about 20 percent smaller than that of the other two patterns. They recommended a combination of minimum rib height of 0.03 bar diameter and rib spacing of 0.3 bar diameter as the optimum geometry for deformed bars to limit splitting effect and to increase bond strength.

Darwin and Graham (1993a, 1993b) conducted 156 beam-end specimen tests, studying the effect of deformation pattern on bond strength. The principal parameters in the study were rib height, rib spacing, relative rib area, and degree of confinement from concrete cover and transverse reinforcement. Specially machined 1 in. (25.4 mm) diameter bars were used in the study, along with conventional bars for comparison. The machined bars had three different rib heights, 0.050, 0.075 and 0.100 in. (1.27, 1.91, and 2.54 mm), with center-to-center rib spacings ranging from

0.263 to 2.2 in. (6.68 to 55.9 mm), producing relative rib areas of 0.20, 0.10 and 0.05. Darwin and Graham concluded that bond strength is independent of deformation pattern if the bar is under relatively low confinement (small concrete cover and no transverse reinforcement) and bond strength is governed by a splitting failure of the concrete. However, if additional confinement is provided by transverse reinforcement, bond strength increases with an increase in relative rib area. They found that the bond force-slip response of bars is related to the relative rib area of the bars, but independent of the specific combination of rib height and spacing. The initial stiffness of the load-slip curve increases with an increase in relative rib area. Darwin and Graham also observed that, when tested in beam-end specimens, bars with the longitudinal ribs oriented in a vertical plane (paralleled to the splitting cracks) provide higher bond strength than bars with the longitudinal ribs oriented in a horizontal plane (perpendicular to the splitting cracks).

Cairns and Jones (1995) investigated 14 different bar geometries using lapped joint test specimens. The lapped joints were confined by stirrups. The relative rib area of the tested bars ranged from 0.031 to 0.090. The inclination of the transverse ribs varied from 40° to 90° and the rib face angle varied from 28° to 51°. Bars were placed in two ways, either alignment A0 (with the plane of two longitudinal ribs parallel to the concrete splitting face) or alignment A90 (with the plane of longitudinal ribs perpendicular to the concrete splitting face). Cairns and Jones reported that there were no significant effects of rib inclination and rib face angle on bond strength, but that, as observed by Darwin and Graham (1993a, 1993b), the alignment of ribs influenced bond strength: the bond force for alignment A0 was higher than for alignment A90. They found that relative rib area plays an important

role on bond strength. The test results indicated that doubling relative rib area could reduce lap and anchorage length by 20 percent.

In a recent study by Darwin, Tholen, Idun, and Zuo (1995a, 1996a), Idun and Darwin (1995), and Tholen and Darwin (1996), 83 beam-splice specimens and 58 beam-end specimens were tested to study the effect of relative rib area on bond strength. The tests involved commercially produced reinforcing bars with high relative rib areas ranging from 0.101 to 0.140 and conventional bars with relative rib areas ranging from 0.068 to 0.087. The tests also included some specimens to study the effect of relative rib area on the splice strength of epoxy-coated bars. The test results indicated that the splice strength of uncoated bars is not affected by the deformation pattern if the bars are not confined by transverse reinforcement. For bars confined by transverse reinforcement, splice strength increases with increases in bar diameter and relative rib area. For coated bars, under all conditions of confinement, splice strength increases with relative rib area.

1.2.2 Effect of Bar Position

As early as 1913, Abrams (1913) observed that bond strength could be affected by bar position during concrete placement. The bond strength of bars with a horizontal position during casting concrete was much lower than the bond strength of bars with a vertical position due to settlement of concrete. Clark (1947, 1949) found that the bond strengths of the beam and pull-out specimens were greater when the bars were near the bottom than when they were near the top of the specimens. Top-bar effects have also been reported by Collier (1947), Menzel (1952), Ferguson and Thompson (1962, 1965), Thompson et al. (1975), Luke et al. (1981), Zekany et al.

(1981), Donahey and Darwin (1983, 1985), Altowaiji et al. (1984, 1986), Brettmann et al. (1984, 1986), and DeVries et al. (1991).

The reduction of the bond strength of top-cast bars can be explained due to bleeding and settlement of the concrete below the bar. The effects of the depth of concrete under the bars and slump of concrete have been shown in several studies (Menzel 1952, Ferguson and Thompson 1965, Luke et al. 1981, Zekany et al. 1981, Brettmann et al. 1984, 1986). These studies have demonstrated that the bond strength of top-cast bars decreases with increasing depth of concrete below the bar and increasing concrete slump.

CUR (1963) found that the bond strength ratio of top-cast to bottom-cast bars decreases significantly as cover decreases. The effect of cover was also reported by Donahey and Darwin (1983).

In the study by Jeanty, Mitchell and Mirza (1988), the top-bar factor was found to be about 1.22 for beam-development specimens. Zekany et al. (1981) reported an average splice strength ratio of top-cast to bottom-cast bar as 0.9 with a standard deviation of 0.08.

The top-bar effect was first introduced to ACI Building Code in 1951 (ACI 318-51). Top bars were defined as horizontal bars with more than 12 in. of fresh concrete cast in the member below the bars. Based on the test results of Clark (1946), a reduction factor of 0.7 was used for the allowable bond stress of top bars in ACI 318-51. In ACI 318-71 (1971), the top-bar effect was accounted for by multiplying the development length by a factor of 1.4, the approximate inverse of the 0.7 reduction factor. This factor was reduced to 1.3 in ACI 318-89.

1.2.3 Effect of Epoxy Coating

The earliest study on bond of epoxy-coated bars was carried out by Mathey and Clifton (1976). They investigated the effect of coating thickness on bond strength using pullout tests. They found that, for bars with an epoxy coating between 1 to 11 mils (0.0254 to 0.279 mm) in thickness, bond strength was only about 6 percent lower than for the uncoated bars. However, for bars with a coating thickness of 25 mils (0.635 mm), the bond force was considerably (56%) lower than for the uncoated bars.

Johnston and Zia (1982) studied the effect of epoxy coating on bond strength using slab and beam-end specimens. The coating thickness of the epoxy-coated bars was between 6.7 and 11.1 mils (0.170 to 0.282 mm). The specimens were confined by transverse reinforcement. They reported that the slab specimens with coated bars had slightly larger deflection and wider cracks than those with uncoated bars. Compared with the uncoated bars, the bond strength of coated bars was about 4% lower for the slab specimens and 15% lower for the beam-end specimens. Based on their test results, Johnston and Zia recommended an increase of 15% in the development length when coated bars are used in place of uncoated bars.

Treecce and Jirsa (1987, 1989) tested 21 beam-splice specimens without transverse reinforcement in the splice region. They used 10 specimens with No. 6 bars and 11 specimens with No. 11 bars. Twelve of the specimens contained epoxy-coated bars with coating thicknesses between 4.5 and 14 mils (0.114 to 0.356 mm). Seventeen specimens contained top-cast bars; four contained bottom-cast bars. Concrete strength ranged from 3860 to 12,600 psi (26.6 to 86.9 MPa). Four of the No. 6 bar specimens had cover less than or equal to the maximum size of the aggregate, which is believed to reduce bond strength (Donahey and Darwin 1985).

An average bond strength reduction of 34% was obtained from the tests. The work by Treece and Jirsa is the basis of the development length modification factor for epoxy-coated bars in the ACI Building Code (1989, 1995) and AASHTO Bridge Specification (1989, 1992, 1996). In the ACI Code, the development length is multiplied by a factor of 1.5 for the epoxy-coated bars with a cover of less than $3d_b$ or clear spacing between the bars less than $6d_b$ and 1.2 for other cases, with a maximum of 1.7 for the product of top-cast bar factor and epoxy-coating factor. In the AASHTO Bridge Specifications (1989, 1992), the three factors are 1.5, 1.15, and 1.7, respectively.

Choi, Hadje-Ghaffari, Darwin, and McCabe (1990, 1991) investigated the effect of epoxy coating on the bond strength, considering the roles of coating thickness, bar size and deformation pattern. Beam-end and splice specimens containing No. 5, No. 6, No. 8, and No. 11 bottom-cast bars with three deformation patterns were used in the study. Coating thickness ranged from 3 to 17 mils (0.076 to 0.432 mm). Using the test results of beam-end specimens, Choi et al. observed that coating thickness has little effect on the reduction of bond strength due to epoxy coating for No. 6 and larger bars. However, for No. 5 bars, the C/U ratio decreases with increasing coating thickness. The results of beam-end specimens also indicated that, in general, C/U ratio decreases as bar size increases and epoxy coating is less detrimental to bond strength of bars with higher relative rib areas. The average bond strength ratio for epoxy-coated bars to uncoated bars, C/U, was observed to be 0.82 for 15 splice specimens.

Hester, Salamizavaregh, Darwin, and McCabe (1991, 1993) conducted 65 beam and slab splice tests. No. 6 and No. 8 bars with three deformation patterns were used in this study. The average coating thickness ranged from 6 to 11 mils (0.152 to

0.279 mm). The test results were analyzed, along with the results of an additional 48 splice specimens from other studies. They found a significant reduction in splice strength due to epoxy coating. However, the extent of the reduction was less than used to select the development and splice length modification factors in the 1989 AASHTO Bridge Specification and 1989 ACI Building Code. The results indicated that the decrease in splice strength caused by epoxy coating is independent on the degree of transverse reinforcement. They also observed that transverse reinforcement improves splice strength for both uncoated and coated splices. This improvement is approximately the same for both uncoated and coated bars. They recommended a single development length modification factor of 1.35 for bars not confined by transverse reinforcement and 1.2 for bars with a minimum amount of transverse reinforcement.

DeVries, Moehle, and Hester (1991) tested 36 beam-splice specimens containing top-cast and bottom-cast bars. Both coated and uncoated bars were used. The ratio of bottom-cast to top-cast bar strength ranged from 1.01 to 1.3. DeVries et al. concluded that the effects of casting position and epoxy coating appeared not to be cumulative. They recommended the use of development length modification factors of 1.3 for uncoated top-cast bars and 1.5 for epoxy-coated bars regardless of casting position.

In a recent study by Idun and Darwin (1995), beam-end and beam-splice specimens were used to study the effect of relative rib area on bond strength for both uncoated and epoxy-coated bars. They found that epoxy coating has a less detrimental effect on bond strength for high relative rib rear bars, matching the results of the study by Choi et al. (1990a, 1990b, 1991). Idun and Darwin also conducted coefficient of friction tests for both coated and uncoated reinforcing steel. The

coefficients of friction obtained were 0.56 for uncoated steel and 0.49 for epoxy-coated steel. Using the results of the coefficient of friction tests and a theoretical relation between C/U ratio and rib face angle developed by Hadje-Ghaffari et al. (1991), Idun and Darwin observed that epoxy coating should cause the least reduction in bond strength for rib face angles greater than 43°. This finding was generally supported by the results of their beam-end tests.

Tan, Darwin, Tholen, and Zuo (1996) extended the work of Idun and Darwin (1995). They found that an increase in the relative rib area improves the relative splice strength of epoxy-coated to uncoated bars, whether or not the splices are confined by transverse reinforcement, i.e. transverse reinforcement does not affect relative splice strength. Tan et al. recommended a development length modification factor of 1.2 for epoxy-coated high relative rib area bars.

1.2.4 Effect of High-Strength Concrete

Azizinamini et al. (1993, 1995) studied the effect of high strength concrete on bond strength using beam-splice tests. The tests included both bottom-cast and top-cast bars with one bar diameter (d_b) of concrete cover. The test results indicated that the bond stress, u ($u = f_s d_b / 4l_s$, where f_s = stress, and l_s = splice length), normalized with respect to square root of concrete compressive strength, $\sqrt{f'_c}$, decreases with an increase in concrete compressive strength and that this rate of decrease increases as splice length increases. Azizinamini et al. noted that the bearing capacity of concrete is related to f'_c , whereas the tensile capacity is related to $\sqrt{f'_c}$. Therefore, the rate of increase of the bearing capacity with an increase in concrete strength is greater than the rate of increase of the tensile capacity. For high strength concrete, the higher bearing capacity of the concrete prevents crushing of concrete in front of bar ribs, which reduces local slip. They concluded that, in the case of high strength concrete,

fewer ribs participate in resisting applied forces than in the case of normal strength concrete, which, coupled with small concrete cover, results in a splitting failure of the concrete prior to achieving a uniform bond stress distribution at ultimate. Another observation is that top-cast splices show slightly higher bond strength than bottom-cast splices in high strength concrete. Azizinamini et al. believed that the later observation is due to the lower quality of concrete underneath top-cast bars which reduces the bearing capacity of concrete adjacent to the ribs of the bars, allowing more crushing of concrete along the splice length, greater slip, and a more uniform distribution of bond stress. The participation of more ribs along the splice length, in turn, results in higher bond strength. Azizinamini et al. also concluded that, due to the brittle failure behavior of splices in high strength concrete, a minimum stirrup requirement is necessary for the splices in high strength concrete to ensure an adequate level of ductility.

Esfahani and Rangan (1995) investigated the influence of concrete strength on bond strength using both beam-end and beam-splice tests. Concrete strengths ranged from 26 MPa (3770 psi) to 75 MPa (10880 psi) for the beam-end specimens and from 66 MPa (9570 psi) to 98 MPa (14,210 psi) for the beam-splice specimens. No confining transverse reinforcement was used. Esfahani and Rangan observed that the extent of concrete crushing in front of ribs in beam-end specimens varied depending on the concrete strength. For normal strength concrete [$f'_c = 26$ MPa (3370 psi)], concrete crushing always occurred for both small and large concrete covers. For 50 MPa (7250 psi) concrete, concrete crushing only occurred for large concrete cover. For 75 MPa (10,880 psi) concrete, no concrete crushing was observed. They also found that, for the same C/d_b ratio (C = minimum value of bottom cover, side cover, and one-half of the center-to-center bar spacing), bond strength normalized with respect to square root of the concrete compressive strength was, in contrast to

Azizinamini et al. (1993, 1995), higher for high strength concrete than for normal strength concrete.

1.2.5 Bond Behavior of Bars under Reversed Cyclic Loading

In a study of bond stress-slip behavior under repeated loading, Morita and Kaku (1973) found that after loading in one direction, the bond stress-slip curve for loading in the reverse direction is almost identical to the monotonic envelope (the curve when loading the first time) in that direction. Once a peak slip is reached, a considerable reduction in bond resistance is produced at lower slip values for subsequent loading. They also found that, for a constant slip value, a moderate deterioration of the peak bond stress occurs under cyclic loading, which is not significantly affected by the loading history.

Eligehausen et al. (1983) studied the local bond stress-slip relationship of deformed bars under monotonic and cyclic loading. Beam-column joint specimens were used. The key parameters included bar size and spacing, confining reinforcement, concrete strength, transverse pressure, and loading rate. As observed by Morita and Kaku (1973), deterioration of bond strength and stiffness increases with increasing peak slip values and number of cycles, and is larger for full reversals of slip than for half cycles (loading in one direction only). The initial part of the stress-slip curve for bars under reversed cyclic loading is similar to the monotonic envelope. As the load increases and cycling progresses, the concrete in front of bar ribs crushes and shears. When the load is reversed, large slip occurs before the ribs bear against concrete in the other direction, resulting in a permanent slip. Cyclic loading beyond the slip values corresponding to a bond stress of 80% of its ultimate strength results in rapid deterioration of bond strength and stiffness.

The slip of bars in beam-column joints under load reversals plays an important role in the ability of reinforced concrete frames to resist seismic loading (Durrani and Wight 1982, Zhu and Jirsa 1983, Ciampi et al. 1983). Based on "push-pull" tests of bars embedded in beam-column specimens, Ciampi et al. found that, to reduce the slip, an anchorage length of about 25 and 35 bar diameters is necessary for Grade 40 and 50 deformed bars, respectively. Zhu and Jirsa (1983) reevaluated available test results of beam-column joints under load reversals. They concluded that ratios of column width to beam bar diameter of 20 to 22 are appropriate to avoid bond damage with a relative interstory drift of 0.03. Based on their evaluations, ratios of bar diameter to column dimension of 1/20 for normal weight concrete and 1/26 for lightweight concrete were chosen for beam-column joints subjected to earthquake loading (ACI 318-95).

1.2.6 Design Equations

Expressions for development and splice strength have been empirically based. Studies by Mathey and Watstein (1961) and Ferguson and Thompson (1962) provided the basis for the 1963 ACI Building Code (ACI 318-63) expressions to determine development length. Flexural bond was introduced to describe the bond stress induced by force transfer between concrete and steel bars in tension. In the studies, the ultimate bond stress was found to be a function of the ratio of the development or embedment length to the bar diameter, l_d/d_b , and the square root of concrete compressive strength, $\sqrt{f'_c}$. In ACI 318-63 the ultimate bond stress, u_u , for both flexural and anchorage bond was limited to

$$u_u = \frac{9.5\sqrt{f'_c}}{d_b} \leq 800 \text{ psi (5.52 MPa)} \quad (1.1)$$

The equilibrium condition, $A_s f_s = u_u \pi d_b l_d$, gives

$$u_u = \frac{f_s A_s}{4l_d} \quad (1.2)$$

where f_s = stress in the bar, in psi, and A_s = the area of the bar, in in.²

Development and embedment lengths were obtained using Eqs. (1.1) and (1.2).

Beginning with the 1971 Building Code (ACI 318-71), development length could be calculated directly by assuming that bond stresses are uniformly distributed along the bar and that, within the development length, the bar must develop 125 percent of its yield strength, which gives

$$u_u \pi d_b l_d = A_s (1.25 f_y) \quad (1.3)$$

so that,

$$l_d = \frac{A_s (1.25 f_y)}{\pi d_b (9.5 \sqrt{f'_c} / d_b)} \approx \frac{0.04 A_s f_y}{\sqrt{f'_c}} \quad (1.4)$$

where f_y = yield strength of the bar.

In a statistical study of the bond strength of reinforcing bars, Orangun, Jirsa, and Breen (1975, 1977) developed an expression for development and splice strength in terms of average bond stress :

$$u = \left(1.2 + \frac{3C_m}{d_b} + \frac{50d_b}{l_d} + \frac{A_{tr}f_{yt}}{500sd_b} \right) \sqrt{f'_c} \quad (1.5)$$

with the limit

$$\frac{A_{tr}f_{yt}}{500sd_b} \leq 3 \quad (1.6)$$

in which C_m = smaller of the minimum concrete cover or one-half of the clear spacing between bars, in in.; A_{tr} = area of the transverse reinforcement normal to the plane of splitting through the anchored bars, in in.²; f_{yt} = yield strength of transverse reinforcement, in psi; and s = spacing of the transverse reinforcement, in in. Eq. (1.5) was based on the test results of 62 beams, including 4 with side-cast bars, 1 with top-cast bars, and 57 with bottom-cast bars.

Based on the recommendations of ACI Committee 408, Bond and Development of Reinforcement [which were based on the work of Orangun et al. (1975, 1977)], the 1989 ACI Building Code (ACI 318-89) classified developed and spliced bars into three categories. Different equations and factors were used to account for the effects of bar size, concrete cover and clear spacing of developed bars, and confinement provided by transverse reinforcement. A maximum limit of 100 psi (0.69 MPa) for $\sqrt{f'_c}$ was applied due to insufficient experimental data for concrete strengths over 10,000 psi (69.0 MPa). The procedures used to determine development lengths in ACI 318-89 were very complex because of multiple equations and multiple categories based on concrete cover, clear spacing between developed bars, and confinement by transverse reinforcement.

To reduce the complexity of development length design, the 1995 ACI Building Code (ACI 318-95) offered simpler procedures for calculating development

and splice length that, like the procedures in ACI 318-89, were based on the work by Orangun et al. (1975, 1977). The new procedures not only simplify the design process, but also reflect development and splice strength better than any previous codes. In ACI 318-95, development and splice length can be calculated using either simplified expressions or a more detailed equation. Two criteria are applied for selecting the simplified equations to be used in design. If (1) neither the clear spacing between bars nor the cover is less than d_b and at least minimum stirrups or ties required by the code are used throughout the development length, l_d , or (2) the clear spacing between bars is not less than $2 d_b$ and the cover is not less than $1 d_b$, for bottom-cast uncoated bars in normal weight concrete, $l_d/d_b = f_y/(25\sqrt{f'_c})$ for No. 6 and smaller bars and $l_d/d_b = f_y/(20\sqrt{f'_c})$ for No. 7 and larger bars. For the cases that do not meet either of the two criteria, $l_d/d_b = 3 f_y/(50\sqrt{f'_c})$ for No. 6 and smaller bars and $l_d/d_b = 3 f_y/(40\sqrt{f'_c})$ for No. 7 and larger bars.

The more detailed equation in ACI 318-95 is

$$\frac{l_d}{d_b} = \frac{3}{40} \frac{\lambda f_y}{\sqrt{f'_c} \left(\frac{c + K_{tr}}{d_b} \right)} \quad (1.7)$$

where $\lambda = 0.8$ for No. 6 and smaller bars and 1.0 for No. 7 and larger bars, c = smaller of the distance from the center of the bar to the nearest concrete surface or one-half of the center-to-center spacing of the developed or spliced bars, $K_{tr} = A_{tr}f_y/(1500sn)$, n = the number of bars being developed or spliced, and $(c+K_{tr})/d_b \leq 2.5$. For a Class B splice (area of reinforcing bars is not more than twice that required by analysis over the entire splice length or more than one-half the total bars is spliced within the

required splice length), l_d is multiplied by a factor of 1.3 to obtain the splice length, the same factor used in ACI 318-89.

Using dummy variable regression techniques on the results of 147 development and splice tests, Darwin, McCabe, Idun, and Schoenekase (1992a, 1992b) developed an equation for bars that are not confined by transverse reinforcement.

$$\frac{A_b f_s}{\sqrt{f'_c}} = 6.67 l_s (c_m + 0.5 d_b) \left(0.92 + 0.08 \frac{c_M}{c_m} \right) + 300 A_b \quad (1.8)$$

in which A_b = area of the developed or spliced bar, in in.^2 , l_s = development or splice length, and c_m and c_M = minimum and maximum, respectively, of the concrete bottom cover or, the smaller of one-half of the clear spacing between bars or the concrete side cover. On the left side of Eq. (1.9), the total bond force is normalized with respect to $\sqrt{f'_c}$ to take into account the effect of different concrete strength. Eq. 1.8 includes the parameters of development/splice length, concrete cover, bar spacing, bar size, and c_M/c_m . It has to be noted that, of the 147 specimens, 20 contained side-cast bars and 33 contained top-cast bars.

In more recent studies, Darwin, Zuo, Tholen, and Idun (1995b, 1995c, 1996b) and Idun and Darwin (1995) used a large data base, including 133 splice and development specimens in which the bars were not confined by transverse reinforcement and 166 specimens in which the bars were confined by transverse reinforcement, to develop the design criteria. Unlike the previous studies [Orangun et al. (1975, 1977) and Darwin et al. (1992a, 1992b)], only bottom-cast bars were included in the analysis. One of the major observations in the studies was that $f'_c^{1/4}$

better represents the effect of concrete strength on development and splice strength than the more traditional $f'_c^{1/2}$. Another major observation involved the role played by the relative rib area, R_r , which was shown to have an important effect on the bond strength of bars confined by transverse reinforcement. The analyses confirmed that the relationship between bond force and development/splice length is linear but not proportional and that the yield strength of transverse reinforcement does not play a role in the effectiveness of the transverse reinforcement in development/splice strength. By applying LRFD concepts and Monte Carlo techniques, reliability-based strength reduction factors, ϕ , were also obtained. Based on the studies, the best-fit equation in terms of ultimate bond force, $T_b = A_b f_s$ in lb, for the bars without transverse reinforcement is

$$\frac{A_b f_s}{f'_c^{1/4}} = [63l_d(c_m + 0.5d_b) + 2130A_b] \left(0.1 \frac{c_M}{c_m} + 0.9 \right) \quad (1.9)$$

The equation for the bars with transverse reinforcement is

$$\frac{A_b f_s}{f'_c^{1/4}} = [63l_d(c_m + 0.5d_b) + 2130A_b] \left(0.1 \frac{c_M}{c_m} + 0.9 \right) + 2226t_r t_d \frac{NA_r}{n} + 66 \quad (1.10)$$

in which c_M = maximum of c_b and c_s , c_m = minimum of c_b and c_s , c_b = bottom cover, c_s = minimum of c_{si} + 0.25 (in.) and c_{so} , c_{si} = one-half of clear bar spacing, c_{so} = side cover, n = number of developed or spliced bars along the plane of splitting, N = number of transverse bars, $t_r = 9.6 R_r + 0.28$; and $t_d = 0.72 d_b + 0.28$. A design equation to determine development and splice length was obtained by dropping the final term of 66 in Eq. (1.10), setting $f_s = f_y$, and applying the reliability-based strength-reduction factor, $\phi_d = 0.9$ (Darwin et al. 1995c, Idun and Darwin 1995).

$$\frac{l_d}{d_b} = \frac{\frac{f_y}{f'_c}^{1/4} - 1900 \left(0.1 \frac{c_m}{c_m} + 0.9 \right)}{72 \left(\frac{c + K_{tr}}{d_b} \right)} \quad (1.11)$$

in which $c = (c_m + 0.5 d_b)(0.1 c_m / c_m + 0.9)$, $K_{tr} = 35.5 t_r t_d A_{tr} / s_n$, and $(c + K_{tr}) / d_b \leq 4.0$.

1.3 Discussion

The reinforcing bar deformation patterns currently used in the United States were established in 1940's based on the work of Clark (1946, 1949) and have not changed since. To date, studies have addressed the effects of numerous parameters on the bond strength, such as bar geometry, confinement by transverse reinforcement, bar spacing, concrete strength, epoxy coating, and casting position. However, little effort has been made to improve the bond strength by developing new deformation patterns.

A large scale research program, underway at the University of Kansas since 1991, is the first major study aimed at developing new deformation patterns and improving development characteristics of steel reinforcing bars since the work of Clark (1946, 1949). In the first phase of the study, Darwin and Graham (1993a, 1993b) demonstrated that the relative rib area of deformed bars plays a significant role in bond strength. Their work provided guidelines for designing bars with new deformation patterns, i.e., with high relative rib areas.

In the second phase of the study, Darwin et al. (1995a, 1995b, 1995c, 1996a, 1996b), Idun and Darwin (1995), and Tholen and Darwin (1996) tested 83 beam-splice specimens and 58 beam-end specimens containing both coated and uncoated

commercially produced conventional and high relative rib area bars. The studies indicated that using high relative area bars can reduce splice lengths by up to 26 percent compared to those obtained with conventional bars when the bars are confined by transverse reinforcement. The studies also showed that, under all conditions of confinement, coated high relative rib area bars provide higher bond strengths than coated conventional bars. Design equations were developed based on a large data base to accurately represent the development and splice strength of bottom-cast bars, including the effect of relative rib area.

1.4 Objective and Scope

The objective of this study is to extend the research started by Darwin and Graham (1993a, 1993b) and continued by Darwin et al. (1995a, 1995b, 1995c, 1996a, 1996b) to improve the development characteristics of reinforcing bars and to complete the picture describing the performance of high relative rib area bars.

The experimental work involves beam-splice tests using No. 5, No. 8, and No. 11 conventional and high relative rib area bars and reversed cyclic loading tests using No. 8 high relative rib area and conventional bars. The key parameters are relative rib area, concrete properties (compressive strength, quantity and type of coarse aggregate), bar position and bar arrangement, epoxy coating, and degree of confinement. Concrete strengths range from 4000 psi to over 15,000 psi (27.6 to 103.4 MPa). The effects of top-cast reinforcement, unsymmetrically placed splices, and multiple layers of bars are investigated. Matched coated and uncoated conventional and high relative rib area bars are tested to evaluate the role played by relative rib area on the development and splice strength of epoxy-coated bars.

Conventional and high relative rib area bars are tested to understand the bond behavior of high relative rib area bars under reversed cyclic loading.

Based on the splice test results and an increased data base, including results of all available bottom-cast development and splice tests from North America, improved design equations are developed using linear regression techniques. For evaluating the effect of concrete strength, the power of f'_c is tested to find the best-fit equations. Monte Carlo techniques are applied to obtain reliability-based strength-reduction factors. The strength reduction factor for high relative rib area epoxy-coated bars is obtained using the test results from both this and previous studies at the University of Kansas.

CHAPTER 2: BEAM SPLICE TESTS

2.1 General

This chapter describes the beam splice test program, including test specimens, materials, procedures, and results. The purpose of the experiments is to evaluate bond performance of high relative rib area bars. The key parameters are bar size, relative rib area, ratio of rib width to rib spacing, bar surface condition (epoxy-coated or uncoated), degree of confinement provided by transverse reinforcement, bar placement and arrangement, concrete strength, and coarse aggregate type and quantity. One hundred and forty beam-splice specimens were tested, including 94 specimens in which the splices were confined by stirrups and 46 specimens in which the splices were not confined by stirrups. Ten deformation patterns were evaluated. The specimens included 9 matched pairs containing top-cast and bottom-cast bars, 10 pairs containing symmetrically and unsymmetrically placed splices, 30 pairs containing coated and uncoated bars, and 1 pair containing two layers of bars.

2.2 Test Specimens

Beam-splice specimens were cast in groups to investigate the key parameters. The groups contained 2 to 6 specimens. The specimens were 16 ft (4.877 m) long, with nominal widths of 12 or 18 in. (305 or 457 mm) and nominal depths of 15.5 or 16 in. (394 or 406 mm).

Splice lengths ranged from 16 to 40 in. (406 to 1016 mm). Except for the specimens in group 22 and specimens 23b.5 and 23b.6, the beams contained two or three No. 5, No. 8, or No. 11 bars spliced at the middle of the specimens and were tested as inverted simply supported beam (Figs. 2.1 and 2.2). Distances between the

ends of the splices and the supports were greater than the depth of the beams. The specimens in group 22 and specimens 23b.5 and 23b.6 were tested as simply supported beams, with one concentrated load at the middle of the span for group 22 (Fig. 2.3) and two concentrated loads in the span for specimens 23b.5 and 23b.6 (Fig. 2.4) to study the effect of shear force on splice strength. For these specimens, the splices were shifted to one side, 17 in. (432 mm) away from the closest concentrated load.

No. 3, No. 4, or No. 5 closed stirrups were evenly spaced in the splice region for specimens used to study the effect of confinement by transverse reinforcement on splice strength. No. 3 stirrups were placed at a 6 in. (152 mm) spacing outside of the constant moment region to provide shear strength. Longitudinal No. 4, No. 5, and No. 6 bars were used on the compression side of the beams to support stirrups for specimens containing No. 5, No. 8, and No. 11 test bars, respectively.

Bottom cover and side cover on the spliced bars ranged from 1.25 to 2.5 in. (32 to 64 mm) and from 1 to 3 in. (25 to 76 mm), respectively. Clear spacing between splices ranged from 1 d_b to 4 d_b , except for the specimens with unsymmetrically arranged splices. The unsymmetrical splice specimens contained three bottom-cast splices; the middle splice was arranged to produce clear spacings of 2 d_b and 6 d_b or 1 d_b and 7 d_b for No. 8 bars, and 1 d_b and 2.5 d_b for No. 11 bars (Fig. 2.1).

Specimens 37.1 and 37.2 were designed to investigate the behavior of beams with multiple spliced layers. The specimens contained two layers of bottom-cast bars (Fig. 2.5). Each layer had two bars. The bottom and side covers were 2 in. (51 mm) and the clear spacing between the two layers of bars was 1 in. (25 mm). The two specimens were identical, except that specimen 37.1 contained two spliced bars in the

first layer and two continuous bars in the second layer, while both layers were spliced in specimen 37.2. No stirrups were used in the splice region for the two specimens. Actual specimen dimensions are given in Table 2.1.

2.3 Materials

2.3.1 Reinforcing Steel

All reinforcing bars were rolled deformed bars satisfying ASTM A 615. Ten deformation patterns were evaluated, including 4 conventional patterns, designated 8C0A, 8N0, 11N0, and 11B0, and 6 experimental patterns, designated 5C3, 8C1, 8F1, 8N1, 8N3, and 11F3. In bar designations, the first number of the designation (one or two digits) is the bar size; the middle letter identifies the manufacturer [B = Birmingham Steel Corporation, C = Chaparral Steel, N = North Star Steel Company, and F = AmeriSteel (formerly Florida Steel Corporation and identified as such in the balance of this report)]; the trailing number identifies the deformation pattern; and the last letter is used if bars with the same deformation pattern are produced from different heats of steel. The relative rib areas ranged from 0.065 to 0.087 for the conventional patterns, and from 0.101 to 0.141 for the experimental patterns. Reinforcing bars used as transverse reinforcement also met the requirements of ASTM A 615. Bar properties for the test bars are given in Table 2.2. Yield strengths for transverse reinforcement are reported in Table 2.1. Yield strengths are based on an average of three tests.

Epoxy coatings were applied commercially in accordance with ASTM A 775 to bars from the same steel heat as the uncoated bars. Coating thicknesses were measured at 20 points along the test bars within the splice length using a magnetic pull-off gage (Mikrotest III Thickness Gage). The average coating thicknesses

ranged from 6.3 to 16.8 mils (0.16 to 0.43 mm) and are reported in Table 2.2. The bar surface condition of transverse reinforcing bars in the splice region matched the surface condition of the spliced bars. Bar properties (steel heat, yield strength, and deformation pattern) of spliced bars and transverse reinforcement were the same in the matched pairs of coated and uncoated splice specimens.

2.3.2 Concrete

Concrete was supplied by a local ready-mix plant. Six series of concrete mixes were used to study the effects of concrete properties (concrete strength and type and quantity of coarse aggregate) on splice strength. The mixes are designated as NNL, NHL, HNL, HHL, NNB, and HHB, in which the first letter indicates concrete strength {N = normal strength [$f'_c < 8000$ psi (55.2 MPa)], H = high strength [$f'_c \geq 8000$ psi (55.2 MPa)]}; the second letter indicates the amount of coarse aggregate content (N = normal, H = high); and the last letter indicates the type of coarse aggregate (L = limestone, B = basalt).

For normal-strength concrete, the water-cement ratio (w/c) was 0.45 for NNL concrete, and 0.44 for NHL concrete. For high-strength concrete, the water-cementitious material ratio (w/cm) ranged from 0.22 to 0.40. Water reducing and superplasticizing admixtures (ASTM C 494 Types A, F and/or G), silica fume and fly ash were used in the high-strength concrete. Type I portland cement and Kansas river sand were used in all concretes. The crushed limestone and basalt coarse aggregates had a nominal maximum size of 3/4 in. (19 mm). Compressive strengths based on 1 in. (25 mm) square by 3 in. (76 mm) prisms were about 15,000 psi (103 MPa) for the limestone and about 50,000 psi (345 MPa) for the basalt. The coarse aggregate content ranged between 1586 and 1661 lb/yd³ (941 and 985 kg/m³) for the concretes

with normal amounts of coarse aggregate, and were about 15 to 20 percent higher, 1803 to 1908 lb/yd³ (1070 to 1132 kg/m³), for the concretes with high amounts of coarse aggregate.

All specimens in a test group were cast from the same batch of concrete. Air contents ranged from 1.5% to 4.7%. Slumps ranged from 2.0 to 4.0 in. (50 to 100 mm) for beams with bottom-cast splices containing normal-strength concrete, from 5.0 to 11.0 in. (125 to 280 mm) for beams with bottom-cast splices containing high-strength concrete, and from 3.0 to 6.0 in. (75 to 150 mm) for beams containing top-cast splices. Compressive strengths ranged from 4250 to 6300 psi (29.3 to 43.4 MPa) for normal-strength concrete, and from 8370 to 15,650 psi (57.7 to 107.9 MPa) for high-strength concrete. Compressive strength was determined based on an average of at least three 6 × 12 in. (152 × 304 mm) cylinders for strengths lower than 12,500 psi (86.2 MPa), and at least three 4 × 8 in. (102 × 204 mm) cylinders for strengths higher than 12,500 psi (86.2 MPa). Testing ages ranged from 7 to 30 days, except for groups 31, 32 39, and 40 which had testing ages in excess of 120 days. Mix proportions and concrete properties are summarized in Table 2.3.

To ensure both uniformity and workability of high-strength concrete, water, cement, fly ash, and sand were loaded and mixed for 10 minutes in the truck at the ready-mix plant, followed by the addition of superplasticizer and continued mixing for about one minute. Silica fume was then added. After two minutes of mixing, the coarse aggregate was added. Additional superplasticizer was added before casting if the slump was not high enough.

2.4 Specimen Manufacture

2.4.1 Formwork

Forms were made of 3/4 in. (19 mm) thick plywood, 2 x 4 studs, and all-thread rods. The plywood (Driform 90 No-oil panels, manufactured by Champion International Corp.) had a polymeric resin coating that did not require the use of a release agent. The forms were held together using clip angles and bolts at end joints and 2 x 4 studs with all-thread rods outside of the forms spaced at 3.2 ft (975 mm). Some all-thread rods [1/4 in. (6 mm) diameter] extended through the forms to hold the reinforcing cage in place. Joints in the forms were sealed with flexible caulk to prevent leakage.

2.4.2 Reinforcing Cage

The reinforcing cage consisted of top and bottom longitudinal bars and transverse stirrups, and was assembled in the forms using wire tires. To prevent interlock of the bar ribs, spliced bars were tired together using four to six wire tires in such a way that one bar had longitudinal ribs horizontal while the other had longitudinal ribs vertical. Markings on the bars were not included in the splice region. Side cover and clear spacing between spliced bars were controlled by tiring the bars to all-thread rods. For bottom-cast specimens, the bottom cover was controlled by supporting the test bars on steel chairs at the bottom of the forms. For top-cast specimens, test bars were tired on size-controlled stirrups located outside of splice region which were supported on steel chairs at bottom of the forms. For two-layer specimens, the second layer of test bars was tied to position-controlled all-thread rods to keep the clear spacing between two layers constant. No supporting rods or chairs were located closer than 6 inches (152 mm) to the splices. Two No. 8

bars were transversely placed 4 ft (1219 mm) from the ends of the beams as lifting bars. Bars were cleaned with acetone before being placed in the forms and again prior to casting. Cover and bar spacings were measured before casting. The measured covers and bar spacings are given in Table 2.1.

2.4.3 Concrete Placement and Curing

The casting procedure was followed to ensure that the concrete in the splice region was as uniform in quality as possible between specimens in a group. Two specimens in a matched pair were placed side by side. Concrete was placed in two lifts, each approximately one-half of the beam depth. In the first lift, concrete was placed in the end regions of all beams first, followed by the splice regions. In the second lift, concrete was placed in splice regions first, followed by the end regions. Each lift was consolidated using a 1.5 in. (38 mm) square internal vibrator.

After initial set of the concrete, the top surface of the beams was covered with wet burlap and plastic. The burlap was kept wet until the forms were stripped when the concrete strength had reached a strength of at least 3000 psi (20.7 MPa). Except for the specimens in groups 31, 32, 39, and 40, specimens were then allowed to dry until testing. Specimens with the highest strength mixes, groups 31, 32, 39, and 40, remained covered with burlap and plastic sheets and were kept wet after the forms were stripped. The burlap and plastic sheets were removed when the concrete had reached the required strength, and the beams were left to dry until the time of test.

Test cylinders were cast in steel molds. Standard 6 × 12 in. (152 × 304 mm) molds were used for normal-strength concrete, while both 6 × 12 in. (152 × 304 mm) and 4 × 8 in. (102 × 204 mm) molds were used for high-strength concrete. The cylinders were cured in the same manner as the test specimens.

2.5 Test Procedure

Specimens were tested as inverted simply supported beams, with the splices on the upper side. As shown in Fig. 2.6, the beams were supported on pin and roller supports mounted on concrete pedestals. A 2/3 in. (17 mm) thick steel plate was mounted on the bottom of the beam using high strength gypsum cement (Hydrostone) at each support. Load was applied to each beam by two 60-ton hollow-cone hydraulic jacks powered by an Amsler hydraulic testing machine. Load was transferred from the jacks to the test beam at each load location using two 1 1/2 in. (38 mm) diameter steel rods attached to a spreader beam mounted on the top of the test beam. Semi-cylindrical rollers were used on the spreader beam to keep the applied load vertical as the end of the test beam rotated. For the beams with splices in the middle section, the supports were located 5 ft (1524 mm) from the ends of the beams and downward loads were applied 6 in. (152 mm) from the ends of the beams to produce a 6 ft (1.830 m) constant moment region (Figs. 2.1, 2.2 and 2.5). The specimens in group 22 and specimens 23b.5 and 23b.6 were supported 6 in. (152 mm) from the ends of the beams and downward loads were applied within the span to produce shear force in splice region (Figs. 2.3 and 2.4).

Deflections were measured at each load point and the middle of the beam using spring-loaded linear variable differential transformers (LVDTs), except for the specimens in group 22 and specimens 23b.5 and 23b.6, where deflections were measured at the middle of the beams only. The applied load was measured by load cells consisting of four strain gauges mounted on each load rod in a full bridge circuit. The number and width of flexural cracks were measured on the top of the beams in the portion of the constant moment region away from the splices for test

groups 28 through 43. Crack widths were measured using a crack comparitor at estimated bar stresses of 20, 30, and 40 ksi (138, 207, and 278 MPa).

Readings from load cells and LVDTs were acquired using a Hewlett-Packard data acquisition system connected to a computer and stored on a hard disk.

The beams were loaded continuously at a rate of about 3 kips (13.3 kN) per minute until failure, with tests lasting 15 to 20 minutes. All specimens in a group were tested in a single day. The 6 × 12 in. (152 × 304 mm) or 4 × 8 in. (102 × 204 mm) cylinders were tested immediately after the tests were completed.

2.6 Results and Observations

2.6.1 Test Results

Load-deflection curves for all beams are shown in Figs 2.7a - 2.7z. The deflection is the sum of the average deflection at the load points and the deflection at midspan, except for the beams in group 22 and beams 23b.5 and 23b.6 for which only the deflection at midspan was measured.

Moments, and maximum bar stresses in splices at splice failure are given in Table 2.1. Beam self-weight and the weight of the loading system are used to calculate the moment and bar stress. The number of flexural cracks, the maximum crack widths along the cracks, and the crack widths cross the centerlines of the beams at bar stresses of 20, 30, and 40 ksi (138, 207, and 278 MPa) in the constant moment region outside of splice region are given in Tables 2.4a-2.4c. In matched pairs of specimens containing conventional and high relative rib bars confined by stirrups, high relative rib area bars produced a higher bar stress at splice failure, except for specimens containing 8N1 bars (see Chapter 4 for a discussion). Coated bars produced a lower bar stress at splice failure than uncoated bars.

2.6.2 Calculation of Bar Stress at Failure

For determining the experimental bar stress at development or splice failure, working stress analysis has been used in many studies. In this study, an analysis is carried out to compare the experimental bar stresses calculated using three analysis methods: the moment-curvature method, the working stress method, and the ultimate strength method. The specimens used for this analysis include the 299 beams included in the study by Darwin et al. (1995a, 1996a) and the 140 beams tested in the current study. Among the 439 beams, 60 beams contained bars that yielded and 379 beams contained bars that did not yield. Concrete strength for the specimens ranged from 2000 to 16,100 psi (13.8 to 111 MPa). Yield strengths of the steel bars ranged from 57.7 to 114.7 ksi (397.8 to 790.8 MPa). For the moment-curvature method, a parabolic concrete stress-strain curve (see Eq. A.2) and steel stress-strain curves (Figs. A.1 and A.3) are used in the analysis. The details of the analysis is described in Appendix A.

The moment-curvature method should provides better results than the other two methods since it considers the nonlinear behavior of the concrete. To evaluate the relative accuracy of the three methods, bar stresses calculated using the moment-curvature method, f_{sc} , are compared with bar stresses calculated using the working stress method, f_{sw} , and the ultimate strength method, f_{su} . The analysis results and comparisons are shown in Table A.1 and Figs. A.5, A.6, A.7, and A.8.

The comparisons indicate that, for the beams in which the bars did not yield, the working stress method overestimates bar stresses for high-strength concrete and underestimates bar stresses for normal-strength concrete, compared to the moment-curvature method. The difference in the stresses obtained using the two methods

increases as the compressive strain in the extreme concrete fiber increases (Fig. A.5); the f_{sw}/f_{sc} ratios range from 0.940 to 1.010. As expected, in general, the ultimate strength method underestimates the bar stresses for the beams in which the bars did not yield, especially for the beams with high-strength concrete (Fig. A.6), compared to the moment-curvature method; the f_{su}/f_{sc} ratios range from 0.909 to 1.025.

For the beams in which the bars yielded, the f_{sw}/f_{sc} ratios range from 0.970 to 1.056 (Fig. A.7) and the f_{su}/f_{sc} ratios range from 0.949 to 1.021 (Figs. A.8). Figs. A.7 and A.8 show that for the beams in this category containing high-strength concrete, the working stress method overestimates and the ultimate strength method underestimates the bar stresses, compared to the moment-curvature method. For 18 of the specimens with bars that yielded, the experimental moments are greater than the moment capacities determined by moment-curvature method. This difference is possible because the yield strengths of bars can vary significantly. The comparisons of the results of f_{sw}/f_{sc} and f_{su}/f_{sc} ratios in Appendix A (Fig. A.7 and Fig. A.8) indicate that the ultimate strength method is more conservative than the working stress method (see Appendix A for the details of the comparisons).

Based on these comparisons, the moment-curvature method is used to calculate bar stresses at failure for the beams with experimental moments less than the moment capacities obtained using the moment-curvature method, otherwise, the bar stresses are determined using the ultimate strength method.

2.6.3 Failure Observations

Most of the specimens failed by splitting at the tension face within the splice region. Specimens 22.1 and 22.3 failed by concrete crushing and specimen 22.5 was not tested to failure due to the limited capacity of the load system.

For members cast with normal-strength concrete, beams with splices that were not confined by transverse stirrups failed suddenly, with a quick drop in load after the peak load. Beams with splices confined by stirrups exhibited a more ductile behavior, with a slow drop in load after the peak. Compared with normal-strength concrete beams, the high-strength concrete beams failed in a more brittle manner.

Typical failures in the splice region for the beams with normal and high strength concrete are shown in Figs. 2.8 and 2.9, respectively. In general, flexural cracks formed initially on the tension face in the constant moment region. As the load increased, transverse cracks formed at both ends of the splices and extended to the sides of the beam. Longitudinal cracks formed in the splice region near ultimate load. The longitudinal cracks ran along the length of splice above the spliced bars, and formed on the sides of the beam near the level of the splices. Beams with stirrups in the splice region exhibited more cracks in the splice region than those without stirrups. Figs. 2.10 shows the distribution of the flexural cracks in the constant moment region outside of the splice region for beams containing uncoated and coated bars, respectively. Generally, beams containing coated bars had fewer flexural cracks with a larger crack width than beams containing uncoated bars (see Chapter 6 for a discussion). The measured number of cracks and crack widths in the constant moment region outside of the splice region at bar stresses of 20, 30, and 40 ksi (138, 207, and 276 MPa) are presented in Tables 4.4a, 4.4b, and 4.4c, respectively.

The failure modes of the unsymmetrical splice specimens were the same as those of the symmetrical specimens. The beams containing two spliced layers failed in a very brittle manner: the concrete bottom and side covers with a depth up to the second splice layer split out at failure. However, for the beam containing one spliced layer and one continuous layer, the failure mode was similar to that of specimens

containing one-layer bars. The failures of the two-layer bar specimens are shown in Fig. 2.11.

The extent of concrete damage at the steel-concrete interface varied, depending on concrete strength (normal or high concrete strength), bar pattern (conventional or high relative rib area bars), and bar surface condition (with or without epoxy coating). For the normal-strength concrete specimens, the damage was the same as observed by Idun and Darwin (1995) and Tholen and Darwin (1996): for specimens with uncoated bars, concrete damage was more extensive near the discontinuous ends of spliced bars; for conventional bars, the damage consisted of crushed concrete between the bar ribs, while for high relative rib area bars, the damage consisted of both crushing and shearing; and for epoxy-coated bars, concrete at the interface had a smooth, glassy surface and exhibited little damage and, in general, the higher the confinement provided by transverse reinforcement, the greater the damage at the steel-concrete interface near the discontinuous ends of spliced bars.

For the high-strength concrete specimens, the concrete damage at the interface was as follows: for uncoated bars without stirrups in the splice region, the interface showed little or no concrete damage; for uncoated bars with stirrups (both conventional and high relative rib area bars) concrete damage at the interface was similar to that observed in normal-strength concrete beams, but the damage occurred over a longer region (about 3/4 of the splice length); for the specimens containing 8N1 bars confined by stirrups, the concrete at the interface appeared to be crushed or sheared off along almost the whole splice length (see Chapter 4 for a discussion); and the damage for the epoxy-coated bars was the same as observed for epoxy-coated bars in normal-strength concrete.

CHAPTER 3: EFFECTS OF SPLICE PLACEMENT AND ARRANGEMENT ON SPLICE STRENGTH

3.1 General

In this chapter, the effects of splice placement and arrangement on splice strength are evaluated. The evaluations are based on the test results of nine pairs of bottom/top-cast specimens, ten pairs of symmetrical/unsymmetrical specimens and one pair of two-layer bar specimens. The effect of shear force on splice strength is addressed briefly.

For the evaluations, the bar stresses in the matched pairs of the specimens are used to make the comparisons. The splice strength ratios for the matched pairs are normalized with respect to Eqs. 3.1 and 3.2 to eliminate the effects of minor differences in concrete cover and bar clear spacing between the specimens. The normalized splice strength ratio is obtained by dividing the ratio of experimental bar stress by the ratio of predicted bar stress based on Eq. 3.1 and Eq. 3.2, as appropriate. As described in Chapter 5, Eq. 3.1 and Eq. 3.2, respectively, were developed based on a statistical analysis of 171 splice and development specimens in which the bars were not confined by transverse reinforcement in splice/development region and 245 specimens in which the bars were confined by transverse reinforcement.

$$\frac{A_b f_s}{f'_c} = [59.8 l_s(c_{min} + 0.5 d_b) + 2350 A_b] \left(0.1 \frac{c_{max}}{c_{min}} + 0.9 \right) \quad (3.1)$$

$$\begin{aligned} \frac{A_b f_s}{f'_c} &= [59.8 l_s(c_{min} + 0.5 d_b) + 2350 A_b] \left(0.1 \frac{c_{max}}{c_{min}} + 0.9 \right) \\ &\quad + \left(31.14 t_r t_d \frac{N_A \pi}{n} + 3.99 \right) f'_c^{1/2} \end{aligned} \quad (3.2)$$

where A_b = single spliced bar area in in.²
 f_s = bar stress at failure in psi
 f'_c = concrete compressive strength in psi
 l_s = splice length in in.
 c_{min}, c_{max} = minimum or maximum value of c_s , or c_b ($c_{max}/c_{min} \leq 3.5$) in.
 c_s = $\min(c_{so}, c_{si} + 0.25$ in.) in in.
 t_r = $9.6 R_r + 0.28$
 t_d = $0.78 d_b + 0.22$
 N = number of stirrups in splice or region
 A_{tr} = area of each stirrups crossing the potential plane of splitting adjacent to the reinforcement being spliced
 n = number of bars being spliced along the plane of splitting
 $f'_c^{1/4}$ and $f'_c^{1/2}$ are in psi.

The data base for Eq. 3.1 and Eq. 3.2 consists of specimens in which bottom-cast spliced/developed bars were symmetrically placed with respect to the specimen centerline. The equations take into account the effects of concrete strength, cover, bar spacing, development/splice length, bar size, degree of confinement from transverse reinforcement, and bar deformation pattern. Eq. 3.1 is similar to the equation developed by Darwin et al. (1995b, 1996b) (see Eq. 1.10 in Chapter 1), with slight differences in the coefficients of l_s and A_b . The major difference between Eq. 3.2 and the expression developed by Darwin et al. (1995b, 1996b) for bars confined by transverse reinforcement (see Eq. 1.10 in Chapter 1) is that the contribution to bond strength of transverse reinforcement is not only a function of relative rib area (t_r), bar size (t_d) and degree of transverse reinforcement (NA_{tr}/n), but is more sensitive

to the concrete compressive strength ($f'_c^{3/4}$ instead of $f'_c^{1/4}$) than apparent from the earlier analysis.

3.2 Top-cast High Relative Rib Area Reinforcing Bars

Top-cast bars are weaker than bottom-cast bars due to bleeding and settlement of the concrete below the bar, which has been demonstrated in earlier studies (see Chapter 1 for the references). In ACI 318-89, based on the studies by Jirsa and Breen (1979) and Jeanty et al. (1988), the so-called top-bar effect is taken into account in design by multiplying the development length for bottom-cast bars by the 1.3. This design requirement remains unchanged in ACI 318-95. However, in the earlier studies, only conventional bars were tested to determine the top-cast bar effect.

To study the relative bond strengths of top-cast high R_r bars, nine matched pairs of bottom/top-cast splice specimens containing either high R_r or conventional bars were tested in this study. In the nine pairs of specimens, 5 pairs contained uncoated high R_r bars (5C3, 8N1, and 8F1), 2 pairs contained coated high R_r bars (5C3 and 8N1), and 2 pairs contained uncoated conventional bars (8N0 and 8C0A). Six pairs of specimens were not confined by stirrups in the splice region, including 3 pairs with uncoated high R_r bars, 2 pairs with coated high R_r bars, and 1 pair with uncoated conventional bars. Three pairs were confined by stirrups, including 2 pairs with uncoated high R_r bars and 1 pair with uncoated conventional bars. Concrete slumps ranged from 3.75 to 5.5 in. (95 to 140 mm). The test results and comparisons are summarized in Table 3.1.

The test results show that, like conventional bars, top-cast high R_r bars have a lower splice strength than bottom-cast bars. In fact, the normalized splice strength ratio of bottom-cast to top-cast bars (Bottom/Top) is quite similar for conventional

and high R_t bars. For high R_t bars, the average Bottom/Top ratios are 1.026 and 1.198 for the specimens without and with stirrups, respectively, while for conventional bars, the ratios are 1.033 and 1.138. The comparisons also indicate that, for both high R_t and conventional bars, the Bottom/Top ratios are lower for the splices without stirrups than for the splices with stirrups. This may be the result of greater support provided to top bars by reinforcing cages with stirrups in the splice region than by cages without stirrups in the splice region. As a result, concrete settlement would have affected the strength of top splices in beams with stirrups more than top splices in beams without stirrups.

For coated bars, the Bottom/Top ratio is 1.059 for 5C3 bars without stirrups and 1.035 for 8N1 bars with stirrups. Comparing the splice strength of uncoated bottom-cast bars to coated top-cast bars in matched pairs (specimens 25.1 and 25.4 for 5C3 bar and 24.1 and 24.4 for 8N1 bar), it is noted that the normalized splice strength ratio for uncoated bottom-cast bar to coated top-cast bars is 0.986 for 5C3 bar and 1.151 for 8N1. These values are much less than the upper limit of 1.7 in ACI 318-95 on the total development length modification factor for epoxy-coated top-cast bars with concrete cover less than $3 d_b$ or clear spacing less than that $6 d_b$. The current results match conclusions by Treece and Jirsa (1987, 1989) and Hadje-Ghaffari et al. (1992, 1994) that the effects of casting position and epoxy coating on splice strength are not cumulative.

3.3 Unsymmetrical Arrangement of Splices

In earlier studies, including most of the tests in this study, developed bars and splices were placed symmetrically across the width of the test specimens. The development and splice design criteria in the ACI 318-95 were established based on

symmetrically placed bars. In practice, however, bars are often placed unsymmetrically or nonuniformly across the width of a beam to avoid interference between beam and column bars at joints.

In design, the minimum clear spacing between bars is usually used to determine the required development or splice length in the case of nonuniform bar placement. However, questions have been raised as to the applicability of design criteria based on uniform bar spacing test results to members with nonuniform bar spacing, and no data exists on the bond behavior of unsymmetrically or nonuniformly placed bars (Lee 1993).

To study the behavior of nonuniformly placed splices, ten matched pairs of specimens with symmetrical and unsymmetrical splice arrangements were tested. Of the ten pairs of specimens, 5 contained bars that were confined by stirrups in the splice region and 5 contained bars that were not confined by stirrups. All of the specimens contained three bottom-cast splices. As shown in Fig. 2.1, the splices for the unsymmetrical splice specimens were arranged with nominal clearing spacings of 1 in./.7 in. (25.4 mm/179 mm) or 2 in./.6 in. (51 mm/152 mm) for No. 8 bars and 1.5 in./3.5 in. (38 mm/89 mm) for No. 11 bars, while the symmetrical specimens had nominal clearing spacings of 4 in. (102 mm) for No. 8 bars and 2.5 in. (64 mm) for No. 11 bars (see Fig. 2.2). Concrete strength ranged from 4250 to 10,500 psi (29.3 to 72.4 MPa). The test results and the comparisons are presented in Table 3.2.

The comparisons in Table 3.2 show that, for the splices not confined by stirrups, the normalized strength ratios of unsymmetrical to symmetrical splices (US/S) range from 0.926 to 1.076, with an average of 0.986. For the splices confined by stirrups, the US/S ratios range from 0.988 to 1.085, with an average of 1.023. The average US/S ratio for all of 10 pairs of specimens is 1.004. These values indicate no

measurable effect of unsymmetrical bar placement on splice strength and suggest that the average clear spacing across a section is the appropriate clear spacing parameter for use in design. It has to be noted that, compared with the test results, using minimum clear spacing in the design for the unsymmetrical splices is too conservative. Table 3.2 shows that, for the unsymmetrical specimens, the test/predicted stress ratios (f_s/f_{sI}) range from 0.921 to 1.058, with an average of 0.975, if using the average clearing spacing of the bars across the width of the specimens. The ratios (f_s/f_{sII}) range from 0.998 to 1.244, with an average of 1.151, if using the minimum clearing spacing of the bars.

3.4 Multiple Splice Layers

Little information about the behavior of multiple splice layers exists in the literature. In a study on the development of bundled reinforcing bars, Jirsa et al. (1995) tested and evaluated development specimens containing one or two layers of bundled bars. They found that the inner layer of bars had little effect on the performance of the outer layer. The bond strength of the outer layer for the specimens containing two layers of bars was close to the bond strength of a similar specimen with one layer of bars. Splitting failure occurred for both of the one-layer and two-layer specimens. For two-layer specimens, splitting occurred through both the inner and outer (horizontal) layer planes. A transfer of stress from the outer layer to the inner layer occurred near the peak load. ACI 318-95 requires the use of "clear spacing of bars being developed" in development/splice design. In practice, however, splice length is often determined based on clear spacing between splices in a layer, instead of clear spacing between layers.

In this study, specimens 37.1 and 37.2 were designed and tested to investigate the splice strength of bars placed in two layers. The two specimens (Fig. 2.5) were identical, except that specimen 37.1 contained one spliced layer (bottom layer) and one continuous layer, while specimen 37.2 contained two spliced layers. The clear spacing between the two layers was 1 in. (25.4 mm), which is less than the bottom and the side covers [2 in. (30.8 mm)], and less than one-half of the clear spacing between splices across the width of the specimens [2 in. (30.8 mm)].

As described in Chapter 2, both of the specimens failed by concrete splitting. The failure mode for the beam containing one spliced layer and one continuous layer (specimen 37.1) was similar to that for the beams containing only one layer of bars. For the specimen containing two spliced layers (specimen 37.2), the failure was very brittle, with concrete splitting on the bottom and side of the specimen up to the second layer of bars, indicating that both spliced layers failed.

The limited test results and the comparisons, shown in Table 3.3, indicate no significant difference in splice strength between the specimen containing two spliced layers and the specimen containing one spliced layer and one continuous layer. The bar stress in the bottom layer at failure is 61.40 ksi (423 MPa) for the specimen with two spliced layers (Specimen 37.2) and 59.97 ksi (413 MPa) for the specimen with one spliced layer and one continuous layer (specimen 37.1). The splice strength ratio of specimen 37.2 to specimen 37.1 is 1.024. The comparison indicates that the splice strength of beams with two-spliced layers is not affected by the inner spliced layer, matching the observations by Jirsa et al. (1995).

In specimen 37.1, 50% of bars were spliced at a section (Class A splice according to ACI 318-95), while all of the bars were spliced in specimen 37.2 (Class B splice). ACI 318-95 requires an increase in splice length of 30%, based on the

development length, for Class B splices. A comparison of specimens 37.1 and 37.2 shows that splice strength is not sensitive to the number of splices at a location, but only to the geometry of the sections.

Table 3.3 shows that the use of clear spacing between two spliced layers as the clear spacing parameter in Eq. 3.1 results in a test/predicted stress ratio of 1.172, which is about 24% higher than the test/predicted stress ratio using the clear spacing across the width of the specimen. However, the use of the clear spacing between the splices in a single layer results in predicted splice strengths that are higher than the experimental strengths for both specimens (14% higher for specimen 37.1 and 11% higher for specimen 37.2). The observations indicate that, when the clear spacing between layers is less than the clear spacing between splices in a layer, using the clear spacing within a layer overestimates the splice strength, but using the clear spacing between layers underestimates the splice strength. Since the number of the tests is limited, more study is needed before the effects of multiple layer bars on splice strength is understood.

3.5 Effect of Shear Force on Splice Strength

Splices subjected to shear (or moment gradient) occur commonly in real structures. The effect of shear on splice strength has been studied before. Based on 24 tests on the influence of shear on splice strength, Jirsa and Breen (1981) concluded that the level of shear along splices has an inconsequential effect on the splice strength. Only negligible changes in splice strength were observed, with substantial increases in the level of shear. Lukose et al. (1982) compared the behavior of splices in a region with varying moment to the similar splices in a constant moment region. They found that the strength of the splices in the region of varying moment was

higher than that in the constant moment region. Their explanation for this observation is that for splices in the constant moment region, splitting damage progresses from both ends of splices. However, for splices subjected a varying moment, splitting damage progresses from the more highly stressed end. Less damage is expected near the end with the lower stress.

In this study, the specimens in test group 22 and specimens 23b.5 and 23b.6 were tested to evaluate the effect of shear on splice strength. Table 3.4 gives the test results and comparisons for specimens 22.3, 22.5, and 23b.5. These specimens contained uncoated bars. Specimen 23b.6 contained coated bars and is not included in Table 3.4. The results for specimen 22.1 are not included in Table 3.4 because the specimen failed by crushing concrete at the middle of the beam span due to the poor quantity of the concrete (honeycomb was found in the compression zone of the beam, which was caused by poor vibrating during placement), but are given in Table 2.1. Specimen 22.3 exhibited a flexural failure, with bar yielding and concrete crushing on the compression face at the middle of the span, instead of a splitting failure. Specimen 22.5 was not tested to failure because the loading capacity of the test apparatus had been reached. Even so, the bar stresses of specimens 22.3 and 22.5 exceed the values predicted by Eq. 3.1 or Eq. 3.2. Specimen 23b.5 failed by splitting concrete (splice failure), with a test/predicted bar stress ratio of 1.095. The ratios of the minimum bar stress at the end of the splices closest to the reaction to the maximum bar stress at the other end of the splices (closest to the applied load) at failure ranged from 0.56 to 0.66. Table 3.4 shows that the bar stresses at failure are higher than the stresses predicted by Eqs. 3.1 or 3.2, with the test/prediction ratios ranging from 1.046 (plus) to 1.126. The test results match the observation by Lukose

et al. (1982) that the performance of splices in the presence of shear is always better than in a constant moment region.

CHAPTER 4: EFFECTS OF CONCRETE AND REINFORCING BAR PROPERTIES

4.1 General

In a previous study of high relative rib area (R_r) bars, Darwin et al. (1995a, 1996a) evaluated the effects of type of coarse aggregate in concrete and confinement provided by stirrups, as well as R_r , on splice strength. They found that the type of coarse aggregate significantly affects splice strength for bars that are confined by stirrups. However, due to the limited number of tests, their evaluations did not address the effect of coarse aggregate type on splice strength for bars that are not confined by transverse reinforcement, nor did they address the effect of coarse aggregate quantity on splice strength under any condition of confinement.

Darwin et al. (1995b, 1996b) found that the 1/4 power of the concrete compressive strength, $f'_c^{1/4}$, successfully characterized the effect of concrete strength on splice strength for bars both confined and not confined by transverse reinforcement. Darwin et al. (1995a, 1995b, 1996a, 1996b) also found that the additional strength provided by confining steel, T_s , normalized with respect to $f'_c^{1/4}$, is a function of the “effective transverse reinforcement”, NA_{tr}/n , in which N is the number of transverse stirrups or ties in the splice region; A_{tr} is the area of each stirrup or tie crossing the potential plane of splitting adjacent to the reinforcing bars being developed or spliced, in in^2 ; and n is the number of reinforcing bars being developed or spliced along the plane of splitting. The yield strength of the transverse reinforcement was found to have no measurable effect on T_s (Darwin et al. 1995b & 1996b, Azizinamini et al. 1995, Sakurada et al. 1993, and Maeda et al. 1991). The data base used by Darwin et al., however, included only a small number of specimens

made with high-strength concrete (HSC). Thus, with more data available on HSC specimens, the question arises as to whether or not the 1/4 power of f'_c is still appropriate for characterizing the contribution of concrete strength to bond.

This chapter presents the evaluations of the test results for the effects of concrete strength, quantity and type of coarse aggregate, bar size, relative rib area, and rib spacing on splice strength. Ten deformation patterns, including conventional and high relative rib area bars, are evaluated. Only specimens containing uncoated, bottom-cast bars are included. For the evaluations, the current results are combined with those reported by Darwin et al. (1995a, 1996a), Hester et al. (1991, 1993), and Choi et al. (1990, 1991) on splice specimens similar to the current NNL concrete (Normal strength concrete containing Normal quantity of Limestone coarse aggregate) specimens. Specimens 8.3 and 10.5 tested by Darwin et al. (1995a, 1996a) contained NNB (B = basalt) concrete. The previous test results are summarized in Tables 4.1, 4.2 and 4.3. The current test results are presented in Table 2.1.

The evaluations presented in this chapter are based on the assumption that the total force in a bar at splice failure, T_b , equals the sum of a concrete contribution, T_c , and a transverse reinforcement (steel) contribution, T_s .

$$T_b = T_c + T_s \quad (4.1)$$

T_c is determined using Eq. 3.1 (see derivation as Eq. 5.5 in Chapter 5), which is

$$\frac{T_c}{f'_c^{1/4}} = [59.8 l_s(c_{\min} + 0.5 d_b) + 2350 A_b] \left(0.1 \frac{c_{\max}}{c_{\min}} + 0.9 \right) \quad (4.2)$$

As demonstrated in Chapter 5, Eq. 4.2 was developed based on a statistical analysis of 171 development/splice specimens and accurately represents the splice strength for the splices not confined by transverse reinforcement.

Test-to-prediction splice strength ratios are used to evaluate the effects of concrete properties and reinforcing bars for bars that are not confined by transverse stirrups, in which the test splice strengths are determined based on test results ($A_b f_s / f'_c^{1/4}$) and the predicted splice strengths are determined using Eq. 4.2. For bars that are confined by stirrups, the evaluations are carried out using linear regression techniques comparing $A_b f_s / f'_c^{1/4}$ versus NA_{tr}/n .

The evaluations in this chapter will be used in Chapter 5 to determine the appropriate power of f'_c to characterize the effect of concrete strength on T_c and T_s , to develop expressions for the effects of R_t and bar size on T_s , and to establish development/splice design criteria based on a broadened data base.

4.2 Effects of Concrete Properties

As described in Chapter 2, six concretes, containing different types and quantities of coarse aggregate (limestone or basalt and “normal” or “high” content) and having different compressive strength levels (normal or high), were used to study the effects of concrete properties on splice strength. Coarse aggregate contents ranged from 1586 lb/yd³ (941 kg/m³) to 1661 lb/yd³ (985 kg/m³) for concrete containing a “normal” quantity of coarse aggregate [NNL, NNB, or HNL in which the first letter represents the concrete strength level (N = normal and H = high), the second letter represents the quantity of coarse aggregate (N = normal and H = high), and the last letter represents the type of coarse aggregate (L = limestone and B = basalt)] and from 1803 lb/yd³ (1070 kg/m³) to 1908 lb/yd³ (1132 kg/m³) for concrete

containing a “high” quantity of coarse aggregate (HHL, HHB, or HNL). Concrete compressive strengths for the specimens used for the evaluation ranged from 3810 psi (26.3 MPa) to 6450 psi (44.5 MPa) for normal-strength concrete (NSC) and from 8370 psi (57.5 MPa) to 15,640 psi (107.8 MPa) for high-strength concrete (HSC).

4.2.1 Splices without Transverse Reinforcement

The specimens that did not contain stirrups within the splice region include 35 containing NNL concrete [9 from the current study, 12 from Darwin et al. (1995a, 1996a), 8 from Choi et al. (1990, 1991), and 7 from Hester et al. (1991, 1993)], 2 containing NNB concrete [Darwin et al. (1995a)], 6 containing NHL concrete, 4 containing HHL concrete, and 9 containing HHB concrete.

Effects of coarse aggregate

Table 4.4 summarizes the range and mean of the test/prediction ratios for the splices not confined by stirrups cast in specimens with NNL, NHL, HHL, NNB, and HHB concretes. The results show no measurable difference in the test/prediction ratios for concretes containing the same type of coarse aggregate, regardless of coarse aggregate content or concrete strength, but do show a difference based on the type of coarse aggregate. For concretes containing limestone, the average test/predication ratios are 1.002, 1.007 and 0.963 for NNL, NHL and HHL concretes, respectively. In contrast, for concretes containing basalt, the average test/prediction ratios, 1.107 and 1.133 for NNB and HHB concretes, respectively, are more than 10% higher. Thus for the splices not confined by stirrups, concrete containing basalt aggregate produced higher splice strengths than the concrete containing limestone aggregate. This observation can be explained based on a study of Kozul and Darwin (1997) using the same aggregate which showed that concrete containing basalt yields a similar flexural

strength but a significantly higher fracture energy (two times plus) than concrete of similar compressive strength containing limestone for all compressive strengths evaluated [3670-13,970 psi (25-97 MPa)].

Effect of concrete strength

Fig. 4.1 compares test/prediction ratio to concrete strength for splice specimens with concretes containing limestone and basalt coarse aggregates. The figure shows that concrete containing basalt coarse aggregate produces a higher splice strength than concrete containing limestone aggregate. The figure also shows that the test/prediction ratio increases slightly for concrete containing basalt and decreases for concrete containing limestone as concrete strength increases. The change in test/prediction ratios may be due to an insufficient number of tests for specimens containing NSC with basalt (only 2 specimens) and HSC with limestone [only 4 specimens including only 1 specimen with $f'_c > 10,000$ psi (69.6 MPa)]. In Fig. 4.2, dummy variable regression is applied to the data shown in Fig. 4.1, based on the assumption that the effect of concrete strength on splice strength is the same for limestone and basalt aggregates, limiting the effect of the different number of tests for normal and high strength concrete in each group. Fig. 4.2 shows that the best-fit lines are virtually horizontal and that the intercept of the best-fit line for the specimens with concrete containing basalt is about 15% greater than that for the specimens with concrete containing limestone.

Since the "prediction" used is based on Eq. 4.1, these observations illustrate that, for the splices not confined by stirrups, (1) $f'_c^{1/4}$ accurately characterizes the effect of concrete strength on bond and (2) stronger coarse aggregates produce higher splice strengths.

4.2.2 Splices with Transverse Reinforcement

To investigate the effects of concrete properties on the strength of splices confined by transverse reinforcement, the additional bond force due to the confinement provided by transverse reinforcement, T_s , is obtained by subtracting the bond force due to the concrete contribution, T_c , which is calculated using Eq. 4.2, from the experimentally determined total bond force, T_b . Comparisons of $T_s/f'_c^{1/4}$ with NA_{tr}/n are used in the following evaluations.

Effects of coarse aggregate

Fig. 4.3 compares $T_s/f'_c^{1/4}$ with $t_r NA_{tr}/n$ for No. 8 conventional bar splices in normal and high strength concretes containing a “normal” or a “high” quantity of limestone coarse aggregate; $t_r = 9.6 R_r + 0.28$, as obtained by Darwin et al. (1995a, 1996a) based on the tests and analyses of splice specimens using No. 5, No. 8, and No. 11 conventional and high R_r bars in normal-strength concrete. The reason for using t_r as a parameter is to eliminate the effect of differences in R_r (R_r ranges from 0.065 to 0.085) from the current analysis of the effects of concrete properties.

$T_s/f'_c^{1/4}$, as shown in Fig. 4.3, is higher for normal and high strength concretes containing a “high” quantity of coarse aggregate (NHL and HHL) than for concretes containing a “normal” quantity of coarse aggregate (NNL and HNL), illustrating that concrete containing a higher quantity of coarse aggregate produces higher additional splice strength due to the confinement of transverse reinforcement. Thus, the current analysis suggests that the quantity of coarse aggregate has a measurable effect on T_s .

Fig. 4.4 compares $T_s/f'_c^{1/4}$ with NA_{tr}/n for one high relative rib area bar, 8N3 ($R_r = 0.119$), in NNL, HNL and HHL concretes. The term of t_r is not used in Fig. 4.4 because only a single R_r value is involved in the plot. As with conventional bars (Fig. 4.3), Fig. 4.4 shows that for high R_r bars, the additional splice strength provided by

stirrups is higher for concrete containing a higher coarse aggregate content than for concrete containing a "normal" coarse aggregate content. The difference in this case is less than observed for conventional bars.

$T_s/f'_c^{1/4}$ is compared with NA_{tr}/n in Figs. 4.5 and 4.6 for bars in NSC and HSC containing different types of coarse aggregate (limestone and basalt). In Fig. 4.5, all bars (conventional No. 8 bars and 8N3, 8F1 high R_r bars) were cast in NSC with a "normal" quantity of coarse aggregate. $T_s/f'_c^{1/4}$ is higher for all of the bar patterns shown in Fig. 4.5 for concrete containing basalt than for concrete containing limestone. A similar observation is obtained in Fig. 4.6 for conventional No. 8 bars (8N0): concrete containing basalt aggregate produces substantially higher values of $T_s/f'_c^{1/4}$, even though the concrete compressive strengths are the same. The observations in Figs. 4.5 and 4.6 match those made by Darwin et al. (1995a, 1996a).

Effect of concrete strength

Figs. 4.3 and 4.4 show that for both conventional and high R_r bars, $T_s/f'_c^{1/4}$ is higher for HSC than for NSC. Fig 4.7 compares $T_s/f'_c^{1/4}$ with NA_{tr}/n for No. 8 conventional bars and No. 8 and No. 11 high R_r bars (8N3 and 11F3) in NSC and HSC containing limestone coarse aggregate, ignoring the effects of coarse aggregate content. For each bar pattern, the values of $T_s/f'_c^{1/4}$ are greater for HSC than for NSC, indicating that a higher power of f'_c than 1/4 may be needed to characterize the effect of concrete strength on T_s . Fig. 4.7 also shows that the difference in $T_s/f'_c^{1/4}$ between HSC and NSC for No. 8 conventional bars is greater than that for No. 8 high R_r bars, implying that concrete strength may affect T_s more for conventional bar than for high R_r bars.

The comparisons shown in Figs. 4.2 to 4.7 indicate that concrete properties (especially compressive strength and type of coarse aggregate) have measurable

effects on the bond strength provided by both the concrete, in absence of transverse reinforcement, and by transverse reinforcement. These effects, in addition to differences in R_r , may be the reason why test results for specimens containing developed or spliced bars confined by stirrups exhibit high scatter from study to study.

4.3 Effects of Reinforcing Bars

Darwin et al. (1995a, 1996a) demonstrated that for splices not confined by stirrups, splice strength is unaffected by relative rib area, while for splices confined by stirrups, splice strength increases as relative rib area increases. Darwin et al. also found that bar size affects the additional bond force, T_s , provided by transverse reinforcement: the higher the bar size, the higher the value of T_s . In this study, the test results of Darwin et al. (1995a, 1996a) are combined with the current results to examine the role played by R_r on splice strength. The effect of the rib width/spacing ratio on splice strength is also studied to determine the need for a limitation on the rib width/spacing ratio for high R_r bars. Flexural crack densities and crack widths for high R_r bars and conventional bars are compared to study the serviceability of members containing high R_r bars.

4.3.1 Effects of Relative Rib Area and Bar Size

Splices without transverse reinforcement

Table 4.5 summarizes the splice strength test/prediction ratios for high R_r and conventional bars not confined by stirrups. The test/prediction ratios are classified into two categories based on the type of coarse aggregate (limestone or basalt). The comparisons show that relative rib area does not affect splice strength for the splices

not confined by stirrups, matching the observations of Darwin et al. (1995a, 1996a). The average test/prediction ratio is 0.989 for high R_r bars in concrete containing limestone coarse aggregate, compared to 1.010 for conventional bars. The average test/prediction ratio is 1.133 for high R_r bars in concrete containing basalt coarse aggregate, compared to 1.123 for conventional bars.

Splices with transverse reinforcement

$T_s/f'_c^{1/4}$ is compared with NA_g/n in Fig. 4.8 for No. 5, No. 8 and No. 11 bars in normal-strength concrete containing "normal" amounts of limestone coarse aggregate (NNL). Fig. 4.8 shows that, as observed by Darwin et al. (1995a, 1996a), relative rib area and bar size affect the additional splice strength due to confining transverse reinforcement, with the value of $T_s/f'_c^{1/4}$ increasing with an increase of R_r or bar size. The same observation can also be made in Fig. 4.7 for No. 8 conventional bars and 8N3 and 11F3 high R_r bars in high-strength concrete and in Fig. 4.9 for 8N0, 8N3 and 8F1 bars in NNB concrete.

4.3.2 Limitation of Rib Width/Spacing Ratio

Studying the effect of rib width on bond strength is important for high R_r bars because the ribs of high R_r bars are closer than those of conventional bars. In a study using machined bars [bars fabricated from cold rolled steel with 1 in. (25.4 mm) diameter, bamboo deformation pattern, flat top surface of ribs, and 60° deformation face angle] in beam-end specimens, Tholen and Darwin (1996) observed a significant reduction in bond strength if the rib width/spacing ratio is greater than 0.67 for the bars not confined by stirrups and 0.45 for the bars confined by stirrups (in this case, the rib width/spacing ratio represents the ratio of the width of rib top surface to center-to-center spacing between ribs). Their observations indicate the following

fact: if ribs are too close, not enough concrete will be between the ribs to resist the shear force transferred from the ribs, resulting in pullout rather than splitting failure, reducing the bond strength.

All of the bars tested in this study and by Darwin et al. (1995a, 1996a)] had flat top rib surfaces. It has to be noted, however, that not all commercially produced reinforcing bars have flat top surfaces. Many have rounded top rib surfaces, which raises a question as to how to determine the rib width. From a practical point of view, the argument can be made that rib width measured at a fraction of the rib height (for example 1/2 or 3/4) would have more meaning than the width at the top of the rib. In the current study, measurements are made at the top and bottom of the ribs. The rib widths at 1/2 and 3/4 rib height are then determined based on interpolation. The measurements of the rib widths and average rib width/spacing ratios for all of the bars tested in this study and by Darwin et al. (1995a, 1996a) are given in Table 4.6.

The effect of rib width on the splice strength of rolled bars is investigated using the 8N3 and 8N1 bars. The bars have similar values of R_f ($R_f = 0.119$ for 8N3 bar and 0.121 for 8N1 bar), while the 8N3 bar has a smaller rib width/spacing ratio than the 8N1 bar: the rib width/spacing ratios are 0.303 and 0.363 at 3/4 rib height for the 8N3 and 8N1 bars, respectively, and 0.362 and 0.438 at 1/2 rib height.

Table 4.7 compares splice strength test/prediction ratios for 8N3 and 8N1 bars with splices not confined by stirrups in concrete containing limestone coarse aggregate. The average test/predication ratio for six specimens containing 8N3 bars is 0.980. The average test/prediction ratio for four specimens containing 8N1 bars is 0.998. The comparison shows no measurable difference between the 8N3 and 8N1 bars. However, the picture changes for the splices confined by stirrups. As shown in Fig. 4.10, the 8N1 bars show a significant reduction in the additional splice strength

due to confinement by stirrups, compared to the 8N3 bars. In Fig. 4.10, the intercepts of the best-fit lines ($T_s/f'_c{}^{1/4}$ versus NA_{tr}/n) are forced to be zero for an easier comparison. Although the relative rib area of the 8N1 bar is slightly greater than that of the 8N3 bar, the slope of the best-fit line for 8N1 bars (2077) is 25% lower than that for the 8N3 bars, indicating that the additional bond strength, $T_s/f'_c{}^{1/4}$, is 25% lower for the 8N1 bars than for the 8N3 bars. In the tests, the concrete at the interface was crushed and sheared off along the whole splice length for the 8N1 bars, indicating a pullout failure. For the 8N3 bars, however, only the concrete near the discontinuous ends of the spliced bars was crushed. This observation supports the conclusion by Tholen and Darwin (1996) that a reduction of bond strength occurs if bar ribs are too close, or more precisely if rib width/spacing ratio is higher than a certain limit.

It is noted that the rib width/spacing limit for high R_r bars (0.45) recommended by Tholen and Darwin (1996) is based on the tests of beam-end specimens with machined bars. The rib widths of the machined bars are constant around the ribs. For the commercially produced bars used in this study, however, the rib widths vary around the ribs. The rib widths presented in Table 4.6 represent average values. Table 4.6 shows that the 8N1 bar has the greatest rib width/spacing ratio of the bars used in this study. The 5C3 bar has the next highest value of rib width/spacing ratio (0.385 at 1/2 rib height and 0.318 at 3/4 rib height). However, since no specimens with 5C3 bars confined by stirrups were tested, this bar cannot be used in the current evaluation. The next highest rib width/spacing ratio is 0.362 at 1/2 rib height and 0.303 at 3/4 rib height for the 8N3 bar or 0.358 at 1/2 rib height and 0.314 at 3/4 rib height for the 5C2 bar. The test results (presented in Chapter 4) indicate that, with the exception of the 8N1 bars, all of the high R_r bars in Table 4.6

exhibited good performance. Therefore, based on the bars tested in this study and by Darwin et al. (1995a, 1996a), safe upper bounds on rib width-spacing ratio for high R_r bars appear to be 0.36 at 1/2 rib height and/or 0.31 at 3/4 rib height. Somewhat higher limiting values on the rib width-spacing ratio may exist, but additional tests are needed before those values can be established.

4.3.3 Flexural Crack Density and Width

Tholen and Darwin (1996) evaluated the load-deflection and moment-rotation behavior of the beams containing continuous conventional and high R_r bars. They concluded that an increase in relative rib area does not affect the displacement and moment-rotation behavior of beams. They also found that the crack patterns and distribution of flexural cracks are nearly identical for matched pairs of beams containing conventional and high R_r bars.

To further understand the flexural crack behavior of members containing high R_r bars, the crack density, maximum flexural crack width along each crack, and the sum of the crack widths on the center lines of the beams in the constant moment region outside of the splice region were measured at estimated bar stresses of 20, 30, and 40 ksi (138, 207, and 276 MPa). Fifteen matched pairs of specimens contained high R_r and conventional bars. The flexural crack density is obtained by dividing the total number of cracks in the constant moment region outside of splice region by the corresponding length. The concrete strength of the specimens ranged from 5230 to 15650 psi (36 to 108 MPa). The bars in the specimens included No. 8 and No. 11 high R_r and conventional bars (8C1, 8F1, 8N1, 8N3, and 11F3 high R_r bars and 8C0A, 8N0, and 11B0 conventional bars). The flexural crack densities, maximum crack widths, and sums of the crack widths at a bar stress of 40 ksi (276 MPa) are

given in Table 4.8. The values at the bar stresses of 20 and 30 ksi (138 and 207 MPa) are given in Tables 4.9 and 4.10.

The ratios of flexural crack density, maximum crack width, and sum of crack widths of the specimens with high R_r bars to the same properties of the specimens with conventional bars for the matched pairs are used for comparison. As shown in Table 4.8, at a bar stress of 40 ksi (276 MPa), the ranges of the flexural crack densities are identical for high R_r and conventional bars [from 1.615 to 3.692 cracks/ft (5.299 to 12.113 cracks/m)]. The maximum crack widths range from 0.006 to 0.013 in. (0.152 to 0.330 mm) for high R_r bars and from 0.006 to 0.014 in. (0.152 to 0.356 mm) for conventional bars. The ranges of the sum of crack widths are also identical for high R_r and conventional bars [from 0.048 to 0.079 in. (1.129 to 2.007 mm)]. The comparisons show that, at a bar stress of 40 ksi (276 MPa), there is no measurable difference in flexural crack density or maximum crack width between the beams containing high R_r and conventional bars; the average flexural crack density ratio and the average maximum crack width ratio for the 15 matched pairs of specimens are 1.019 and 0.999, respectively. However, the sum of crack widths is slightly smaller for the beams with high R_r bars than for the beams with conventional bars, with an average ratio of 0.940. Similar observations can be obtained at the lower bar stress levels [20 and 30 ksi (138 and 207 MPa), Tables 4.9 and 4.10]. These comparisons indicate that an increase in relative rib area may result in a small reduction in total crack width, but does not otherwise affect the flexural crack behavior of beams.

CHAPTER 5: DEVELOPMENT LENGTH CRITERIA

5.1 General

Darwin et al. (1995b, 1996b) carried out a statistical analysis, based on a data base including 133 development and splice specimens in which the bars were not confined by transverse reinforcement and 166 specimens in which the bars were confined by transverse reinforcement, to develop tensile bond design criteria. The expressions (Eqs. 1.9 and 1.10) that were developed using regression techniques accurately represent the development and splice strength of reinforcing bars. One of the important observations from the analysis is that the 1/4 power of the concrete compressive strength better represents the effect of concrete strength on the development and splice strength than the 1/2 power which has been traditionally used. The expression (Eq. 1.10) for the development and splice strength of bars confined by transverse reinforcement includes the effect of the bar relative rib area. The reliability-based strength reduction factor, $\phi_d = 0.9$, included in the design equation for determining development/splice length (Eq. 1.11) was developed using Monte Carlo analyses (Darwin et al. 1995c, Idun and Darwin 1995).

The data base used by Darwin et al. (1995b, 1996b) included only a small number of specimens containing high-strength concrete [HSC, $f'_c \geq 8000$ psi (55.2 MPa)], 9 out of 133 specimens in which the bars were not confined by transverse reinforcement and 11 out of 166 specimens in which the bars were confined by transverse reinforcement.

In this chapter, the design criteria for development and splice lengths are reevaluated using techniques similar to those used by Darwin et al. (1995b, 1995c, 1996b). The reevaluation is based on a larger data base that includes the test results

used by Darwin et al (1995b, 1996b) plus additional test results from the current study and elsewhere (Kadoriku 1994, Hatfield et al. 1996). The new data base includes 171 specimens containing developed or spliced bars not confined by transverse reinforcement and 245 specimens containing bars confined by transverse reinforcement. All of the specimens in the data base are bottom cast. Compared to the data base used by Darwin et al. (1995b, 1996b), the number of specimens containing high strength-concrete has increased from 7% to 19% (32 out of 171) for bars not confined by transverse reinforcement and from 7% to 25% (62 out of 245) for bars confined by transverse reinforcement. The power of concrete compressive strength (f'_c), p , used to characterize the effect of concrete strength on the development/splice strength is studied and a strength reduction factor, ϕ , for a new design equation is obtained using Monte Carlo simulation. The new expressions are compared to the design expressions in ACI 318-95.

5.2 Bars Not Confined by Transverse Reinforcement

5.2.1 Development/Splice Strength Model and Variables

The development/splice strength model developed by Darwin et al. (1995b, 1996b) is used in this study. The model is obtained as follows.

At first, a dummy variable regression analysis (Draper and Smith 1981) based on bar size is carried out comparing $A_b f / f'_c^P$ (test) versus $l_d(c_{min} + 0.5 d_b)$. The slope of the relationship (coefficient C_1) and intercept at $A_b f / f'_c^P = 0$ (coefficient C_2) for each bar size can then be determined. The values of C_2 are roughly proportional to the bar area. Therefore, a weighted average multiplier for A_b (C_3) is determined for the full data set. Replacing C_2 by $C_3 A_b$, the expression becomes

$$\frac{T_c}{f'_c P} = \frac{A_b f_s}{f'_c P} = C_1 l_d (c_{min} + 0.5 d_b) + C_3 A_b \quad (5.1)$$

Using the right side as the predicted strength, another dummy variable analysis based on bar size is carried out for the test/prediction ratio, T/P, versus c_{max}/c_{min} . c_{min} and c_{max} are the minimum and maximum of c_b (bottom cover) and c_s , in which c_s is defined as the smaller value of c_{so} (side cover) and the effective value of c_{si} (one-half of the clear spacing). The slope of the relationship (coefficient C_4) and intercept at $T/P = 0$ (coefficient C_5) for each bar size are then obtained. This gives an expression of the form

$$\frac{T}{P} = C_4 \frac{c_{max}}{c_{min}} + C_5 \quad (5.2)$$

Replacing the individual values of C_5 by the weighted average intercept, C_6 , combining Eq. 5.1 with Eq. 5.2, and adjusting the coefficients C_1 , C_3 , C_4 , and C_6 , so that the term $(C_4 c_{max}/c_{min} + C_6) = 1$ at $c_{max}/c_{min} = 1$, gives the final equation as

$$\frac{T_c}{f'_c P} = \frac{A_b f_s}{f'_c P} = [K_1 l_d (c_{min} + 0.5 d_b) + K_2 A_b] \left(K_3 \frac{c_{max}}{c_{min}} + K_4 \right) \quad (5.3)$$

in which

$$K_1 = C_1 (C_4 + C_6)$$

$$K_2 = C_3 (C_4 + C_6)$$

$$K_3 = C_4/(C_4 + C_6)$$

$$K_4 = C_6/(C_4 + C_6)$$

A_b = single developed or spliced bar area, in in.²

f_s = bar stress at failure, in psi

f'_c = concrete compressive strength, in psi

l_d = development or splice length, in in.

c_{min}, c_{max} = minimum or maximum value of c_s , or c_b

c_s = min(c_{so} , effective c_{si}), in in.

T_c = $A_b f_s$ in lb, f'_c^p , in psi.

For illustration, the coefficients C_i and K_i are provided in Tables 5.1 and 5.2 for an effective value of $c_{si} = c_{si} + 0.25$ in. and for $p = 1/4$ and $1/2$, respectively.

The left side of Eq. 5.3 represents the experimental development/splice strength, while the right side represents the predicted development/splice strength. The relationship between development/splice strength and development/splice length is linear, but not proportional. The power of f'_c , p , should be suitable to characterize the effect of concrete strength for both normal and high strength concrete.

Effect of concrete cover and bar spacing

Figs. 5.1a and 5.1b show the splitting failure modes for bond. In Fig. 5.1a, the concrete bottom cover, c_b , is smaller than either the concrete side cover, c_{so} , or one half of the bar clear spacing, c_{si} , and, therefore, controls the splitting failure. In Fig. 5.1b, the side cover or one-half of the bar clear spacing is smaller than the bottom cover and, therefore, controls the splitting failure. In ACI 318-95, the effective value of c_{si} is equal to c_{si} . In the Canadian code (CSA Standard A23.3-94), however, a greater value (two-thirds of the center-to-center spacing of the bars being developed minus one-half of the bar diameter = $4/3 c_{si} + 1/6 d_b$) is used as the effective value of c_{si} . Darwin et al. (1995a, 1996a) found that using $c_{si} + 0.25$ in. as the effective value of c_{si} gives a better match between test development/splice strength and predicted strength than using the actual value of c_{si} . The fact that the effective value of c_{si} is greater than the actual value is most likely "due to the longer effective crack lengths

that occur when concrete splits between the bars" (Darwin et al. 1995b, 1996b) (Fig. 5.1b).

In this study, two approaches are used to find the best definition for the effective value of c_{si} , (1) adding a constant value to c_{si} and (2) multiplying c_{si} by a constant. A series of dummy variable analyses are carried out based on bar size, using Eq. 5.3 and the 171 test results for the bars without confining transverse reinforcement. Different values of the power of f'_c , p , and different values of the constants that are added to or multiplied by c_{si} are evaluated. The coefficients, K_1 , K_3 , K_4 , and K_5 , for the different values of p (from 0.20 to 0.50) and different effective values of c_{si} (from $1.0c_{si}$ to $1.7c_{si}$ and from $c_{si} + 0.24$ in. to $c_{si} + 0.40$ in.) are summarized in Table B.1.

The analyses show that using $1.6c_{si}$ as the effective value of c_{si} gives the best match (smallest value of coefficient of variation, COV, for the test/prediction strength ratios using Eq. 5.3) for the values of p evaluated. Table 5.3 gives the comparisons of the overall test/prediction ratios for different powers of f'_c and different effective values of c_{si} (c_{si} , $c_{si} + 0.25$ in., and $1.6c_{si}$). The overall test/prediction ratios using all definitions of the effective c_{si} are given in Table B.2. Table 5.3 shows that, for each definition of the effective c_{si} , $p = 0.25$ gives the smallest COV. For $p = 0.25$, the values of COV are 1.072, 1.043, and 1.026 for effective values of c_{si} equal to c_{si} , $c_{si} + 0.25$ in., and $1.6c_{si}$, respectively. Table 5.3 also shows that for a given definition of the effective value of c_{si} , the COV is largely insensitive to p for values between 0.24 and 0.26 (COV's are between 0.1072 and 0.1073 for c_{si} , between 0.1043 and 0.1044 for $c_{si} + 0.25$ in., and between 0.1026 and 0.1027 for $1.6c_{si}$). When adding a constant to c_{si} , for the range studied, the COV decreases with an increase in the constant, but is greater than the COV for $1.6c_{si}$.

Although $1.6c_{si}$ gives the best match for development/splice strength for bars not confined by transverse reinforcement, it does not give the best results for bars confined by transverse reinforcement. A later analysis for bars confined by transverse reinforcement (Section 5.3) shows that $1.6c_{si}$ overestimates the effective crack length between confined bars. Using $1.6c_{si}$, the assumed splitting cracks change from a horizontal plane (clear spacing between developed/spliced bars controls, Fig. 5.1b) to a vertical plane (bottom cover controls, Fig. 5.1a) for some specimens in which splitting was actually controlled by the clearing ~~spacing~~ spacing. Based on the observations described in Section 5.3, $c_{si} + 0.25$ in. is selected as the effective value of c_{si} for development/splice designs both with and without transverse reinforcement.

For an effective value of $c_{si} = c_{si} + 0.25$ in. and $p = 1/4$, Eq. 5.3 becomes

$$\frac{T_c}{f'_c^{1/4}} = \frac{A_b f_s}{f'_c^{1/4}} = [59.8 l_d(c_{min} + 0.5 d_b) + 2350 A_b] \left(0.1 \frac{c_{max}}{c_{min}} + 0.9 \right) \quad (5.4)$$

By way of comparison using the effective value of $c_{si} = c_{si} + 0.25$ in. along with the more traditional value $p = 1/2$, Eq. 5.3 becomes

$$\frac{T_c}{f'_c^{1/2}} = \frac{A_b f_s}{f'_c^{1/2}} = [8.45 l_d(c_{min} + 0.5 d_b) + 177.6 A_b] \left(0.17 \frac{c_{max}}{c_{min}} + 0.83 \right) \quad (5.5)$$

In Eqs. 5.4 and 5.5, $c_{max}/c_{min} \leq 3.5$, since test data are not available for larger values.

Effect of concrete strength

The previous analysis shows that $p = 1/4$ gives the lowest COV for the beams in the data base. The COV, however, only gives the relative accuracy of the predicted results for the data base, as a whole. It does not represent a measure of

accuracy for specific values of f'_c . Darwin et al. (1995b, 1996b) found that the traditional $p = 1/2$ gives a good representation of bond strengths for concrete compressive strengths between 4500 and 7500 psi (31.0 and 51.7 MPa), while $p = 1/4$ gives a good representation for both normal and high strength concretes [f'_c between 2160 and 15,120 psi (14.9 and 104.3 MPa)].

In this study, the test results of the 171 specimens containing bars without transverse reinforcement are plotted versus the results predicted by Eq. 5.5 ($p = 1/2$, and $c_{si} + 0.25$ in. as the effective value of c_{si}), using dummy variable regression based on concrete strength (Fig. 5.2). The concrete compressive strengths are classified into eight groups, 2500 to 3500 psi (17.2 to 24.1 MPa), 3500 to 4500 psi (24.1 to 31.0 MPa), 4500 to 5500 psi (31.0 to 37.9 MPa), 5500 to 6500 psi (37.9 to 44.8 MPa), 6500 to 10,500 psi (44.8 to 72.4 MPa), 10,500 to 13,500 psi (72.8 to 93.1 MPa), 13,500 to 14,500 psi (93.1 to 100.0 MPa), and 14,500 to 16,100 psi (100.0 to 111.0 MPa).

As observed by Darwin et al. (1996a, 1996b), in Fig. 5.2, the best-fit lines representing the categories of concrete strength are scattered, and the intercepts of the best-fit lines decrease as concrete strength increases, indicating that using $p = 1/2$ gives a biased prediction of development/splice strength.

Based on these observations, a series of dummy variable analyses is applied for test versus predicted bond strength based on concrete strength, using $c_{si} + 0.25$ in. as the effective value of c_{si} and different powers of f'_c , p . The range of the relative intercepts is used to evaluate the spread of data for different values of p . A relative intercept is obtained by dividing the intercept of the best-fit line representing each concrete strength group by the range between the maximum and minimum predicted bond strengths obtained for the data base using Eq. 5.3. A smaller range of the

relative intercept represents a lower spread of the data. The analysis results are given in Table 5.4, and the ranges of the relative intercepts are plotted versus the power of f'_c in Fig. 5.3. As shown in the figure, $p = 0.24$ gives the smallest range of the relative intercepts, matching the results obtained by Darwin et al. (1995a, 1995b). Considering the analysis results for the effect of concrete cover and bar spacing ($p = 1/4$ gives the lowest COV) and for convenience, $p = 1/4$ is selected for characterizing the effect of concrete strength, as shown in Eq. 5.4.

Test bond strengths are plotted versus predicted bond strength using $p = 1/4$ (Eq. 5.4) and dummy variable analysis based on concrete strength in Fig. 5.4. The best-fit lines for the different categories of concrete strength nearly coincide, indicating that $f'_c^{1/4}$ accurately represents the effect of concrete strength on the development/splice strength of bars not confined by transverse reinforcement.

5.2.2 Comparison with Test Results

Specimen properties, test results and the predicted results using Eqs. 5.4 and 5.5 for the 171 specimens are presented in Table 5.5. As shown in Table 5.5, the mean ratio of test-to-predicted strength is 1.0 using both the 1/4 and 1/2 powers of f'_c , with a coefficient of variation (COV) of 0.104 using the 1/4 power of f'_c and a COV of 0.152 using the 1/2 power of f'_c . The ratios of test-to-predicted strength using Eqs. 5.4 and 5.5 are plotted versus concrete compressive strength, f'_c , for the 171 test specimens in Figs. 5.5a and 5.5b, respectively. Fig. 5.5a shows that the best-fit line for the 1/4 power of f'_c is virtually horizontal, indicating that there is no bias in the prediction of development/splice strength using Eq. 5.5 as a function of concrete strength over the range of f'_c evaluated (2610 to 15650 psi). However, as foretold by Fig. 5.2, Fig. 5.5b shows that the test/prediction ratio decreases as concrete strength

increases. The use of the 1/2 power of f'_c obviously overestimates the development/splice strength for high-strength concrete. This, again, indicates that the 1/4 power of f'_c does a better job than the 1/2 power of f'_c in characterizing the contribution of concrete strength to bond.

5.3 Bars with Confining Transverse Reinforcement

The additional bond strength provided by transverse reinforcement can be determined using Eq. 5.6, based on the assumption that the maximum bond force in a bar at development/splice failure is expressed as the sum of a concrete contribution, T_c , and a transverse reinforcement contribution, T_s .

$$T_s = T_b - T_c \quad (5.6)$$

in which, T_b is the experimental bond force and T_c is determined using Eq. 5.4.

The test results of Hester et al. (1991, 1993), Darwin et al. (1995a, 1996a) and this study are used for the following analysis and the analyses presented in Sections 5.3.1 through 5.3.3 because similar materials, test specimens, and test procedures were used. The test results for the 8N1 bars confined by transverse reinforcement are not used in this chapter because the 8N1 bars had a high ratio of rib width to rib spacing, which increased the tendency for a pullout failure and caused a reduced bond strength compared to that of bars with lower ratios of rib width to rib spacing (see Chapter 4).

The analysis presented in Section 5.2.1 shows that using $1.6c_{si}$ as the effective value of c_{si} gives the best match between test and predicted results for bars not confined by transverse reinforcement. However, for bars confined by transverse reinforcement, $1.6c_{si}$ does not give good results. Comparisons of $T_s/f'_c^{1/4}$ versus the

effective transverse reinforcement, NA_{tr}/n [N = number of stirrups in the splice region, A_{tr} = area of each stirrup or tie crossing the potential plane of splitting adjacent to the bars, and n = number of bars being developed or spliced; Darwin et al. (1995b, 1996b) demonstrated that $T_s/f'_c^{1/4}$ is a function of NA_{tr}/n], show that, in general, $c_{si} + 0.25$ in. produces a better match with test results (higher coefficient of determination, r^2 , for $T_s/f'_c^{1/4}$ versus NA_{tr}/n) than $1.6c_{si}$ or the other definitions of the effective value of c_{si} . Table 5.6 gives the comparisons of the values of r^2 for specimens with bars confined by transverse reinforcement in normal strength concrete. In the 11 groups of bars, the values of r^2 are highest for 6 groups of bars when using the effective value of $c_{si} = c_{si} + 0.25$ in. (5N0, 8C1, 8F1, 8N3, 11F3, and conventional No. 11 in the concrete with limestone aggregate). The values of r^2 are highest for two groups when using the effective value of $c_{si} = 1.6c_{si}$ (5C2 and conventional No. 8 bars in the concrete with limestone aggregate). One group has the same value of r^2 when using $c_{si} + 0.25$ in. or $1.6c_{si}$ (8F1 bars in the concrete with basalt aggregate) and two groups have the highest r^2 when using the actual c_{si} (8N0 and 8N3 bars in the concrete with basalt aggregate – in this case the values of r^2 are higher when using $c_{si} + 0.25$ in. than when using $1.6c_{si}$). $1.6c_{si}$ overestimates the effective crack length between confined bars, which, in turn, overestimates the concrete contribution to bond strength. An another disadvantage of using the larger effective value of c_{si} is that the assumed splitting cracks change from a horizontal plane to a vertical plane for some specimens in which splitting was actually controlled by the clear spacing. This incorrectly changes the value of NA_{tr}/n for beams with more than two spliced bars, resulting in a lower r^2 (8C1 and 11F3 bars; see Table 5.6). Based on these observations, $c_{si} + 0.25$ in. is used for both confined bars and bars not confined by transverse reinforcement.

5.3.1 Effect of Concrete Strength

The evaluations of the test results presented in Chapter 4 show that high strength concrete (HSC) produces a higher additional bond force due to transverse reinforcement normalized with respect to $f'_c^{1/4}$ ($T_s/f'_c^{1/4}$) than normal strength concrete (NSC). Therefore, a value of the power of f'_c , p , higher than 1/4 is expected to characterize the effect of concrete strength on T_s .

To capture the main behavior of developed/spliced bars confined by transverse reinforcement as a function of f'_c , values of p equal to 1/4, 1/2, 3/4 and 1.0 are selected to evaluate the effect of concrete strength on T_s . In this case, comparisons are limited to members cast with concrete containing limestone coarse aggregate. The concrete strengths for specimens with bars designated as 8N3 ($R_r = 0.119$) and 11F3 ($R_r = 0.127$) and No. 8 conventional bars ranged from normal to high strength. Therefore, these three bar patterns are used in the first step of the evaluation. For each bar, T_s normalized with respect to f'_c^p is plotted versus NA_{tr}/n . Then the best-fit lines for each value of p are obtained. In general, the closer the coefficient of determination, r^2 , is to 1.0, the better the correlation between T_s/f'_c^p and NA_{tr}/n , which, in turn, indicates the better value of p to characterize the effect of concrete strength. The values of r^2 for the different values of p are summarized in Table 5.7. The results show that $p = 3/4$ produces the highest r^2 for high relative rib area (R_r) bars: $r^2 = 0.9160$ for the 8N3 bars and $r^2 = 0.6554$ for the 11F3 bars. For No. 8 conventional bars, $p = 1.0$ produces the highest r^2 (0.7136). For all three bar patterns, $p = 1/4$ produces the lowest r^2 values (0.7618 for the 8N3 bars, 0.5718 for the 11F3 bars and 0.5104 for No. 8 conventional bars).

The values of $T_s/f'_c^{3/4}$ are plotted versus NA_{tr}/n in Figs. 5.6a and 5.7a for 8N3 and 11F3 bars, respectively. The values of T_s/f'_c are plotted versus NA_{tr}/n in Fig.

5.8a for No. 8 conventional bars. The figures show that when the additional bond forces, T_s , are normalized with respect to $f'_c^{3/4}$ for 8N3 and 11F3 bars and f'_c for No. 8 conventional bars, the data points for HSC and NSC overlap, resulting in the higher values of the coefficient of determination. For comparison, the values of $T_s/f'_c^{1/4}$ are plotted versus NA_{tr}/n in Figs. 5.6b, 5.7b, and 5.8b for 8N3, 11F3, and No. 8 conventional bars, respectively. These figures show that the bond forces normalized with respect to $f'_c^{1/4}$ are higher for HSC than for NSC.

These observations also suggest that the effect of R_r on bond strength may be less for HSC than for NSC, matching the observations described in Chapter 4. To derive a single equation for both high R_r and conventional bars, $p = 3/4$ is initially selected for characterizing the effect of concrete strength on the additional bond strength due to transverse reinforcement. This selection will be verified and the other values of p (1/4, 1/2, and 1.0) will be used for further evaluation of the effect of concrete strength and for comparisons in the later analyses, including a wider range of test data.

Figs. 5.9 and 5.10 compare $T_s/f'_c^{3/4}$ versus NA_{tr}/n for splices confined by transverse reinforcement and cast in concretes containing limestone and basalt coarse aggregates, respectively. The figures illustrate that, in general, $T_s/f'_c^{3/4}$ increases with increasing relative rib area, as well as with increasing bar size, matching observations by Darwin et al. (1995a, 1996a) for the bars cast in normal strength concrete and using $f'_c^{1/4}$ to normalize T_s . The slopes, intercepts, and coefficients of determination of the best-fit lines for all of the test bars are given in Table 5.8. $p = 1/4$ gives the highest r^2 for five bar sizes and patterns that were tested only with normal strength concrete (No. 11 conventional, 5C2, and 8C1 bars in the concrete with limestone and 8F1 and 8N3 bars in the concrete with basalt. For two other bars cast only with NSC

(No. 5 conventional and 8F1 bars in the concrete with limestone) $p = 1.0$ gives the highest r^2 . As described before, for high R_r bars cast in both NSC and HSC (8N3 and 11F3) $p = 3/4$ gives the highest r^2 , while for conventional bars cast in both NSC and HSC concrete (No. 8 conventional bars), $p = 1.0$ gives the highest r^2 . In the cases where $p = 1/4$ gives the highest values of r^2 , r^2 is not particularly sensitive to p , while in cases where $p = 3/4$ or larger gives the highest values of r^2 , r^2 exhibits significant sensitivity to p .

The next step of the analysis is to establish the relationship between the additional bond strength due to transverse reinforcement, T_s , and parameters such as relative rib area, R_r , bar size, d_b , effective transverse reinforcement, NA_{tr}/n , and power of f'_c , p . Procedures similar to those used by Darwin et al (1995a, 1996a) are used in this study.

Based on the results of the best-fit lines for each group of data presented in Table 5.8, the relationships between T_s/f'_c^p and NA_{tr}/n are replaced with linear functions that have zero intercept at $NA_{tr}/n = 0$ and cross the best-fit lines at $NA_{tr}/n = 1.0$, taking the form

$$\frac{T_s}{f'_c^p} = (m + b) \frac{NA_{tr}}{n} = M \frac{NA_{tr}}{n} \quad (5.7)$$

in which m and b are the slope and intercept of the best-fit lines, respectively, corresponding to the values of p presented in Table 5.8. In Eq. 5.7, M is the modified slope which combines the effects of relative rib area and bar size in one parameter. The expression provides a conservative representation for the relationship between T_s/f'_c^p and NA_{tr}/n for the test bars with a positive intercept, which is the case for most of the bars (1 high R_r and 1 conventional bar for $p = 1/4$ and $1/2$, 2 high R_r and 1

conventional bar for $p = 3/4$, and 3 high R_r and 1 conventional bar for $p = 1.0$ have negative intercepts). It is found that using $NA_{tr}/n = 1.0$ to establish the modified slope gives a better match with the test results. Therefore, $M = m + b$ is used in Eq. 5.7. The differences in the procedures to establish Eq. 5.7 between this study and the previous study (Darwin et al. 1995b, 1996b) are (1) different powers of f'_c are evaluated in this study and (2) the modified slope, M , is obtained based on $NA_{tr}/n = 1.0$, $M = m + b$, in this study, instead of $NA_{tr}/n = 2.0$, $M = (2m + b)/2$.

5.3.2 Effect of Relative Rib Area

To determine the effects of R_r and bar size on T_s , it is first assumed that changes in T_s due to changes in R_r are independent of bar size and concrete properties. For $p = 3/4$, the values of M developed using Eq. 5.7 are plotted versus R_r in Fig. 5.11 for No. 5, No. 8, and No. 11 bars cast with concrete containing limestone coarse aggregate and No. 8 bars cast with concrete containing basalt coarse aggregate for the data provided in Table 5.8. In Fig. 5.11, each data point represents a single value of R_r , except that the weighted average values of R_r are used for the conventional No. 8 and No. 11 bars because a range of R_r values was used for these test bars.

The best-fit lines of M versus R_r are obtained for each of the four groups of test bars, as shown in Fig. 5.11, and the values of M corresponding to $R_r = 0.075$ ($M_{R_r=0.075}$) are then determined using the best-fit equations, in which $R_r = 0.075$ is the midway point in the range of conventional bars tested. The individual values of M are normalized with respect to $M_{R_r=0.075}$ to obtain the factor $t_r = M / M_{R_r=0.075}$ for each group of bars. This approach should, presumably, remove the effects of bar size and concrete properties so that t_r only represents the effect of R_r .

The values of t_r are plotted versus R_r in Fig. 5.12 for $p = 3/4$, and linear regression yields the best-fit equation for $p = 3/4$ as

$$t_r = 9.6R_r + 0.28 \quad (5.8)$$

with a coefficient of determination $r^2 = 0.942$.

Eq. 5.8 is identical to the equation developed by Darwin et al. (1995a, 1996a) using test results for the bars in normal strength concrete and T_s normalized with respect to $f'_c^{1/4}$. The strong correlation between t_r and R_r supports the initial assumption of that the effect of R_r on T_s is independent of bar size and concrete properties.

5.3.3 Effect of Bar Size

Once the effect of R_r is determined, the effect of bar size on T_s can be obtained by dividing the values of M by t_r from Eq. 5.8. This step removes the effect of R_r from M and converts the original values of M to values corresponding to bars with $R_r = 0.075$. A linear regression of M/t_r versus d_b for the bars cast in limestone concrete (Fig. 5.13) gives

$$\frac{M}{t_r} = 20.7d_b + 5.77 \quad (5.9)$$

with $r^2 = 0.951$.

Assuming that this expression can be generalized to the other concretes, Eq. 5.9 is normalized with respect to M/t_r for $d_b = 1$ in. to obtain an expression representing the effect of bar size on T_s .

$$t_d = 0.78d_b + 0.22 \quad (5.10)$$

The values of m , b , M , $M_{R_r=0.075}$, and M/t_r using $p = 3/4$ are summarized in Table 5.9. Compared to the equation developed by Darwin et al. (1995a, 1996a) ($t_d = 0.72d_b + 0.28$), the slope in Eq. 5.10 is slightly higher, while the intercept is slightly lower.

For the other values of p (1/4, 1/2, and 1.0) the terms of t_r and t_d can be obtained using the procedures described above. A summary of the best-fit equations for t_r and t_d terms using different values of p is presented in Table 5.10. It is noted that using $p = 1.0$ produces the highest values of coefficient of determination, r^2 , for t_r and t_d terms ($r^2 = 0.957$ for t_r and $r^2 = 0.970$ for t_d as shown in Table 5.10). Lower levels of r^2 for using $p = 1/4$ and 1/2 indicate less linearity in the relationships between T_s and the effects of R_r and bar size. Although $p = 1.0$ appears to be the best for the t_r and t_d terms, it is not selected for characterizing the effect of concrete strength on T_s because an analysis including a wider range of data (Section 5.3.4) indicates that using $p = 1.0$ overpredicts T_s for splices in high strength concrete.

For $p = 3/4$, the expression combining the effects of R_r , d_b , and NA_{tr}/n gives

$$t_r t_d N A_{tr} / n = (9.6 R_r + 0.28) (0.78d_b + 0.22) N A_{tr} / n \quad (5.11)$$

5.3.4 Expression for Development/Splice Strength

The additional bond strength contributed by transverse reinforcement normalized with respect to $f'_c P$ ($T_s/f'_c P$) can be expressed as a linear function of $t_r t_d N A_{tr} / n$.

$$\frac{T_s}{f'_c P} = K_1 t_r t_d \frac{N A_{tr}}{n} + K_2 \quad (5.12)$$

in which T_s is in lb; f'_c^p is in psi; t_r and t_d are given in Table 5.9 for each value of p ; for $p = 3/4$, the combined term of $t_r t_d N A_{tr}/n$ is given in Eq. 5.11; and K_1 and K_2 are the slope and intercept that can be determined using regression techniques.

At first, a data base that includes 212 specimens containing uncoated bottom-cast developed/spliced bars, including the 166 specimens used by Darwin et al. (1995b, 1996b) and 46 specimens from the current study, is used to develop an expression for T_s . After the expression is developed, an independent set of tests from Kadoriku (1994) is used to evaluate the appropriateness of the selected power of f'_c and the accuracy of the expression. The independent set is then incorporated in the full data set to obtain an improved expression.

Darwin et al. (1995b, 1996b) found that specimens with $l_d/d_b < 16$ exhibit especially low strengths and that the test/prediction ratios are consistently below 1.0 for the specimens with $(c + K_{tr})/d_b > 4.0$ (see Eq. 1.12), in which $K_{tr} = 35.3 t_r t_d N A_{tr}/n$, $t_r = 9.6 R_r + 0.28$, and $t_d = 0.72 d_b + 0.28$. Their analyses showed that high values of $(c + K_{tr})/d_b$ cause the mode of bond failure to change from splitting to pullout. With pullout failure, bond strength is limited by the strength of the concrete between the ribs of the bar rather than by the clamping forces provided by the surrounding concrete and the transverse steel, which causes a drop in bond strength in relation to the predicted strength. Therefore, the 49 specimens with $l_d/d_b < 16$ and $(c + K_{tr})/d_b > 4.0$ used by Darwin et al. are removed from the 212 specimens [Note: $(c + K_{tr})/d_b \leq 4.0$ for all of the specimens containing splices confined by stirrups tested in the current study].

With the data removed, a series of dummy variable analyses, based on study and bar size, is applied using Eq. 5.12 for different values of p (1/4, 1/2, 3/4, and 1.0).

The dummy variable regression technique is used to limit the effects on the analysis of variations in concrete properties or other differences between test sites.

Of the remaining 163 specimens, R_r is known for 152 specimens based on measurements made on the bars or based on data provided in the original papers. The other 11 specimens contained conventional bars for which R_r is unknown and average values of R_r , obtained by Darwin et al. (1995b, 1996b) based on bar samples from previous studies (Choi et al. 1990, 1991, Hester et al. 1991, 1993, Darwin et al. 1995a, 1996a, Rezansoff et al. 1991, 1993, and Azizinamini et al. 1995), are used. For the 11 bars, the average values of R_r are 0.0752 for No. 5 (16 mm) bars, 0.0748 for No. 6 (19 mm) bars, 0.0731 for No. 8 (25 mm) bars, and 0.0674 for No. 11 (36 mm) bars. For Canadian "metric bars" included in the data base (Rezansoff et al. 1991, 1993), the normal metric sizes are converted exactly to customary units for the analysis. Concrete compressive strengths for the 163 specimens range from 1820 to 15,760 psi (13 to 109 MPa) [Note: specimen 15G-12B-P9 tested by DeVries (1991) had the highest value of f'_c , 16,100 psi (111 MPa), in the data base. However, this specimen is not used for the analysis because I_d/d_b is less than 16]. Values of R_r range from 0.059 to 0.140. Full data for the 163 specimens are included in Table 5.11.

The results of the dummy variable analyses are shown in Figs 5.14a-5.14d and Table 5.12. Based on the dummy variable analyses and using weighted mean intercepts at $T_s/f'_c^p = 0$, the best-fit expressions are

for $p = 1/4$,

$$\frac{T_s}{f'_c^{1/4}} = 1977(t_r t_d)_{p=1/4} \frac{NA_{tr}}{n} + 455 \quad (5.13a)$$

with $r^2 = 0.787$;

for $p = 1/2$,

$$\frac{T_s}{f'_c^{1/2}} = 247(t_r t_d)_{p=1/2} \frac{NA_{tr}}{n} + 40.4 \quad (5.13b)$$

with $r^2 = 0.836$;

for $p = 3/4$,

$$\frac{T_s}{f'_c^{3/4}} = 30.9(t_r t_d)_{p=3/4} \frac{NA_{tr}}{n} + 3.59 \quad (5.13c)$$

with $r^2 = 0.858$;

and for $p = 1.0$,

$$\frac{T_s}{f'_c} = 3.823(t_r t_d)_{p=1.0} \frac{NA_{tr}}{n} + 0.322 \quad (5.13d)$$

with $r^2 = 0.860$.

Expressions with higher values of r^2 better represent the relationship between T_s/f'_c^p and the selected combination of parameters. r^2 is highest (0.860) for $p = 1.0$. For $p = 3/4$, r^2 (0.858) is just slightly lower. $p = 1/4$ produces the lowest value of r^2 (0.786). The results indicate that, at this point, the selections of $p = 1.0$ and $3/4$ give the nearly same level of confidence.

Combining Eqs. 5.13a - 5.13d with Eq. 5.4, predicted strengths and test/predicted strength ratios can be obtained for each value of p . The predicted strength and test/predicted strength ratios for the 163 specimens are summarized in Table B.3. The overall average of the test/predicted strength ratios is 1.0 for all of the values of p evaluated. $p = 3/4$ provides the second lowest coefficient of variation, COV (0.120), which is slightly higher than the lowest COV, provided by $p = 1/2$ (0.116). The COV is highest for $p = 1.0$ (0.132).

The COV values, however, only reflect the accuracy of the predictions for the overall data base. The best value of p for characterizing the effect of concrete strength should provide unbiased predictions for both NSC and HSC. This means

that, for the appropriate value of p , the best-fit line of the test/predicted strength ratio versus concrete compressive strength should be horizontal. To evaluate the power of f'_c that best characterizes the effect of concrete strength on T_s , a series of dummy variable analyses is carried out, based on study, for test/prediction ratios versus f'_c using Eqs. 5.13a - 5.13d. The results of the dummy variable analyses are summarized in Table 5.13 and Fig. 5.15. In Fig. 5.15, each line represents the best-fit line of test/prediction ratio versus f'_c , with the slopes and weighted intercepts from the analysis given in Table 5.13. The figure shows that the slope of the best-fit line decreases with an increase of the value of p . $p = 3/4$ gives the smallest positive slope, while $p = 1.0$ gives a negative slope. The best-fit line for $p = 3/4$ is virtually horizontal. This indicates that, among the values of p evaluated ($1/4$, $1/2$, $3/4$, and 1.0), $p = 3/4$ gives the best predictions of bond strength for both NSC and HSC. The use of $p = 1.0$ overestimates the bond strength for the bars in HSC. It seems that the best value of p is between 0.75 and 1.0 , (approximately 0.8 , according to an estimation based on the slopes of the lines shown in Fig. 5.15). For convenience, $p = 3/4$ is selected.

To evaluate the appropriateness of the selected value of p and the accuracy of Eq. 5.13c, an independent set of 33 splice specimens tested by Kadoriku (1994) is used to compare the test/prediction ratios for Eqs. 5.13a - 5.13d and the corresponding values of p . For this series, concrete compressive strength ranged from 3072 to 10,980 psi (21.2 to 75.7 MPa). A single bar size, 19 mm, was used. Since R_r was not reported, $R_r = 0.748$ is used [the mean value for No. 6 (19 mm) conventional bars (Darwin et al 1995b, 1996b)]. The specimen details are included in Table 5.11. The test/prediction ratios using Eqs. 5.13a - 5.13d are given in Table 5.14. The comparisons indicate that Eq. 5.13c for $p = 3/4$ provides the lowest COV value

(0.085) for the 33 specimens. The test/prediction ratios using different values of p (1/4, 1/2, 3/4 and 1.0) are plotted versus f'_c in Fig. 5.16, showing the same characteristics as in Fig. 5.15: $p = 3/4$ provides the smallest positive slope of the best-fit lines and $p = 1.0$ gives a negative slope. This analysis shows that, among the values of p evaluated, $p = 3/4$ is the most appropriate for use in characterizing the effect of concrete strength on T_s .

Adding the 33 specimens in the data base, a reanalysis is carried out using $p = 3/4$ for the 196 specimens, which yields

$$\frac{T_s}{f'_c^{3/4}} = 30.98 t_r t_d \frac{NA_{tr}}{n} + 3.91 \quad (5.14)$$

with $r^2 = 0.855$. The dummy variable analysis results are given in Table 5.15 and Fig. 5.17.

Combining Eq. 5.4 and Eq. 5.14, dropping the mean intercept, 3.91, replacing N by l_d/s , where s is the spacing of transverse reinforcement or ties, and solving for the development/splice length, l_d , gives

$$l_d = -\frac{A_b \left[\frac{f_s}{f'_c^{1/4}} - 2350 \left(0.1 \frac{c_{max}}{c_{min}} + 0.9 \right) \right]}{59.8 \left[(c_{min} + 0.5 d_b) \left(0.1 \frac{c_{max}}{c_{min}} + 0.9 \right) + 0.518 \frac{t_r t_d A_{tr}}{sn} f'_c^{1/2} \right]} \quad (5.15)$$

Modifying Eq. 5.15 to express l_d in terms of d_b by replacing A_b by $\pi d_b^2/4$ gives

$$\frac{l_d}{d_b} = \frac{\left[\frac{f_s}{f'_c^{1/4}} - 2350 \left(0.1 \frac{c_{max}}{c_{min}} + 0.9 \right) \right]}{76.1 \left(\frac{c + K_{tr}}{d_b} \right)} \quad (5.16)$$

in which $c = (c_{\min} + 0.5 d_b)(0.1 c_{\max}/c_{\min} + 0.9)$ and $K_{tr} = (0.518 t_r t_d A_{tr}/sn) f'_c^{1/2}$. The principal difference between the terms $(c + K_{tr})/d_b$ obtained in the current study and the equation developed by Darwin et al. (1995b, 1996b) is that the K_{tr} from this study includes the effect of concrete strength.

To examine the limits of $(c + K_{tr})/d_b$ using the new expression for K_{tr} , the test/prediction ratios based on the sum of Eqs. 5.4 and 5.14 are plotted versus $(c + K_{tr})/d_b$ in Fig. 5.18. The figure shows that the test/prediction ratios are below 1.0 for the specimens with $(c + K_{tr})/d_b > 4.0$. Based on this observation, a reanalysis is carried out for the 191 specimens with $(c + K_{tr})/d_b \leq 4.0$. The results of the reanalysis are given in Table 5.16 and Fig. 5.19. The best-fit expression changes only slightly from Eq. 5.14.

$$\frac{T_s}{f'_c^{3/4}} = 31.14 t_r t_d \frac{NA_{tr}}{n} + 3.99 \quad (5.17)$$

with $r^2 = 0.856$.

Combining Eq. 5.4 with Eq. 5.17 gives the expression of total bond strength.

$$\begin{aligned} \frac{T_b}{f'_c^{1/4}} &= \frac{T_c + T_s}{f'_c^{1/4}} = [59.8 l_d (c_{\min} + 0.5 d_b) + 2350 A_b] \left(0.1 \frac{c_{\max}}{c_{\min}} + 0.9 \right) \\ &\quad + \left(31.14 t_r t_d \frac{NA_{tr}}{n} + 3.99 \right) f'_c^{1/2} \end{aligned} \quad (5.18)$$

Dropping the intercept 3.99 and solving for l_d in terms of A_b and d_b gives, respectively,

$$l_d = \frac{A_b \left[\frac{f_s}{f'_c^{1/4}} - 2350 \left(0.1 \frac{c_{\max}}{c_{\min}} + 0.9 \right) \right]}{59.8 \left[(c_{\min} + 0.5 d_b) \left(0.1 \frac{c_{\max}}{c_{\min}} + 0.9 \right) + 0.52 \frac{t_r t_d A_{tr}}{sn} f'_c^{1/2} \right]} \quad (5.19)$$

$$\frac{l_d}{d_b} = \frac{\left[\frac{f_s}{f'_c} - 2350 \left(0.1 \frac{c_{\max}}{c_{\min}} + 0.9 \right) \right]}{76.1 \left(\frac{c + K_{tr}}{d_b} \right)} \quad (5.20)$$

A

in which t_r and t_d are determined by Eqs. 5.6 and 5.8, $K_{tr} = (0.52 t_r t_d / s_n) f'_c^{1/2}$, and $(c + K_{tr})/d_b \leq 4.0$.

Eqs. 5.18 - 5.20 are the final expressions for evaluating the bond strength of bars confined by transverse reinforcement. The test/predicted strength ratios using Eq. 5.18 and the new definition of K_{tr} for the 213 specimens with $l_d/d_b \geq 16$ [including 17 specimens with $(c + K_{tr})/d_b > 4.0$, in which $K_{tr} = 35.1 t_r t_d A_{tr} / s_n$ developed by Darwin et al. (1995b, 1996b)] are plotted versus $(c + K_{tr})/d_b$ in Fig. 5.20 to evaluate the test/predicted strength ratios versus $(c + K_{tr})/d_b$ for all beams in the data base with transverse reinforcement and $l_d/d_b \geq 16$. As before, the test/predicted strength ratios for the additional 17 specimens are lower than 1.0. The test/predicted strength ratios are plotted versus $(c + K_{tr})/d_b$ in Fig. 5.21 using Eq. 5.18 for the 191 specimens used to develop Eq. 5.18 and in Fig. 5.22 using Eq. 5.20, setting $(c + K_{tr})/d_b \leq 4.0$, for all 213 specimens. The figures show that Eqs 5.18 - 5.20 provide accurate predictions for specimens with $(c + K_{tr}) \leq 4.0$ and the limit of $(c + K_{tr})/d_b \leq 4.0$ is appropriate for development/splice designs.

The details for all 245 specimens with transverse reinforcement in the data base, the predicted development/splice strengths using Eq. 5.18, and the test/prediction ratios are given in Table 5.11. For the 191 specimens used to develop Eq. 5.18, the average test/predicted strength ratio is 1.001 and the COV is 0.115. A

comparison of the test and predicted results is shown in Fig. 5.23 for the 191 specimens.

For design purposes, Eq. 5.20 can be conservatively simplified by setting $c_{\max}/c_{\min} = 1$ and dropping the 0.25 term in the definition of the effective c_{si} ($c_{si} + 0.25$ in.), which gives

$$\frac{l_d}{d_b} = \frac{\frac{f_s}{f_c^{1/4}} - 2350}{76.1 \left(\frac{c + K_{tr}}{d_b} \right)} \quad (5.21)$$

in which $c = (c_{\min} + 0.5 d_b)$, $c_{\min} = \min(c_s, c_b)$, $c_s = \min(c_{so}, c_{si})$. The definition of K_{tr} following Eq. 5.20 remains unchanged.

5.4 Effect of Bar Stress on Development/Splice Strength

An analysis by Darwin et al. (1995b, 1996b) demonstrates that yielding of developed/spliced bars has no effect on the bond strength of bars not confined by transverse reinforcement, and results in an increase in the bond strength of bars confined by transverse reinforcement. Their conclusion does not support the concern of others that yielding of developed/spliced bars will result in a reduction in bond strength (Orangun et al. 1975, Harajli 1994). An evaluation of the test/prediction results in the current study supports the conclusions of Darwin et al. (1995b, 1996b).

For the 19 specimens without transverse reinforcement that yielded prior to bond failure [that is, the calculated bar stresses at the peak loads are greater than or equal to the bar yield strengths (see Appendix A)], the test/predicted strength ratios range from 0.754 to 1.262 with an average of 0.981, compared to the test/predicted strength ratios for the 143 specimens that did not yield, which range from 0.732 to 1.317 with an average of 1.008. As before (Darwin et al. 1995b, 1996b), there is no

significant effect of yielding on the bond strength of bars not confined by transverse reinforcement.

Of the 191 specimens with bars confined by transverse reinforcement used to develop Eq. 5.18, 43 specimens yielded prior to bond failure. The test/predicted strength ratios range from 0.833 to 1.312 with an average of 1.088 for the 43 specimens and from 0.761 to 1.244 with an average of 0.971 for the 148 specimens that did not yield. This comparison shows that yielding of bars with confining transverse reinforcement results in an increase in bond strength, again matching the observations of Darwin et al. (1995b, 1996b) and indicating that earlier concerns about a reduction in bond strength due to yielding of bars were unwarranted.

5.5 Design Expression for Development/Splice Length

Eqs. 5.18 - 5.21 provide predictions of development/splice strength. To obtain design expressions, a strength reduction (ϕ) factor must be added to reduce the level of risk caused by the variability in the applied loads and the resistance of the members.

This section describes the calculation of a reliability-based ϕ -factor for developed/spliced high R_r and conventional bars. Bars both with and without confining transverse reinforcement are considered. A design expression for development/splice length is obtained which incorporates the ϕ -factor. The development/splice lengths calculated for high R_r bars are then compared to those calculated for conventional bars. The design expression obtained from this study is also compared to the expressions in ACI 318-95.

5.5.1 Strength Reduction (ϕ) Factor

The approach used by Darwin et al. (1995c) to obtain the ϕ -factor for bond, ϕ_b , is used in this study and is briefly described as follows.

Overall approach

Converting Eqs. 5.20 and 5.21 back to a form that can be used to predict $T_b = A_b f_s$ gives, respectively,

$$T_b = A_b f_s = f_c^{1/4} \left\{ [59.8 l_d(c_{min} + 0.5 d_b) + 2350 A_b] \left(0.1 \frac{c_{min}}{c_{max}} + 0.9 \right) + 31.14 t_r t_d \frac{l_d A_u}{sn} f_c^{1/2} \right\} \quad (5.22)$$

$$T_b = A_b f_s = f_c^{1/4} \left\{ [59.8 l_d(c_{min} + 0.5 d_b) + 2350 A_b] + 31.14 t_r t_d \frac{l_d A_u}{sn} f_c^{1/2} \right\} \quad (5.23)$$

in which t_r and t_d are determined by Eqs. 5.8 and 5.10, respectively; and c_s (used to determine c_{min} and c_{max}) is defined appropriately in the expressions following Eqs. 5.20 and 5.21, respectively. Eq. 5.23 is, in general, more conservative than Eq. 5.22, but will provide the same strength as Eq. 5.22 when $c_{min} = c_{max}$.

It is noted that, in design, the bar force $A_b f_s$ that appears on the left side of Eqs. 5.22 and 5.23, has already been increased by a factor of $1/\phi$, in which ϕ is the strength reduction factor for the main loading, before development/splice design is undertaken. So as not to double-count ϕ -factors, the resistance to which the ϕ_b is applied corresponds to $\phi A_b f_s$ (equivalent to the factored load) (Darwin et al. 1995c). That is,

$$\phi A_b f_s \geq \phi_b [\text{right side of Eq. 5.22 or 5.23}] \quad (5.24)$$

from which

$$A_b f_s \geq \phi_d [\text{right side of Eq. 5.22 or 5.23}] \quad (5.25)$$

where $\phi_d = \phi_b/\phi$ is the effective ϕ -factor for use in determining development/splice lengths.

To obtain the value of ϕ_b (and ultimately ϕ_d), a selection of the desired level of reliability, represented by the reliability index (β), must be determined. The expression of β for bond is obtained by Darwin et al. (1995c).

$$\beta = \frac{\ln(\bar{r} / \phi_b \bar{q})}{\sqrt{V_r^2 + V_{\phi q}^2}} \quad (5.26)$$

where

$$r = \frac{R}{R_n} = \frac{X(1)R_p}{R_n} \quad (5.27)$$

in which R is the random variable for resistance, $X(1)$ is the test-to-predicted load capacity random variable, and R_p is the predicted capacity random variable; \bar{r} and V_r are the mean and COV of r , respectively; and q is loading random variable given by

$$q = \frac{\left[X(2) + X(3) \left(\frac{Q_L}{Q_D} \right)_n \right]}{\gamma_D + \gamma_L \left(\frac{Q_L}{Q_D} \right)_n} \quad (5.28)$$

in which $X(2)$, $X(3)$ = actual-to-nominal dead and live load random variables,

$$\left(\frac{Q_L}{Q_D} \right)_n = \text{nominal ratio of live load } (Q_L) \text{ to dead load } (Q_D) ,$$

γ_D, γ_L = load factors for dead and live loads,

\bar{q} = mean value of q ;

$$V_{\phi q} = \frac{\left[\overline{X(2)} V_{Q_d} \right]^2 + \left[\overline{X(3)} \left(\frac{Q_L}{Q_d} \right) V_{Q_L} \right]^2 \right]^{1/2}}{\overline{X(2)} + \overline{X(3)} \left(\frac{Q_L}{Q_d} \right)} \quad (5.29)$$

in which V_{Q_d} and V_{Q_L} are COV of Q_d and Q_L , respectively, $\overline{X(2)}$ and $\overline{X(3)}$ are mean values of $X(2)$ and $X(3)$, respectively.

Solving for ϕ_b from Eq. 5.26 gives

$$\phi_b = \frac{\bar{r}}{\bar{q}} e^{-(V_r^2 + V_{\phi q}^2)^{1/2} \beta} \quad (5.30)$$

Resistance random variable

The resistance random variable, r , is obtained from Eq. 5.27, in which $X(1)$ is based on a comparison of test results with Eq. 5.18. The mean of $X(1)$, $\overline{X(1)}$, can be obtained from the analyses presented in Sections 5.2 and 5.3: $\overline{X(1)} = 1.0$ for bars both with and without confining transverse reinforcement. The coefficient of variation $V_{X(1)}$ is equal to the coefficient of variation associated with the predictive equation (or model) itself, V_m , which can be represented as (Darwin et al. 1995c)

$$V_m = \sqrt{V_{TP}^2 - V_{ls}^2 - V_{R_r}^2} \quad (5.31)$$

in which V_{TP} = COV obtained directly from the comparison of measured and predicted bond strengths; V_{ls} = COV representing uncertainties in the measured loads and differences in the actual material and geometric properties for the specimens

from values used to calculate the predicted strength; and $V_{R_r} = \text{COV}$ representing the uncertainty due to the unknown values of R_r for some members containing bars with confining transverse reinforcement. For reinforced concrete, $V_s \approx 0.07$ (Grant et al. 1978). V_{R_r} is zero for the members containing bars without confining transverse reinforcement and is 0.02 for the bars with confining transverse reinforcement (Darwin et al. 1995c). From Section 5.2, $V_{T/P} = 0.1043$ for bars without confining transverse reinforcement, resulting in $V_m = \sqrt{0.1043^2 - 0.07^2} = 0.077$. From Section 5.3, $V_{T/P} = 0.115$ for bars with confining transverse reinforcement, resulting in $V_m = \sqrt{0.115^2 - 0.07^2 - 0.02^2} = 0.089$.

The individual values of the predicted capacity random variable, R_p , are obtained for hypothetical beams using the Monte Carlo method. R_p can be determined using Eq. 5.18 in terms of $A_b f_s$

$$R_p = A_b f_s = f'_c^{1/4} \left\{ [59.8 l_d(c_{\min} + 0.5 d_b) + 2350 A_b] \left(0.1 \frac{c_{\max}}{c_{\min}} + 0.9 \right) + \left(31.14 t_r t_d \frac{N A_{tr}}{n} + 3.99 \right) f'_c^{1/2} \right\} \quad (5.32)$$

The nominal strength, R_n , is calculated using Eq. 5.22 and 5.23 with the specified concrete strength and the nominal dimensions of the member.

The expressions for the other variables included in R_n , such as concrete compressive strength, f'_c , the developed/spliced length, l_d , the member width, b , the cover, c_b , the side cover, c_{so} , and the relative rib area R_r , are exactly the same as those used by Darwin et al. (1995c). These expressions are not repeated here.

The mean values of r , \bar{r} , and COV of r , V_r , can be obtained using Monte Carlo simulations of a selected number of beams. The normal distribution function is used for all random variables.

Loading random variable

The term of q in Eq. 5.28 represents the loading random variable. It depends on random variables $X(2)$ and $X(3)$, load factors for dead and live load, γ_D and γ_L , and the nominal live load-to-dead load ratio, $(Q_L/Q_D)_n$. γ_D and γ_L are selected as 1.4 and 1.7 as used for ACI 318-95 and AASHTO 1996, and as 1.2 and 1.6 as used for ASCE 7-97. Values of $(Q_L/Q_D)_n$ of 0.5, 1.0, and 1.5 are selected for evaluating the reliability of reinforced concrete structures.

As with the study by Darwin et al. (1995c), $\beta = 3.5$ is selected to ensure that probability of a bond failure is lower than the probability of a failure in bending for beams or in combined bending and compression for columns. It produces a probability of failure equal to approximately 1/5 of that obtained with $\beta = 3.0$ [$\beta = 3.0$ for reinforced concrete beams and columns (Ellingwood et al. 1980)].

For reinforced concrete, $\overline{X(2)} = \bar{Q}_D / Q_{Dn} = 1.03$, $V_{Q_D} = 0.093$, $\overline{X(3)} = \bar{Q}_L / Q_{Ln} = 0.975$, and $V_{Q_L} = 0.25$ (Ellingwood et al. 1980 and Darwin et al. 1995c), in which \bar{Q}_D and \bar{Q}_L are the means of dead and live load random variables, respectively, Q_{Dn} and Q_{Ln} are the normal dead and live load random variables, and V_{Q_D} and V_{Q_L} are the COV's of the dead and live load random variables.

Monte Carlo simulation

Sixty-three beams in which the bars are not confined by transverse reinforcement and 252 beams (in 4 groups of 63 each) in which the bars are confined by transverse reinforcement are used for the simulations. The values of l_d for each beam is calculated using Eq. 5.23, with the right side multiplied by an assumed initial

value of 0.90 for ϕ_d and $f_s = 60$ ksi. Concrete strengths of 3000, 4000, 6000, 8000, 10,000, 12,000, 13,000, 14,000, 15,000, and 16,000 psi (21, 28, 41, 55, 70, 83, 90, 96, 103, and 110 MPa) are evaluated. The mean values of R_r , 0.0727 and 0.1275, are used for conventional and high R_r bars, respectively, (Darwin et al. 1995c). The data for the beams used in the analysis are given in Tables 5.17a and 5.17b for bars not confined and confined by transverse reinforcement, respectively.

One-thousand Monte Carlo simulations for each of the 63 beams without transverse reinforcement and 250 simulations for each of the 252 beams with transverse reinforcement are carried out, in which the predicted strengths are calculated using Eq. 5.18.

Strength reduction factor

The individual predicted strengths are used to calculate the mean and COV of r (\bar{r} and V_r). \bar{q} and $V_{\phi q}$ are calculated using Eq. 5.28 and Eq. 5.29 based on the selected load factors (γ_D and γ_L) and live load-to-dead load ratios $[(Q_L/Q_D)_n]$. ϕ_b is calculated using Eq. 5.30 and the value of $\phi_d = \phi/\phi_b$ is then obtained. The results of the analysis are presented in Table 5.18.

Load factors 1.4 and 1.7 - For Eq. 5.22 which is based on Eq. 5.20 (the more accurate of the two equations), ϕ_b equals 0.975, 0.941, and 0.907 for bars without confining transverse reinforcement at live-to-dead load ratios of 0.5, 1.0, and 1.5, respectively, and 0.976, 0.950, and 0.921 (for $R_r = 0.0727$) and 0.971, 0.944, and 0.914 (for $R_r = 0.1275$) for bars with confining transverse reinforcement.

For the more simplified expression, Eq. 5.23 based on Eq. 5.21, ϕ_b equals 0.945, 0.923, and 0.897 for bars without confining transverse reinforcement at live-to-dead load ratios of 0.5, 1.0, and 1.5, respectively, and 1.035, 1.012, and 0.985 (for

$R_r = 0.0727$) and 1.014, 0.990, and 0.962 (for $R_r = 0.1275$) for bars with confining transverse reinforcement.

Load factors 1.2 and 1.6 - The values of ϕ_d increase slightly for load factors of 1.2 and 1.6 compared to load factors of 1.4 and 1.7 (Note: $\phi_{bending}$ decreases to 0.8 from 0.9). The live-to-dead load ratio of 1.5 produces the lowest value of ϕ_d : using Eq. 5.22, ϕ_d equals to 0.930 for bars without confining transverse reinforcement and 0.944 (for $R_r = 0.0727$) and 0.937 (for $R_r = 0.1275$) for bars with confining transverse reinforcement. Using Eq. 5.23, the respective values are 0.920, 1.010, and 0.987.

Table 5.18 shows that the values of ϕ_d are greater for the bars with confining transverse reinforcement than those without confining transverse reinforcement. An increase in live-to-dead load ratio results in an decrease in ϕ_d factors, matching the observations of Darwin et al. (1995c). As with the results obtained by Darwin et al. (1995c), $\phi_d = 0.9$ is generally conservative and satisfactory for application with Eqs. 5.22 and 5.23 for both sets of load factors.

5.5.2 Design Expressions

Multiplying the right side of Eqs. 5.22 and 5.23 by $\phi_d = 0.90$, setting $f_s = f_y$, and solving for l_d/d_b gives, respectively,

$$\frac{l_d}{d_b} = \frac{\left[\frac{f_y}{f'_c} - 2100 \left(0.1 \frac{c_{\max}}{c_{\min}} + 0.9 \right) \right]}{68 \left(\frac{c + K_r}{d_b} \right)} \quad (5.33)$$

$$\frac{l_d}{d_b} = \frac{\frac{f_y}{f'_c^{1/4}} - 2100}{68 \left(\frac{c + K_{tr}}{d_b} \right)} \quad (5.34)$$

in which $l_d/d_b \geq 16$, $c = (c_{min} + 0.5 d_b) (0.1 c_{max}/c_{min} + 0.9)$ for Eq. 5.33 where $c_s = \min(c_{so}, c_{si} + 0.25 \text{ in.})$ and $c = (c_{min} + 0.5 d_b)$ for Eq. 5.34 where $c_s = \min(c_{so}, c_{si})$, $K_{tr} = (0.52 t_r t_d A_{tr}/sn) f'_c^{1/2}$ ≤ 4.0 , $c_{min} = \min(c_s, c_b)$, $c_{max} = \max(c_s, c_b)$, $t_r = 9.6 R_r + 0.28$, and $t_d = 0.78 d_b + 0.22$.

Eq. 5.33 is similar to the equation developed by Darwin et al. (1995b, 1996b) (Eq. 1.11 in Chapter 1), except that the constants in the denominator and numerator are slightly different (2100 versus 1900 and 68 versus 72, respectively) and that the definition of K_{tr} is different. In Eq. 1.11, the 1/4 power of f'_c is used to characterize the effect of concrete strength on T_s based on an analysis using a data base that included only a small number of specimens cast with high strength concrete, which is the same as the power used to normalize T_c , the concrete contribution to bond strength. Thus, K_{tr} in Eq. 1.11 is only a function of bar size, relative rib area, and confining transverse reinforcement. In Eq. 5.33, the 3/4 power of f'_c is used to characterize the effect of concrete strength on T_s based on the analysis of a larger data base, including more specimens cast with high strength concrete. Therefore, K_{tr} in Eq. 5.33 is not only a function of bar size, relative rib area, and confining transverse reinforcement, but also a function of $f'_c^{1/2}$.

5.6 Comparison to ACI 318-95 Design Criteria

The major differences between Eqs. 5.33 and 5.34 and the design criteria in ACI 318-95 are as follows.

- (1) Eqs. 5.33 and 5.34 are developed based on the data base containing 90% splice specimens and 10% development specimens. Therefore, using Eqs. 5.33 and 5.34 results in identical lengths for spliced and developed bars, removing the requirement to multiply development lengths, l_d , by 1.3 (ACI 318-95) to obtain splice lengths.
- (2) Development/splice length is a linear function of bar stress, f_s , or bar yield strength, f_y , in Eqs 5.33 and 5.34, but not proportional to f_s or f_y as it is in ACI 318-95.
- (3) The effect of concrete strength is represented by $f'_c^{1/4}$, instead of $f'_c^{1/2}$, for the developed/spliced bars without confining transverse reinforcement and by $f'_c^{3/4}$, instead of $f'_c^{1/2}$, for the contribution to bond strength provided by transverse reinforcement. The impact of these changes is greatest for high-strength concrete. Eqs. 5.33 and 5.34 can be applied for f'_c up to 16,000 psi (110 MPa). ACI 318-95 limits the value of $f'_c^{1/2}$ to 100 psi [$f'_c = 10,000$ psi (69.0 MPa)] due to a lack of data for high-strength concrete.
- (4) Eqs. 5.33 and 5.34 take into account the effect of R_r on development/splice strength for bars confined by transverse reinforcement, producing shorter development/splice lengths for high R_r bars. R_r is not considered in ACI 318-95.

For the purpose of comparisons, the 63 hypothetical beams with bars not confined by transverse reinforcement and the 252 beams with bars confined by transverse reinforcement used in Section 5.4.1 to determine the development/splice strength reduction factor, as well as the data base used to develop Eqs. 5.33 and 5.44, are used to study the economy of conventional and high R_r bars and the safety and economy of the design criteria (1) developed in this study and (2) in ACI 318-95.

Development/splice lengths are determined using Eqs. 5.33 and 5.34 and the "detailed" equation of ACI 318-95 (for development lengths, l_d , and 1.3 l_d for splice lengths) which is (for bottom-cast uncoated bars in normal weight concrete)

$$\frac{l_d}{d_b} = \frac{3}{40} \frac{f_y}{\sqrt{f'_c}} \frac{\gamma}{\left(\frac{c + K_{tr}}{d_b} \right)} \quad (5.35)$$

where l_d (l_s) \geq 12 in. (305 mm); $\sqrt{f'_c} \leq 100$ psi; $\gamma = 0.8$ for No. 6 and smaller bars and 1.0 for No. 7 and larger bars; $c = \min(c_b, c_{so}, c_{si}) + 0.5 d_b$; $K_{tr} = A_{tr} f_{yt}/1500sn$ and $(c + K_{tr})/d_b \leq 2.5$; f_{yt} = yield strength of transverse reinforcement; s = spacing of transverse reinforcement; and n = number of bars being developed along the plane of splitting.

5.6.1 Bars not Confined by Transverse Reinforcement

Table 5.19 gives the calculated development and splice lengths and the comparisons between Eqs. 5.33 and 5.34 and the ACI 318-95 design criteria for the 63 hypothetical beams with bars not confined by transverse reinforcement. The comparisons show that the ratios of development lengths obtained by Eq. 5.34 (the more simplified expression) to those obtained using ACI criteria range from 1.061 to 1.407 for normal-strength concrete [$f'_c < 8000$ psi (55 MPa)], with an average of 1.165, and from 0.994 to 1.275 for high-strength concrete, with an average of 1.119. The ratios of development lengths obtained by Eq. 5.33 to those obtained using ACI criteria range from 0.796 to 1.194 for normal-strength concrete, with an average of 1.037, and from 0.874 to 1.275 for high-strength concrete, with an average of 1.047. The ratios of splice lengths obtained by Eq. 5.34 to those obtained using ACI criteria are between 0.816 to 1.082 for normal-strength concrete, with an average of 0.896,

and between 0.764 and 0.980 for high-strength concrete, with an average of 0.861. The ratios of splice lengths obtained by Eq. 5.33 to those obtained using the ACI criteria are between 0.673 and 0.980 for normal-strength concrete, with an average of 0.806, and between 0.613 and 0.980 for high-strength concrete, with an average of 0.801. The comparisons indicate that Eqs. 5.33 and 5.34 result in an increase in development lengths and a decrease in splice lengths compared to the values obtained under the provision of ACI 318-95. The comparison results are similar to those obtained by Darwin et al. (1995b, 1996b).

Table 5.19 also compares development and splice lengths using different equations for different bar sizes. The development lengths calculated using Eq. 5.33 is, on average, 6% and 10% longer than that calculated using the ACI criteria for No. 6 and No. 8 bars, respectively, but 2% shorter for No. 11 bars. Eq. 5.34 produces 11% to 15% longer development lengths than the ACI criteria for all bar sizes. Eq. 5.33 produces 18% and 15% shorter splice lengths for No. 6 and No. 8 bars, respectively, and about 25% shorter splice lengths for No. 9 and No. 11 bars compared to the ACI criteria.

Table 5.20 and Figs. 5.24 through 5.26 compare test and predicted strengths using Eq. 5.33 and the ACI criteria for specimens in the data base with bars not confined by transverse reinforcement and $l_d \geq 12$ in. (305 mm) (137 specimens). Using the ACI criteria, the factor of 1.3 is not applied for the spliced bars. The comparisons show that Eq. 5.33 provides more accurate predictions than the ACI criteria. The average test/prediction ratios using Eq. 5.33 are 1.153, with a COV of 0.111, and 1.120, with an COV of 0.114 for No. 6 and smaller bars and No. 7 and larger bars, respectively (Note: there are no specimens with No. 7 bars in the data base), which are lower than those obtained using the ACI criteria, 1.219 with a COV

of 0.264 for No. 6 and smaller bars and 1.219 with a COV of 0.291 for No. 7 and larger bars, respectively.

The safety provided by Eq. 5.33 and the ACI criteria can be evaluated using the percentage of the specimens with test/prediction ratios less than 1.0. The higher the percentage is, the lower the safety margin. Fig. 5.24 compares the distributions of test/prediction ratios using Eq. 5.33 and the ACI criteria for the specimens in Table 5.20. Using Eq. 5.33, 9% of the specimens have test/prediction ratios less than 1.0, while using the ACI criteria, 18% of the specimens have test/prediction ratios less than 1.0. Figs. 5.25 and 5.26 show the distributions of the test/prediction ratios for the specimens with No. 7 and larger bars and with No. 6 and smaller bars, respectively. For the specimens containing No. 7 and larger bars, 10% of the specimens have test/prediction ratios less than 1.0 when using Eq. 5.33 versus 16% when using the ACI criteria. For the specimens containing No. 6 and smaller bars, the percentage decreases to 4% for Eq. 5.33, but increases to 32% for the ACI criteria due to a use of the 0.8 factor for No. 6 and smaller bars. The latter percentage is unreasonably high. Figs. 5.24 through 5.26 also show that the percentage of the specimens with test/prediction ratios higher than 1.2 is higher when using the ACI criteria than when using Eq. 5.33.

The comparisons indicate that, the new equations produce more accurate and more economic results than the ACI criteria. A 10% or 20% percent saving can be obtained for splice lengths using Eq. 5.34 or Eq. 5.33, compared to the ACI criteria. The safety margin for the ACI criteria is lower than that for Eq. 5.33. Especially, for No. 6 and smaller bars, the safety margin is much lower for using the ACI criteria than for using the new equations.

5.6.2 Bars Confined by Transverse Reinforcement

Comparison of high relative rib area bars with conventional bars

Table 5.21 compares the development and splice lengths calculated using Eq. 5.33, Eq. 5.34 and the ACI design criteria for the 252 hypothetical beams. The average ratios of l_d for high R_r bars to those for conventional bars are 0.862 and 0.835 using Eqs. 5.33 and 5.34, respectively, for normal-strength concrete and 0.958 and 0.900 for high-strength concrete. Similar to the observations by Darwin et al. (1995b, 1996b), average reductions of 14 and 16 percent in development and splice lengths can be expected, depending on which of the expressions is used, with the use of high R_r bars and normal-strength concrete. Using high-strength concrete, the reductions in development and splice lengths using high R_r bars decrease to 4 and 10 percent using Eq. 5.33 and 5.34, respectively, because of the requirement that l_d/d_b must be ≥ 16 . Table 5.21 shows that, of the 112 beams with high-strength concrete, development/splice lengths are limited to $16d_b$ for 69 and 83 beams using conventional and high R_r bars, respectively, by Eq. 5.33 and 40 and 68 beams by Eq. 5.34. This results in the same development/splice lengths for both conventional and high R_r bars.

Comparison with ACI 318-95

As shown in Table 5.21, based on Eqs. 5.33 and 5.34, development lengths for conventional bars in normal-strength concrete, average 97 and 126 percent, respectively, of those obtained using ACI 318-95, while splice lengths obtained with the two expressions average 74 and 97 percent, respectively, of those obtained using ACI 318-95; these percentages are reduced to 83 and 105 percent for development lengths and 64 and 81 percent for splice lengths if using high R_r bars.

Using Eqs. 5.33 and 5.34, development lengths for conventional bars in high-strength concrete average 87 and 100 percent, respectively, of those obtained with ACI 318-95, while the splice lengths average 67 and 77 percent, respectively, of the splice lengths obtained using ACI 318-95; these percentages are reduced to 83 and 90 percent for development lengths and 64 and 69 percent for splice lengths if using high R_r bars.

Table 5.21 shows that the ratios of development/splice lengths calculated using Eq. 5.33 or 5.34 to development/splice lengths calculated using the ACI criteria are greater for small bars (No. 6) than for larger bars (No. 8, No. 9 and No. 11). On average, the development lengths calculated using Eq. 5.33 are 4% longer than that using the ACI criteria for No. 6 conventional bars, but about 10% shorter for No. 8 and larger conventional bars. The development lengths calculated using Eq. 5.34 are 39% and 8% longer than those obtained using the ACI criteria for conventional No. 6 and No. 8 bars, respectively, and 2% longer for conventional No. 9 and No. 11 bars. For high R_r bars the ratio of l_d (l_s) calculated using Eq. 5.33 to that calculated using the ACI criteria decreases significantly from 0.956 (0.735) for No. 6 bars to 0.778, 0.800, and 0.774 (0.599, 0.615, and 0.595) for No. 8, No. 9, and No. 11 bars, respectively, and the ratio of l_d (l_s) calculated using Eq. 5.34 to that calculated using the ACI criteria decreases from 1.206 (0.928) for No. 6 bars to 0.929, 0.888, and 0.861 (0.715, 0.683, and 0.662) for No. 8, No. 9, and No. 11 bars, respectively. This comparison not only indicates that, for high R_r bars, the new equations produce shorter development/splice lengths than the ACI criteria, but also raises a question as to the safety of the ACI criteria and the new equations: for both conventional and high R_r bars, the ratios of l_d and l_s obtained using the new equations to those obtained using the ACI criteria are higher for small bars (No. 6) than for larger bars (No. 8,

No. 9, and No. 11). The safety of the new equations and the ACI criteria is discussed next.

Table 5.22 and Figs. 5.27 through 5.29 compare the test/prediction ratios obtained using Eq. 5.33 and the ACI criteria for the specimens from the data base containing bars confined by transverse reinforcement, with $l_d/d_b \geq 16$ and $l_d \geq 12$ in. (305 mm) (207 specimens). Table 5.22 shows that the average test/prediction ratio using Eq. 5.33 is greater for No. 6 and smaller bars (1.254, with a COV of 0.099) than for No. 7 and larger bars (1.153, with a COV of 0.143), while the average test/prediction ratio using the ACI criteria is smaller for No. 6 and smaller bars (1.010, with a COV of 0.207) than for No. 7 and larger bars (1.357, with a COV of 0.270). The comparisons indicate that Eq. 5.33 provide a more accurate prediction (smaller COV) than the ACI criteria. The difference between the test/prediction ratios for No. 6 and smaller bars and those for No. 7 and larger bars is smaller when using Eq. 5.33 than when using the ACI criteria. The average test/prediction ratio for No. 6 and smaller bars is much smaller than that for No. 7 and larger bars when using the ACI criteria.

Fig. 5.27 compares the distribution of the test/prediction ratios using Eq. 5.33 and the ACI criteria. Seven percent of the specimens have a test/prediction ratio less than 1.0 when using Eq. 5.33. The number of the specimens with test/prediction ratios less than 1.0 more than doubles to 16% when using the ACI criteria. Figs. 5.28 and 5.29 compare the distributions of the test/prediction ratios for No. 7 and larger bars and for No. 6 and smaller bars, respectively. Fig. 5.28 shows that 7% of the specimens containing No. 7 and larger bars have a test/prediction ratio less than 1.0 when using the ACI criteria, compared to 8% when using Eq. 5.33, indicating that, for No. 7 and larger bars confined by transverse reinforcement, the safety margins of

the ACI criteria and Eq. 5.33 are about the same. Fig. 5.29 shows that a whopping 56% of the specimens containing No. 6 and smaller bars have test/prediction ratios less than 1.0 when using the ACI criteria, compared to 2% when using Eq. 5.33. The ACI criteria are clearly unsafe for No. 6 and smaller bars. In practice, no failure has been observed for No. 6 and smaller developed/spliced bars because other safety factors are used in design. The fact is, however, that, compared to the other safety factors used in design, the safety margin provided by the ACI criteria for No. 6 and smaller bars is significantly lower than provided for No. 7 and larger bars.

Similar to the observations for bars without confining reinforcement, Fig. 5.28 shows that the number of the specimens containing No. 7 and larger bars with test/prediction ratios greater than 1.2 is 75% greater when using the ACI criteria than that when using Eq. 5.33. For obvious reasons, the same statement cannot be made for No. 6 and smaller bars.

The comparisons indicate, in general, that use of the new expressions could result in significant savings in development and splice lengths. More savings can be expected when using the new expressions in conjunction with high R_r bars. Compared with ACI 318-95, the new expressions provide greater savings with high-strength concrete than with normal-strength concrete. The new expressions also provide more accurate predictions than the ACI criteria. The ACI criteria are more conservative for No. 7 and larger bars than Eq. 5.33, and appear unsafe for No. 6 and smaller bars.

CHAPTER 6: SPLICE STRENGTH OF EPOXY-COATED HIGH RELATIVE RIB AREA REINFORCING BARS

6.1 General

Previous studies (Choi et al. 1991, 1992, Darwin et al. 1995a, 1996a, Tan et al. 1996) have demonstrated that the relative bond strength of epoxy-coated reinforcing bars increases as the relative rib area (R_r) increases and that the detrimental effect of epoxy coating is lower for high R_r bars than that for conventional bars. Based on an evaluation of 10 matched pairs of splice specimens containing bottom-cast epoxy-coated and uncoated high R_r bars, Darwin et al. (1995a, 1996a) obtained a C/U ratio (splice strength ratio of epoxy-coated bars to uncoated bars) of 0.88, compared to C/U ratio of 0.74, the average for conventional bars (Hester et al. 1991, 1993). In an extension of the study by Darwin et al. (1995a, 1996a), Tan et al. (1996) evaluated 20 matched pairs of splice specimens containing bottom-cast coated and uncoated high R_r bars, including 10 pairs reported by Darwin et al. (1995a, 1996a). They recommended that the development length modification factor of 1.5 used in ACI 318-95 and the 1996 AASHTO Bridge Specifications for epoxy-coated bars with a cover less than 3 bar diameters or a clear bar spacing less than 6 bar diameters be reduced to 1.2 for epoxy-coated high R_r bars. Tan et al. also observed that transverse reinforcement and total confinement provided by concrete cover and transverse reinforcement have no effect on the C/U ratio, matching earlier conclusions by Hester et al. (1991, 1993). The tests of high R_r bars by Darwin et al. (1995a, 1996a) and Tan et al. (1996) involved normal-strength concrete (NSC) for most of the specimens. Other than 3 pairs of specimens reported by Tan et al., no information exists for high R_r bars in high-strength concrete (HSC).

In this study, a total of 36 matched pairs of beam-splice specimens containing epoxy-coated and uncoated bars in both NSC and HSC were tested to evaluate the splice strength of epoxy-coated high R_r bars. In the 36 pairs, 30 containing only bottom-cast bars that failed with splitting of concrete are used for the evaluations [of these, 8 pairs were previously reported by Tan et al. (1996)]. The remaining 6 pairs are not included in the evaluations: 2 pairs previously reported by Tan et al. (1996) contained top-cast bars; 1 pair contained the 8N1 bars confined by stirrups (the 8N1 bars had a high rib width/spacing ratio that caused a reduction in splice strength, as described in Chapter 4); and the specimens containing uncoated bars in the other 3 pairs failed by crushing concrete at the compression face or did not fail due to limited capacity of the loading system. In addition to the 30 pairs of specimens, test results for 7 matched pairs of splice tests by Choi et al. (1990, 1991), 15 matched pairs of splice tests by Hester et al. (1991, 1993), and 10 matched pairs of splice tests by Darwin et al. (1995a, 1996a) are used for the overall evaluation. The specimens and test procedures used in the previous studies (Choi et al. 1990, 1991, Hester et al. 1991, 1993, Darwin et al. 1995a, 1996a) were similar to those in the current study. The test results of Darwin et al. (1995a, 1995b), Hester et al. (1991, 1993), and Choi et al. (1990, 1991) are included in Tables 4.1, 4.2, and 4.3, respectively. The current test results are included in Table 2.1.

Combining the test results of the current and previous studies provides 29 matched pairs of the specimens containing conventional bars and 33 matched pairs containing high R_r bars. The R_r values range from 0.060 to 0.086 for conventional bars and from 0.101 to 0.141 for high R_r bars. Thirty five pairs contained normal-strength concrete, with f'_c between 4000 and 6500 psi (27.6 and 44.8 MPa) and 27

pairs contained high-strength concrete, with f'_c between 8000 and 16,000 psi (55.2 and 110 MPa).

The C/U ratios for high R_r bars are compared to those for conventional bars. The effects of concrete properties (compressive strength and type of coarse aggregate) on the relative splice strength of epoxy-coated bars are evaluated. Development/splice length modification factors are obtained for epoxy-coated high R_r bars in normal and high strength concrete.

6.2 Splice Strength Ratio, C/U

To eliminate the effects of minor differences in concrete cover and bar clear spacing between the two matched specimens, the splice strength ratio of coated (C) to uncoated (U) bars for each matched pair of specimens is normalized with respect to Eq. 5.4 or 5.18 for uncoated bar splices not confined or confined by transverse reinforcement, respectively. Therefore, the normalized splice strength ratio of coated to uncoated bars, C/U, is obtained by dividing the experimental stress ratio of coated to uncoated bars by the predicted stress ratio using Eq. 5.4 or 5.18.

As described in Chapter 5, Eqs. 5.4 and 5.18 were developed to predict the development/splice strength for the bottom-cast uncoated bars, based on the statistical analyses of 171 development and splice specimens in which the bars were not confined by transverse reinforcement and 245 specimens in which the bars were confined by transverse reinforcement. Concrete compressive strengths for the specimens ranged between 2500 and 16,000 psi (17.2 and 110.3 MPa). Eqs. 5.4 and 5.18 take into account the effects of concrete strength, concrete cover, bar clear spacing, development/splice length, transverse reinforcement, bar size, and relative rib area of bars.

Tables 6.1 and 6.2 present the C/U ratios for high R_r and conventional bars, respectively. As shown in Table 6.1, the C/U ratios for high R_r bars range from 0.787 to 1.074, with an average of 0.889, for normal-strength concrete [f'_c less than 8000 psi (55.2 MPa); Note: the maximum compressive strength in this group was actually 5250 psi (36.2 MPa)], from 0.793 to 0.979, with an average of 0.889, for f'_c between 8000 and 10,000 psi (55.2 to 69.0 MPa), and from 0.683 to 0.902, with an average of 0.796, for f'_c greater than 10,000 psi (69.0 MPa). The overall average C/U ratio for high R_r bars is 0.843. The average C/U ratios for f'_c less than 8000 psi (55.2 MPa) and between 8000 psi (55.2 MPa) and 10,000 psi (69.0 MPa) are the same and only slightly higher than the average C/U ratios obtained by Darwin et al. (1995a, 1996a) and Tan et al. (1996). The average C/U ratio for high R_r bars in concrete with f'_c greater than 10000 psi (69.0 MPa) is about 10% lower than the C/U ratios for lower strength concrete.

Table 6.2 shows that the C/U ratios for conventional bars are between 0.611 and 0.941, with an average of 0.759, for normal-strength concrete [maximum compressive strength was 6450 psi (44.5 MPa)] and between 0.668 and 0.893, with an average of 0.776, for f'_c greater than 10,000 psi (69.0 MPa) [there were no matched specimens with f'_c between 8000 and 10,000 psi (55.2 and 69.0 MPa)]. The average C/U ratios for f'_c less than 8000 psi (55.2 MPa) and greater than 10,000 psi (69.0 MPa) are very close and result in an overall C/U ratio of 0.763 for the evaluated range of f'_c [4000-16,000 psi (27.6-110.3 MPa)]. This C/U value is slightly higher than the overall average C/U ratio of 0.74 obtained by Hester et al. (1991, 1993) using a data base including 113 splice tests.

The comparison between high R_r and conventional bars shows that for concrete compressive strength less 10,000 psi, the average C/U ratio of high R_r bars

(0.889) contrasts sharply with the average C/U ratio of 0.74 for conventional bars obtained by Hester et al. (1991, 1993) and the average C/U ratio of 0.66 for the 21 beam splices tests (Treece and Jirsa 1987, 1989) used to establish the current development length modification factors for epoxy-coated bars (ACI 318-95, ASSHTO 1996). For concrete with $f'_c > 10,000$ psi (69.0 MPa), the average C/U ratio for high R_r bars decreases from 0.889 to 0.796, but is still higher than the C/U ratio for conventional bars (7% higher compared to 0.74). The comparisons indicate that coated high R_r bars require shorter development and splice lengths than conventional bars when using normal-strength concrete. The advantage of coated high R_r bars is reduced when using high-strength concrete.

6.3 Effect of Concrete Properties

6.3.1 Type of Coarse Aggregate

Table 6.3 compares normalized C/U ratios for No. 8 conventional bars in HSC, No. 8 high R_r bars in NSC and No. 11 high R_r bar in HSC. Limestone and basalt were used as coarse aggregates. The test results for the 18 matched pairs of specimens show a consistent tendency for the concrete containing basalt coarse aggregate to provide higher C/U ratios than the concrete containing limestone aggregate. The average difference in C/U is 6%.

This observation indicates that a harder coarse aggregate may improve the relative bond strength of epoxy-coated bars. The limited number of tests contributing to the observation, however, indicate that more work is needed before this conclusion can be firmly established.

6.3.2 Concrete Strength

In the previous section, the observation was made that the C/U ratio of high R_r bars is lower for high-strength concrete than that for normal-strength concrete. In Fig. 6.1, the values of C/U for different values of R_r are plotted versus concrete compressive strength, f'_c . The data include No. 8 conventional bars ($R_r = 0.06$ - 0.086 with average of 0.071) and No. 8 and No. 11 high R_r bars [8C1 ($R_r = 0.101$), 8N3 ($R_r = 0.119$), and 11F3 ($R_r = 0.127$)]. Concrete compressive strength ranges from 4090 to 15,650 psi (28.2 to 107.9 MPa). No. 11 conventional bars ($R_r = 0.071$) and No. 5 and No. 6 bars are not included in Fig. 6.1 due to insufficient tests using high-strength concrete. The figure shows that the slopes of the best-fit lines are negative for all high R_r bars plotted, but positive for No. 8 conventional bars. For the range of concrete strengths studied, the slopes of the best-fit lines decrease (become more negative) as R_r increases. The best-fit lines indicate that as concrete compressive strength increases from 4000 to 16,000 psi (27.6 to 110.3 MPa), C/U decreases from 0.809 to 0.779 for 8C1 bars, from 0.899 to 0.809 for 8N3 bars, and from 0.869 to 0.765 for 11F3 bars, while increasing from 0.746 to 0.776 for No. 8 conventional bars.

Fig. 6.2 shows the general trends of C/U versus f'_c for all matched pairs of specimens. The dashed line represents the best-fit line for all conventional bars and the continuous line represents all high R_r bars, showing the same tendencies as exhibited in Fig. 6.1. Fig. 6.2 also shows that there seems to be a sharp reduction in C/U for high R_r bars once f'_c exceeds 10,000 psi (69 MPa).

6.4 Effect of Relative Rib Area

The effect of relative rib area on relative splice strength, C/U, is illustrated in Figs. 6.3 and 6.4 for the splices in normal-strength and high-strength concrete,

respectively. In the figures, dummy variable regression is applied based on bar size, producing slopes of the best-fit lines of 2.37 for normal-strength concrete and 1.47 for high-strength concrete. For normal-strength concrete, C/U increases by 0.17 as R_r increases from 0.07 to 0.14. For high-strength concrete, C/U increases by 0.10 as R_r increases from 0.07 to 0.14, indicating a reduction in the benefit of high R_r bars on the relative splice strength for the coated bars in high-strength concrete.

6.5 Flexural Cracking

Table 6.4 provides comparisons of maximum flexural crack widths, flexural crack densities (number of cracks per foot), and sums of crack widths at the beam centerline in the constant moment region outside of the splice region at a bar stress of 40 ksi for matched pairs of specimens containing epoxy-coated and uncoated bars. Table 6.4 shows that, at a bar stress of 40 ksi, the beams with epoxy-coated bars had larger crack widths and lower crack densities than the beams with uncoated bars, while the sum of crack widths at the centerline of the beams are the same for the beams containing coated and uncoated bars. C/U ratios for maximum crack width, crack density, and sum of crack widths range from 1.158 to 1.579 with an average of 1.390, from 0.435 to 1.000 with an average of 0.766, and from 0.624 to 1.254 with an average of 1.023, respectively. Table 6.4 also shows that there is no significant difference in the ratios of crack density and maximum crack width between the beams with high R_r bars (1.367 and 0.767) and the beams with conventional bars (1.436 and 0.748). Since the sums of crack widths for only one pair of specimens containing conventional bars were recorded, no comparison of the sum of crack widths can be made between coated high R_r and conventional bars. Observations made at bar stresses of 20 and 30 ksi (see Table C.1 and C.2) are similar to those made at 40 ksi,

except that at a bar stress of 20 ksi, the sum of crack widths is slightly greater (averaging 8% higher) for uncoated bars than for coated bars.

6.6 Development Length Modification Factor for High R_r Bars

The development and splice length of bottom-cast uncoated bars can be determined using Eq. 5.19, repeated here as

$$l_d = \frac{A_b \left[\frac{f_s}{f'_c} - 2350 \left(0.1 \frac{c_{\max}}{c_{\min}} + 0.9 \right) \right]}{59.8 \left[(c_{\min} + 0.5d_b) \left(0.1 \frac{c_{\max}}{c_{\min}} + 0.9 \right) + \frac{0.52t_r t_d A_u f_c^{1/2}}{sn} \right]} \quad (6.1)$$

For epoxy-coated bars, Eq. 6.1 becomes

$$l_{d,epoxy} = \frac{A_b \left[\frac{f_s}{f'_c} - 2350 \left(0.1 \frac{c_{\max}}{c_{\min}} + 0.9 \right) \right]}{59.8 \left[(c_{\min} + 0.5d_b) \left(0.1 \frac{c_{\max}}{c_{\min}} + 0.9 \right) + \frac{0.52t_r t_d A_u f_c^{1/2}}{sn} \right]} \quad (6.2)$$

A development length modification factor for epoxy-coated bars can be obtained by dividing Eq. 6.2 by Eq. 6.1 and assuming $c_{\max} = c_{\min}$

$$MF = \frac{l_{d,epoxy}}{l_d} = \frac{\frac{f_s}{f'_c} - 2350}{\frac{f_s}{f'_c} - 2350} \quad (6.3)$$

For grade 60 steel, concrete compressive strengths ranging from 4000 to 10,000 psi (27.6 to 69.0 MPa), and using $C/U = 0.889$ (average value for high R_t bars, see Table 6.1), Eq. 6.3 yields modification factors between 1.14 and 1.18. For concrete compressive strengths ranging from 10,000 to 16,000 psi (69.0 to 110.3 MPa) and using $C/U = 0.796$ (average value, Table 6.1), Eq. 6.3 yields modification factors between 1.42 and 1.46. Therefore, as recommended by Darwin et al. (1995a, 1996a) and Tan et al. (1996), the modification factor can be conservatively reduced from 1.5 (the value used by ACI 318-95 and AASHTO 1996) to 1.2 for epoxy-coated high R_t bars in the concrete with f'_c less than 10,000 psi (69.0 MPa). For f'_c between 10,000 and 16,000 psi (69.0 and 110.3 MPa), the modification factor for the epoxy-coated high R_t bars should remain 1.5, as for epoxy-coated conventional bars.

CHAPTER 7: REVERSED CYCLIC LOADING TESTS

7.1 General

Reversed cyclic loading can produce severe deterioration of bond stiffness (Ciampi et al. 1982, Balazs and Koch 1991, ACI Committee 408 1992). Earlier studies have demonstrated that the behavior of beam-column joints plays an important role in the ability of reinforced concrete frames to resist earthquake forces (Meinheit and Jirsa 1977, Briss et al. 1978, Ehsani 1982, Durrani and Wight 1982, Leon 1989). The slip of beam and column bars through the joints is one of the main reasons for loosing stiffness in frames (Durrani and Wight 1982, Zhu and Jirsa 1983). To reduce the slip, a ratio of bar diameter to column dimension of approximately 1/25 for Grade 40 steel or 1/35 for Grade 60 steel is necessary (Ciampi et al. 1982), which would result in a very large joints. Based on an evaluation of available test results by Zhu and Jirsa (1983), ratios of bar diameter to column dimension of 1/20 for normal weight concrete and 1/26 for lightweight concrete were chosen for buildings subject to seismic loading (ACI 318-95).

Darwin and Graham (1993a, 1993b) used beam-end specimens to evaluate the bond strength of machined bars with different relative rib areas (R_r) under monotonic loading. They observed that the initial stiffness of the load-slip curves increases with an increase in relative rib area. Thus, it can be reasoned that the bond behavior of bars under cyclic loading should improve as the relative rib area increases.

This chapter presents the tests and evaluation of specimens used to study the bond behavior of high R_r bars under reversed cyclic loading. The behavior of high R_r bars is compared to that of conventional bars.

7.2 Test Specimens

Six high R_r and six conventional No. 8 (25 mm) reinforcing bars (2 dummy and 10 test bars) were embedded in two concrete specimens (Fig 7.1). The concrete specimens were 16 ft long, 16 in. (406 mm) high and 12 in. (305 mm) wide. The bars were embedded horizontally through the middle of the specimens, at a spacing of 2.5 ft (762 mm). The bars had bonded lengths of 10 in. (254 mm). Two No. 5 longitudinal bars were placed at the bottom and the top of the specimens to provide flexural strength for moving the specimens. No transverse reinforcement was used.

7.3 Materials

7.3.1 Reinforcing Steel

All bars met the requirements of ASTM A 615, except that the high R_r bars had no bar markings. The high R_r bars, designated 8N3, have a relative rib area of 0.119 and a yield strength of 80.57 ksi (555.5 MPa). The conventional bars, designated 8C0A, have a relative rib area of 0.085 and a yield strength of 69.50 ksi (479.2 MPa). Yield strengths were determined from tests of three samples of each bar. Bar properties are given in Table 7.1.

7.3.2 Concrete

Air-entrained concrete was supplied by a local ready-mix plant. The concrete contained Type I portland cement, 3/4 in. (19 mm) maximum size crushed limestone coarse aggregate, and Kansas River sand. The water/cement ratio was 0.44. The concrete compressive strength was 5170 psi (35.6 MPa) at the time of testing. The test ages were 20 days for test bars 3 through 6 and 21 days for test bars 7 through 12.

Bars 1 and 2 (as dummy bars) were tested at the ages of 18 and 19 days. Concrete properties are given in Table 7.2.

7.4 Concrete Placement and Curing

The formwork for the specimens was the same as described in Section 2.4. The test bars were placed through the forms horizontally. Polyvinyl chloride (PVC) pipes were placed on both sides of the forms for each bar as bond breakers to produce a 10 in. (254 mm) bonded length and to prevent a cone type failure at the concrete surfaces.

The two specimens were cast from one batch of concrete. The concrete was placed from one end of a specimen to the other end in two lifts. Each lift was vibrated using a 1.5 in. (38 mm) square vibrator.

The specimens were cured in the forms and covered with wet burlap and plastic sheets for 7 days before the forms were removed. After the forms were removed, the specimens were left to dry until the time of testing. Standard 6 × 12 in. (152 × 304 mm) test cylinders were cast in steel molds and cured in the same manner as the test specimens.

7.5 Test Procedures

The test setup is shown in Fig. 7.2. Load was applied to a bar by two 60 ton jacks on opposite sides of the specimen. Loads were transferred to the specimen through reaction frames. The frames had two supports spaced with a clear distance of 24 in. (607 mm), so that compressive struts originating at the loading apparatus would not intersect the test region. As shown in Fig. 7.2, a 0.5 in. (13 mm) gap between the jack and the anchor plate insured that when the load was applied to one

side of the specimen, no load was applied to the other side of the specimen. Five reversed cycles with peak loads of 10, 15, and 20 kips (44.5, 66.7, 89.0 kN) were applied at a rate of about 5 kips (22.2 kN) per minute.

Bar slips were measured using two spring-loaded linear variable differential transformers (LVDTs) on each side of the specimen. LVDTs were attached to the bars and bore against the faces of the concrete specimen. Loads were measured using load cells that were placed between the reaction frames and the jacks. Readings from the load cells and LVDTs were acquired using a Hewlett-Packard data acquisition system connected to a computer. Tests on bars 3 through 12 were completed within 36 hours. Bars 1 and 2 were used to evaluate the test apparatus and loading procedure. Three 6 x 12 in. (152 x 304 mm) concrete cylinders were tested at the end of each day's tests. The reported concrete strength represents the average of the six tests (note: the average of the three cylinders tested on day 20 was 5140 psi (35.4 MPa) and the average of the three cylinders tested on day 21 was 5200 psi (35.9 MPa)).

7.6 Test Results and Evaluation

The loaded and unloaded end slips for each test bar at the peak loads [10, 15 and 20 kips (44.5, 66.7, 89.0 kN)] are summarized in Table 7.3, except for bar 12 which was overloaded [20 kips (89 kN)] during cycle 3, resulting in a flexural crack at the bar and an unusually high value of slip. The elastic deformation of the bars at the loaded end between the bonded length and the LVDT has been subtracted from the recorded values to give the best estimate of the actual slips. The reported slips are based on the average readings from the two LVDTs.

The load-slip curves for the bars are shown in Fig. 7.3a to 7.3r. In the curves, the slips of a bar on one side of the specimen are plotted in one figure, including the loaded-end slips corresponding to the loading on one side of the specimen and the unloaded-end slips corresponding to the loading on the other side, because these slips were measured by the same LVDTs. Slip in the direction from the right to the left side of the specimen is defined as "positive" slip, while slip in the opposite direction is defined as "negative" slip. Loading on the bars on the left side of the specimen is defined as "positive" loading, while loading on the right side is defined as "negative" loading. As expected, the unloaded end slips are smaller than the loaded end slips, and the load-unloaded end slip curves are initially much steeper than the load-loaded end slip curves. The curves show that bond stiffness decreases and slip increases as the number of loading cycles increases. The magnitude of the slip increase is much higher at the higher load levels [15 and 20 kips (66.7 and 89.0 kN)] than that at the lowest load level [10 kips (44.5 kN)]. These observations indicate a deterioration of bond under reversed cyclic loading. The load-slip curves exhibit pinching near zero load. This phenomenon is mainly due to an rigid body movement of the bars, as explained by Eligehausen et al. (1983). As the load increases and cycling progresses, the concrete in the front of bar ribs crushes and shears. When the load is reversed, large slip occurs before the bar bears against the concrete and bond stress again increases, causing a rigid body movement of the bars.

The average loaded end and unloaded end slips at each peak load are summarized in Table 7.4 for high R_t and conventional bars (averages for 4 high R_t bars and for 5 conventional bars). The comparisons show that the maximum loaded and unloaded end slips at peak loads for high R_t bars are consistently smaller than those for conventional bars. The loaded end slip of high R_t bars averages 60 to 70

percent of the slip of the conventional bars at all three load levels [10, 15, and 20 kips (44.5, 66.7 and 89.0 kN)]. The unloaded end slip of high R_r bars averages 30 percent, 40 percent, and 50 percent of the slip of the conventional bars at the peak loads of 10, 15, and 20 kips (44.5, 66.7, 89.0 kN), respectively.

In Figs. 7.4 and 7.5, the average slips of high R_r and conventional bars at each peak load are plotted as a function of the number of loading cycles. Fig. 7.4 shows the loaded end slips on the left side and unloaded end slips on the right side of the specimens under the loads applied on the bars on the left side of the specimens (left loading case, see Fig. 7.2). Fig. 7.5 shows the loaded end slip on the right side and the unloaded end slips on the left side of the specimens for the right side loading case. The loads corresponding to unloaded end slips are multiplied by -1 for easier comparison. Figs. 7.4 and 7.5 show that the loaded and unloaded end slips increase as the peak load and number of load cycles increase for both high R_r and conventional bars and that the slips are greater for conventional bars than for high R_r bars. At the lowest peak load [10 kips (44.8 kN)], the increase in slip with an increase in loading cycle is about the same for high R_r and conventional bars [about 0.0002 in. (0.005 mm) increase in loaded end slip as the number of cycles increases from 1 to 5]. However, at higher peak loads [15 and 20 kips (66.7 and 89.0 kN)], like the total slips, the increases in slip with an increase in loading cycle are lower for high R_r bars than for conventional bars. At a peak load of 15 kips (66.7 kN), with an increase in loading cycle from 6 to 10, the average increase in (left and right side) loaded end slip for high R_r bars is only 55 percent of that for conventional bars. At a peak load of 20 kips (89.0 kN), with an increase in loading cycle from 11 to 15, the ratio of incremental slips for high R_r bars to those for conventional bars increases to 70 percent.

The comparisons in Table 7.4 and Figs. 7.4 and 7.5 demonstrate that the slip of high R_r bars is significantly smaller than the slip of conventional bars under reversed cyclic loading and that high R_r bars exhibit less bond deterioration under reversed cyclic loading than conventional bars. Therefore, it can be expected that reinforced concrete members and frame joints that are affected by bond deterioration under seismic loading will exhibit better performance if reinforced with high R_r bars than if reinforced with conventional bars.

CHAPTER 8: SUMMARY AND CONCLUSIONS

8.1 Summary

The bond strengths of uncoated and epoxy-coated high relative rib area (R_r) and conventional bars are studied. Development and splice design criteria are developed using a large data base. The effect of deformation pattern on bond behavior under reversed cyclic loading is investigated.

One hundred and forty beam-splice specimens are used to investigate the effects of deformation properties, bar placement and arrangement, concrete properties, and epoxy coating on development/splice strength. For analysis, test results from this study are combined with results from the previous studies [15 tests by Choi et al. (1990, 1991), 32 tests by Hester et al. (1991, 1993), and 83 tests by Darwin et al. (1995a, 1996a)]. Relative rib areas range from 0.065 to 0.141. Six series of concrete mixes with compressive strengths ranging from 3400 to 15,400 psi (23.4 to 106.2 MPa), quantities of coarse aggregate ranging from 1586 to 1908 lb/yd³ (914 to 1132 kg/m³), and two types of coarse aggregate (limestone and basalt) are used to study the effects of concrete properties on bond strength. Limitations on the ratio of bar rib width to rib spacing for high R_r bars are obtained from the current test results.

Development/splice design equations are developed based on a data base of 488 bottom-cast development/splice specimens, including 245 specimens containing uncoated bars confined by transverse reinforcement, 171 specimens containing uncoated bars not confined by transverse reinforcement, and 62 specimens containing epoxy-coated bars. The design equations account for the effects of bar size, relative rib area, confinement provided by transverse reinforcement, epoxy-coating, and

concrete strength. A reliability-based development/splice strength reduction (ϕ) factor, obtained using LRFD concepts and Monte Carlo techniques, is incorporated in the design expressions.

Specimens containing No. 8 (25 mm) conventional and high R_t bars are used to study the bond behavior of the bars under reversed cyclic loading.

8.2 Observations and Conclusions

The following observations and conclusions are obtained based on the results and analyses presented in this report.

8.2.1 Effects of Bar Placement and Arrangement

1. The "top-bar effect" of high relative rib area bars is similar to that of conventional bars.
2. No significant difference exists between symmetrically and unsymmetrically placed splices. The average clear spacing between developed/spliced bars across a section should replace the minimum clear spacing for use in design.
3. For specimens with two-layers of bars, the bond strength of the specimen containing two layers of spliced bars is similar to that of the specimen containing one layer of spliced bars and one layer of continuous bars. More study is needed to understand the effect of multiple layers of bars on development/splice strength.
4. Bars spliced in a region of varying moment have a higher bond strength than those spliced in a constant moment region.

8.2.2 Effect of Concrete Properties

1. The type of coarse aggregate in concrete has a significant effect on splice strength under all conditions of confinement. Concrete with stronger coarse aggregate provides higher splice strength.
2. For specimens with uncoated bars confined by transverse reinforcement, the quantity of coarse aggregate in concrete has a measurable effect on bond strength. For the range of coarse aggregate content investigated in this study [1586 to 1908 lb/yd³ (914 to 1132 kg/m³)], the concrete with higher coarse aggregate content produced the greater contribution to splice strength due to the presence of transverse reinforcement.
3. For specimens containing spliced bars not confined by transverse reinforcement, the compressive strength, f'_c , to the 1/4 power best characterizes the effect of concrete strength on splice strength. $f'_c^{3/4}$ successfully characterizes the effect of concrete strength on the splice strength provided by transverse reinforcement.

8.2.3 Effects of Bar Properties

1. The splice strength of uncoated bars not confined by transverse reinforcement is not affected by relative rib area of the bars. The splice strength of bars confined by transverse reinforcement increases with an increase in relative rib area.
2. Splice strength increases with an increase in bar diameter.
3. A reduction in splice strength will occur if the ratio of rib width to rib spacing is too high. Limitations on the ratio of rib width to rib spacing of 0.36 at 1/2 rib height and/or 0.31 at 3/4 rib height are suggested for high R_r bars.

4. The maximum flexural crack width and crack density are similar in beams with high R_r and conventional bars. The total width of flexural cracks is slightly smaller in beams with high R_r bars than in beams with conventional bars.

8.2.4 New Design Expressions

1. Eqs. 5.18 through 5.20 accurately represent the development/splice strength for bottom-cast uncoated bars. The equations include the effects of concrete strength, relative rib area, bar size, and confinement provided by both concrete and transverse reinforcement.
2. With the incorporation of a reliability-based strength reduction (ϕ) factor, the new design expressions are identical for development and splice length, removing the requirement to multiply development lengths, l_d , by 1.3 (ACI 318-95) to obtain splice lengths.
3. The use of high R_r bars, with an average R_r of 0.1275, confined by transverse reinforcement can provide a 14 to 17 percent decrease in development/splice length for normal-strength concrete and a 5 to 10 percent decrease for high-strength concrete when compared to conventional bars, depending on which equation is selected (Eq. 5.33 or Eq. 5.34). The lower savings for high-strength concrete are due to limitations on minimum development/splice lengths, not lower efficiency in bond.
4. Compared to the design criteria in ACI 318-95:
 - (a) For bars not confined by transverse reinforcement, the new design expressions (Eq. 5.33 or Eq. 5.34) provide, on average, an increase (5 or 14%, depending on the expression selected) in development length, but a substantial

decrease (20 or 12%) in splice length. The increase is higher and the decrease is smaller for small bars than for larger bars.

- (b) For conventional bars confined by transverse reinforcement, depending on the expression selected (Eq. 5.33 or Eq. 5.34), development lengths average 3 percent lower to 26 percent higher for bars cast in normal-strength concrete and average up to 13 percent lower for bars cast in high-strength concrete. However, splice lengths average 3 to 25 percent lower for bars cast in normal-strength concrete and 23 to 33 percent lower for bars cast in high-strength concrete. As for bars not confined by transverse reinforcement, the increase in development length is smaller and the decrease in development/splice length is greater for small bars than for larger bars.
- (c) For high R_r bars confined by transverse reinforcement, a greater saving is obtained. Using the new expressions, the development lengths of high R_r bars average up to 36 percent lower than the development lengths of conventional bars calculated using ACI 318-95 for both normal-strength and high-strength concretes.
5. The safety margins provided by the new design expressions are higher than those provided by the design criteria in ACI 318-95. ACI 318-95 appears to be unsafe for No. 6 and smaller developed bars.

8.2.5 Effect of Epoxy Coating

1. Epoxy-coated high R_r bars provide higher splice strengths than epoxy-coated conventional bars. Under all conditions of confinement, development/splice lengths of coated high R_r bars cast in normal-strength concrete average 20 percent shorter than those of conventional coated bars.

2. The relative splice strength of epoxy-coated high R_r bars cast in normal-strength concrete is higher than that of the bars cast in high-strength concrete. There is a sharp reduction in relative splice strength once concrete compressive strength exceeds 10,000 psi (69 MPa).
3. A development/splice length modification factor of 1.2 is suggested for use with high R_r bars cast in concrete with $f'_c \leq 10,000$ (69 MPa). For coated high R_r bars cast in concrete with $f'_c > 10,000$ (69 MPa), the same development/splice length modification factor conventionally used for conventional bars (1.5) should be used.

8.2.6 Reversed Cyclic Loading Tests

High R_r bars exhibit lower slips and less deterioration of bond under reversed cyclic loading than conventional bars.

8.3 Suggestions for Further Study

A principal goal of the current and earlier studies at the University of Kansas (Darwin and Graham 1993a, 1993b, Brown et al. 1993, Darwin et al. 1995a, 1995b, Darwin et al. 1995d, 1996b, Darwin et al. 1995c, Idun and Darwin 1995, Tan et al. 1996, Tholen and Darwin 1996) has been to better understand the bond behavior of reinforcing bars. While many aspects of the bond performance of both conventional and high relative rib area bars have been addressed, further studies are needed in the following areas.

1. Bond performance of multiple layer developed/splice bars.
2. Bond strength of conventional and high relative rib area bars cast in high-strength concrete.

3. Effect of rib width on bond strength and limitations of rib width/spacing for high relative rib area bars.
4. Bond performance of epoxy-coated high relative rib area bars in high strength concrete.
5. Effect of bar rib face angle on bond strength of epoxy-coated bars.
6. Fatigue behavior of high relative rib area bars.
7. Finite element analysis of spliced reinforcing bars.
8. Development of a rational rather than empirical design procedure for development/splice length.

REFERENCES

- AASHTO Highway Sub-Committee on Bridges and Structures. (1989). *Standard Specifications for Highway Bridges*, 14th Edition, American Association of State Highway and Transportation Officials, Washington, DC.
- AASHTO Highway Sub-Committee on Bridges and Structures. (1992). *Standard Specifications for Highway Bridges*, 15th Edition, American Association of State Highway and Transportation Officials, Washington, DC.
- AASHTO Highway Sub-Committee on Bridges and Structures. (1996). *Standard Specifications for Highway Bridges*, 15th Edition, American Association of State Highway and Transportation Officials, Washington, DC.
- Abrams, D. A. (1913). "Tests of Bond Between Concrete and Steel," *Bulletin No. 71*, Engineering Experiment Station, University of Illinois, Urbana, IL, Dec., 238 pp.
- ACI Committee 318. (1951). *Building Code Requirements for Reinforced Concrete (ACI 318-51)*, American Concrete Institute, Detroit, MI.
- ACI Committee 318. (1963). *Building Code Requirements for Reinforced Concrete (ACI 318-63)*, American Concrete Institute, Detroit, MI, 144 pp.
- ACI Committee 318. (1971). *Building Code Requirements for Reinforced Concrete (ACI 318-71)*, American Concrete Institute, Detroit, MI.
- ACI Committee 318. (1977). *Building Code Requirements for Reinforced Concrete (ACI 318-77)*, American Concrete Institute, Detroit, MI.
- ACI Committee 318. (1983). *Building Code Requirements for Reinforced Concrete (ACI 318-83)*, American Concrete Institute, Detroit, MI.
- ACI Committee 318. (1989). *Building Code Requirements for Reinforced Concrete (ACI 318-89) and Commentary - ACI 318R-89*, American Concrete Institute, Detroit, MI, 353 pp.
- ACI Committee 318. (1995). *Building Code Requirements for Structural Concrete (ACI 318-95) and Commentary (ACI 318R-95)*, American Concrete Institute, Farmington Hills, MI, 369 pp.
- ACI Committee 408. (1990). *Suggested Development, Splice, and Standard Hook Provisions for Deformed Bars in Tension (ACI 408.R-90)*, American Concrete Institute, Detroit, MI, 3 pp.
- ACI Committee 408. (1992). "Bond Under Cyclic Loading," *State-of-the-Art Report (ACI 408.2R-92)*, American Concrete Institute, Detroit, MI, 32 pp.
- Altowaiji, Wisam A. K.; Darwin, David; and Donahey, Rex C. (1984). "Preliminary Study of the Effect of Revibration on Concrete-Steel Bond Strength," *SL Report No. 84-2*, University of Kansas Center for Research, Lawrence, Kansas, Nov., 29 pp.

Altowaiji, Wisam A. K.; Darwin, David; and Donahey, Rex C. (1986). "Bond of Reinforcement to Revibrated Concrete," *ACI Journal, Proceedings* Vol. 83, No. 6, Nov.-Dec., pp. 98-107.

ASCE (1995). *Minimum Design Loads for Buildings and Other Structures, ASCE 7-95*, American Society of Civil Engineers, New York.

ASTM A 305-47T (1947). "Tentative Specifications for Minimum Requirements for Deformations of Deformed Steel Bars for Concrete Reinforcement," American Society for Testing and Materials, Philadelphia, PA.

ASTM A305-49 (1949). "Specifications for Minimum Requirements for Deformations of Deformed Steel Bars for Concrete Reinforcement," American Society for Testing and Materials, Philadelphia, PA.

ASTM A 615/A 615M-95b. (1996). "Standard Specification for Deformed and Plain Billet-Steel Bars for Concrete Reinforcement," *1996 Annual Book of ASTM Standards*, Vol. 1.04, American Society for Testing and Materials, West Conshohocken, PA, pp. 302-307.

ASTM A 616/A 616M-95b. (1996). "Standard Specification for Rail-Steel Deformed and Plain Bars for Concrete Reinforcement," *1996 Annual Book of ASTM Standards*, Vol. 1.04, American Society for Testing and Materials, West Conshohocken, PA, pp. 308-312.

ASTM A 617/A 617M-95b. (1996). "Standard Specification for Axle-Steel Deformed and Plain Bars for Concrete Reinforcement," *1996 Annual Book of ASTM Standards*, Vol. 1.04, American Society for Testing and Materials, West Conshohocken, PA, pp. 313-317.

ASTM A 706/A 706M-95b. (1996). "Standard Specification for Low-Alloy Steel Deformed Bars for Concrete Reinforcement," *1996 Annual Book of ASTM Standards*, Vol. 1.04, American Society for Testing and Materials, West Conshohocken, PA, pp. 344-348.

ASTM A 722-90. (1996). "Standard Specification for Uncoated High-Strength Steel Bar for Prestressing Concrete," *1996 Annual Book of ASTM Standards*, Vol. 1.04, American Society for Testing and Materials, West Conshohocken, PA, pp. 359-362.

ASTM A 775/A 775M-95. (1996). "Standard Specification for Epoxy-Coated Reinforcing Steel Bars," *1996 Annual Book of ASTM Standards*, Vol. 1.04, American Society for Testing and Materials, West Conshohocken, PA, pp. 408-414.

Azizinamini, A.; Stark, M.; Roller, John H.; and Ghosh, S. K. (1993). "Bond Performance of Reinforcing Bars Embedded in High-Strength Concrete," *ACI Structural Journal*, Vol. 95, No. 5, Sept.-Oct., pp. 554-561.

Azizinamini, A.; Chisala, M.; and Ghosh, S. K. (1995). "Tension Development Length of Reinforcing Bars Embedded in High-Strength Concrete," *Engineering Structures*, Vol. 17, No. 7, pp. 512-522.

- Balazs, Gyorgy. L., and Koch, Rainer (1995). "Bond Characteristics Under Reversed Cyclic Loading," *Annual Journal on Research and Testing of Materials*, Vol. 6, Germany, pp. 47-62.
- Bashur, Fuad K., and Darwin, David (1976). "Nonlinear Model for Reinforced Concrete Slabs," *SL Report* No. 76-03, University of Kansas Center for Research, Lawrence, Kansas, December, 128 pp.
- Bashur, Fuad K., and Darwin, David (1978). "Nonlinear Model for Reinforced Concrete Slabs," *Journal of the Structural Division, ASCE*, V. 104 No. 1, Jan., pp. 157-170.
- Brettmann, Barrie B.; Darwin, David; and Donahey, Rex C. (1984). "Effects of Superplasticizers on Concrete-Steel Bond Strength," *SL Report* 84-1, University of Kansas Center for Research, Lawrence, Kansas, April, 32 pp.
- Brettmann, Barrie B.; Darwin, David; and Donahey, Rex C. (1986). "Bond of Reinforcement to Superplasticized Concrete," *ACI Journal, Proceedings* Vol. 83, No. 1, Jan.-Feb., pp. 98-107.
- Briss, G. R.; Paulay, T.; and Park, R. (1978). "Elastic Behavior of Earthquake Resistant R. C. Interior Beam-Column Joints," *Report* 78-13, University of Canterbury, Department of Civil Engineering, Christchurch, New Zealand, Feb.
- Cairns, J. and Jones, K. (1995). "Influence of Rib geometry on Strength of Lapped Joints: An Experimental and Analytical Study," *Magazine of Concrete Research*, 47, No. 172, Sept., pp. 253-262.
- Chamberlin, S. J. (1956). "Spacing of Reinforcement in Beams," *ACI Journal, Proceedings* Vol. 53, No. 1, July, pp. 113-134.
- Chamberlin, S. J. (1958). "Spacing of Spliced Bars in Beams," *ACI Journal, Proceedings* Vol. 54, No. 8, Feb., pp. 689-698.
- Chinn, James; Ferguson, Phil M.; and Thompson, J. Neils (1955). "Lapped Splices in Reinforced Concrete Beams," *ACI Journal, Proceedings* Vol. 52, No. 2, Oct., pp. 201-214.
- Choi, Oan Chul; Hadje-Ghaffari, Hossain; Darwin, David; and McCabe, Steven L. (1990a). "Bond of Epoxy-Coated Reinforcement to Concrete: Bar Parameters," *SL Report* 90-1, University of Kansas Center for Research, Lawrence, Kansas, Jan., 43 pp.
- Choi, Oan Chul; Darwin, David; and McCabe, Steven L. (1990b). "Bond Strength of Epoxy-Coated Reinforcement to Concrete," *SM Report* No. 25, University of Kansas Center for Research, Lawrence, Kansas, July, 217 pp.
- Choi, Oan Chul; Hadje-Ghaffari, Hossain; Darwin, David; and McCabe, Steven L. (1991). "Bond of Epoxy-Coated Reinforcement: Bar Parameters," *ACI Materials Journal*, Vol. 88, No. 2, Mar.-Apr., pp. 207-217.

- Ciampi, V.; Eligehausen, R.; Bertero, V. V.; and Popov, E. P. (1982). "Analytical Model for Deformed Bar Bond Under Generalized Excitations," *Report No. UCB/EERC-82/23*, Earthquake Engineering Research Center, University of California at Berkeley, November.
- Clark, A. P. (1946). "Comparative Bond Efficiency of Deformed Concrete Reinforcing Bars," *ACI Journal, Proceedings* Vol. 43, No. 4, Dec., pp. 381-400.
- Clark, A. P. (1949). "Bond of Concrete Reinforcing Bars," *ACI Journal, Proceedings* Vol. 46, No. 3, Nov., pp. 161-184.
- Collier, S. T. (1947). "Bond Characteristics of Commercial and Prepared Reinforcing Bars," *ACI Journal, Proceedings* Vol. 43, No. 10, June, pp. 1125-2233.
- CSA STANDARD A23.3-94 (1994). "*Design of Concrete Structures*," Canadian Standards Association, Ontario, Canada.
- CUR (1963), Commissie voor Uitvoering van Research Ingesteld door de Betonvereniging. "Onderzoek naar de samenwerking van geprofileerd staal met beton," *Report No. 23*, The Netherlands (Translation No. 112, 1964, Cement and Concrete Association, London, "An Investigation of the Bond of Deformed Steel Bars with Concrete"), 28 pp.
- Darwin, David; McCabe, Steven L.; Idun, Emmanuel K.; and Schoenekase, Steven P. (1992a). "Development Length Criteria: Bars Without Transverse Reinforcement," *SL Report 92-1*, University of Kansas Center for Research, Lawrence, Kansas, Apr., 62 pp.
- Darwin, David; McCabe, Steven L.; Idun, Emmanuel K.; and Schoenekase, Steven P. (1992b). "Development Length Criteria: Bars Not Confined by Transverse Reinforcement," *ACI Structural Journal*, Vol. 89, No. 6, Nov.-Dec., pp. 709-720.
- Darwin, David, and Graham, Ebenezer K. (1993a). "Effect of Deformation Height and Spacing on Bond Strength of Reinforcing Bars," *SL Report 93-1*, University of Kansas Center for Research, Lawrence, Kansas, Jan., 68 pp.
- Darwin, David, and Graham, Ebenezer K. (1993b). "Effect of Deformation Height and Spacing on Bond Strength of Reinforcing Bars," *ACI Structural Journal*, Vol. 90, No. 6, Nov.-Dec., pp. 646-657.
- Darwin, David; Tholen, Michael L.; and Idun, Emmanuel K.; and Zuo, Jun; (1995a). "Splice Strength of High Relative Rib Area Reinforcing Bars," *SL Report 95-3*, University of Kansas Center for Research, Lawrence, Kansas, May, 58 pp.
- Darwin, David; Zuo, Jun; Tholen, Michael L.; and Idun, Emmanuel K. (1995b). "Development Length Criteria for Conventional and High Relative Rib Area Reinforcing Bars," *SL Report 95-4*, University of Kansas Center for Research, Lawrence, Kansas, May, 70 pp.

- Darwin, David; Idun, Emmanuel K.; Zuo, Jun; and Tholen, Michael L. (1995c). "Reliability-Based Strength Reduction Factor for Bond," *SL Report 95-5*, University of Kansas Center for Research, Lawrence, Kansas, May, 47 pp.
- Darwin, David; Tholen, Michael L.; and Idun, Emmanuel K.; and Zuo, Jun; (1996a). "Splice Strength of High Relative Rib Area Reinforcing Bars," *ACI Structural Journal*, Vol. 93, No. 1, Jan.-Feb., pp. 95-107.
- Darwin, David; Zuo, Jun; Tholen, Michael L.; and Idun, Emmanuel K. (1996b). "Development Length Criteria for Conventional and High Relative Rib Area Reinforcing Bars," *ACI Structural Journal*, Vol. 93, No. 3, May-June, pp. 347-359.
- DeVries, Richard A.; Moehle, Jack P.; and Hester, Weston. (1991). "Lap Splice Strength of Plain and Epoxy-Coated Reinforcement," *Report No. UCB/SEMM-91/02*, University of California, Berkeley, California, Jan., 86 pp.
- Donahey, Rex C., and Darwin, David. (1983). "Effects of Construction Procedures on Bond in Bridge Decks," *SM Report No. 7*, University of Kansas Center for Research, Lawrence, Kansas, 129 pp.
- Donahey, Rex C., and Darwin, David. (1985). "Bond of Top-Cast Bars in Bridge Decks," *ACI Journal, Proceedings* Vol. 82, No. 1, Jan.-Feb., pp. 57-66.
- Draper, N. R., and Smith H. (1981). *Applied Regression Analysis*, Second Edition, John Wiley & Sons, Inc., pp. 241-249.
- Durrani, A. J., and Wight, J. K. (1982). "Experimental and Analytical Study of Internal Beam to Column Connections Subjected to Reversed Cyclic Loading," *Report No. UMEE 82R3*, Department of Civil Engineering, University of Michigan, July, 275 pp.
- Elgehausen, Rolf; Popov, Egor P.; and Bertero, V. V. (1983). "Local Bond Stress-Slip Relationships of Deformed Bars Under Generalized Excitations," *Report No. UCB/EERC-83/23*, Earthquake Engineering Center, University of California at Berkeley, October, 169 pp.
- Ehsani, M. R. (1982). "Behavior of Exterior Reinforced Concrete Beam to Column Connections Subjected to Earthquake Type Loading," *Report No. UMEE 82RS*, Department of Civil Engineering, University of Michigan, July, 275 pp.
- Ellingwood, Bruce; Galambos, Theodore V.; MacGregor, James G.; and Cornell, C. Allin (1980). "Development of a Probability Based Criterion for American National Standard A58," *NBS Special Publication 577*, U.S. Dept. of Commerce, Washington, D.C., June, 222 pp.
- Esfahani, M. R., and Rangan, B. V. (1996). "Studies on Bond Between Concrete and Reinforcing Bars," School of Civil Engineering, Curtin University of Technology, Perth, Western Australia, 315 pp.

Ferguson, Phil M., and Thompson, J. Neils. (1962). "Development Length of High Strength Reinforcing Bars in Bond," *ACI Journal, Proceedings* Vol. 59, No. 7, July, pp. 887-922.

Ferguson, Phil M., and Thompson, J. Neils. (1965). "Development Length for Large High Strength Reinforcing Bars," *ACI Journal, Proceedings* Vol. 62, No. 1, Jan., pp. 71-91.

Grant, Leon H.; Mirza, S. Ali; and MacGregor, James G. (1978). "Monte Carlo Study of Strength of Concrete Columns," *ACI Journal, Proceedings* Vol. 75, No. 8, Aug., pp 348-358.

Hadje-Ghaffari, Hossain; Darwin, David; and McCabe, Steven L. (1992). "Bond of Epoxy-Coated reinforcement to Concrete: Cover, Casting Position, Slump, and Consolidation," *SL Report* No. 92-3. University of Kansas Center for Research, Lawrence, Kansas, July, 42 pp.

Hadje-Ghaffari, Hossain; Choi, Oan Chul; Darwin, David; and McCabe, Steven L. (1994). "Bond of Epoxy-Coated reinforcement to Concrete: Cover, Casting Position, Slump, and Consolidation," *ACI Structural Journal*, Vol. 91, No. 1, Jan.-Feb., pp. 59-68.

Harajli, M. H. (1994). "Development/Splice Strength of Reinforcing Bars Embedded in Plain and Fiber Reinforced Concrete," *ACI Structural Journal*, Vol. 91, No. 5, Sep.-Oct., pp. 511-520.

Hatfield, Erleen; Azizinamini, Atorod; and Pavel, Rob (1996), "Minimum Stirrups Requirements for Tension Splices in High Strength Concrete," *Abstract* No. 130, 4th International Symposium on Utilization of High-Strength/High-performance Concrete, Paris, 10 pp.

Hester, Cynthia J.; Salamizavaregh, Shahin; Darwin, David; and McCabe, Steven L. (1991). "Bond of Epoxy-Coated Reinforcement to Concrete: Splices," *SL Report* 91-1, University of Kansas Center for Research, Lawrence, Kansas, May, 66 pp.

Hester, Cynthia J.; Salamizavaregh, Shahin; Darwin, David; and McCabe, Steven L. (1993). "Bond of Epoxy-Coated Reinforcement: Splices," *ACI Structural Journal*, Vol. 90, No. 1, Jan.-Feb., pp. 89-102.

Idun, Emmanuel K., and Darwin, David. (1995). "Improving the Development Characteristics of Steel Reinforcing Bars," *SM Report* No. 41, University of Kansas Center for Research, Lawrence, Kansas, Aug., 267 pp.

Jeanty, Paul R.; Mitchell, Denis; and Mirza M. Saeed (1988). "Investigation of 'Top Bar' Effects in Beams," *ACI Structural Journal*, Vol. 85, No. 3., May-June, pp. 251-257.

Jirsa, J. O., and Breen, J. E., (1981), "Influence of Casting Position and Shear on Development and Splice Length - Design Recommendation," *Research Report* No. 242-3F, Center for Transportation Research, The University of Texas at Austin

- Jirsa, J. O.; Chen, W.; Grant, D. B.; and Elizondo, R. (1995). "Development of Bundled Reinforcing Steel," *Research Report* No. 1363-2F, Center for Transportation Research, The University of Texas at Austin, December, 116 pp.
- Johnston, David W., and Zia, Paul (1982). "Bond Characteristics of Epoxy Coated Reinforcing Bars," *Report* No. FHWA-NC-82-002, Federal Highway Administration, Washington, DC, 163 pp.
- Kadoriku, Junichi (1994). "Study on Behavior of Lap Splices in High-Strength Reinforced Concrete Members," Doctorate Thesis, Kobe University, March, Japan, 201 pp.
- Kozul, Rozalija, and Darwin, David (1997). "Effects of Aggregate Type, Size, and Content on Concrete Strength and Fracture Energy," *SM Report* No. 43, University of Kansas Center for Research, Lawrence, Kansas, June, 83 pp.
- Lee, D. D. (1993). "Disc. 89-S68," *ACI Structural Journal* Vol. 90, No. 5, Sept.-Oct., pp. 581-583.
- Leon, Roberto T. (1989). "Interior Joints with Variable Anchorage Lengths," *Journal of Structural Engineering*, American Society of Civil Engineers, V. 115, No. 9, Sept., pp. 2261-2275.
- Losberg, Anders, and Olsson, Per-Ake. (1979). "Bond Failure of Deformed Reinforcing Bars Based on the Longitudinal Splitting Effect of the Bars," *ACI Journal, Proceedings* Vol. 76, No. 1, Jan., pp. 5-18.
- Luke, J. J.; Hamad, B. S.; Jirsa, J. O.; and Breen, J. E. (1981). "The Influence of Casting Position on Development and Splice Length of Reinforcing Bars," *Research Report* No. 242-1, Center for Transportation Research, Bureau of Engineering Research, University of Texas at Austin, June, 153 pp.
- Lukose, K.; Gergely, P.; and White, R. N., (1982) "Behavior of Reinforced Concrete Lapped Splices for Inelastic Cyclic Loading," *ACI Journal, Proceedings* Vol. 79, No. 5, Sept.-Oct., pp355-365.
- Lutz, L. A.; Gergely, P.; and Winter, G. (1966). "The Mechanics of Bond and Slip of Deformed Reinforcing Bars in Concrete," *Report* No. 324, Department of Structural Engineering, Cornell University, Aug., 306 pp.
- Lutz, L. A., and Gergely, P. (1967). "Mechanics of Bond and Slip of Deformed Bars in Concrete," *ACI Journal, Proceedings* Vol. 64, No. 11, Nov., pp. 711-721.
- Maeda, M.; Otani, S.; and Aoyama, H. (1991). "Bond Splitting Strength in Reinforced Concrete Members," *Transactions of the Japan Concrete Inst.*, Vol. 13, pp. 581-588.
- Mathey, Robert G., and Clifton, James R. (1976). "Bond of Coated Reinforcing Bars in Concrete," *Journal of the Structural Division*, ASCE, Vol. 102, No. ST1, Jan., pp. 215-229.

Mathey, Robert G., and Watstein, David. (1961). "Investigation of Bond in Beam and Pull-Out Specimens with High-Yield-Strength Deformed Bars," ACI Journal, *Proceedings* Vol. 57, No. 9, Mar., pp. 1071-1090.

Meinheit, D. F., and Jirsa, J. O. (1977). "Shear Strength of Reinforced Concrete Beam-Column Joints," *Report No. 77-1*, Department of Civil Engineering, Structures Research Laboratory, University of Texas at Austin, Jan.

Menzel, Carl A. (1952). "Effect of Settlement of Concrete on Results of Pullout Tests," *Research Department Bulletin 41*, Research and Development laboratories of the Portland Cement Association, Nov., 49 pp.

Morita, S. and Kaku, T. (1973). "Local Bond Stress-Slip Relationship and Repeated Loading," *Proceedings*, IABSE Symposium on "Resistance and Ultimate Deformability of Structures Acted on by Well Defined Repeated Loads," Lisbon.

Nilson, Arthur H. (1997). *Design of Concrete Structures*, Twelfth Edition, The McGraw-hill Companies, Inc., pp. 40-59.

Orangun, C. O.; Jirsa, J. O.; and Breen, J. E. (1975). "The Strength of Anchored Bars: A Reevaluation of Test Data on Development Length and Splices," *Research Report No. 154-3F*, Center for Highway Research, The University of Texas at Austin, Jan., 78 pp.

Orangun, C. O.; Jirsa, J. O.; and Breen, J. E. (1977). "A Reevaluation of Test Data on Development Length and Splices," ACI Journal, *Proceedings* Vol. 74, No. 3, Mar., pp. 114-122.

Rehm, G. (1957). "The Fundamental Law of Bond," *Proceedings*, Symposium on Bond and Crack Formation in Reinforced Concrete, Stockholm, RILEM, Paris, (published by Tekniska Hogskolans Rotaprinttrychkeri, Stockholm, 1958).

Rehm, G. (1961). "Über die Grundlagen des Verbundes Zwischen Stahl und Beton." *Deutscher Ausschuss für Stahlbeton*. No. 1381, pp. 59, (C & CA Library Translation No. 134, 1968. "The Basic Principle of the Bond between Steel and Concrete.").

Rezanoff, T.; Konkankar, U. S.; and Fu, Y. C. (1991). "Confinement Limits for Tension Lap Splices under Static Loading," *Report*, University of Saskatchewan, Saskatoon, Sask., Aug., 24 pp.

Rezanoff, T.; Akanni, A.; and Sparling, B. (1993). "Tensile Lap Splices under Static Loading: A Review of the Proposed ACI 318 Code Provisions," *ACI Structural Journal*, Vol. 90, No. 4, July-Aug., pp. 374-384.

Sakurada, T; Morohashi, N.; Tanaka, R. (1993). "Effect of Transverse Reinforcement on Bond Splitting Strength of Lap Splices," *Transactions of the Japan Concrete Inst.*, Vol. 15, pp. 573-580.

Skorobogatov, S. M., and Edwards, A. D. (1979). "The Influence of the Geometry of Deformed Steel Bars on Their Bond Strength in Concrete," *Institute of Civil Engineers*, Proceedings Vol. 67, Part 2, June, pp. 327-339.

Soretz, S., and Holzenbein, H. (1979). "Influence of Rib Dimensions of Reinforcing Bars on Bond and Bendability," *ACI Journal, Proceedings* Vol. 76, No. 1, Jan., pp. 111-127.

Tan, Changzheng; Darwin, David; Tholen, Michael L.; and Zuo, Jun. (1996). "Splice Strength of Epoxy-Coated High Relative Rib Area Bars," *SL Report 96-2*, University of Kansas Center for Research, Lawrence, Kansas, May, 69 pp.

Tholen, M. L., and Darwin, David (1996). "Effects of Deformation Properties on the Bond of Reinforcing Bars," *SL Report 96-3*, University of Kansas Center for research, Lawrence, Kansas, October, 370 pp.

Thompson, M. A.; Jirsa, J. O.; Breen, J. E.; and Meinheit, D. F. (1975). "The Behavior of Multiple Lap Splices in Wide Sections," *Research Report* No. 154-1, Center for Highway Research, The University of Texas at Austin, Feb., 75 pp.

Treece, Robert A., and Jirsa, James O. (1987). "Bond Strength of Epoxy-Coated Reinforcing Bars," *PMFSEL Report* No. 87-1, Phil M. Ferguson Structural Engineering Laboratory, The University of Texas at Austin, Jan., 85 pp.

Treece, Robert A., and Jirsa, James O. (1989). "Bond Strength of Epoxy-Coated Reinforcing Bars," *ACI Materials Journal*, Vol. 86, No. 2, Mar.-Apr., pp. 167-174.

Zekany, A. J.; Neumann, S.; and Jirsa, J. O. (1981). "The Influence of Shear on Lapped Splices in Reinforced Concrete," *Research Report* No. 242-2, Center for Transportation Research, Bureau of Engineering Research, University of Texas at Austin, July, 88 pp.

Zhu, Songchao, and Jirsa, James O. (1983). "A Study of Bond Deterioration in Reinforced Concrete Beam-Column Joints," *PMFSEL Report* No. 83-1, Phil M. Ferguson Structural Engineering Laboratory, The University of Texas at Austin, July, 69 pp.

Table 2.1
Splice specimen properties and test results

Specimen Label +	Bar Designation	n	l_s (in)	b (in)	h (in)	d_b (in)	c_{sa} (in)	c_{si} (in)	c_b (in)	d (in)	f_c (psi)	N	d_s (in)	f_y (ksi)	P (kips)	M_u (k-in)	f_{s++} (ksi)
19.1-B-S-U	8N3	3	36	18.14	16.162	1.000	1.954	1.930	1.961	13.66	4250	0		38.18	2095	73.513	
19.2-B-N-U	8N3	3	36	18.06	16.129	1.000	2.016	1.883	1.929	13.66	4250	0		35.26	1937	67.853	
19.3-B-S-U	8N3	3	30	18.10	16.066	1.000	2.063	1.898	1.903	13.62	4250	3	0.375	64.55	37.02	2031	71.428
19.4-B-N-U	8N3	3	30	18.13	16.07	1.000	2.032	1.891	1.897	13.63	4250	3	0.375	64.55	40.04	2194	77.276
20.1-B-S-U	11F3	3	40	18.05	16.199	1.410	2.008	1.313	1.840	13.61	5080	8	0.500	84.70	69.84	3805	71.084
20.2-B-N-U	11F3	3	40	18.05	16.15	1.410	2.000	1.297	1.848	13.56	5080	8	0.500	84.70	70.18	3824	71.81
20.3-B-S-U	11F3	3	40	18.07	16.151	1.410	2.000	1.313	1.822	13.58	5080	5	0.500	84.70	67.30	3668	68.515
20.4-B-N-U	11F3	3	40	18.10	16.258	1.410	2.040	1.297	1.868	13.64	5080	5	0.500	84.70	66.82	3643	67.647
20.5-B-S-C	8N3	3	40	12.03	15.631	1.000	1.500	0.660	1.243	13.85	5080	0		25.87	1419	49.535	
20.6-B-S-U	8N3	3	40	12.08	15.597	1.000	1.516	0.672	1.300	13.76	5080	0		29.61	1621	57.149	
21.1-B-S-U	8N3	3	24	12.05	15.655	1.000	1.766	0.484	1.470	13.65	4330	6	0.625	62.98	37.27	2033	73.879
21.2-B-S-C	8N3	3	24	12.13	15.762	1.000	1.813	0.492	1.462	13.76	4330	6	0.625	62.98	35.15	1918	68.769
21.3-B-S-U	8N3	3	25	12.10	16.134	1.000	1.655	0.578	1.492	13.65	4330	5	0.625	62.98	38.43	2096	76.249
21.4-B-S-C	8N3	3	25	12.06	16.171	1.000	1.524	0.613	1.850	13.78	4330	5	0.625	62.98	35.35	1929	69.103
21.5-B-S-U	8N3	2	25	12.14	15.544	1.000	1.641	2.219	1.421	13.58	4330	5	0.500	64.92	26.67	1460	77.35
21.6-B-S-C	8N3	2	25	12.14	15.501	1.000	1.516	2.172	1.376	13.59	4330	2	0.500	64.92	22.49	1235	65.083
22.1-B-S-U*	11F3	2	32	12.11	15.685	1.410	2.391	0.703	1.413	13.53	6300	8	0.375	71.25	56.46	2161	59.465
22.2-B-S-C	11F3	2	32	12.10	15.671	1.410	2.313	0.688	1.436	13.49	6300	8	0.375	71.25	67.63	2569	71.351
22.3-B-S-U*	11F3	2	33	11.98	15.662	1.410	1.289	1.234	1.428	13.49	6300	6	0.375	71.25	67.87	2577	71.661
22.4-B-S-C	11F3	2	33	12.06	15.647	1.410	1.282	1.250	1.390	13.51	6300	6	0.375	71.25	65.66	2497	69.152
22.5-B-S-U**	11F3	2	33	17.86	16.094	1.410	3.422	2.469	2.767	12.58	6300	0		82.61	3149	62.407	
22.6-B-S-C	11F3	2	33	17.87	16.467	1.410	3.438	2.172	2.724	13.00	6700	0		94.16	3536	67.548	
23a.1-B-S-U	8N3	3	21	18.28	16.09	1.000	2.164	1.852	1.931	13.62	9080	4	0.375	71.25	42.51	2326	78.873
23a.2-B-S-C	8N3	3	21	18.28	16.09	1.000	2.063	1.859	1.933	13.69	9080	4	0.375	71.25	33.82	1857	62.476
23a.3-B-N-U	8N3	3	21	18.18	16.17	1.000	2.055	1.902	1.902	13.66	9080	4	0.375	71.25	43.86	2399	80.57
23a.4-B-S-U	8N3	3	21	18.13	16.103	1.000	2.008	1.898	1.930	13.69	9080	4	0.375	71.25	42.88	2346	79.153
23a.5-B-S-U	8N3	2	22	18.19	16.163	1.000	2.000	1.891	1.938	13.63	9320	0		22.72	1248	62.244	
23a.6-B-S-U	8N3	2	29	12.24	16.11	1.000	2.031	1.875	1.919	13.67	9320	0		27.25	1493	75.467	

Table 2.1
Splice specimen properties and test results (continued)

Specimen Label +	Bar Designation	n	l_s (in)	b (in)	h (in)	d_b (in)	c_{so} (in)	c_{si} (in)	c_b (in)	d (in)	f_c (psi)	N	d_s (in)	f_y (ksi)	P (kips)	M_u (k-in)	f_s++ (ksi)
23b.1-B-S-U	8N3	3	18	12.15	16.215	1.000	1.469	0.711	1.951	13.73	8370	5	0.500	64.92	41.87	2281	79.04
23b.2-B-S-C	8N3	3	18	12.10	16.108	1.000	1.454	0.711	1.903	13.67	8370	5	0.500	94.92	37.21	2029	70.51
23b.3-B-S-U	8N3	2	20	18.23	16.321	1.000	3.032	3.859	3.057	12.72	8370	0			24.02	1328	71.64
23b.4-B-S-C	8N3	2	20	18.18	16.114	1.000	3.047	3.813	3.041	12.53	8370	0			23.17	1282	70.24
23b.5-B-S-U	11F3	2	25	12.03	16.244	1.410	2.032	1.125	1.939	13.56	4500	5	0.500	64.92	32.37	1954	54.80
23b.6-B-S-C	11F3	2	25	12.04	16.095	1.410	2.001	1.125	1.905	13.44	4500	5	0.500	64.92	26.40	1605	45.10
24.1-B-S-U	8N1	2	32	12.14	16.122	1.000	2.000	1.875	1.903	13.69	4300	0			21.54	1185	61.91
24.2-B-S-C	8N1	2	32	12.15	16.172	1.000	2.000	1.875	1.878	13.77	4300	0			19.36	1067	55.32
24.3-T-S-U	8N1	2	32	12.08	16.043	1.000	2.000	1.875	2.000	13.52	4300	0			20.56	1132	59.93
24.4-T-S-C	8N1	2	32	12.07	16.044	1.000	2.000	1.875	2.102	13.42	4300	0			18.84	1039	55.38
25.1-B-S-U	5C3	3	17	12.19	16.271	0.625	1.985	1.023	1.556	14.37	4490	0			14.59	808	63.72
25.2-B-S-C	5C3	3	17	12.16	16.124	0.625	2.016	0.992	1.530	14.25	4490	0			15.45	854.2	67.58
25.3-T-S-U	5C3	3	17	12.12	16.141	0.625	2.032	0.984	1.460	14.28	4490	0			14.65	811.2	64.33
25.4-T-S-C	5C3	3	17	12.28	16.12	0.625	2.047	0.961	1.422	14.28	4490	0			13.92	772.1	62.98
26.1-B-S-U	8N1	3	30	12.03	16.113	1.000	1.563	0.656	1.888	13.77	4956	6	0.375	71.25	33.38	1824	64.59
26.2-T-S-U	8N1	3	30	12.08	16.133	1.000	1.578	0.633	1.969	13.64	4956	6	0.375	71.25	28.43	1557	55.43
26.3-B-S-U	8N1	3	40	12.11	16.194	1.000	1.547	0.652	1.889	13.78	4956	0			32.34	1769	62.51
26.4-T-S-U	8N1	3	40	12.03	16.07	1.000	1.493	0.664	2.047	13.50	4956	0			30.78	1685	60.83
26.5-B-S-U	8N0	3	40	12.15	16.165	1.000	1.500	0.684	1.891	13.75	4956	0			33.21	1816	64.35
26.6-T-S-U	8N0	3	40	12.06	16.217	1.000	1.500	0.656	2.000	13.69	4956	0			32.13	1758	62.53
27.1-B-S-U	8N1	3	23	12.22	15.584	1.000	1.907	0.484	1.447	13.61	10810	6	0.375	71.25	43.27	2357	79.98
27.2-B-S-U	8N0	3	23	12.12	15.515	1.000	2.000	0.477	1.415	13.71	10810	6	0.375	64.92	42.70	2326	78.52
27.3-B-S-U	8N1	3	18	12.06	15.534	1.000	1.938	0.461	1.473	13.53	10810	5	0.500	64.92	42.29	2303	79.21
27.4-B-S-U	8N0	3	18	12.15	15.503	1.000	2.000	0.457	1.442	13.54	10810	5	0.500	64.92	40.78	2222	77.21
27.5-B-S-U	8N1	3	18	18.16	15.612	1.000	4.016	0.941	1.427	13.66	10810	4	0.500	64.92	41.74	2284	77.07
27.6-B-S-U	8N0	3	18	18.12	15.619	1.000	4.032	0.930	1.442	13.65	10810	4	0.500	64.92	43.02	2353	78.42
28.1-B-S-U	11F3	2	25	11.71	16.069	1.410	2.188	0.766	1.900	13.42	12610	5	0.375	71.25	48.63	2646	71.23
28.2-B-S-C	11F3	2	25	12.13	16.202	1.410	2.188	0.734	1.939	13.52	12610	5	0.375	71.25	37.35	2038	54.17

Table 2.1
Splice specimen properties and test results (continued)

Specimen Label +	Bar Designation	n	l_s (in)	b (in)	h (in)	d_b (in)	c_{so} (in)	c_{si} (in)	c_b (in)	d (in)	f_c (psi)	N	d_s (in)	f_y (ksi)	P (kips)	M_u (k-in)	f_s^{++} (ksi)
28.3-B-S-U	11F3	3	28	18.10	16.094	1.410	2.172	1.242	1.901	13.45	12610	4	0.375	71.25	68.89	3752	67.03
28.4-B-S-C	11F3	3	28	18.09	16.157	1.410	2.063	1.211	1.893	13.52	12610	4	0.375	71.25	47.14	2577	45.62
28.5-B-S-U	11F3	2	30	18.09	16.198	1.410	1.977	4.031	1.999	13.45	12610	0			35.40	1944	50.89
28.6-B-S-C	11F3	2	30	18.11	16.215	1.410	2.016	3.984	1.946	13.52	12610	0			29.13	1605	41.76
29.1-B-S-U	8N1	3	20	12.06	15.644	1.000	1.766	0.492	1.441	13.68	10620	5	0.375	71.25	44.26	2410	80.98
29.2-B-S-U	8N0	3	20	12.14	15.599	1.000	1.875	0.484	1.478	13.60	10620	5	0.375	71.25	46.07	2508	83.65
29.3-B-S-U	8N1	3	18	12.13	15.638	1.000	1.859	0.484	1.470	13.64	10620	6	0.375	71.25	41.62	2267	78.23
29.4-B-S-U	8N0	3	18	12.17	15.6	1.000	1.938	0.492	1.418	13.66	10620	6	0.375	71.25	41.94	2284	77.96
29.5-B-S-U	8N1	3	16	18.10	15.653	1.000	3.906	0.965	1.470	13.66	10620	4	0.375	71.25	41.02	2244	75.79
29.6-B-S-U	8N0	3	16	18.17	15.648	1.000	3.906	0.980	1.414	13.71	10620	4	0.375	71.25	42.25	2311	77.72
30.1-B-S-U	11F3	2	25	12.19	16.152	1.410	2.375	0.688	1.891	13.51	13220	3	0.375	71.25	45.63	2485	66.07
30.2-B-S-C	11F3	2	25	12.07	16.137	1.410	2.344	0.734	1.847	13.54	13220	3	0.375	71.25	35.28	1926	51.00
30.3-B-S-U	11F3	3	28	18.02	16.105	1.410	1.953	1.273	1.889	13.47	13220	2	0.375	71.25	68.97	3756	66.88
30.4-B-S-C	11F3	3	28	18.04	16.098	1.410	2.031	1.227	1.864	13.49	13220	2	0.375	71.25	55.87	3049	54.09
30.5-B-S-U	11F3	2	30	18.12	16.146	1.410	2.063	4.016	1.956	13.44	13220	0			46.72	2555	66.95
30.6-B-S-C	11F3	2	30	18.14	15.999	1.410	2.141	3.859	1.988	13.26	13220	0			37.42	2052	54.47
31.1-B-S-U	8N1	2	16	12.12	15.483	1.000	2.000	1.875	1.522	13.43	12890	2	0.375	71.25	24.32	1333	68.25
31.2-B-S-C	8N1	2	16	12.20	15.535	1.000	2.000	1.813	1.488	13.52	12890	2	0.375	71.25	20.39	1121	56.94
31.3-B-S-U	8N0	2	16	12.15	15.483	1.000	1.969	1.938	1.438	13.52	12890	2	0.375	71.25	23.39	1282	65.21
31.4-B-S-C	8N0	2	16	12.08	15.629	1.000	1.969	1.875	1.404	13.70	12890	2	0.375	71.25	19.12	1052	52.72
31.5-B-S-U	8N1	3	22	12.26	15.584	1.000	1.828	0.508	1.494	13.56	12890	0			32.73	1787	61.43
31.6-B-S-U	8C0A	3	22	12.17	15.485	1.000	1.719	0.539	1.492	13.44	12890	0			33.47	1827	63.42
32.1-B-S-U	11F3	2	32	12.17	16.169	1.000	2.000	0.984	1.904	13.52	14400	0			43.86	2390	63.33
32.2-B-S-U	11B0	2	32	12.14	16.16	1.000	2.000	1.063	1.916	13.51	14400	0			42.55	2319	61.49
32.3-B-S-U	11F3	2	32	18.14	16.146	1.000	1.969	4.016	1.947	13.45	14400	0			42.41	2323	60.64
32.4-B-S-U	11B0	2	28	18.20	16.173	1.000	2.031	4.047	1.935	13.50	14400	0			42.85	2346	61.01
33.1-B-S-U	8N1	3	18	12.16	16.03	1.000	2.031	0.426	1.954	13.55	5360	6	0.500	64.92	31.37	1714	61.32
33.2-B-S-U	8C0A	3	18	12.10	16.124	1.000	1.953	0.395	1.913	13.66	5360	6	0.500	64.92	31.69	1732	61.42

Table 2.1
Splice specimen properties and test results (continued)

Specimen Label +	Bar Designation	n	l_s (in)	b (in)	h (in)	d_b (in)	c_{so} (in)	c_{si} (in)	c_b (in)	d (in)	f_c (psi)	N	d_s (in)	f_y (ksi)	P (kips)	M_u (k-in)	f_s++ (ksi)
33.3-B-S-U	8N1	3	18	18.14	16.127	1.000	2.070	1.918	1.969	13.63	5360	4	0.375	71.25	30.27	1665	57.60
33.4-B-S-U	8C0A	3	18	18.12	16.13	1.000	2.063	1.914	1.936	13.64	5360	4	0.375	71.25	30.67	1687	58.32
33.5-B-S-U	8N1	2	22	12.14	16.326	1.000	2.047	1.875	1.928	13.87	5230	2	0.375	71.25	20.12	1108	56.46
33.6-B-S-U	8C0A	2	22	12.17	16.261	1.000	2.094	1.688	1.891	13.82	5230	2	0.375	71.25	20.57	1132	57.94
34.1-B-S-U	8N1	3	24	18.13	16.123	1.000	2.063	1.938	1.941	13.66	5440	0			30.48	1677	57.88
34.2-B-N-U	8N1	3	24	18.17	16.05	1.000	2.070	1.945	1.918	13.61	5440	0			32.52	1787	61.97
34.3-B-S-U	8C0A	3	24	18.12	16.022	1.000	2.080	1.844	1.981	13.49	5440	0			30.64	1685	58.94
34.4-B-N-U	8C0A	3	24	18.21	16.02	1.000	2.045	1.883	1.936	13.53	5440	0			30.51	1679	58.49
35.1-B-S-U	8F1	2	20	12.08	16.17	1.000	1.453	2.375	1.938	13.69	5330	5	0.375	71.25	24.08	1321	68.44
35.2-T-S-U	8F1	2	20	12.25	16.23	1.000	1.422	2.328	2.159	13.54	5330	5	0.375	71.25	19.54	1076	56.21
35.3-B-S-U	8C0A	2	20	12.08	16.07	1.000	1.500	2.266	1.920	13.60	5330	5	0.375	71.25	21.58	1186	61.77
35.4-T-S-U	8C0A	2	20	12.16	16.24	1.000	1.640	2.211	1.938	13.75	5330	5	0.375	71.25	19.65	1082	55.61
36.1-B-S-U	8N1	3	24	12.16	15.522	1.000	1.938	0.484	1.446	13.55	5060	6	0.625	62.98	39.21	2137	77.39
36.2-B-S-U	8N1	3	21	12.13	15.508	1.000	1.969	0.484	1.421	13.56	5060	7	0.500	64.92	34.50	1883	67.75
36.3-B-S-U	8C0A	3	26	18.17	16.102	1.000	2.016	1.836	2.000	13.55	5060	0			32.68	1796	62.78
36.4-B-N-U	8C0A	3	26	18.14	16.101	1.000	2.031	1.828	1.988	13.56	5060	0			31.35	1724	60.17
37.1-B-D-U***	8C0A	2	32	12.11	16.261	1.000	2.000	1.813	1.965	12.70	4800	0			32.81	1794	59.97
37.2-B-D-U****	8C0A	2	32	12.14	16.158	1.000	2.000	1.781	1.954	12.60	4800	0			33.27	1818	61.40
37.3-B-S-C	8F1	3	21	12.11	15.52	1.000	1.891	0.469	1.500	13.48	4800	7	0.500	64.92	31.78	1736	62.92
37.4-B-S-U	8F1	3	21	12.07	15.505	1.000	2.000	0.484	1.503	13.47	4800	7	0.500	64.92	37.02	2019	73.78
38.1-B-N-U	8C0A	3	26	18.25	16.101	1.000	1.938	1.953	1.802	13.75	5080	0			28.64	1578	54.18
38.2-B-S-U	8C0A	3	26	18.17	16.139	1.000	2.125	1.844	2.075	13.51	5080	0			31.41	1728	60.51
38.3-B-S-U	8N1	3	24	12.08	15.442	1.000	1.938	0.500	1.446	13.47	5080	6	0.625	62.98	34.82	1900	68.93
38.4-B-S-U	8N1	3	21	12.13	15.492	1.000	1.969	0.484	1.437	13.53	5080	7	0.500	64.92	31.12	1700	61.12
38.5-B-S-U	8N1	2	24	12.16	15.624	1.000	2.047	1.875	1.450	13.65	5080	6	0.375	71.25	23.74	1302	67.83
38.5-B-S-U	8N1	2	26	12.17	16.098	1.000	1.969	1.938	1.754	13.64	5080	2	0.375	71.25	20.87	1094	56.86
39.1-B-S-C	8C1	3	16	12.16	15.527	1.000	1.859	0.469	1.502	13.51	14450	4	0.375	71.25	30.65	1675	57.61
39.2-B-S-U	8C1	3	16	12.18	15.48	1.000	1.906	0.516	1.475	13.49	14450	4	0.375	71.25	38.59	2103	69.74

Table 2.1
Splice specimen properties and test results (continued)

Specimen Label +	Bar Designation	n	l_s (in)	b (in)	h (in)	d_b (in)	c_{so} (in)	c_{si} (in)	c_b (in)	d (in)	f_c (psi)	N	d_s (in)	f_y (ksi)	P (kips)	M_u (k-in)	f_g++ (ksi)
39.3-B-S-U	8N0	3	16	12.17	15.452	1.000	1.891	0.488	1.477	13.45	14450	4	0.375	71.25	41.43	2257	77.96
39.4-B-S-C	8N0	3	16	12.09	15.465	1.000	1.813	0.500	1.470	13.47	14450	4	0.375	71.25	30.04	1641	56.64
39.5-B-S-C	8C1	3	21	12.15	15.495	1.000	1.813	0.516	1.508	13.47	14450	0			26.26	1438	49.56
39.6-B-S-U	8C1	3	21	12.19	15.409	1.000	1.953	0.508	1.505	13.59	14450	0			36.10	1969	67.38
40.1-B-S-U	11F3	2	23	12.16	15.478	1.410	2.031	1.000	1.473	13.26	15650	4	0.375	71.25	45.38	2471	66.60
40.2-B-S-C	11F3	2	23	12.16	15.49	1.410	2.023	1.023	1.459	13.28	15650	4	0.375	71.25	37.66	2053	55.16
40.3-B-S-C	11N0	2	23	12.15	15.484	1.410	1.953	1.063	1.435	13.31	15650	4	0.375	71.25	26.80	1467	39.25
40.4-B-S-U	11N0	2	23	12.09	15.521	1.410	2.000	1.063	1.451	13.33	15650	4	0.375	71.25	40.32	2197	58.83
40.5-B-S-U	8N0	2	17	12.11	16.041	1.000	2.000	1.875	1.846	13.67	15650	0			24.00	1316	65.81
40.6-B-S-C	8N0	2	17	12.26	16.231	1.000	2.000	1.906	1.823	13.88	15650	0			21.66	1190	58.53
41.1-B-S-U	8N3	2	16	12.14	15.552	1.000	2.000	1.844	1.522	13.49	10180	2	0.375	71.25	23.52	1289	66.16
41.2-B-S-U	8N3	3	16	12.16	15.531	1.000	1.875	0.469	1.515	13.38	10180	4	0.625	62.98	44.34	2414	83.02
41.3-B-S-U	8N3	3	16	12.11	16.091	1.000	1.891	0.461	1.890	13.56	10180	4	0.500	64.92	41.87	2281	79.35
41.4-B-S-U	8N0	3	16	12.20	15.531	1.000	1.906	0.484	1.476	13.40	10180	4	0.625	62.98	40.28	2194	77.27
41.5-B-N-U	8C0A	3	16	18.32	16.04	1.000	2.016	1.875	1.977	13.51	10500	2	0.375	71.25	34.86	1935	66.01
41.6-B-S-U	8C0A	3	16	18.22	16.167	1.000	2.000	1.875	1.984	13.63	10500	2	0.375	71.25	35.26	1934	65.38
42.1-B-S-U	8N0	2	16	12.11	15.986	1.000	2.000	1.859	1.864	13.50	11930	2	0.375	71.25	22.97	1260	64.32
42.2-B-S-C	8N0	2	16	12.09	15.976	1.000	2.016	1.859	1.816	13.64	11930	2	0.375	71.25	17.12	944	47.64
42.3-B-S-C	8N0	3	16	12.11	16.007	1.000	1.906	0.500	1.848	13.64	11930	4	0.500	64.92	27.99	1531	52.45
42.4-B-S-U	8N0	3	16	12.17	16.091	1.000	1.906	0.500	1.829	13.74	11930	4	0.500	64.92	38.07	2076	70.70
42.5-B-S-U	8N0	3	16	12.18	15.358	1.000	1.906	0.500	1.476	13.62	11930	4	0.625	62.98	41.60	2266	77.92
42.6-B-S-C	8N0	3	16	12.15	15.516	1.000	1.906	0.500	1.456	13.53	11930	4	0.625	62.98	34.94	1906	65.90
43.1-B-S-C	8N3	2	16	12.15	16.072	1.000	2.000	1.844	1.903	13.63	11530	2	0.375	71.25	18.68	1029	51.96
43.2-B-S-U	8N3	2	16	12.06	16.059	1.000	2.031	1.875	1.844	13.68	11530	2	0.375	71.25	23.49	1288	64.95
43.3-B-S-U	8N3	3	16	12.22	16.067	1.000	1.844	0.500	1.859	13.83	11530	4	0.500	64.92	42.70	2326	78.81
43.4-B-S-C	8N3	3	16	12.09	16.072	1.000	1.828	0.500	1.956	13.58	11530	4	0.500	64.92	33.79	1844	63.63
43.5-B-S-C	8N3	3	16	12.07	15.544	1.000	1.875	0.500	1.464	13.54	11530	4	0.625	62.98	39.46	2150	74.50
43.6-B-S-U	8N3	3	16	12.07	15.484	1.000	1.891	0.500	1.492	13.62	11530	4	0.625	62.98	45.16	2458	82.73

Note: Refer to last page of table for footnotes.

Table 2.1
Splice specimen properties and test results (continued)

Specimen Label +	Bar Designation	n	l_s (in)	b (in)	h (in)	d_b (in)	c_{so} (in)	c_{si} (in)	c_b (in)	d (in)	f'_c (psi)	N	d_s (in)	f'_s (ksi)	P (kips)	M_u (k-in)	f_s^{++} (ksi)
------------------	-----------------	---	------------	--------	--------	------------	---------------	---------------	------------	--------	--------------	---	------------	--------------	----------	--------------	------------------

+ Specimen label:

G.P-C-A-S, G = group number (19-43), P = casting order in the group (1-6), C = casting position of test bars (B = bottom cast bar, T = top cast bar), A = bar arrangement (S = symmetrical splices, N = unsymmetrical splices, D = two layers of bars), S = surface condition of test bars (U = uncoated, C = epoxy coated)

++ Bar stress is computed using the moment-curvature method if M_u does not exceed the moment capacity from moment-curvature analysis, otherwise f'_s is computed using the ultimate strength method; M_u and f'_s include effects of beam self weight and loading system.

* Beam failed by crushing concrete at middle section.

** Beam did not fail due to the limited capacity of loading system.

*** First layer contained spliced bars and second layer contained continuous bars.

**** Both layers were spliced bars.

1 in. = 25.4 mm; 1 psi = 6.895 kPa; 1 ksi = 6.895 MPa; 1 kip = 4.445 kN; 1 k-in. = 0.113 kN-m

Table 2.2
Properties of reinforcing bars

Bar * Designation	Yield Strength (ksi)	Nominal Diameter (in.)	Weight (lb/ft)	% Light or Heavy	Rib Spacing (in.)	Rib Width**		Rib Width+ Rib Spacing		Rib Height		Relative Rib Area	Coating+++ Thickness (mils)
						I (in.)	II (in.)	I (in.)	II (in.)	ASTM (in.)	Avg.++ (in.)		
5C3	62.98	0.625	1.033	1.0%L	0.258	0.082	0.100	0.318	0.386	0.047	0.043	0.141	7.8
8C0A	69.50	1.000	2.615	2.1%L	0.598	0.146	0.173	0.243	0.288	0.066	0.063	0.085	-
8N0	77.96	1.000	2.594	2.8%L	0.650	0.138	0.165	0.212	0.253	0.057	0.054	0.069	10.1
8C1	67.69	1.000	2.592	5.3%L	0.504	0.149	0.178	0.296	0.353	0.064	0.060	0.101	13.3
8F1	75.42	1.000	2.600	2.6%L	0.471	0.123	0.140	0.261	0.297	0.078	0.074	0.140	16.8
8N1	79.70	1.000	4.733	2.4%H	0.441	0.160	0.193	0.363	0.438	0.073	0.068	0.121	10.2
8N3	80.57	1.000	2.730	2.2%H	0.487	0.148	0.177	0.303	0.362	0.072	0.068	0.119	12.1
11N0	65.54	1.410	5.157	2.9%L	0.911	0.194	0.234	0.212	0.257	0.079	0.072	0.072	8.1
11B0	66.69	1.410	5.102	4.0%L	0.825	0.156	0.187	0.188	0.226	0.070	0.070	0.070	-
11F3	77.77	1.410	5.145	3.2%L	0.615	0.157	0.204	0.255	0.332	0.090	0.127	0.127	6.3

* Bar Designation

#AAB, # = bar size (No. 5, No.8, or No.11), AA = bar manufacturer and deformation pattern:

B0 Conventional Birmingham Steel bars

C0 Conventional Chaparral Steel bar

C1, C3 New Chaparral Steel bar

N0 Conventional North Star Steel bar

F1, F3 New Florida Steel bar

N1, N3 New North Star Steel bar

B = different letter that is presented if the bar had the same deformation pattern as reported by Darwin et al. (1995a), but were produced from different steel heat.

** Average rib width at: I - 3/4 height of ribs
II - 1/2 height of ribs

+ Ratio of rib width to rib spacing corresponding to rib width I and II

++ Average rib height between longitudinal ribs

+++ Average coating thicknesses for epoxy-coated bars belonging to bar designation

1 in. = 25.4 mm; 1 ksi = 6.895 MPa, 1 lb/ft = 1.49 kg/m, 1 mil = 0.0254 mm

Table 2.3
Concrete mix proportions (lb/yd³) and properties

Group	Concrete Series*	w/cm Ratio**	Cement (lb/yd ³)	Water (lb/yd ³)	Fine Agg.*** (lb/yd ³)	Coarse Agg. (lb/yd ³)	Fly Ash (lb/yd ³)	Silica Fume [†] (lb/yd ³)	Superplasticizer Type F (oz/yd ³)	Superplasticizer Type G (oz/yd ³)	Retarder Type A (oz/yd ³)	Slump (in.)	Concrete Temperature (F°)	Air Content (%)	Test Age (days)	Cylinder Strength (psi)
19	NNL	0.44	511	225	1564	1661	0	0	0	0	0	2.00	59	3.3	4250	
20	NNL	0.44	511	225	1564	1661	0	0	0	0	0	2.25	66	3.4	5080	
21	NNL	0.44	511	225	1564	1661	0	0	0	0	0	2.50	74	3.2	4330	
22	NNB	0.35	886	310	1209	1568	0	0	0	0	0	2.25	93	2.1	6300	
														14	6700	
23a	HHL	0.33	548	182	1427	1803	0	83	132	44	0	3.50	66	1.9	8	9080
23b-1	HHL	0.33	548	182	1427	1803	0	83	132	44	0	4.50	56	1.6	8	8370
23b-2++	NNL	0.33	511	225	1427	1661	0	0	0	0	0	3.00	51	3.0	10	4500
24	NNL	0.44	511	225	1564	1661	0	0	0	58	0	4.00	87	2.6	9	4300
25	NNL	0.44	511	225	1564	1661	0	0	0	58	0	3.75	90	3.9	13	4490
26	NNL	0.44	602	265	1444	1661	0	0	0	0	0	5.00	65	2.4	19	4956
27	HHL	0.33	548	182	1427	1803	0	83	132	44	0	5.50	47	1.3	27	10810
28	HHL	0.24	786	202	1030	1858	47	94	207	0	21	9.50	64	0.9	19	12610
29	HHB	0.31	561	170	1368	1908	0	99	381	0	16	5.25	50	2.1	23	10620
30	HHB	0.22	695	166	1282	1857	41	82	291	0	47	8.25	64	1.8	20	13220
31	HHB	0.22	773	180	1140	1857	45	91	283	0	78	8.50	70	1.9	127	12890
32	HHB	0.22	773	180	1140	1857	45	91	283	0	78	8.50	63	1.8	127	14400
33-1	NHL	0.45	605	272	1270	1849	0	0	0	0	0	3.00	78	1.6	8	5360
33-2++	NHL	0.45	605	272	1270	1849	0	0	0	0	0	5.50	82	1.7	8	5230
34	NHL	0.45	605	272	1270	1849	0	0	0	0	0	2.25	84	1.6	12	5440
35	NNL	0.44	602	265	1444	1661	0	0	0	0	0	5.50	75	3.0	13	5330
36	NHL	0.45	605	272	1270	1849	0	0	0	0	0	3.00	79	1.8	7	5060
37	NNL	0.44	511	225	1564	1661	0	0	0	0	0	2.50	78	4.5	22	4800
38	NNL	0.44	511	225	1564	1661	0	0	0	0	0	2.00	55	3.4	15	5080
39	HHB	0.22	696	168	1283	1854	41	82	329	0	47	7.00	56	1.8	119	14450
40	HHB	0.22	696	168	1283	1854	41	82	329	0	47	8.00	58	1.6	135	15650
41-1	HHL	0.33	548	182	1427	1803	0	83	132	44	0	4.00	53	2.0	25	10180
41-2++	HHL	0.33	548	182	1427	1803	0	83	132	44	0	8.00	62	2.0	15	10500

Table 2.3
Concrete mix proportions (lb/yd³) and properties (continued)

Group	Concrete	w/cm	Cement	Water	Fine	Coarse	Fly	Silica	Superplasticizer	Retarder	Slump	Concrete	Air	Test	Cylinder	
	Series*	Ratio**		Agg.***	Agg.	Ash	Fume ⁺	Type F	Type G	Type A		Temperature	Content	Age	Strength	
			(lb/yd ³)	(oz/yd ³)	(oz/yd ³)	(in.)	(F°)	(%)	(days)	(psi)						
42	HNL	0.24	810	226	1155	1600	122	81	608	0	108	11.00	56	1.9	15	11930
43	HNL	0.24	810	226	1155	1600	122	81	608	0	108	10.50	65	1.8	16	11530

* Series of Concrete, SCA:

S = Concrete Strength [N = normal strength ($f_c < 8000$ psi), H = high strength ($f_c \geq 8000$ psi)]

C = coarse aggregate content in concrete (N = normal content, H = high content)

A = type of coarse aggregate,

L - Crushed Limestone from Fogel's Quarry, Ottawa, KS

Bulk Specific Gravity (SSD) = 2.58; Absorption = 2.7%; Maximum Size = 3/4 in.

Unit Weight = 90.5 lb/ft³

B - Basalt from Iron Mountain Trap Rock Company

Bulk Specific Gravity (SSD) = 2.64; Absorption = 0.44%; Maximum Size = 3/4 in.

Unit Weight = 95.5 lb/ft³

** water-cement ratio or water-cementitious material ratio

*** Kansas River Sand from Lawrence Sand Co., Lawrence, KS

+ Silica Fume from Master Builders Technologies, Inc.

++ For specimen No. 5 and No. 6 in the group

1 lb/yd³ = 0.5993 kg/m³; 1 oz = 29.57 cm³; 1 psi = 6.895 kPa; 1 in. = 25.4 mm

Table 2.4a
Number of cracks and crack widths at a bar stress of 20 ksi

Specimen Label*	Bar Designation	Number of Cracks +		Max. Crack Width ++		Sum of Crack Widths **	
		East Side	West Side	East Side (in.)	West Side (in.)	East Side (in.)	West Side (in.)
28.1-B-S-U	11F3	4	4	0.004	0.003	0.013	0.011
28.2-B-S-C	11F3	3	3	0.003	0.003	0.008	0.009
28.3-B-S-U	11F3	4	4	0.003	0.003	0.011	0.011
28.4-B-S-C	11F3	3	3	0.005	0.004	0.010	0.010
28.5-B-S-U	11F3	3	3	0.003	0.003	0.008	0.008
28.6-B-S-C	11F3	2	3	0.004	0.004	0.008	0.009
29.1-B-S-U	8N1	7	4	0.002	0.001	0.009	0.004
29.2-B-S-U	8N0	6	5	0.001	0.001	0.006	0.005
29.3-B-S-U	8N1	5	5	0.001	0.001	0.005	0.005
29.4-B-S-U	8N0	6	7	0.001	0.001	0.006	0.007
29.5-B-S-U	8N1	3	4	0.001	0.001	0.003	0.004
29.6-B-S-U	8N0	3	4	0.001	0.001	0.003	0.004
30.1-B-S-U	11F3	4	3	0.002	0.003	0.007	0.008
30.2-B-S-C	11F3	3	2	0.003	0.003	0.008	0.005
30.3-B-S-U	11F3	5	4	0.002	0.002	0.006	0.006
30.4-B-S-C	11F3	3	3	0.002	0.002	0.006	0.004
30.5-B-S-U	11F3	2	2	0.003	0.003	0.005	0.005
30.6-B-S-C	11F3	2	2	0.002	0.002	0.004	0.004
31.1-B-S-U	8N1	2	2	0.002	0.002	0.004	0.004
31.2-B-S-C	8N1	2	2	0.002	0.003	0.004	0.005
31.3-B-S-U	8N0	2	3	0.002	0.002	0.004	0.006
31.4-B-S-C	8N0	2	2	0.002	0.003	0.004	0.005
31.5-B-S-U	8N1	4	4	0.002	0.002	0.006	0.008
31.6-B-S-U	8C0A	3	3	0.002	0.002	0.006	0.006
32.1-B-S-U	11F3	3	3	0.005	0.003	0.009	0.009
32.2-B-S-U	11B0	4	3	0.004	0.004	0.014	0.010
32.3-B-S-U	11F3	2	2	0.003	0.003	0.006	0.006
32.4-B-S-U	11B0	2	2	0.004	0.004	0.007	0.009
33.1-B-S-U	8N1	4	4	0.002	0.003	0.006	0.008
33.2-B-S-U	8C0A	4	4	0.002	0.002	0.008	0.008
33.3-B-S-U	8N1	2	2	0.002	0.003	0.005	0.004
33.4-B-S-U	8C0A	2	2	0.002	0.002	0.004	0.004
33.5-B-S-U	8N1	3	2	0.002	0.002	0.006	0.004
33.6-B-S-U	8C0A	4	2	0.003	0.003	0.008	0.005
34.1-B-S-U	8N1	2	2	0.002	0.003	0.003	0.006
34.2-B-N-U	8N1	2	2	0.003	0.002	0.005	0.004
34.3-B-S-U	8C0A	3	2	0.002	0.002	0.006	0.004
34.4-B-N-U	8C0A	2	3	0.002	0.002	0.004	0.005
35.1-B-S-U	8F1	3	2	0.002	0.002	0.006	0.004
35.2-T-S-U	8F1	3	2	0.002	0.002	0.006	0.004
35.3-B-S-U	8C0A	3	2	0.002	0.002	0.006	0.004
35.4-T-S-U	8C0A	3	2	0.002	0.002	0.006	0.004
36.1-B-S-U	8N1	4	4	0.002	0.002	0.008	0.008
36.2-B-S-U	8N1	3	4	0.003	0.002	0.007	0.008
36.3-B-S-U	8C0A	2	2	0.003	0.003	0.005	0.005
36.4-B-N-U	8C0A	2	2	0.002	0.003	0.004	0.005
37.1-B-D-U	8C0A	3	3	0.003	0.003	0.007	0.008
37.2-B-E-U	8C0A	4	3	0.002	0.002	0.008	0.006
37.3-B-S-C	8F1	5	5	0.002	0.003	0.008	0.011
37.4-B-S-U	8F1	4	4	0.003	0.003	0.009	0.009
38.1-B-N-U	8C0A	2	3	0.002	0.002	0.004	0.006
38.2-B-S-U	8C0A	3	3	0.003	0.002	0.008	0.006
38.3-B-S-U	8N1	4	4	0.002	0.002	0.008	0.008
38.4-B-S-U	8N1	5	4	0.003	0.002	0.010	0.007

Table 2.4a
Number of cracks and crack widths at a bar stress of 20 ksi (continued)

Label*	Specimen Designation	Number of Cracks +		Max. Crack Width ++		Sum of Crack Widths **	
		East Side	West Side	East Side (in.)	West Side (in.)	East Side (in.)	West Side (in.)
38.5-B-S-U	8N1	2	3	0.002	0.002	0.004	0.006
38.6-B-S-U	8N1	2	3	0.002	0.002	0.004	0.006
39.1-B-S-C	8N1	3	4	0.003	0.003	-	-
39.2-B-S-U	8C1	3	5	0.003	0.003	-	-
39.3-B-S-U	8N0	3	3	0.003	0.003	-	-
39.4-B-S-C	8N0	3	2	0.003	0.003	-	-
39.5-B-S-C	8C1	3	3	0.004	0.004	-	-
39.6-B-S-U	8C1	4	4	0.003	0.003	-	-
40.1-B-S-U	11F3	4	3	0.003	0.005	-	-
40.2-B-S-C	11F3	3	3	0.003	0.006	-	-
40.3-B-S-C	11N0	3	2	0.006	0.006	-	-
40.4-B-S-U	11N0	5	4	0.003	0.003	-	-
40.5-B-S-U	8N0	1	0	0.003	0.000	-	-
40.6-B-S-C	8N0	3	2	0.003	0.005	-	-
41.1-B-S-U	8N3	2	3	0.001	0.002	-	-
41.2-B-S-U	8N3	5	6	0.002	0.002	-	-
41.3-B-S-U	8N3	5	5	0.002	0.002	-	-
41.4-B-S-U	8N0	6	4	0.002	0.002	-	-
41.5-B-N-U	8C0	1	2	0.002	0.004	-	-
41.6-B-S-U	8C0	2	2	0.002	0.002	-	-
42.1-B-S-U	8N0	-	-	-	-	-	-
42.2-B-S-C	8N0	-	-	-	-	-	-
42.3-B-S-C	8N0	-	-	-	-	-	-
42.4-B-S-U	8N0	-	-	-	-	-	-
42.5-B-S-U	8N0	-	-	-	-	-	-
42.6-B-S-C	8N0	-	-	-	-	-	-
43.1-B-S-C	8N3	4	3	0.004	0.003	-	-
43.2-B-S-U	8N3	3	3	0.004	0.003	-	-
43.3-B-S-U	8N3	4	5	0.002	0.003	-	-
43.4-B-S-C	8N3	3	4	0.005	0.005	-	-
43.5-B-S-C	8N3	3	5	0.003	0.003	-	-
43.6-B-S-U	8N3	4	5	0.003	0.002	-	-

* See Table 2.1 for notation of the specimen label

** Sum of flexural cracks width on east and west sides of splices in constant moment region, but outside of splice region, at a bar stress of 40 ksi

+ Number of flexural cracks in the constant moment region, but outside splice region, at a bar stress of 40 ksi;
West Side = west side of splice region; East Side = east side of splice region

++ Maximum flexural crack width in the constant moment region, but outside splice region, at a bar stress of 40 ksi

Table 2.4b
Number of cracks and crack widths at a bar stress of 30 ksi

Specimen Label*	Bar Designation	Number of Cracks +		Max. Crack Width ++		Sum of Crack Widths **	
		East Side	West Side	East Side (in.)	West Side (in.)	East Side (in.)	West Side (in.)
28.1-B-S-U	11F3	5	5	0.007	0.007	0.025	0.026
28.2-B-S-C	11F3	4	4	0.012	0.012	0.035	0.034
28.3-B-S-U	11F3	5	4	0.006	0.007	0.022	0.026
28.4-B-S-C	11F3	5	3	0.006	0.009	0.031	0.028
28.5-B-S-U	11F3	3	3	0.009	0.009	0.023	0.024
28.6-B-S-C	11F3	2	3	0.013	0.012	0.026	0.032
29.1-B-S-U	8N1	8	8	0.004	0.003	0.017	0.016
29.2-B-S-U	8N0	8	7	0.003	0.003	0.019	0.014
29.3-B-S-U	8N1	7	7	0.003	0.004	0.016	0.016
29.4-B-S-U	8N0	7	8	0.003	0.003	0.016	0.019
29.5-B-S-U	8N1	7	6	0.003	0.003	0.014	0.011
29.6-B-S-U	8N0	6	8	0.003	0.003	0.012	0.014
30.1-B-S-U	11F3	5	5	0.005	0.006	0.020	0.020
30.2-B-S-C	11F3	4	3	0.008	0.008	0.022	0.018
30.3-B-S-U	11F3	5	5	0.006	0.005	0.020	0.018
30.4-B-S-C	11F3	4	4	0.007	0.007	0.019	0.021
30.5-B-S-U	11F3	2	3	0.008	0.009	0.015	0.019
30.6-B-S-C	11F3	3	2	0.008	0.009	0.016	0.017
31.1-B-S-U	8N1	5	6	0.005	0.005	0.018	0.020
31.2-B-S-C	8N1	4	4	0.007	0.007	0.022	0.020
31.3-B-S-U	8N0	3	4	0.005	0.006	0.014	0.018
31.4-B-S-C	8N0	4	4	0.006	0.007	0.022	0.023
31.5-B-S-U	8N1	5	5	0.006	0.006	0.024	0.023
31.6-B-S-U	8C0A	5	6	0.007	0.006	0.021	0.023
32.1-B-S-U	11F3	4	4	0.007	0.008	0.018	0.021
32.2-B-S-U	11B0	4	4	0.008	0.008	0.029	0.022
32.3-B-S-U	11F3	3	4	0.009	0.008	0.022	0.022
32.4-B-S-U	11B0	3	3	0.009	0.009	0.025	0.023
33.1-B-S-U	8N1	4	4	0.007	0.006	0.016	0.019
33.2-B-S-U	8C0A	4	4	0.006	0.006	0.023	0.022
33.3-B-S-U	8N1	4	4	0.006	0.006	0.020	0.018
33.4-B-S-U	8C0A	4	4	0.005	0.005	0.018	0.018
33.5-B-S-U	8N1	4	4	0.005	0.005	0.017	0.018
33.6-B-S-U	8C0A	4	4	0.006	0.006	0.017	0.020
34.1-B-S-U	8N1	4	3	0.005	0.005	0.018	0.013
34.2-B-N-U	8N1	4	4	0.006	0.005	0.019	0.017
34.3-B-S-U	8C0A	4	3	0.008	0.007	0.017	0.018
34.4-B-N-U	8C0A	4	4	0.006	0.007	0.017	0.023
35.1-B-S-U	8F1	3	4	0.006	0.006	0.017	0.015
35.2-T-S-U	8F1	4	3	0.007	0.009	0.024	0.020
35.3-B-S-U	8C0A	4	4	0.006	0.006	0.019	0.021
35.4-T-S-U	8C0A	4	4	0.007	0.007	0.022	0.021
36.1-B-S-U	8N1	4	4	0.005	0.005	0.020	0.019
36.2-B-S-U	8N1	4	6	0.007	0.005	0.021	0.023
36.3-B-S-U	8C0A	2	4	0.007	0.006	0.013	0.017
36.4-B-N-U	8C0A	3	4	0.006	0.006	0.013	0.017
37.1-B-D-U	8C0A	4	3	0.006	0.007	0.016	0.020
37.2-B-E-U	8C0A	4	3	0.006	0.006	0.020	0.018
37.3-B-S-C	8F1	5	5	0.004	0.003	0.018	0.012
37.4-B-S-U	8F1	6	6	0.005	0.005	0.023	0.022
38.1-B-N-U	8C0A	3	3	0.006	0.006	0.017	0.016
38.2-B-S-U	8C0A	3	3	0.008	0.008	0.022	0.019

Table 2.4b
Number of cracks and crack widths at a bar stress of 30 ksi (continued)

Specimen Label*	Bar Designation	Number of Cracks +		Max. Crack Width ++		Sum of Crack Widths **	
		East Side	West Side	East Side (in.)	West Side (in.)	East Side (in.)	West Side (in.)
38.3-B-S-U	8N1	4	5	0.006	0.005	0.020	0.018
38.4-B-S-U	8N1	5	5	0.006	0.007	0.025	0.023
38.5-B-S-U	8N1	4	4	0.005	0.005	0.016	0.017
38.6-B-S-U	8N1	4	4	0.006	0.005	0.018	0.015
39.1-B-S-C	8N1	4	5	0.009	0.009	-	-
39.2-B-S-U	8C1	6	6	0.008	0.006	-	-
39.3-B-S-U	8N0	7	7	0.009	0.007	-	-
39.4-B-S-C	8N0	5	5	0.008	0.009	-	-
39.5-B-S-C	8C1	5	5	0.009	0.009	-	-
39.6-B-S-U	8C1	5	5	0.008	0.007	-	-
40.1-B-S-U	11F3	5	3	0.007	0.009	-	-
40.2-B-S-C	11F3	4	4	0.009	0.009	-	-
40.3-B-S-C	11N0	4	3	0.009	0.009	-	-
40.4-B-S-U	11N0	5	5	0.008	0.009	-	-
40.5-B-S-U	8N0	4	5	0.007	0.007	-	-
40.6-B-S-C	8N0	4	3	0.009	0.009	-	-
41.1-B-S-U	8N3	5	4	0.006	0.006	-	-
41.2-B-S-U	8N3	7	7	0.005	0.005	-	-
41.3-B-S-U	8N3	6	7	0.005	0.005	-	-
41.4-B-S-U	8N0	6	6	0.006	0.004	-	-
41.5-B-N-U	8C0	5	4	0.005	0.006	-	-
41.6-B-S-U	8C0	5	5	0.005	0.005	-	-
42.1-B-S-U	8N0	5	4	0.007	0.007	-	-
42.2-B-S-C	8N0	3	4	0.009	0.009	-	-
42.3-B-S-C	8N0	5	5	0.008	0.007	-	-
42.4-B-S-U	8N0	5	5	0.006	0.007	-	-
42.5-B-S-U	8N0	6	6	0.005	0.005	-	-
42.6-B-S-C	8N0	7	5	0.006	0.009	-	-
43.1-B-S-C	8N3	5	5	0.009	0.008	-	-
43.2-B-S-U	8N3	5	5	0.008	0.007	-	-
43.3-B-S-U	8N3	6	5	0.006	0.006	-	-
43.4-B-S-C	8N3	5	5	0.008	0.010	-	-
43.5-B-S-C	8N3	5	6	0.007	0.009	-	-
43.6-B-S-U	8N3	5	6	0.007	0.006	-	-

* See Table 2.1 for notation of the specimen label

** Sum of flexural cracks width on east and west sides of splices in constant moment region, but outside of splice region, at a bar stress of 40 ksi

+ Number of flexural cracks in the constant moment region, but outside splice region, at a bar stress of 40 ksi;
 West Side = west side of splice region; East Side = east side of splice region

++ Maximum flexural crack width in the constant moment region, but outside splice region, at a bar stress of 40 ksi

Table 2.4c
Number of cracks and crack widths at a bar stress of 40 ksi

Specimen Label*	Bar Designation	Number of Cracks +		Max. Crack Width ++		Sum of Crack Widths **	
		East Side	West Side	East Side (in.)	West Side (in.)	East Side (in.)	West Side (in.)
28.1-B-S-U	11F3	5	6	0.013	0.013	0.048	0.053
28.2-B-S-C	11F3	4	4	0.018	0.018	0.049	0.050
28.3-B-S-U	11F3	5	6	0.009	0.014	0.034	0.042
28.4-B-S-C	11F3	5	3	0.018	0.017	0.046	0.043
28.5-B-S-U	11F3	3	4	0.015	0.015	0.038	0.037
28.6-B-S-C	11F3	2	3	-	-	-	-
29.1-B-S-U	8N1	8	8	0.007	0.005	0.024	0.024
29.2-B-S-U	8N0	8	8	0.006	0.006	0.032	0.022
29.3-B-S-U	8N1	7	8	0.007	0.007	0.033	0.026
29.4-B-S-U	8N0	8	8	0.007	0.007	0.028	0.030
29.5-B-S-U	8N1	8	8	0.006	0.006	0.025	0.026
29.6-B-S-U	8N0	7	8	0.006	0.006	0.023	0.024
30.1-B-S-U	11F3	5	5	0.009	0.009	0.03	0.029
30.2-B-S-C	11F3	4	3	0.013	0.013	0.038	0.036
30.3-B-S-U	11F3	6	5	0.010	0.009	0.031	0.030
30.4-B-S-C	11F3	4	4	0.015	0.015	0.037	0.039
30.5-B-S-U	11F3	3	3	0.016	0.015	0.031	0.035
30.6-B-S-C	11F3	2	3	0.018	0.018	0.033	0.027
31.1-B-S-U	8N1	6	6	0.009	0.009	0.036	0.039
31.2-B-S-C	8N1	4	4	0.011	0.011	0.036	0.036
31.3-B-S-U	8N0	5	6	0.010	0.009	0.033	0.035
31.4-B-S-C	8N0	4	4	0.011	0.011	0.04	0.041
31.5-B-S-U	8N1	5	6	0.010	0.010	0.042	0.037
31.6-B-S-U	8C0A	5	6	0.010	0.010	0.034	0.036
32.1-B-S-U	11F3	4	4	0.012	0.013	0.028	0.037
32.2-B-S-U	11B0	4	4	0.012	0.013	0.041	0.035
32.3-B-S-U	11F3	3	4	0.012	0.011	0.033	0.041
32.4-B-S-U	11B0	4	4	0.015	0.016	0.044	0.041
33.1-B-S-U	8N1	5	4	0.010	0.010	0.031	0.033
33.2-B-S-U	8C0A	4	4	0.010	0.010	0.039	0.036
33.3-B-S-U	8N1	4	4	0.009	0.009	0.029	0.030
33.4-B-S-U	8C0A	4	5	0.009	0.009	0.035	0.033
33.5-B-S-U	8N1	5	4	0.010	0.010	0.038	0.032
33.6-B-S-U	8C0A	4	4	0.010	0.010	0.035	0.036
34.1-B-S-U	8N1	4	4	0.009	0.010	0.038	0.031
34.2-B-N-U	8N1	4	4	0.010	0.010	0.035	0.037
34.3-B-S-U	8C0A	4	4	0.013	0.010	0.031	0.036
34.4-B-N-U	8C0A	5	5	0.012	0.010	0.035	0.036
35.1-B-S-U	8F1	4	5	0.010	0.010	0.031	0.031
35.2-T-S-U	8F1	4	3	0.013	0.015	0.042	0.037
35.3-B-S-U	8C0A	4	4	0.010	0.011	0.036	0.039
35.4-T-S-U	8C0A	4	3	0.013	0.013	0.041	0.037
36.1-B-S-U	8N1	4	4	0.009	0.009	0.032	0.030
36.2-B-S-U	8N1	5	6	0.010	0.009	0.033	0.035
36.3-B-S-U	8C0A	3	4	0.010	0.009	0.028	0.034
36.4-B-N-U	8C0A	3	4	0.010	0.008	0.026	0.029
37.1-B-D-U	8C0A	4	3	0.010	0.010	0.031	0.030
37.2-B-E-U	8C0A	4	3	0.010	0.010	0.033	0.029
37.3-B-S-C	8F1	5	4	0.011	0.011	0.022	0.021
37.4-B-S-U	8F1	6	6	0.009	0.010	0.042	0.043
38.1-B-N-U	8C0A	3	4	0.010	0.010	0.030	0.031

Table 2.4c
Number of cracks and crack widths at a bar stress of 40 ksi (continued)

Specimen Label*	Bar Designation	Number of Cracks +		Max. Crack Width ++		Sum of Crack Widths **	
		East Side	West Side	East Side (in.)	West Side (in.)	East Side (in.)	West Side (in.)
38.2-B-S-U	8C0A	3	3	0.010	0.010	0.029	0.030
38.3-B-S-U	8N1	5	6	0.009	0.008	0.029	0.026
38.4-B-S-U	8N1	5	6	0.010	0.010	0.039	0.038
38.5-B-S-U	8N1	5	4	0.010	0.010	0.034	0.035
38.6-B-S-U	8N1	4	4	0.010	0.009	0.031	0.034
39.1-B-S-C	8N1	5	6	0.016	0.013	-	-
39.2-B-S-U	8C1	7	6	0.010	0.010	-	-
39.3-B-S-U	8N0	7	6	0.011	0.009	-	-
39.4-B-S-C	8N0	6	5	0.016	0.013	-	-
39.5-B-S-C	8C1	5	5	0.016	0.014	-	-
39.6-B-S-U	8C1	5	5	0.011	0.010	-	-
40.1-B-S-U	11F3	5	6	0.011	0.013	-	-
40.2-B-S-C	11F3	4	5	0.016	0.015	-	-
40.3-B-S-C	11N0	4	3	0.010	0.009	-	-
40.4-B-S-U	11N0	5	5	0.013	0.012	-	-
40.5-B-S-U	8N0	5	5	0.010	0.010	-	-
40.6-B-S-C	8N0	4	3	0.016	0.015	-	-
41.1-B-S-U	8N3	6	5	0.010	0.010	-	-
41.2-B-S-U	8N3	7	8	0.009	0.009	-	-
41.3-B-S-U	8N3	6	8	0.010	0.009	-	-
41.4-B-S-U	8N0	7	8	0.009	0.009	-	-
41.5-B-N-U	8C0	5	5	0.009	0.009	-	-
41.6-B-S-U	8C0	5	6	0.009	0.009	-	-
42.1-B-S-U	8N0	6	6	0.010	0.010	-	-
42.2-B-S-C	8N0	4	4	0.016	0.015	-	-
42.3-B-S-C	8N0	5	5	0.016	0.016	-	-
42.4-B-S-U	8N0	6	7	0.011	0.010	-	-
42.5-B-S-U	8N0	7	6	0.010	0.010	-	-
42.6-B-S-C	8N0	7	5	0.012	0.016	-	-
43.1-B-S-C	8N3	5	5	0.015	0.013	-	-
43.2-B-S-U	8N3	6	6	0.010	0.011	-	-
43.3-B-S-U	8N3	6	6	0.010	0.010	-	-
43.4-B-S-C	8N3	5	5	0.013	0.015	-	-
43.5-B-S-C	8N3	5	6	0.013	0.015	-	-
43.6-B-S-U	8N3	7	6	0.010	0.010	-	-

* See Table 2.1 for notation of the specimen label

** Sum of flexural cracks width on east and west sides of splices in constant moment region, but outside of splice region, at a bar stress of 40 ksi

+ Number of flexural cracks in the constant moment region, but outside splice region, at a bar stress of 40 ksi;
 West Side = west side of splice region; Ease Side = east side of splice region

++ Maximum flexural crack width in the constant moment region, but outside splice region, at a bar stress of 40 ksi

Table 3.1
Comparison of bottom-cast and top-cast splice specimens

Specimen Label [†]	Bar Designation	Cast Position	Surface Condition	Concrete Slump (in)	Transverse Stirrups	f _s (Test) (ksi)	f _s * (Prediction) (ksi)	Bottom** Top
24.1-B-S-U	8N1	Bottom	uncoated	4.00	w/o	61.78	67.25	1.058
24.3-T-S-U	8N1	Top	uncoated	4.00	w/o	59.83	68.91	
24.2-B-S-C	8N1	Bottom	coated	4.00	w/o	55.21	66.82	1.035
24.4-T-S-C	8N1	Top	coated	4.00	w/o	55.27	69.26	
25.1-B-S-U	5C3	Bottom	uncoated	3.75	w/o	63.73	61.98	0.975
25.3-T-S-U	5C3	Top	uncoated	3.75	w/o	64.32	61.00	
25.2-B-S-C	5C3	Bottom	coated	3.75	w/o	67.59	61.21	1.059
25.4-T-S-C	5C3	Top	coated	3.75	w/o	62.98	60.39	
26.3-B-S-U	8N1	Bottom	uncoated	5.00	w/o	62.34	61.46	1.046
26.4-T-S-U	8N1	Top	uncoated	5.00	w/o	60.74	62.62	
26.5-B-S-U	8N0	Bottom	uncoated	5.00	w/o	64.24	62.01	1.033
26.6-T-S-U	8N0	Top	uncoated	5.00	w/o	62.41	62.21	
26.1-B-S-U	8N1	Bottom	uncoated	5.00	w/	64.74	66.79	1.172
26.2-T-S-U	8N1	Top	uncoated	5.00	w/	55.35	66.94	
35.1-B-S-U	8F1	Bottom	uncoated	5.50	w/	68.24	68.53	1.224
35.2-T-S-U	8F1	Top	uncoated	5.50	w/	56.07	68.91	
35.3-B-S-U	8C0A	Bottom	uncoated	5.50	w/	61.54	61.06	1.138
35.4-T-S-U	8C0A	Top	uncoated	5.50	w/	55.40	62.55	
For 3 pairs of uncoated high R _t bars w/o stirrups:							Max.	1.058
							Min.	0.975
							Avg.	1.026
For 1 pair of uncoated conventional bars w/o stirrups:							1.033	
For 2 pairs of uncoated high R _t bars w/ stirrups							Max.	1.224
							Min.	1.172
							Avg.	1.198
For 1 pair of uncoated conventional bars w/ stirrups:							1.138	
For all 5 pairs of uncoated high R _t bars:							Max.	1.224
							Min.	0.975
							Avg.	1.095
For all 2 pairs of uncoated conventional bars :							Max.	1.033
							Min.	1.138
							Avg.	1.085
For 2 pairs of coated high R _t bars w/o stirrups:							Max.	1.035
							Min.	1.059
							Avg.	1.047

+ See Table 2.2 for specimen label notation

* Predicted bar stress using Eq. 3.1 and Eq. 3.2 for the splices not confined and confined by stirrups in splice region, respectively.

** Normalized splice strength ratio of Bottom-cast to Top-cast splice specimens

1 in. = 25.4 mm; 1 psi = 6.895 kPa; 1 ksi = 6.895 MPa

Table 3.2
Comparison of symmetrical and unsymmetrical splice specimens

Specimen Label *	Bar Designation	l_s (in.)	f_c (psi)	Clear Spacing*		Avg. c_{si} (in)	Min. c_{si} (in)	Transverse Stirrups	f_s (Test) (ksi)	Predicted Stress**		US+	Test/Prediction	
				Small (in)	Large (in)					f_{sl} (ksi)	f_{sll} (ksi)		$\frac{f_s}{f_{sl}}$	$\frac{f_s}{f_{sll}}$
19.1-B-S-U	8N3	36.0	4250	3.875	3.844	1.930	w/o	73.53	73.03			0.925		
19.2-B-N-U	8N3	36.0	4250	2.000	5.531	1.883	1.000	w/o	67.86	72.82	60.92		0.932	1.114
34.1-B-S-U	8N1	24.0	5440	3.813	3.938	1.938	w/o	57.78	58.70			1.075		
34.2-B-N-U	8N1	24.0	5440	1.938	5.844	1.945	0.969	w/o	61.86	58.44	49.97		1.058	1.238
34.3-B-S-U	8C0A	24.0	5440	3.563	3.813	1.844	w/o	58.70	59.25			1.004		
34.4-B-N-U	8C0A	24.0	5440	2.031	5.500	1.883	1.016	w/o	58.29	58.58	50.52		0.995	1.154
36.3-B-S-U	8C0A	26.0	5060	3.578	3.766	1.836	w/o	62.53	61.41			0.960		
36.4-B-N-U	8C0A	26.0	5060	1.125	6.188	1.828	0.563	w/o	59.94	61.30	48.20		0.978	1.244
38.2-B-S-U	8C0A	26.0	5080	3.688	3.688	1.844	w/o	60.54	62.73			0.958		
38.1-B-N-U	8C0A	26.0	5080	1.000	6.813	1.953	0.500	w/o	54.17	58.60	46.85		0.924	1.156
19.3-B-S-U	8N3	30.0	4250	3.750	3.844	1.898	w/	71.46	75.50			1.085		
19.4-B-N-U	8N3	30.0	4250	2.000	5.563	1.891	1.000	w/	77.31	75.31	62.45		1.026	1.238
20.1-B-S-U	11F3	40.0	5080	2.625	2.625	1.313	w/	71.09	76.41			1.011		
20.2-B-N-U	11F3	40.0	5080	1.531	3.656	1.297	0.766	w/	71.79	76.29	71.91		0.941	0.998
20.3-B-S-U	11F3	40.0	5080	2.625	2.625	1.313	w/	68.53	66.99			0.987		
20.4-B-N-U	11F3	40.0	5080	1.531	3.656	1.297	0.766	w/	67.67	66.98	62.62		1.010	1.081
23a.1-B-S-U	8N3	21.0	9080	3.688	3.719	1.852	w/	78.64	87.96			1.031		
23a.3-B-N-U	8N3	21.0	9080	1.984	5.625	1.902	0.992	w/	80.57	87.45	71.85		0.921	1.121
41.6-B-S-U	8C0A	16.0	10500	3.750	3.750	1.875	w/	65.38	68.63			1.010		
41.5-B-N-U	8C0A	16.0	10500	1.000	6.500	1.875	0.500	w/	66.01	68.60	56.61		0.962	1.166
For 5 pairs w/o stirrups:										Max.	1.075	1.058	1.244	
										Min.	0.925	0.924	1.114	
										Average	0.985	0.977	1.181	
For 5 pairs w/ stirrups:										Max.	1.085	1.026	1.238	
										Min.	0.987	0.921	0.998	
										Average	1.025	0.972	1.121	
For all 10 pairs:										Max	1.085	1.058	1.244	
										Min.	0.925	0.921	0.998	
										Average	1.005	0.975	1.151	
										Std	0.050	0.047	0.078	
										COV	0.050	0.048	0.068	

+ See Table 2.2 for specimen label notation

++ Normalized splice strength ratio of unsymmetrical to symmetrical splice specimens based on f_{sll}

* Clear spacing between splices

** Predicted bar stress using Eq. 3.1 and Eq. 3.2 for the specimens not confined or confined by stirrups in splice region;

f_{sl} = predicted bar stress using average clear bar spacing

f_{sll} = predicted bar stress using minimum clear bar spacing for unsymmetrical specimens only

1 in. = 25.4 mm; 1 psi = 6.895 kPa; 1 ksi = 6.895 MPa

Table 3.3: Comparison of splice strength between one spliced layer and two spliced layers

Specimen Label	l_s	d_b	c_{so}	c_b	c_{si} H *	c_{si} V **	f_c	f_s (Test)	Predicted f_{sh}^+ (ksi)	Predicted f_{sv}^{++} (ksi)	Test/Prediction Ratio	$f_s(37.2)^{+++}$ f_s/f_{sh}	f_s/f_{sv}	$f_s(37.1)$
37.1-B-D-U***	32	1.000	2.000	1.965	1.813	-	4800	59.97	69.39	-	0.864			
37.2-B-D-U****	32	1.000	2.000	1.954	1.781	0.500	4800	61.40	69.21	52.40	0.887	1.172	1.024	

* One half of clear spacing (horizontal) between splices in one layer

** One half of clear spacing (vertical) between two spliced layers

*** The bottom layer was spliced and the second layer consisted of continuous bars

**** Both layers were spliced

+ Bar stress calculated using Eq. 3.1 and $c_{si} H$

++ Bar stress calculated using Eq. 3.1 and $c_{si} V$

+++ Ratio of test bar stress of specimen 37.2 to specimen 37.1

1 in. = 25.4 mm; 1 psi = 6.895 kPa; 1 ksi = 6.895 MPa

Table 3.4
Effect of shear force on splice strength

Specimen No.	Bar Designation	l_s (in)	f_c (psi)	Transverse Stirrups	Max. $f_s +$ (Test)	$\frac{\text{Min } f_s ++}{\text{Max } f_s}$ (Predicted)	$f_s +++,$ (ksi)	Test Prediction
22.3	11F3	33.0	6300	w/	71.66*	0.56	63.64	1.126
22.5	11F3	33.0	6300	w/o	> 62.41**	0.57	59.68	> 1.046
23b.5	11F3	25.0	4500	w/	54.80	0.66	50.04	1.095

+ Maximum bar stress at the end of the splices closest to the applied load (see Figs. 2.3 and 2.4)

++ Ratio of minimum to maximum bar stresses in splices; the minimum stress occurred at the end of the splice closest to the reaction support

+++ Predicted bar stress determined using Eqs. 3.1 and 3.2 for the splices that were not confined and confined by stirrups, respectively

*

Specimen exhibited flexural failure, with bar yielding and concrete crushing at the middle section of the beam; splices did not fail

** Beam was not tested to failure due to capacity of loading system

1 in. = 25.4 mm, 1 psi = 6.895 kPa, 1 ksi = 6.895 MPa

Table 4.1
Splice specimen properties and test results from Darwin et al. (1995a, 1996a)

Specimen No. +	Bar ++ Designation	R _r	n	l _s (in.)	d _b (in.)	b (in.)	h (in.)	c _{so} (in.)	c _{si} (in.)	c _b (in.)	l (in.)	l _c (in.)	d (in.)	f _c (psi)	N	d _s (in.)	f _y (ksi)	f _{yt} (ksi)	M _u (k-in.)	f _s * (ksi)
1.1	8C1	0.101	2	16.00	1.000	16.08	17.22	2.969	2.938	2.938	13.00	4.00	13.76	5020	-	-	67.69	-	1021	51.78
1.2	8C1	0.101	2	16.00	1.000	24.06	16.25	2.032	2.281	1.938	13.00	4.00	13.79	5020	-	-	67.69	-	1746	44.77
1.3	8C1	0.101	3	16.00	1.000	16.07	16.21	2.032	1.438	1.938	13.00	4.00	13.75	5020	-	-	67.69	-	1310	45.22
1.4	8C1**	0.101	3	16.00	1.000	16.11	16.20	2.032	1.375	1.938	13.00	4.00	13.74	5020	-	-	67.69	-	1079	37.15
1.5	8C1	0.101	3	16.00	1.000	16.07	16.19	2.063	1.375	1.938	13.00	4.00	13.74	5020	5	0.500	67.69	70.75	1518	52.54
1.6	8C1	0.101	3	16.00	1.000	16.05	16.19	2.063	1.438	1.938	13.00	4.00	13.74	5020	3	0.500	67.69	70.75	1511	52.30
2.1	8S0	0.071	2	24.00	1.000	12.12	15.56	2.250	1.706	1.328	16.00	6.00	13.70	5250	7	0.375	64.52	69.92	1214	62.81
2.2	8F1	0.140	2	24.00	1.000	12.12	15.52	2.125	1.801	1.406	16.00	6.00	13.58	5250	7	0.375	75.42	69.92	1526	77.78
2.3	8F1	0.140	2	24.00	1.000	12.11	16.06	2.125	1.780	1.969	16.00	6.00	13.56	5250	4	0.375	75.42	69.92	1413	74.12
2.4	8F1	0.140	2	24.00	1.000	12.13	15.64	2.000	1.914	1.313	16.00	6.00	13.79	5250	-	-	75.42	-	1059	54.29
2.5	8F1	0.140	2	24.00	1.000	12.13	16.01	2.063	1.856	1.813	16.00	6.00	13.67	5250	-	-	75.42	-	1138	58.97
2.6	8F1**	0.140	2	24.00	1.000	12.12	16.19	2.000	1.917	1.938	16.00	6.00	13.67	5250	-	-	75.42	-	961	49.52
3.4	8C0	0.085	2	24.00	1.000	12.14	16.26	2.110	1.857	2.000	16.00	6.00	13.73	5110	4	0.375	64.72	69.92	1087	56.07
3.5	8C0	0.085	3	28.00	1.000	12.17	16.17	1.001	0.965	1.906	16.00	6.00	13.74	3810	8	0.375	64.72	69.92	1479	53.05
4.1	8S0	0.071	2	24.00	1.000	12.16	15.49	2.063	1.926	1.250	16.00	6.00	13.72	4090	6	0.500	64.52	70.75	1211	63.33
4.2	8F1	0.140	2	24.00	1.000	12.17	15.59	2.094	1.848	1.313	16.00	6.00	13.74	4090	8	0.375	75.42	69.92	1403	73.54
4.4	8C1	0.101	2	24.00	1.000	12.15	15.47	2.032	1.978	1.219	16.00	6.00	13.73	4090	4	0.375	67.69	69.92	1141	59.55
4.5	8C1	0.101	2	24.00	1.000	12.12	16.15	2.063	1.936	1.844	16.00	6.00	13.79	4090	-	-	67.69	-	994	51.50
4.6	8C1**	0.101	2	24.00	1.000	12.16	16.23	2.094	1.926	2.000	16.00	6.00	13.79	4090	-	-	67.69	-	808	41.97
5.1	8SH0	0.065	3	24.00	1.000	18.22	15.57	2.016	1.914	1.250	16.00	6.00	13.79	4190	7	0.375	65.70	69.92	1888	65.43
5.2	8F1	0.140	3	24.00	1.000	18.16	15.62	2.078	1.867	1.359	16.00	6.00	13.73	4190	7	0.375	75.42	69.92	1902	66.26
5.3	8F1	0.140	2	24.00	1.000	12.11	15.50	2.063	1.849	1.281	16.00	6.00	13.68	4190	7	0.375	75.42	69.92	1311	68.83
5.4	8SH0	0.065	2	24.00	1.000	12.12	15.46	1.985	1.980	1.250	16.00	6.00	13.68	4190	7	0.375	65.70	69.92	1137	59.50
5.5	8C0	0.085	2	24.00	1.000	12.12	15.60	2.063	1.904	1.406	16.00	6.00	13.67	4190	4	0.375	64.72	69.92	896	46.74
5.6	8F1	0.140	2	22.00	1.000	12.11	15.69	2.094	1.807	1.313	16.00	6.00	13.84	4190	5	0.500	75.42	70.75	1297	67.22
6.1	8SH0	0.065	3	24.00	1.000	12.18	16.12	2.063	0.422	1.906	16.00	6.00	13.69	4220	8	0.500	65.70	66.42	1797	64.71
6.2	8F1	0.140	3	24.00	1.000	12.11	16.15	2.000	0.438	2.000	16.00	6.00	13.62	4220	8	0.500	75.42	66.42	2115	76.21
6.3	8F1	0.140	2	16.00	1.000	12.13	15.51	2.000	1.906	1.344	16.00	6.00	13.63	4220	2	0.375	75.42	64.55	887	46.39
6.4	8C0	0.085	2	16.00	1.000	12.11	15.45	2.094	1.844	1.344	16.00	6.00	13.58	4220	2	0.375	64.72	64.55	703	36.83

Table 4.1

Splice specimen properties and test results from Darwin et al. (1995a, 1996a) (continued)

Specimen No. +	Bar ++	R _t	n	l _s (in.)	d _b (in.)	b (in.)	h (in.)	c _{sd} (in.)	c _{si} (in.)	c _b (in.)	l (in.)	l _e (in.)	d (in.)	f _c (psi)	N	d _s (in.)	f _y (ksi)	f _u (ksi)	M _u (k-in.)	f _i * (ksi)
No. +	Designation																			
6.5	8F1	0.140	2	24.00	1.000	12.10	16.13	2.000	1.906	1.969	16.00	6.00	13.63	4220	-	-	75.42	-	1031	54.06
6.6	8F1**	0.140	2	24.00	1.000	12.15	16.13	2.032	1.875	1.969	16.00	6.00	13.63	4220	-	-	75.42	-	955	50.01
7.1	8C1	0.140	2	16.00	1.000	12.00	16.18	2.079	1.797	1.875	16.00	6.00	13.77	4160	2	0.375	67.69	64.55	908	47.05
7.2	8C1	0.101	2	18.00	1.000	12.06	15.45	1.469	2.531	1.313	16.00	6.00	13.72	4160	5	0.500	67.69	84.70	1081	56.37
7.5	8F1	0.140	3	24.00	1.000	11.97	16.17	2.032	0.399	2.000	16.00	6.00	13.64	4160	8	0.500	75.42	84.70	2068	75.42
7.6	8C1	0.101	2	16.00	1.000	12.01	16.22	2.032	1.969	1.938	16.00	6.00	13.77	4160	2	0.375	67.69	64.55	862	44.62
8.1	8N0	0.069	3	24.00	1.000	12.13	16.23	2.032	0.453	1.953	16.00	6.00	13.76	3830	8	0.500	77.96	84.70	1983	72.14
8.2	8N3	0.119	3	24.00	1.000	12.16	16.20	2.047	0.430	1.969	16.00	6.00	13.69	3830	8	0.500	80.57	84.70	2247	85.08
8.3	8N0	0.072	2	24.00	1.000	12.11	16.05	2.000	1.953	2.000	16.00	6.00	13.53	3830	-	-	77.96	-	1171	62.38
8.4	8N3	0.119	2	16.00	1.000	12.10	16.35	2.063	1.891	1.906	16.00	6.00	13.91	3830	2	0.375	80.57	64.55	959	49.37
9.1	8N3	0.119	2	24.00	1.000	12.14	16.19	2.032	1.875	1.954	16.00	6.00	13.70	4230	2	0.375	80.57	64.55	1126	64.16
9.2	8F1	0.140	2	18.00	1.000	12.10	15.67	2.063	1.844	1.290	16.00	6.00	13.84	4230	6	0.375	75.42	64.55	1351	70.02
9.3	8N0	0.069	2	24.00	1.000	12.19	16.12	2.094	1.907	1.818	16.00	6.00	13.78	4230	2	0.375	77.96	64.55	1076	55.75
9.4	8F1	0.140	2	24.00	1.000	12.11	16.17	2.016	1.891	1.915	16.00	6.00	13.72	4230	2	0.375	75.42	64.55	1259	65.82
10.1	8N3**	0.119	2	26.00	1.000	12.15	16.16	2.016	1.907	1.896	16.00	6.00	13.78	4250	-	-	80.57	-	1120	58.36
10.2	8N3	0.119	2	26.00	1.000	12.13	16.25	2.063	1.875	1.933	16.00	6.00	13.78	4250	-	-	80.57	-	1191	61.84
10.3	8N0	0.069	2	26.00	1.000	12.11	16.09	2.094	1.844	1.798	16.00	6.00	13.77	4250	2	0.375	77.96	64.55	1144	59.45
10.4	8N0	0.069	2	20.00	1.000	12.07	16.19	2.079	1.875	1.916	16.00	6.00	13.75	4250	5	0.500	77.96	84.70	1204	62.68
11.1	8F1	0.140	3	18.00	1.000	12.20	16.14	2.000	0.453	1.928	16.00	6.00	13.68	4380	6	0.500	75.42	84.70	1902	68.52
11.2	8N0	0.069	2	18.00	1.000	12.19	16.13	2.094	1.844	1.881	16.00	6.00	13.72	4380	4	0.500	77.96	84.70	1202	62.58
11.3	8N3	0.119	2	18.00	1.000	12.13	16.08	2.063	1.844	1.943	16.00	6.00	13.60	4380	4	0.500	80.57	84.70	1200	63.11
11.4	8F1	0.140	2	24.00	1.000	12.15	16.23	2.094	1.844	1.928	16.00	6.00	13.77	4380	2	0.375	75.42	64.55	1217	63.15
12.1	5N0	0.082	4	10.00	0.625	12.07	15.56	1.875	0.521	1.335	13.00	4.00	13.90	4120	2	0.500	66.39	84.70	708	45.63
12.2	5C2	0.109	4	10.00	0.625	12.12	15.57	1.953	0.516	1.297	13.00	4.00	13.94	4120	2	0.500	61.83	84.70	711	45.68
12.3	5N0	0.082	3	10.00	0.625	12.14	15.50	2.032	1.039	1.291	13.00	4.00	13.88	4120	1	0.375	66.39	64.55	573	48.67
12.4	5C2	0.109	3	10.00	0.625	12.12	15.56	2.063	1.032	1.264	13.00	4.00	13.96	4120	1	0.375	61.83	64.55	618	52.21
13.1	5C2	0.109	3	12.00	0.625	12.18	15.51	1.532	1.289	1.303	13.00	4.00	13.88	4110	1	0.375	61.83	64.55	659	56.06
13.2	5N0	0.082	3	12.00	0.625	12.11	15.50	1.563	1.266	1.315	13.00	4.00	13.86	4110	1	0.375	66.39	64.55	661	56.35

Table 4.1
Splice specimen properties and test results from Darwin et al. (1995) (continued)

Specimen No. +	Bar ++ Designation	R _r	n	l _s (in.)	d _b (in.)	b (in.)	h (in.)	c _{so} (in.)	c _{si} (in.)	c _b (in.)	l (in.)	l _e (in.)	d (in.)	f _c (psi)	N	d _s (in.)	f _y (ksi)	f _{yA} (ksi)	M _u (k-in.)	f _s * (ksi)
13.3	5C2**	0.109	3	16.00	0.625	12.15	15.52	2.047	1.000	1.325	13.00	4.00	13.92	4110	-	-	61.83	-	661	54.13
13.4	5C2	0.109	3	16.00	0.625	12.19	15.60	2.094	1.016	1.354	13.00	4.00	13.92	4110	-	-	61.83	-	710	60.26
14.1	8C1	0.101	3	36.00	1.000	12.12	16.26	2.032	0.484	1.877	13.00	4.00	13.86	4200	3	0.375	67.69	64.55	1725	61.19
14.2	8C1	0.101	3	21.00	1.000	12.19	16.13	2.016	0.469	1.897	13.00	4.00	13.72	4200	7	0.500	67.69	84.70	1788	64.24
14.3	5C2	0.109	3	17.00	0.625	12.14	15.51	2.032	1.031	1.295	13.00	4.00	13.89	4200	-	-	61.83	-	743	61.83
14.4	5C2**	0.109	3	17.00	0.625	12.14	15.59	2.063	1.000	1.320	13.00	4.00	13.89	4200	-	-	61.83	-	57.58	
14.5	5N0	0.082	2	12.00	0.625	12.13	15.45	1.594	3.156	1.210	13.00	4.00	13.91	4200	2	0.375	66.39	64.55	482	60.29
14.6	5C2	0.109	2	12.00	0.625	12.05	15.49	1.532	3.188	1.277	13.00	4.00	13.89	4200	2	0.375	61.83	64.55	507	61.83
15.1	11F3	0.127	2	27.00	1.410	12.11	16.11	1.516	1.500	1.902	16.00	6.00	13.46	5250	9	0.500	77.77	84.70	2449	69.11
15.2	11N0	0.072	2	27.00	1.410	12.11	16.12	1.610	1.469	1.924	16.00	6.00	13.46	5250	9	0.500	65.54	84.70	2287	64.28
15.3	11N0	0.072	2	40.00	1.410	12.04	16.19	1.516	1.531	1.820	16.00	6.00	13.63	5250	10	0.375	65.54	64.55	2287	63.40
15.4	11F3	0.127	2	40.00	1.410	12.08	16.13	1.563	1.469	1.884	16.00	6.00	13.50	5250	10	0.375	77.77	64.55	2808	78.90
15.5	11F3	0.127	2	40.00	1.410	18.05	16.12	3.063	2.984	1.908	16.00	6.00	13.47	5250	-	-	77.77	-	2013	54.51
15.6	11F3**	0.127	2	40.00	1.410	18.07	16.10	2.922	3.063	1.932	16.00	6.00	13.42	5250	-	-	77.77	-	1787	48.46
16.1	11F3**	0.127	2	40.00	1.410	18.04	15.93	3.063	2.906	1.833	16.00	6.00	13.35	5180	-	-	77.77	-	1799	49.13
16.2	11F3	0.127	2	40.00	1.410	18.07	16.28	3.016	2.969	1.895	16.00	6.00	13.64	5180	-	-	77.77	-	1974	52.75
16.3	11F3	0.127	2	40.00	1.410	18.03	16.16	3.047	2.969	1.791	16.00	6.00	13.62	5180	4	0.375	77.77	64.55	2312	62.06
16.4	11B0	0.070	2	40.00	1.410	18.06	16.00	3.063	3.000	1.846	16.00	6.00	13.45	5180	4	0.375	66.69	64.55	2272	61.84
17.3	11F3	0.127	2	38.00	1.410	18.03	16.12	3.047	2.984	1.888	16.00	6.00	13.48	4710	8	0.375	77.77	64.55	2558	70.06
17.4	11B0	0.070	2	38.00	1.410	18.07	16.09	3.094	3.000	1.866	16.00	6.00	13.52	4710	8	0.375	66.69	64.55	2451	66.69
17.5	11B0	0.070	2	30.00	1.410	18.09	16.09	3.079	3.000	1.907	16.00	6.00	13.48	4710	7	0.500	66.69	84.70	2175	59.30
17.6	11F3	0.127	2	30.00	1.410	18.07	16.20	3.063	2.969	1.911	16.00	6.00	13.54	4710	7	0.500	77.77	84.70	2572	70.12
18.1	11F3	0.127	2	40.00	1.410	18.05	16.11	1.485	4.500	1.845	16.00	6.00	13.52	4700	10	0.375	77.77	64.55	3007	80.90
18.2	11F3**	0.127	2	40.00	1.410	18.07	16.14	2.984	3.000	1.922	16.00	6.00	13.48	4700	6	0.375	77.77	64.55	2134	58.17
18.3	11F3	0.127	2	40.00	1.410	18.05	16.08	3.032	3.000	1.911	16.00	6.00	13.43	4700	6	0.375	77.77	64.55	2564	70.58
18.4	11B0	0.070	2	40.00	1.410	18.08	16.23	3.016	3.031	1.871	16.00	6.00	13.62	4700	6	0.375	66.69	64.55	2791	66.69

Note: Refer to last page of the table for footnotes.

Table 4.1
Splice specimen properties and test results from Darwin et al. (1995a, 1996a) (continued)

-
- + Specimen No.:
G.P, G = group number (1-18), P = casting order in the group (1-6); Note: Groups 8-11 cast in concrete containing a "normal" quantity of basalt coarse aggregate and the other groups cast in concrete containing a "normal" quantity of limestone coarse aggregate.
 - ++ Bar Designation:
#AA, # = bar size (No. 5, No.8, or No.11), AA = bar manufacturer and deformation pattern:
 B0 Conventional Birmingham Steel bars
 C0 Conventional Chaparral Steel bar
 N0 Conventional North Star Steel bar
 S0 Conventional Structural Metals, Inc, bar
 SH0 Conventional Sheffield Steel Bar
 C1, C2 New Chaparral Steel bars
 F1, F3 New Florida Steel bars
 N3 New North Star Steel bar
 - * Bar stress is computed using moment-curvature method if M_u does not exceed the moment capacity from moment-curvature analysis, otherwise f_s is computed using ultimate strength method; M_u and f_s include effects of beam self weight and loading system.
 - ** Spliced bars were coated

1 in. = 25.4 mm; 1 psi = 6.895 kPa; 1 ksi = 6.895 MPa; 1 kip = 4.448 kN; 1 k-in. = 0.113 kN-m

Table 4.2
Splice specimen properties and test results from Hester et al. (1991, 1993)

Specimen No. +	Bar ++ Designation	R _r	n	l _s (in.)	d _b (in.)	c _{so} (in.)	c _{si} (in.)	c _b (in.)	b (in.)	h (in.)	d (in.)	f _c (psi)	l (in.)	l _e (in.)	N	d _s (in.)	f _y (ksi)	f _u (ksi)	M _u (k-in.)	f _s * (ksi)
1.1	8N0	0.078	3	16.00	1.000	2.000	1.500	2.000	16.00	16.00	13.50	5990	13.00	4.00	-	-	63.80	-	1433	50.13
1.2	8N0	0.078	3	16.00	1.000	2.000	1.500	2.000	16.00	16.00	13.50	5990	13.00	4.00	2	0.375	63.80	77.30	1604	56.18
1.4	8N0**	0.078	3	16.00	1.000	2.000	1.500	2.000	16.00	16.00	13.50	5990	13.00	4.00	2	0.375	63.80	77.30	1214	42.40
2.1	8C0	0.071	3	16.00	1.000	2.000	1.500	1.840	16.00	16.33	13.99	6200	13.00	4.00	-	-	69.00	-	1376	46.25
2.2	8C0	0.071	3	16.00	1.000	2.000	1.500	1.830	16.00	16.28	13.95	6200	13.00	4.00	2	0.375	69.00	54.10	1305	43.98
2.3	8C0**	0.071	3	16.00	1.000	2.000	1.500	1.750	16.00	16.39	14.14	6200	13.00	4.00	-	-	69.00	-	1146	38.04
2.4	8C0**	0.071	3	16.00	1.000	2.000	1.500	1.780	16.00	16.31	14.03	6200	13.00	4.00	2	0.375	69.00	54.10	1124	37.61
3.1	8S0	0.070	3	16.00	1.000	2.000	1.500	2.040	16.09	16.23	13.69	6020	13.00	4.00	-	-	71.10	-	1361	46.86
3.2	8S0	0.070	3	16.00	1.000	2.000	1.500	2.080	16.06	16.24	13.66	6020	13.00	4.00	2	0.375	71.10	68.90	1348	46.51
3.3	8S0**	0.070	3	16.00	1.000	2.000	1.500	2.060	16.09	16.53	13.97	6020	13.00	4.00	-	-	71.10	-	911	30.61
3.4	8S0**	0.070	3	16.00	1.000	2.000	1.500	2.070	16.09	16.18	13.61	6020	13.00	4.00	2	0.375	71.10	68.90	921	31.81
4.1	8S0	0.070	3	16.00	1.000	2.000	1.500	2.100	16.08	16.22	13.62	6450	13.00	4.00	-	-	71.00	-	1228	42.36
4.2	8S0	0.070	3	16.00	1.000	2.000	1.500	2.040	16.09	16.36	13.82	6450	13.00	4.00	2	0.375	71.10	68.90	1384	47.05
4.3	8S0	0.070	3	16.00	1.000	2.000	1.500	2.100	16.09	16.28	13.68	6450	13.00	4.00	3	0.375	71.10	68.90	1456	50.06
4.4	8S0**	0.070	3	16.00	1.000	2.000	1.500	2.110	16.05	16.22	13.61	6450	13.00	4.00	-	-	71.00	-	884	30.45
4.5	8S0**	0.070	3	16.00	1.000	2.000	1.500	2.000	16.05	16.27	13.77	6450	13.00	4.00	3	0.375	71.10	68.90	932	31.72
4.6	8S0**	0.070	3	16.00	1.000	2.000	1.500	2.030	16.03	16.18	13.65	6450	13.00	4.00	3	0.375	71.10	68.90	887	30.46
5.1	8C0	0.071	3	16.00	1.000	2.000	1.500	2.050	16.09	16.27	13.72	5490	13.00	4.00	-	-	69.00	-	1158	39.86
5.2	8C0	0.071	3	16.00	1.000	2.000	1.500	2.060	16.10	16.42	13.86	5490	13.00	4.00	2	0.375	69.00	54.10	1367	46.62
5.3	8C0	0.071	3	16.00	1.000	2.000	1.500	2.060	16.09	16.12	13.56	5490	13.00	4.00	3	0.375	69.00	54.10	1244	43.39
5.4	8C0**	0.071	3	16.00	1.000	2.000	1.500	2.010	16.09	16.28	13.77	5490	13.00	4.00	-	-	69.00	-	931	31.87
5.5	8C0**	0.071	3	16.00	1.000	2.000	1.500	2.060	16.06	16.44	13.88	5490	13.00	4.00	3	0.375	69.00	54.10	1024	34.79
6.1	8C0	0.071	3	22.75	1.000	2.000	1.500	2.150	16.06	16.19	13.54	5850	13.00	4.00	-	-	69.00	-	1489	51.99
6.2	8C0	0.071	3	22.75	1.000	2.000	1.500	2.170	16.06	16.20	13.53	5850	13.00	4.00	3	0.375	69.00	54.10	1620	56.66
6.3	8C0	0.071	3	22.75	1.000	2.000	1.500	2.160	16.03	16.17	13.51	5850	13.00	4.00	4	0.375	69.00	54.10	1595	55.87
6.4	8C0**	0.071	3	22.75	1.000	2.000	1.500	2.000	16.06	16.16	13.66	5850	13.00	4.00	-	-	69.00	-	952	32.80
6.5	8C0**	0.071	3	22.75	1.000	2.000	1.500	2.130	16.06	16.25	13.62	5850	13.00	4.00	3	0.375	69.00	54.10	1027	35.51
6.6	8C0**	0.071	3	22.75	1.000	2.000	1.500	2.180	16.09	16.22	13.54	5850	13.00	4.00	4	0.375	69.00	54.10	1112	38.71
7.1	8C0	0.071	2	16.00	1.000	2.000	4.000	2.120	16.03	16.20	13.58	5240	13.00	4.00	-	-	69.00	-	885	45.40
7.2	8C0	0.071	2	16.00	1.000	2.000	4.000	2.030	16.00	16.30	13.77	5240	13.00	4.00	3	0.375	69.00	54.10	1019	51.57
7.3	8C0**	0.071	2	16.00	1.000	2.000	4.000	2.120	16.00	16.22	13.60	5240	13.00	4.00	-	-	69.00	-	759	38.78
7.4	8C0**	0.071	2	16.00	1.000	2.000	4.000	2.080	16.00	16.20	13.62	5240	13.00	4.00	3	0.375	69.00	54.10	759	38.78

Note: Refer to last page of the table for footnote

Table 4.2 (continued)
Splice specimen properties and test results from Hester et al. (1991, 1993)

-
- + Specimen No.:
G,P, G = group number (1-7), P = casting order in the group (1-3); Note: All groups cast in concrete containing a "normal" quantity of limestone coarse aggregate.
 - ++ Bar Designation:
#AA, # = bar size (No.8), AA = bar manufacturer and deformation pattern:
C0 Conventional Chaparral Steel bar
N0 Conventional North Star Steel bar
S0 Conventional Structural Metals, Inc, bar
 - * Bar stress is computed using moment-curvature method if M_u does not exceed the moment capacity from moment-curvature analysis, otherwise f_c is computed using ultimate strength method; M_u and f_c include effects of beam self weight and loading system.
 - ** Spliced bars were coated.

1 in. = 25.4 mm; 1 psi = 6.895 kPa; 1 ksi = 6.895 MPa; 1 kip = 4.447 kN; 1 k-in. = 0.113 kN-m

Table 4.3
Splice specimen properties and test results from Choi et al. (1990, 1991)

Specimen No. +	Bar ++ Designation	R _r	n	l _s (in.)	d _b (in.)	c _{so} (in.)	c _{sl} (in.)	c _b (in.)	b (in.)	h (in.)	d (in.)	f _c (psi)	l (in.)	l _c (in.)	N	d _s (in.)	f _y (ksi)	f _{yt} (ksi)	M _u (k-in.)	f _s * (ksi)
1.1	5N0	0.086	2	12.00	0.625	2.000	2.000	1.000	10.50	16.00	14.69	5360	12.00	4.00	-	-	63.80	-	521	61.51
1.2	5N0	0.086	3	12.00	0.625	2.000	2.000	1.000	15.75	16.00	14.69	5360	12.00	4.00	-	-	63.80	-	813	64.00
1.3	5N0**	0.086	3	12.00	0.625	2.000	2.000	1.000	15.75	16.00	14.69	5360	12.00	4.00	-	-	63.80	-	609	47.93
2.1	6S0	0.060	2	12.00	0.750	2.000	2.000	1.000	11.00	16.01	14.63	6010	12.00	4.00	-	-	63.80	-	543	45.75
2.2	6S0**	0.060	2	12.00	0.750	2.000	2.000	1.000	11.00	16.01	14.63	6010	12.00	4.00	-	-	63.80	-	511	43.06
2.3	6C0	0.079	2	12.00	0.750	2.000	2.000	1.000	11.00	16.01	14.63	6010	12.00	4.00	-	-	70.90	-	610	51.40
2.4	6C0**	0.079	2	12.00	0.750	2.000	2.000	1.000	11.00	16.01	14.63	6010	12.00	4.00	-	-	70.90	-	466	39.26
3.1	8S0	0.064	2	16.00	1.000	2.000	2.000	1.500	12.00	16.00	14.00	5980	12.00	4.00	-	-	67.00	-	854	42.82
3.2	8S0**	0.064	2	16.00	1.000	2.000	2.000	1.500	12.00	16.00	14.00	5980	12.00	4.00	-	-	67.00	-	768	43.37
3.3	8N0	0.080	2	16.00	1.000	2.000	2.000	1.500	12.00	16.00	14.00	5980	12.00	4.00	-	-	63.80	-	858	43.02
3.4	8N0	0.080	2	16.00	1.000	2.000	2.000	1.500	12.00	16.00	14.00	5980	12.00	4.00	-	-	63.80	-	737	36.96
4.1	11S0	0.071	2	24.00	1.410	2.000	2.000	2.000	13.65	16.01	13.30	5850	15.00	6.00	-	-	64.60	-	1459	40.22
4.2	11S0**	0.071	2	24.00	1.410	2.000	2.000	2.000	13.65	16.01	13.30	5850	15.00	6.00	-	-	64.60	-	1053	29.03
4.3	11C0	0.069	2	24.00	1.410	2.000	2.000	2.000	13.65	16.01	13.30	5850	15.00	6.00	-	-	63.10	-	1372	37.82
4.4	11C0	0.069	2	24.00	1.410	2.000	2.000	2.000	13.65	16.01	13.30	5850	15.00	6.00	-	-	63.10	-	1128	31.09

+ Specimen No.:

G.P, G = group number (1-4), P = casting order in the group (1-4); All groups cast in concrete containing a "normal" quantity of limestone coarse aggregate.

++ Bar Designation:

#AA, # = bar size (No.8), AA = bar manufacturer and deformation pattern:

C0 Conventional Chaparral Steel bar

N0 Conventional North Star Steel bar

S0 Conventional Structural Metals, Inc, bar

* Bar stress is computed using moment-curvature method if M_u does not exceed the moment capacity from moment-curvature analysis, otherwise f_s is computed using ultimate strength method; M_u and f_s include effects of beam self weight and loading system.

** Spliced bars were coated.

1 in. = 25.4 mm; 1 psi = 6.895 kPa; 1 ksi = 6.895 MPa; 1 kip = 4.448 kN; 1 k-in. = 0.113 kN-m

Table 4.4
Effect of concrete properties on splice strength of the
splices not confined by transverse reinforcement

Concrete +	Number of Tests	Test/Prediction Ratio ++		
		Maximum	Minimum	Average
NNL	35	1.251	0.895	1.002
NHL	6	1.060	0.982	1.007
HHL	4	0.996	0.882	0.963
NNB	2	1.150	1.064	1.107
HHB	9	1.274	0.986	1.133

+ See Table 2.3 for the notation

++ Test-to-predicted splice strength ratio; test strength = $A_b f_s / f_c^{1/4}$, determined from the test results; predicted strength is determined using Eq. 4.2; predicted strengths for individual specimens are presented in Table 5.5

Table 4.5
Effect of deformation pattern on splice strength for the
splices not confined by transverse reinforcement

Coarse Aggregate	Bar + Deformation	Number of Tests	Test/Prediction Ratio		
			Maximum	Minimum	Average
Limestone	Conventional	22	1.251	0.895	1.010
	High R _r	23	1.069	0.882	0.989
Basalt	Conventional	5	1.206	1.068	1.123
	High R _r	6	1.274	0.986	1.133

+ Conventional bars: R_r = 0.069 - 0.087

High R_r Bars: R_r = 0.101 - 0.141

Table 4.6
Measurements of bar rib widths and rib width/spacing ratios

Bar	R_r	Avg. Spacing S_r (in.)	Avg. Top Width (in.)	Avg. Bottom Width (in.)	Avg. Width I * at 1/2 Height (in.)	Avg. Width II ** at 3/4 Height (in.)	Width I S_r	Width II S_r
					Avg. Width I * at 1/2 Height (in.)	Avg. Width II ** at 3/4 Height (in.)	Width I S_r	Width II S_r
5C2	0.109	0.275	0.074	0.123	0.098	0.086	0.358	0.314
5C3	0.141	0.258	0.064	0.134	0.099	0.082	0.385	0.318
8C0A	0.085	0.598	0.106	0.239	0.173	0.139	0.289	0.233
8N0	0.069	0.650	0.111	0.217	0.164	0.138	0.252	0.212
8C1	0.101	0.504	0.120	0.237	0.178	0.149	0.354	0.296
8F1	0.140	0.471	0.106	0.174	0.140	0.123	0.298	0.262
8N1	0.121	0.441	0.127	0.260	0.193	0.160	0.438	0.363
8N3	0.119	0.487	0.119	0.234	0.176	0.148	0.362	0.303
11B0	0.072	0.825	0.124	0.249	0.187	0.156	0.226	0.189
11N0	0.070	0.911	0.153	0.316	0.234	0.193	0.257	0.212
11F3	0.127	0.615	0.110	0.298	0.204	0.157	0.332	0.255

* Interpolation at 1/2 rib height based on measurements on top and bottom rib width

** Interpolation at 3/4 rib height based on measurements on top and bottom rib width

Table 4.7
Effect of rib width/spacing ratio on splice strength for the splices not confined by stirrups

Bar Deformation	R_r	W_r/S_r *	No. of Tests	Test/Prediction Ratio		
				Maximum	Minimum	Average
8N3	0.119	0.362	6	1.007	0.932	0.98
8N1	0.121	0.438	4	1.06	0.93	0.996

* W_r = rib width at 1/2 height of ribs

S_r = center-to-center rib spacing

Table 4.8
Comparison of flexural crack density and flexural crack width at a bar stress
of 40 ksi between high relative rib area and conventional bars
in matched pairs of specimens

Specimen No	Bar + Designation	Length Outside of Splice Region (ft)	Total No. of Cracks	Avg. Max. Crack Width (in.)	Crack * Density (cracks/ft)	Sum of ** Crack Widths (in.)	Ratios of High R _r /Conv. ***			
							Crack Density	Max. Crack Width	Sum of Crack Widths	
29.1	8N1	4.33	16	0.0060	3.692	0.048	1.000	1.000	0.889	
29.2	8N0	4.33	16	0.0060	3.692	0.054				
29.3	8N1	4.50	15	0.0070	3.333	0.055	0.938	1.000	0.948	
29.4	8N0	4.50	16	0.0070	3.556	0.058				
29.5	8N1	4.67	16	0.0060	3.429	0.051	1.067	1.000	1.063	
29.6	8N0	4.67	15	0.0060	3.214	0.048				
31.5	8N1	4.17	11	0.0100	2.640	0.075	1.000	1.000	1.071	
31.6	8C0A	4.17	11	0.0100	2.640	0.070				
32.1	11F3	3.33	8	0.0125	2.400	0.065	1.000	1.000	0.890	
32.2	11B0	3.33	8	0.0125	2.400	0.073				
33.1	8N1	4.50	9	0.0100	2.000	0.064	1.125	1.000	0.853	
33.2	8C0A	4.50	8	0.0100	1.778	0.075				
33.3	8N1	4.50	8	0.0090	1.778	0.059	0.889	1.000	0.868	
33.4	8C0A	4.50	9	0.0090	2.000	0.068				
33.5	8N1	4.17	9	0.0100	2.160	0.070	1.125	1.000	0.986	
33.6	8C0A	4.17	8	0.0100	1.920	0.071				
35.1	8F1	4.33	9	0.0100	2.077	0.062	1.125	0.952	0.827	
35.3	8C0A	4.33	8	0.0105	1.846	0.075				
35.2	8F1	4.33	7	0.0140	1.615	0.079	1.000	1.077	1.000	
35.4	8C0A	4.33	7	0.0130	1.615	0.079				
39.2	8C1	4.67	13	0.0100	2.786	-	1.000	1.000		
39.3	8N0	4.67	13	0.0100	2.786	-				
40.1	11F3	4.08	11	0.0120	2.694	-	1.100	0.960		
40.4	11N0	4.08	10	0.0125	2.449	-				
43.2	8N3	4.67	12	0.0105	2.571	-	1.000	1.050		
42.1	8N0	4.67	12	0.0100	2.571	-				
43.3	8N3	4.67	12	0.0100	2.571	-	0.923	0.952		
42.4	8N0	4.67	13	0.0105	2.786	-				
43.6	8N3	4.67	13	0.0100	2.786	-	1.000	1.000		
42.5	8N0	4.67	13	0.0100	2.786	-				
							Average	1.019	0.999	0.940
							Max.	1.125	1.077	1.071
							Min.	0.889	0.952	0.827
							St.Dev.	0.075	0.032	0.087

+ 8C0A, 8N0, and 11N0 are conventional bars ($R_r = 0.069 - 0.085$).

8C1, 8F1, 8N1, 8N3, and 11F3 are high relative rib area (R_r) bars ($R_r = 0.101 - 0.140$).

++ Total number of flexural cracks in constant moment region outside of splice region

+++ Average maximum flexural crack width on east and west sides of splice region in constant moment region

* Number of flexural cracks in unit foot length

** Sum of flexural crack widths cross the center of the beam on the east and west sides of splices in constant moment region outside of splice region

*** Ratios for crack density or maximum crack width or sum of crack widths of high R_r

to conventional bars

1 in. = 25.4 mm, 1 ft = 0.305 m, 1 ksi = 6.895 MPa

Table 4.9
Comparison of flexural crack density and flexural crack width at a bar stress
of 20 ksi between high relative rib area and conventional bars
in matched pairs of specimens

Specimen No	Bar + Designation	Length Outside of Splice Region (ft)	Total No. of Cracks	Avg. Max. Crack Width (in.)	Crack * Density (cracks/ft)	Sum of** Crack Widths (in.)	Ratios of High R./Conv.***			
							Crack Density	Max. Crack Width	Sum of Crack Widths	
29.1	8N1	4.33	11	0.0015	2.538	0.013	1.000	1.000	1.182	
29.2	8N0	4.33	11	0.0015	2.538	0.011				
29.3	8N1	4.50	10	0.0010	2.222	0.011	0.769	1.000	0.846	
29.4	8N0	4.50	13	0.0010	2.889	0.013				
29.5	8N1	4.67	7	0.0010	1.500	0.004	1.000	1.000	0.571	
29.6	8N0	4.67	7	0.0010	1.500	0.007				
31.5	8N1	4.17	8	0.0020	1.920	0.014	1.333	1.000	1.273	
31.6	8C0A	4.17	6	0.0020	1.440	0.011				
32.1	11F3	3.33	6	0.0040	1.800	0.018	0.750	1.000	0.783	
32.2	11B0	3.33	8	0.0040	2.400	0.023				
33.1	8N1	4.50	8	0.0020	1.778	0.014	1.000	1.000	0.875	
33.2	8C0A	4.50	8	0.0020	1.778	0.016				
33.3	8N1	4.50	4	0.0025	0.889	0.009	1.000	1.250	1.125	
33.4	8C0A	4.50	4	0.0020	0.889	0.008				
33.5	8N1	4.17	5	0.0020	1.200	0.010	0.833	0.667	0.769	
33.6	8C0A	4.17	6	0.0030	1.440	0.013				
35.1	8F1	4.33	5	0.0020	1.154	0.008	1.000	1.000	0.800	
35.3	8C0A	4.33	5	0.0020	1.154	0.010				
35.2	8F1	4.33	5	0.0020	1.154	0.010	1.000	1.000	1.000	
35.4	8C0A	4.33	5	0.0020	1.154	0.010				
39.2	8C1	4.67	8	0.0030	1.714	-	1.333	1.000		
39.3	8N0	4.67	6	0.0030	1.286	-				
40.1	11F3	4.08	7	0.0040	1.714	-	0.778	1.333		
40.4	11N0	4.08	9	0.0030	2.204	-				
43.2	8N3	4.67	6	0.0035	1.286	-	1.000	1.000		
42.1	8N0	4.67	6	0.0035	1.286	-				
43.3	8N3	4.67	9	0.0025	1.929	-	1.000	0.833		
42.4	8N0	4.67	9	0.0030	1.929	-				
43.6	8N3	4.67	8	0.0030	1.714	-	0.667	1.000		
42.5	8N0	4.67	12	0.0030	2.571	-				
							Average	0.964	1.006	0.922
							Max.	1.333	1.333	1.273
							Min.	0.667	0.667	0.571
							St.Dev.	0.190	0.149	0.218

+ 8C0A, 8N0, and 11N0 are conventional bars ($R_t = 0.069 - 0.085$).

8C1, 8F1, 8N1, 8N3, and 11F3 are high relative rib area ($R_t = 0.101 - 0.140$).

++ Total number of flexural cracks in constant moment region outside of splice region

+++ Average maximum flexural crack width on east and west sides of splice region in constant moment region

* Number of flexural cracks in unit foot length

** Sum of flexural crack widths cross the center of the beam on the east and west sides of splices in constant moment region outside of splice region

*** Ratios for crack density or maximum crack width or sum of crack widths of high R_t to conventional bars

1 in. = 25.4 mm, 1 ft = 0.305 m, 1 ksi = 6.895 MPa

Table 4.10
Comparison of flexural crack density and flexural crack width at a bar stress
of 30 ksi between high relative rib area and conventional bars
in matched pairs of specimens

Specimen No	Bar + Designation	Length Outside of Splice Region (ft)	Total No. of Cracks	Avg. Max. Crack Width (in.)	Crack * Density (cracks/ft)	Sum of ** Crack Widths (in.)	Ratios of High R _r /Conv. ***		
							Crack Density	Max. Crack Width	Sum of Crack Widths
29.1	8N1	4.33	16	0.0035	3.692	0.033	1.067	1.000	1.000
29.2	8N0	4.33	15	0.0035	3.462	0.033			
29.3	8N1	4.50	14	0.0040	3.111	0.035	0.933	1.000	1.129
29.4	8N0	4.50	15	0.0040	3.333	0.031			
29.5	8N1	4.67	13	0.0030	2.786	0.025	0.929	1.000	0.962
29.6	8N0	4.67	14	0.0030	3.000	0.026			
31.5	8N1	4.17	10	0.0055	2.400	0.047	1.000	0.846	1.068
31.6	8C0A	4.17	10	0.0065	2.400	0.044			
32.1	11F3	3.33	8	0.0075	2.400	0.043	1.000	0.938	0.768
32.2	11B0	3.33	8	0.0080	2.400	0.056			
33.1	8N1	4.50	8	0.0065	1.778	0.035	1.000	1.083	0.778
33.2	8C0A	4.50	8	0.0060	1.778	0.045			
33.3	8N1	4.50	8	0.0055	1.778	0.038	1.000	1.100	0.927
33.4	8C0A	4.50	8	0.0050	1.778	0.041			
33.5	8N1	4.17	8	0.0050	1.920	0.035	1.000	0.833	0.833
33.6	8C0A	4.17	8	0.0060	1.920	0.042			
35.1	8F1	4.33	7	0.0060	1.615	0.032	0.875	1.091	0.800
35.3	8C0A	4.33	8	0.0055	1.846	0.040			
35.2	8F1	4.33	7	0.0080	1.615	0.044	1.167	1.143	1.023
35.4	8C0A	4.33	6	0.0070	1.385	0.043			
39.2	8C1	4.67	12	0.0070	2.571	-	0.923	0.875	-
39.3	8N0	4.67	13	0.0080	2.786	-			
40.1	11F3	4.08	8	0.0080	1.959	-	0.800	0.941	-
40.4	11N0	4.08	10	0.0085	2.449	-			
43.2	8N3	4.67	12	0.0075	2.571	-	1.333	1.071	-
42.1	8N0	4.67	9	0.0070	1.929	-			
43.3	8N3	4.67	11	0.0060	2.357	-	1.100	0.923	-
42.4	8N0	4.67	10	0.0065	2.143	-			
43.6	8N3	4.67	10	0.0065	2.143	-	0.833	1.000	-
42.5	8N0	4.67	12	0.0065	2.571	-			
							Average	0.997	0.990
							Max.	1.333	1.143
							Min.	0.800	0.833
							St.Dev.	0.134	0.096
									0.129

+ 8C0A, 8N0, and 11N0 are conventional bars ($R_r = 0.069 - 0.085$).

+ 8C1, 8F1, 8N1, 8N3, and 11F3 are high relative rib area (R_r) bars ($R_r = 0.101 - 0.140$).

++ Total number of flexural cracks in constant moment region outside of splice region

+++ Average maximum flexural crack width on east and west sides of splice region in constant moment region

* Number of flexural cracks in unit foot length

** Sum of flexural crack widths cross the center of the beam on the east and west sides of splices in constant moment region outside of splice region

*** Ratios for crack density or maximum crack width or sum of crack widths of high R_r ,

to conventional bars 1 in. = 25.4 mm, 1 ft = 0.305 m, 1 ksi = 6.895 MPa

Table 5.1
Coefficients obtained in the derivation of Eq. 5.4 ($p = 1/4$)

Bar Size	No. of Specimens	C_2^{**}	C_2/A_b	C_5^{++}
No. 3	2	431.5	3922.8	1.0419
No. 4	16	541.3	2706.6	0.8763
No. 5	5	944.1	3045.6	0.9524
No. 6	33	1066.4	2423.6	0.8069
No. 8	63	1845.0	2335.4	0.8472
No. 9	3	3396.4	3396.4	0.9813
No. 11	47	3864.3	2477.1	0.8232
No. 14	2	5076.3	2256.1	0.8590
Slope, C_1^*		63.22		
Weighted Average, C_3			2483.1	
Slope, C_4^+		0.103		
Weighted Average Intercept, C_6				0.843
$K_1 = C_1(C_4 + C_6) = 59.85$		$K_2 = C_3(C_4 + C_6) = 2350.9$		
$K_3 = C_4/(C_4 + C_6) = 0.10$		$K_4 = C_6/(C_4 + C_6) = 0.90$		

* Slope of the best-fit lines of $A_b f_s / f_c^{1/4}$ versus $l_d(c_{min} + 0.5d_b)$ from dummy variable regression based on bar size

** Intercepts of the best-fit lines of $A_b f_s / f_c^{1/4}$ versus $l_d(c + 0.5d_b)$ from dummy variable regression based on bar size

+ Slope of the best-fit lines of T/P versus c_{max}/c_{min} from dummy variable regression based on bar size, where
 $T = T/f_c^{1/4} = A_b f_s / f_c^{1/4}$, $P = C_1 l_d(c_{min} + 0.5d_b) + C_3 A_b$

++ Intercepts of the best-fit lines of T/P versus c_{max}/c_{min} from dummy variable regression based on bar size, where $c_{min} = \min(c_b, c_s)$, $c_{max} = \max(c_b, c_s)$, and $c_s = \min(c_{so}, c_{si} + 0.25 \text{ in.})$

Table 5.2
Coefficients obtained in the derivation of Eq. 5.5 ($p = 1/2$)

Bar Size	No. of Specimens	C_2^{**}	C_2/A_b	C_5^{++}
No. 3	2	45.5	413.7	1.0182
No. 4	16	53.3	266.7	0.8898
No. 5	5	81.8	264.0	0.8783
No. 6	33	102.6	233.2	0.7982
No. 8	63	121.2	153.4	0.7429
No. 9	3	336.9	336.9	0.9594
No. 11	47	249.3	159.8	0.6844
No. 14	2	578.8	257.2	0.9022
Slope, C_1^*		9.13		
Weighted Average, C_3			191.9	
Slope, C_4^+		0.162		
Weighted Average Intercept, C_6				0.764
$K_1 = C_1(C_4 + C_6) = 8.45$		$K_2 = C_3(C_4 + C_6) = 177.6$		
$K_3 = C_4/(C_4 + C_6) = 0.17$		$K_4 = C_6/(C_4 + C_6) = 0.83$		

* Slope of the best-fit lines of $A_b f_s / f_c^{1/2}$ versus $l_d(c_{min} + 0.5d_b)$ from dummy variable regression based on bar size

** Intercepts of the best-fit lines of $A_b f_s / f_c^{1/2}$ versus $l_d(c + 0.5d_b)$ from dummy variable regression based on bar size

+ Slope of the best-fit lines of T/P versus c_{max}/c_{min} from dummy variable regression based on bar size, where

$$T = T_c / f_c^{1/2} = A_b f_s / f_c^{1/2}, P = C_1 l_d(c_{min} + 0.5d_b) + C_3 A_b$$

++ Intercepts of the best-fit lines of T/P versus c_{max}/c_{min} from dummy variable regression based on bar size, where $c_{min} = \min(c_b, c_s)$, $c_{max} = \max(c_b, c_s)$, and $c_s = \min(c_{so}, c_{si} + 0.25 \text{ in.})$

Table 5.3
Summary of test/prediction ratios using Eq. 5.3 for different powers of f'_c
and definitions of effective value of c_{si}

Effect Value of c_{si}	Test/Predication ratio		
	c_{si}	$c_{si}+0.25$	$1.6 c_{si}$
$f_c^{0.20}$			
Max	1.3046	1.3259	1.3353
Min	0.7001	0.7036	0.7105
Mean	1.0002	1.0001	0.9999
St. Dev.	0.1099	0.1069	0.1052
COV	0.1099	0.1069	0.1053
$f_c^{0.22}$			
Max	1.3137	1.3027	1.3128
Min	0.7103	0.7142	0.7215
Mean	0.9992	0.9989	0.9990
St. Dev.	0.1081	0.1052	0.1035
COV	0.1082	0.1053	0.1036
$f_c^{0.23}$			
Max	1.3189	1.3060	1.3042
Min	0.7158	0.7199	0.7273
Mean	1.0001	1.0000	0.9999
St. Dev.	0.1076	0.1047	0.1030
COV	0.1076	0.1047	0.1030
$f_c^{0.24}$			
Max	1.3236	1.3104	1.2941
Min	0.7211	0.7254	0.7330
Mean	1.0000	0.9999	0.9999
St. Dev.	0.1073	0.1044	0.1027
COV	0.1073	0.1044	0.1027
$f_c^{0.25}$			
Max	1.3323	1.3150	1.2956
Min	0.7286	0.7310	0.7386
Mean	1.0029	1.0000	0.9999
St. Dev.	0.1075	0.1043	0.1026
COV	0.1072	0.1043	0.1026
$f_c^{0.26}$			
Max	1.3331	1.3195	1.2993
Min	0.7318	0.7365	0.7436
Mean	1.0000	1.0000	0.9998
St. Dev.	0.1072	0.1044	0.1027
COV	0.1072	0.1044	0.1027

Table 5.3 (continued)
Summary of test/prediction ratios using Eq. 5.3 for different powers of f'_c
and definitions of effective value of c_{si}

Effect Value of c_{si}	Test/Predication ratio		
	c_{si}	$c_{si}+0.25$	$1.6 c_{si}$
$f_c^{0.27}$			
Max	1.3377	1.3239	1.3030
Min	0.7371	0.7352	0.7345
Mean	1.0000	1.0000	0.9998
St. Dev.	0.1074	0.1047	0.1030
COV	0.1074	0.1047	0.1030
$f_c^{0.3}$			
Max	1.3515	1.3370	1.3132
Min	0.7178	0.7083	0.7137
Mean	1.0000	0.9999	0.9997
St. Dev.	0.1093	0.1068	0.1036
COV	0.1093	0.1068	0.1037
$f_c^{0.4}$			
Max	1.3951	1.3783	1.3475
Min	0.6326	0.6245	0.6242
Mean	0.9996	0.9994	0.9992
St. Dev.	0.1257	0.1243	0.1229
COV	0.1258	0.1243	0.1230
$f_c^{0.5}$			
Max	1.4354	1.4162	1.3779
Min	0.5561	0.5491	0.5491
Mean	0.9992	0.9990	0.9987
St. Dev.	0.1524	0.1522	0.1515
COV	0.1525	0.1523	0.1517

Table 5.4
Results of dummy variable analyses for $A_b f_s / f'_c$ versus the right side of Eq. 5.3
based on concrete compressive strength

f'_c (ksi)	No. of Tests	p=0.2		p=0.22		p=0.23		p=0.24		p=0.25		p=0.26		p=0.27		p=0.3		p=0.4		p=0.5	
		K	K/R	K	K/R	K	K/R	K	K/R												
2.5-3.5	21	256.0	0.0096	336.8	0.0147	361.1	0.0171	382.2	0.0196	397.6	0.0221	408.5	0.0246	415.0	0.0270	415.5	0.0343	316.0	0.0576	196.6	0.0792
3.5-4.5	57	264.3	0.0099	271.8	0.0119	267.5	0.0127	265.0	0.0136	261.0	0.0145	256.1	0.0154	250.1	0.0163	228.6	0.0189	147.2	0.0268	83.7	0.0337
4.5-5.5	39	161.0	0.0060	179.7	0.0079	175.5	0.0083	176.6	0.0091	176.0	0.0098	174.6	0.0105	171.9	0.0112	160.2	0.0132	105.2	0.0192	59.3	0.0239
5.5-6.5	20	297.4	0.0111	281.6	0.0123	264.6	0.0126	253.3	0.0130	241.8	0.0134	230.7	0.0139	219.5	0.0143	187.7	0.0155	103.5	0.0189	52.8	0.0213
6.5-10.5	5	413.5	0.0155	330.9	0.0145	282.9	0.0134	248.5	0.0128	217.5	0.0121	190.4	0.0115	166.0	0.0108	108.7	0.0090	18.8	0.0034	-3.6	-0.0015
10.5-13.5	7	724.4	0.0271	546.9	0.0239	453.5	0.0215	384.3	0.0197	323.3	0.0180	270.7	0.0163	224.3	0.0146	119.4	0.0099	-20.6	-0.0038	-36.4	-0.0146
13.5-14.5	12	818.5	0.0306	580.8	0.0254	461.7	0.0219	372.6	0.0191	295.1	0.0164	229.1	0.0138	171.8	0.0112	46.8	0.0039	-93.0	-0.0170	-82.4	-0.0332
14.5-16.0	10	760.9	0.0285	495.0	0.0216	362.0	0.0172	264.7	0.0136	180.9	0.0101	110.8	0.0067	50.8	0.0033	-74.8	-0.0062	-181.5	-0.0331	-134.1	-0.0540
Slope		0.955		0.948		0.947		0.945		0.942		0.940		0.937		0.929		0.9024		0.8751	
r^2		0.971		0.971		0.970		0.970		0.969		0.969		0.968		0.967		0.9599		0.9514	
Max. Prediction		27641		23646		21785		20123		18584		17166		15855		12494		5647.5		2552.2	
Min. Prediction		914		772.2		706.9		648.8		595.3		546.4		501.4		387.66		164.45		69.785	
Range of Prediction, R		26727		22874		21078		19475		17989		16620		15353		12107		5483		2482.4	
Max. of K/R		0.0306		0.0254		0.0219		0.0197		0.0221		0.0246		0.0270		0.0343		0.0576		0.0792	
Min. of K/R		0.0060		0.0079		0.0083		0.0091		0.0098		0.0067		0.0033		-0.0062		-0.0331		-0.0540	
Range of K/R		0.0246		0.0175		0.0136		0.0107		0.0123		0.0179		0.0237		0.0405		0.0907		0.1332	

K = Intercept

Prediction = predicted bond strength = right side of Eq. 5.3 using $c_{si} + 0.25$ in. as the effective value of c_{si}

R = Range of Prediction = Max. Prediction - Min. Prediction

K/R = relative intercept

Range of K/R = Max. K/R - Min. K/R

Table 5.5
Data and test/prediction ratios for developed and spliced bars
without confining reinforcement

Test No.	n	l_d	d_b	c_{s0}	c_{s1}	c_b	b	h	d	f_c	f_y	f_t^*	$T_c/f_c^{1/2}$	$T_c/f_c^{1/4}$	$T_e/f_c^{1/2}$	$T_e/f_c^{1/4}$	Test	Test		
																		Eq. 5.5**	Eq. 5.4*	
Chinn (1956)																				
D31	1	5.50	0.375	1.470		0.830	3.69	-	-	4700	79.00	60.70	98	810	76	640	1.292	1.265		
D36	1	5.50	0.375	1.470		0.560	3.69	-	-	4410	79.00	49.21	82	667	69	588	1.180	1.135		
D10	1	7.00	0.750	1.060		1.480	3.62	-	-	4370	57.00	26.41	176	1429	174	1699	1.010	0.841		
D20	1	7.00	0.750	1.125		1.420	3.75	-	-	4230	57.00	27.12	183	1479	174	1705	1.052	0.867		
D22	1	7.00	0.750	1.095		0.800	3.69	-	-	4480	57.00	23.97	158	1289	157	1582	1.004	0.815		
D13	1	11.00	0.750	2.905		1.440	7.31	-	-	4820	57.00	49.14	311	2595	290	2455	1.076	1.057		
D14	1	11.00	0.750	1.095		0.830	3.69	-	-	4820	57.00	32.82	208	1733	200	1885	1.038	0.919		
D15	1	11.00	0.750	2.875		0.620	7.25	-	-	4290	57.00	42.45	285	2308	276	2303	1.033	1.002		
D21	1	11.00	0.750	2.905		1.470	7.31	-	-	4480	57.00	43.53	286	2341	291	2467	0.983	0.949		
D29	1	11.00	0.750	1.095		1.390	3.69	-	-	7480	57.00	44.62	227	2111	225	2055	1.011	1.027		
D3	2	11.00	0.750	1.500	0.500	1.500	9.00	-	-	4350	57.00	37.15	248	2013	214	1951	1.159	1.031		
D32	1	11.00	0.750	2.875		1.470	7.25	-	-	4700	57.00	46.24	297	2457	290	2462	1.023	0.998		
D38	1	11.00	0.750	1.560		1.520	4.62	-	-	3160	57.00	28.50	223	1673	255	2287	0.873	0.732		
D39	1	11.00	0.750	1.095		1.560	3.69	-	-	3160	57.00	28.05	220	1646	230	2086	0.953	0.789		
D5	1	11.00	0.750	2.000		1.500	5.50	-	-	4180	57.00	44.76	305	2449	267	2343	1.142	1.045		
D6	2	11.00	0.750	1.500	0.625	1.160	7.25	-	-	4340	57.00	33.48	224	1815	205	1917	1.090	0.947		
D7	1	11.00	0.750	1.060		1.270	3.62	-	-	4450	57.00	34.15	225	1840	219	2017	1.030	0.912		
D8	2	11.00	0.750	1.500	0.625	1.480	7.25	-	-	4570	57.00	36.28	236	1942	217	1985	1.087	0.978		
D9	1	11.00	0.750	1.060		1.440	3.62	-	-	4380	57.00	35.33	235	1911	224	2049	1.047	0.933		
D34	1	12.50	0.750	1.060		1.490	3.62	-	-	3800	57.00	37.46	267	2099	246	2192	1.089	0.958		
D12	1	16.00	0.750	1.125		1.620	3.75	-	-	4530	57.00	46.37	303	2487	302	2578	1.004	0.965		
D17	1	16.00	0.750	1.095		0.800	3.69	-	-	3580	57.00	40.56	398	2307	252	2238	1.184	1.031		
D19**	1	16.00	0.750	2.905		1.700	7.31	-	-	4230	57.00	57.60	390	3142	402	3233	0.970	0.972		
D23	1	16.00	0.750	1.060		0.780	3.62	-	-	4450	57.00	39.70	262	2139	249	2216	1.053	0.965		
D24	1	16.00	0.750	2.875		0.810	7.25	-	-	4450	57.00	43.37	286	2336	342	2720	0.837	0.859		
D30	1	16.00	0.750	1.095		1.560	3.69	-	-	7480	57.00	53.04	270	2509	297	2544	0.909	0.986		
D4	2	16.00	0.750	1.500	0.500	1.500	9.00	-	-	4470	57.00	47.40	312	2550	269	2321	1.158	1.099		
D40	1	16.00	0.750	2.940		0.750	7.38	-	-	5280	57.00	50.69	307	2617	345	2727	0.891	0.960		
D25**	1	24.00	0.750	1.060		1.530	3.62	-	-	5100	57.00	57.00	351	2968	397	3231	0.885	0.919		
D26	1	24.00	0.750	1.095		0.750	3.69	-	-	5100	57.00	56.82	350	2959	330	2770	1.060	1.068		
D35	1	24.00	0.750	1.060		1.450	3.62	-	-	3800	57.00	56.91	406	3189	392	3207	1.036	0.994		
D33	1	20.25	1.410	1.990		1.550	6.80	-	-	4830	57.00	28.60	642	5352	695	6578	0.924	0.814		
Chamberlin (1956)																				
SII15	1	6.00	0.500	0.500		1.000	6.00	6.00	4.75	4470	-	34.55	103	845	86	813	1.201	1.040		
SII16	1	6.00	0.500	0.750		1.000	6.00	6.00	4.75	4470	-	38.17	114	934	91	856	1.253	1.090		
SII31	1	6.00	0.500	0.500		1.000	6.00	6.00	4.75	5870	-	39.60	103	905	86	813	1.201	1.113		
SII32	1	6.00	0.500	0.750		1.000	6.00	6.00	4.75	5870	-	46.33	121	1059	91	856	1.328	1.236		
SII33	1	6.00	0.500	1.000		1.000	6.00	6.00	4.75	5870	-	48.43	126	1107	99	919	1.278	1.205		
SII11	1	10.67	0.500	0.500		1.000	6.00	6.00	4.75	3680	-	41.39	136	1063	121	1043	1.131	1.019		
SII27	1	10.67	0.500	0.500		1.000	6.00	6.00	4.75	5870	-	46.40	121	1060	121	1043	1.004	1.016		
SII28	1	10.67	0.500	0.750		1.000	6.00	6.00	4.75	5870	-	49.30	129	1126	133	1145	0.969	0.984		
SII29	1	10.67	0.500	1.000		1.000	6.00	6.00	4.75	5870	-	49.30	129	1126	148	1267	0.868	0.889		
SIV53	1	12.00	0.500	2.000	0.500	1.000	6.00	6.00	4.75	4540	-	47.43	141	1156	145	1227	0.973	0.942		
SII23	1	16.00	0.750	0.750		1.000	9.00	9.00	7.63	4470	-	41.93	276	2256	243	2181	1.134	1.035		
Chamberlin (1958)																				
3a	2	6.00	0.500	0.300	1.500	1.000	6.00	6.00	4.75	4450	50.00	32.94	99	807	86	813	1.148	0.992		
3b	2	6.00	0.500	0.500	1.000	1.000	6.00	6.00	4.75	4450	50.00	33.16	99	812	86	813	1.156	0.999		
3c	2	6.00	0.500	0.500	0.500	1.000	6.00	6.00	4.75	4450	50.00	33.65	101	824	86	813	1.173	1.014		
4a	1	6.00	0.500	2.500		1.000	6.00	6.00	4.75	4370	50.00	42.75	129	1052	124	1056	1.042	0.996		
4b	1	6.00	0.500	2.250		1.000	6.00	6.00	4.75	4370	50.00	44.02	133	1083	120	1033	1.111	1.048		
4c	1	6.00	0.500	2.000		1.000	6.00	6.00	4.75	4370	50.00	43.44	131	1069	116	1010	1.136	1.058		
Ferguson and Breen (1965)																				
8R18a	2	18.00	1.000	3.250	3.265	1.750	17.03	14.97	12.72	3470	99.00	41.60	558	4282	553	4645	1.009	0.922		
8R24a	2	24.00	1.000	3.250	3.310	1.670	17.12	15.03	12.86	3530	99.00	59.53	792	6101	674	5441	1.175	1.121		
8F30a	2	30.00	1.000	3.250	3.295	1.530	17.09	14.97	12.94	3030	74.00	53.48	768	5695	780	6116	0.984	0.931		
8F36a**	2	36.00	1.000	3.250	3.330	1.410	17.16	15.00	13.09	4650	63.50	66.22	767	6335	881	6747	0.870	0.939		
8F36b	2	36.00	1.000	3.250	3.220	1.400	16.94	15.03	13.13	3770	74.00	61.90	796	6241	880	6733	0.905	0.927		
8F36k	2	36.00	1.000	1.420	1.425	1.380	9.69	15.09	13.21	3460	74.00	55.84	750	5752	716	5921	1.048	0.971		
8F39a**	2	39.00	1.000	3.250	3.280	1.530	17.06	15.09	13.06	3650	63.50	72.90	953	7409	964	7332	0.989	0.101		
8F42a**	2	42.00	1.000	3.250	3.345	1.500	17.19	15.09	13.09	2660	63.50	65.93	1010	7253	1019	7				

Table 5.5 (continued)
Data and test/prediction ratios for developed and spliced bars
without confining reinforcement

Test No.	n	l _d	d _b	c _{so}	c _{si}	c _b	b	h	d	f _c	f _y	f _u *	T _c /f _c ^{1/2}	T _c /f _c ^{1/4}	T _c /f _c ^{1/2}	T _c /f _c ^{1/4}	Test		Test		
																	Eq. 5.5 ⁺⁺	Eq. 5.4 ⁺	Eq. 5.5 Eq. 5.4	Eq. 5.5 Eq. 5.4	
				(in.)	(in.)	(in.)	(in.)	(in.)	(in.)	(psi)	(ksi)	(ksi)	(in. ²)	(in. ²)	(in. ²)	(in. ²)					
11F42a	2	57.75	1.410	4.590	4.590	1.480	24.00	18.00	15.82	3530	65.00	64.57	1695	13067	1823	13568	0.930	0.963			
11F48a**	2	66.00	1.410	4.590	4.620	1.530	24.16	18.03	15.80	3140	73.00	73.91	2058	15402	2042	14985	1.008	1.028			
11F48b**	2	66.00	1.410	4.590	4.665	1.580	24.15	18.22	15.93	3330	65.00	72.24	1953	14835	2054	15101	0.951	0.982			
11R48a	2	66.00	1.410	4.590	4.670	1.500	24.16	18.02	15.83	5620	93.00	82.81	1723	14920	2034	14917	0.847	1.000			
11R48b	2	66.00	1.410	4.590	4.700	2.060	24.22	18.19	15.43	3100	93.00	73.20	2051	15303	2199	16369	0.933	0.935			
11F60a**	2	82.50	1.410	4.590	4.575	1.590	23.97	18.09	15.83	2610	73.00	84.80	2589	18508	2479	17816	1.045	1.039			
11F60b**	2	82.50	1.410	4.590	4.590	1.500	24.00	18.09	15.92	4090	65.00	78.02	1903	15219	2450	17541	0.777	0.868			
11R60a	2	82.50	1.410	4.590	4.590	1.410	24.00	18.12	16.01	2690	93.00	77.19	2322	16720	2423	17280	0.958	0.968			
11R60b	2	82.50	1.410	4.590	4.575	1.750	24.00	18.03	15.58	3460	93.00	90.35	2396	18378	2537	18338	0.944	1.002			
Thompson et al. (1975)																					
6-12-4/2/2-6/6	6	12.00	0.750	2.000	2.000	2.000	33.00	13.00	10.63	3730	61.70	57.96	418	3263	319	2738	1.309	1.192			
8-18-4/3/2-6/6	6	18.00	1.000	2.000	2.000	3.000	36.00	13.00	9.50	4710	59.30	57.00	656	5435	565	4775	1.162	1.138			
8-18-4/3/2-5-4/6	6	18.00	1.000	2.500	2.000	3.000	36.00	13.00	9.50	2920	59.30	50.86	744	5466	590	4977	1.260	1.098			
8-24-4/2/2-6/6	6	24.00	1.000	2.000	2.000	2.000	36.00	13.00	10.50	3105	59.30	51.89	736	5491	647	5445	1.136	1.009			
11-25-6/2/3-5/5	5	25.00	1.410	3.000	3.000	2.000	44.06	13.01	10.30	3920	66.30	45.00	1121	8873	921	8095	1.218	1.096			
11-30-4/2/2-6/6	6	30.00	1.410	2.000	2.000	2.000	40.88	13.01	10.30	2865	60.50	39.56	1153	8436	963	8519	1.198	0.990			
11-30-4/2/4-6/6	6	30.00	1.410	4.000	2.000	2.000	44.88	13.01	10.30	3350	63.40	45.90	1237	9413	983	8625	1.258	1.091			
11-30-4/2/2-7.4/6	4	30.00	1.410	2.700	2.000	2.000	44.88	13.01	10.30	4420	63.30	58.48	1372	11189	983	8625	1.396	1.297			
11-45-4/1/2-6/6	6	45.00	1.410	2.000	2.000	1.000	40.88	13.01	11.30	3520	60.50	46.72	1228	9462	1083	9080	1.135	1.042			
14-60-4/2/2-5/5	5	60.00	1.693	2.000	2.000	2.000	37.50	16.15	13.30	2865	57.70	48.13	2023	14801	1843	15501	1.098	0.955			
14-60-4/2/4-5/5	5	60.00	1.693	4.000	2.000	2.000	41.50	16.00	13.15	3200	57.70	56.64	2253	16944	1882	15695	1.197	1.080			
Zekany (1981)																					
9-33-B-N	5	16.00	1.128	2.000	1.423	2.000	27.25	16.00	13.44	5650	62.80	47.77	636	5510	496	4578	1.281	1.204			
N-N-80B	4	22.00	1.410	2.000	1.849	2.000	27.25	16.01	13.30	3825	60.10	38.53	972	7642	780	7225	1.246	1.058			
Choi et al. (1990, 1991)																					
1.1	2	12.00	0.625	2.000	2.000	1.000	10.50	16.00	14.69	5360	63.80	61.51	260	2229	220	1837	1.183	1.213			
1.2**	3	12.00	0.625	2.000	2.000	1.000	15.75	16.00	14.69	5360	63.80	64.00	271	2319	220	1837	1.231	1.262			
2.3	2	12.00	0.750	2.000	2.000	1.000	11.00	16.01	14.63	6010	70.90	51.34	291	2566	255	2223	1.145	1.154			
2.1	2	12.00	0.750	2.000	2.000	1.000	11.00	16.01	14.63	6010	63.80	45.67	259	2282	255	2223	1.018	1.027			
3.3	2	16.00	1.000	2.000	2.000	1.500	12.00	16.00	14.00	5980	63.80	43.00	439	3863	434	3896	1.012	0.992			
3.1	2	16.00	1.000	2.000	2.000	1.500	12.00	14.00	12.00	5980	67.00	42.81	437	3846	434	3896	1.008	0.987			
4.3	2	24.00	1.410	2.000	2.000	2.000	13.65	16.01	13.30	5850	63.10	37.93	774	6765	826	7548	0.937	0.896			
4.1	2	24.00	1.410	2.000	2.000	2.000	13.65	16.01	13.30	5850	64.60	40.37	823	7201	826	7548	0.997	0.954			
Hester et al. (1991, 1993)																					
1.1	3	16.00	1.000	2.000	1.500	2.000	16.00	16.00	13.50	5990	63.80	50.13	512	4501	455	4067	1.124	1.107			
2.1	3	16.00	1.000	2.000	1.500	1.840	16.00	13.33	13.99	6200	69.00	46.25	464	4118	448	4030	1.035	1.022			
3.1	3	16.00	1.000	2.000	1.500	2.040	16.09	16.23	13.69	6020	71.10	46.86	477	4202	457	4076	1.044	1.031			
4.1	3	16.00	1.000	2.000	1.500	2.100	16.08	16.22	13.62	6450	71.10	42.36	417	3734	460	4089	0.907	0.913			
5.1	3	16.00	1.000	2.000	1.500	2.050	16.09	16.27	13.72	5490	69.00	39.86	425	3658	457	4078	0.929	0.897			
6.1	3	22.75	1.000	2.000	1.500	2.150	16.06	16.19	13.54	5850	69.00	51.99	537	4696	595	5030	0.902	0.934			
7.1	2	16.00	1.000	2.000	4.000	2.120	16.03	16.20	13.58	5240	69.00	45.40	495	4215	483	4274	1.025	0.986			
Rezansoff et al. (1993)																					
2a	3	29.53	0.992	1.827	0.994	2.008	13.58	12.99	10.49	3958	64.52	60.24	742	5885	631	5194	1.175	1.133			
2b	3	29.53	0.992	1.827	0.994	2.008	13.58	12.99	10.49	3799	64.52	60.48	760	5970	631	5194	1.204	1.149			
5a	3	35.43	1.177	1.819	1.183	2.008	15.43	20.00	17.40	4031	68.87	56.96	973	7756	852	7107	1.142	1.091			
5b	3	34.29	1.177	1.819	1.183	2.008	15.43	20.00	17.40	3726	68.87	67.50	1200	9374	1014	8221	1.183	1.140			
Azizinamini et al. (1993)																					
BB-8-5-23	2	23.00	1.000	1.500	1.000	1.000	9.00	14.00	12.50	5290	77.85	47.30	514	4381	432	3920	1.190	1.118			
AB83-8-15-41	2	41.00	1.000	1.500	1.000	1.000	9.00	14.00	12.50	15120	77.85	72.67	467	5177	660	5534	0.707	0.936			
BB-11-5-24	2	24.00	1.410	1.410	1.770	1.410	12.00	16.00	13.89	5080	70.80	29.82	653	5511	706	6701	0.925	0.822			
BB-11-5-40	2	40.00	1.410	1.410	1.770	1.410	12.00	16.00	13.89	5080	70.80	43.44	951	8026	992	8725	0.870	0.979			
BB-11-12-24	2	24.00	1.410	1.410	1.770	1.410	12.00	16.00	13.89	12730	70.80	44.40	614	6521	706	6701	0.870	0.973			
B-11-12-40	2	40.00	1.410	1.410	1.770	1.410	12.00	16.00	13.89	13000	70.80	58.47	800	8543	992	8725	0.807	0.979			
BB-11-11-45	3	45.00	1.410	1.410	1.680	1.410	18.00	18.00	15.89	109											

Table 5.5 (continued)
Data and test/prediction ratios for developed and spliced bars
without confining reinforcement

Test No.	n	l_d	d_b	c_{so}	c_s	c_b	b	h	d	f_c	f_y	f_i^*	$T_c/f_c^{1/2}$	$T_e/f_c^{1/4}$	$T_e/f_c^{1/2}$	$T_e/f_c^{1/4}$	Test	Test	Eq. 5.5**	Eq. 5.4*	Eq. 5.5	Eq. 5.4	
	(in.)	(in.)	(in.)	(in.)	(in.)	(in.)	(in.)	(in.)	(in.)	(psi)	(ksi)	(ksi)	(in. ²)	(in. ³)	(in. ³)	(in. ²)							
Darwin et al. (1995a, 1996a)																							
1.1	2	16.00	1.000	2.969	2.938	2.938	16.08	17.22	13.76	5020	67.69	51.78	577	4859	606	5151	0.952	0.943					
1.2	2	16.00	1.000	2.032	2.281	1.938	24.06	16.25	13.79	5020	67.69	44.77	499	4202	474	4209	1.054	0.998					
1.3	3	16.00	1.000	2.032	1.406	1.938	16.07	16.21	13.75	5020	67.69	45.22	504	4244	444	3986	1.135	1.065					
2.4	2	24.00	1.000	2.000	1.914	1.313	12.13	15.64	13.79	5250	75.42	54.29	592	5039	553	4692	1.070	1.074					
2.5	2	24.00	1.000	2.063	1.856	1.813	12.13	16.01	13.67	5250	75.42	58.97	643	5473	624	5247	1.031	1.043					
4.5	2	24.00	1.000	2.063	1.936	1.844	12.12	16.15	13.79	4090	67.69	51.50	636	5088	628	5282	1.013	0.963					
6.5	2	24.00	1.000	2.000	1.906	1.969	12.10	16.13	13.63	4220	75.42	54.06	657	5299	643	5409	1.023	0.980					
8.3	2	24.00	1.000	2.000	1.953	2.000	12.11	16.05	13.53	3830	77.96	62.38	796	6264	647	5445	1.230	1.151					
10	2	26.00	1.000	2.063	1.875	1.933	12.13	16.25	13.78	4250	80.57	61.84	749	6051	683	5677	1.098	1.066					
13	3	16.00	0.625	2.094	1.016	1.354	12.19	15.60	13.92	4110	61.83	60.26	291	2333	272	2254	1.073	1.035					
14.3**	3	17.00	0.625	2.032	1.031	1.295	12.14	15.51	13.89	4200	61.83	61.83	296	2381	285	2351	1.040	1.013					
16	2	40.00	1.410	3.063	2.984	1.908	18.05	16.12	13.47	5250	77.77	54.51	1174	9989	1280	10516	0.917	0.950					
16	2	40.00	1.410	3.016	2.969	1.895	18.07	16.28	13.64	5180	77.77	52.75	1143	9700	1272	10470	0.899	0.926					
Current Study																							
25.1**	3	16.50	0.625	1.985	1.023	1.556	12.19	16.27	14.37	4490	62.98	63.72	295	2413	287	2344	1.029	1.029					
19.1	3	36.00	1.000	1.953	1.930	1.961	18.14	16.16	13.66	4250	80.57	73.51	891	7193	887	7140	1.004	1.007					
19.2	3	36.00	1.000	2.016	1.883	1.929	18.06	16.13	13.66	4250	80.57	67.85	822	6639	886	7117	0.928	0.933					
20.6	3	40.00	1.000	1.516	0.672	1.300	12.09	15.60	13.76	5080	80.57	57.15	633	5348	664	5473	0.954	0.977					
23a.5	2	22.00	1.000	2.000	1.891	1.938	18.19	16.16	13.63	9320	80.57	62.24	509	5005	597	5080	0.854	0.985					
23a.6	2	29.00	1.000	2.031	1.875	1.919	12.24	16.11	13.67	9320	80.57	75.47	618	6068	740	6086	0.834	0.997					
23b.3	2	19.50	1.000	3.031	3.859	3.057	18.23	16.32	12.72	8370	80.57	71.64	619	5917	723	5979	0.855	0.990					
24.1	2	32.00	1.000	2.000	1.875	1.903	12.14	16.12	13.69	4300	79.70	61.91	746	6040	797	6488	0.936	0.931					
26.3	3	40.00	1.000	1.547	0.652	1.889	12.11	16.19	13.78	4960	79.70	62.52	701	5885	728	5781	0.963	1.018					
26.5	3	40.00	1.000	1.500	0.684	1.891	12.15	16.17	13.75	4960	77.96	64.36	722	6058	734	5828	0.984	1.040					
31.5	3	22.00	1.000	1.828	0.508	1.494	12.26	15.58	13.56	12890	79.70	61.43	427	4555	436	3852	0.981	1.182					
31.6	3	22.00	1.000	1.719	0.539	1.492	12.17	15.49	13.44	12890	69.50	63.42	441	4702	437	3869	1.009	1.215					
34.1	3	24.00	1.000	2.063	1.938	1.941	18.13	16.12	13.66	5440	79.70	57.88	620	5324	642	5394	0.965	0.987					
34.2	3	24.00	1.000	2.070	1.945	1.918	18.17	16.05	13.61	5440	79.70	61.97	664	5701	639	5369	1.039	1.062					
34.3	3	24.00	1.000	2.080	1.844	1.981	18.12	16.02	13.49	5440	69.50	58.94	631	5422	649	5444	0.973	0.996					
34.4	3	24.00	1.000	2.045	1.883	1.936	18.21	16.02	13.53	5440	69.50	58.49	626	5380	640	5383	0.978	1.000					
36.3	3	26.00	1.000	2.016	1.836	2.000	18.17	16.10	13.55	5060	69.50	62.78	597	5881	690	5748	1.010	1.023					
36.4	3	26.00	1.000	2.031	1.828	1.988	18.14	16.10	13.56	5060	69.50	60.17	668	5636	689	5737	0.969	0.982					
38.1	3	26.00	1.000	1.938	1.953	1.802	18.25	16.10	13.75	5080	69.50	53.96	598	5049	654	5477	0.914	0.922					
38.2	3	26.00	1.000	2.125	1.844	2.075	18.17	16.14	13.51	5080	69.50	60.30	668	5643	707	5865	0.945	0.962					
39.6	3	21.00	1.000	1.953	0.516	1.505	12.19	15.41	13.59	14450	67.69	67.38	443	4855	425	3779	1.043	1.285					
40.5	2	17.00	1.000	2.000	1.875	1.846	12.11	16.04	13.67	15650	77.96	65.81	416	4649	484	4277	0.859	1.087					
28.5	2	30.00	1.410	1.977	4.031	1.999	18.09	16.20	13.45	12610	77.77	50.89	707	7492	959	8486	0.738	0.883					
30.5	2	30.00	1.410	2.063	4.016	1.956	18.12	16.15	13.44	13220	77.77	66.95	908	9740	960	8486	0.946	1.148					
32.1	2	32.00	1.410	2.000	0.984	1.904	12.17	16.17	13.52	14400	77.77	63.33	823	9019	875	7778	0.940	1.160					
32.2	2	32.00	1.410	2.000	1.063	1.916	12.14	16.16	13.51	14400	66.69	61.49	799	8757	887	7873	0.901	1.112					
32.3	2	32.00	1.410	1.969	4.016	1.947	18.14	16.15	13.45	14400	77.77	60.64	788	8635	996	8750	0.791	0.987					
32.4	2	28.00	1.410	2.031	4.047	1.935	18.20	16.17	13.50	14400	66.69	61.01	793	8688	909	8127	0.872	1.069					
For all 171 specimens :																							
Max. 1.396 1.297																							
Min. 0.549 0.732																							
Mean 1.001 1.005																							
St. Dev. 0.152 0.105																							
COV 0.152 0.104																							
For 152 specimens with $f_i < f_y$:																							
Max. 1.396 1.297																							
Min. 0.549 0.754																							
Mean 1.014 1.008																							
St. Dev. 0.144 0.101																							
COV 0.142 0.100																							
For 19 specimens with $f_i \geq f_y$:																							

- * Bar stress is computed using the moment-curvature method if M_u is not in excess of the moment capacity from moment-curvature analysis; otherwise f_s is computed using the ultimate strength method

Table 5.5 (continued)
Data and test/prediction ratios for developed and spliced bars
without confining reinforcement

** specimens with $f_s \geq f_y$

$$+ \quad \text{Eq. 5.4} = \frac{T_c}{f'_c^{1/4}} = \frac{A_b f_s}{f'_c^{1/4}} = [59.8l_d(c_{\min} + 0.5d_b) + 2350A_b] \left(0.1 \frac{c_{\max}}{c_{\min}} + 0.9 \right)$$

$$++ \quad \text{Eq. 5.5} = \frac{T_c}{f'_c^{1/2}} = \frac{A_b f_s}{f'_c^{1/2}} = [8.45l_d(c_{\min} + 0.5d_b) + 177.6A_b] \left(0.17 \frac{c_{\max}}{c_{\min}} + 0.83 \right)$$

1 in. = 25.4 mm; 1 psi = 6.895 kPa; 1 ksi = 6.895 MPa

Table 5.6
Comparisons of the coefficients of determination for the best-fit lines
of $T_s/f'_c^{1/4}$ versus NA_{tr}/n for bars in normal strength concrete
using c_{si} , $c_{si} + 0.25$ in., and $1.6c_{si}$ as the effective values of c_{si}

Bar*	r^2 **		
	c_{si}	$c_{si} + 0.25$ in.	$1.6c_{si}$
5N0(L)	0.200	0.742	0.688
5C2(L)	0.079	0.427	0.501
Conv. No. 8(L)	0.598	0.661	0.713
8N0(B)	0.854	0.781	0.780
8C1(L)	0.620	0.731	0.382
8N3(L)	0.943	0.948	0.941
8N3(B)	0.833	0.794	0.793
8F1(L)	0.821	0.841	0.840
8F1(B)	0.865	0.963	0.963
11F3(L)	0.509	0.568	0.316
Conv. No. 11(L)	0.782	0.797	0.794

* (L) = Bars in the concrete containing limestone coarse aggregate
 (B) = Bars in the concrete containing basalt coarse aggregate

** Coefficient of determination for $f'_c^{1/4}$ versus NA_{tr}/n

Table 5.7

**Comparisons of coefficients of determination for the best-fit lines of $T_s/f'_c P$ versus NA_{tr}/n for high relative rib area and conventional bars
(T_s in lb, $f'_c P$ in psi, and A_{tr} in in.²)**

Bar * Designation	No. of Tests		$r^2 **$			
	NSC +	HSC ++	$p = 1/4$	$p = 1/2$	$p = 3/4$	$p = 1$
Conv. No. 8	23	9	0.4839	0.5816	0.6607	0.7112
8N3	5	10	0.7618	0.8968	0.9160	0.8679
11F3	11	2	0.5718	0.6348	0.6553	0.6551

* Notation of bar designation is the same as in Table 2.2

** Coefficient of determination for the best-fit line of $T_s/f'_c P$ versus NA_{tr}/n

+ Normal strength concrete containing limestone coarse aggregate;
 $f'_c < 8000$ psi

++ High strength concrete containing limestone coarse aggregate;
 8000 psi $\leq f'_c \leq 16,000$ psi

1 lb = 4.448 N; 1 psi = 6.895 kPa; 1 in. = 25.4 mm

Table 5.8
Results of best-fit lines for $T_s/f'_c P$ versus NA_{tr}/n
(T_s in lb, $f'_c P$ in psi, and A_{tr} in in.²)

Bars * Test	No. of Test	Weighted Mean R_t	$p = 1/4$			$p = 1/2$			$p = 3/4$			$p = 1.0$		
			m^+	b^{++}	r^{+++}									
11F3 (L)	13	0.127	2419	1551	0.5718	318.5	145.9	0.6348	40.75	13.76	0.6553	5.11	1.302	0.6551
8F1 (L)	12	0.140	2816	75	0.8412	352.1	3.4	0.8641	44.00	-0.26	0.8804	5.50	-0.113	0.8907
8N3 (L)	15	0.119	2476	628	0.7617	310.7	41.9	0.8968	38.87	1.62	0.9160	4.85	-0.156	0.8678
Conv. No. 11 (L)	6	0.071	1871	460	0.7875	218.5	59.2	0.7854	25.51	7.58	0.7816	2.98	0.966	0.7758
8C1 (L)	7	0.101	1869	130	0.7304	232.6	14.7	0.7219	28.94	1.65	0.7126	3.60	0.185	0.7029
Conv. No. 8 (L)	32	0.075	2303	-89	0.5104	264.8	-16.9	0.6021	30.81	-2.70	0.6735	3.62	-0.396	0.7136
5C2 (L)	4	0.109	1408	133	0.4273	173.8	16.8	0.4263	21.45	2.13	0.4252	2.65	0.269	0.4240
Conv. No. 5 (L)	4	0.082	1282	103	0.7416	158.7	12.9	0.7440	19.65	1.63	0.7464	2.43	0.206	0.7486
Conv. No. 8 (B)	10	0.069	1076	1235	0.1210	186.1	97.4	0.3041	28.25	6.68	0.4993	4.02	0.303	0.6403
8N3 (B)	4	0.119	3471	-105	0.7938	440.2	-15.2	0.7831	55.84	-2.16	0.7727	7.08	-0.302	0.7625
8F1 (B)	4	0.140	3769	121	0.9611	464.3	15.5	0.9576	57.19	1.97	0.9539	7.05	0.252	0.9501

* (L): bars in concrete containing limestone coarse aggregate

(B): bars in concrete containing basalt coarse aggregate

+ Slope of the best-fit line

++ Intercept of the best-fit line

+++ Coefficient of determination of the best-fit line

1 lb = 4.448 N; 1 psi = 6.895 kPa; 1 in. = 25.4 mm

Table 5.9
Analysis of effects of relative rib area, R_r , and bar diameter, d_b , on increase in splice strength, represented by $T_s/f_c^{3/4}$, provided by transverse reinforcement, represented by NA_{tr}/n (T_s in lb, $f_c^{3/4}$ in psi, and A_{tr} in in.²)

Bars *	No. of Tests	Weighted Mean R_r	m^+	b^{++}	Mean *** Slope, M	$M_{R_r=0.075}^{****}$	t_r^{**}	$t_d = M/t_r^{***}$
Conv. No. 5 (L)	4	0.082	19.66	1.632	21.290	20.70	1.029	19.69
5C2 (L)	4	0.109	21.45	2.128	23.577		1.139	17.55
Conv. No. 8 (L)	32	0.075	30.81	-2.695	28.118	26.92	1.045	27.74
8C1 (L)	7	0.101	28.94	1.652	30.591		1.137	24.17
8N3 (L)	15	0.119	38.87	1.617	40.485		1.504	28.12
8F1 (L)	12	0.140	44.01	-0.259	43.747		1.625	26.62
Conv. No. 11 (L)	6	0.071	25.51	7.580	33.093	34.62	0.956	33.95
11F3 (L)	13	0.127	40.75	13.760	54.508		1.574	35.92
Conv. No. 8 (B)	10	0.069	28.25	6.678	34.928	37.33	0.936	36.56
8F1 (B)	4	0.140	57.19	1.973	59.163		1.585	36.00
8N3 (B)	4	0.119	55.84	-2.156	53.686		1.438	37.28

* (L): bars in concrete containing limestone coarse aggregate
 (B): bars in concrete containing basalt coarse aggregate

** $t_r = M/M_{R_r=0.075}$

*** $t_r = 9.6 R_r + 0.28$ (used to calculate t_d)

+ Slope of the best-fit line

++ Intercept of the best-fit line

+++ $M = (m + b)$

**** Based on best-fit line for each bar size and concrete type

1 lb = 4.448 N; 1 psi = 6.895 kPa; 1 in. = 25.4 mm

Table 5.10
Summary of the expressions for t_r and t_d terms using different p values

p^*	Expression of t_r		Expression of t_d	
	$t_r =$	r^2^{**}	$t_d =$	r^2^{**}
1/4	$7.9 R_r + 0.41$	0.764	$0.87 d_b + 0.13$	0.828
1/2	$8.8 R_r + 0.34$	0.882	$0.83 d_b + 0.17$	0.902
3/4	$9.6 R_r + 0.28$	0.942	$0.78 d_b + 0.22$	0.951
1.0	$10.3 R_r + 0.23$	0.957	$0.73 d_b + 0.27$	0.970

* Power of concrete compressive strength, f_c , used to normalize the additional bond force provided by transverse reinforcement, T_s

** Coefficient of determination of the best-fit line

Table 5.11
Data and test/prediction ratios for developed and spliced bars
with confining reinforcement

Specimen No.	n	l_u	d_b	R_r	c_{se}	c_s	b	h	d	d_t	N°	f_c	f_t	f_y	ϵ_y	$T_b/f_c^{1/4}$	$T_b/f_c^{1/4}$	Test																					
																			Test	Eq. 5.18**	Prediction																		
(in.)																																							
Mathey and Waitzman (1961)**																																							
4-7-2**	1	7.00	0.50	0.0960	3.75		1.75	8.00	18.00	16.00	0.50	2	4210	88.71	114.70	114.70	2202	2306	0.955																				
4-7-1**	1	7.00	0.50	0.0960	3.75		1.75	8.00	18.00	16.00	0.50	2	4265	92.21	114.70	114.70	2282	2312	0.987																				
4-10.5-3***	1	10.50	0.50	0.0960	3.75		1.75	8.00	18.00	16.00	0.50	3	3675	113.71	114.70	114.70	2921	2992	0.976																				
4-10.5-2***	1	10.50	0.50	0.0960	3.75		1.75	8.00	18.00	16.00	0.50	3	4055	115.26	114.70	114.70	3889	3046	0.948																				
4-14-2***	1	14.00	0.50	0.0960	3.75		1.75	8.00	18.00	16.00	0.50	4	3710	100.69	114.70	114.70	2580	3741	0.690																				
8-21-1***	1	21.00	1.00	0.0880	3.50		1.50	8.00	18.00	16.00	0.50	5	4235	62.16	97.00	114.70	6087	7482	0.813																				
8-28-1***	1	28.00	1.00	0.0880	3.50		1.50	8.00	18.00	16.00	0.50	7	4485	77.79	97.00	114.70	7509	9440	0.795																				
8-28-2***	1	28.00	1.00	0.0880	3.50		1.50	8.00	18.00	16.00	0.50	7	3700	72.59	97.00	114.70	7353	9115	0.807																				
8-34-1***	1	34.00	1.00	0.0880	3.50		1.50	8.00	18.00	16.00	0.50	9	3745	93.63	97.00	114.70	9455	10803	0.875																				
8-14-1***	1	14.00	1.00	0.0880	3.50		1.50	8.00	18.00	16.00	0.50	4	3585	33.51	97.00	114.70	3421	5913	0.579																				
8-34-2***	1	34.00	1.00	0.0880	3.50		1.50	8.00	18.00	16.00	0.50	9	3765	91.10	97.00	114.70	9188	10814	0.850																				
8-14-2***	1	14.00	1.00	0.0880	3.50		1.50	8.00	18.00	16.00	0.50	4	4055	42.63	97.00	114.70	4220	6035	0.699																				
8-7-1**	1	7.00	1.00	0.0880	3.50		1.50	8.00	18.00	16.00	0.50	2	4005	28.63	97.00	114.70	2843	4189	0.679																				
8-21-2***	1	21.00	1.00	0.0880	3.50		1.50	8.00	18.00	16.00	0.50	5	3495	53.62	97.00	114.70	5509	7251	0.760																				
Ferguson and Breen (1965)**																																							
8F36c	2	36.00	1.000	0.0731	3.250	3.295	1.470	17.09	14.97	13.00	0.252	6	2740	62.56	74.00	52.00	6831	7523	0.908																				
8F36d*	2	36.00	1.000	0.0731	3.250	3.280	1.530	17.06	15.00	12.97	0.252	10	3580	74.74	74.00	52.00	7633	8077	0.945																				
8F36e*	2	36.00	1.000	0.0731	3.250	3.310	1.470	17.12	14.91	12.94	0.252	6	4170	77.38	74.00	52.00	7597	7684	0.989																				
8F36f*	2	36.00	1.000	0.0731	3.250	3.280	1.500	17.06	15.09	13.04	0.252	10	3780	77.64	74.00	52.00	7822	8063	0.970																				
8F36g*	2	36.00	1.000	0.0731	3.250	3.265	1.530	17.03	14.97	12.94	0.252	6	3070	75.34	74.00	52.00	7996	7654	1.045																				
8F36h	2	36.00	1.000	0.0731	3.250	3.265	1.590	17.03	15.09	13.00	0.252	14	1910	57.88	74.00	52.00	6917	8126	0.851																				
8F36j	2	36.00	1.000	0.0731	3.250	3.310	1.500	17.12	15.03	13.02	0.252	14	1820	66.98	74.00	52.00	8101	7961	1.018																				
8F30b	2	30.00	1.000	0.0731	3.250	3.270	1.500	17.04	15.03	13.03	0.252	6	2610	58.62	74.00	52.00	6479	6751	0.960																				
11R36a	2	49.50	1.410	0.0674	4.590	4.620	2.020	24.06	18.05	15.33	0.375	11	3020	85.26	93.00	42.00	17941	15970	1.123																				
Thompson et al. (1975)**																																							
11-30-4/2/2-6/6-S5	6	30.00	1.410	0.0674	2.000	2.000	2.000	40.88	13.00	10.30	0.375	6	3063	49.06	65.00	68.00	10287	10127	1.016																				
11-20-4/2/2-6/6-SP**	6	22.00	1.410	0.0674	2.000	2.000	2.000	40.88	13.00	10.30	0.375	7	3620	43.61	67.30	67.30	8770	9225	0.951																				
11-20-4/2/2-6/6-S5**	6	15.00	1.410	0.0674	2.000	2.000	2.000	40.88	13.00	10.30	0.375	4	3400	41.92	67.30	67.30	8565	7300	1.173																				
8-15-4/2/2-6/6-S5**	6	15.00	1.000	0.0727	2.000	2.000	2.000	36.00	13.00	10.50	0.375	3	3507	58.66	61.10	61.10	6022	4929	1.222																				
Zekany et al. (1981)***																																							
9-53-B**	5	16.00	1.128	0.0727	2.000	1.500	2.000	27.25	16.00	13.44	0.236	4	5700	57.79	62.80	70.00	6651	5107	1.302																				
11-40-B-A**	4	22.00	1.410	0.0674	2.000	2.000	2.000	27.25	16.00	13.30	0.236	5	5425	45.28	60.10	70.00	8230	8131	1.012																				
2-4.5-80-B**	4	22.00	1.410	0.0674	2.000	2.000	2.000	27.25	16.00	13.30	0.236	5	4200	43.16	60.10	74.50	8363	8022	1.043																				
2-5-40-B(4)**	4	22.00	1.410	0.0674	2.000	2.000	2.000	27.25	16.00	13.30	0.236	4	3850	42.31	60.10	70.00	8379	7885	1.063																				
3-5-53-B**	4	22.00	1.410	0.0674	2.000	2.000	2.000	27.25	16.00	13.30	0.375	4	3775	40.09	60.10	60.30	7979	8497	0.959																				
2-4.5-53-B**	4	22.00	1.410	0.0674	2.000	2.000	2.000	27.25	16.00	13.30	0.236	5	4125	42.62	60.10	74.50	8297	8015	1.035																				
11-53-B**	4	22.00	1.410	0.0674	2.000	2.000	2.000	27.25	16.00	13.30	0.236	5	4025	43.00	60.10	70.00	8421	8005	1.052																				
11-40-B-D**	4	22.00	1.410	0.0674	2.000	2.000	2.000	27.25	16.00	13.30	0.236	5	5050	46.03	60.10	70.00	8518	8099	1.052																				
11-53-B-D**	4	22.00	1.410	0.0674	2.000	2.000	2.000	27.25	16.00	13.30	0.236	5	4125	34.23	60.10	70.00	6662	8015	0.831																				
3-5-40-B**	4	22.00	1.410	0.0674	2.000	2.000	2.000	27.25	16.00	13.30	0.375	4	3750	38.82	60.10	60.30	7738	8493	0.911																				
DeVries et al. (1991)***																																							
8Q-9B-P6**	2	9.00	0.750	0.0799	1.875	1.125	1.125	11.00	16.00	14.50	0.375	3	8850	70.16	76.63	78.58	3183	3152	1.010																				
8N-9B-P6**	2	9.00	0.750	0.0799	1.625	2.438	1.250	11.10	16.00	14.38	0.375	3	8300	56.34	76.63	78.58	2597	3116	0.834																				
8G-22B-P9	2	22.00	1.128	0.0727	1.500	1.744	1.125	11.00	16.00	14.31	0.375	4	7460	52.74	66.40	78.58	5675	6338	0.895																				
8N-18B-P9**	2	18.00	1.128	0.0727	1.375	1.932	1.500	11.10	16.00	13.94	0.375	3	7660	51.63	70.35	78.58	5519	5791	0.953																				
8G-16B-P9**	2	16.00	1.128	0.0727	1.375	1.869	1.063	11.00	16.00	14.37	0.375	3	7460	42.34	66.40	78.58	4556	5318	0.857																				
8G-18B-P9**	2	18.00	1.128	0.0727	1.688	1.557	1.250	11.00	16.00	14.19	0.375	3	8610	52.25	70.35	78.58	5424	5846	0.928																				
10N-12B-P9**	2	12.00	1.128	0.0727	1.938	1.307	1.188	1																															

Table 5.11 (continued)
Data and test/prediction ratios for developed and spliced bars
with confining reinforcement

Specimen No.	n	l _b	d _b	R _r	c ₁₀	c ₂₀	c ₃₀	b	h	d	d _s	N*	f _c	f _t	f _r	f _s	T _s /f _c ^{1/4}	T _s /f _c ^{1/4}	Test
																	Test	Eq. 5.18** Prediction	
Rezansoff et al. (1991)***																			
20-6-2	2	18.15	0.768	0.0799	1.000	2.980	1.000	11.02	12.99	11.61	0.313	5	4277	70.77	72.50	62.08	4069	3524	1.155
20-6-3*	2	15.39	0.768	0.0799	1.000	2.980	1.000	11.02	12.99	11.61	0.313	6	3886	75.23	72.50	62.08	4431	3379	1.311
20-6-4*	2	22.09	0.768	0.0799	1.000	2.980	1.000	11.02	12.99	11.61	0.313	3	4045	77.86	72.50	62.08	4539	3564	1.274
20-8-11*	2	16.34	0.992	0.0731	1.000	2.530	1.000	11.02	13.00	11.50	0.313	13	4466	75.00	65.54	62.08	7110	5569	1.277
20-8-9	2	18.70	0.992	0.0731	1.500	2.030	1.500	11.02	13.00	11.00	0.313	9	4205	61.10	65.54	62.08	5880	5669	1.037
20-8-10**	2	15.12	0.992	0.0731	1.500	2.030	1.500	11.02	13.00	11.00	0.313	12	4408	65.16	65.54	62.08	6198	5743	1.079
20-8-4*	2	18.70	0.992	0.0731	1.000	2.530	1.000	11.02	13.00	11.50	0.313	13	5220	71.05	65.54	62.08	6478	5966	1.086
20-8-12	2	16.34	0.992	0.0731	1.500	2.030	1.500	11.02	13.00	11.00	0.313	11	4350	65.38	65.54	62.08	6239	5721	1.091
20-8-2	2	21.77	0.992	0.0731	1.000	2.530	1.000	11.02	13.00	11.50	0.313	11	5742	65.36	65.54	62.08	5819	6009	0.968
20-8-3	2	26.10	0.992	0.0731	1.000	2.530	1.000	11.02	13.00	11.50	0.313	9	5510	64.59	65.54	62.08	5810	6006	0.967
20-8-6*	2	26.10	0.992	0.0731	1.000	2.530	1.000	11.02	13.00	11.50	0.313	9	4770	75.37	65.54	62.08	7028	5877	1.196
20-8-7	2	26.10	0.992	0.0731	1.500	2.030	1.500	11.02	13.00	11.00	0.313	4	4495	62.30	65.54	62.08	5897	5828	1.012
20-8-8	2	21.77	0.992	0.0731	1.500	2.030	1.500	11.02	13.00	11.00	0.313	7	4350	60.52	65.54	62.08	5776	5757	1.003
20-8-5*	2	21.77	0.992	0.0731	1.000	2.530	1.000	11.02	13.00	11.50	0.313	11	4770	76.01	65.54	62.08	7088	5811	1.220
20-8-4*	2	18.70	0.992	0.0731	1.000	2.530	1.000	11.02	13.00	11.50	0.313	13	4335	71.94	65.54	62.08	6871	5747	1.196
20-8-21**	2	15.35	0.992	0.0731	1.260	2.270	1.500	11.02	13.00	11.00	0.313	7	3378	46.58	60.90	52.21	4735	4832	0.980
20-8-13	2	28.70	0.992	0.0731	1.180	2.350	1.000	11.02	13.00	11.50	0.313	4	3509	52.17	64.38	52.21	5254	5255	1.000
20-8-14	2	23.11	0.992	0.0731	1.180	2.350	1.000	11.02	13.00	11.50	0.313	6	3277	54.51	64.38	52.21	5584	4986	1.120
20-8-15	2	20.31	0.992	0.0731	1.180	2.350	1.000	11.02	13.00	11.50	0.313	7	3625	55.74	64.38	52.21	5567	4924	1.131
20-8-16	2	28.70	0.992	0.0731	1.180	2.350	1.000	11.02	13.00	11.50	0.313	4	3291	56.14	60.90	52.21	5744	5230	1.098
20-8-18	2	17.44	0.992	0.0731	1.180	2.350	1.000	11.02	13.00	11.50	0.313	8	3349	56.07	60.90	52.21	5712	4750	1.203
20-8-19	2	21.65	0.992	0.0731	1.260	2.270	1.500	11.02	13.00	11.00	0.313	4	3219	45.41	60.90	52.21	4672	4927	0.948
20-8-17*	2	20.31	0.992	0.0731	1.180	2.350	1.000	11.02	13.00	11.50	0.313	7	3480	60.90	60.90	52.21	6145	4900	1.254
20-8-20	2	17.32	0.992	0.0731	1.260	2.270	1.500	11.02	13.00	11.00	0.313	6	3291	45.78	60.90	52.21	4684	4739	0.988
20-9-1	2	19.69	1.177	0.0727	2.000	2.140	1.500	12.99	21.72	17.91	0.444	7	3538	59.66	67.28	60.05	8393	7641	1.098
20-9-2	2	25.59	1.177	0.0727	2.000	2.140	1.500	12.99	24.03	17.91	0.444	5	3378	66.15	67.28	60.05	9414	7725	1.219
20-11-4**	2	18.90	1.406	0.0674	2.020	1.670	1.508	12.99	20.00	17.79	0.444	10	4350	48.03	66.12	83.40	9167	10275	0.892
20-11-2*	2	26.57	1.406	0.0674	2.020	1.670	2.295	12.99	20.00	17.00	0.444	11	4355	69.92	69.02	83.40	13356	12477	1.071
20-11-1*	2	37.99	1.406	0.0674	2.020	1.670	2.295	12.99	20.00	17.00	0.444	5	4770	69.02	69.02	83.40	12872	12091	1.065
20-11-3	2	26.61	1.406	0.0674	2.020	1.670	1.508	12.99	20.00	17.79	0.444	7	4466	53.02	66.12	83.40	10053	10369	0.970
20-11-8	2	34.29	1.406	0.0674	2.000	1.690	1.000	12.99	22.70	18.30	0.444	10	3349	63.30	66.12	60.05	12896	11432	1.128
20-11-5	2	27.01	1.406	0.0674	2.000	1.690	2.000	12.99	21.27	17.30	0.444	9	3625	65.82	66.12	60.05	13148	11356	1.158
20-11-6	2	34.72	1.406	0.0674	2.000	1.690	2.000	12.99	24.06	17.30	0.444	6	3625	55.80	66.12	60.05	11147	11519	0.968
20-11-7	2	27.20	1.406	0.0674	2.000	1.690	1.000	12.99	21.54	18.30	0.444	12	3291	52.59	66.12	60.05	10762	11285	0.954
Rezansoff et al. (1993)***																			
6	3	22.05	0.992	0.0731	1.827	0.502	2.008	11.61	12.99	10.49	0.313	8	3625	52.50	64.52	84.10	5243	5032	1.042
1b*	2	29.53	0.992	0.0731	1.827	0.520	2.008	8.66	12.99	10.49	0.250	6	3799	69.82	64.52	63.80	6892	5505	1.252
1a*	2	29.53	0.992	0.0731	1.827	0.520	2.008	8.66	12.99	10.49	0.250	6	3958	74.05	64.52	63.80	7235	5521	1.310
7**	3	14.76	0.992	0.0731	1.827	0.502	2.008	11.61	12.99	10.49	0.630	4	3625	47.93	64.52	68.15	4787	5788	0.827
3a*	3	29.53	0.992	0.0731	1.827	0.502	2.008	11.61	12.99	10.49	0.250	6	3958	69.76	64.52	63.80	6816	5322	1.281
3b	3	29.53	0.992	0.0731	1.827	0.502	2.008	11.61	12.99	10.49	0.250	6	3799	61.57	64.52	63.80	6078	5310	1.145
8**	3	11.81	0.992	0.0731	1.827	0.994	2.008	13.58	12.99	10.49	0.630	3	3625	34.50	64.52	68.15	3446	4967	0.694
4b*	3	44.29	1.177	0.0727	1.819	0.573	2.008	2.99	20.00	17.40	0.250	5	3726	68.87	68.87	63.80	9564	7783	1.229
9*	3	33.46	1.177	0.0727	1.819	0.573	2.008	12.99	20.00	17.40	0.445	10	3886	76.40	68.87	68.87	10499	8630	1.217
10*	3	22.05	1.177	0.0727	1.819	0.573	2.008	12.99	20.00	17.40	0.250	7	4089	70.99	68.87	68.15	9632	8515	1.131
4a	3	35.43	1.177	0.0727	1.819	0.573	2.008	12.99	20.00	17.40	0.250	4	4031	62.56	68.87	63.80	8519	6879	1.238
Azizinamini et al. (1995 at CTL)****																			
ABS-11-15-57-55-50*	2	57.50	1.410	0.0674	1.410	1.770	1.410	12.00	16.00	13.89	0.252	6	15120	75.96	73.70	58.98	10686	12830	0.833
Azizinamini et al. (1995 at UNL)***																			
ABS-11-15-45S-60	3	45.00	1.410	0.0590	1.410	1.680	1.410	18.00	18.00	15.89	0.375	4	14890	70.48	70.50	71.80	9953	11707	0.850
ABS-11-15-45S-100*	3	45.00	1.410	0.0590	1.410	1.680	1.410	18.00	18.00	15.89	0.375	6	14850	76.79	70.50	71.80	10851	12634	0.859
ABS-11-15-40S																			

Table 5.11 (continued)
Data and test/prediction ratios for developed and spliced bars
with confining reinforcement

Specimen No.	n	l _d	d _b	R _r	c _{so}	c _{st}	c _b	b	d	d _t	N*	f _c	f _s	f _y	f _u	T _v /f _c ^{1/4}	T _v /f _c ^{1/4}	Test Eq. 5.18 ^{**}	Prediction
					(in.)	(in.)	(in.)	(in.)	(in.)	(in.)	(in.)	(psi)	(ksi)	(ksi)	(ksi)	(in. ²)	(in. ²)		
1.6	3	16.00	1.000	0.1010	2.063	1.438	1.938	16.05	16.19	13.74	0.500	3	5200	52.30	67.69	70.50	4908	5390	0.911
2.1	2	24.00	1.000	0.0710	2.250	1.706	1.328	12.12	15.36	15.70	0.375	7	5250	62.81	64.52	69.92	5839	6647	0.877
2.2 [*]	2	24.00	1.000	0.1400	2.125	1.801	1.406	12.12	15.52	13.58	0.375	7	5250	77.60	75.42	69.92	7202	7903	0.911
2.3	2	24.00	1.000	0.1400	2.125	1.780	1.969	12.11	16.06	13.56	0.375	4	5250	74.12	75.42	69.92	6879	7313	0.941
3.4	2	24.00	1.000	0.0850	2.110	1.857	2.000	12.14	16.26	13.73	0.375	4	5110	56.07	64.72	69.92	5239	6829	0.767
3.5	3	28.00	1.000	0.0850	1.001	0.965	1.906	12.17	16.17	13.74	0.375	8	3810	53.05	64.72	69.92	5334	6243	0.854
4.1	2	24.00	1.000	0.0710	2.063	1.926	1.250	12.16	15.49	13.72	0.500	6	4090	63.33	64.52	70.75	6256	7199	0.869
4.2***	2	24.00	1.000	0.1400	2.094	1.848	1.313	12.17	15.59	13.74	0.375	8	4090	73.54	75.42	69.92	7265	7815	0.930
4.4	2	24.00	1.000	0.1010	2.032	1.978	1.219	12.15	15.47	13.73	0.375	4	4090	59.55	67.69	69.92	5882	5958	0.987
5.1	3	24.00	1.000	0.0650	2.016	1.914	1.250	18.22	15.57	13.79	0.375	7	4190	65.43	65.70	69.92	6425	6293	1.021
5.2	3	24.00	1.000	0.1400	2.078	1.867	1.359	18.16	15.62	13.73	0.375	7	4190	66.26	75.42	96.92	6506	7534	0.864
5.3	2	24.00	1.000	0.1400	2.063	1.849	1.281	12.11	15.50	13.68	0.375	7	4190	68.83	75.42	69.92	6759	7452	0.907
5.4	2	24.00	1.000	0.0650	1.985	1.980	1.250	12.12	15.46	13.68	0.375	7	4190	59.50	65.70	69.92	5843	6282	0.930
5.5	2	24.00	1.000	0.0850	2.063	1.904	1.406	12.12	15.60	13.67	0.375	4	4190	46.74	64.72	69.92	4590	6034	0.761
5.6***	2	22.00	1.000	0.1400	2.094	1.807	1.313	12.11	15.69	13.84	0.500	5	4190	67.22	75.42	70.75	6600	8003	0.825
6.1	3	24.00	1.000	0.0650	2.063	0.422	1.906	12.18	16.12	13.69	0.500	8	4220	64.71	65.70	66.42	6342	6393	0.992
6.2 [*]	3	24.00	1.000	0.1400	2.000	0.438	2.006	12.11	16.15	13.62	0.500	8	4220	77.57	75.42	66.42	7603	7992	0.951
6.3	2	16.00	1.000	0.1400	2.000	1.906	1.344	12.13	15.51	13.63	0.375	2	4220	46.39	75.42	64.55	4547	4777	0.952
6.4	2	16.00	1.000	0.0850	2.094	1.844	1.344	12.11	15.45	13.58	0.375	2	4220	36.83	64.72	64.55	3610	4568	0.790
7.1	2	16.00	1.000	0.1400	2.079	1.797	1.375	12.00	16.18	13.77	0.375	2	4160	47.05	75.42	64.55	4628	5139	0.901
7.2***	2	18.00	1.000	0.1010	1.469	2.531	1.313	12.06	16.18	13.72	0.500	5	4160	56.37	67.69	84.70	5545	6612	0.839
7.5 [*]	3	24.00	1.000	0.1400	2.032	0.399	2.000	12.17	16.17	13.64	0.500	8	4160	75.73	75.42	84.70	7450	7960	0.936
7.6	2	16.00	1.000	0.1010	2.032	1.969	1.938	12.01	16.22	13.77	0.375	2	4160	44.62	67.69	64.55	4389	5017	0.875
8.1	3	24.00	1.000	0.0690	2.032	0.453	1.953	12.13	16.23	13.76	0.500	8	3830	72.14	77.96	84.70	7244	6399	1.132
8.2 [*]	3	24.00	1.000	0.1190	2.047	0.430	1.969	12.16	16.20	13.69	0.500	8	3830	85.08	80.57	84.70	8544	7384	1.157
8.4	2	16.00	1.000	0.1190	2.063	1.891	1.906	12.10	16.35	13.91	0.375	2	3830	49.37	77.96	64.55	4958	5041	0.983
9.1	2	24.00	1.000	0.1190	2.032	1.875	1.954	12.14	16.19	13.70	0.375	2	4230	64.16	80.57	64.55	6285	6291	0.999
9.2	2	18.00	1.000	0.1400	2.063	1.844	1.290	12.10	15.67	13.84	0.375	6	4230	70.02	75.42	64.55	6859	6433	1.066
9.3	2	24.00	1.000	0.0690	2.094	1.907	1.818	12.19	16.12	13.78	0.375	2	4230	55.75	77.96	64.55	5461	5940	0.919
9.4	2	24.00	1.000	0.1400	2.016	1.891	1.915	12.11	16.17	13.72	0.375	2	4230	65.82	75.42	64.55	6447	6311	1.018
10.3	2	26.00	1.000	0.0690	2.094	1.844	1.798	12.11	16.09	13.77	0.375	2	4250	59.45	77.96	64.55	5817	6199	0.938
10.4***	2	20.00	1.000	0.0690	2.079	1.875	1.916	12.07	16.19	13.75	0.500	5	4250	62.68	77.96	84.70	6133	6954	0.882
11.1	3	18.00	1.000	0.1400	2.000	0.453	1.928	12.20	16.14	13.68	0.500	6	4380	68.52	75.42	84.70	6654	6633	1.003
11.2	2	18.00	1.000	0.0690	2.094	1.844	1.881	12.19	16.13	13.72	0.500	4	4380	62.58	77.96	84.70	6077	6283	0.967
11.3***	2	18.00	1.000	0.1190	2.063	1.844	1.943	12.13	16.08	13.60	0.500	4	4380	63.11	80.57	84.70	6129	7115	0.861
11.4	2	24.00	1.000	0.1400	2.094	1.844	1.928	12.15	16.23	13.77	0.375	2	4380	63.15	75.42	64.55	6385	6385	0.960
14.1	3	36.00	1.000	0.1010	2.032	0.484	1.877	12.12	16.26	13.86	0.375	3	4200	61.19	67.69	64.55	6005	6027	0.996
14.2	3	21.00	1.000	0.1010	2.016	0.469	1.897	12.19	16.13	13.72	0.500	7	4200	64.24	67.69	84.70	6304	6547	0.963
15.1***	2	27.00	1.410	0.1270	1.516	1.500	1.902	12.11	16.11	13.46	0.500	9	5250	69.11	77.77	84.70	12665	15734	0.805
15.2***	2	27.00	1.410	0.0720	1.610	1.469	1.924	12.11	16.12	13.46	0.500	9	5250	64.28	65.54	84.70	11780	13027	0.904
15.4 [*]	2	40.00	1.410	0.1270	1.563	1.469	1.884	12.08	16.13	13.50	0.375	10	5250	78.90	77.77	64.55	14459	14461	1.000
15.5	2	40.00	1.410	0.0720	1.516	1.531	1.820	12.04	16.19	13.63	0.375	10	5250	63.40	65.54	64.55	11619	12620	0.921
16.3	2	40.00	1.410	0.1270	3.047	2.969	1.791	18.03	16.16	13.62	0.375	4	5180	62.06	77.77	64.55	11412	12544	0.910
16.4	2	40.00	1.410	0.0700	3.063	3.000	1.846	18.06	16.00	13.45	0.375	4	5180	61.84	66.69	64.55	11371	11935	0.953
17.4 [*]	2	38.00	1.410	0.0700	3.094	3.000	1.866	18.07	16.09	13.52	0.375	8	4710	66.69	66.69	64.55	12558	12764	0.984
17.5	2	30.00	1.410	0.0700	3.079	3.000	1.907	18.09	16.09	13.48	0.500	7	4710	59.30	66.69	84.70	11167	12887	0.867
17.3	2	38.00	1.410	0.1270	3.047	2.984	1.888	18.03	16.12	13.48	0.375	8	4710	70.06	77.77	64.55	13193	14127	0.934
17.6***	2	30.00	1.410	0.1270	3.063	2.969	1.911	18.07	16.20	13.54	0.500	7	4710	70.12	77.77	84.70	13205	15037	0.878
18.1 [*]	2	40.00	1.410	0.1270	1.485	4.500	1.845	18.05	16.11	13.52	0.375	10	4700	80.90	77.77	64.55	15242	14024	1.087
18.3	2	40.00	1.410	0.1270	3.032	3.000	1.911	18.05	16.08	13.43	0.375	6	4700	70.58	77.77	64.55	13298	13557	0.981
18.4 [*]	2	40.00	1.410	0.0700	3.016	3.031	1.871	18.08	16.23	13.62	0.375	6	4700	66.69	64.55	12565	12468	1.008	
Current Study ^{**}																			
19.3	3	30.00	1.000	0.1190	2.063	1.898	1.903	18.10	16.07	13.62	0.375	3	4250	71.46	80.57	64.55	6992	7429	0.941
19.4	3	30.00	1.000	0.1190	2.031	1.891	1.897	18.13	16.07	13.63	0.375	3	4250	77.31	80.57	64.55	7564	7410	1.021
21.1	3	24.00	1.000	0.1190	1.766	0.484	1.470	12.05	15.66	13.65	0.625	6	4330	73.88	80.57	62.98	7195	7856	0.916
21.3	3	25.00	1.000	0.1190	1.609	0.578	1.942	12.10	16.13	13.65	0.625	5	4330	76.25	80.57	62.98	7426	7623	0.974
21.5	2	25.00	1.000	0.1190	1.641	2.219	1.421	12.14	15.54	1.42	0.500	5	4330	77.35	80.57	64.92	7533	7968	0.945
23a.1	3	21.00	1.000	0.1190	2.117	1.852	1.931	18.28	16.09	13.66	0.375	4	5080	78.87	80.57	71.25	6383	7184	0.889
23a.3 [*]	3	21.00	1.000	0.1190	2.055	1.902	1.902	18.18	16.17	13.70	0.375	4	5080	80.57	80.57	71.25	6520	7143	0.913
23a.4	3	21.00	1.000	0.1190	2.008														

Table 5.11 (continued)
Data and test/prediction ratios for developed and spliced bars
with confining reinforcement

Specimen No.	n	l _d	d _b	R _r	c _{so}	c _d	c _b	b	h	d	d _s	N*	f _c	f _t	f _y	f _{st}	T _v /f _c ^{1/4}	T _v /f _c ^{1/4}	Test		
																			Eq. 5.18**	Prediction	
27.6*	3	18.00	1.000	0.0690	4.031	0.930	1.442	18.12	15.62	13.68	0.500	4	10810	78.42	77.96	64.92	6075	5783	1.051		
29.2*	3	20.00	1.000	0.0690	1.875	0.484	1.478	12.14	15.60	13.62	0.375	5	10620	83.65	77.96	71.25	6510	5187	1.255		
29.4*	3	18.00	1.000	0.0690	1.938	0.492	1.418	12.17	15.60	13.68	0.375	6	10620	77.96	77.96	71.25	6067	5222	1.162		
29.6	3	16.00	1.000	0.0690	3.906	0.980	1.414	18.17	15.65	13.73	0.375	4	10620	77.72	77.96	71.25	6049	4860	1.244		
31.3	2	16.00	1.000	0.0690	1.969	1.938	1.438	12.15	15.48	13.52	0.375	2	12890	65.21	77.96	71.25	4835	5032	0.961		
33.2	3	18.00	1.000	0.0850	1.953	0.395	1.913	12.10	16.12	13.71	0.500	6	5360	61.42	69.50	64.92	5671	5859	0.968		
33.4	3	18.00	1.000	0.0850	2.063	1.914	1.936	18.12	16.13	13.69	0.375	4	5360	58.32	69.50	71.25	5384	5829	0.924		
33.6	2	23.00	1.000	0.0850	2.094	1.688	1.891	12.17	16.26	13.87	0.375	2	5230	57.94	69.50	71.25	5382	5811	0.926		
35.1	2	20.00	1.000	0.1400	1.453	2.375	1.938	12.08	16.17	13.73	0.375	5	5330	68.44	75.42	71.25	6328	6647	0.952		
35.3	2	20.00	1.000	0.0850	1.500	2.266	1.920	12.08	16.07	13.65	0.375	5	5330	61.77	69.50	71.25	5711	5941	0.961		
37.4	3	21.00	1.000	0.1400	2.000	0.484	1.503	12.07	15.51	13.47	0.500	7	4800	73.78	75.42	64.92	7002	7298	0.959		
39.2*	3	16.00	1.000	0.1010	1.906	0.508	1.475	12.18	15.48	13.49	0.375	4	14450	69.74	67.69	71.25	5025	5197	0.967		
39.3*	3	16.00	1.000	0.0690	1.891	0.488	1.477	12.17	15.45	13.45	0.375	4	14450	77.96	77.96	71.25	5617	4857	1.157		
41.1	2	16.00	1.000	0.1190	2.000	1.844	1.522	12.14	15.55	13.49	0.375	2	10180	66.16	80.57	71.25	5203	5292	0.983		
41.2***	3	16.00	1.000	0.1190	1.875	0.469	1.515	12.16	15.53	13.52	0.625	4	10180	83.02	80.57	62.98	6529	7442	0.877		
41.3	3	16.00	1.000	0.1190	1.891	0.461	1.890	12.11	16.09	13.72	0.500	4	10180	79.35	80.57	64.92	6240	6293	0.992		
41.4	3	16.00	1.000	0.0690	1.906	0.484	1.476	12.20	15.53	13.55	0.375	4	10180	77.27	77.96	62.98	6077	6187	0.982		
41.5	3	16.00	1.000	0.0850	2.016	1.875	1.977	18.32	16.04	13.41	0.375	2	10500	66.01	69.50	71.25	5151	5364	0.960		
41.6	3	16.00	1.000	0.0850	2.000	1.875	1.984	18.22	16.17	13.53	0.375	2	10500	65.38	69.50	71.25	5102	5365	0.951		
42.1	2	16.00	1.000	0.0690	2.000	1.859	1.864	12.11	15.99	13.60	0.375	2	11930	64.32	77.96	71.25	4862	5287	0.920		
42.4	3	16.00	1.000	0.0690	1.906	0.500	1.829	12.17	16.09	13.74	0.500	4	11930	70.70	77.96	64.92	5344	5632	0.949		
42.5***	3	16.00	1.000	0.0690	1.906	0.500	1.476	12.18	15.36	13.36	0.625	4	11930	77.92	77.96	62.98	5890	6426	0.917		
43.2	2	16.00	1.000	0.1190	2.031	1.875	1.844	12.06	16.06	13.68	0.375	2	11530	64.95	80.57	71.25	4952	5612	0.882		
43.3***	3	16.00	1.000	0.1190	1.844	0.500	1.859	12.22	16.07	13.67	0.500	4	11530	78.81	80.57	64.92	6008	6460	0.930		
43.6***	3	16.00	1.000	0.1190	1.891	0.500	1.497	12.07	15.48	13.45	0.625	4	11530	82.73	80.57	62.98	6307	7702	0.819		
20.1	3	40.00	1.410	0.1270	2.008	1.313	1.840	18.05	16.20	13.65	0.500	8	5080	71.08	77.77	84.70	13135	14204	0.925		
20.2	3	40.00	1.410	0.1270	2.000	1.297	1.848	18.05	16.15	13.56	0.500	8	5080	71.81	77.77	84.70	13269	14181	0.936		
20.3	3	40.00	1.410	0.1270	2.000	1.313	1.822	16.07	15.15	13.62	0.500	5	5080	68.52	77.77	84.70	12660	12443	1.017		
20.4	3	40.00	1.410	0.1270	2.039	1.297	1.868	18.10	16.26	13.64	0.500	5	5080	67.65	80.57	84.70	12500	12442	1.005		
28.1	2	25.00	1.410	0.1270	2.188	0.766	1.900	11.71	16.07	13.46	0.375	5	12610	71.23	77.77	71.25	10486	11022	0.951		
28.3	3	28.00	1.410	0.1270	2.172	1.242	1.901	18.10	16.09	13.49	0.375	4	12610	67.03	77.77	71.25	9867	10017	0.985		
30.1	2	25.00	1.410	0.1270	2.375	0.688	1.891	12.19	16.15	13.56	0.375	3	13220	66.07	77.77	71.25	9613	9533	1.008		
30.3	3	28.00	1.410	0.1270	2.031	1.953	1.273	1.889	18.02	16.11	13.51	0.375	2	13220	66.88	77.77	71.25	9729	9069	1.073	
40.1	2	23.00	1.410	0.0720	2.000	1.063	1.451	12.09	15.52	13.33	0.375	4	15650	58.83	65.54	71.25	8205	9198	0.892		
Kadrikou (1994)**																					
PB-01	2	14.96	0.748	0.0748	1.421	2.988	1.122	11.81	9.84	8.35	0.370	2	8932	83.56	102.68	59.295	3777	3384	1.116		
PB-02	2	22.44	0.748	0.0748	1.421	2.988	1.122	11.81	9.84	8.35	0.370	3	8932	100.59	102.68	59.295	4547	4232	1.075		
PB-04	2	22.44	0.748	0.0748	1.421	2.988	1.122	11.81	9.84	8.35	0.370	3	3243	63.41	102.68	59.295	3693	3790	0.974		
PB-05	2	29.92	0.748	0.0748	1.421	2.988	1.122	11.81	9.84	8.35	0.370	4	3243	82.08	102.68	59.295	4780	4574	1.045		
PB-06*	2	37.40	0.748	0.0748	1.421	2.988	1.122	11.81	9.84	8.35	0.370	5	3243	105.93	102.68	59.295	6169	5357	1.152		
PB-15*	2	22.44	0.748	0.0748	1.421	2.988	1.122	11.81	9.84	8.35	0.370	3	10980	107.64	105.15	59.295	4621	4352	1.062		
PB-16	2	22.44	0.748	0.0748	1.421	2.988	1.122	11.81	9.84	8.35	0.370	3	8832	91.65	95.14	59.295	4155	4225	0.983		
PB-19	2	22.44	0.748	0.0748	1.421	2.988	1.122	11.81	9.84	8.35	0.370	3	4082	86.96	105.15	59.295	4781	3872	1.235		
PB-20*	2	22.44	0.748	0.0748	1.421	2.988	1.122	11.81	9.84	8.35	0.370	3	4082	78.02	76.87	59.295	4290	3872	1.108		
PB-21	2	14.96	0.748	0.0748	1.421	2.988	1.122	11.81	9.84	8.35	0.370	2	4082	59.04	76.87	59.295	3246	3077	1.055		
PB-23	2	22.44	0.748	0.0748	1.421	2.988	1.122	11.81	9.84	8.35	0.370	3	3072	55.91	76.87	59.295	3300	3773	0.875		
PB-24	2	22.44	0.748	0.0748	1.421	2.988	1.122	11.81	9.84	8.35	0.370	3	3072	60.03	64.10	59.295	3543	3773	0.939		
PB-25	2	14.96	0.748	0.0748	1.421	2.988	1.122	11.81	9.84	8.35	0.370	2	3072	44.05	64.10	59.295	2600	2992	0.869		
PB-27	2	22.44	0.748	0.0748	1.421	2.201	1.122	10.24	9.84	8.35	0.370	3	8832	93.74	95.14	59.295	4250	4192	1.014		
PB-31	2	14.96	0.748	0.0748	1.421	2.988	1.122	11.81	9.84	8.35	0.370	4	8832	72.86	76.87	59.295	3303	3379	0.977		
SI-01	2	22.44	0.748	0.0748	3.543	4.803	1.122	19.69	11.81	10.31	0.252	7	9216	113.19	122.23	199.12	5077	4914	1.033		
SI-0																					

Table 5.11 (continued)
Data and test/prediction ratios for developed and spliced bars
with confining reinforcement

Specimen No.	n	l_d	d_b	R_r	c_{\max}	c_d	b	h	d	d_s	N*	f'_c	f_t	f_y	f_{st}	$T_y/f'_c{}^{1/4}$	$T_y/f'_c{}^{1/4}$	Test	
	(in.)	(in.)	(in.)	(in.)	(in.)	(in.)	(in.)	(in.)	(in.)	(in.)	(in.)	(psi)	(ksi)	(ksi)	(ksi)	(in. ²)	(in. ²)	Eq. 5.18** Test	
PB-16	2	22.44	0.748	0.0748	1.142	3.268	1.122	11.81	9.84	8.35	0.394	2	8832	91.65	95.14	60.30	4155	4041	1.028
PB-11*	2	22.44	0.748	0.0748	1.142	3.268	1.122	11.81	9.84	8.35	0.394	5	8832	105.98	105.15	60.30	4804	4661	1.031
PB-13	2	22.44	0.748	0.0748	1.142	3.268	1.122	11.81	9.84	8.35	0.236	6	3072	62.39	105.15	60.30	3683	3633	1.014
PB-24	2	22.44	0.748	0.0748	1.142	3.268	1.122	11.81	9.84	8.35	0.394	2	3072	60.03	64.10	60.30	3543	3633	0.975
PB-14	2	22.44	0.748	0.0748	1.142	3.268	1.122	11.81	9.84	8.35	0.394	5	3072	70.49	105.15	60.30	4161	3998	1.041
For all 245 specimens:																			
																		Max. 1.311	
																		Min. 0.579	
																		Mean 0.979	
																		St. Dev. 0.128	
																		COV 0.131	
For the 191 specimens with $l_d/d_b \geq 16$ and $(c + K_{tr})/d_b \leq 4.0$ [$K_{tr} = (0.52 t_d A_{tr}/sn) f'_c{}^{1/2}$]																			
																		Max. 1.312	
																		Min. 0.761	
																		Mean 1.001	
																		St. Dev. 0.115	
																		COV 0.115	
For the 43 specimens with $f_t \geq f_y$ and with $l_d/d_b \geq 16$ and $(c + K_{tr})/d_b \leq 4.0$ [$K_{tr} = (0.52 t_d A_{tr}/sn) f'_c{}^{1/2}$]																			
																		Max. 1.311	
																		Min. 0.833	
																		Mean 1.088	
																		St. Dev. 0.136	
																		COV 0.125	
For the 148 specimens with $f_t < f_y$ and with $l_d/d_b \geq 16$ and $(c + K_{tr})/d_b \leq 4.0$ [$K_{tr} = (0.52 t_d A_{tr}/sn) f'_c{}^{1/2}$]																			
																		Max. 1.244	
																		Min. 0.761	
																		Mean 0.978	
																		St. Dev. 0.095	
																		COV 0.097	

* Number of transverse stirrups crossing l_d with 2 legs per stirrups, except for Thompson et al. (1975) [6 legs.]

** Specimens with $l_d/d_b < 16$ which are removed from the 245 specimens

*** Specimens with $(c + K_{tr})/d_b > 4.0$ which are removed from the 245 specimens,
where $K_{tr} = 31.51 t_d A_{tr}/sn$ and $t_d = 0.72 d_b + 0.28$ developed by Darwin et al. (1995a, 1995b)]

**** Specimens with $(c + K_{tr})/d_b > 4.0$ which are removed from the 196 specimens,
where $K_{tr} = 0.518 t_d A_{tr}/sn$ and $t_d = 0.78 d_b + 0.22$ developed in the current study

+ Specimens with $f_t \geq f_y$

$$++ \quad \text{Eq. 5.18} = \frac{T_h}{f'_c{}^{1/4}} = \frac{T_c + T_s}{f'_c{}^{1/4}} = [59.8 l_d (c_{\max} + 0.5 d_b) + 2350 A_b] \left(0.1 \frac{c_{\max}}{c_{\min}} + 0.9 \right) + \left(3114 t_d \frac{N A_{tr}}{n} + 399 \right) f'_c{}^{1/2}$$

+++ R_r is known based on measurements made on the bars or based on data provided in the original papers

++++ R_r is determined based on Darwin et al. (1995b, 1996b)

1 in. = 25.4 mm; 1 psi = 6.895 kPa; 1 ksi = 6.895 MPa

Table 5.12

Results of dummy variable analyses, based on study and bar size, of increase in bond force due to transverse reinforcement, T_s , normalized with respect to $f'_c P$ versus $t_r t_d N A_{tr}/n$ for 163 beams (T_s in lb, $f'_c P$ in psi, and A_{tr} in in.²)

Study	Bar Size	No. of Tests	Intercept			
			p = 1/4	p = 1/2	p = 3/4	p = 1.0
Ferguson and Breen (1965)	No. 8 No. 11	8 1	-248.80	-24.85	-2.09	-0.11
Thompson et al. (1975)	No. 11	1				
DeVries et al. (1991)	No. 9	1				
Hester et al. (1991, 1993)	No. 8	10	-177.23	-24.41	-3.26	-0.43
Rezansoff et al. (1991)	No. 20M No. 25M No. 30M No. 35M	3 19 2 7	1134.56 808.89 1273.90 565.47	141.04 98.30 178.40 84.56	17.58 12.14 25.08 12.91	2.20 1.51 3.51 1.93
Rezansoff (1993)	No. 25M No. 30M	5 4	1345.59 1818.77	171.60 231.96	21.95 29.80	2.81 3.84
Azizinamini et al. (1995 at CTL)	No. 11	1				
Azizinamini et al. (1995 at UNL)	No. 11	3	-90.20	-57.79	-11.02	-1.69
Darwin et al. (1995a, 1996a)	No. 5 L No. 8 L	8 53	86.56 242.37	9.43 4.55	1.01 -1.96	0.11 -0.49
and Current Study	No. 11 L No. 8 B No. 11 B	16 17 4	298.49 814.81 1232.21	6.11 77.27 71.95	-2.18 7.37 1.64	-0.56 0.71 -0.45
Weighted Average Intercept			455.34	40.42	3.59	0.32
Slope			1977.76	247.57	30.90	3.82
r ²			0.787	0.837	0.858	0.860

1 lb = 4.448 N, 1 psi = 6.895 kPa, 1 in. = 25.4 mm

Table 5.13
Results of dummy variable analyses, based on study, for test/prediction ratio
versus f'_c using Eqs. 5.13a - 5.13d for 163 tests

Study	No. of Tests	Intercept			
		$p = 1/4^+$	$p = 1/2^{++}$	$p = 3/4^{+++}$	$p = 1.0^{++++}$
Ferguson and Breen (1965)	9	0.872	0.926	0.976	1.023
Thompson et al. (1975)	1				
Devries et al. (1991)	1				
Hester et al. (1991, 1993)	10	0.757	0.821	0.885	0.948
Rezanoff et al. (1991)	31	0.981	1.042	1.101	1.157
Rezanoff et al. (1993)	9	1.083	1.145	1.203	1.259
Azizinamini (1995 at CTL)	1				
Azizinamini (1995 at UNL)	3	0.641	0.732	0.824	0.917
Darwin et al. (L)* (1995a, 1996a)	77	0.834	0.882	0.929	0.976
Darwin et al. (B)* (1995a, 1996a)	21	0.907	0.968	1.027	1.084
Weighted Average Intercept		0.880	0.935	0.989	1.041
Slope		2.04E-05	1.155E-05	2.01E-06	-8.05E-06

* Bars in concrete containing limestone coarse aggregate

** Bars in concrete containing basalt coarse aggregate

+ Power of f'_c used to normalize T_s in Eq. 5.13a

++ Power of f'_c used to normalize T_s in Eq. 5.13b

+++ Power of f'_c used to normalize T_s in Eq. 5.13c

++++ Power of f'_c used to normalize T_s in Eq. 5.13d

Table 5.14
Test/predicted splice strength ratios, using Eqs. 5.13a - 5.13d,
for specimens tested by Kadoriku (1994)

Specimen + Label	f_c (psi)	Test/Predicted Splice Strength Ratio**			
		p = 1/4*	p = 1/2	p = 3/4	p = 1.0
PB-01	8932	1.157	1.148	1.130	1.102
PB-02	8932	1.121	1.108	1.086	1.055
PB-04	3243	0.911	0.950	0.981	1.004
PB-05	3243	0.986	1.023	1.051	1.073
PB-06	3243	1.094	1.130	1.157	1.179
PB-15	10980	1.140	1.112	1.074	1.025
PB-16	8832	1.025	1.013	0.993	0.966
PB-19	4082	1.179	1.216	1.244	1.264
PB-20	4082	1.058	1.091	1.116	1.134
PB-21	4082	0.995	1.035	1.065	1.087
PB-23	3072	0.814	0.852	0.881	0.903
PB-24	3072	0.874	0.914	0.946	0.970
PB-25	3072	0.797	0.842	0.876	0.903
PB-27	8832	1.054	1.043	1.024	0.998
PB-31	8832	1.012	1.005	0.990	0.966
S1-01	9216	1.083	1.067	1.043	1.011
S1-02	9216	1.088	1.071	1.047	1.015
S1-03	9216	0.972	0.957	0.935	0.907
S1-04	9216	0.808	0.796	0.778	0.754
S2-01	6500	1.079	1.083	1.081	1.073
S2-02	6500	1.084	1.088	1.086	1.078
S2-03	6500	1.075	1.079	1.076	1.068
S2-04	6500	1.060	1.064	1.061	1.054
S2-05	6500	1.052	1.056	1.053	1.046
S3-01	4907	1.032	1.050	1.062	1.069
S3-03	4907	1.062	1.079	1.090	1.096
S3-05	4907	0.975	0.993	1.004	1.011
PB-10	8832	1.191	1.182	1.164	1.137
PB-16	8832	1.063	1.055	1.039	1.015
PB-11	8832	1.114	1.082	1.041	0.992
PB-13	3072	0.942	0.987	1.021	1.046
PB-24	3072	0.907	0.950	0.982	1.007
PB-14	3072	0.964	1.011	1.048	1.078
	Max.	1.191	1.216	1.244	1.264
	Min.	0.797	0.796	0.778	0.754
	Mean	1.023	1.034	1.037	1.033
	St. Dev.	0.103	0.093	0.089	0.091
	COV	0.101	0.090	0.085	0.088

* Power used to characterize T_s

** Predicted strength = Eq. 5.13a for p = 1/4
= Eq. 5.13b for p = 1/2
= Eq. 5.13c for p = 3/4
= Eq. 5.13d for p = 1.0

+ Specimen details are given in Table 5.11.

1 psi = 6.895 kPa

Table 5.15
Results of dummy variable analysis, based on study and bar size, of increase in
bond force due to transverse reinforcement, T_s , normalized
with respect to $f'_c^{3/4}$ versus $t_r t_d N A_{tr} / n$ for 196 beams
(T_s in lb, $f'_c^{3/4}$ in psi, and A_{tr} in in.²)

Study	Bar Size	No. of Specimens	Intercept
Ferguson and Breen (1965)	No. 8 No. 11	8 1	-2.127
Thompson et al. (1975)	No. 11	1	
DeVries et al. (1991)	No. 9	1	
Hester et al. (1991, 1993)	No. 8	10	-3.281
Rezanoff et al. (1991)	No. 20M No. 25M No. 30M No. 35M	3 19 2 7	17.552 12.082 24.994 11.769
Rezanoff (1991)	No. 25M No. 30M	5 4	21.923 29.729
Azizinamini et al. (1995 at CTL)	No. 11	1	
Azizinamini et al. (1995 at UNL)	No. 11	3	-11.086
Darwin et al. (1995a, 1996a) and Current Study	No. 5 L No. 8 L No. 11 L No. 8 B No. 11 B	8 52 17 17 4	1.001 -2.023 -2.312 7.322 1.590
Kadoriku (1994)	No. 19M	33	5.750
Weighted Average Intercept			3.912
Slpoe			30.99
r^2			0.8550

1 lb = 4.448 N, 1 psi = 6.895 kPa, 1 in. = 25.4 mm

Table 5.16

Results of dummy variable analysis, based on study and bar size, of increase in bond force due to transverse reinforcement, T_s , normalized with respect to $f'_c^{3/4}$ versus $t_r t_d A_{tr}/n$ for 191 beams with $(c + K_{tr})/d_b \leq 4$
 $[K_{tr} = (0.518 t_r t_d A_{tr}/sn) f'_c^{1/2}]$ (T_s in lb, $f'_c^{3/4}$ in psi, and A_{tr} in in.²)

Study	Bar Size	No. of Specimens	Intercept
Ferguson and Breen (1965)	No. 8	8	-2.196
	No. 11	1	
Thompson et al. (1975)	No. 11	1	
DeVries et al. (1991)	No. 9	1	
Hester et al. (1991, 1993)	No. 8	10	-3.311
Rezansoff et al. (1991)	No. 20M	3	17.503
	No. 25M	19	11.986
	No. 30M	2	24.831
	No. 35M	7	12.515
Rezansoff (1991)	No. 25M	5	21.880
	No. 30M	4	29.607
Azizinamini et al. (1995 at CTL)	No. 11	1	
Azizinamini et al. (1995 at UNL)	No. 11	3	-11.202
Darwin et al. (1995a, 1996a)	No. 5 L	8	0.980
and Current Study	No. 8 L	49	-2.069
	No. 11 L	16	-2.541
	No. 8 B	17	7.236
	No. 11 B	4	1.496
Kadoriku (1994)	No. 19M	33	5.709
Weighted Average Intercept			3.988
Slope			31.14
r^2			0.8556

1 lb = 4.448 N, 1 psi = 6.895 kPa, 1 in. = 25.4 mm

Table 5.17a
Data for hypothetical beams without confining transverse reinforcement

Beam No.	n	l_d^* (in.)	d_b (in.)	b (in.)	h (in.)	f_c (psi)	c_{si} (in.)	c_{so} (in.)	c_b (in.)
1	2	32.92	0.750	8.0	12.0	4000	0.500	2.000	2.000
2	2	19.24	0.750	12.0	12.0	4000	2.500	2.000	2.000
3	2	32.81	1.000	12.0	12.0	4000	2.000	2.000	2.000
4	2	54.99	1.270	12.0	12.0	4000	1.460	2.000	2.000
5	2	72.02	1.410	12.0	12.0	4000	1.180	2.000	2.000
6	2	19.24	0.750	24.0	12.0	4000	8.500	2.000	2.000
7	4	19.24	0.750	24.0	12.0	4000	2.333	2.000	2.000
8	6	24.87	0.750	24.0	12.0	4000	1.100	2.000	2.000
9	8	31.84	0.750	24.0	12.0	4000	0.571	2.000	2.000
10	2	32.81	1.000	24.0	12.0	4000	8.000	2.000	2.000
11	4	32.81	1.000	24.0	12.0	4000	2.000	2.000	2.000
12	6	47.10	1.000	24.0	12.0	4000	0.800	2.000	2.000
13	2	50.05	1.270	24.0	12.0	4000	7.460	2.000	2.000
14	4	51.83	1.270	24.0	12.0	4000	1.640	2.000	2.000
15	2	59.89	1.410	24.0	12.0	4000	7.180	2.000	2.000
16	4	65.74	1.410	24.0	12.0	4000	1.453	2.000	2.000
17	2	21.14	0.750	12.0	24.0	3000	2.500	2.000	2.000
18	2	19.24	0.750	12.0	24.0	4000	2.500	2.000	2.000
19	2	16.78	0.750	12.0	24.0	6000	2.500	2.000	2.000
20	2	15.18	0.750	12.0	24.0	8000	2.500	2.000	2.000
21	2	14.02	0.750	12.0	24.0	10000	2.500	2.000	2.000
22	2	13.11	0.750	12.0	24.0	12000	2.500	2.000	2.000
23	2	12.73	0.750	12.0	24.0	13000	2.500	2.000	2.000
24	2	12.38	0.750	12.0	24.0	14000	2.500	2.000	2.000
25	2	12.06	0.750	12.0	24.0	15000	2.500	2.000	2.000
26	2	11.77	0.750	12.0	24.0	16000	2.500	2.000	2.000
27	2	36.06	1.000	12.0	24.0	3000	2.000	2.000	2.000
28	2	32.81	1.000	12.0	24.0	4000	2.000	2.000	2.000
29	2	28.62	1.000	12.0	24.0	6000	2.000	2.000	2.000
30	2	25.89	1.000	12.0	24.0	8000	2.000	2.000	2.000
31	2	23.91	1.000	12.0	24.0	10000	2.000	2.000	2.000
32	2	22.37	1.000	12.0	24.0	12000	2.000	2.000	2.000
33	2	21.71	1.000	12.0	24.0	13000	2.000	2.000	2.000
34	2	21.12	1.000	12.0	24.0	14000	2.000	2.000	2.000
35	2	20.57	1.000	12.0	24.0	15000	2.000	2.000	2.000
36	2	20.07	1.000	12.0	24.0	16000	2.000	2.000	2.000
37	2	60.46	1.270	12.0	24.0	3000	1.460	2.000	2.000
38	2	54.99	1.270	12.0	24.0	4000	1.460	2.000	2.000
39	2	47.93	1.270	12.0	24.0	6000	1.460	2.000	2.000
40	2	43.33	1.270	12.0	24.0	8000	1.460	2.000	2.000
41	2	39.99	1.270	12.0	24.0	10000	1.460	2.000	2.000
42	2	37.39	1.270	12.0	24.0	12000	1.460	2.000	2.000
43	2	36.29	1.270	12.0	24.0	13000	1.460	2.000	2.000
44	2	35.28	1.270	12.0	24.0	14000	1.460	2.000	2.000
45	2	34.37	1.270	12.0	24.0	15000	1.460	2.000	2.000
46	2	33.52	1.270	12.0	24.0	16000	1.460	2.000	2.000
47	2	79.23	1.410	12.0	24.0	3000	1.180	2.000	2.000
48	2	72.02	1.410	12.0	24.0	4000	1.180	2.000	2.000
49	2	62.69	1.410	12.0	24.0	6000	1.180	2.000	2.000
50	2	56.63	1.410	12.0	24.0	8000	1.180	2.000	2.000
51	2	52.22	1.410	12.0	24.0	10000	1.180	2.000	2.000
52	2	48.79	1.410	12.0	24.0	12000	1.180	2.000	2.000
53	2	47.33	1.410	12.0	24.0	13000	1.180	2.000	2.000
54	2	46.01	1.410	12.0	24.0	14000	1.180	2.000	2.000
55	2	44.80	1.410	12.0	24.0	15000	1.180	2.000	2.000
56	2	43.69	1.410	12.0	24.0	16000	1.180	2.000	2.000
57	4	22.54	0.750	18.0	24.0	4000	1.333	2.000	2.000
58	6	32.92	0.750	18.0	24.0	4000	0.500	2.000	2.000
59	2	32.81	1.000	18.0	24.0	4000	5.000	2.000	2.000
60	4	43.36	1.000	18.0	24.0	4000	1.000	2.000	2.000
61	2	50.05	1.270	18.0	24.0	4000	4.460	2.000	2.000
62	4	73.77	1.270	18.0	24.0	4000	0.640	2.000	2.000
63	2	59.89	1.410	18.0	24.0	4000	4.180	2.000	2.000

* Predicted development/splice length based on Eq. 5.33, using $\phi_d = 0.9$ and $f_y = 60$ ksi

1 in. = 25.4 mm; 1 psi = 6.895 kPa; 1 ksi = 6.895 MPa

Table 5.17b
Data for hypothetical beams with confining transverse reinforcement

Beam No.	n	l_d^* $R_t=0.1275$	d_b $R_t=0.0727$	b	h	f_c	c_{si}	c_{so}	c_b	d_s	s	A_w/n
Group I												
1	2	15.89	18.57	0.75	8.00	12.00	4000	0.50	2.00	2.00	0.375	4.81 0.110
2	2	12.80	12.91	0.75	12.00	12.00	4000	2.50	2.00	2.00	0.375	4.81 0.110
3	2	18.65	20.97	1.00	12.00	12.00	4000	2.00	2.00	2.00	0.375	4.75 0.110
4	2	28.67	32.99	1.27	12.00	12.00	4000	1.46	2.00	2.00	0.375	4.68 0.110
5	2	35.20	41.15	1.41	12.00	12.00	4000	1.18	2.00	2.00	0.375	4.65 0.110
6	2	12.80	12.91	0.75	24.00	12.00	4000	8.50	2.00	2.00	0.375	4.81 0.110
7	4	13.54	14.35	0.75	24.00	12.00	4000	2.33	2.00	2.00	0.375	4.81 0.055
8	6	17.75	18.71	0.75	24.00	12.00	4000	1.10	2.00	2.00	0.375	4.81 0.037
9	8	22.46	23.65	0.75	24.00	12.00	4000	0.57	2.00	2.00	0.375	4.81 0.028
10	2	18.65	20.97	1.00	24.00	12.00	4000	8.00	2.00	2.00	0.375	4.75 0.110
11	4	22.16	23.72	1.00	24.00	12.00	4000	2.00	2.00	2.00	0.375	4.75 0.055
12	6	31.52	33.71	1.00	24.00	12.00	4000	0.80	2.00	2.00	0.375	4.75 0.037
13	2	27.11	30.91	1.27	24.00	12.00	4000	7.46	2.00	2.00	0.375	4.68 0.110
14	4	33.76	36.56	1.27	24.00	12.00	4000	1.64	2.00	2.00	0.375	4.68 0.055
15	2	31.77	36.45	1.41	24.00	12.00	4000	7.18	2.00	2.00	0.375	4.65 0.110
16	4	41.64	45.50	1.41	24.00	12.00	4000	1.45	2.00	2.00	0.375	4.65 0.055
17	2	15.58	16.33	0.75	12.00	24.00	3000	2.50	2.00	2.00	0.375	10.81 0.110
18	2	13.78	14.53	0.75	12.00	24.00	4000	2.50	2.00	2.00	0.375	10.81 0.110
19	2	12.00	12.22	0.75	12.00	24.00	6000	2.50	2.00	2.00	0.375	10.81 0.110
20	2	12.00	12.00	0.75	12.00	24.00	8000	2.50	2.00	2.00	0.375	10.81 0.110
21	2	12.00	12.00	0.75	12.00	24.00	10000	2.50	2.00	2.00	0.375	10.81 0.110
22	2	12.00	12.00	0.75	12.00	24.00	12000	2.50	2.00	2.00	0.375	10.81 0.110
23	2	12.00	12.00	0.75	12.00	24.00	13000	2.50	2.00	2.00	0.375	10.81 0.110
24	2	12.00	12.00	0.75	12.00	24.00	14000	2.50	2.00	2.00	0.375	10.81 0.110
25	2	12.00	12.00	0.75	12.00	24.00	15000	2.50	2.00	2.00	0.375	10.81 0.110
26	2	12.00	12.00	0.75	12.00	24.00	16000	2.50	2.00	2.00	0.375	10.81 0.110
27	2	25.70	27.13	1.00	12.00	24.00	3000	2.00	2.00	2.00	0.375	10.75 0.110
28	2	22.66	24.09	1.00	12.00	24.00	4000	2.00	2.00	2.00	0.375	10.75 0.110
29	2	18.77	20.18	1.00	12.00	24.00	6000	2.00	2.00	2.00	0.375	10.75 0.110
30	2	16.27	17.66	1.00	12.00	24.00	8000	2.00	2.00	2.00	0.375	10.75 0.110
31	2	16.00	16.00	1.00	12.00	24.00	10000	2.00	2.00	2.00	0.375	10.75 0.110
32	2	16.00	16.00	1.00	12.00	24.00	12000	2.00	2.00	2.00	0.375	10.75 0.110
33	2	16.00	16.00	1.00	12.00	24.00	13000	2.00	2.00	2.00	0.375	10.75 0.110
34	2	16.00	16.00	1.00	12.00	24.00	14000	2.00	2.00	2.00	0.375	10.75 0.110
35	2	16.00	16.00	1.00	12.00	24.00	15000	2.00	2.00	2.00	0.375	10.75 0.110
36	2	16.00	16.00	1.00	12.00	24.00	16000	2.00	2.00	2.00	0.375	10.75 0.110
37	2	41.41	44.28	1.27	12.00	24.00	3000	1.46	2.00	2.00	0.375	10.68 0.110
38	2	36.30	39.14	1.27	12.00	24.00	4000	1.46	2.00	2.00	0.375	10.68 0.110
39	2	29.79	32.56	1.27	12.00	24.00	6000	1.46	2.00	2.00	0.375	10.68 0.110
40	2	25.64	28.32	1.27	12.00	24.00	8000	1.46	2.00	2.00	0.375	10.68 0.110
41	2	22.69	25.28	1.27	12.00	24.00	10000	1.46	2.00	2.00	0.375	10.68 0.110
42	2	20.43	22.94	1.27	12.00	24.00	12000	1.46	2.00	2.00	0.375	10.68 0.110
43	2	20.32	21.96	1.27	12.00	24.00	13000	1.46	2.00	2.00	0.375	10.68 0.110
44	2	20.32	21.07	1.27	12.00	24.00	14000	1.46	2.00	2.00	0.375	10.68 0.110
45	2	20.32	20.32	1.27	12.00	24.00	15000	1.46	2.00	2.00	0.375	10.68 0.110
46	2	20.32	20.32	1.27	12.00	24.00	16000	1.46	2.00	2.00	0.375	10.68 0.110
47	2	52.62	56.80	1.41	12.00	24.00	3000	1.18	2.00	2.00	0.375	10.65 0.110
48	2	45.89	50.01	1.41	12.00	24.00	4000	1.18	2.00	2.00	0.375	10.65 0.110
49	2	37.37	41.33	1.41	12.00	24.00	6000	1.18	2.00	2.00	0.375	10.65 0.110
50	2	31.98	35.77	1.41	12.00	24.00	8000	1.18	2.00	2.00	0.375	10.65 0.110
51	2	28.15	31.79	1.41	12.00	24.00	10000	1.18	2.00	2.00	0.375	10.65 0.110
52	2	25.24	28.74	1.41	12.00	24.00	12000	1.18	2.00	2.00	0.375	10.65 0.110
53	2	24.03	27.46	1.41	12.00	24.00	13000	1.18	2.00	2.00	0.375	10.65 0.110
54	2	22.94	26.30	1.41	12.00	24.00	14000	1.18	2.00	2.00	0.375	10.65 0.110
55	2	22.56	25.25	1.41	12.00	24.00	15000	1.18	2.00	2.00	0.375	10.65 0.110
56	2	22.56	24.29	1.41	12.00	24.00	16000	1.18	2.00	2.00	0.375	10.65 0.110
57	4	15.92	16.84	0.75	18.00	24.00	4000	1.33	2.00	2.00	0.500	10.81 0.100
58	6	22.74	24.08	0.75	18.00	24.00	4000	0.50	2.00	2.00	0.500	10.81 0.067
59	2	19.89	21.97	1.00	18.00	24.00	4000	5.00	2.00	2.00	0.500	10.75 0.200
60	4	28.61	30.77	1.00	18.00	24.00	4000	1.00	2.00	2.00	0.500	10.75 0.100
61	2	29.19	32.63	1.27	18.00	24.00	4000	4.46	2.00	2.00	0.500	10.68 0.200
62	4	45.50	49.84	1.27	18.00	24.00	4000	0.64	2.00	2.00	0.500	10.68 0.100
63	2	34.38	38.63	1.41	18.00	24.00	4000	4.18	2.00	2.00	0.500	10.65 0.200

Table 5.17b (continued)
Data for hypothetical beams with confining transverse reinforcement

Beam No.	n	l_d	d_b	b	h	f_c	c_{si}	c_{so}	c_b	d_s	s	A_{sr}/n
		$R_r=0.1275$	$R_r=0.0727$	(in.)	(in.)	(in.)	(in.)	(in.)	(in.)	(in.)	(in.)	(in. ²)
Group 2												
1	2	12.83	15.36	0.75	8.50	12.00	4000	0.75	2.00	2.00	0.500	6.00
2	2	12.83	15.36	0.75	8.50	12.00	4000	0.75	2.00	2.00	0.500	6.00
3	2	18.83	22.58	1.00	10.00	12.00	4000	1.00	2.00	2.00	0.500	6.00
4	2	25.56	30.67	1.27	11.62	12.00	4000	1.27	2.00	2.00	0.500	6.00
5	2	29.11	34.95	1.41	12.46	12.00	4000	1.41	2.00	2.00	0.500	6.00
6	2	12.83	15.36	0.75	8.50	12.00	4000	0.75	2.00	2.00	0.500	6.00
7	4	16.78	18.80	0.75	14.50	12.00	4000	0.75	2.00	2.00	0.500	6.00
8	6	18.70	20.32	0.75	20.50	12.00	4000	0.75	2.00	2.00	0.500	6.00
9	8	19.83	21.18	0.75	26.50	12.00	4000	0.75	2.00	2.00	0.500	6.00
10	2	18.83	22.58	1.00	10.00	12.00	4000	1.00	2.00	2.00	0.500	6.00
11	4	24.68	27.69	1.00	18.00	12.00	4000	1.00	2.00	2.00	0.500	6.00
12	6	27.53	29.95	1.00	26.00	12.00	4000	1.00	2.00	2.00	0.500	6.00
13	2	25.56	30.67	1.27	11.62	12.00	4000	1.27	2.00	2.00	0.500	6.00
14	4	33.55	37.67	1.27	21.78	12.00	4000	1.27	2.00	2.00	0.500	6.00
15	2	29.11	34.95	1.41	12.46	12.00	4000	1.41	2.00	2.00	0.500	6.00
16	4	38.24	42.95	1.41	23.74	12.00	4000	1.41	2.00	2.00	0.500	6.00
17	2	15.25	17.98	0.75	8.50	24.00	3000	0.75	2.00	2.00	0.500	6.00
18	2	12.83	15.36	0.75	8.50	24.00	4000	0.75	2.00	2.00	0.500	6.00
19	2	12.00	12.11	0.75	8.50	24.00	6000	0.75	2.00	2.00	0.500	6.00
20	2	12.00	12.00	0.75	8.50	24.00	8000	0.75	2.00	2.00	0.500	6.00
21	2	12.00	12.00	0.75	8.50	24.00	10000	0.75	2.00	2.00	0.500	6.00
22	2	12.00	12.00	0.75	8.50	24.00	12000	0.75	2.00	2.00	0.500	6.00
23	2	12.00	12.00	0.75	8.50	24.00	13000	0.75	2.00	2.00	0.500	6.00
24	2	12.00	12.00	0.75	8.50	24.00	14000	0.75	2.00	2.00	0.500	6.00
25	2	12.00	12.00	0.75	8.50	24.00	15000	0.75	2.00	2.00	0.500	6.00
26	2	12.00	12.00	0.75	8.50	24.00	16000	0.75	2.00	2.00	0.500	6.00
27	2	22.35	26.40	1.00	10.00	24.00	3000	1.00	2.00	2.00	0.500	6.00
28	2	18.83	22.58	1.00	10.00	24.00	4000	1.00	2.00	2.00	0.500	6.00
29	2	16.00	17.85	1.00	10.00	24.00	6000	1.00	2.00	2.00	0.500	6.00
30	2	16.00	16.00	1.00	10.00	24.00	8000	1.00	2.00	2.00	0.500	6.00
31	2	16.00	16.00	1.00	10.00	24.00	10000	1.00	2.00	2.00	0.500	6.00
32	2	16.00	16.00	1.00	10.00	24.00	12000	1.00	2.00	2.00	0.500	6.00
33	2	16.00	16.00	1.00	10.00	24.00	13000	1.00	2.00	2.00	0.500	6.00
34	2	16.00	16.00	1.00	10.00	24.00	14000	1.00	2.00	2.00	0.500	6.00
35	2	16.00	16.00	1.00	10.00	24.00	15000	1.00	2.00	2.00	0.500	6.00
36	2	16.00	16.00	1.00	10.00	24.00	16000	1.00	2.00	2.00	0.500	6.00
37	2	30.30	35.82	1.27	11.62	24.00	3000	1.27	2.00	2.00	0.500	6.00
38	2	25.56	30.67	1.27	11.62	24.00	4000	1.27	2.00	2.00	0.500	6.00
39	2	20.32	24.29	1.27	11.62	24.00	6000	1.27	2.00	2.00	0.500	6.00
40	2	20.32	20.35	1.27	11.62	24.00	8000	1.27	2.00	2.00	0.500	6.00
41	2	20.32	20.32	1.27	11.62	24.00	10000	1.27	2.00	2.00	0.500	6.00
42	2	20.32	20.32	1.27	11.62	24.00	12000	1.27	2.00	2.00	0.500	6.00
43	2	20.32	20.32	1.27	11.62	24.00	13000	1.27	2.00	2.00	0.500	6.00
44	2	20.32	20.32	1.27	11.62	24.00	14000	1.27	2.00	2.00	0.500	6.00
45	2	20.32	20.32	1.27	11.62	24.00	15000	1.27	2.00	2.00	0.500	6.00
46	2	20.32	20.32	1.27	11.62	24.00	16000	1.27	2.00	2.00	0.500	6.00
47	2	34.50	40.80	1.41	12.46	24.00	3000	1.41	2.00	2.00	0.500	6.00
48	2	29.11	34.95	1.41	12.46	24.00	4000	1.41	2.00	2.00	0.500	6.00
49	2	22.57	27.69	1.41	12.46	24.00	6000	1.41	2.00	2.00	0.500	6.00
50	2	22.56	23.21	1.41	12.46	24.00	8000	1.41	2.00	2.00	0.500	6.00
51	2	22.56	22.56	1.41	12.46	24.00	10000	1.41	2.00	2.00	0.500	6.00
52	2	22.56	22.56	1.41	12.46	24.00	12000	1.41	2.00	2.00	0.500	6.00
53	2	22.56	22.56	1.41	12.46	24.00	13000	1.41	2.00	2.00	0.500	6.00
54	2	22.56	22.56	1.41	12.46	24.00	14000	1.41	2.00	2.00	0.500	6.00
55	2	22.56	22.56	1.41	12.46	24.00	15000	1.41	2.00	2.00	0.500	6.00
56	2	22.56	22.56	1.41	12.46	24.00	16000	1.41	2.00	2.00	0.500	6.00
57	4	16.78	18.80	0.75	14.50	24.00	4000	0.75	2.00	2.00	0.500	6.00
58	6	18.70	20.32	0.75	20.50	24.00	4000	0.75	2.00	2.00	0.500	6.00
59	2	18.83	22.58	1.00	10.00	24.00	4000	1.00	2.00	2.00	0.500	6.00
60	4	24.68	27.69	1.00	18.00	24.00	4000	1.00	2.00	2.00	0.500	6.00
61	2	25.56	30.67	1.27	11.62	24.00	4000	1.27	2.00	2.00	0.500	6.00
62	4	33.55	37.67	1.27	21.78	24.00	4000	1.27	2.00	2.00	0.500	6.00
63	2	29.11	34.95	1.41	12.46	24.00	4000	1.41	2.00	2.00	0.500	6.00

Table 5.17b (continued)
Data for hypothetical beams with confining transverse reinforcement

Beam No.	n	l_d $R_f=0.1275$	d_b $R_f=0.0727$	b	h	f_c	c_{si}	c_{so}	c_b	d_s	s	A_{tr}/n	
Group 3													
1	2	15.29	18.04	0.75	8.00	12.00	4000	0.50	2.00	2.00	0.500	8.00	0.200
2	2	15.29	18.04	0.75	8.00	12.00	4000	0.50	2.00	2.00	0.500	8.00	0.200
3	2	23.28	27.76	1.00	9.00	12.00	4000	0.50	2.00	2.00	0.500	8.00	0.200
4	2	32.16	38.48	1.27	10.35	12.00	4000	0.64	2.00	2.00	0.500	8.00	0.200
5	2	36.90	44.22	1.41	11.05	12.00	4000	0.71	2.00	2.00	0.500	8.00	0.200
6	2	15.29	18.04	0.75	8.00	12.00	4000	0.50	2.00	2.00	0.500	8.00	0.200
7	4	19.54	21.64	0.75	13.00	12.00	4000	0.50	2.00	2.00	0.500	8.00	0.100
8	6	21.53	23.19	0.75	18.00	12.00	4000	0.50	2.00	2.00	0.500	8.00	0.067
9	8	22.69	24.04	0.75	23.00	12.00	4000	0.50	2.00	2.00	0.500	8.00	0.050
10	2	23.28	27.76	1.00	9.00	12.00	4000	0.50	2.00	2.00	0.500	8.00	0.200
11	4	30.27	33.83	1.00	15.00	12.00	4000	0.50	2.00	2.00	0.500	8.00	0.100
12	6	33.64	36.48	1.00	21.00	12.00	4000	0.50	2.00	2.00	0.500	8.00	0.067
13	2	32.16	38.48	1.27	10.35	12.00	4000	0.64	2.00	2.00	0.500	8.00	0.200
14	4	42.03	47.09	1.27	17.97	12.00	4000	0.64	2.00	2.00	0.500	8.00	0.100
15	2	36.90	44.22	1.41	11.05	12.00	4000	0.71	2.00	2.00	0.500	8.00	0.200
16	4	48.34	54.21	1.41	19.51	12.00	4000	0.71	2.00	2.00	0.500	8.00	0.100
17	2	18.14	21.09	0.75	8.00	24.00	3000	0.50	2.00	2.00	0.500	8.00	0.200
18	2	15.29	18.04	0.75	8.00	24.00	4000	0.50	2.00	2.00	0.500	8.00	0.200
19	2	12.00	14.24	0.75	8.00	24.00	6000	0.50	2.00	2.00	0.500	8.00	0.200
20	2	12.00	12.00	0.75	8.00	24.00	8000	0.50	2.00	2.00	0.500	8.00	0.200
21	2	12.00	12.00	0.75	8.00	24.00	10000	0.50	2.00	2.00	0.500	8.00	0.200
22	2	12.00	12.00	0.75	8.00	24.00	12000	0.50	2.00	2.00	0.500	8.00	0.200
23	2	12.00	12.00	0.75	8.00	24.00	13000	0.50	2.00	2.00	0.500	8.00	0.200
24	2	12.00	12.00	0.75	8.00	24.00	14000	0.50	2.00	2.00	0.500	8.00	0.200
25	2	12.00	12.00	0.75	8.00	24.00	15000	0.50	2.00	2.00	0.500	8.00	0.200
26	2	12.00	12.00	0.75	8.00	24.00	16000	0.50	2.00	2.00	0.500	8.00	0.200
27	2	27.72	32.58	1.00	9.00	24.00	3000	0.50	2.00	2.00	0.500	8.00	0.200
28	2	23.28	27.76	1.00	9.00	24.00	4000	0.50	2.00	2.00	0.500	8.00	0.200
29	2	17.89	21.80	1.00	9.00	24.00	6000	0.50	2.00	2.00	0.500	8.00	0.200
30	2	16.00	18.13	1.00	9.00	24.00	8000	0.50	2.00	2.00	0.500	8.00	0.200
31	2	16.00	16.00	1.00	9.00	24.00	10000	0.50	2.00	2.00	0.500	8.00	0.200
32	2	16.00	16.00	1.00	9.00	24.00	12000	0.50	2.00	2.00	0.500	8.00	0.200
33	2	16.00	16.00	1.00	9.00	24.00	13000	0.50	2.00	2.00	0.500	8.00	0.200
34	2	16.00	16.00	1.00	9.00	24.00	14000	0.50	2.00	2.00	0.500	8.00	0.200
35	2	16.00	16.00	1.00	9.00	24.00	15000	0.50	2.00	2.00	0.500	8.00	0.200
36	2	16.00	16.00	1.00	9.00	24.00	16000	0.50	2.00	2.00	0.500	8.00	0.200
37	2	38.26	45.11	1.27	10.35	24.00	3000	0.64	2.00	2.00	0.500	8.00	0.200
38	2	32.16	38.48	1.27	10.35	24.00	4000	0.64	2.00	2.00	0.500	8.00	0.200
39	2	24.77	30.28	1.27	10.35	24.00	6000	0.64	2.00	2.00	0.500	8.00	0.200
40	2	20.32	25.23	1.27	10.35	24.00	8000	0.64	2.00	2.00	0.500	8.00	0.200
41	2	20.32	21.73	1.27	10.35	24.00	10000	0.64	2.00	2.00	0.500	8.00	0.200
42	2	20.32	20.32	1.27	10.35	24.00	12000	0.64	2.00	2.00	0.500	8.00	0.200
43	2	20.32	20.32	1.27	10.35	24.00	13000	0.64	2.00	2.00	0.500	8.00	0.200
44	2	20.32	20.32	1.27	10.35	24.00	14000	0.64	2.00	2.00	0.500	8.00	0.200
45	2	20.32	20.32	1.27	10.35	24.00	15000	0.64	2.00	2.00	0.500	8.00	0.200
46	2	20.32	20.32	1.27	10.35	24.00	16000	0.64	2.00	2.00	0.500	8.00	0.200
47	2	43.89	51.82	1.41	11.05	24.00	3000	0.71	2.00	2.00	0.500	8.00	0.200
48	2	36.90	44.22	1.41	11.05	24.00	4000	0.71	2.00	2.00	0.500	8.00	0.200
49	2	28.44	34.82	1.41	11.05	24.00	6000	0.71	2.00	2.00	0.500	8.00	0.200
50	2	23.35	29.03	1.41	11.05	24.00	8000	0.71	2.00	2.00	0.500	8.00	0.200
51	2	22.56	25.02	1.41	11.05	24.00	10000	0.71	2.00	2.00	0.500	8.00	0.200
52	2	22.56	22.56	1.41	11.05	24.00	12000	0.71	2.00	2.00	0.500	8.00	0.200
53	2	22.56	22.56	1.41	11.05	24.00	13000	0.71	2.00	2.00	0.500	8.00	0.200
54	2	22.56	22.56	1.41	11.05	24.00	14000	0.71	2.00	2.00	0.500	8.00	0.200
55	2	22.56	22.56	1.41	11.05	24.00	15000	0.71	2.00	2.00	0.500	8.00	0.200
56	2	22.56	22.56	1.41	11.05	24.00	16000	0.71	2.00	2.00	0.500	8.00	0.200
57	4	19.54	21.64	0.75	13.00	24.00	4000	0.50	2.00	2.00	0.500	8.00	0.100
58	6	21.53	23.19	0.75	18.00	24.00	4000	0.50	2.00	2.00	0.500	8.00	0.067
59	2	23.28	27.76	1.00	9.00	24.00	4000	0.50	2.00	2.00	0.500	8.00	0.200
60	4	30.27	33.83	1.00	15.00	24.00	4000	0.50	2.00	2.00	0.500	8.00	0.100
61	2	32.16	38.48	1.27	10.35	24.00	4000	0.64	2.00	2.00	0.500	8.00	0.200
62	4	42.03	47.09	1.27	17.97	24.00	4000	0.64	2.00	2.00	0.500	8.00	0.100
63	2	36.90	44.22	1.41	11.05	24.00	4000	0.71	2.00	2.00	0.500	8.00	0.200

Table 5.17b (continued)
Data for hypothetical beams with confining transverse reinforcement

Beam No.	n	l_d $R_r=0.1275$	l_d $R_r=0.0727$	d_b	b	h	f'_c	c_{si}	c_{so}	c_b	d_s	s	A_{sr}/n
Group 4													
1	2	12.00	13.53	0.75	8.00	12.00	4000	0.50	2.00	2.00	0.500	4.00	0.200
2	2	12.00	13.53	0.75	8.00	12.00	4000	0.50	2.00	2.00	0.500	4.00	0.200
3	2	16.00	20.44	1.00	9.00	12.00	4000	0.50	2.00	2.00	0.500	4.00	0.200
4	2	21.88	28.18	1.27	10.35	12.00	4000	0.64	2.00	2.00	0.500	4.00	0.200
5	2	25.05	32.31	1.41	11.05	12.00	4000	0.71	2.00	2.00	0.500	4.00	0.200
6	2	12.00	13.53	0.75	8.00	12.00	4000	0.50	2.00	2.00	0.500	4.00	0.200
7	4	15.29	18.04	0.75	13.00	12.00	4000	0.50	2.00	2.00	0.500	4.00	0.100
8	6	17.88	20.29	0.75	18.00	12.00	4000	0.50	2.00	2.00	0.500	4.00	0.067
9	8	19.54	21.64	0.75	23.00	12.00	4000	0.50	2.00	2.00	0.500	4.00	0.050
10	2	16.00	20.44	1.00	9.00	12.00	4000	0.50	2.00	2.00	0.500	4.00	0.200
11	4	23.28	27.76	1.00	15.00	12.00	4000	0.50	2.00	2.00	0.500	4.00	0.100
12	6	27.51	31.53	1.00	21.00	12.00	4000	0.50	2.00	2.00	0.500	4.00	0.067
13	2	21.88	28.18	1.27	10.35	12.00	4000	0.64	2.00	2.00	0.500	4.00	0.200
14	4	32.16	38.48	1.27	17.97	12.00	4000	0.64	2.00	2.00	0.500	4.00	0.100
15	2	25.05	32.31	1.41	11.05	12.00	4000	0.71	2.00	2.00	0.500	4.00	0.200
16	4	36.90	44.22	1.41	19.51	12.00	4000	0.71	2.00	2.00	0.500	4.00	0.100
17	2	13.22	16.20	0.75	8.00	24.00	3000	0.50	2.00	2.00	0.500	4.00	0.200
18	2	12.00	13.53	0.75	8.00	24.00	4000	0.50	2.00	2.00	0.500	4.00	0.200
19	2	12.00	12.00	0.75	8.00	24.00	6000	0.50	2.00	2.00	0.500	4.00	0.200
20	2	12.00	12.00	0.75	8.00	24.00	8000	0.50	2.00	2.00	0.500	4.00	0.200
21	2	12.00	12.00	0.75	8.00	24.00	10000	0.50	2.00	2.00	0.500	4.00	0.200
22	2	12.00	12.00	0.75	8.00	24.00	12000	0.50	2.00	2.00	0.500	4.00	0.200
23	2	12.00	12.00	0.75	8.00	24.00	13000	0.50	2.00	2.00	0.500	4.00	0.200
24	2	12.00	12.00	0.75	8.00	24.00	14000	0.50	2.00	2.00	0.500	4.00	0.200
25	2	12.00	12.00	0.75	8.00	24.00	15000	0.50	2.00	2.00	0.500	4.00	0.200
26	2	12.00	12.00	0.75	8.00	24.00	16000	0.50	2.00	2.00	0.500	4.00	0.200
27	2	19.43	24.57	1.00	9.00	24.00	3000	0.50	2.00	2.00	0.500	4.00	0.200
28	2	16.00	20.44	1.00	9.00	24.00	4000	0.50	2.00	2.00	0.500	4.00	0.200
29	2	16.00	16.00	1.00	9.00	24.00	6000	0.50	2.00	2.00	0.500	4.00	0.200
30	2	16.00	16.00	1.00	9.00	24.00	8000	0.50	2.00	2.00	0.500	4.00	0.200
31	2	16.00	16.00	1.00	9.00	24.00	10000	0.50	2.00	2.00	0.500	4.00	0.200
32	2	16.00	16.00	1.00	9.00	24.00	12000	0.50	2.00	2.00	0.500	4.00	0.200
33	2	16.00	16.00	1.00	9.00	24.00	13000	0.50	2.00	2.00	0.500	4.00	0.200
34	2	16.00	16.00	1.00	9.00	24.00	14000	0.50	2.00	2.00	0.500	4.00	0.200
35	2	16.00	16.00	1.00	9.00	24.00	15000	0.50	2.00	2.00	0.500	4.00	0.200
36	2	16.00	16.00	1.00	9.00	24.00	16000	0.50	2.00	2.00	0.500	4.00	0.200
37	2	26.67	33.84	1.27	10.35	24.00	3000	0.64	2.00	2.00	0.500	4.00	0.200
38	2	21.88	28.18	1.27	10.35	24.00	4000	0.64	2.00	2.00	0.500	4.00	0.200
39	2	20.32	21.42	1.27	10.35	24.00	6000	0.64	2.00	2.00	0.500	4.00	0.200
40	2	20.32	20.32	1.27	10.35	24.00	8000	0.64	2.00	2.00	0.500	4.00	0.200
41	2	20.32	20.32	1.27	10.35	24.00	10000	0.64	2.00	2.00	0.500	4.00	0.200
42	2	20.32	20.32	1.27	10.35	24.00	12000	0.64	2.00	2.00	0.500	4.00	0.200
43	2	20.32	20.32	1.27	10.35	24.00	13000	0.64	2.00	2.00	0.500	4.00	0.200
44	2	20.32	20.32	1.27	10.35	24.00	14000	0.64	2.00	2.00	0.500	4.00	0.200
45	2	20.32	20.32	1.27	10.35	24.00	15000	0.64	2.00	2.00	0.500	4.00	0.200
46	2	20.32	20.32	1.27	10.35	24.00	16000	0.64	2.00	2.00	0.500	4.00	0.200
47	2	30.53	38.79	1.41	11.05	24.00	3000	0.71	2.00	2.00	0.500	4.00	0.200
48	2	25.05	32.31	1.41	11.05	24.00	4000	0.71	2.00	2.00	0.500	4.00	0.200
49	2	22.56	24.57	1.41	11.05	24.00	6000	0.71	2.00	2.00	0.500	4.00	0.200
50	2	20.32	20.32	1.27	10.35	24.00	8000	0.64	2.00	2.00	0.500	4.00	0.200
51	2	20.32	20.32	1.27	10.35	24.00	10000	0.64	2.00	2.00	0.500	4.00	0.200
52	2	20.32	20.32	1.27	10.35	24.00	12000	0.64	2.00	2.00	0.500	4.00	0.200
53	2	20.32	20.32	1.27	10.35	24.00	13000	0.64	2.00	2.00	0.500	4.00	0.200
54	2	20.32	20.32	1.27	10.35	24.00	14000	0.64	2.00	2.00	0.500	4.00	0.200
55	2	20.32	20.32	1.27	10.35	24.00	15000	0.64	2.00	2.00	0.500	4.00	0.200
56	2	20.32	20.32	1.27	10.35	24.00	16000	0.64	2.00	2.00	0.500	4.00	0.200
57	4	15.29	18.04	0.75	13.00	24.00	4000	0.50	2.00	2.00	0.500	4.00	0.100
58	6	17.88	20.29	0.75	18.00	24.00	4000	0.50	2.00	2.00	0.500	4.00	0.067
59	2	16.00	20.44	1.00	9.00	24.00	4000	0.50	2.00	2.00	0.500	4.00	0.200
60	4	23.28	27.76	1.00	15.00	24.00	4000	0.50	2.00	2.00	0.500	4.00	0.100
61	2	21.88	28.18	1.27	10.35	24.00	4000	0.64	2.00	2.00	0.500	4.00	0.200
62	4	32.16	38.48	1.27	17.97	24.00	4000	0.64	2.00	2.00	0.500	4.00	0.100
63	2	25.05	32.31	1.41	11.05	24.00	4000	0.71	2.00	2.00	0.500	4.00	0.200

* Predicted development/splice length based on Eq. 5.33, using $\phi_d = 0.9$ and $f_y = 60 \text{ ksi}$

1 in. = 25.4 mm; 1 psi = 6.895 kPa; 1 ksi = 6.895 MPa

Table 5.18
Strength reduction (ϕ) factor for bond

(a) $\gamma_D = 1.4$ $\gamma_L = 1.7$ $\phi_{\text{bonding}} = 0.9$ $\beta = 3.5$

	Without Stirrups			With Stirrups				
Eq. 5.22								
Avg. R_r	N/A					0.0727		
\bar{r}	0.962					1.029		
V_r	0.094					0.120		
$(Q_D/Q_L)_n$	0.5	1.0	1.5	0.5	1.0	1.5	0.5	1.0
\bar{q}	0.675	0.647	0.631	0.675	0.647	0.631	0.675	0.647
$V_{\phi q}$	0.102	0.131	0.152	0.102	0.131	0.152	0.102	0.131
ϕ_b	0.877	0.847	0.816	0.879	0.855	0.829	0.874	0.849
ϕ_d	0.975	0.941	0.907	0.976	0.950	0.921	0.971	0.944
Eq. 5.23								
Avg. R_r	N/A					0.0727		
\bar{r}	1.035					1.152		
V_r	0.134					0.14		
$(Q_D/Q_L)_n$	0.5	1.0	1.5	0.5	1.0	1.5	0.5	1.0
\bar{q}	0.675	0.647	0.631	0.675	0.647	0.631	0.675	0.647
$V_{\phi q}$	0.102	0.131	0.152	0.102	0.131	0.152	0.102	0.131
ϕ_b	0.851	0.831	0.808	0.931	0.911	0.886	0.912	0.866
ϕ_d	0.945	0.923	0.897	1.035	1.012	0.985	1.014	0.990

(b) $\gamma_D = 1.2$ $\gamma_L = 1.6$ $\phi_{\text{bonding}} = 0.8$ $\beta = 3.5$

	Without Stirrups			With Stirrups				
Eq. 5.22								
Avg. R_r	N/A					0.0727		
\bar{r}	0.962					1.029		
V_r	0.094					0.120		
$(Q_D/Q_L)_n$	0.5	1.0	1.5	0.5	1.0	1.5	0.5	1.0
\bar{q}	0.759	0.716	0.693	0.759	0.716	0.693	0.759	0.716
$V_{\phi q}$	0.102	0.131	0.152	0.102	0.131	0.152	0.102	0.131
ϕ_b	0.780	0.765	0.744	0.781	0.772	0.755	0.777	0.767
ϕ_d	0.975	0.956	0.930	0.976	0.965	0.944	0.971	0.959
Eq. 5.23								
Avg. R_r	N/A					0.0727		
\bar{r}	1.035					1.152		
V_r	0.134					0.14		
$(Q_D/Q_L)_n$	0.5	1.0	1.5	0.5	1.0	1.5	0.5	1.0
\bar{q}	0.759	0.716	0.693	0.759	0.716	0.693	0.759	0.716
$V_{\phi q}$	0.102	0.131	0.152	0.102	0.131	0.152	0.102	0.131
ϕ_b	0.756	0.751	0.736	0.828	0.823	0.808	0.811	0.805
ϕ_d	0.945	0.938	0.920	1.035	1.029	1.010	1.014	1.006

Table 5.19
Data, development and splice lengths for hypothetical beams
without confining transverse reinforcement

Beam No.	n	d _b (in.)	b (in.)	h (in.)	f _c (psi)	c _{st} (in.)	c _{so} (in.)	c _b (in.)	Eq.5.33 l _d (in.)	Eq.5.34 ^a l _d (in.)	ACI 318-95		Eq.5.33 ACI l _d (in.)	Eq.5.34 ACI l _s (in.)	Eq.5.33 ACI l _s (in.)	Eq.5.34 ACI l _s (in.)
											l _d (in.)	l _s (in.)				
1	2	0.75	8.0	12.0	4000	0.50	2.00	2.00	32.11	51.47	36.59	47.57	0.877	1.407	0.675	1.082
2	2	0.75	12.0	12.0	4000	2.50	2.00	2.00	18.96	18.96	17.08	22.20	1.111	1.111	0.854	0.854
3	2	1.00	12.0	12.0	4000	2.00	2.00	2.00	32.03	32.03	28.46	37.00	1.125	1.125	0.866	0.866
4	2	1.27	12.0	12.0	4000	1.46	2.00	2.00	53.80	61.64	54.78	71.21	0.982	1.125	0.755	0.866
5	2	1.41	12.0	12.0	4000	1.18	2.00	2.00	70.60	84.45	75.04	97.56	0.941	1.125	0.724	0.866
6	2	0.75	24.0	12.0	4000	8.50	2.00	2.00	18.96	18.96	17.08	22.20	1.111	1.111	0.854	0.854
7	4	0.75	24.0	12.0	4000	2.33	2.00	2.00	18.96	18.96	17.08	22.20	1.111	1.111	0.854	0.854
8	6	0.75	24.0	12.0	4000	1.10	2.00	2.00	24.45	30.53	21.71	28.22	1.126	1.407	0.866	1.082
9	8	0.75	24.0	12.0	4000	0.57	2.00	2.00	31.10	47.59	33.83	43.98	0.919	1.407	0.707	1.082
10	2	1.00	24.0	12.0	4000	8.00	2.00	2.00	32.03	32.03	28.46	37.00	1.125	1.125	0.866	0.866
11	4	1.00	24.0	12.0	4000	2.00	2.00	2.00	32.03	32.03	28.46	37.00	1.125	1.125	0.866	0.866
12	6	1.00	24.0	12.0	4000	0.80	2.00	2.00	45.72	61.59	54.73	71.15	0.835	1.125	0.643	0.866
13	2	1.27	24.0	12.0	4000	7.46	2.00	2.00	49.01	49.01	43.55	56.62	1.125	1.125	0.866	0.866
14	4	1.27	24.0	12.0	4000	1.64	2.00	2.00	50.73	56.77	50.44	65.58	1.006	1.125	0.774	0.866
15	2	1.41	24.0	12.0	4000	7.18	2.00	2.00	58.85	52.29	67.98	1.125	1.125	0.866	0.866	
16	4	1.41	24.0	12.0	4000	1.45	2.00	2.00	64.53	73.75	65.54	85.20	0.985	1.125	0.757	0.866
17	2	0.75	12.0	24.0	3000	2.50	2.00	2.00	20.92	20.92	19.72	25.63	1.061	1.061	0.816	0.816
18	2	0.75	12.0	24.0	4000	2.50	2.00	2.00	18.96	18.96	17.08	22.20	1.111	1.111	0.854	0.854
19	2	0.75	12.0	24.0	6000	2.50	2.00	2.00	16.43	16.43	13.94	18.13	1.178	1.178	0.906	0.906
20	2	0.75	12.0	24.0	8000	2.50	2.00	2.00	14.78	12.00	12.07	15.70	1.224	0.994	0.942	0.764
21	2	0.75	12.0	24.0	10000	2.50	2.00	2.00	13.58	12.00	12.00	15.60	1.132	1.000	0.871	0.769
22	2	0.75	12.0	24.0	12000	2.50	2.00	2.00	12.65	12.00	12.00	15.60	1.054	1.000	0.811	0.769
23	2	0.75	12.0	24.0	13000	2.50	2.00	2.00	12.26	12.00	12.00	15.60	1.021	1.000	0.786	0.769
24	2	0.75	12.0	24.0	14000	2.50	2.00	2.00	12.00	12.00	12.00	15.60	1.000	1.000	0.769	0.769
25	2	0.75	12.0	24.0	15000	2.50	2.00	2.00	12.00	12.00	12.00	15.60	1.000	1.000	0.769	0.769
26	2	0.75	12.0	24.0	16000	2.50	2.00	2.00	12.00	12.00	12.00	15.60	1.000	1.000	0.769	0.769
27	2	1.00	12.0	24.0	3000	2.00	2.00	2.00	35.34	35.34	32.86	42.72	1.075	1.075	0.827	0.827
28	2	1.00	12.0	24.0	4000	2.00	2.00	2.00	32.03	32.03	28.46	37.00	1.125	1.125	0.866	0.866
29	2	1.00	12.0	24.0	6000	2.00	2.00	2.00	27.75	27.75	23.24	30.21	1.194	1.194	0.919	0.919
30	2	1.00	12.0	24.0	8000	2.00	2.00	2.00	24.97	24.97	20.12	26.16	1.241	1.241	0.954	0.954
31	2	1.00	12.0	24.0	10000	2.00	2.00	2.00	22.94	22.94	18.00	23.40	1.275	1.275	0.980	0.980
32	2	1.00	12.0	24.0	12000	2.00	2.00	2.00	21.37	21.37	18.00	23.40	1.187	1.187	0.913	0.913
33	2	1.00	12.0	24.0	13000	2.00	2.00	2.00	20.70	20.70	18.00	23.40	1.150	1.150	0.885	0.885
34	2	1.00	12.0	24.0	14000	2.00	2.00	2.00	20.09	20.09	18.00	23.40	1.116	1.116	0.859	0.859
35	2	1.00	12.0	24.0	15000	2.00	2.00	2.00	19.54	19.54	18.00	23.40	1.085	1.085	0.835	0.835
36	2	1.00	12.0	24.0	16000	2.00	2.00	2.00	19.03	19.03	18.00	23.40	1.057	1.057	0.813	0.813
37	2	1.27	12.0	24.0	3000	1.46	2.00	2.00	59.39	68.01	63.25	82.23	0.939	1.075	0.722	0.827
38	2	1.27	12.0	24.0	4000	1.46	2.00	2.00	53.80	61.64	54.78	71.21	0.982	1.125	0.755	0.866
39	2	1.27	12.0	24.0	6000	1.46	2.00	2.00	46.56	53.41	44.73	58.14	1.041	1.194	0.801	0.919
40	2	1.27	12.0	24.0	8000	1.46	2.00	2.00	41.86	48.05	38.73	50.35	1.081	1.241	0.831	0.954
41	2	1.27	12.0	24.0	10000	1.46	2.00	2.00	38.44	44.15	34.64	45.04	1.109	1.275	0.853	0.980
42	2	1.27	12.0	24.0	12000	1.46	2.00	2.00	35.78	41.13	34.64	45.04	1.033	1.187	0.794	0.913
43	2	1.27	12.0	24.0	13000	1.46	2.00	2.00	34.65	39.84	34.64	45.04	1.000	1.150	0.769	0.885
44	2	1.27	12.0	24.0	14000	1.46	2.00	2.00	33.62	38.67	34.64	45.04	0.970	1.116	0.747	0.859
45	2	1.27	12.0	24.0	15000	1.46	2.00	2.00	32.68	37.61	34.64	45.04	0.943	1.085	0.726	0.835
46	2	1.27	12.0	24.0	16000	1.46	2.00	2.00	31.82	36.62	34.64	45.04	0.918	1.057	0.707	0.813
47	2	1.41	12.0	24.0	3000	1.18	2.00	2.00	78.01	93.17	86.65	112.65	0.900	1.075	0.692	0.827
48	2	1.41	12.0	24.0	4000	1.18	2.00	2.00	70.60	84.45	75.04	97.56	0.941	1.125	0.724	0.866
49	2	1.41	12.0	24.0	6000	1.18	2.00	2.00	61.02	73.17	61.27	79.65	0.996	1.194	0.766	0.919
50	2	1.41	12.0	24.0	8000	1.18	2.00	2.00	54.79	65.83	53.06	68.98	1.033	1.241	0.794	0.954
51	2	1.41	12.0	24.0	10000	1.18	2.00	2.00	50.26	60.49	47.46	61.70	1.059	1.275	0.815	0.980
52	2	1.41	12.0	24.0	12000	1.18	2.00	2.00	46.74	56.34	47.46	61.70	0.985	1.187	0.757	0.913
53	2	1.41	12.0	24.0	13000	1.18	2.00	2.00	45.24	54.58	47.46	61.70	0.953	1.150	0.733	0.885
54	2	1.41	12.0	24.0	14000	1.18	2.00	2.00	43.88	52.98	47.46	61.70	0.925	1.116	0.711	0.859
55	2	1.41	12.0	24.0	15000	1.18	2.00	2.00	42.64	51.52	47.46	61.70	0.898	1.085	0.691	0.835
56	2	1.41	12.0	24.0	16000	1.18	2.00	2.00	41.50	50.17	47.46	61.70	0.874	1.057	0.673	0.813
57	4	0.75	18.0	24.0	4000	1.33	2.00	2.00	22.18	26.36	18.74	24.36	1.183	1.407	0.910	1.082
58	6	0.75	18.0	24.0	4000	0.50	2.00	2.00	32.11	51.47	36.59	47.57	0.877	1.407	0.675	1.082
59	2	1.00	18.0	24.0	4000	5.00	2.00	2.00	32.03	32.03	28.46	37.00	1.125	1.125	0.866	0.866
60	4	1.00	18.0	24.0	4000	1.00	2.00	2.00	42.16	53.38	47.43	61.66	0.889	1.125	0.684	0.866

Table 5.19 (continued)
Data, development and splice lengths for hypothetical beams
without confining transverse reinforcement

Beam No.	n	d_b (in.)	b (in.)	h (in.)	f'_c (psi)	c_{si} (in.)	c_{so} (in.)	c_b (in.)	Eq. 5.33 ⁺ l_d (in.)	Eq. 5.34 ⁺⁺ l_d (in.)	ACI 318-95		Eq. 5.33	Eq. 5.34	Eq. 5.33	Eq. 5.34	
											l_d (in.)	l_s (in.)	ACI l_d	ACI l_d	ACI l_s	ACI l_s	
61	2	1.27	18.0	24.0	4000	4.46	2.00	2.00	49.01	49.01	43.55	56.62	1.125	1.125	0.866	0.866	
62	4	1.27	18.0	24.0	4000	0.64	2.00	2.00	71.67	101.29	90.01	117.01	0.796	1.125	0.613	0.866	
63	2	1.41	18.0	24.0	4000	4.18	2.00	2.00	58.85	58.85	52.29	67.98	1.125	1.125	0.866	0.866	
$+ \quad \text{Eq. 5.33} = \frac{l_d}{d_b} = \frac{\frac{f_y}{f'_c} - 2100 \left(0.1 \frac{c_{\max}}{c_{\min}} + 0.9 \right)}{68 \left(\frac{c + K_{tr}}{d_b} \right)}$ $++ \quad \text{Eq. 5.34} = \frac{l_d}{d_b} = \frac{\frac{f_y}{f'_c} - 2100}{68 \left(\frac{c + K_{tr}}{d_b} \right)}$											For $f'_c < 8000$ psi :		Max.	1.194	1.407	0.919	1.082
											Min.		0.796	1.061	0.613	0.816	
											Average		1.037	1.165	0.798	0.896	
$+ \quad \text{Eq. 5.33} = \frac{l_d}{d_b} = \frac{\frac{f_y}{f'_c} - 2100 \left(0.1 \frac{c_{\max}}{c_{\min}} + 0.9 \right)}{68 \left(\frac{c + K_{tr}}{d_b} \right)}$ $++ \quad \text{Eq. 5.34} = \frac{l_d}{d_b} = \frac{\frac{f_y}{f'_c} - 2100}{68 \left(\frac{c + K_{tr}}{d_b} \right)}$										For $f'_c \geq 8000$ psi :		Max.	1.275	1.275	0.980	0.980	
										Min.		0.874	0.994	0.673	0.764		
										Average		1.047	1.119	0.806	0.861		
$+ \quad \text{Eq. 5.33} = \frac{l_d}{d_b} = \frac{\frac{f_y}{f'_c} - 2100 \left(0.1 \frac{c_{\max}}{c_{\min}} + 0.9 \right)}{68 \left(\frac{c + K_{tr}}{d_b} \right)}$ $++ \quad \text{Eq. 5.34} = \frac{l_d}{d_b} = \frac{\frac{f_y}{f'_c} - 2100}{68 \left(\frac{c + K_{tr}}{d_b} \right)}$										For all:		Max.	1.275	1.407	0.980	1.082	
										Min.		0.796	0.994	0.613	0.764		
										Average		1.042	1.144	0.801	0.880		
$+ \quad \text{Eq. 5.33} = \frac{l_d}{d_b} = \frac{\frac{f_y}{f'_c} - 2100 \left(0.1 \frac{c_{\max}}{c_{\min}} + 0.9 \right)}{68 \left(\frac{c + K_{tr}}{d_b} \right)}$ $++ \quad \text{Eq. 5.34} = \frac{l_d}{d_b} = \frac{\frac{f_y}{f'_c} - 2100}{68 \left(\frac{c + K_{tr}}{d_b} \right)}$										For No. 6 Bars		Max.	1.224	1.407	0.942	1.082	
										Min.		0.877	0.994	0.675	0.764		
										Average		1.061	1.150	0.816	0.885		
$+ \quad \text{Eq. 5.33} = \frac{l_d}{d_b} = \frac{\frac{f_y}{f'_c} - 2100 \left(0.1 \frac{c_{\max}}{c_{\min}} + 0.9 \right)}{68 \left(\frac{c + K_{tr}}{d_b} \right)}$ $++ \quad \text{Eq. 5.34} = \frac{l_d}{d_b} = \frac{\frac{f_y}{f'_c} - 2100}{68 \left(\frac{c + K_{tr}}{d_b} \right)}$										For No. 8 Bars		Max.	1.275	1.275	0.980	0.980	
										Min.		0.835	1.057	0.643	0.813		
										Average		1.108	1.141	0.852	0.878		
$+ \quad \text{Eq. 5.33} = \frac{l_d}{d_b} = \frac{\frac{f_y}{f'_c} - 2100 \left(0.1 \frac{c_{\max}}{c_{\min}} + 0.9 \right)}{68 \left(\frac{c + K_{tr}}{d_b} \right)}$ $++ \quad \text{Eq. 5.34} = \frac{l_d}{d_b} = \frac{\frac{f_y}{f'_c} - 2100}{68 \left(\frac{c + K_{tr}}{d_b} \right)}$										For No. 9 Bars		Max.	1.125	1.275	0.866	0.980	
										Min.		0.796	1.057	0.613	0.813		
										Average		1.007	1.115	0.775	0.858		
$+ \quad \text{Eq. 5.33} = \frac{l_d}{d_b} = \frac{\frac{f_y}{f'_c} - 2100 \left(0.1 \frac{c_{\max}}{c_{\min}} + 0.9 \right)}{68 \left(\frac{c + K_{tr}}{d_b} \right)}$ $++ \quad \text{Eq. 5.34} = \frac{l_d}{d_b} = \frac{\frac{f_y}{f'_c} - 2100}{68 \left(\frac{c + K_{tr}}{d_b} \right)}$										For No. 11 Bars		Max.	1.125	1.275	0.866	0.980	
										Min.		0.874	1.057	0.673	0.813		
										Average		0.981	1.143	0.755	0.880		

1 in. = 25.4 mm, 1psi = 6.895 kPa

Table 5.20
Test/prediction ratios for developed and spliced bars without
confining transverse reinforcement using Eq. 5.33 and ACI 318-95 criteria

Test No.*	l_d (in.)	d_b (in.)	f'_c (psi)	f'_s Test (ksi)	f'_s (Prediction)		Test/Prediction Ratio	
					Eq. 5.33+ (ksi)	ACI++ (ksi)	Test Eq. 5.33	Test ACI
Chinn (1956)								
D34	12.50	0.750	3800	37.46	34.87	26.21	1.074	1.429
D12	16.00	0.750	4530	46.37	42.84	47.86	1.083	0.969
D17	16.00	0.750	3580	40.56	35.07	33.33	1.157	1.217
D19	16.00	0.750	4230	57.60	52.80	57.81	1.091	0.996
D23	16.00	0.750	4450	39.70	36.67	36.53	1.083	1.087
D24	16.00	0.750	4450	43.37	45.02	37.48	0.963	1.157
D30	16.00	0.750	7480	53.04	47.92	60.27	1.107	0.880
D4	16.00	0.750	4470	47.40	38.46	27.73	1.232	1.709
D40	16.00	0.750	5280	50.69	47.09	38.75	1.076	1.308
D25	24.00	0.750	5100	57.00	55.28	72.87	1.031	0.782
D26	24.00	0.750	5100	56.82	47.41	57.13	1.198	0.995
D35	24.00	0.750	3800	56.91	50.99	62.90	1.116	0.905
D33	20.25	1.410	4830	28.60	31.39	26.60	0.911	1.075
Chamberlin (1956)								
SIV53	12.00	0.500	4540	47.43	45.50	32.34	1.042	1.466
SII23	16.00	0.750	4470	41.93	36.13	35.66	1.161	1.176
Ferguson and Breen (1965)								
8R18a	18.00	1.000	3470	41.60	40.45	39.76	1.028	1.046
8R24a	24.00	1.000	3530	59.53	47.60	41.26	1.251	1.443
8F30a	30.00	1.000	3030	53.48	51.51	44.70	1.038	1.197
8F36a	36.00	1.000	4650	66.22	63.25	62.52	1.047	1.059
8F36b	36.00	1.000	3770	61.90	59.89	56.00	1.034	1.105
8F36k	36.00	1.000	3460	55.84	51.55	53.08	1.083	1.052
8F39a	39.00	1.000	3650	72.90	64.71	63.77	1.127	1.143
8F42a	42.00	1.000	2660	65.93	62.65	57.76	1.052	1.141
8F42b	42.00	1.000	3830	73.54	67.82	67.58	1.084	1.088
8R42a	42.00	1.000	3310	72.21	67.11	66.37	1.076	1.088
8R48a	48.00	1.000	3040	74.43	71.19	69.87	1.046	1.065
8R64a	64.00	1.000	3550	91.70	93.64	102.70	0.979	0.893
8R80a	80.00	1.000	3740	98.61	113.35	130.47	0.870	0.756
IIR24a	33.00	1.410	3720	52.30	43.86	32.06	1.192	1.631
IIR30a	41.25	1.410	4030	59.03	49.24	35.39	1.199	1.668
IIF36a	49.50	1.410	4570	64.66	57.84	49.48	1.118	1.307
IIF36b	49.50	1.410	3350	60.09	53.33	41.79	1.127	1.438
IIF42a	57.75	1.410	3530	64.57	59.85	50.28	1.079	1.284
IIF48a	66.00	1.410	3140	73.91	64.19	55.44	1.151	1.333
IIP48b	66.00	1.410	3330	72.24	65.64	58.37	1.101	1.238
IIR48a	66.00	1.410	5620	82.81	73.90	73.17	1.120	1.132
IIR48b	66.00	1.410	3100	73.20	69.89	68.14	1.047	1.074
IIF60a	82.50	1.410	2610	84.80	72.86	64.87	1.164	1.307
IIF60b	82.50	1.410	4090	78.02	80.26	78.02	0.972	1.000
IIR60a	82.50	1.410	2690	77.19	71.21	60.69	1.084	1.272
IIR60b	82.50	1.410	3460	90.35	80.47	79.90	1.123	1.131
Thompson et al. (1975)								
6-12-4/2/2-6/6	12.00	0.750	3730	57.96	43.34	32.57	1.338	1.780
8-18-4/3/2-6/6	18.00	1.000	4710	57.00	44.88	51.47	1.270	1.107
8-18-4/3/2.5-4/6	18.00	1.000	2920	50.86	41.52	32.42	1.225	1.569
8-24-4/2/2-6/6	24.00	1.000	3105	51.89	46.13	44.58	1.125	1.164
11-25-6/2/3-5/5	25.00	1.410	3920	45.00	36.66	28.40	1.227	1.585
11-30-4/2/2-6/6	30.00	1.410	2865	39.56	35.67	29.13	1.109	1.358
11-30-4/2/4-6/6	30.00	1.410	3350	45.90	37.56	31.50	1.222	1.457
11-30-4/2/2.7-4/6	30.00	1.410	4420	58.48	40.25	36.18	1.453	1.616
11-45-4/1/2-6/6	45.00	1.410	3520	46.72	40.03	30.53	1.167	1.530
14-60-4/2/2-5/5	60.00	1.693	2865	48.13	45.01	42.53	1.069	1.132
14-60-4/2/4-5/5	60.00	1.693	3200	56.64	46.85	44.94	1.209	1.260
Zekany (1981)								
9-53-B-N	16.00	1.128	5650	47.77	35.47	25.04	1.347	1.908
N-N-80B	22.00	1.410	3825	38.53	32.52	23.30	1.185	1.653

Table 5.20 (continued)
Test/prediction ratios for developed and spliced bars without
confining transverse reinforcement using Eq. 5.33 and ACI 318-95 criteria

Test No.*	l_a (in.)	d_b (in.)	f'_c (psi)	f_t Test (ksi)	f_t (Prediction)		Test/Prediction Ratio	
					Eq. 5.33+ (ksi)	ACI++ (ksi)	Test Eq. 5.33	Test ACI
<i>Choi et al. (1990, 1991)</i>								
1-5N0120U	12.00	0.625	5360	61.51	45.57	39.36	1.350	1.563
1-5N0120U	12.00	0.625	5360	64.00	45.57	49.20	1.405	1.301
2-6C0120U	12.00	0.750	6010	51.34	39.66	37.90	1.295	1.355
2-6S0120U	12.00	0.750	6010	45.67	39.66	37.90	1.152	1.205
3-8N0160U	16.00	1.000	5980	43.00	38.86	41.24	1.107	1.043
3-8S0160U	16.00	1.000	5980	42.81	38.86	32.99	1.102	1.297
4-11C0240U	24.00	1.410	5850	37.93	37.79	33.30	1.004	1.139
4-11S0240U	24.00	1.410	5850	40.37	37.79	33.30	1.068	1.212
<i>Hester et al. (1991, 1993)</i>								
1-8N3160U	16.00	1.000	5990	50.13	40.58	33.02	1.235	1.518
2-8C3160U	16.00	1.000	6200	46.25	40.56	33.60	1.140	1.377
3-8S3160U	16.00	1.000	6020	46.86	40.72	33.10	1.151	1.415
4-8S3160U	16.00	1.000	6450	42.36	41.57	34.27	1.019	1.236
5-8C3160U	16.00	1.000	5490	39.86	39.82	31.61	1.001	1.261
6-8C3220U	22.75	1.000	5850	51.99	49.92	46.40	1.041	1.120
7-8C3160U	16.00	1.000	5240	45.40	41.26	38.61	1.100	1.176
<i>Rezanoff et al. (1993)</i>								
2a	29.53	0.992	3958	60.24	47.56	37.50	1.266	1.606
2b	29.53	0.992	3799	60.48	47.08	36.73	1.285	1.646
5a	35.43	1.177	4031	56.96	46.54	38.35	1.224	1.485
5b	44.29	1.177	3726	67.50	52.77	46.09	1.279	1.465
<i>Azizinamini et al. (1993)</i>								
BB-8-5-23	23.00	1.000	5290	47.30	37.92	33.46	1.247	1.414
AB83-8-15-41	41.00	1.000	15120	72.67	69.66	82.00	1.043	0.886
BB-11-5-24	24.00	1.410	5080	29.82	32.39	24.26	0.921	1.229
BB-11-5-40	40.00	1.410	5080	43.44	42.16	40.44	1.030	1.074
BB-11-12-24	24.00	1.410	12730	44.40	40.75	34.04	1.090	1.304
B-11-12-40	40.00	1.410	13000	58.47	53.32	56.74	1.097	1.031
BB-11-11-45	45.00	1.410	10900	48.63	54.72	63.83	0.889	0.762
BB-11-15-36	36.00	1.410	14550	56.95	51.67	51.06	1.102	1.115
BB-11-5-36	36.00	1.410	6170	46.93	41.69	40.11	1.126	1.170
BB-11-13-40	40.00	1.410	13600	57.34	53.93	56.74	1.063	1.011
BB-11-15-13	13.00	1.410	14330	29.76	33.27	18.44	0.895	1.614
AB83-11-15-57.5	57.50	1.410	13870	71.39	67.93	81.56	1.051	0.875
AB89-11-15-80	80.00	1.410	15120	73.88	87.46	113.48	0.845	0.651
<i>Hatfield et al. (1996)</i>								
BB2-8-15-36	36.00	1.000	14450	77.19	90.12	120.00	0.856	0.643
BB3-8-15-36	36.00	1.000	14450	72.75	63.28	72.00	1.150	1.010
BB3-8-15-30	30.00	1.000	15040	66.74	57.14	60.00	1.168	1.112
BB2-8-15-20	20.00	1.000	15040	70.61	60.91	66.67	1.159	1.059
BB2-11-15-36	36.00	1.410	14450	70.35	73.04	85.11	0.963	0.827
BB3-11-15-36	36.00	1.410	14450	57.23	51.10	50.22	1.120	1.140
BB2-11-15-28	28.00	1.410	15040	69.46	62.55	66.19	1.110	1.049
BB2-11-15-42	42.00	1.410	15040	73.48	82.20	99.29	0.894	0.740
BB2-11-15-45B	45.00	1.410	15520	76.21	59.17	62.77	1.288	1.214
BB2-11-15-45D	45.00	1.410	15520	77.16	59.17	62.77	1.304	1.229
<i>Darwin et al. (1995a, 1996a)</i>								
1.1	16.00	1.000	5020	51.78	49.21	37.79	1.052	1.370
1.2	16.00	1.000	5020	44.77	40.20	36.85	1.114	1.215
1.3	16.00	1.000	5020	45.22	38.06	28.81	1.188	1.570
2.4	24.00	1.000	5250	54.29	45.31	42.04	1.198	1.292
2.5	24.00	1.000	5250	58.97	50.70	53.63	1.163	1.100
4.5	24.00	1.000	4090	51.50	47.95	47.97	1.074	1.074
6.5	24.00	1.000	4220	54.06	49.48	50.02	1.093	1.081
8.3	24.00	1.000	3830	62.38	48.62	48.58	1.283	1.284
10.2	26.00	1.000	4250	61.84	52.03	53.67	1.188	1.152
13.4	16.00	0.625	4110	60.26	52.37	46.50	1.151	1.296
14.3	17.00	0.625	4200	61.83	54.93	63.17	1.126	0.979
15.5	40.00	1.410	5250	54.51	51.23	63.49	1.064	0.859

Table 5.20 (continued)
Test/prediction ratios for developed and spliced bars without
confining transverse reinforcement using Eq. 5.33 and ACI 318-95 criteria

Test No.*	l_d (in.)	d_b (in.)	f'_c (psi)	f'_s Test (ksi)	f'_s (Prediction)		Test/Prediction Ratio	
					Eq. 5.33+ (ksi)	ACI++ (ksi)	Test Eq. 5.33	Test ACI
16.2	40.00	1.410	5180	52.75	49.78	50.20	1.060	1.051
Current Study								
25.1	16.50	0.625	4490	63.72	55.68	50.40	1.144	1.264
19.1	36.00	1.000	4250	73.51	65.47	95.04	1.123	0.774
19.2	36.00	1.000	4250	67.85	65.26	74.56	1.040	0.910
20.6	40.00	1.000	5080	57.15	52.44	44.55	1.090	1.283
23a.5	22.00	1.000	9320	62.24	56.64	67.70	1.099	0.919
23a.6	29.00	1.000	9320	75.47	67.89	88.66	1.112	0.851
23b.3	19.50	1.000	8370	71.64	64.93	59.47	1.103	1.205
24.1	32.00	1.000	4300	61.91	59.65	66.45	1.038	0.932
26.3	40.00	1.000	4960	62.52	55.06	43.28	1.135	1.444
26.5	40.00	1.000	4960	64.36	55.51	44.46	1.159	1.448
31.5	22.00	1.000	12890	61.43	46.54	29.56	1.320	2.078
31.6	22.00	1.000	12890	63.42	46.75	30.48	1.357	2.081
34.1	24.00	1.000	5440	57.88	52.58	57.53	1.101	1.006
34.2	24.00	1.000	5440	61.97	52.33	57.06	1.184	1.086
34.3	24.00	1.000	5440	58.94	53.07	55.32	1.111	1.066
34.4	24.00	1.000	5440	58.49	52.47	56.24	1.115	1.040
36.3	26.00	1.000	5060	62.78	55.03	57.60	1.141	1.090
36.4	26.00	1.000	5060	60.17	54.93	57.41	1.095	1.048
38.1	26.00	1.000	5080	53.96	52.48	56.88	1.028	0.949
38.2	26.00	1.000	5080	60.30	56.21	57.91	1.073	1.041
39.6	21.00	1.000	14450	67.38	46.98	28.44	1.434	2.370
40.5	17.00	1.000	15650	65.81	54.27	53.18	1.213	1.238
28.5	30.00	1.410	12610	50.89	51.47	53.95	0.989	0.943
30.5	30.00	1.410	13220	66.95	52.08	53.54	1.286	1.250
32.1	32.00	1.410	14400	63.33	48.77	36.26	1.299	1.747
32.2	32.00	1.410	14400	61.49	49.36	37.93	1.246	1.621
32.3	32.00	1.410	14400	60.64	54.86	56.91	1.105	1.065
32.4	28.00	1.410	14400	61.01	50.95	49.57	1.197	1.231
For No. 6 and smaller bars					Max.	1.405	1.780	
					Min.	0.963	0.782	
					Average	1.153	1.219	
					St.Dev.	0.111	0.264	
					COV	0.096	0.217	
% of specimens with test/prediction ratio < 1.0					4.5%	31.8%		
For No. 7 and larger bars					Max.	1.453	2.370	
					Min.	0.845	0.643	
					Average	1.120	1.219	
					St.Dev.	0.114	0.291	
					COV	0.102	0.239	
% of specimens with test/prediction ratio < 1.0					10.4%	15.7%		
For all					Max.	1.453	2.370	
					Min.	0.845	0.643	
					Average	1.125	1.219	
					St.Dev.	0.114	0.286	
					COV	0.101	0.234	
% of specimens with test/prediction ratio < 1.0					9.5%	18.2%		

* Specimens with $l_d \geq 12$ in.

$$+ \quad \text{Eq. 5.33} = \frac{\frac{f'_s}{f'_c} - 2100 \left(0.1 \frac{c_{\max}}{c_{\min}} + 0.9 \right)}{\frac{68 \left(c + K_{tr} \right)}{d_b}}$$

++ ACI 318-95 "detailed" Equation; the factor of 1.3 is not applied for spliced bars
 1 in = 25.4 mm, 1 psi = 6.895 kPa, 1 ksi = 6.895 MPa

Table 5.21
Data, development and splice lengths for hypothetical beams
with confining transverse reinforcement

Beam No.*	l_d by Eq. 5.33+		l_d by Eq. 5.34++		ACI 318-95		l_d (High R _c)		Eq. 5.33		Eq. 5.34		Eq. 5.33		Eq. 5.34		Eq. 5.33		Eq. 5.34	
	Conv. ^{***}	High R _c ^{**}	Conv.	High R _c	l_d (in.)	l_d (in.)	l_d (in.)	l_d (Conv.)	Eq. 5.33	Eq. 5.34	Eq. 5.33	Eq. 5.34	Eq. 5.33	Eq. 5.34						
Group 1	(in.)	(in.)	(in.)	(in.)	(in.)	(in.)	(in.)	(in.)	Eq. 5.33	Eq. 5.34	Conv.	Conv.	Conv.	Conv.	Conv.	Conv.	High R _c	High R _c	ACI l_d	ACI l_d
1	22.13	18.96	30.71	25.23	17.89	23.26	0.857	0.822	1.237	1.716	0.951	1.320	1.060	1.410	0.815	1.085				
2	15.18	13.71	26.23	22.13	17.08	22.20	0.903	0.844	0.889	1.536	0.684	1.182	0.803	1.296	0.618	0.997				
3	24.68	21.96	35.67	30.27	29.32	38.12	0.890	0.849	0.841	1.216	0.647	0.936	0.749	1.032	0.576	0.794				
4	38.88	33.84	45.80	39.00	40.34	52.44	0.870	0.851	0.964	1.135	0.741	0.873	0.839	0.967	0.645	0.744				
5	48.60	41.63	55.09	46.41	49.95	64.94	0.856	0.842	0.973	1.103	0.748	0.848	0.833	0.929	0.641	0.715				
6	15.18	13.71	26.23	22.13	17.08	22.20	0.903	0.844	0.889	1.536	0.684	1.182	0.803	1.296	0.618	0.997				
7	16.86	15.91	31.70	28.50	17.08	22.20	0.944	0.899	0.987	1.856	0.760	1.428	0.932	1.669	0.717	1.284				
8	22.04	20.93	34.06	31.53	22.39	29.11	0.950	0.926	0.984	1.521	0.757	1.170	0.935	1.408	0.719	1.083				
9	28.06	26.66	41.15	38.36	27.25	35.42	0.950	0.932	1.030	1.510	0.792	1.162	0.979	1.408	0.753	1.083				
10	24.68	21.96	35.67	30.27	29.32	38.12	0.890	0.849	0.841	1.216	0.647	0.936	0.749	1.032	0.576	0.794				
11	27.87	26.06	42.76	38.63	29.32	38.12	0.935	0.903	0.951	1.458	0.731	1.122	0.889	1.317	0.684	1.013				
12	39.86	37.29	51.71	47.61	44.23	57.50	0.936	0.921	0.901	1.169	0.693	0.899	0.843	1.076	0.649	0.828				
13	36.38	31.95	45.80	39.00	40.34	52.44	0.878	0.851	0.902	1.135	0.694	0.873	0.792	0.967	0.609	0.744				
14	42.99	39.73	54.67	49.51	48.32	62.82	0.924	0.906	0.890	1.131	0.684	0.870	0.822	1.025	0.632	0.788				
15	42.91	37.45	51.03	43.49	46.20	60.06	0.873	0.852	0.929	1.104	0.714	0.850	0.811	0.941	0.624	0.724				
16	53.55	49.06	60.82	55.13	54.65	71.05	0.916	0.906	0.980	1.113	0.754	0.856	0.898	1.009	0.691	0.776				
17	19.09	18.23	36.72	33.67	24.13	31.37	0.955	0.917	0.791	1.522	0.608	1.171	0.755	1.395	0.581	1.073				
18	17.07	16.20	32.44	29.44	20.90	27.17	0.949	0.907	0.817	1.552	0.628	1.194	0.775	1.408	0.596	1.083				
19	14.47	13.59	26.96	24.07	17.07	22.18	0.940	0.893	0.848	1.580	0.652	1.215	0.796	1.411	0.613	1.085				
20	12.78	12.00	23.44	20.68	14.78	19.21	0.939	0.882	0.865	1.586	0.663	1.220	0.812	1.399	0.625	1.076				
21	12.00	12.00	20.93	18.27	13.22	17.18	1.000	0.873	0.908	1.583	0.698	1.218	0.908	1.382	0.698	1.063				
22	12.00	12.00	19.00	16.45	13.22	17.18	1.000	0.866	0.908	1.438	0.698	1.106	0.908	1.245	0.698	0.957				
23	12.00	12.00	18.20	15.69	13.22	17.18	1.000	0.862	0.908	1.377	0.698	1.059	0.908	1.187	0.698	0.913				
24	12.00	12.00	17.47	15.01	13.22	17.18	1.000	0.859	0.908	1.321	0.698	1.016	0.908	1.135	0.698	0.873				
25	12.00	12.00	16.80	14.39	13.22	17.18	1.000	0.856	0.908	1.271	0.698	0.978	0.908	1.089	0.698	0.837				
26	12.00	12.00	16.20	13.83	13.22	17.18	1.000	0.854	0.908	1.226	0.698	0.943	0.908	1.046	0.698	0.805				
27	31.72	30.07	49.49	45.58	43.03	55.94	0.948	0.921	0.737	1.150	0.567	0.885	0.699	1.059	0.537	0.815				
28	28.30	26.63	43.77	39.91	37.27	48.45	0.941	0.912	0.759	1.175	0.584	0.904	0.715	1.071	0.550	0.824				
29	23.90	22.24	36.45	32.72	30.43	39.56	0.931	0.898	0.785	1.198	0.604	0.922	0.731	1.076	0.562	0.827				
30	21.05	19.41	31.76	28.17	26.35	34.26	0.922	0.887	0.799	1.205	0.614	0.927	0.737	1.069	0.567	0.822				
31	18.99	17.38	28.39	24.93	23.57	30.64	0.915	0.878	0.806	1.204	0.620	0.927	0.737	1.058	0.567	0.814				
32	17.40	16.00	25.81	22.48	23.57	30.64	0.919	0.871	0.738	1.095	0.568	0.842	0.679	0.954	0.522	0.734				
33	16.73	16.00	24.72	21.45	23.57	30.64	0.956	0.868	0.710	1.049	0.546	0.807	0.679	0.910	0.522	0.700				
34	16.12	16.00	23.74	20.53	23.57	30.64	0.992	0.865	0.684	1.007	0.526	0.775	0.679	0.871	0.522	0.670				
35	16.00	16.00	22.85	19.70	23.57	30.64	1.000	0.862	0.679	0.970	0.522	0.746	0.679	0.836	0.522	0.643				
36	16.00	16.00	22.04	18.94	23.57	30.64	1.000	0.859	0.679	0.935	0.522	0.719	0.679	0.803	0.522	0.618				
37	51.85	48.53	63.26	58.42	57.19	74.35	0.936	0.923	0.906	1.106	0.697	0.851	0.848	1.021	0.653	0.786				
38	46.06	42.75	56.00	51.21	49.53	64.39	0.928	0.914	0.930	1.131	0.715	0.870	0.863	1.034	0.664	0.795				
39	38.61	35.37	46.70	42.06	40.44	52.58	0.916	0.901	0.955	1.155	0.734	0.888	0.874	1.040	0.673	0.800				
40	33.82	30.65	40.72	36.25	35.02	45.53	0.906	0.890	0.966	1.163	0.743	0.894	0.875	1.035	0.673	0.796				
41	30.36	27.28	36.43	32.12	31.33	40.72	0.898	0.882	0.969	1.163	0.746	0.895	0.871	1.025	0.670	0.789				
42	27.71	24.71	33.15	28.98	31.33	40.72	0.892	0.874	0.884	1.058	0.680	0.814	0.789	0.925	0.607	0.712				
43	26.59	23.63	31.76	27.67	31.33	40.72	0.889	0.871	0.849	1.014	0.653	0.780	0.754	0.883	0.580	0.679				
44	25.58	22.66	30.52	26.49	31.33	40.72	0.886	0.868	0.816	0.974	0.628	0.749	0.723	0.846	0.556	0.650				
45	24.66	21.78	29.38	25.42	31.33	40.72	0.883	0.865	0.787	0.938	0.605	0.721	0.695	0.812	0.535	0.624				
46	23.81	20.97	28.35	31.33	40.72	0.881	0.863	0.760	0.905	0.585	0.696	0.670	0.780	0.515	0.600					
47	66.61	61.76	77.55	71.13	71.07	92.39	0.927	0.917	0.937	1.091	0.721	0.839	0.869	1.001	0.668	0.770				
48	58.95	54.15	68.51	62.19	61.55	80.01	0.918	0.908	0.958	1.113	0.737	0.856	0.880	1.010	0.677	0.777				
49	49.13	44.47	56.94	50.87	50.25	65.33	0.905	0.893	0.978	1.133	0.752	0.872	0.885	1.012	0.681	0.779				
50	42.83	38.33	49.53	43.71	43.52	56.58	0.895	0.882	0.984	1.138	0.757	0.875	0.881	1.004	0.677	0.773				
51	38.30	33.95	44.22	38.63	38.93	50.61	0.887	0.874	0.984	1.136	0.757	0.874	0.872	0.992	0.671	0.763				
52	34.82	30.62	40.16	34.79	38.93	50.61	0.879	0.866	0.89											

Table 5.21 (continued)
Data, development and splice lengths for hypothetical beams
with confining transverse reinforcement

Beam No.*	l_d by Eq. 5.33+		l_d by Eq. 5.34++		ACI 318-95		l_d (High R.)		Eq. 5.33		Eq. 5.34		Eq. 5.33		Eq. 5.34		Eq. 5.33		Eq. 5.34	
	Conv.***	High R.**	Conv.	High R.	l_d	l_d	l_d (Conv.)	Eq. 5.33	Eq. 5.34											
	(in.)	(in.)	(in.)	(in.)	(in.)	(in.)	(in.)	Eq. 5.33	Eq. 5.34	Conv.	Conv.	Conv.	Conv.	Conv.	Conv.	High R.	High R.	High R.	High R.	
Group 2																				
1	18.23	15.25	22.65	18.37	17.08	22.20	0.837	0.811	1.067	1.327	0.921	1.021	0.893	1.076	0.687	0.827				
2	18.23	15.25	22.65	18.37	17.08	22.20	0.837	0.811	1.067	1.327	0.821	1.021	0.893	1.076	0.687	0.827				
3	26.72	22.32	31.13	25.43	28.46	37.00	0.835	0.817	0.939	1.094	0.722	0.841	0.784	0.893	0.603	0.687				
4	36.23	30.24	40.32	33.10	36.14	46.99	0.835	0.821	1.002	1.116	0.771	0.858	0.837	0.916	0.643	0.705				
5	41.25	34.41	45.10	37.10	41.02	53.33	0.834	0.823	1.006	1.099	0.774	0.846	0.839	0.904	0.645	0.696				
6	18.23	15.25	22.65	18.37	17.08	22.20	0.837	0.811	1.067	1.327	0.821	1.021	0.893	1.076	0.687	0.827				
7	22.27	19.90	28.94	25.18	23.23	37.00	0.893	0.870	1.246	1.619	0.959	1.246	1.113	1.409	0.857	1.084				
8	24.05	22.15	31.88	28.73	20.40	26.52	0.921	0.901	1.179	1.563	0.907	1.202	1.086	1.408	0.835	1.083				
9	25.05	23.48	33.59	30.92	21.96	28.54	0.937	0.920	1.141	1.530	0.878	1.177	1.069	1.408	0.823	1.083				
10	26.72	22.32	31.13	25.43	28.46	37.00	0.835	0.817	0.939	1.094	0.722	0.841	0.784	0.893	0.603	0.687				
11	32.71	29.19	39.33	34.45	32.84	42.69	0.892	0.876	0.996	1.198	0.766	0.921	0.889	1.049	0.684	0.807				
12	35.35	32.53	43.11	39.07	36.59	47.57	0.920	0.906	0.966	1.178	0.743	0.906	0.889	1.068	0.684	0.821				
13	36.23	30.24	40.32	33.10	36.14	46.99	0.835	0.821	1.002	1.116	0.771	0.858	0.837	0.916	0.643	0.705				
14	44.42	39.60	50.57	44.49	44.62	58.01	0.892	0.880	0.995	1.133	0.766	0.872	0.888	0.997	0.683	0.767				
15	41.25	34.41	45.10	37.10	41.02	53.33	0.834	0.823	1.006	1.099	0.774	0.846	0.839	0.904	0.645	0.696				
16	50.60	45.10	56.40	49.70	50.85	66.11	0.891	0.881	0.995	1.109	0.765	0.853	0.887	0.977	0.682	0.752				
17	21.22	18.01	26.54	21.85	19.72	25.63	0.849	0.823	1.076	1.346	0.828	1.035	0.914	1.108	0.703	0.852				
18	18.23	15.25	22.65	18.37	17.08	22.20	0.837	0.811	1.067	1.327	0.821	1.021	0.893	1.076	0.687	0.827				
19	14.51	12.00	17.88	14.19	13.94	18.13	0.827	0.793	1.041	1.283	0.801	0.987	0.861	1.018	0.662	0.783				
20	12.21	12.00	14.97	12.00	12.07	15.70	0.983	0.802	1.011	1.240	0.778	0.954	0.994	1.094	0.764	0.764				
21	12.00	12.00	12.96	12.00	12.00	15.60	1.000	0.926	1.000	1.080	0.769	0.831	1.000	1.000	0.769	0.769				
22	12.00	12.00	12.00	12.00	12.00	15.60	1.000	1.000	1.000	1.000	0.769	0.769	1.000	1.000	0.769	0.769				
23	12.00	12.00	12.00	12.00	12.00	15.60	1.000	1.000	1.000	1.000	0.769	0.769	1.000	1.000	0.769	0.769				
24	12.00	12.00	12.00	12.00	12.00	15.60	1.000	1.000	1.000	1.000	0.769	0.769	1.000	1.000	0.769	0.769				
25	12.00	12.00	12.00	12.00	12.00	15.60	1.000	1.000	1.000	1.000	0.769	0.769	1.000	1.000	0.769	0.769				
26	12.00	12.00	12.00	12.00	12.00	15.60	1.000	1.000	1.000	1.000	0.769	0.769	1.000	1.000	0.769	0.769				
27	31.07	26.35	36.38	30.17	32.86	42.72	0.848	0.829	0.946	1.107	0.727	0.851	0.802	0.918	0.617	0.706				
28	26.72	22.32	31.13	25.43	28.46	37.00	0.835	0.817	0.939	1.094	0.722	0.841	0.784	0.893	0.603	0.687				
29	21.31	17.43	24.66	19.71	23.24	30.21	0.818	0.799	0.917	1.061	0.706	0.816	0.750	0.848	0.577	0.653				
30	17.97	16.00	20.69	16.29	20.12	26.16	0.891	0.787	0.893	1.028	0.687	0.791	0.795	0.809	0.612	0.623				
31	16.00	16.00	17.95	16.00	18.00	23.40	1.000	0.891	0.889	0.997	0.684	0.767	0.889	0.889	0.684	0.684				
32	16.00	16.00	16.00	16.00	18.00	23.40	1.000	0.890	0.889	0.998	0.684	0.768	0.889	0.889	0.684	0.684				
33	16.00	16.00	16.00	16.00	18.00	23.40	1.000	0.890	0.889	0.998	0.684	0.768	0.889	0.889	0.684	0.684				
34	16.00	16.00	16.00	16.00	18.00	23.40	1.000	0.890	0.889	0.998	0.684	0.768	0.889	0.889	0.684	0.684				
35	16.00	16.00	16.00	16.00	18.00	23.40	1.000	0.890	0.889	0.998	0.684	0.768	0.889	0.889	0.684	0.684				
36	16.00	16.00	16.00	16.00	18.00	23.40	1.000	0.890	0.889	0.998	0.684	0.768	0.889	0.889	0.684	0.684				
37	42.10	35.66	47.04	39.21	41.74	54.26	0.847	0.834	1.009	1.127	0.776	0.867	0.854	0.940	0.657	0.723				
38	36.23	30.24	40.32	33.10	36.14	46.99	0.835	0.821	1.002	1.116	0.771	0.858	0.837	0.916	0.643	0.705				
39	28.94	23.63	32.02	25.72	29.51	38.37	0.817	0.803	0.980	1.085	0.754	0.835	0.801	0.872	0.616	0.671				
40	24.42	20.32	26.91	21.29	25.56	33.23	0.832	0.791	0.955	1.053	0.735	0.810	0.795	0.833	0.612	0.641				
41	21.27	20.32	23.38	20.32	22.86	29.72	0.955	0.869	0.930	1.023	0.716	0.787	0.889	0.889	0.684	0.684				
42	20.32	20.32	20.75	20.32	22.86	29.72	1.000	0.979	0.889	0.908	0.684	0.698	0.889	0.889	0.684	0.684				
43	20.32	20.32	20.32	20.32	22.86	29.72	1.000	1.000	0.889	0.889	0.684	0.684	0.889	0.889	0.684	0.684				
44	20.32	20.32	20.32	20.32	22.86	29.72	1.000	1.000	0.889	0.889	0.684	0.684	0.889	0.889	0.684	0.684				
45	20.32	20.32	20.32	20.32	22.86	29.72	1.000	1.000	0.889	0.889	0.684	0.684	0.889	0.889	0.684	0.684				
46	20.32	20.32	20.32	20.32	22.86	29.72	1.000	1.000	0.889	0.889	0.684	0.684	0.889	0.889	0.684	0.684				
47	47.92	40.57	52.58	43.91	47.37	61.58	0.847	0.835	1.012	1.110	0.778	0.854	0.857	0.927	0.659	0.713				
48	41.25	34.41	45.10	37.10	41.02	53.33	0.834	0.823	1.006	1.099	0.774	0.846	0.839	0.904	0.645	0.696				
49	32.96	26.91	35.84	28.85	33.49	43.54	0.816	0.805	0.984	1.070	0.757	0.823	0.803	0.861	0.618	0.663				
50	27.82	22.56	30.15	23.90	29.01	37.71	0.811	0.793	0.959	1.039	0.738	0.799	0.778	0.824	0.598	0.634				
51	24.25	22.56	26.20	22.56	25.94	33.73	0.930	0.861	0.935	1.010	0.719	0.777	0.870	0.870	0.669	0.669				
52	22.56	22.56	23.26	22.56	25.94	33.73	1.000	0												

Table 5.21 (continued)
Data, development and splice lengths for hypothetical beams
with confining transverse reinforcement

Beam No.*	l_d by Eq. 5.33+		l_d by Eq. 5.34++		ACI 318-95		l_d (High R.)	l_d (Conv.)	Eq. 5.33		Eq. 5.34		Eq. 5.33		Eq. 5.34		Eq. 5.33		Eq. 5.34		
	Conv.***	High R.**	Conv.	High R.	l_d	l_d			Eq. 5.33	Eq. 5.34	ACI l_d										
Group 3																					
1	21.50	18.26	29.59	24.08	17.08	22.20	0.849	0.814	1.259	1.733	0.969	1.333	1.069	1.410	0.823	1.085					
2	21.50	18.26	29.59	24.08	17.08	22.20	0.849	0.814	1.259	1.733	0.969	1.333	1.069	1.410	0.823	1.085					
3	33.12	27.80	44.38	35.80	35.58	46.25	0.839	0.807	0.931	1.248	0.716	0.960	0.781	1.006	0.601	0.774					
4	45.76	38.29	57.57	46.67	50.55	65.72	0.837	0.811	0.905	1.139	0.696	0.876	0.757	0.923	0.583	0.710					
5	52.52	43.89	64.42	52.33	58.70	76.30	0.836	0.812	0.895	1.097	0.688	0.844	0.748	0.892	0.575	0.686					
6	21.50	18.26	29.59	24.08	17.08	22.20	0.849	0.814	1.259	1.733	0.969	1.333	1.069	1.410	0.823	1.085					
7	25.76	23.28	37.57	32.81	23.29	30.27	0.904	0.873	1.106	1.614	0.851	1.241	1.000	1.409	0.769	1.084					
8	27.58	25.63	41.29	37.32	26.50	34.45	0.929	0.904	1.041	1.558	0.801	1.199	0.967	1.408	0.744	1.083					
9	28.58	26.99	43.44	40.07	28.46	37.00	0.944	0.923	1.004	1.526	0.773	1.174	0.948	1.408	0.730	1.083					
10	33.12	27.80	44.38	35.80	35.58	46.25	0.839	0.807	0.931	1.248	0.716	0.960	0.781	1.006	0.601	0.774					
11	40.27	36.08	57.11	49.48	47.43	61.66	0.896	0.866	0.849	1.204	0.653	0.926	0.761	1.043	0.585	0.802					
12	43.40	40.05	63.14	56.70	53.36	69.37	0.923	0.898	0.813	1.183	0.626	0.910	0.751	1.062	0.577	0.817					
13	45.76	38.29	57.57	46.67	50.55	65.72	0.837	0.811	0.905	1.139	0.696	0.876	0.757	0.923	0.583	0.710					
14	55.89	49.95	73.51	63.98	64.84	84.29	0.894	0.870	0.862	1.134	0.663	0.872	0.770	0.987	0.593	0.739					
15	52.52	43.89	64.42	52.33	58.70	76.30	0.836	0.812	0.895	1.097	0.688	0.844	0.748	0.892	0.575	0.686					
16	64.27	57.37	82.03	71.51	74.06	96.28	0.893	0.872	0.868	1.108	0.668	0.852	0.775	0.966	0.596	0.743					
17	24.98	21.52	34.62	28.61	19.72	25.63	0.861	0.826	1.267	1.756	0.975	1.350	1.091	1.451	0.840	1.116					
18	21.50	18.26	29.59	24.08	17.08	22.20	0.849	0.814	1.259	1.733	0.969	1.333	1.069	1.410	0.823	1.085					
19	17.16	14.27	23.40	18.63	13.94	18.13	0.832	0.796	1.231	1.678	0.947	1.291	1.023	1.336	0.787	1.028					
20	14.46	12.00	19.61	15.38	12.07	15.70	0.830	0.784	1.197	1.624	0.921	1.349	0.994	1.274	0.764	0.980					
21	12.57	12.00	16.99	13.17	12.00	15.60	0.955	0.775	1.048	1.416	0.806	1.089	1.000	1.098	0.769	0.844					
22	12.00	12.00	15.05	12.00	12.00	15.60	1.000	0.797	1.000	1.255	0.769	0.965	1.000	1.000	0.769	0.769					
23	12.00	12.00	14.26	12.00	12.00	15.60	1.000	0.842	1.000	1.188	0.769	0.914	1.000	1.000	0.769	0.769					
24	12.00	12.00	13.55	12.00	12.00	15.60	1.000	0.886	1.000	1.129	0.769	0.868	1.000	1.000	0.769	0.769					
25	12.00	12.00	12.91	12.00	12.00	15.60	1.000	0.930	1.000	1.076	0.769	0.828	1.000	1.000	0.769	0.769					
26	12.00	12.00	12.33	12.00	12.00	15.60	1.000	0.973	1.000	1.028	0.769	0.791	1.000	1.000	0.769	0.769					
27	38.61	32.89	52.08	42.66	41.08	53.40	0.852	0.819	0.940	1.268	0.723	0.975	0.801	1.038	0.616	0.799					
28	33.12	27.80	44.38	35.80	35.58	46.25	0.839	0.807	0.931	1.248	0.716	0.960	0.781	1.006	0.601	0.774					
29	26.29	21.60	34.95	27.59	29.05	37.76	0.822	0.789	0.905	1.203	0.696	0.926	0.744	0.950	0.572	0.731					
30	22.07	17.86	29.21	22.71	25.16	32.70	0.809	0.777	0.877	1.161	0.673	0.893	0.710	0.903	0.546	0.694					
31	19.13	16.00	25.25	19.41	22.50	29.25	0.837	0.769	0.850	1.122	0.654	0.863	0.711	0.863	0.547	0.664					
32	16.93	16.00	22.33	17.00	22.50	29.25	0.945	0.762	0.753	0.992	0.579	0.763	0.711	0.756	0.547	0.581					
33	16.03	16.00	21.13	16.03	22.50	29.25	0.998	0.759	0.712	0.939	0.548	0.722	0.711	0.712	0.547	0.548					
34	16.00	16.00	20.06	16.00	22.50	29.25	1.000	0.798	0.711	0.892	0.547	0.686	0.711	0.711	0.547	0.547					
35	16.00	16.00	19.10	16.00	22.50	29.25	1.000	0.838	0.711	0.849	0.547	0.653	0.711	0.711	0.547	0.547					
36	16.00	16.00	18.24	16.00	22.50	29.25	1.000	0.877	0.711	0.877	0.547	0.624	0.711	0.711	0.547	0.547					
37	53.32	45.28	67.43	55.52	58.38	75.89	0.849	0.823	0.913	1.155	0.703	0.889	0.776	0.951	0.597	0.732					
38	45.76	38.29	57.57	46.67	50.55	65.72	0.837	0.811	0.905	1.139	0.696	0.876	0.757	0.923	0.583	0.710					
39	36.37	29.79	45.44	36.05	41.28	53.66	0.819	0.793	0.881	1.101	0.678	0.847	0.722	0.873	0.555	0.672					
40	30.57	24.66	38.04	29.72	35.75	46.47	0.807	0.781	0.855	1.064	0.658	0.819	0.690	0.831	0.531	0.640					
41	26.53	21.14	32.93	25.43	31.97	41.57	0.797	0.772	0.830	1.030	0.638	0.792	0.661	0.795	0.509	0.612					
42	23.51	20.32	29.15	22.31	31.97	41.57	0.864	0.765	0.735	0.912	0.566	0.701	0.636	0.698	0.489	0.537					
43	22.27	20.32	27.60	21.03	31.97	41.57	0.912	0.762	0.697	0.863	0.536	0.664	0.636	0.658	0.489	0.506					
44	21.16	20.32	26.21	20.32	31.97	41.57	0.960	0.775	0.662	0.820	0.509	0.631	0.636	0.636	0.489	0.489					
45	20.32	20.32	24.97	20.32	31.97	41.57	1.000	0.814	0.636	0.746	0.489	0.601	0.636	0.636	0.489	0.489					
46	20.32	20.32	23.85	20.32	31.97	41.57	1.000	0.852	0.636	0.746	0.489	0.574	0.636	0.636	0.489	0.489					
47	61.19	51.89	75.41	62.21	67.78	88.11	0.848	0.825	0.903	1.113	0.694	0.856	0.766	0.918	0.589	0.706					
48	52.52	43.89	64.42	52.33	58.70	76.30	0.836	0.812	0.895	1.097	0.688	0.844	0.748	0.892	0.575	0.686					
49	41.77	34.16	50.90	40.46	47.92	62.30	0.818	0.795	0.872	1.062	0.670	0.817	0.713	0.844	0.548	0.649					
50	35.12	28.28	42.63	33.37	41.50	53.96	0.805	0.783	0.846	1.027	0.651	0.790	0.681	0.804	0.524	0.619					
51	30.49	24.27	36.93	28.57	37.12	48.26	0.796	0.774	0.821	0.995	0.632	0.765	0.654	0.770	0.503	0.592					
52	27.04	22.56	32.70	25.07</																	

Table 5.21 (continued)
Data, development and splice lengths for hypothetical beams
with confining transverse reinforcement

Beam No.*	l_d by Eq. 5.33+		l_d by Eq. 5.34++		ACI 318-95		l_d (High R_c)		Eq. 5.33		Eq. 5.34		Eq. 5.33		Eq. 5.34		Eq. 5.33		Eq. 5.34	
	Conv.***	High R_c **	Conv.	High R_c	l_d (in.)	l_d (in.)	Eq. 5.33	Eq. 5.34	ACI l_d Conv.	Eq. 5.33	Eq. 5.34	ACI l_d Conv.	Eq. 5.33	Eq. 5.34	ACI l_d High R_c	Eq. 5.33	Eq. 5.34	ACI l_d High R_c	Eq. 5.33	Eq. 5.34
Group 4																				
1	16.17	12.76	20.76	15.72	17.08	22.20	0.789	0.757	0.947	1.216	0.728	0.935	0.747	0.920	0.575	0.708	0.575	0.708		
2	16.17	12.76	20.76	15.72	17.08	22.20	0.789	0.757	0.947	1.216	0.728	0.935	0.747	0.920	0.575	0.708	0.575	0.708		
3	24.43	19.06	30.70	23.05	28.46	37.00	0.780	0.751	0.858	1.079	0.660	0.830	0.670	0.810	0.515	0.623	0.515	0.623		
4	33.59	26.11	40.15	30.29	36.14	46.99	0.777	0.754	0.929	1.111	0.715	0.854	0.722	0.838	0.556	0.645	0.556	0.645		
5	38.46	29.86	45.06	34.06	41.48	53.93	0.776	0.756	0.927	1.086	0.713	0.836	0.720	0.821	0.554	0.632	0.554	0.632		
6	16.17	12.76	20.76	15.72	17.08	22.20	0.789	0.757	0.947	1.216	0.728	0.935	0.747	0.920	0.575	0.708	0.575	0.708		
7	21.50	18.26	29.59	24.08	17.08	22.20	0.849	0.814	1.259	1.733	0.969	1.333	1.069	1.410	0.823	1.085	0.823	1.085		
8	24.16	21.33	34.47	29.27	20.77	27.00	0.883	0.849	1.164	1.660	0.895	1.277	1.027	1.409	0.790	1.084	0.790	1.084		
9	25.76	23.28	37.57	32.81	23.29	30.27	0.904	0.873	1.106	1.614	0.851	1.241	1.000	1.409	0.769	1.084	0.769	1.084		
10	24.43	19.06	30.70	23.05	28.46	37.00	0.780	0.751	0.858	1.079	0.660	0.830	0.670	0.810	0.515	0.623	0.515	0.623		
11	33.12	27.80	44.38	35.80	35.58	46.25	0.839	0.807	0.931	1.248	1.176	0.960	0.781	1.006	0.601	0.774	0.601	0.774		
12	37.57	32.82	52.13	43.89	42.69	55.50	0.874	0.842	0.880	1.221	0.677	0.939	0.769	1.028	0.591	0.791	0.591	0.791		
13	33.59	26.11	40.15	30.29	36.14	46.99	0.777	0.754	0.929	1.111	0.715	0.854	0.722	0.838	0.556	0.645	0.556	0.645		
14	45.76	38.29	57.57	46.67	50.55	65.72	0.837	0.811	0.905	1.139	0.696	0.876	0.757	0.923	0.583	0.710	0.583	0.710		
15	38.46	29.86	45.06	34.06	41.48	53.93	0.776	0.756	0.927	1.086	0.713	0.836	0.720	0.821	0.554	0.632	0.554	0.632		
16	52.52	43.89	64.42	52.33	58.70	76.30	0.836	0.812	0.895	1.097	0.688	0.844	0.748	0.892	0.575	0.686	0.575	0.686		
17	19.23	15.41	24.89	19.12	19.72	25.63	0.801	0.768	0.975	1.263	0.750	0.971	0.782	0.970	0.601	0.746	0.601	0.746		
18	16.17	12.76	20.76	15.72	17.08	22.20	0.789	0.757	0.947	1.216	0.728	0.935	0.747	0.920	0.575	0.708	0.575	0.708		
19	12.47	12.00	15.86	12.00	13.94	18.13	0.963	0.757	0.894	1.137	0.688	0.875	0.861	0.861	0.662	0.662	0.662	0.662		
20	12.00	12.00	12.98	12.00	12.07	15.70	1.000	0.925	0.994	1.075	0.764	0.827	0.994	0.994	0.764	0.764	0.764	0.764		
21	12.00	12.00	12.00	12.00	12.00	15.60	1.000	1.000	1.000	1.000	0.769	0.769	1.000	1.000	0.769	0.769	1.000	0.769		
22	12.00	12.00	12.00	12.00	12.00	15.60	1.000	1.000	1.000	1.000	0.769	0.769	1.000	1.000	0.769	0.769	1.000	0.769		
23	12.00	12.00	12.00	12.00	12.00	15.60	1.000	1.000	1.000	1.000	0.769	0.769	1.000	1.000	0.769	0.769	1.000	0.769		
24	12.00	12.00	12.00	12.00	12.00	15.60	1.000	1.000	1.000	1.000	0.769	0.769	1.000	1.000	0.769	0.769	1.000	0.769		
25	12.00	12.00	12.00	12.00	12.00	15.60	1.000	1.000	1.000	1.000	0.769	0.769	1.000	1.000	0.769	0.769	1.000	0.769		
26	12.00	12.00	12.00	12.00	12.00	15.60	1.000	1.000	1.000	1.000	0.769	0.769	1.000	1.000	0.769	0.769	1.000	0.769		
27	29.18	23.11	36.92	28.12	32.86	42.72	0.792	0.762	0.888	1.124	0.683	0.864	0.703	0.856	0.541	0.658	0.541	0.658		
28	24.43	19.06	30.70	23.05	28.46	37.00	0.780	0.751	0.858	1.079	0.660	0.830	0.670	0.810	0.515	0.623	0.515	0.623		
29	18.74	16.00	23.36	17.22	23.24	30.21	0.854	0.737	0.806	1.005	0.620	0.773	0.689	0.741	0.530	0.570	0.530	0.570		
30	16.00	16.00	19.06	16.00	20.12	26.16	1.000	0.839	0.795	0.947	0.612	0.729	0.636	0.795	0.612	0.612	0.612	0.612		
31	16.00	16.00	16.19	16.00	18.00	23.40	1.000	0.988	0.889	0.899	0.684	0.692	0.889	0.889	0.684	0.684	0.889	0.684		
32	16.00	16.00	16.00	16.00	18.00	23.40	1.000	1.000	0.889	0.889	0.684	0.684	0.889	0.889	0.684	0.684	0.889	0.684		
33	16.00	16.00	16.00	16.00	18.00	23.40	1.000	1.000	0.889	0.889	0.684	0.684	0.889	0.889	0.684	0.684	0.889	0.684		
34	16.00	16.00	16.00	16.00	18.00	23.40	1.000	1.000	0.889	0.889	0.684	0.684	0.889	0.889	0.684	0.684	0.889	0.684		
35	16.00	16.00	16.00	16.00	18.00	23.40	1.000	1.000	0.889	0.889	0.684	0.684	0.889	0.889	0.684	0.684	0.889	0.684		
36	16.00	16.00	16.00	16.00	18.00	23.40	1.000	1.000	0.889	0.889	0.684	0.684	0.889	0.889	0.684	0.684	0.889	0.684		
37	40.09	31.64	48.20	36.89	41.74	54.26	0.789	0.765	0.961	1.155	0.739	0.888	0.758	0.884	0.583	0.680	0.583	0.680		
38	33.59	26.11	40.15	30.29	36.14	46.99	0.777	0.754	0.929	1.111	0.715	0.854	0.722	0.838	0.556	0.645	0.556	0.645		
39	25.79	20.32	30.62	22.56	29.51	38.37	0.788	0.740	0.874	1.038	0.672	0.798	0.689	0.768	0.530	0.591	0.530	0.591		
40	21.14	20.32	25.02	20.32	25.56	33.23	0.961	0.812	0.827	0.979	0.636	0.753	0.795	0.795	0.612	0.612	0.612	0.612		
41	20.32	20.32	21.27	20.32	22.86	29.72	1.000	0.955	0.889	0.931	0.684	0.716	0.889	0.889	0.684	0.684	0.889	0.684		
42	20.32	20.32	20.32	20.32	22.86	29.72	1.000	1.000	0.889	0.889	0.684	0.684	0.889	0.889	0.684	0.684	0.889	0.684		
43	20.32	20.32	20.32	20.32	22.86	29.72	1.000	1.000	0.889	0.889	0.684	0.684	0.889	0.889	0.684	0.684	0.889	0.684		
44	20.32	20.32	20.32	20.32	22.86	29.72	1.000	1.000	0.889	0.889	0.684	0.684	0.889	0.889	0.684	0.684	0.889	0.684		
45	20.32	20.32	20.32	20.32	22.86	29.72	1.000	1.000	0.889	0.889	0.684	0.684	0.889	0.889	0.684	0.684	0.889	0.684		
46	20.32	20.32	20.32	20.32	22.86	29.72	1.000	1.000	0.889	0.889	0.684	0.684	0.889	0.889	0.684	0.684	0.889	0.684		
47	45.90	36.18	54.07	41.45	47.90	62.27	0.788	0.767	0.958	1.129	0.737	0.868	0.755	0.865	0.581	0.666	0.581	0.666		
48	38.46	29.86	45.06	34.06	41.48	53.93	0.776	0.756	0.927	1.086	0.713	0.836	0.720	0.821	0.554	0.632	0.554	0.632		
49	29.54	22.56	34.40	25.50	33.87	44.03	0.764	0.741	0.872	1.016	0.671	0.781	0.666	0.753	0.512	0.579	0.512	0.579		
50	21.14	20.32	25.02	20.32	25.56	33.23	0.961	0.812	0.827	0.979	0.636	0.753	0.795	0.795	0.612	0.612	0.612	0.612		
51	20.32	20.32	21.27	20.32	22.86	29.72	1.000	0.955	0.889	0.931	0.684	0.716	0.889	0.889	0.684	0.684	0.889	0.684		
52	20.32	2																		

Table 5.21 (continued)
Data, development and splice lengths for hypothetical beams
with confining transverse reinforcement

Note: Refer to last page of the table for footnote

Table 5.21 (continued)
Data, development and splice lengths for hypothetical beams
with confining transverse reinforcement

* See Table 5.17b for the data of the beams

** High R_r bars; R_r = 0.1275

*** Conventional bars; R_r = 0.0727

$$+ \quad \text{Eq. 5.33} = \frac{l_d}{d_b} = \frac{\frac{f_y}{f'_c^{1/4}} - 2100 \left(0.1 \frac{c_{\max}}{c_{\min}} + 0.9 \right)}{68 \left(\frac{c + K_{tr}}{d_b} \right)}$$

$$++ \quad \text{Eq. 5.34} = \frac{l_d}{d_b} = \frac{\frac{f_y}{f'_c^{1/4}} - 2100}{68 \left(\frac{c + K_{tr}}{d_b} \right)}$$

1 in. = 25.4 mm

Table 5.22
Test/prediction ratios for developed and spliced bars with confining
transverse reinforcement using Eq. 5.33 and ACI 318-95 criteria

Specimen No.*	l_d (in.)	d_b (in.)	R_c	f'_c (psi)	f'_{st} (ksi)	f_s Test (ksi)	f_t (Prediction)		Test/prediction Ratio	
							Eq. 5.33+	ACI++	Test Eq. 5.33	Test ACI
Mathey and Wastein (1961)										
4-14-2	14.00	0.50	0.0960	3710	114.70	100.69	77.70	71.06	1.296	1.417
8-21-1	21.00	1.00	0.0880	4235	114.70	62.16	65.28	45.55	0.952	1.364
8-28-1	28.00	1.00	0.0880	4485	114.70	77.79	81.80	62.51	0.951	1.244
8-28-2	28.00	1.00	0.0880	3700	114.70	72.59	77.96	56.77	0.931	1.279
8-34-1	34.00	1.00	0.0880	3745	114.70	93.63	90.96	69.36	1.029	1.350
8-34-2	34.00	1.00	0.0880	3765	114.70	91.10	91.08	69.54	1.000	1.310
8-21-2	21.00	1.00	0.0880	3495	114.70	53.62	59.11	41.38	0.907	1.296
Ferguson and Breen (1965)										
8F36c	36.00	1.000	0.0731	2740	52.00	62.56	60.08	56.74	1.041	1.103
8F36d	36.00	1.000	0.0731	3580	52.00	74.74	68.84	71.80	1.086	1.041
8F36e	36.00	1.000	0.0731	4170	52.00	77.28	67.76	69.99	1.141	1.104
8F36f	36.00	1.000	0.0731	3780	52.00	77.64	69.60	73.20	1.115	1.061
8F36g	36.00	1.000	0.0731	3070	52.00	75.34	62.82	61.65	1.199	1.222
8F36h	36.00	1.000	0.0731	1910	52.00	57.88	59.69	52.44	0.970	1.104
8F36j	36.00	1.000	0.0731	1820	52.00	66.98	57.78	51.19	1.159	1.308
8F30b	30.00	1.000	0.0731	2610	52.00	58.62	53.12	47.94	1.104	1.223
11R36a	49.50	1.410	0.0674	3020	42.00	85.26	66.83	62.20	1.276	1.371
Thompson et al. (1975)										
11-30-4/2/2-6/6-S5	30.00	1.410	0.0674	3063	68.00	49.06	42.18	39.25	1.163	1.250
DeVries et al. (1991)										
8G-22B-P9	22.00	1.128	0.0727	7460	78.58	52.74	49.79	54.49	1.059	0.968
Hester et al. (1991, 1993)										
1.2	16.00	1.000	0.0780	5990	77.30	56.18	44.22	40.82	1.271	1.376
2.2	16.00	1.000	0.0710	6200	54.10	43.98	43.94	39.15	1.001	1.123
3.2	16.00	1.000	0.0700	6020	68.90	46.51	44.19	40.07	1.053	1.161
4.2	16.00	1.000	0.0700	6450	68.90	47.05	44.99	41.48	1.046	1.134
4.3	16.00	1.000	0.0700	5490	54.10	50.06	46.90	42.83	1.067	1.169
5.2	16.00	1.000	0.0710	5490	54.10	46.62	43.02	36.84	1.084	1.265
5.3	16.00	1.000	0.0710	5490	54.10	43.39	44.61	39.45	0.973	1.100
6.2	22.75	1.000	0.0710	5850	54.10	56.66	54.98	54.49	1.031	1.040
6.3	22.75	1.000	0.0710	5850	54.10	55.87	56.62	57.19	0.987	0.977
7.2	16.00	1.000	0.0710	5240	54.10	51.57	47.98	38.61	1.075	1.336
Rezanoff et al. (1991)										
20-6-2	18.15	0.768	0.0799	4277	62.08	70.77	50.86	51.54	1.392	1.373
20-6-3	15.39	0.768	0.0799	3886	62.08	75.23	47.64	41.66	1.579	1.806
20-6-1	22.09	0.768	0.0799	4045	62.08	77.86	50.88	57.69	1.530	1.350
20-8-11	16.34	0.992	0.0731	4466	62.08	75.00	50.08	36.68	1.498	2.044
20-8-9	18.70	0.992	0.0731	4205	62.08	61.10	50.32	40.74	1.214	1.500
20-8-1	18.70	0.992	0.0731	5220	62.08	71.05	55.75	45.39	1.274	1.565
20-8-12	16.34	0.992	0.0731	4350	62.08	65.38	51.20	36.20	1.277	1.806
20-8-2	21.77	0.992	0.0731	5742	62.08	65.36	57.39	55.43	1.139	1.179
20-8-3	26.10	0.992	0.0731	5510	62.08	64.59	56.82	65.10	1.137	0.992
20-8-6	26.10	0.992	0.0731	4770	62.08	75.37	53.77	60.57	1.402	1.244
20-8-7	26.10	0.992	0.0731	4495	62.08	62.30	52.57	58.80	1.185	1.060
20-8-8	21.77	0.992	0.0731	4350	62.08	60.52	51.52	48.24	1.175	1.255
20-8-5	21.77	0.992	0.0731	4770	62.08	76.01	53.14	50.52	1.430	1.504
20-8-4	18.70	0.992	0.0731	4335	62.08	71.94	51.41	41.37	1.399	1.739
20-8-13	28.70	0.992	0.0731	3509	52.21	52.17	44.60	43.03	1.170	1.213
20-8-14	23.11	0.992	0.0731	3277	52.21	54.51	41.56	39.24	1.312	1.389
20-8-15	20.31	0.992	0.0731	3625	52.21	55.74	41.97	40.04	1.328	1.392
20-8-16	28.70	0.992	0.0731	3291	52.21	56.14	43.74	41.67	1.283	1.347
20-8-18	17.44	0.992	0.0731	3349	52.21	56.07	39.70	33.91	1.412	1.653
20-8-19	21.65	0.992	0.0731	3219	52.21	45.41	40.88	37.44	1.111	1.213
20-8-17	20.31	0.992	0.0731	3480	52.21	60.90	41.37	39.23	1.472	1.552
20-8-20	17.32	0.992	0.0731	3291	52.21	45.78	39.44	33.39	1.161	1.371
20-9-1	19.69	1.177	0.0727	3538	60.05	59.66	46.94	33.16	1.271	1.799
20-9-2	25.59	1.177	0.0727	3378	60.05	66.15	46.95	42.12	1.409	1.570
20-11-2	26.57	1.406	0.0674	4335	83.40	69.92	57.11	41.50	1.224	1.685
20-11-1	37.99	1.406	0.0674	4770	83.40	53.02	47.58	42.18	1.111	1.111
20-11-3	26.61	1.406	0.0674	4466	83.40	60.05	63.30	49.10	1.289	1.257
20-11-8	34.29	1.406	0.0674	3349	60.05			47.03	1.286	1.346

Table 5.22 (continued)
Test/prediction ratios for developed and spliced bars with confining
transverse reinforcement using Eq. 5.33 and ACI 813-95 criteria

Specimen No.*	l _a (in.)	d _b (in.)	R _t	f' _c (psi)	f' _s (ksi)	f _t Test (ksi)	f _t (Prediction)		Test/prediction Ratio	
							Eq. 5.33+	ACI++	Test Eq. 5.33	Test ACI
20-11-5	27.01	1.406	0.0674	3625	60.05	65.82	49.69	38.56	1.324	1.707
20-11-6	34.72	1.406	0.0674	3625	60.05	55.80	50.42	48.88	1.107	1.142
20-11-7	27.20	1.406	0.0674	3291	60.05	52.59	48.26	37.02	1.090	1.421
Rezanoff et al. (1993)										
6	22.05	0.992	0.0731	3625	84.10	52.50	42.93	36.66	1.223	1.432
1b	29.53	0.992	0.0731	3799	63.80	69.82	47.67	35.51	1.465	1.966
1a	29.53	0.992	0.0731	3958	63.80	74.05	48.27	36.25	1.534	2.043
3a	29.53	0.992	0.0731	3958	63.80	69.76	46.44	32.23	1.502	2.164
3b	29.53	0.992	0.0731	3799	63.80	61.57	45.90	31.58	1.342	1.950
4b	44.29	1.177	0.0727	3726	63.80	68.87	48.41	34.31	1.423	2.008
9	33.46	1.177	0.0727	3886	68.87	76.40	54.39	51.85	1.405	1.473
10	22.05	1.177	0.0727	4089	68.15	70.99	54.30	39.92	1.307	1.778
4a	35.43	1.177	0.0727	4031	63.80	62.56	43.40	28.54	1.442	2.192
Azizinamini et al. (1995 at CTL)										
AB83-11-15-57.5S-50	57.50	1.410	0.0674	15120	58.98	75.96	78.29	89.45	0.970	0.849
Azizinamini et al. (1995 at UNL)										
ABS-11-15-45S-60	45.00	1.410	0.0590	14890	71.80	70.48	70.94	77.95	0.993	0.904
ABS-11-15-45S-100	45.00	1.410	0.0590	14850	71.80	76.79	76.76	85.02	1.000	0.903
ABS-11-15-40S-150	40.00	1.410	0.0590	15760	71.80	79.06	80.54	84.99	0.982	0.930
Darwin et al. (1995a, 1996a)										
13.1	12.00	0.625	0.1090	4110	64.55	56.06	49.40	51.29	1.135	1.093
13.2	12.00	0.625	0.0820	4110	64.55	56.35	48.57	51.29	1.160	1.099
14.5	12.00	0.625	0.0820	4200	64.55	60.29	51.70	51.85	1.166	1.163
14.6	12.00	0.625	0.1090	4200	64.55	63.45	54.26	51.85	1.169	1.224
1.5	16.00	1.000	0.1010	5020	70.50	52.54	54.65	37.79	0.961	1.390
1.6	16.00	1.000	0.1010	5020	70.50	52.30	48.81	37.79	1.071	1.384
2.1	24.00	1.000	0.0710	5250	69.92	62.81	61.46	57.97	1.022	1.084
2.2	24.00	1.000	0.1400	5250	69.92	77.60	73.66	57.97	1.053	1.339
2.3	24.00	1.000	0.1400	5250	69.92	74.12	67.92	57.97	1.091	1.279
3.4	24.00	1.000	0.0850	5110	69.92	56.07	62.84	57.19	0.892	0.981
3.5	28.00	1.000	0.0850	3810	69.92	53.05	52.00	56.27	1.020	0.943
4.1	24.00	1.000	0.0710	4090	70.75	63.33	63.08	51.16	1.004	1.238
4.2	24.00	1.000	0.1400	4090	69.92	73.54	68.71	51.16	1.070	1.437
4.4	24.00	1.000	0.1010	4090	69.92	59.55	51.79	51.16	1.150	1.164
5.1	24.00	1.000	0.0650	4190	69.92	65.43	55.14	51.78	1.187	1.264
5.2	24.00	1.000	0.1400	4190	96.92	66.26	65.62	51.78	1.010	1.280
5.3	24.00	1.000	0.1400	4190	69.92	68.83	65.77	51.78	1.047	1.329
5.4	24.00	1.000	0.0650	4190	69.92	59.50	55.03	51.78	1.081	1.149
5.5	24.00	1.000	0.0850	4190	69.92	46.74	52.76	51.78	0.886	0.903
5.6	22.00	1.000	0.1400	4190	70.75	67.22	66.00	47.47	1.018	1.416
6.1	24.00	1.000	0.0650	4220	66.42	64.71	56.13	51.97	1.153	1.245
6.2	24.00	1.000	0.1400	4220	66.42	77.57	70.83	51.97	1.095	1.493
6.3	16.00	1.000	0.1400	4220	64.55	46.39	41.33	33.76	1.123	1.374
6.4	16.00	1.000	0.0850	4220	64.55	36.83	39.41	33.76	0.935	1.091
7.1	16.00	1.000	0.1400	4160	64.55	47.05	44.51	34.40	1.057	1.368
7.2	18.00	1.000	1.0100	4160	84.70	56.37	56.19	38.70	1.003	1.457
7.5	24.00	1.000	0.1400	4160	84.70	75.73	70.30	51.60	1.077	1.468
7.6	16.00	1.000	0.1010	4160	64.55	44.62	43.39	34.40	1.028	1.297
8.1	24.00	1.000	0.0690	3830	84.70	72.14	54.95	49.51	1.313	1.457
8.2	24.00	1.000	0.1190	3830	84.70	85.08	63.79	49.51	1.334	1.718
8.4	16.00	1.000	0.1190	3830	64.55	49.37	42.81	33.01	1.153	1.496
9.1	24.00	1.000	0.1190	4230	64.55	64.16	55.23	52.03	1.162	1.233
9.2	18.00	1.000	0.1400	4230	64.55	70.02	56.56	39.02	1.238	1.794
9.3	24.00	1.000	0.0690	4230	64.55	55.75	52.01	52.03	1.072	1.071
9.4	24.00	1.000	0.1400	4230	64.55	65.82	55.60	52.03	1.184	1.265
10.3	26.00	1.000	0.0690	4250	64.55	59.45	54.44	56.50	1.092	1.052
10.4	20.00	1.000	0.0690	4250	84.70	62.68	61.02	43.46	1.027	1.442
11.1	18.00	1.000	0.1400	4380	84.70	68.52	58.86	39.71	1.164	1.725
11.2	18.00	1.000	0.0690	4380	84.70	62.58	55.61	39.71	1.125	1.576
11.3	18.00	1.000	0.1190	4380	84.70	63.11	57.02	39.71	1.107	1.589
11.4	24.00	1.000	0.1400	4380	64.55	63.15	56.55	52.95	1.117	1.193
14.1	36.00	1.000	0.1010	4200	64.55	61.19	52.72	38.79	1.161	1.577
14.2	21.00	1.000	0.1010	4200	84.70	64.24	57.50	45.37	1.117	1.416
15.1	27.00	1.410	0.1270	5250	84.70	69.11	62.67	46.25	1.103	1.494
15.2	27.00	1.410	0.0720	5250	84.70	64.28	62.08	46.25	1.035	1.390

Table 5.22 (continued)
Test/prediction ratios for developed and spliced bars with confining
transverse reinforcement using Eq. 5.33 and ACI 813-95 criteria

Specimen No.*	l_d (in.)	d_b (in.)	R_t	f'_c (psi)	f'_{yt} (ksi)	f'_s Test (ksi)	f'_s (Prediction)		Test/prediction Ratio	
							Eq. 5.33+	ACI++	Test Eq. 5.33	Test ACI
15.4	40.00	1.410	0.1270	5250	64.55	78.90	69.07	65.26	1.142	1.209
15.5	40.00	1.410	0.0720	5250	64.55	63.40	60.08	66.17	1.055	0.958
16.3	40.00	1.410	0.1270	5180	64.55	62.06	59.52	57.33	1.043	1.083
16.4	40.00	1.410	0.0700	5180	64.55	61.84	56.55	58.39	1.093	1.059
17.4	38.00	1.410	0.0700	4710	64.55	66.69	59.23	61.65	1.126	1.082
17.5	30.00	1.410	0.0700	4710	84.70	59.30	58.75	48.67	1.009	1.218
17.3	38.00	1.410	0.1270	4710	64.55	70.06	65.71	61.65	1.066	1.136
17.6	30.00	1.410	0.1270	4710	84.70	70.12	66.39	48.67	1.056	1.441
18.1	40.00	1.410	0.1270	4700	64.55	80.90	65.19	62.03	1.241	1.304
18.3	40.00	1.410	0.1270	4700	64.55	70.58	62.96	61.17	1.121	1.154
18.4	40.00	1.410	0.0700	4700	64.55	66.69	57.79	60.43	1.154	1.104
Current Study										
19.3	30.00	1.000	0.1190	4250	64.55	71.46	65.74	65.19	1.087	1.096
19.4	30.00	1.000	0.1190	4250	64.55	77.31	65.57	65.19	1.179	1.186
21.1	24.00	1.000	0.1190	4330	62.98	73.88	70.01	52.64	1.055	1.403
21.3	25.00	1.000	0.1190	4330	62.98	76.25	67.84	54.84	1.124	1.391
21.5	25.00	1.000	0.1190	4330	64.92	77.35	71.04	54.84	1.089	1.411
23a.1	21.00	1.000	0.1190	9080	71.25	78.87	75.45	66.70	1.045	1.182
23a.3	21.00	1.000	0.1190	9080	71.25	80.57	75.00	66.70	1.074	1.208
23a.4	21.00	1.000	0.1190	9080	71.25	79.15	75.17	66.70	1.053	1.187
23b.1	17.50	1.000	0.1190	8370	64.92	79.04	67.68	53.37	1.168	1.481
27.2	22.50	1.000	0.0690	10810	64.92	78.52	59.93	54.69	1.310	1.436
27.4	17.50	1.000	0.0690	10810	64.92	77.21	63.36	58.33	1.219	1.324
27.6	18.00	1.000	0.0690	10810	64.92	78.42	62.16	60.00	1.262	1.307
29.2	20.00	1.000	0.0690	10620	71.25	83.65	55.03	49.47	1.520	1.691
29.4	18.00	1.000	0.0690	10620	71.25	77.96	55.44	51.68	1.406	1.509
29.6	16.00	1.000	0.0690	10620	71.25	77.72	51.26	50.16	1.516	1.549
31.3	16.00	1.000	0.0690	12890	71.25	65.21	55.37	53.33	1.178	1.223
33.2	18.00	1.000	0.0850	5360	64.92	61.42	55.27	43.93	1.111	1.398
33.4	18.00	1.000	0.0850	5360	71.25	58.32	54.44	43.93	1.071	1.328
33.6	22.00	1.000	0.0850	5230	71.25	57.94	53.64	53.03	1.080	1.092
35.1	20.00	1.000	0.1400	5330	71.25	68.44	61.70	48.67	1.109	1.406
35.3	20.00	1.000	0.0850	5330	71.25	61.77	55.63	48.67	1.110	1.269
37.4	21.00	1.000	0.1400	4800	64.92	73.78	66.42	48.50	1.111	1.521
39.2	16.00	1.000	0.1010	14450	71.25	69.74	58.71	40.08	1.188	1.740
39.3	16.00	1.000	0.0690	14450	71.25	77.96	54.46	39.66	1.432	1.966
41.1	16.00	1.000	0.1190	10180	71.25	66.16	55.76	53.33	1.187	1.240
41.2	16.00	1.000	0.1190	10180	62.98	83.02	67.14	53.33	1.256	1.557
41.3	16.00	1.000	0.1190	10180	64.92	79.35	67.20	51.28	1.181	1.547
41.4	16.00	1.000	0.0690	10180	62.98	77.27	47.98	37.41	1.610	2.065
41.5	16.00	1.000	0.0850	10500	71.25	66.01	57.48	53.33	1.148	1.238
41.6	16.00	1.000	0.0850	10500	71.25	65.38	57.50	53.33	1.137	1.226
42.1	16.00	1.000	0.0690	11930	71.25	64.32	57.55	53.33	1.118	1.206
42.4	16.00	1.000	0.0690	11930	64.92	70.70	61.65	52.11	1.147	1.357
42.5	16.00	1.000	0.0690	11930	62.98	77.92	69.55	53.33	1.120	1.461
43.2	16.00	1.000	0.1190	11530	71.25	64.95	60.99	53.33	1.065	1.218
43.3	16.00	1.000	0.1190	11530	64.92	78.81	70.08	52.11	1.125	1.512
43.6	16.00	1.000	0.1190	11530	62.98	82.73	69.01	53.33	1.199	1.551
20.1	40.00	1.410	0.1270	5080	84.70	71.08	67.29	67.37	1.056	1.055
20.2	40.00	1.410	0.1270	5080	84.70	71.81	67.18	67.07	1.069	1.071
20.3	40.00	1.410	0.1270	5080	84.70	68.52	58.77	56.57	1.166	1.211
20.4	40.00	1.410	0.1270	5080	84.70	67.65	58.76	56.27	1.151	1.202
28.1	25.00	1.410	0.1270	12610	71.25	71.23	64.17	42.18	1.110	1.689
28.3	28.00	1.410	0.1270	12610	71.25	67.03	58.06	45.91	1.155	1.460
30.1	25.00	1.410	0.1270	13220	71.25	66.07	55.72	33.86	1.186	1.951
30.3	28.00	1.410	0.1270	13220	71.25	66.88	52.86	41.82	1.265	1.599
40.1	23.00	1.410	0.1270	15650	71.25	66.60	63.08	40.32	1.056	1.652
40.4	23.00	1.410	0.0720	15650	71.25	58.83	55.71	41.28	1.056	1.425
Kadoriku (1994)										
PB-01	14.96	0.748	0.0748	8932	59.29473	83.56	59.44	78.76	1.406	1.061
PB-02	22.44	0.748	0.0748	8932	59.29473	100.59	76.18	118.14	1.320	0.851
PB-04	22.44	0.748	0.0748	3243	59.29473	63.41	54.66	71.18	1.160	0.891
PB-05	29.92	0.748	0.0748	3243	59.29473	82.08	66.68	94.91	1.231	0.865
PB-06	37.40	0.748	0.0748	3243	59.29473	105.93	78.70	118.64	1.346	0.893
PB-15	22.44	0.748	0.0748	10980	59.29473	107.64	81.88	125.00	1.315	0.861

Table 5.22 (continued)
Test/prediction ratios for developed and spliced bars with confining
transverse reinforcement using Eq. 5.33 and ACI 813-95 criteria

Specimen No.*	l_d (in.)	d_b (in.)	R_r	f_c (psi)	f_{yt} (ksi)	f_s Test (ksi)	ζ (Prediction)		Test/prediction Ratio	
							Eq. 5.33+	ACI++	Test Eq. 5.33	Test ACI
PB-16	22.44	0.748	0.0748	8832	59.29473	91.65	75.89	117.48	1.208	0.780
PB-19	22.44	0.748	0.0748	4082	59.29473	86.96	58.78	79.86	1.479	1.089
PB-20	22.44	0.748	0.0748	4082	59.29473	78.02	58.78	79.86	1.327	0.977
PB-21	14.96	0.748	0.0748	4082	59.29473	59.04	45.86	53.24	1.288	1.109
PB-23	22.44	0.748	0.0748	3072	59.29473	55.91	53.75	69.28	1.040	0.807
PB-24	22.44	0.748	0.0748	3072	59.29473	60.03	53.75	69.28	1.117	0.866
PB-25	14.96	0.748	0.0748	3072	59.29473	44.05	41.93	46.19	1.051	0.954
PB-27	22.44	0.748	0.0748	8832	59.29473	93.74	75.23	117.48	1.246	0.798
PB-31	14.96	0.748	0.0748	8832	59.29473	72.86	59.21	78.32	1.230	0.930
S1-01	22.44	0.748	0.0748	9216	199.12	113.19	90.26	120.00	1.254	0.943
S1-02	22.44	0.748	0.0748	9216	199.12	113.70	90.26	120.00	1.260	0.947
S1-03	22.44	0.748	0.0748	9216	199.12	101.55	90.26	120.00	1.125	0.846
S1-04	22.44	0.748	0.0748	9216	199.12	84.43	90.26	120.00	0.935	0.704
S2-01	22.44	0.748	0.0748	6500	199.12	103.39	80.27	100.78	1.288	1.026
S2-02	22.44	0.748	0.0748	6500	199.12	103.86	80.27	100.78	1.294	1.031
S2-03	22.44	0.748	0.0748	6500	199.12	102.93	80.27	100.78	1.282	1.021
S2-04	22.44	0.748	0.0748	6500	199.12	101.52	80.27	100.78	1.265	1.007
S2-05	22.44	0.748	0.0748	6500	199.12	100.75	80.27	100.78	1.255	1.000
S3-01	22.44	0.748	0.0748	4907	199.12	92.09	73.26	87.56	1.257	1.052
S3-03	22.44	0.748	0.0748	4907	199.12	109.20	85.32	87.56	1.280	1.247
S3-05	22.44	0.748	0.0748	4907	199.12	87.07	73.26	87.56	1.189	0.994
PB-10	22.44	0.748	0.0748	8832	60.30	102.66	72.25	117.48	1.421	0.874
PB-16	22.44	0.748	0.0748	8832	60.30	91.65	72.25	117.48	1.268	0.780
PB-11	22.44	0.748	0.0748	8832	60.30	105.98	84.49	117.48	1.254	0.902
PB-13	22.44	0.748	0.0748	3072	60.30	62.39	51.63	69.28	1.208	0.900
PB-24	22.44	0.748	0.0748	3072	60.30	60.03	51.63	69.28	1.163	0.866
PB-14	22.44	0.748	0.0748	3072	60.30	70.49	57.18	69.28	1.233	1.017
For No. 6 and smaller Bars							Max.	1.579	1.806	
							Min.	0.935	0.704	
							Average	1.254	1.010	
							St.Dev.	0.125	0.207	
							COV	0.099	0.205	
% of specimens with test/prediction ratio < 1.0								2.4%	56.1%	
For No. 7 and larger bars							Max.	1.610	2.192	
							Min.	0.886	0.849	
							Average	1.153	1.357	
							St.Dev.	0.143	0.270	
							COV	0.124	0.199	
% of specimens with test/prediction ratio < 1.0								8.4%	6.6%	
For all bars							Max.	1.610	2.192	
							Min.	0.886	0.704	
							Average	1.173	1.289	
							St.Dev.	0.145	0.293	
							COV	0.124	0.227	
% of specimens with test/prediction ratio < 1.0								7.2%	16.4%	

* Specimens with $l_d/d_b \geq 16$ and $l_d \geq 12$ in.

$$+ \quad \text{Eq.5.33} = \frac{\frac{f_s}{f'_c} - 2100 \left(0.1 \frac{c_{\max}}{c_{\min}} + 0.9 \right)}{68 \left(\frac{c + K_w}{d_b} \right)}$$

++ ACI 318-95 "detailed" equation; the factor of 1.3 is not applied for spliced bars

1 in. = 25.4 mm, 1 psi = 6.895 kPa, 1 ksi = 6.895 MPa

Table 6.1
Effect of epoxy coating on splice strength for high relative rib area bars

Study	Bar Size	Specimen No. ***	Surface* Condition	Coarse** Aggregate	R _r	f _c (psi)	f _s †		C/U **
							Test (ksi)	Pred. (ksi)	
Darwin et al. (1995a, 1996a) and Current	No. 5	13.4	U	L	0.109	4110	60.26	58.23	0.905
		13.3	C	L	0.109	4110	54.13	57.77	
		14.3	U	L	0.109	4200	61.83	61.05	0.940
		14.4	C			4200	57.58	60.50	
		25.1****	U	L	0.141	4490	63.72	61.89	1.074
		25.2****	C			4490	67.58	61.12	
	No. 8	1.3	U	L	0.101	5020	45.22	42.71	0.831
		1.4	C			5020	37.15	42.24	
		4.5	U	L	0.101	4090	51.50	53.48	0.787
		4.6	C			4090	41.97	55.37	
		39.2	U	B	0.101	14450	69.74	72.15	0.826
		39.1	C			14450	57.61	72.16	
		39.6	U	B	0.101	14450	67.38	52.39	0.734
		39.5	C			14450	49.56	52.46	
		10.2	U	B	0.119	4250	61.84	58.02	0.954
		10.1	C			4250	58.36	57.41	
		20.6****	U	L	0.119	5080	57.15	58.49	0.875
		20.5****	C			5080	49.53	57.93	
		21.1****	U	L	0.119	4330	73.88	80.66	0.931
		21.2****	C			4330	68.77	80.67	
		21.3****	U	L	0.119	4330	76.25	76.13	0.884
		21.4****	C			4330	69.10	78.08	
		21.5****	U	L	0.119	4330	77.35	81.82	0.851
		21.6****	C			4330	65.08	80.87	
		23a.1****	U	L	0.119	9080	78.87	88.77	0.793
		23a.2****	C			9080	62.48	88.67	
		23b.1****	U	L	0.119	8370	79.04	82.23	0.894
		23b.2****	C			8370	70.51	82.02	
		23b.3****	U	L	0.119	8370	71.64	72.40	0.979
		23b.4****	C			8370	70.24	72.49	
		43.2	U	L	0.119	11530	64.95	73.61	0.795
		43.1	C			11530	51.96	74.08	
		43.3	U	L	0.119	11530	78.81	84.74	0.802
		43.4	C			11530	63.63	85.26	
		43.6	U	L	0.119	11530	82.73	101.02	0.902
		43.5	C			11530	74.50	100.87	
		24.1****	U	L	0.121	4300	61.91	66.50	0.899
		24.2****	C			4300	55.32	66.10	
		2.5	U	L	0.140	5250	58.97	56.54	0.820
		2.6	C			5250	49.52	57.89	
		6.5	U	L	0.140	4220	54.06	55.18	0.923
		6.6	C			4220	50.01	55.27	
		37.4	U	L	0.140	4800	73.78	76.89	0.854
		37.3	C			4800	62.92	76.81	

Table 6.1 (continued)
Effect of epoxy coating on splice strength for high relative rib area bars

Study	Bar Size	Specimen No. ^{***}	Surface* Condition	Coarse** Aggregate	R_r	f_c (psi)	f_s^+		C/U ⁺⁺
							Test (ksi)	Pred. (ksi)	
No. 11	15.5	U	L	0.127	5250	54.53	57.38	0.891	
		C	L	0.127	5250	48.46	57.21		
		U	L	0.127	5180	52.75	56.94	0.939	
		C	L	0.127	5180	49.13	56.50		
		U	L	0.127	4700	70.58	71.96	0.825	
		C	L	0.127	4700	58.17	71.93		
		U	L	0.127	4500	54.80	60.06	0.824	
		C	L	0.127	4500	45.10	59.98		
		U	L	0.127	12610	71.23	74.87	0.760	
		C	L	0.127	12610	54.17	74.94		
		U	L	0.127	12610	67.03	68.04	0.683	
		C	L	0.127	12610	45.62	67.79		
		U	L	0.127	12610	50.89	57.65	0.824	
		C	L	0.127	12610	41.76	57.41		
		U	B	0.127	13220	66.07	65.52	0.773	
		C	B	0.127	13220	51.00	65.45		
		U	B	0.127	13220	66.88	62.34	0.815	
		C	B	0.127	13220	54.09	61.89		
		U	B	0.127	13220	66.95	58.33	0.806	
		C	B	0.127	13220	54.47	58.86		
	40.1	U	B	0.127	15650	66.60	74.19	0.827	
	40.2	C	B	0.127	15650	55.16	74.27		

For $f_c < 8000$ psi:

Avg. C/U = 0.889

For $8000 \leq f_c < 10000$ psi:

Avg. C/U = 0.889

For $f_c \geq 10000$ psi:

Avg. C/U = 0.796

For All:

Avg. C/U = 0.843

* U = uncoated; C = coated

** L = limestone

B = basalt

+ Test - bar stress determined from test

Pred. - bar stress determined using Eq. 5.4 or 5.18 for the splices not confined or confined by transverse reinforcement, respectively

++ Normalized splice strength ratio of coated to uncoated bars

*** Specimens in groups from 1 to 18 were tested by Darwin et al. (1995a, 1995b).

**** Specimens previously reported by Tan et al. (1996)

1 psi = 6.895 kPa ; 1 ksi = 6.895 MPa

Table 6.2
Effect of epoxy coating on splice strength for conventional bars

Study	Bar Size (in.)	Specimen No. ⁺⁺⁺	Surface* Condition	Coarse ** Aggregate	R _t	f _c (psi)	f _s ⁺		C/U ⁺⁺
							Test (ksi)	Pred. (ksi)	
Choi et al. (1991, 1992)	No. 5	1.2	U	L	0.086	5360	63.99	50.71	0.749
		1.3	C			5360	47.93	50.71	
	No. 6	2.1	U	L	0.060	6010	45.75	44.48	0.941
		2.2	C			6010	43.06	44.48	
		2.3	U	L	0.079	6010	51.40	44.48	0.764
		2.4	C			6010	39.26	44.48	
	No. 8	3.1	U	L	0.064	5980	42.82	43.37	0.899
		3.2	C			5980	38.51	43.37	
		3.3	U	L	0.080	5980	43.02	43.37	0.859
		3.4	C			5980	36.96	43.37	
Hester et al. (1991, 1993)	No. 8	4.3	U	L	0.069	5850	37.82	42.32	0.822
		4.4	C			5850	31.09	42.32	
		4.1	U	L	0.071	5850	40.22	42.32	0.722
		4.2	C			5850	29.03	42.32	
		3.1	U	L	0.07	6020	46.86	45.44	0.652
		3.3	C			6020	30.61	45.50	
		4.1	U	L	0.07	6450	42.35	46.39	0.719
		4.4	C			6450	30.45	46.42	
		3.2	U	L	0.07	6020	46.52	52.75	0.684
		3.4	C			6020	31.81	52.72	
		4.2	U	L	0.07	6450	47.05	53.82	0.676
		4.5	C			6450	31.72	53.71	
		4.3	U	L	0.07	6450	50.06	55.95	0.611
		4.6	C			6450	30.46	55.77	
		2.1	U	L	0.071	6200	46.26	45.27	0.827
		2.3	C			6200	38.04	45.03	
		5.1	U	L	0.071	5490	39.86	44.43	0.801
		5.4	C			5490	31.87	44.33	
		6.1	U	L	0.071	5850	51.99	55.68	0.636
		6.4	C			5850	32.80	55.22	
		7.1	U	L	0.071	5240	45.39	46.03	0.854
		7.3	C			5240	38.78	46.03	
		2.2	U	L	0.071	6200	43.98	52.64	0.857
		2.4	C			6200	37.61	52.51	
		5.3	U	L	0.071	5490	43.39	52.98	0.802
		5.5	C			5490	34.79	52.98	
		6.2	U	L	0.071	5850	56.67	64.68	0.628
		6.5	C			5850	35.51	64.56	
		6.3	U	L	0.071	5850	55.87	66.51	0.692
		6.6	C			5850	38.71	66.57	
		7.2	U	L	0.071	5240	51.57	56.61	0.750
		7.4	C			5240	38.78	56.73	
		1.2	U	L	0.078	5990	56.19	52.76	0.755
		1.4	C			5990	42.40	52.76	

Table 6.2 (continued)
Effect of epoxy coating on splice strength for conventional bars

Study	Bar Size (in.)	Specimen No. ***	Surface* Condition	Coarse ** Aggregate	R _r	f _c (psi)	f _s +		C/U ++
							Test (ksi)	Pred. (ksi)	
Current	No. 8	31.3	U	B	0.069	12890	65.21	67.86	0.812
		31.4	C			12890	52.72	67.57	
		39.3	U	B	0.069	14450	77.96	67.40	0.726
		39.4	C			14450	56.64	67.40	
		40.5	U	B	0.069	15650	65.81	60.55	0.893
		40.6	C			15650	58.53	60.29	
		42.1	U	L	0.069	11930	64.32	69.94	0.745
		42.2	C			11930	47.64	69.53	
		42.4	U	L	0.069	11930	70.70	74.51	0.741
		42.3	C			11930	52.45	74.60	
		42.5	U	L	0.069	11930	77.92	85.00	0.847
		42.6	C			11930	65.90	84.90	
	No. 11	40.4	U	B	0.072	15650	58.83	65.95	0.668
		40.3	C			15650	39.25	65.89	

For $f_c < 8000$ psi: Avg. C/U = 0.759

Avg. C/U = - .

For $f'_c \geq 10000$ psi: Avg. C/U = 0.77

Avg C/I = 0.77

For $f_c \geq 10000$ psi: Avg. C/U = 0.776

For All: Avg. C/U = 0.763

* U = uncoated ; C = coated

** L = limestone
B = basalt

+ Test - bar stress determined from test
 Pred. - bar stress determined using Eq. 5.4 or 5.18 for the splices not confined or
 confined by transverse reinforcement, respectively

^{††} Normalized splice strength ratio of coated to uncoated bars

Specimens in groups 1 to 18 were tested by Darwin et al. (1995a, 1996a).

$$1 \text{ psi} = 6.895 \text{ kPa}; 1 \text{ ksi} = 6.895 \text{ MPa}$$

Table 6.3
Comparison of C/U ratio for using different types
of coarse aggregate in concrete

Bar *	Concrete **	Coarse + Aggregate	No. of ++ Tests	Average +++ C/U
Designation	Strength Level			
8N0	High	L	3	0.778
	High	B	3	0.811
8N3	Normal	L	4	0.885
	Normal	B	1	0.954
11F3	High	L	3	0.756
	High	B	4	0.805

* See Table 2.2 for the bar designation

** High = high strength, compressive strength = 11,930 - 15,650 psi
 Normal = normal strength, compressive strength = 4250 - 5080 psi

+ L = limestone
 B = basalt

++ Number of matched pair tests

+++ Average normalized splice strength ratio of coated to uncoated bars;
 the splice strength ratio is normalized with respect to Eq. 5.4 or 5.18
 for the splices not confined or confined by transverse reinforcement.

1 psi = 6.985 kPa

Table 6.4
Comparison of flexural crack density and flexural crack width at a bar stress
of 40 ksi between beams containing coated and uncoated bars
in matched pairs of specimens

Specimen No.	Surface Condition	Bar Designation	Length outside of Splice Region (ft)	Total No. of Cracks	Avg. Max. Crack Width (in.)	Crack* Density (in./ft)	Sum of** Crack Widths (in.)	Ratios of C/U***		
								Max. Crack Width	Crack Density	Sum of Crack Widths
28.1	U	11F3	3.92	11	0.0130	2.809	0.101			
28.2	C	11F3	3.92	8	0.0180	2.043	0.099	1.385	0.727	0.980
28.3	U	11F3	3.67	11	0.0115	3.000	0.076			
28.4	C	11F3	3.67	8	0.0175	2.182	0.089	1.522	0.727	1.171
28.5	U	11F3	3.50	7	0.0150	2.000	0.075			
28.6	C	11F3	5.75	5	-	0.870	-		0.435	-
30.1	U	11F3	3.92	10	0.0090	2.553	0.059			
30.2	C	11F3	3.92	7	0.0130	1.787	0.074	1.444	0.700	1.254
30.3	U	11F3	3.67	11	0.0095	3.000	0.061			
30.4	C	11F3	3.67	8	0.0150	2.182	0.076	1.579	0.727	1.246
30.5	U	11F3	3.50	6	0.0155	1.714	0.066			
30.6	C	11F3	3.50	5	0.0180	1.429	0.060	1.161	0.833	0.909
31.1	U	8N1	4.67	12	0.0090	2.571	0.075			
31.2	C	8N1	4.67	8	0.0110	1.714	0.072	1.222	0.667	0.960
31.3	U	8N0	4.67	11	0.0095	2.357	0.078			
31.4	C	8N0	4.67	8	0.0110	1.714	0.081	1.158	0.727	1.038
37.4	U	8F1	4.25	12	0.0095	2.824	0.085			
37.3	C	8F1	4.25	9	0.0110	2.118	0.053	1.158	0.750	0.624
39.2	U	8N1	4.67	13	0.0100	2.786	-			
39.1	C	8N1	4.67	11	0.0145	2.357	-	1.450	0.846	-
39.3	U	8N0	4.67	13	0.0100	2.786	-			
39.4	C	8N0	4.67	11	0.0145	2.357	-	1.450	0.846	-
39.6	U	8C1	4.67	10	0.0105	2.143	-			
39.5	C	8C1	4.67	10	0.0150	2.143	-	1.429	1.000	-
40.1	U	11F3	4.08	11	0.0120	2.694	-			
40.2	C	11F3	4.08	9	0.0155	2.204	-	1.292	0.818	-
40.4	U	11N0	4.08	10	0.0125	2.449	-			
40.3	C	11N0	4.08	7	-	1.714	-		0.700	-
40.5	U	8N0	4.58	10	0.0100	2.182	-			
40.6	C	8N0	4.58	7	0.0155	1.527	-	1.550	0.700	-
42.1	U	8N0	4.67	12	0.0100	2.571	-			
42.2	C	8N0	4.67	8	0.0155	1.714	-	1.550	0.667	-
42.4	U	8N0	4.67	13	0.0105	2.786	-			
42.3	C	8N0	4.67	10	0.0160	2.143	-	1.524	0.769	-
42.5	U	8N0	4.67	13	0.0100	2.786	-			
42.6	C	8N0	4.67	12	0.0140	2.571	-	1.400	0.923	-
43.2	U	8N3	4.67	12	0.0105	2.571	-			
43.1	C	8N3	4.67	10	0.0140	2.143	-	1.333	0.833	-
43.3	U	8N3	4.67	12	0.0100	2.571	-			
43.4	C	8N3	4.67	10	0.0140	2.143	-	1.400	0.833	-
43.6	U	8N3	4.67	13	0.0100	2.786	-			
43.5	C	8N3	4.67	11	0.0140	2.357	-	1.400	0.846	-

Table 6.4 (continued)
Comparison of flexural crack density and flexural crack width at a bar stress
of 40 ksi between beams containing coated and uncoated bars
in matched pairs of specimens

Specimen No.	Surface Condition	Bar Designation	Length outside of Splice Region (ft)	Total No. of Cracks ⁺⁺	Avg. Max. ⁺⁺⁺	Crack* Density	Sum of** Crack Widths (in.)	Ratios of C/U***			
								Max. Crack Width	Crack Density	Sum of Crack Widths	
								Max	1.579	1.000	1.254
								Min.	1.158	0.435	0.624
								Average	1.367	0.767	1.021
								Max.	1.550	0.923	1.038
								Min.	1.158	0.667	1.038
								Average	1.436	0.748	1.038
								Max.	1.579	1.000	1.254
								Min.	1.158	0.435	0.624
								Average	1.390	0.766	1.023

+ U = Uncoated, C = Coated

++ Total number of flexural cracks in the constant moment region outside of the splice region

+++ Average maximum flexural crack width on the west and east sides of splices in the constant moment region

* Number of flexural cracks in unit foot length

** Sum of flexural crack widths cross the centerline of the beam on the east and west sides of splices in the constant moment region outside of the splice region

*** Ratios for crack density or maximum crack width or sum of crack widths of beams with coated bars to beams with uncoated bars

1 in. = 25.4 mm 1 ft = 305 mm, 1 ksi = 6.895 MPa

Table 7.1
Properties of reinforcing bars

Bar * Designation	Yield Strength (ksi)	Nominal Diameter (in.)	Weight (lb/ft)	% Light or Heavy	Rib Spacing (in.)	Rib Width**		Rib Width + Rib Spacing		Rib Height		Relative Rib Area
						I (in.)	II (in.)	I	II	ASTM (in.)	Avg.++ (in.)	
8C0A	69.50	1.000	2.615	2.1%L	0.598	0.146	0.173	0.243	0.288	0.066	0.063	0.085
8N3	80.57	1.000	2.730	2.2%H	0.487	0.148	0.177	0.303	0.362	0.072	0.068	0.119

* Bar Designation

#AAB, # = bar size (No. 5, No.8, or No.11), AA = bar manufacturer and deformation pattern:

C0 Conventional Chaparral Steel bar

N3 New North Star Steel bar

B = different letter that is presented if the bar had the same deformation pattern as reported by Darwin et al. (1995a), but were produced from different steel heat.

1 in. = 25.4 mm; 1 ksi = 6.89 MPa, 1 lb/ft = 1.49 kg/m

** Average rib width at: I - 3/4 height of ribs

II - 1/2 height of ribs

+ Ratio of rib width to rib spacing corresponding to rib width I and II

++ Average rib height between longitudinal ribs

Table 7.2
Concrete mix proportions (lb/yd³) and properties

w/c Ratio	Cement (lb/yd ³)	water (lb/yd ³)	Fine Aggregate.* (lb/yd ³)	Coarse Aggregate ** (lb/yd ³)	Slump (in.)	Concrete Temperature (F°)	Air Content (%)	Test Age (days)	Cylinder Strength (psi)
0.44	511	225	1564	1661	3.25	61	3.6	20-21	5170

* Kansas River Sand from Lawrence Sand Co., Lawrence, KS

** L - Crushed Limestone from Fogel's Quarry, Ottawa, KS

Bulk Specific Gravity (SSD) = 2.58; Absorption = 2.7%; Maximum Size = 3/4 in.

Unit Weight = 90.5 lb/ft³

1 lb/yd³ = 0.5993 kg/m³; 1 oz = 29.57 cm³; 1 psi = 6.89 kPa; 1 in. = 25.4 mm

Table 7.3 Maximum slips under reversed cyclic loading at peak load

Specimen Label +	Cycle No.	Peak Load (kips)	Loading from Left		Loading from Right	
			Loaded End Slip (in.)	Unloaded End Slip (in.)	Loaded End Slip (in.)	Unloaded End Slip (in.)
8C0A-3	1	10	0.00182	0.00010	0.00210	0.00031
	2	10	0.00182	0.00011	0.00227	0.00031
	3	10	0.00180	0.00012	0.00228	0.00041
	4	10	0.00179	0.00014	0.00227	0.00044
	5	10	0.00181	0.00016	0.00233	0.00049
	6	15	0.00299	0.00050	0.00359	0.00098
	7	15	0.00312	0.00064	0.00362	0.00109
	8	15	0.00323	0.00075	0.00367	0.00121
	9	15	0.00331	0.00083	0.00379	0.00130
	10	15	0.00336	0.00089	0.00385	0.00137
	11	20	0.00536	0.00167	0.00600	0.00239
	12	20	0.00598	0.00216	0.00699	0.00311
	13	20	0.00651	0.00261	0.00771	0.00363
	14	20	0.00693	0.00291	0.00808	0.00407
	15	20	0.00715	0.00323	0.00841	0.00432
8N3-4	1	10	0.00075	0.00006	0.00189	0.00017
	2	10	0.00080	0.00009	0.00194	0.00022
	3	10	0.00091	0.00019	0.00188	0.00017
	4	10	0.00099	0.00017	0.00190	0.00011
	5	10	0.00103	0.00015	0.00187	0.00007
	6	15	0.00179	0.00026	0.00318	0.00052
	7	15	0.00192	0.00044	0.00323	0.00060
	8	15	0.00200	0.00050	0.00328	0.00068
	9	15	0.00203	0.00055	0.00329	0.00072
	10	15	0.00204	0.00059	0.00331	0.00075
	11	20	0.00340	0.00126	0.00488	0.00131
	12	20	0.00378	0.00156	0.00518	0.00153
	13	20	0.00394	0.00176	0.00539	0.00173
	14	20	0.00428	0.00208	0.00579	0.00203
	15	20	0.00443	0.00225	0.00600	0.00224

Table 7.3 Maximum slips under reversed cyclic loading at peak load (continued)

Specimen Label +	Cycle No.	Peak Load (kips)	Loading from Left		Loading from Right	
			Loaded End Slip (in.)	Unloaded End Slip (in.)	Loaded End Slip (in.)	Unloaded End Slip (in.)
8C0A-5	1	10	0.00110	0.00100	0.00113	0.00028
	2	10	0.00119	0.00107	0.00112	0.00028
	3	10	0.00126	0.00113	0.00109	0.00031
	4	10	0.00126	0.00119	0.00110	0.00034
	5	10	0.00131	0.00124	0.00106	0.00035
	6	15	0.00245	0.00173	0.00232	0.00079
	7	15	0.00266	0.00195	0.00243	0.00089
	8	15	0.00281	0.00209	0.00252	0.00098
	9	15	0.00283	0.00220	0.00258	0.00105
	10	15	0.00295	0.00227	0.00267	0.00107
	11	20	0.00458	0.00299	0.00435	0.00177
	12	20	0.00490	0.00325	0.00466	0.00204
	13	20	0.00511	0.00344	0.00487	0.00224
	14	20	0.00532	0.00359	0.00507	0.00239
	15	20	0.00555	0.00371	0.00516	0.00255
8N3-6	1	10	0.00027	0.00009	0.00116	0.00015
	2	10	0.00031	0.00009	0.00128	0.00014
	3	10	0.00035	0.00010	0.00125	0.00015
	4	10	0.00035	0.00009	0.00129	0.00015
	5	10	0.00040	0.00009	0.00136	0.00014
	6	15	0.00097	0.00017	0.00233	0.00027
	7	15	0.00107	0.00016	0.00242	0.00031
	8	15	0.00110	0.00019	0.00253	0.00037
	9	15	0.00114	0.00024	0.00248	0.00039
	10	15	0.00117	0.00025	0.00245	0.00046
	11	20	0.00257	0.00083	0.00361	0.00084
	12	20	0.00302	0.00112	0.00385	0.00099
	13	20	0.00327	0.00132	0.00399	0.00109
	14	20	0.00348	0.00146	0.00412	0.00117
	15	20	0.00377	0.00161	0.00423	0.00123

Table 7.3 Maximum slips under reversed cyclic loading at peak load (continued)

Specimen Label +	Cycle No.	Peak Load (kips)	Loading from Left		Loading from Right	
			Loaded End Slip (in.)	Unloaded End Slip (in.)	Loaded End Slip (in.)	Unloaded End Slip (in.)
8C0A-7	1	10	0.00081	0.00020	0.00219	0.00035
	2	10	0.00082	0.00031	0.00238	0.00039
	3	10	0.00082	0.00035	0.00243	0.00043
	4	10	0.00082	0.00035	0.00249	0.00047
	5	10	0.00082	0.00036	0.00255	0.00049
	6	15	0.00172	0.00048	0.00356	0.00075
	7	15	0.00192	0.00060	0.00374	0.00085
	8	15	0.00201	0.00065	0.00390	0.00090
	9	15	0.00215	0.00071	0.00398	0.00097
	10	15	0.00217	0.00073	0.00401	0.00102
	11	20	0.00397	0.00149	0.00569	0.00161
	12	20	0.00459	0.00186	0.00605	0.00184
	13	20	0.00494	0.00215	0.00633	0.00196
	14	20	0.00520	0.00236	0.00658	0.00210
	15	20	0.00541	0.00254	0.00690	0.00232
8N3-8	1	10	0.00110	0.00009	0.00148	0.00020
	2	10	0.00115	0.00005	0.00164	0.00018
	3	10	0.00117	0.00003	0.00171	0.00020
	4	10	0.00112	0.00003	0.00175	0.00021
	5	10	0.00114	0.00003	0.00176	0.00020
	6	15	0.00173	0.00020	0.00273	0.00039
	7	15	0.00184	0.00020	0.00289	0.00042
	8	15	0.00196	0.00022	0.00298	0.00053
	9	15	0.00195	0.00023	0.00303	0.00053
	10	15	0.00200	0.00024	0.00310	0.00056
	11	20	0.00335	0.00086	0.00468	0.00094
	12	20	0.00365	0.00106	0.00496	0.00110
	13	20	0.00387	0.00123	0.00526	0.00124
	14	20	0.00423	0.00145	0.00555	0.00136
	15	20	0.00446	0.00162	0.00582	0.00146

Table 7.3 Maximum slips under reversed cyclic loading at peak load (continued)

Specimen Label +	Cycle No.	Peak Load (kips)	Loading from Left		Loading from Right	
			Loaded End Slip (in.)	Unloaded End Slip (in.)	Loaded End Slip (in.)	Unloaded End Slip (in.)
8C0A-9	1	10	0.00169	0.00013	0.00167	0.00017
	2	10	0.00179	0.00013	0.00176	0.00013
	3	10	0.00192	0.00013	0.00185	0.00013
	4	10	0.00199	0.00018	0.00189	0.00013
	5	10	0.00200	0.00022	0.00193	0.00012
	6	15	0.00344	0.00095	0.00298	0.00044
	7	15	0.00374	0.00109	0.00309	0.00041
	8	15	0.00385	0.00110	0.00343	0.00054
	9	15	0.00397	0.00111	0.00362	0.00058
	10	15	0.00410	0.00112	0.00343	0.00062
	11	20	0.00564	0.00189	0.00493	0.00111
	12	20	0.00603	0.00214	0.00525	0.00130
	13	20	0.00632	0.00235	0.00551	0.00141
	14	20	0.00652	0.00251	0.00551	0.00149
	15	20	0.00672	0.00262	0.00574	0.00162
8N3-10	1	10	0.00068	0.00021	0.00042	0.00025
	2	10	0.00077	0.00019	0.00060	0.00021
	3	10	0.00088	0.00022	0.00078	0.00023
	4	10	0.00090	0.00024	0.00086	0.00024
	5	10	0.00095	0.00026	0.00095	0.00030
	6	15	0.00241	0.00108	0.00153	0.00073
	7	15	0.00241	0.00113	0.00177	0.00082
	8	15	0.00251	0.00118	0.00194	0.00090
	9	15	0.00262	0.00133	0.00201	0.00097
	10	15	0.00277	0.00136	0.00211	0.00105
	11	20	0.00405	0.00209	0.00338	0.00174
	12	20	0.00448	0.00242	0.00395	0.00207
	13	20	0.00485	0.00271	0.00456	0.00243
	14	20	0.00524	0.00303	0.00499	0.00273
	15	20	0.00559	0.00327	0.00528	0.00285

Table 7.3 Maximum slips under reversed cyclic loading at peak load (continued)

Specimen Label +	Cycle No.	Peak Load (kips)	Loading from Left		Loading from Right	
			Loaded End Slip (in.)	Unloaded End Slip (in.)	Loaded End Slip (in.)	Unloaded End Slip (in.)
8C0A-11	1	10	0.00099	0.00083	0.00274	0.00154
	2	10	0.00107	0.00087	0.00280	0.00156
	3	10	0.00112	0.00089	0.00284	0.00161
	4	10	0.00117	0.00095	0.00293	0.00165
	5	10	0.00130	0.00098	0.00297	0.00164
	6	15	0.00274	0.00169	0.00451	0.00233
	7	15	0.00298	0.00191	0.00484	0.00262
	8	15	0.00309	0.00203	0.00536	0.00294
	9	15	0.00320	0.00211	0.00536	0.00301
	10	15	0.00330	0.00216	0.00554	0.00308
	11	20	0.00517	0.00311	0.00833	0.00469
	12	20	0.00603	0.00376	0.00962	0.00585
	13	20	0.00676	0.00434	0.01040	0.00659
	14	20	0.00729	0.00482	0.01103	0.00707
	15	20	0.00766	0.00510	0.01154	0.00750

+ Specimen Label: #AAB-P
#AAB = bar designation (see Table 7.1)
P = Test order (1 to 12)

1 in. = 25.4 mm; 1 kips = 4.448 kN

Table 7.4
Comparisons of average maximum slips under reversed cyclic loading
at peak load for high R_r and conventional bars: (a) loaded end slips,
(b) unloaded end slips

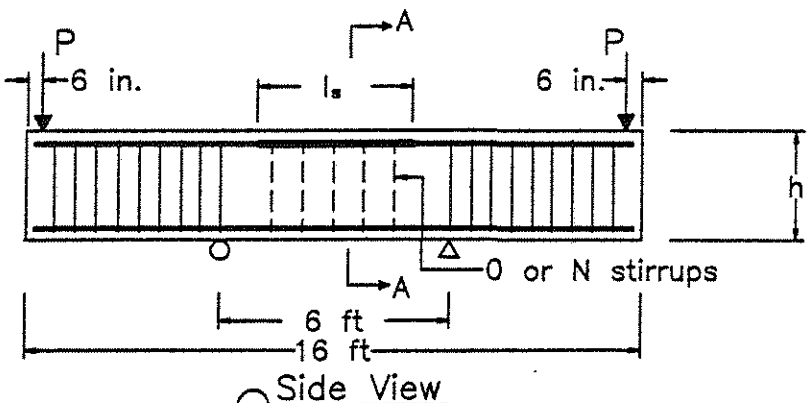
Cycle	Peak Load (kips)	Left Loaded End Slip+		Ratio of ++ High R_r /Conv.	Right Loaded End Slip+		Ratio of ++ High R_r /Conv.
		High R_r (in.)	Conv. (in.)		High R_r (in.)	Conv. (in.)	
1	10	0.00070	0.00128	0.547	0.00124	0.00197	0.630
2	10	0.00076	0.00134	0.567	0.00137	0.00207	0.661
3	10	0.00083	0.00138	0.597	0.00140	0.00210	0.669
4	10	0.00084	0.00141	0.598	0.00145	0.00214	0.679
5	10	0.00088	0.00145	0.609	0.00148	0.00217	0.685
6	15	0.00173	0.00267	0.648	0.00244	0.00339	0.719
7	15	0.00181	0.00289	0.628	0.00258	0.00354	0.728
8	15	0.00190	0.00300	0.633	0.00268	0.00378	0.710
9	15	0.00193	0.00309	0.626	0.00270	0.00387	0.699
10	15	0.00199	0.00317	0.628	0.00274	0.00390	0.702
11	20	0.00334	0.00494	0.676	0.00414	0.00586	0.706
12	20	0.00373	0.00551	0.678	0.00448	0.00652	0.688
13	20	0.00398	0.00593	0.672	0.00480	0.00697	0.689
14	20	0.00431	0.00625	0.689	0.00511	0.00725	0.705
15	20	0.00456	0.00650	0.703	0.00533	0.00755	0.706

Cycle	Peak Load (kips)	Left Unloaded End Slip+		Ratio of ++ High R_r /Conv.	Right Unloaded End Slip+		Ratio of ++ High R_r /Conv.
		High R_r (in.)	Conv. (in.)		High R_r (in.)	Conv. (in.)	
1	10	0.00019	0.00053	0.359	0.00011	0.00045	0.250
2	10	0.00019	0.00053	0.353	0.00011	0.00050	0.213
3	10	0.00019	0.00058	0.323	0.00013	0.00052	0.253
4	10	0.00018	0.00060	0.292	0.00013	0.00056	0.233
5	10	0.00018	0.00062	0.287	0.00013	0.00059	0.222
6	15	0.00048	0.00106	0.451	0.00043	0.00107	0.399
7	15	0.00054	0.00117	0.460	0.00048	0.00124	0.389
8	15	0.00062	0.00131	0.472	0.00052	0.00132	0.395
9	15	0.00065	0.00138	0.470	0.00059	0.00139	0.422
10	15	0.00070	0.00143	0.490	0.00061	0.00144	0.424
11	20	0.00121	0.00231	0.521	0.00126	0.00223	0.564
12	20	0.00142	0.00283	0.503	0.00154	0.00263	0.585
13	20	0.00162	0.00317	0.513	0.00175	0.00298	0.589
14	20	0.00182	0.00343	0.532	0.00200	0.00324	0.619
15	20	0.00194	0.00366	0.531	0.00219	0.00344	0.636

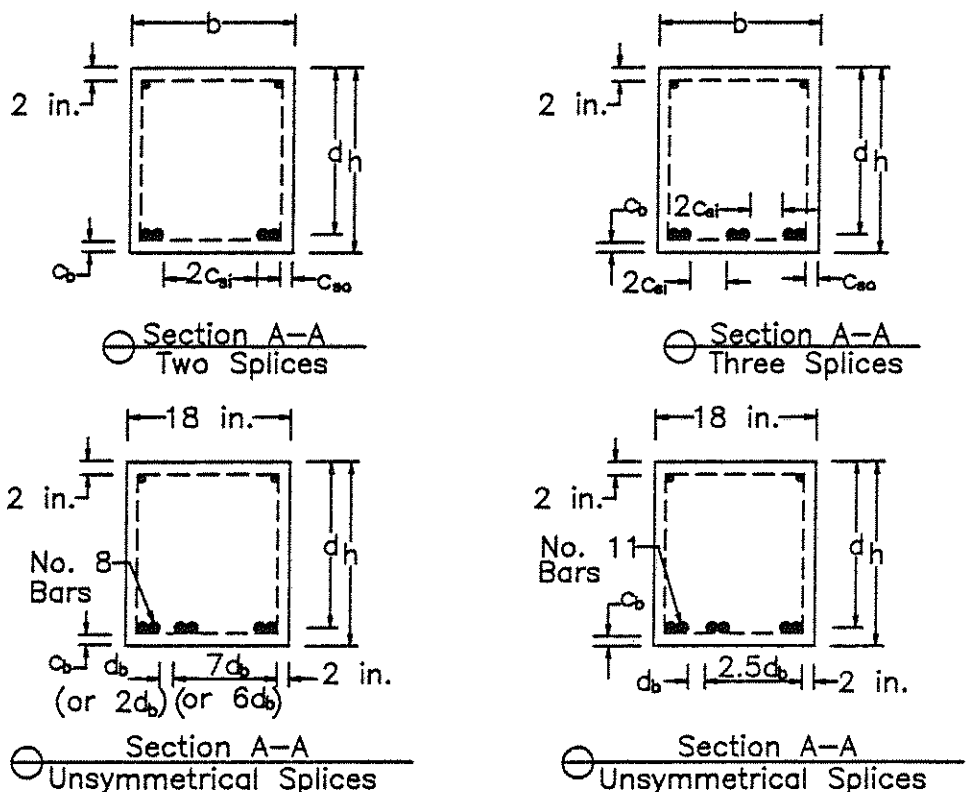
+ Average slips from 4 tests for high R_r bars and 5 tests for conventional bars, respectively.

++ Ratio of slip of high R_r bar to that of conventional bar

1 in. = 24.5 mm; 1 kips = 4.448 kN

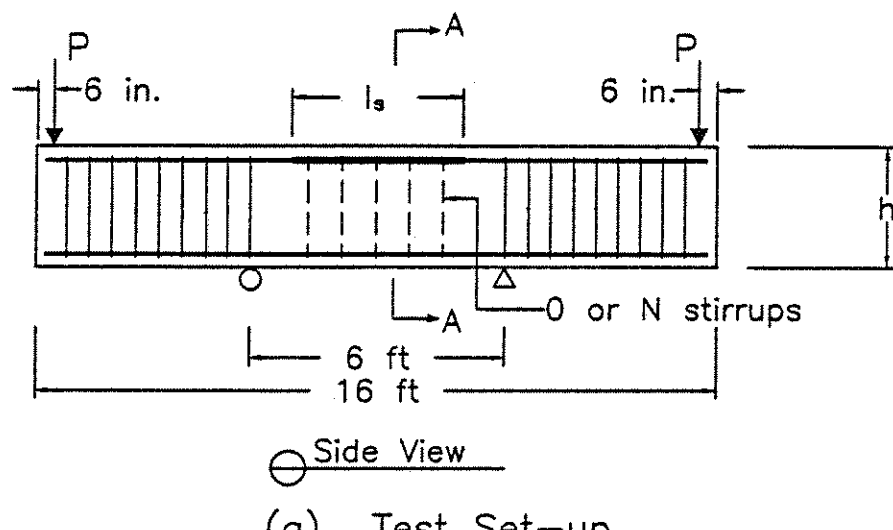


(a) Test Set-up

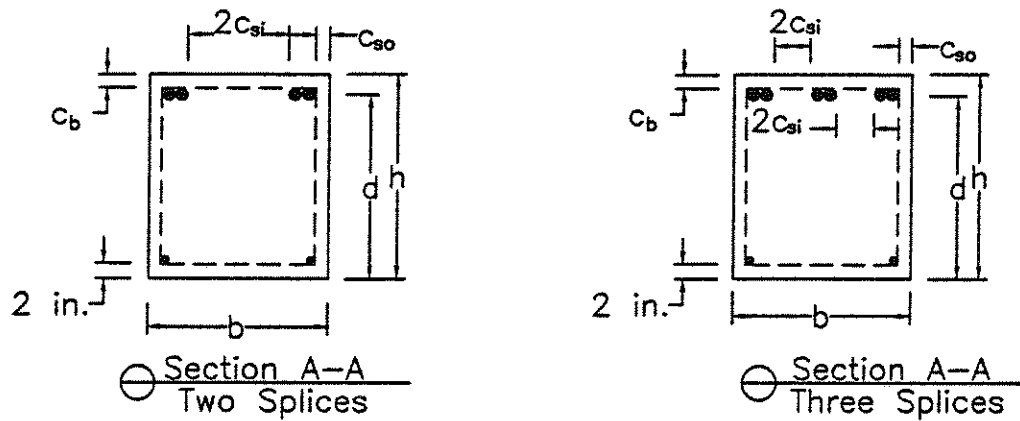


(b) Beam Configuration as Cast

Fig. 2.1 Typical bottom-cast beam splice specimens



(a) Test Set-up



(b) Beam Configuration as Cast

Fig. 2.2 Typical top-cast beam splice specimens

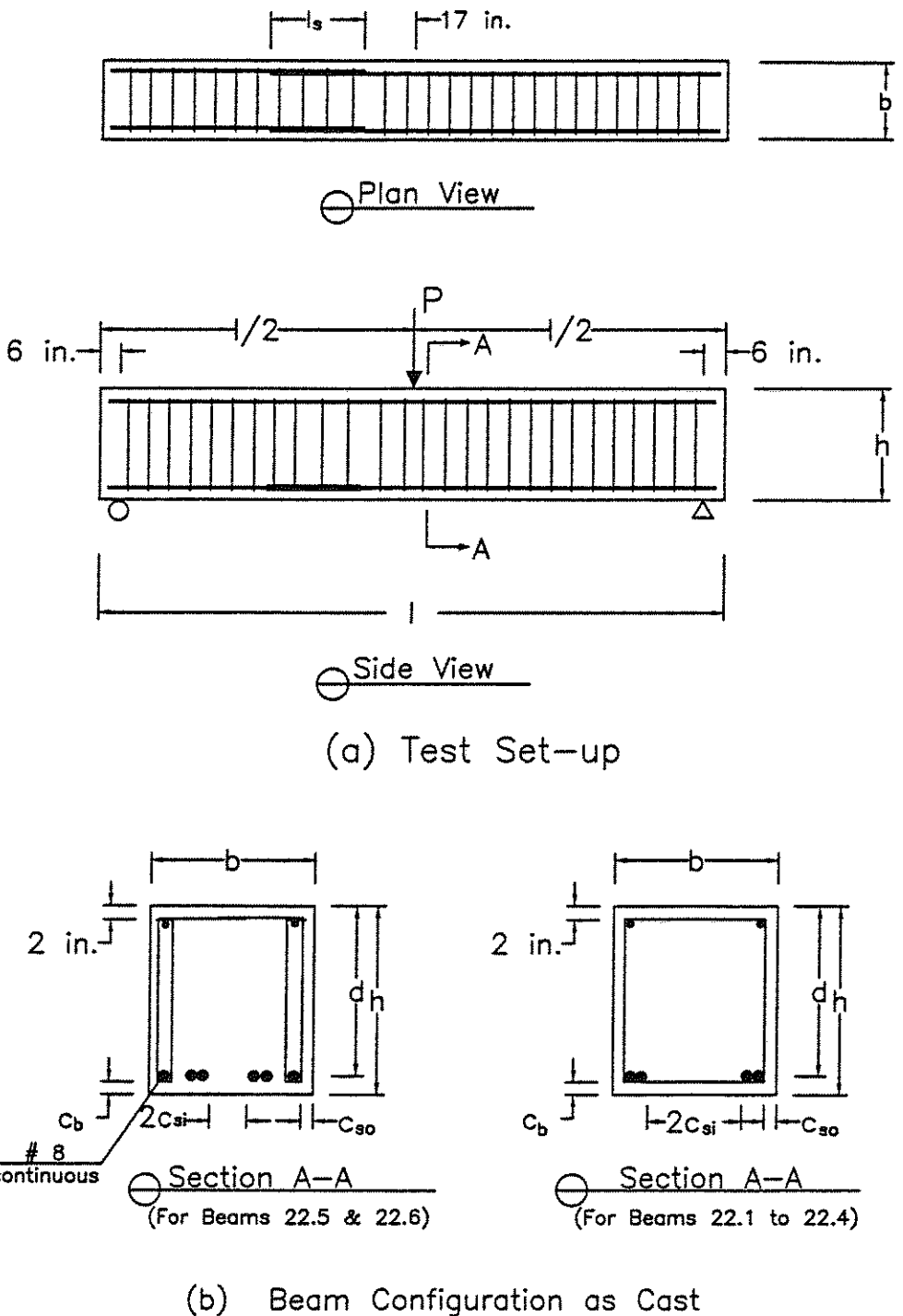


Fig. 2.3 Beam splice specimens in test group 22

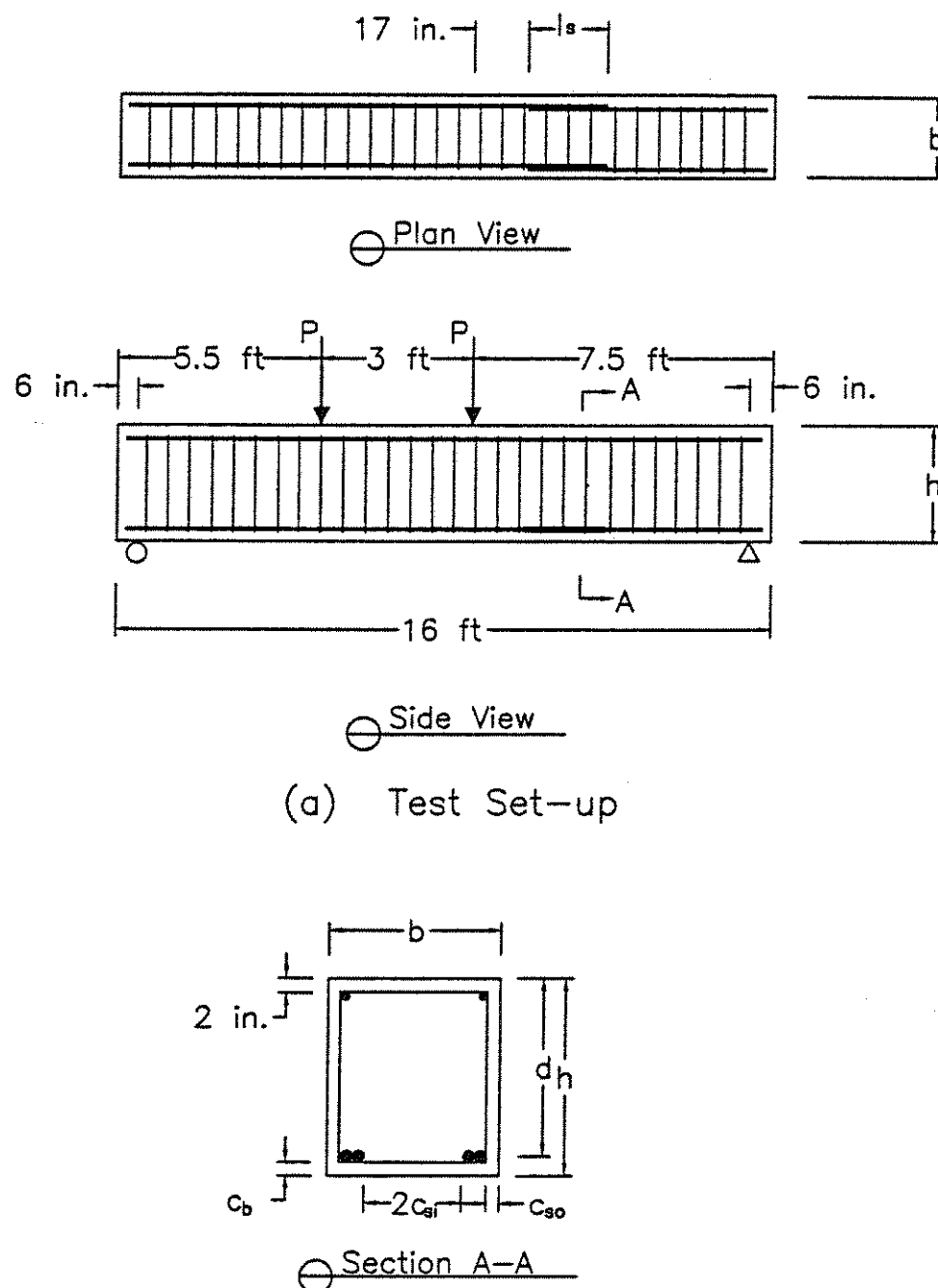
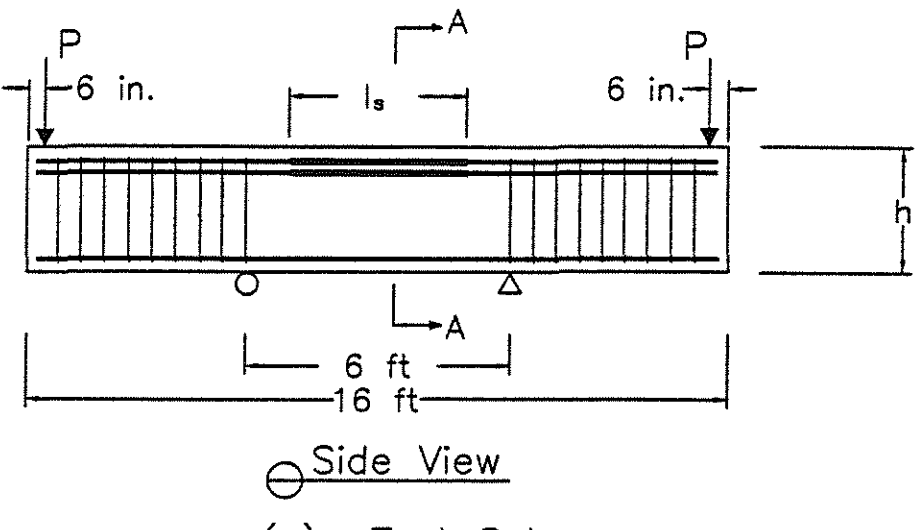
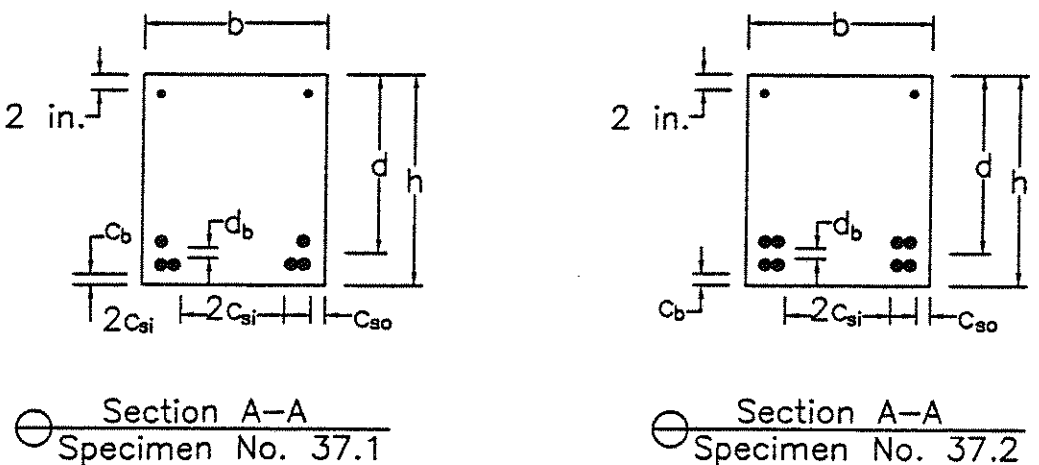


Fig. 2.4 Beam splice specimens 23b.5 and 23b.6



(a) Test Set-up



(b) Beam Configuration as Cast

Fig. 2.5 Beam splice specimens with two layers of bars

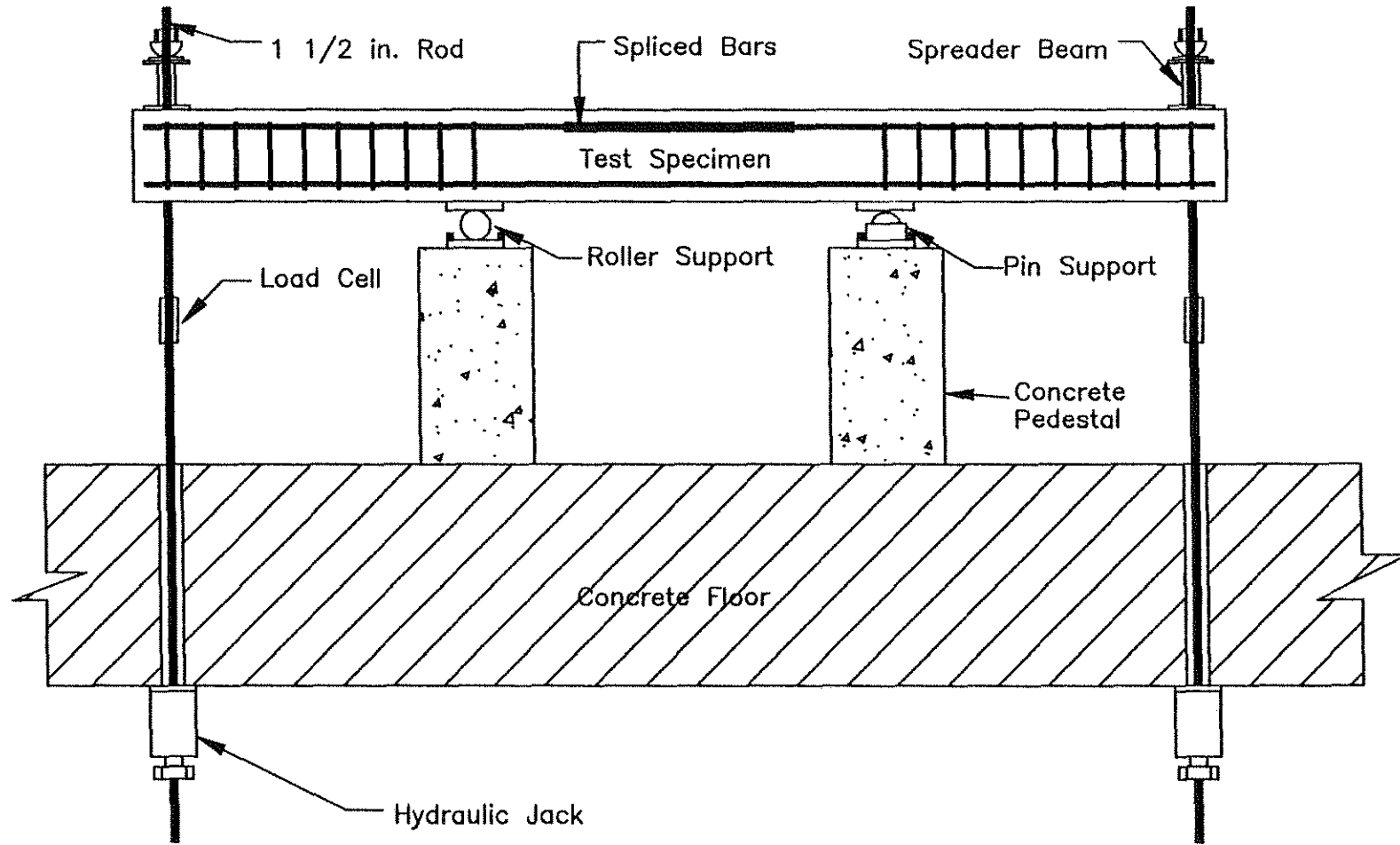


Fig. 2.6 Schematic of splice test setup

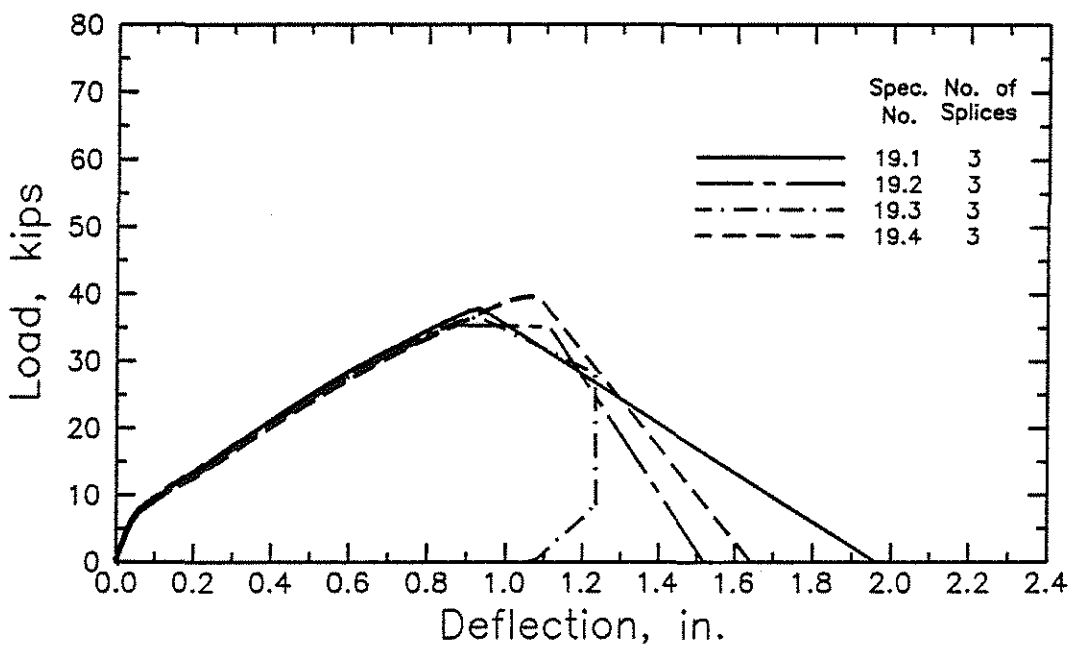


Fig. 2.7a Load-deflection curves for splice specimens in group 19

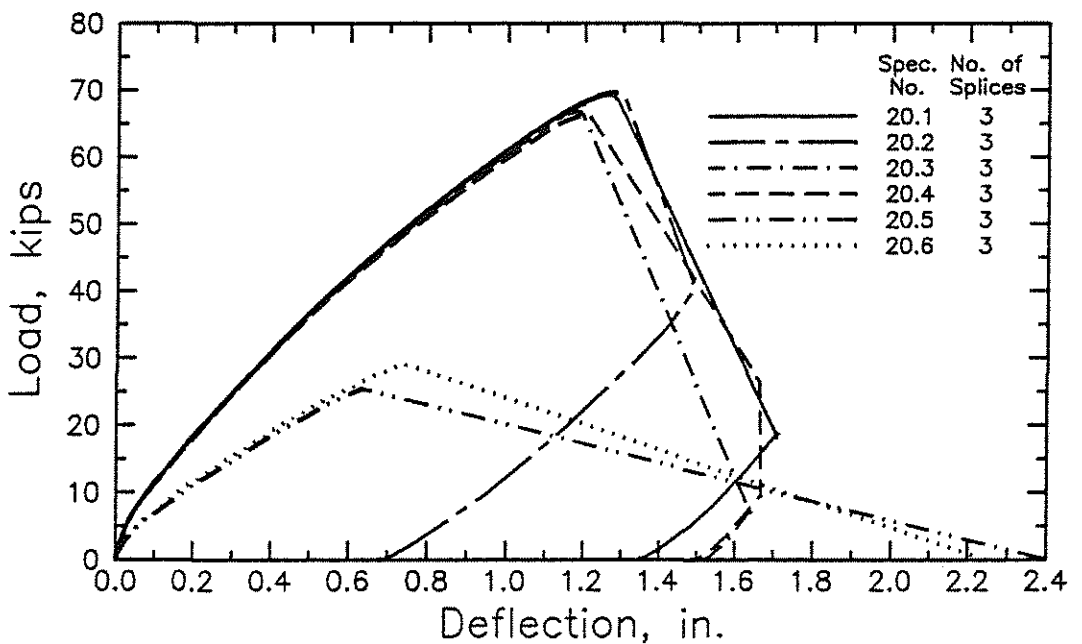


Fig. 2.7b Load-deflection curves for splice specimens in group 20

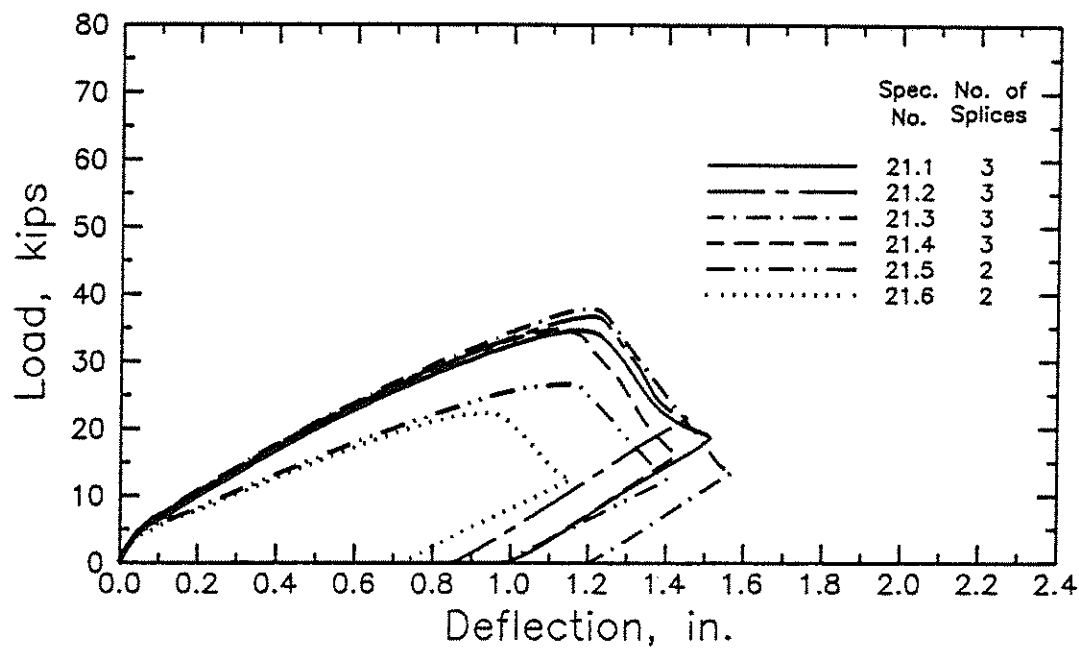


Fig. 2.7c Load-deflection curves for splice specimens in group 21

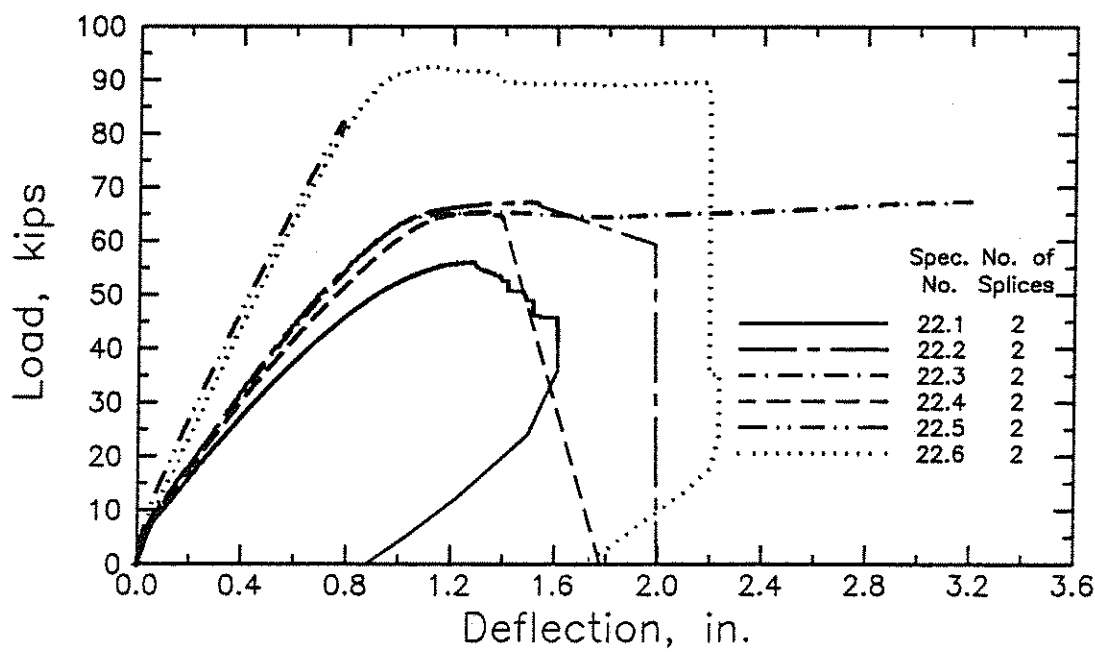


Fig. 2.7d Load-deflection curves for splice specimens in group 22

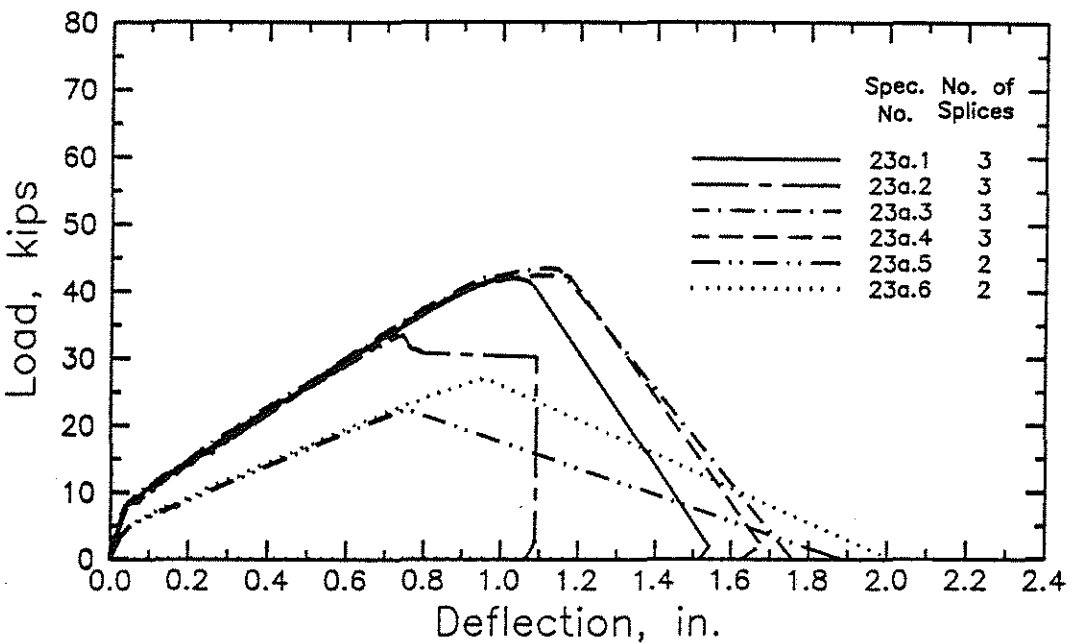


Fig. 2.7e Load-deflection curves for splice specimens in group 23a

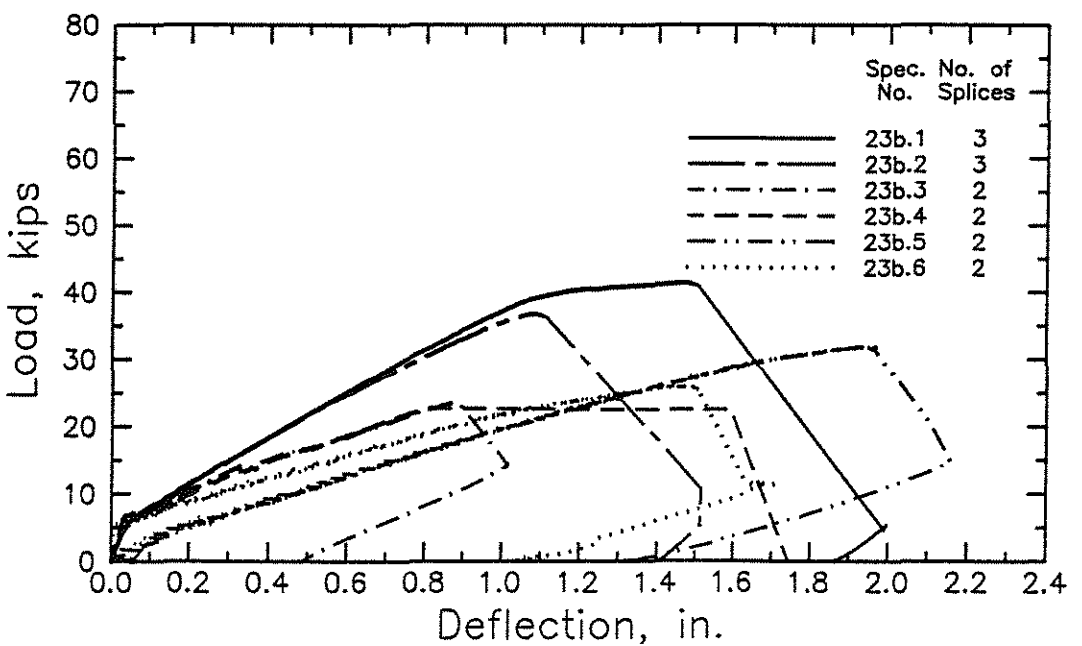


Fig. 2.7f Load-deflection curves for splice specimens in group 23b

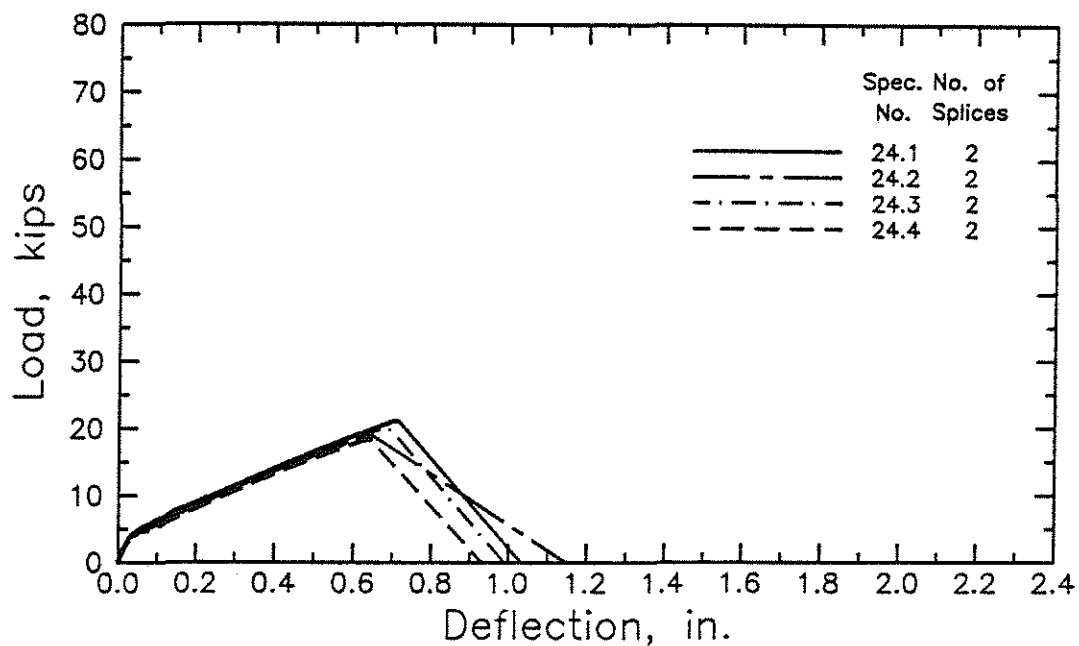


Fig. 2.7g Load-deflection curves for splice specimens in group 24

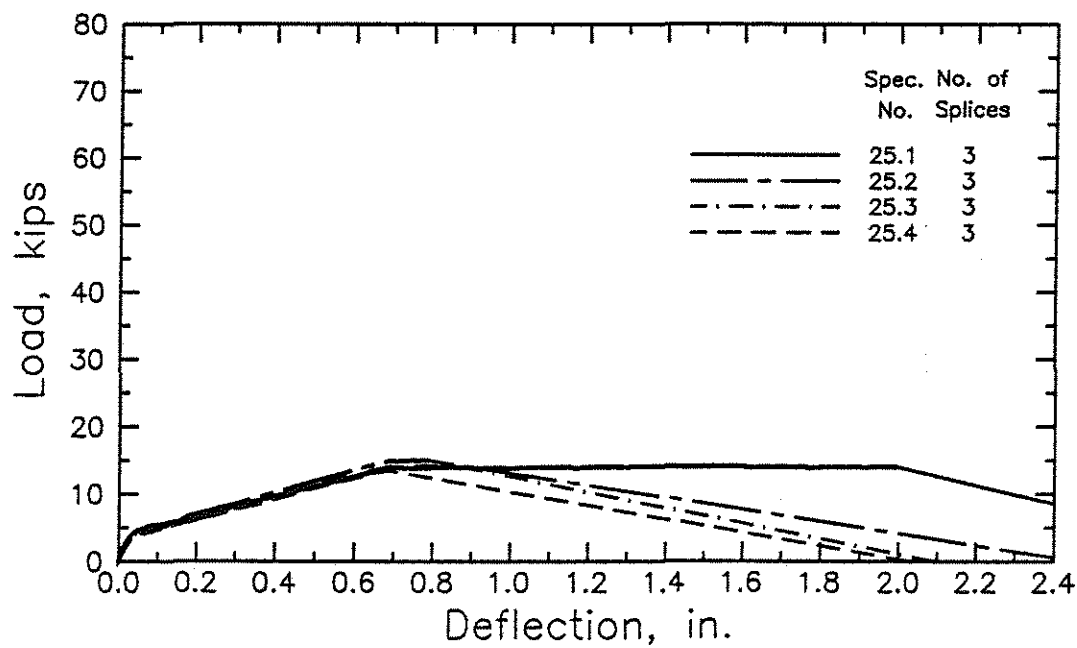


Fig. 2.7h Load-deflection curves for splice specimens in group 25

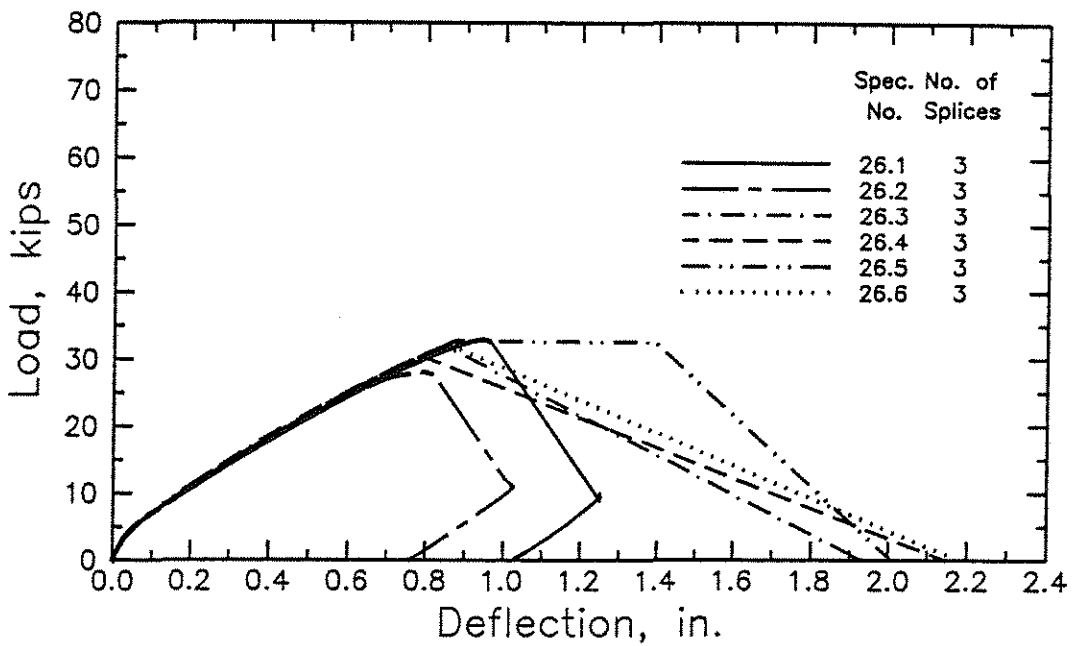


Fig. 2.7i Load-deflection curves for splice specimens in group 26

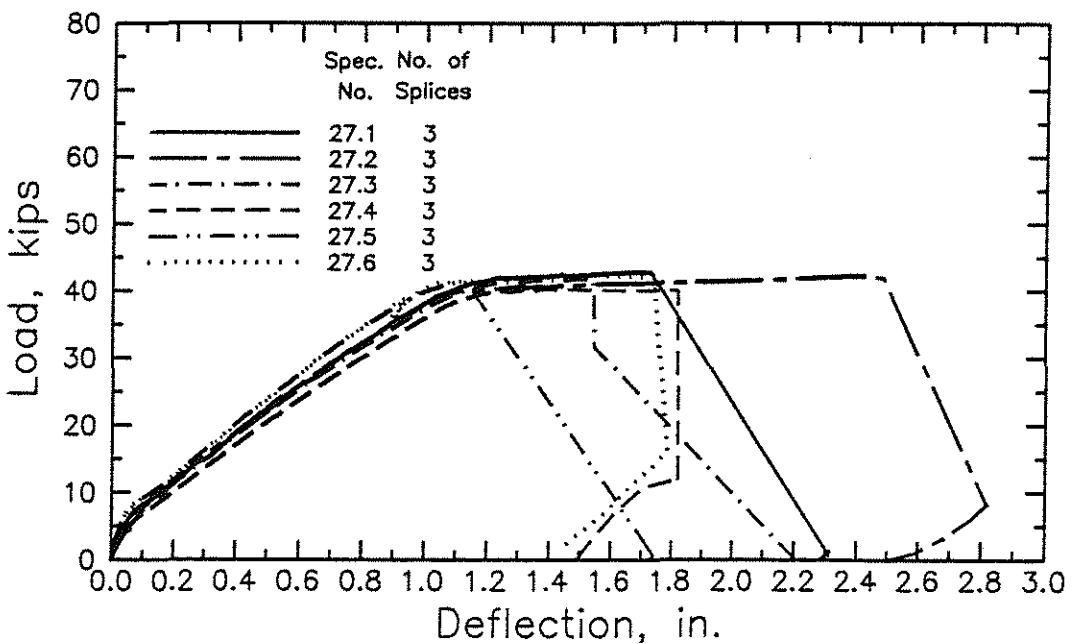


Fig. 2.7j Load-deflection curves for splice specimens in group 27

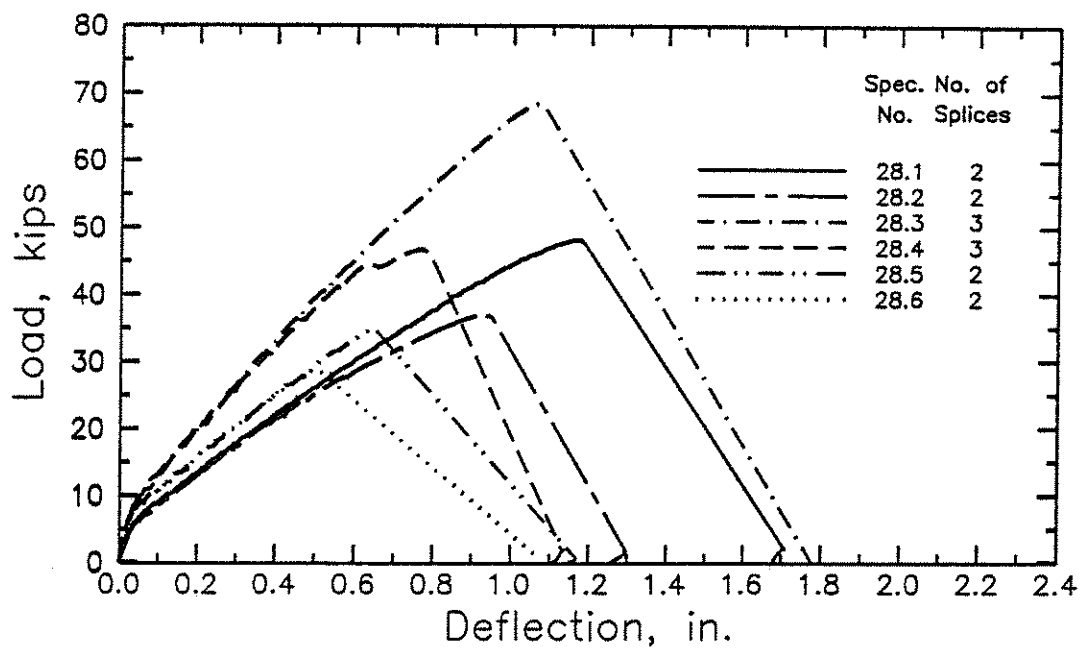


Fig. 2.7k Load-deflection curves for splice specimens in group 28

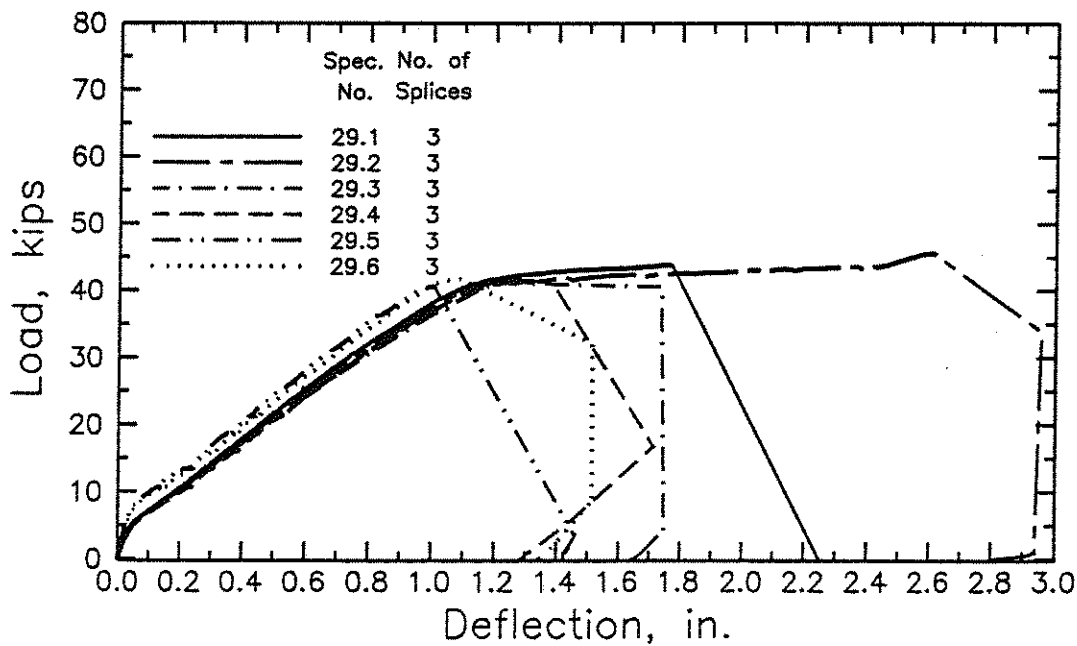


Fig. 2.7l Load-deflection curves for splice specimens in group 29

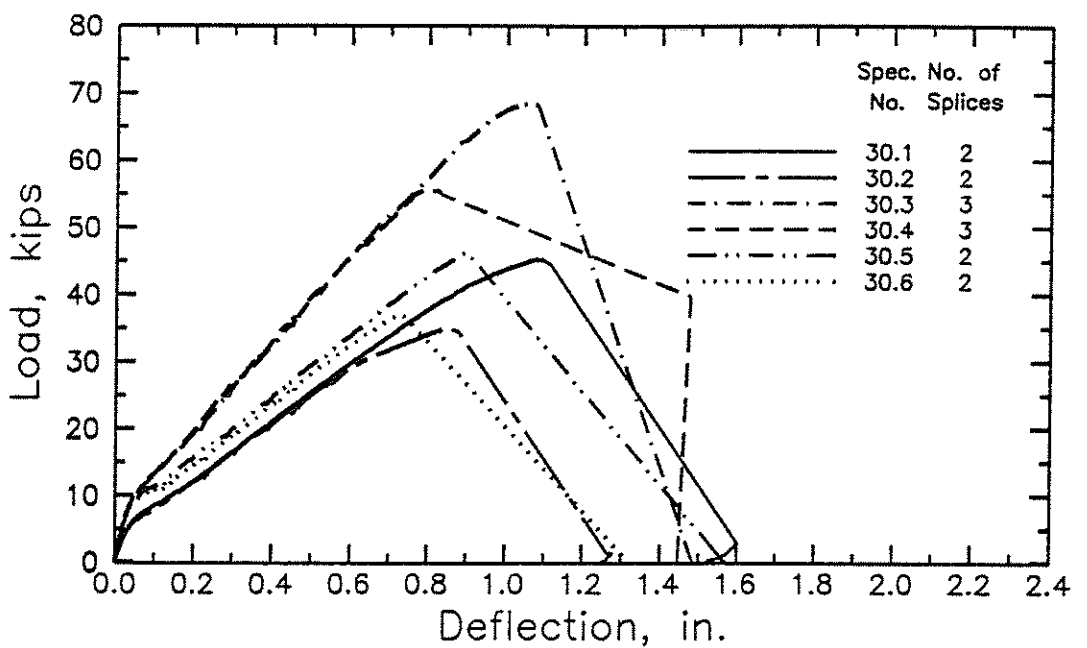


Fig. 2.7m Load-deflection curves for splice specimens in group 30

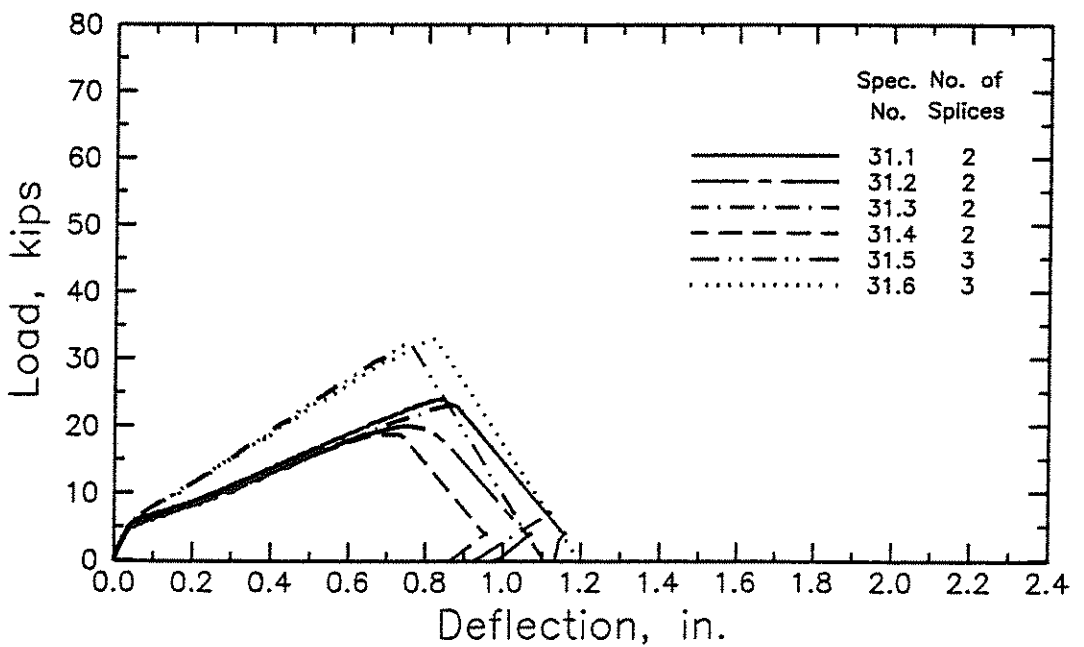


Fig. 2.7n Load-deflection curves for splice specimens in group 31

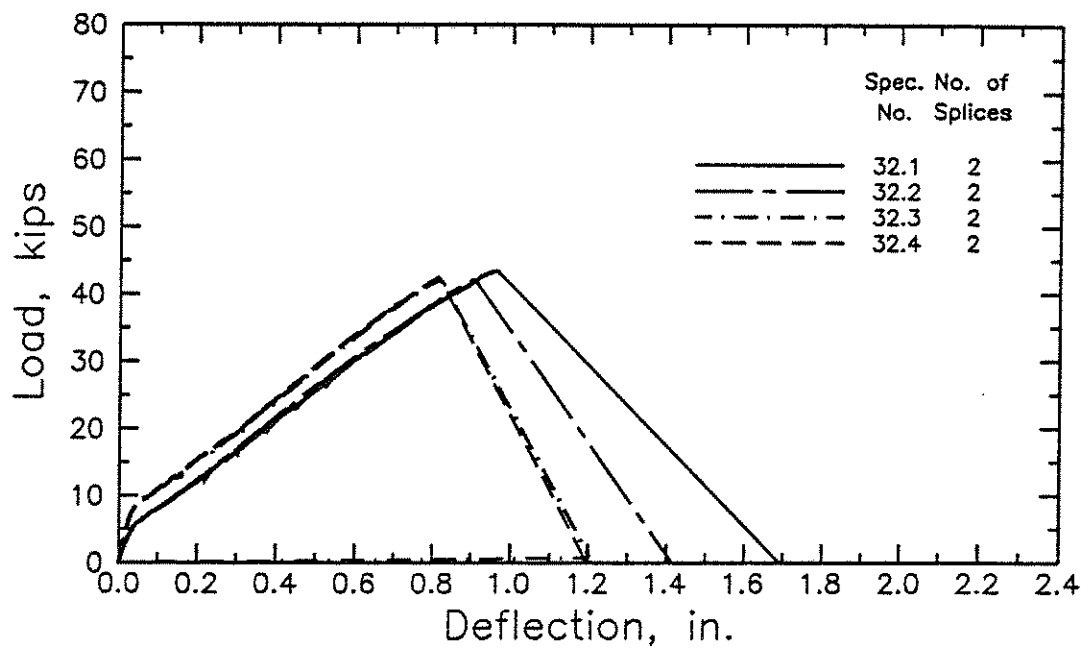


Fig. 2.7o Load-deflection curves for splice specimens in group 32

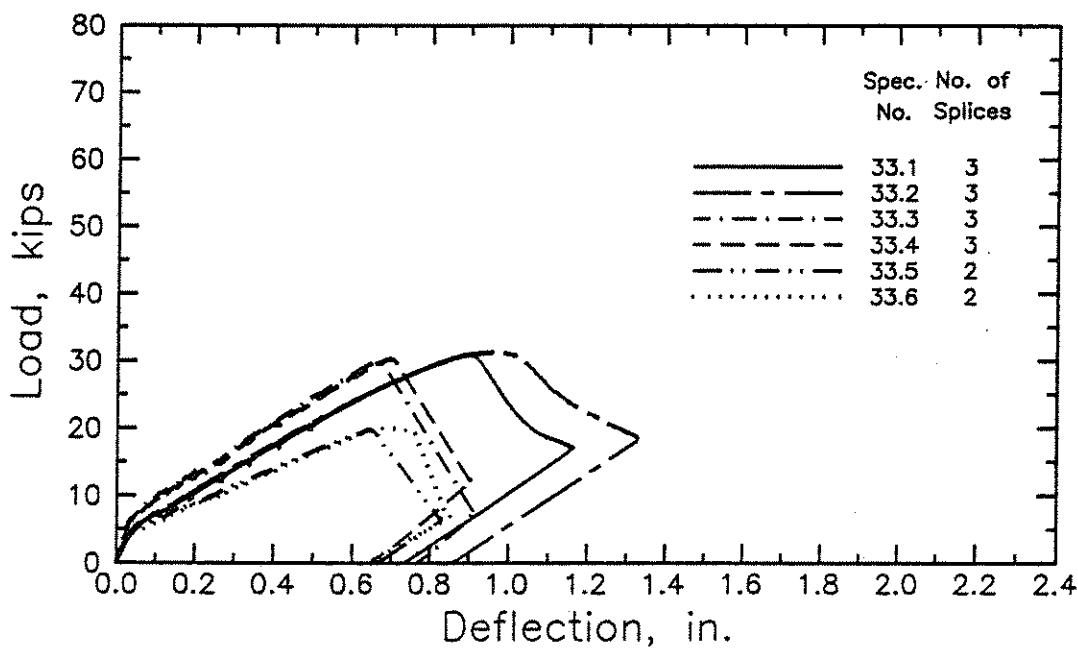


Fig. 2.7p Load-deflection curves for splice specimens in group 33

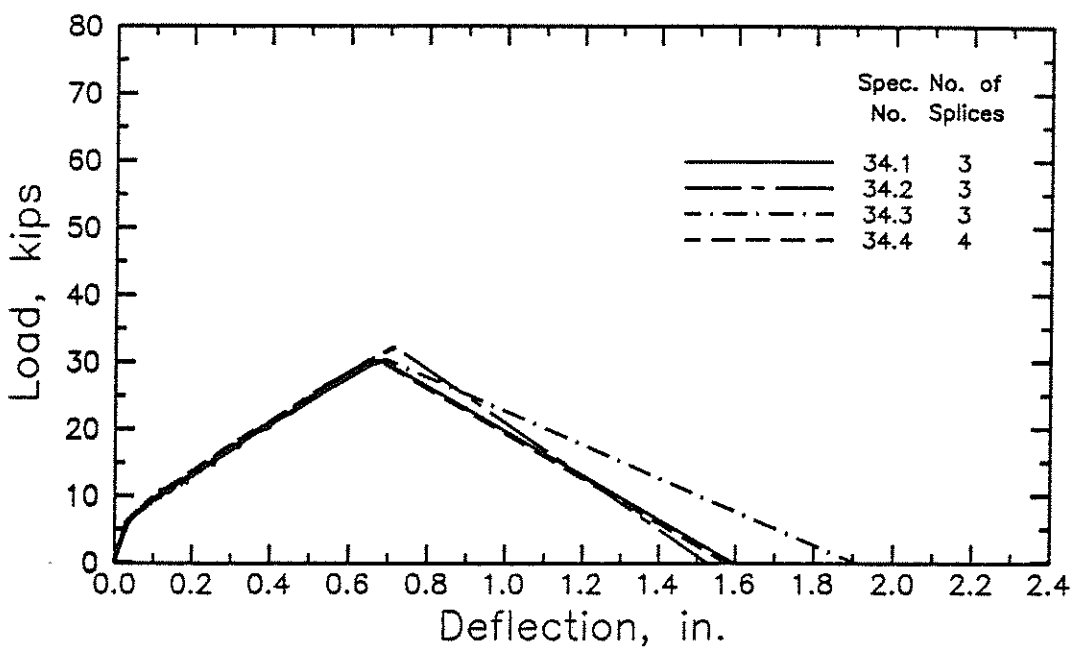


Fig. 2.7q Load-deflection curves for splice specimens in group 34

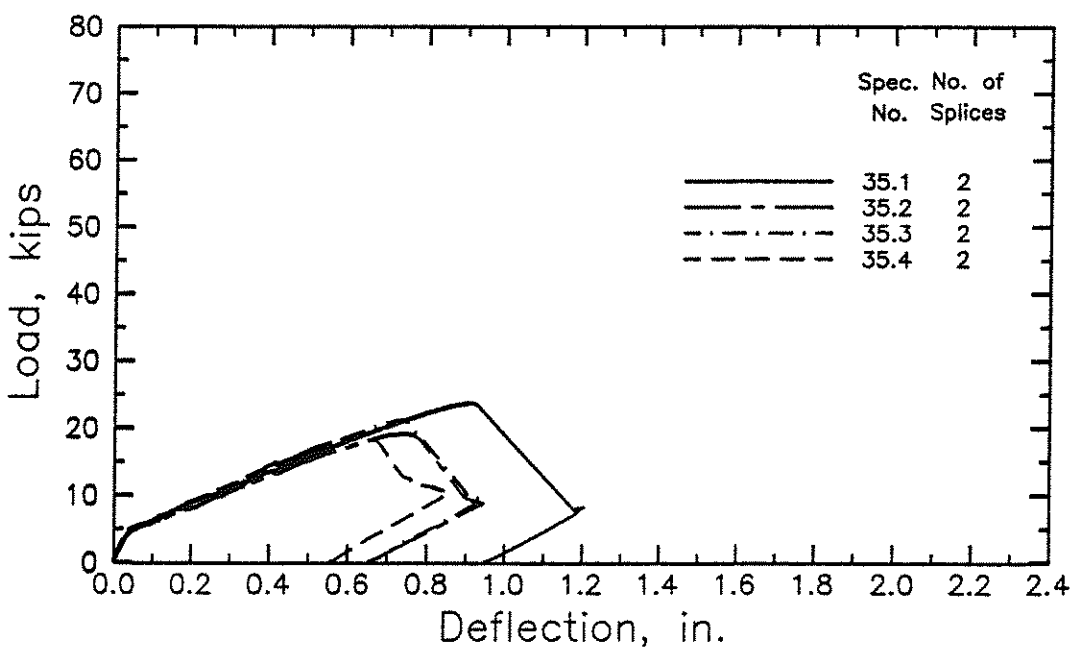


Fig. 2.7r Load-deflection curves for splice specimens in group 35

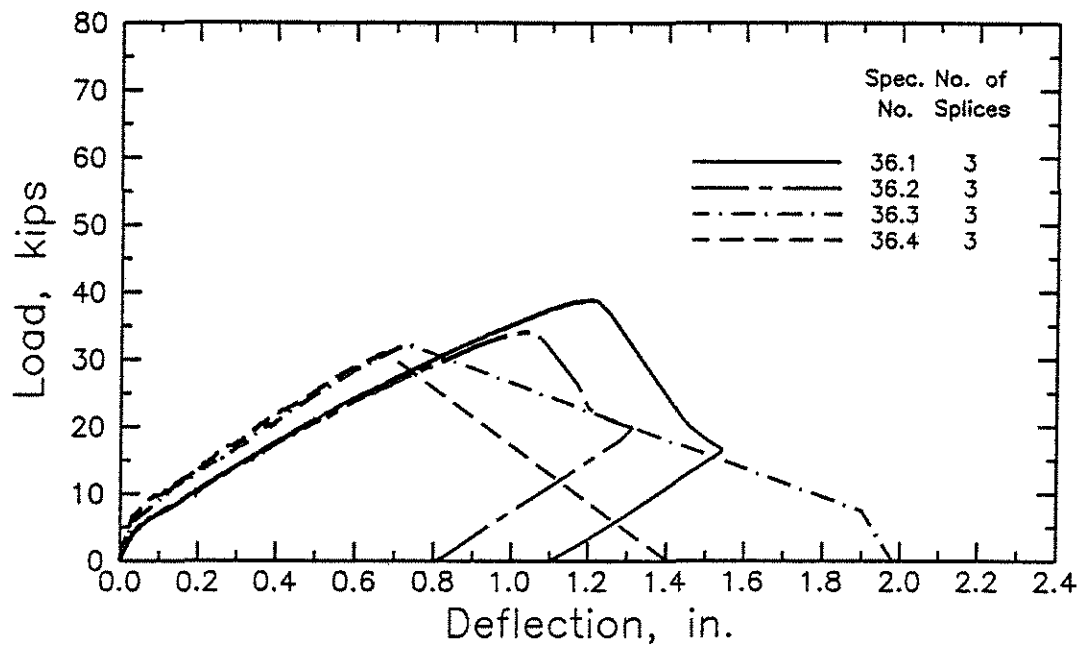


Fig. 2.7s Load-deflection curves for splice specimens in group 36

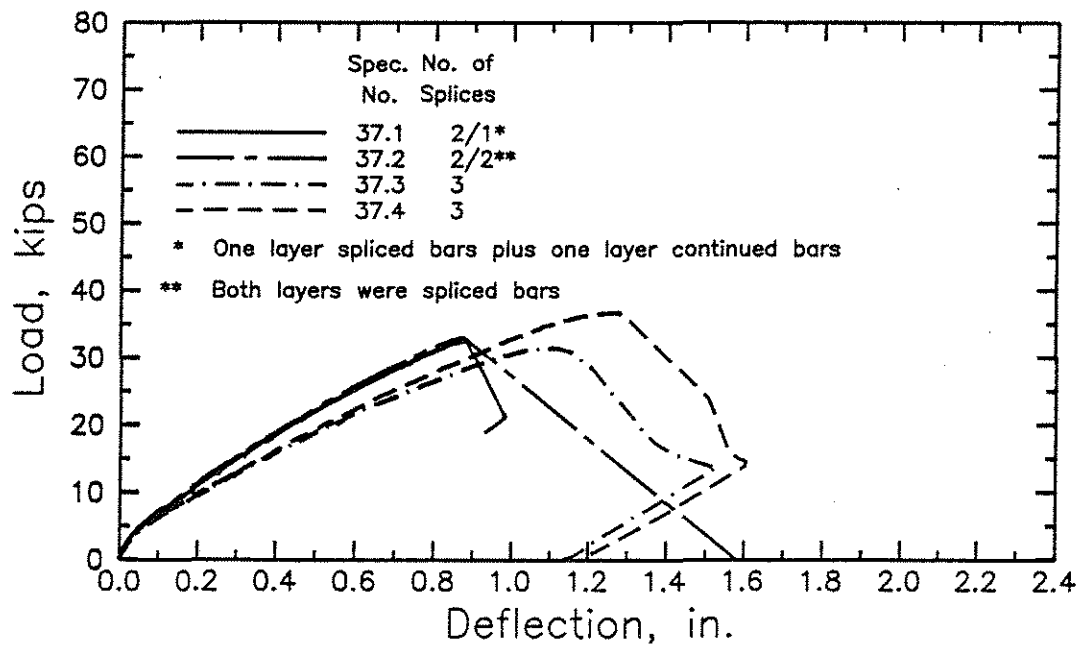


Fig. 2.7t Load-deflection curves for splice specimens in group 37

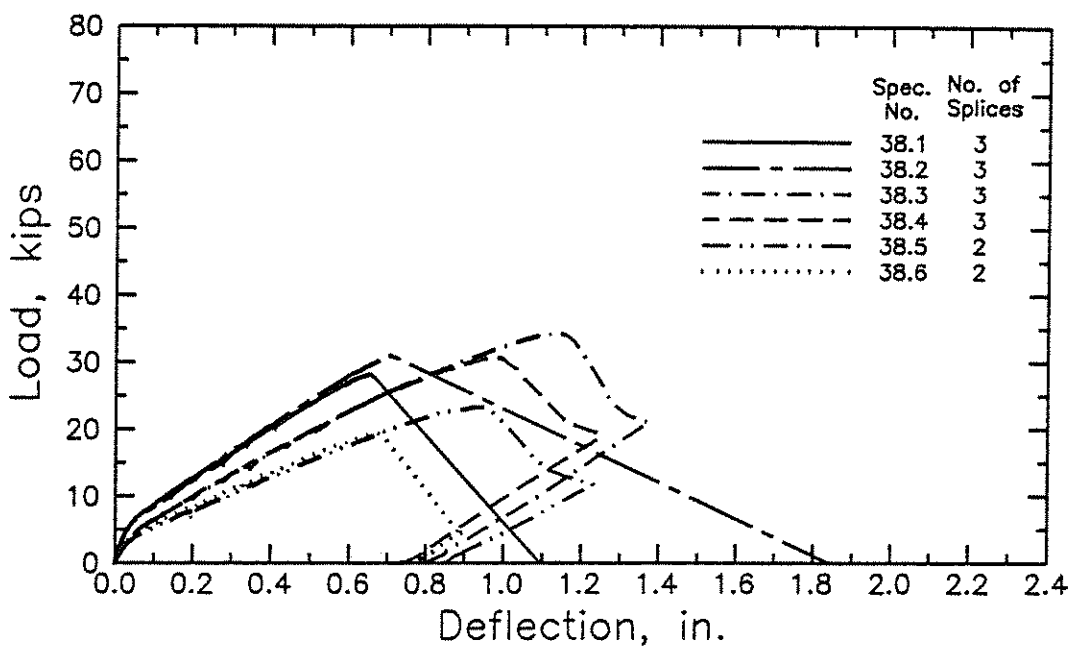


Fig. 2.7u Load-deflection curves for splice specimens in group 38

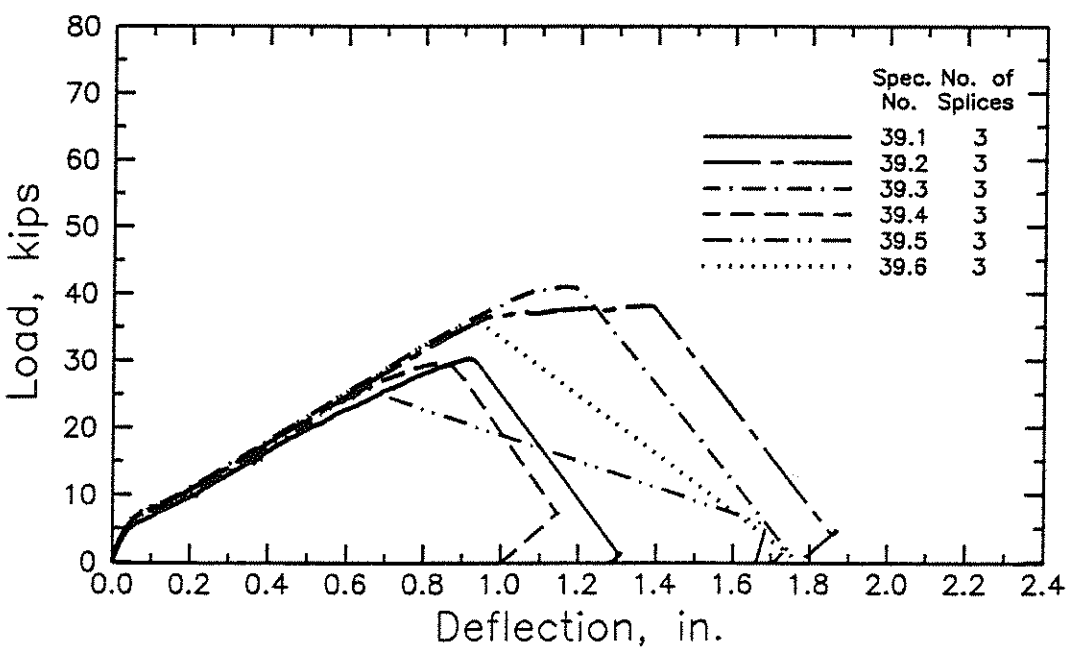


Fig. 2.7v Load-deflection curves for splice specimens in group 39

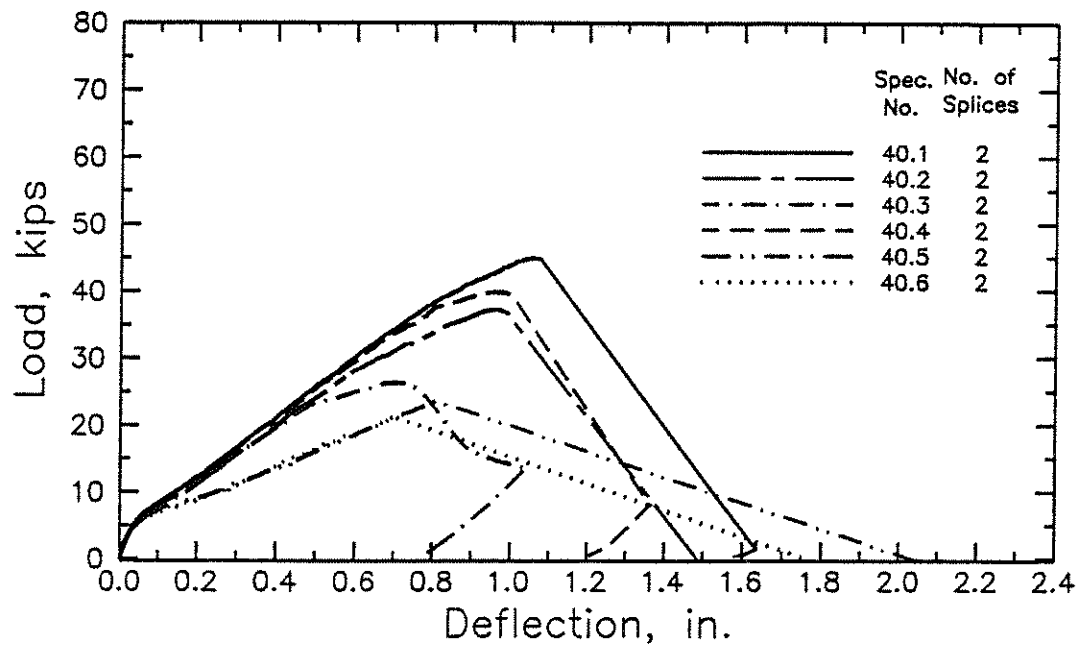


Fig. 2.7w Load-deflection curves for splice specimens in group 40

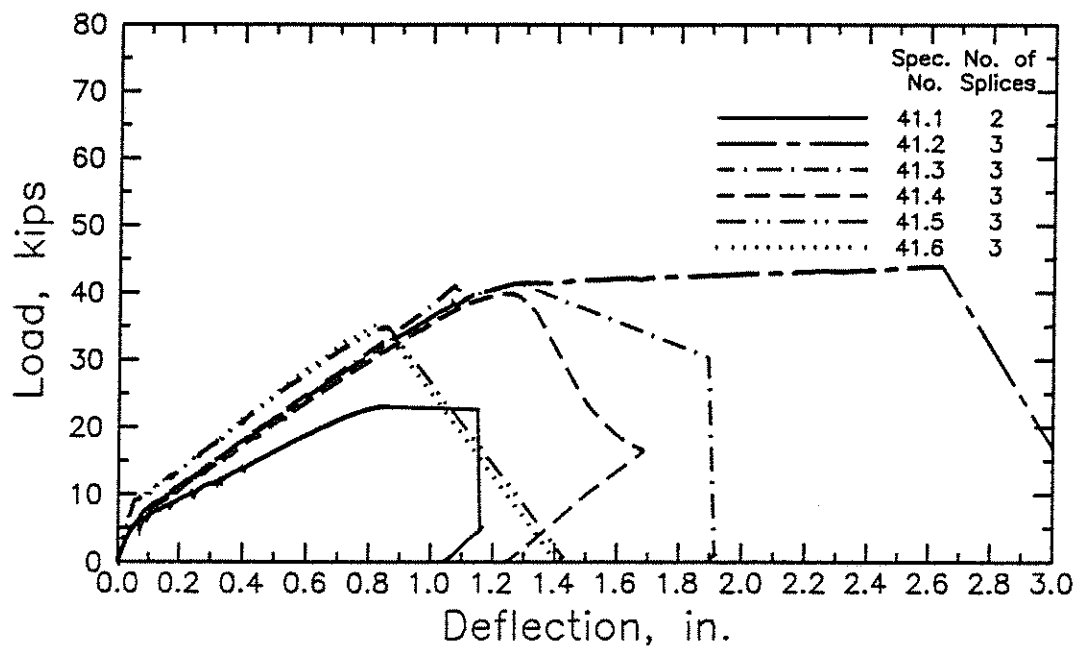


Fig. 2.7x Load-deflection curves for splice specimens in group 41

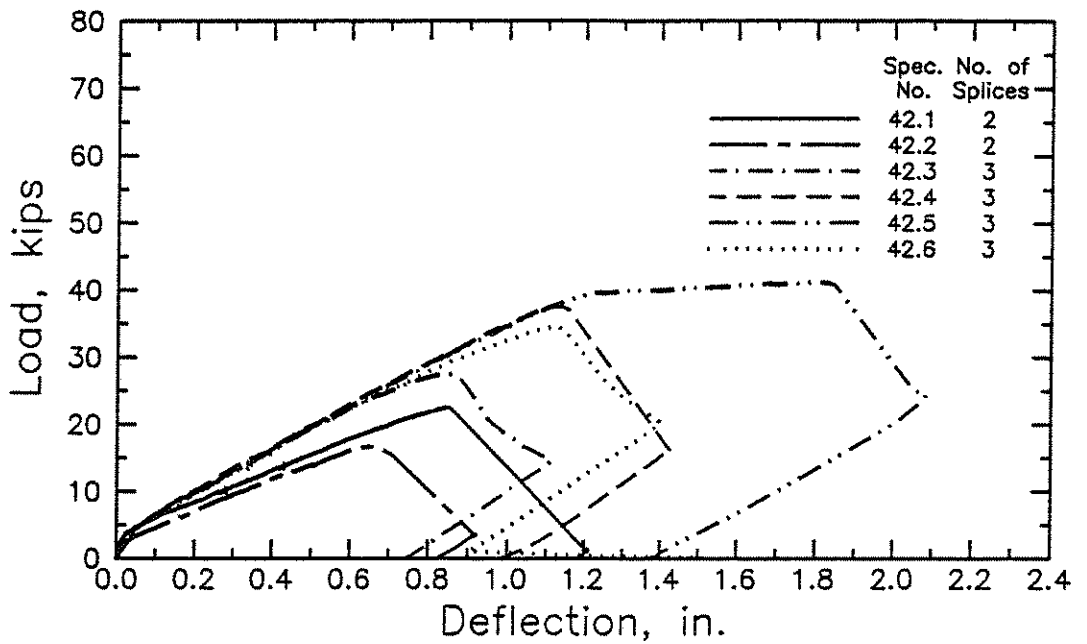


Fig. 2.7y Load-deflection curves for splice specimens in group 42

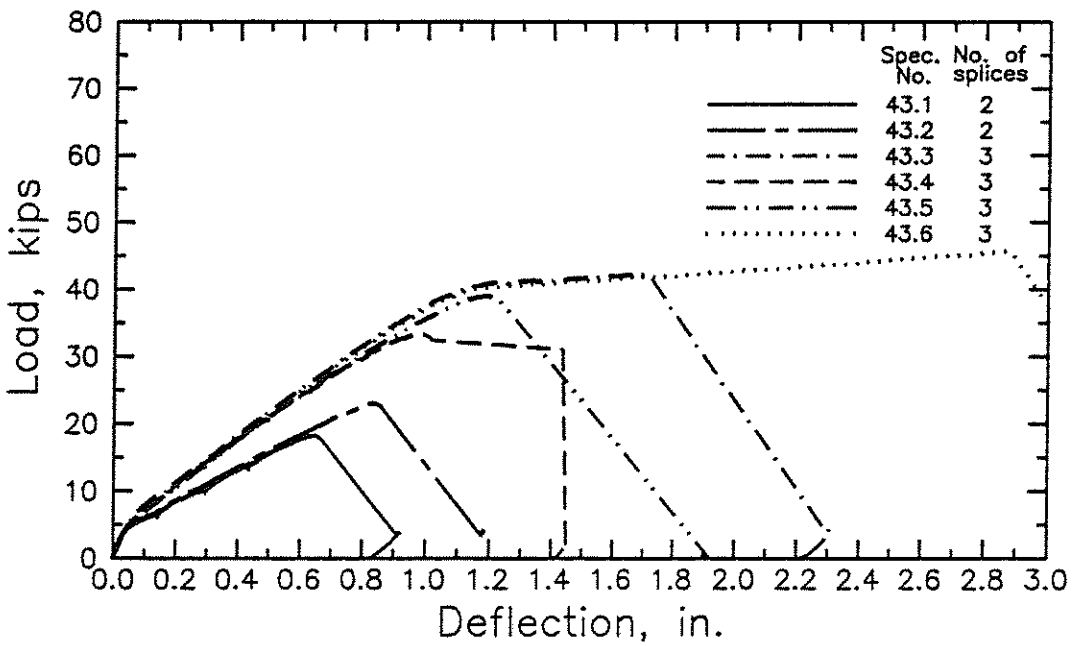


Fig. 2.7z Load-deflection curves for splice specimens in group 43

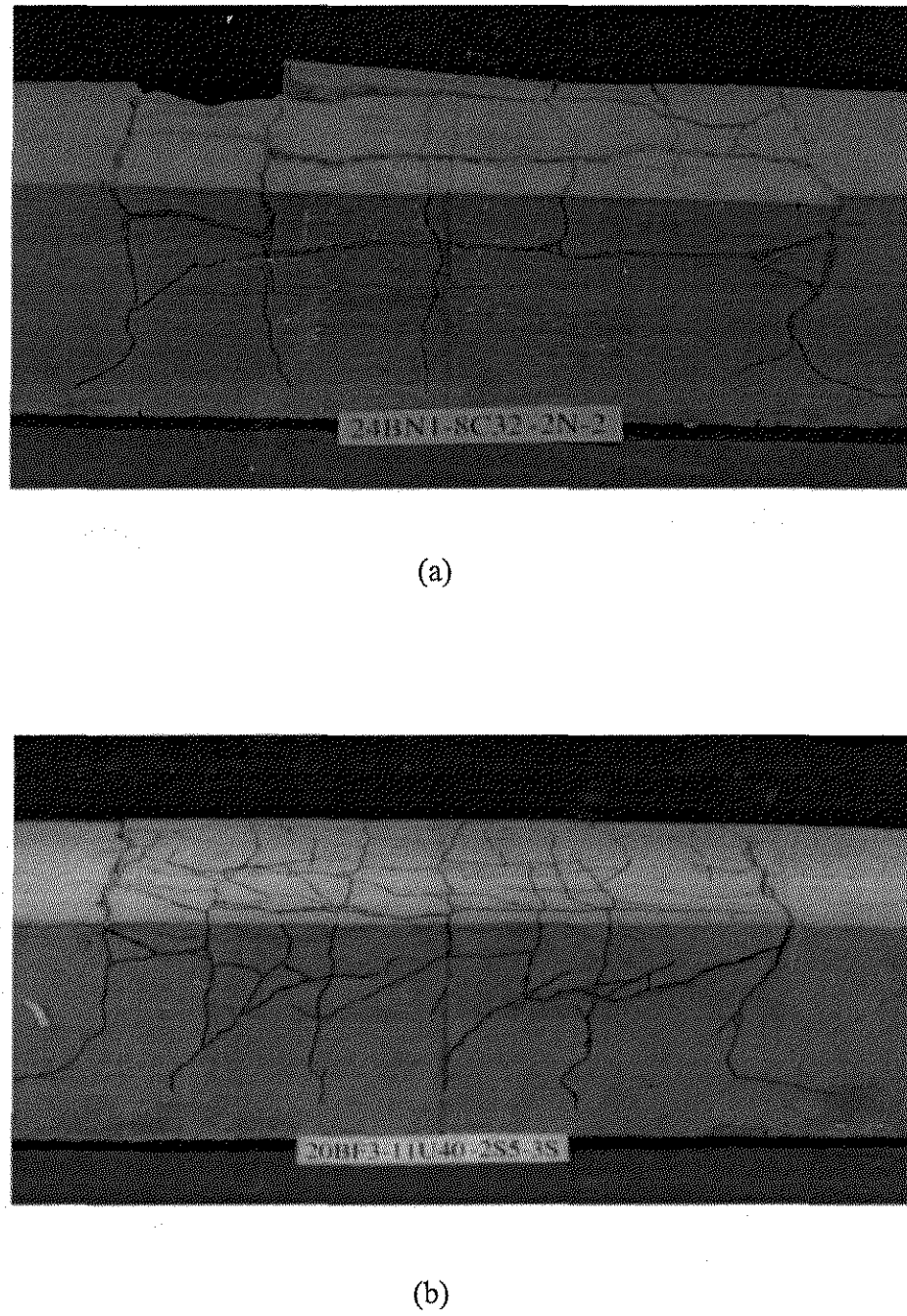
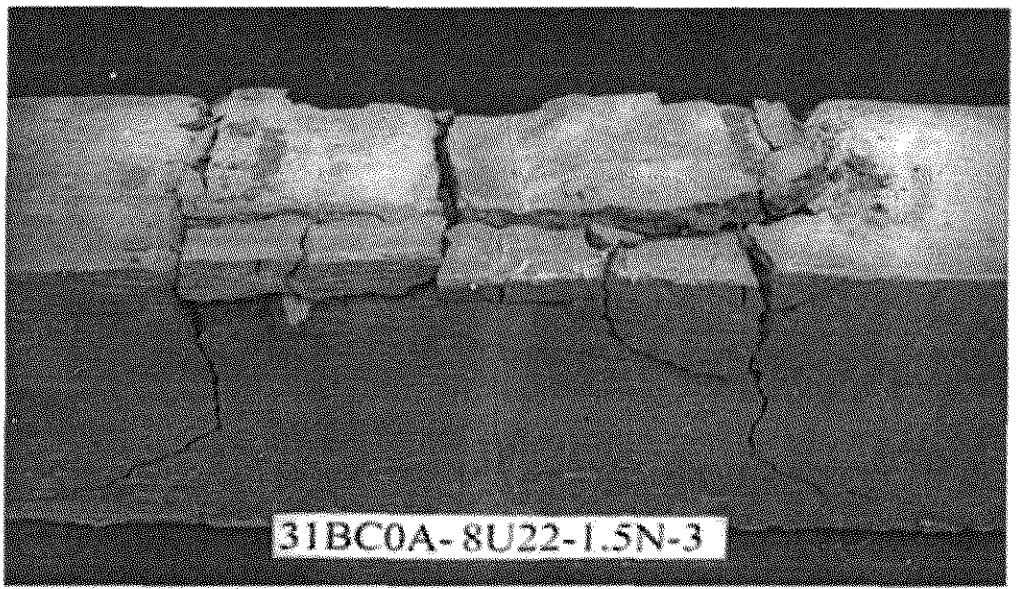


Fig. 2.8 Cracked specimens cast with normal-strength concrete after failure: (a) without stirrups, (b) with stirrups

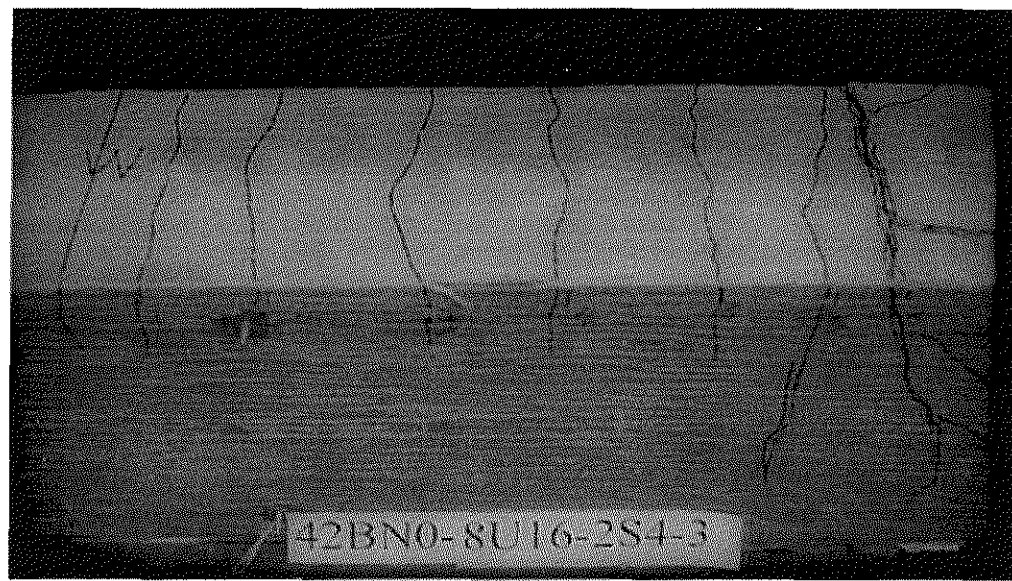


(a)

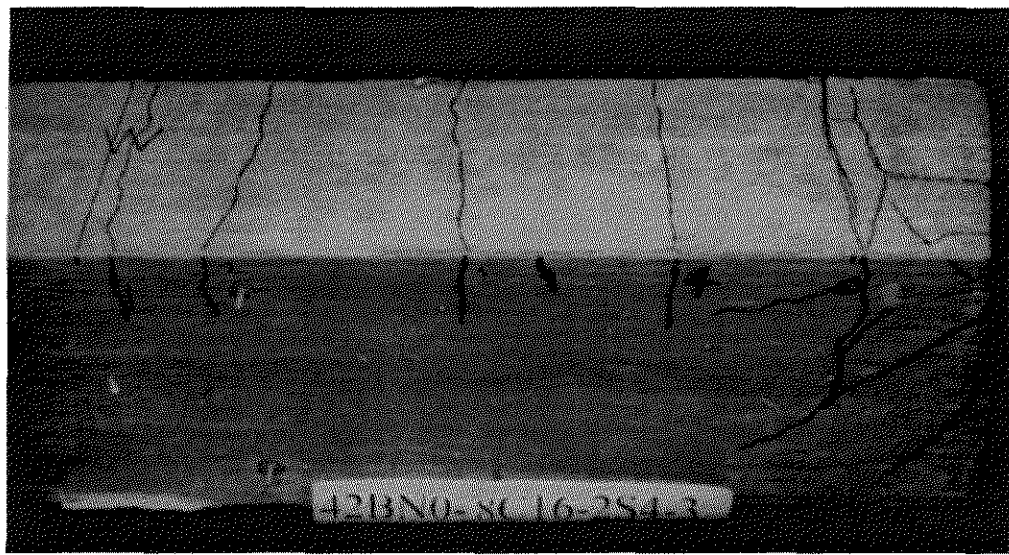


(b)

Fig. 2.9 Cracked specimens cast with high-strength concrete after failure: (a) without stirrups, (b) with stirrups

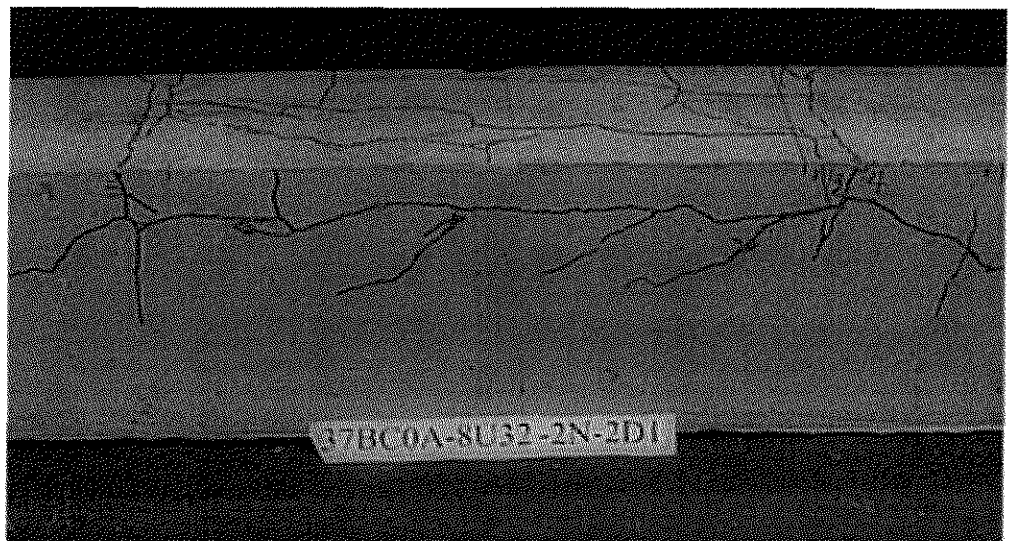


(a)

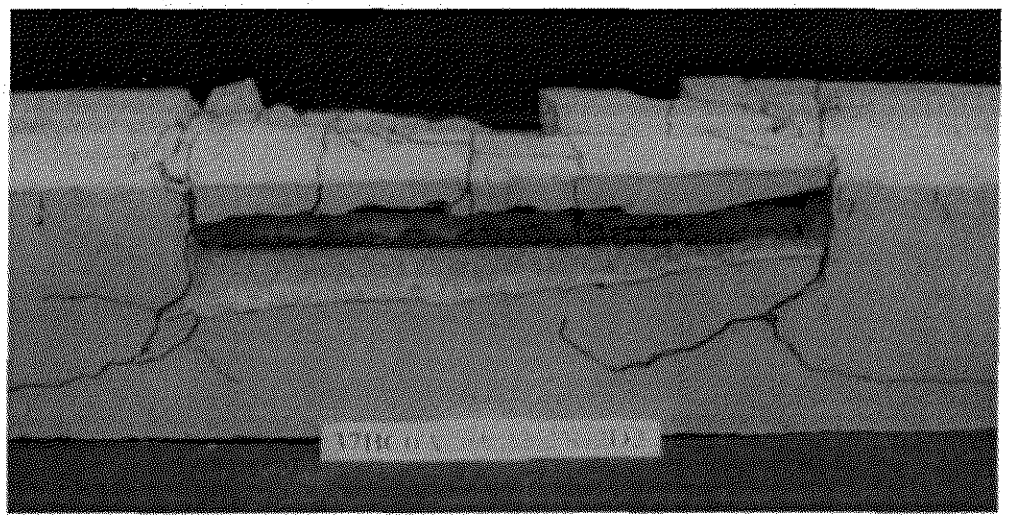


(b)

Fig. 2.10 Flexural crack distribution on west side of splice region: (a) uncoated bars, (b) epoxy-coated bars



(a)



(b)

Fig. 2.11 Cracked specimens with two-layer bars after failure: (a) one spliced layer and one continuous layer, (b) two-spliced layers

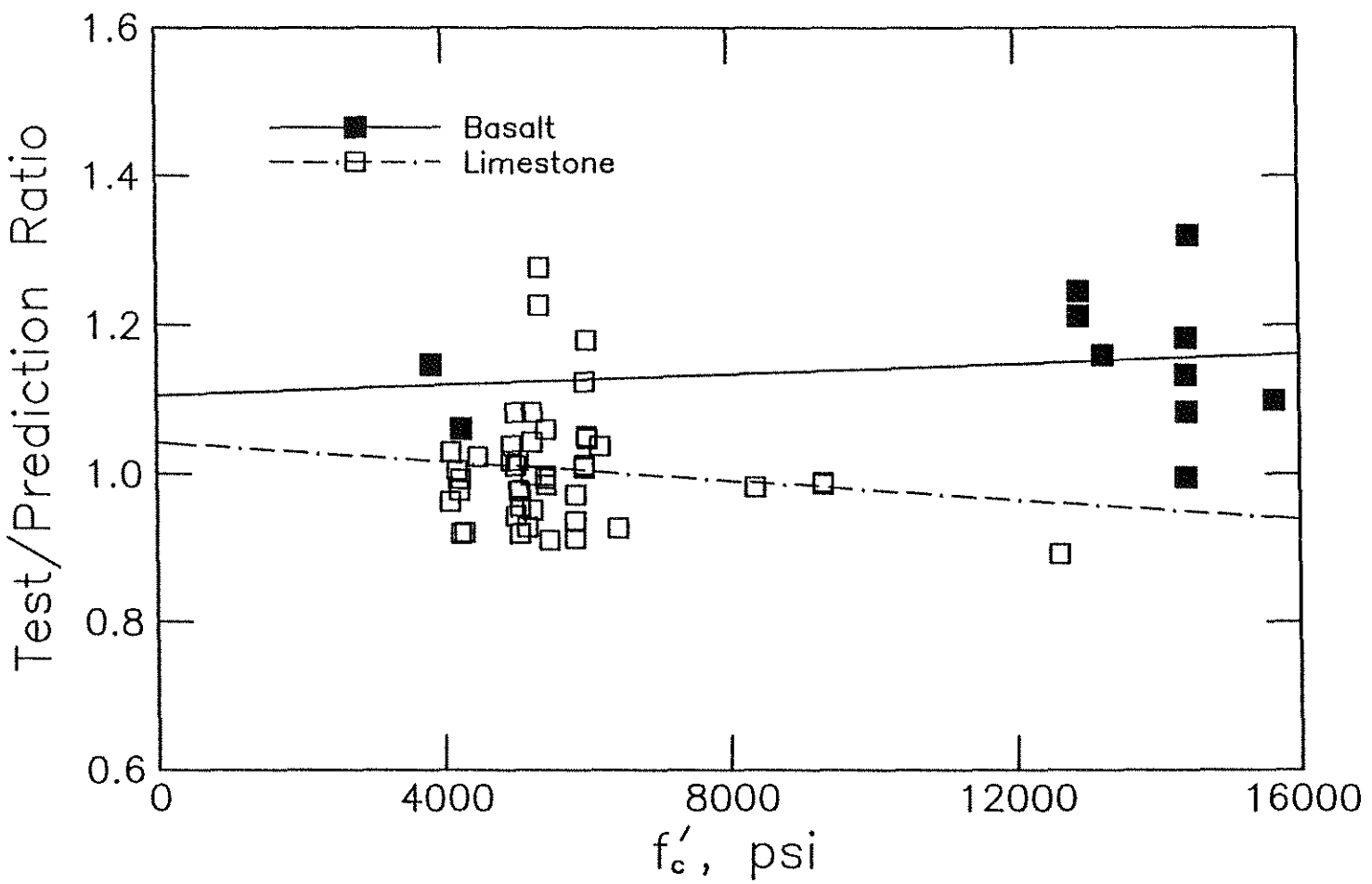


Fig. 4.1 Test/prediction ratio versus concrete compressive strength, f'_c , for splices not confined by transverse reinforcement in concrete containing basalt and limestone coarse aggregates

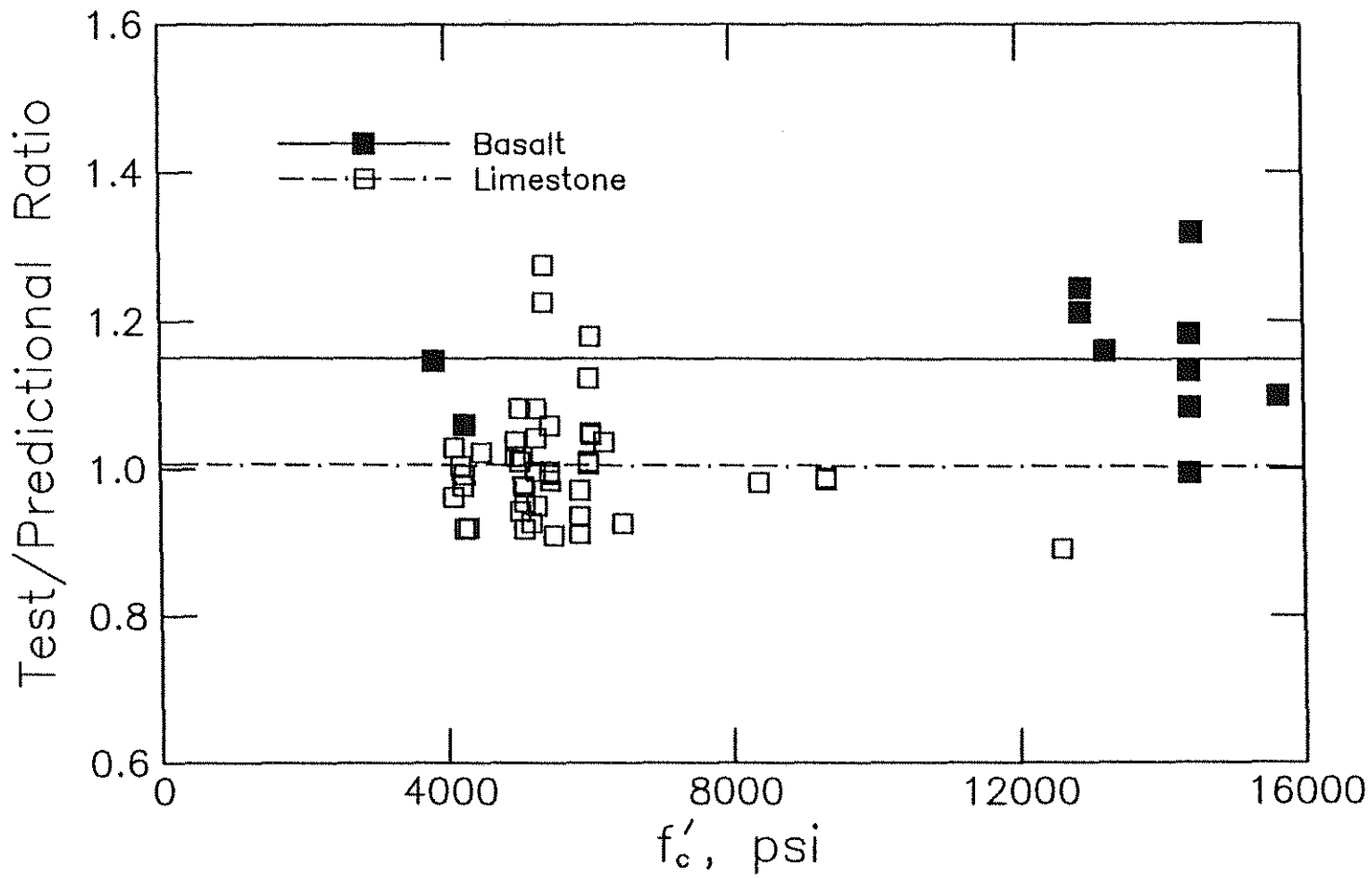


Fig. 4.2 Test/prediction ratio versus concrete compressive strength, f'_c , for splices not confined by transverse reinforcement in concrete containing basalt and limestone coarse aggregates, using dummy variable analysis based on type of coarse aggregate

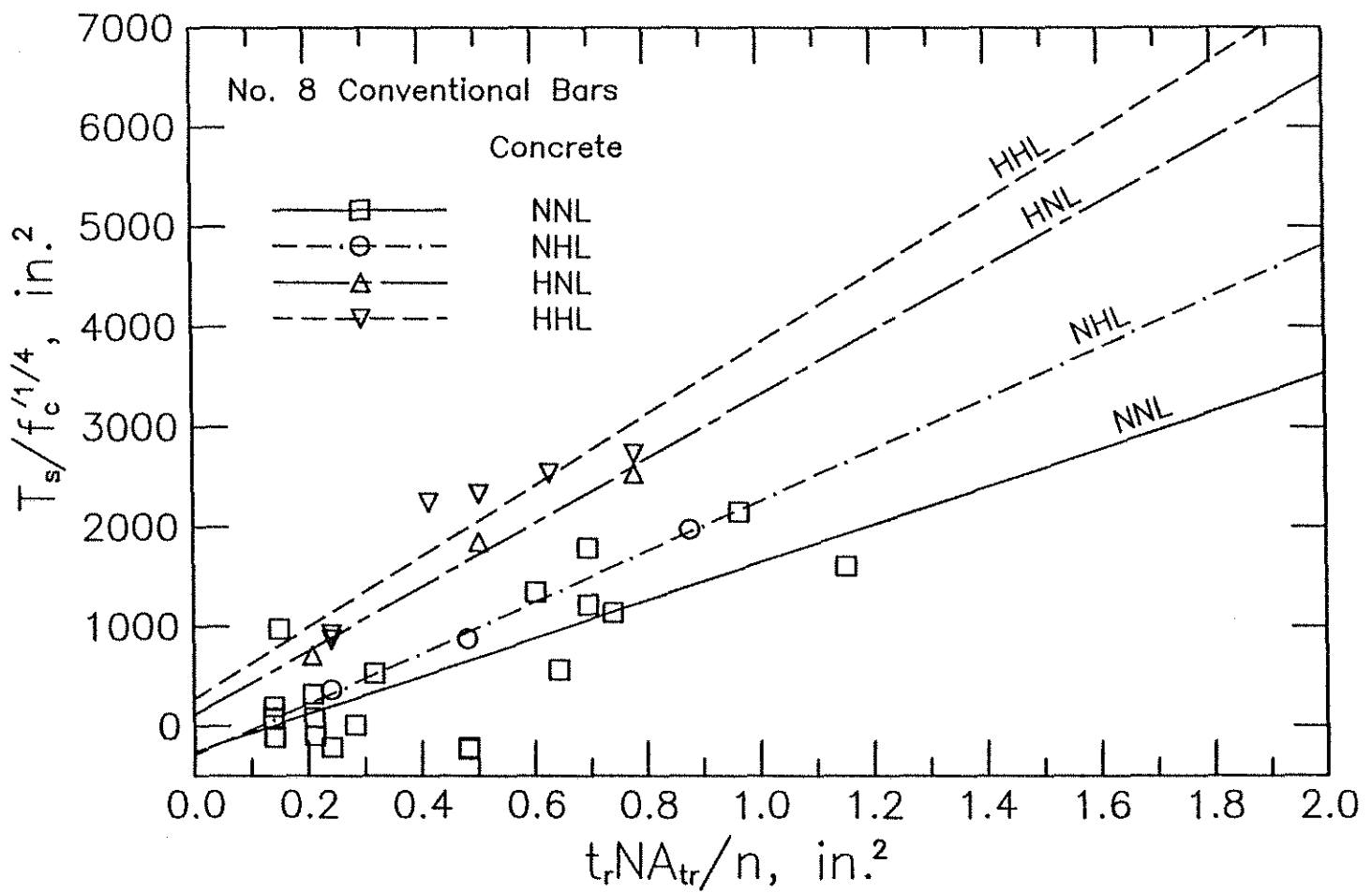


Fig. 4.3 Increase in bond force, T_s , normalized with respect to $f'_c{}^{1/4}$, versus $t_r N A_{tr}/n$ for No. 8 conventional bars in NNL, NHL, HNL, and HHL concretes, showing contributions to splice strength as a function of concrete strength and quantity of coarse aggregate

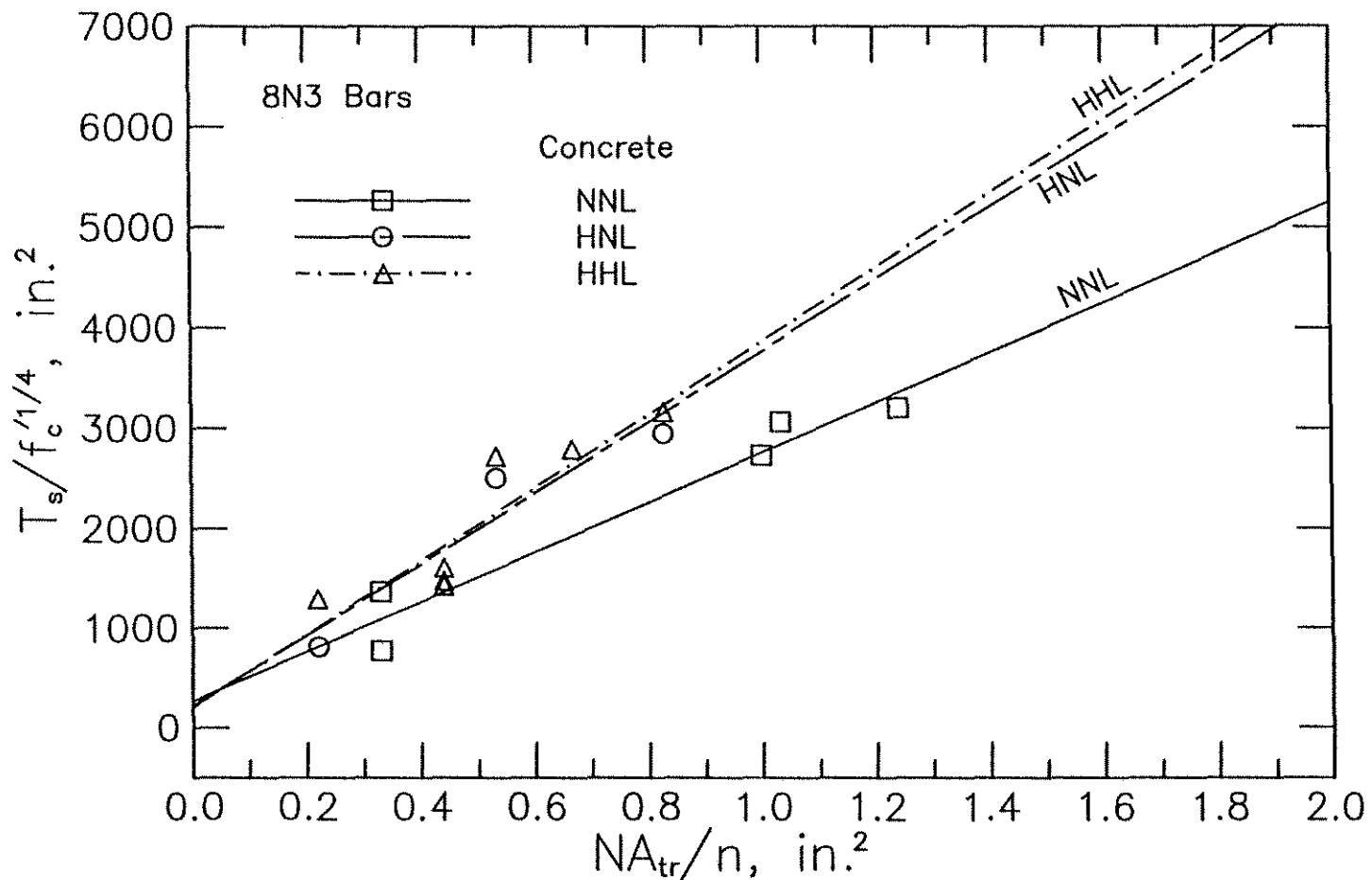


Fig. 4.4 Increase in bond force, T_s , normalized with respect to, $f'_c^{1/4}$ versus N_A_{tr}/n for the 8N3 bars in NNL, HNL, and HHL concrete, showing contributions to splice strength as a function of concrete strength and quantity of coarse aggregate

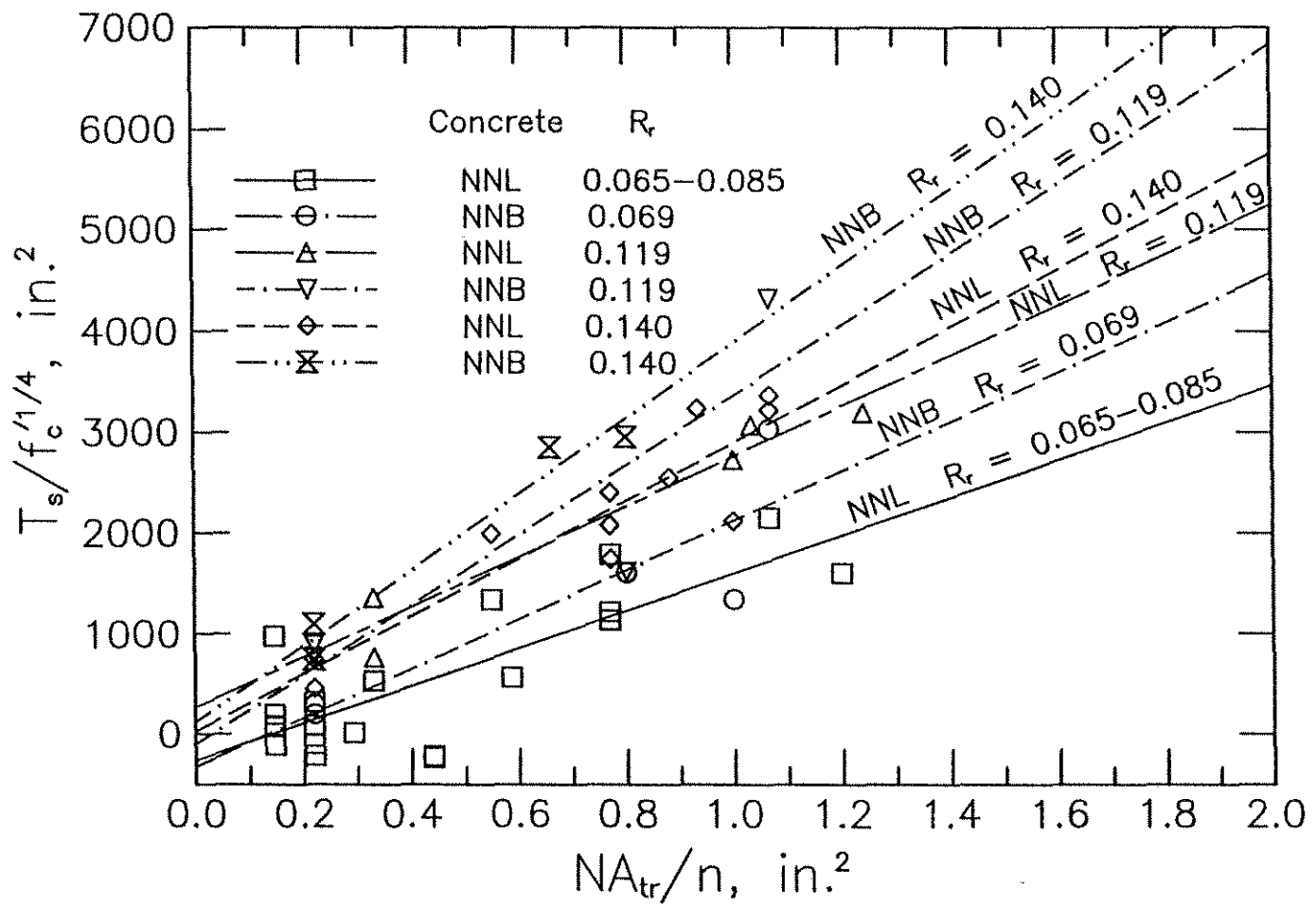


Fig. 4.5 Increase in bond force, T_s , normalized with respect to, $f_c^{1/4}$ versus NA_{tr}/n for No. 8 bars in normal-strength concrete as affected by type of coarse aggregate and relative rib area

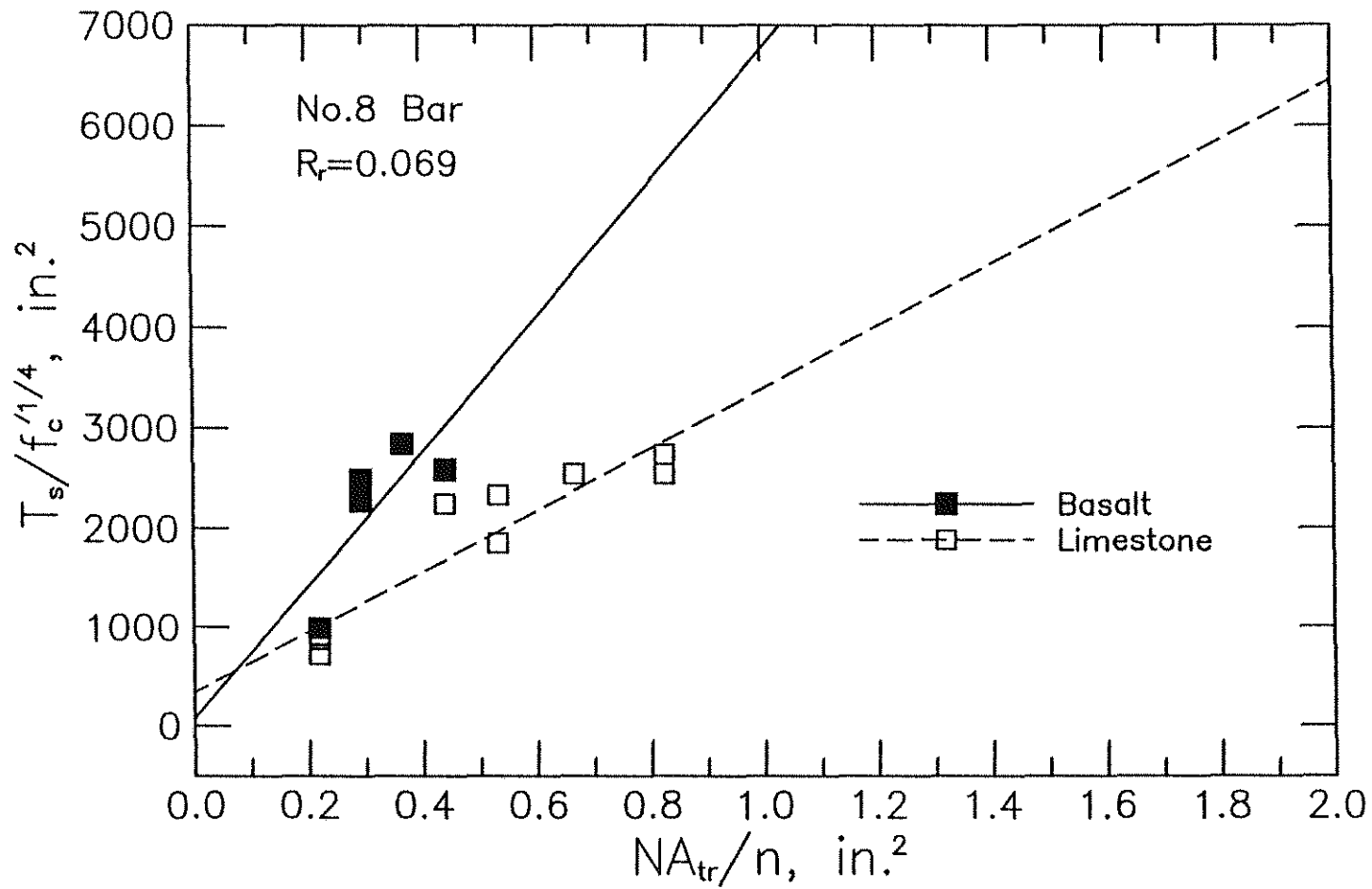


Fig. 4.6 Increase in bond force, T_s , normalized with respect to, $f'_c{}^{1/4}$ versus NA_{tr}/n for No. 8 (8N0) conventional bars in high-strength concrete as affected by type of coarse aggregate

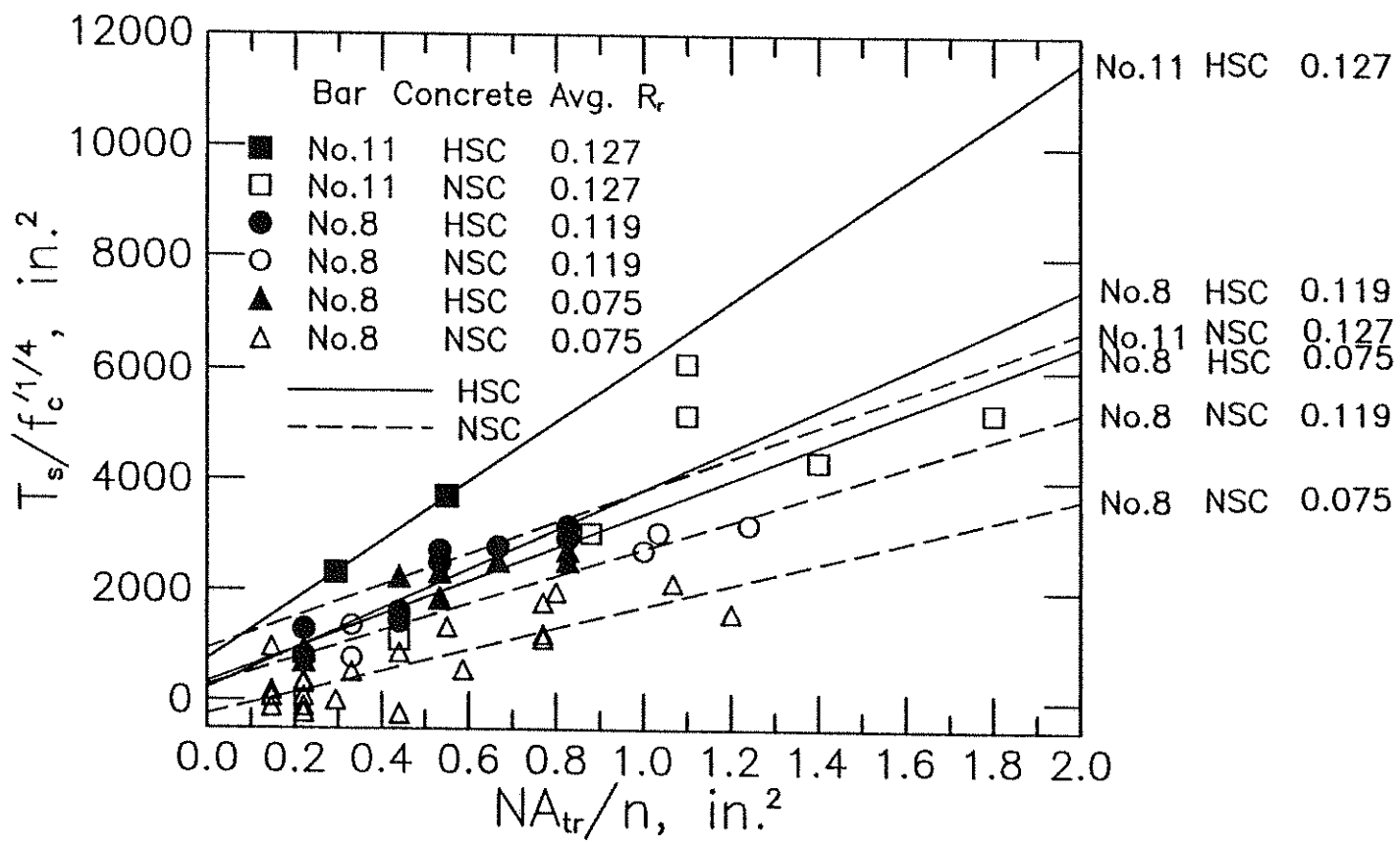


Fig. 4.7 Increase in bond force, T_s , normalized with respect to $f'_c{}^{1/4}$, versus N_A_{tr}/n for No. 8 conventional bars and the 8N3 and 11F3 high R_t bars as affected by concrete strength

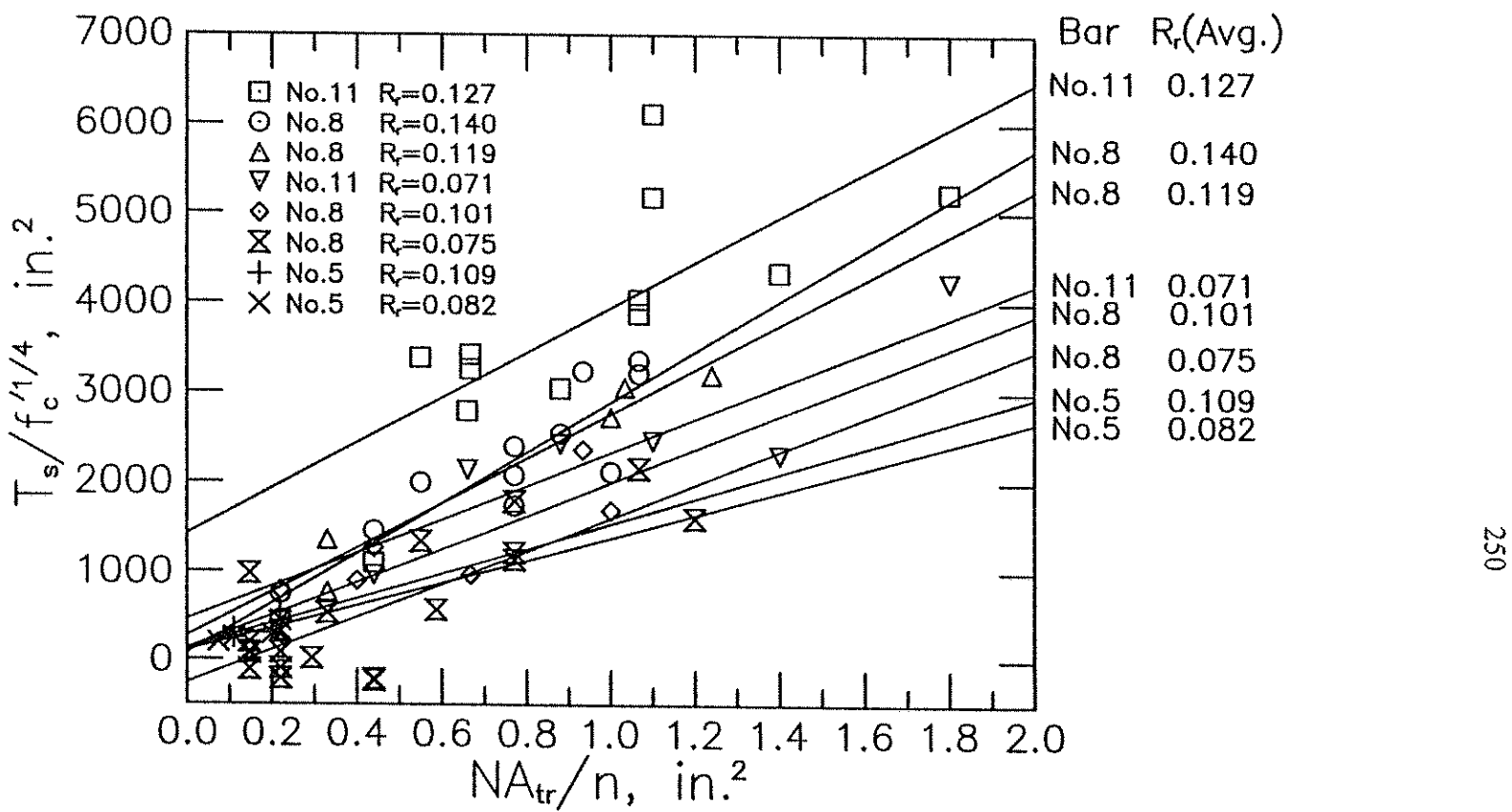


Fig. 4.8 Increase in bond force, T_s , normalized with respect to $f'_c^{1/4}$, versus NA_{tr}/n for bars in NNL concrete as affected by bar size and relative rib area

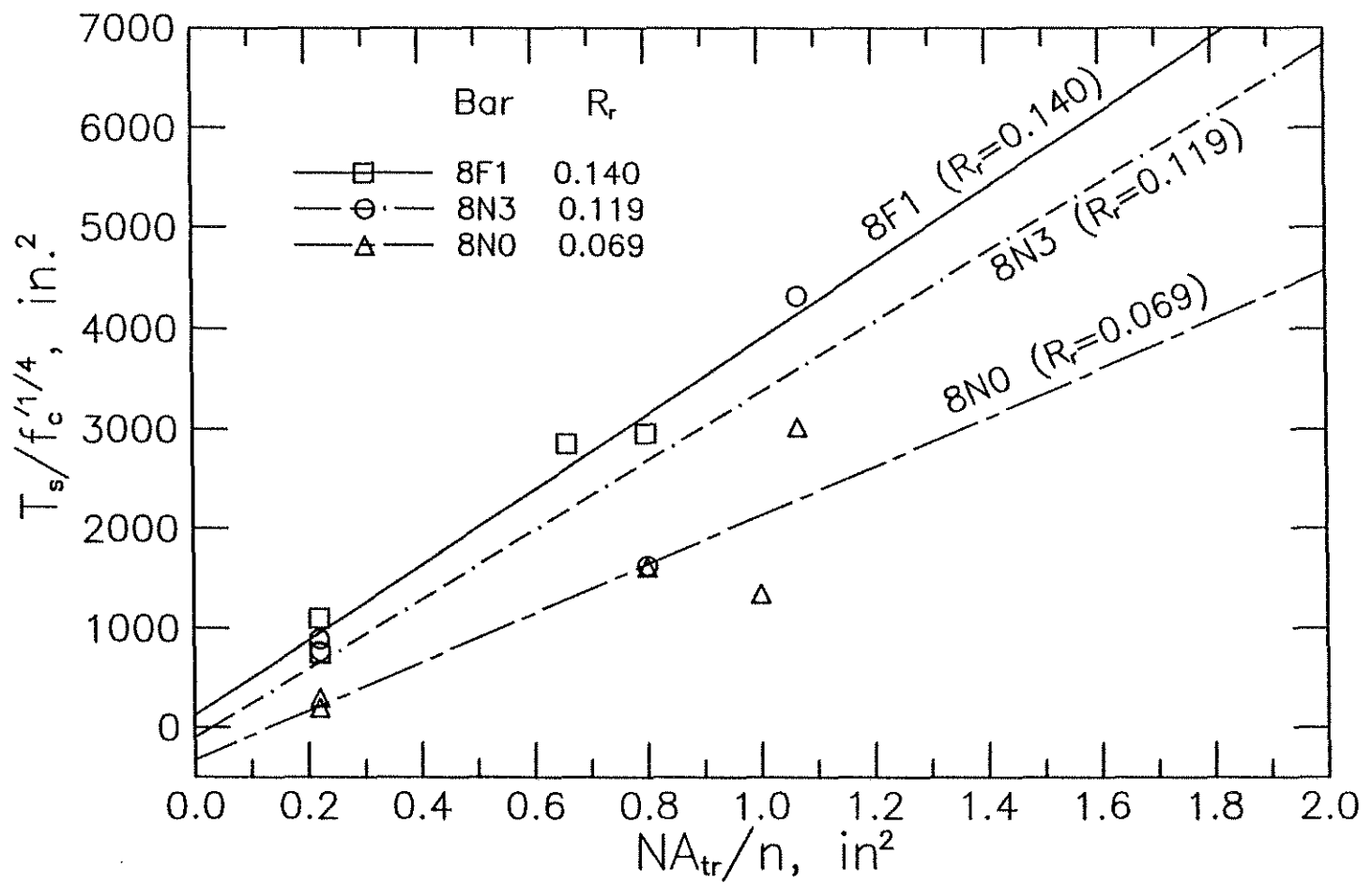


Fig. 4.9 Increase in bond force, T_s , normalized with respect to $f'_c^{1/4}$, versus NA_{tr}/n for No. 8 bars in NNB concrete as affected by relative rib area

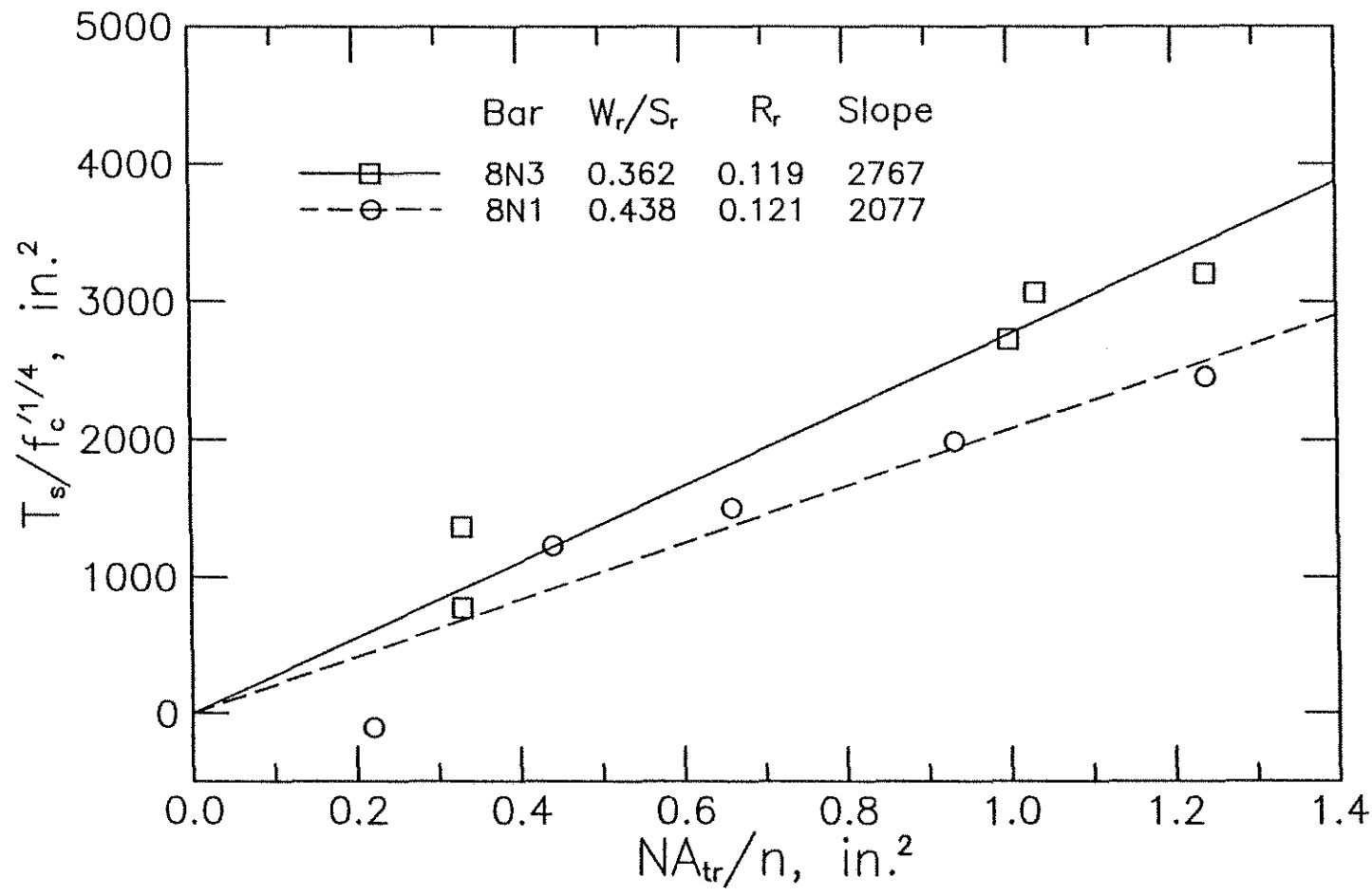


Fig. 4.10 Comparison of increase in bond force, T_s , normalized with respect to $f'_c^{1/4}$, for No. 8 high R_r bars as affected by bar rib width/spacing ratio

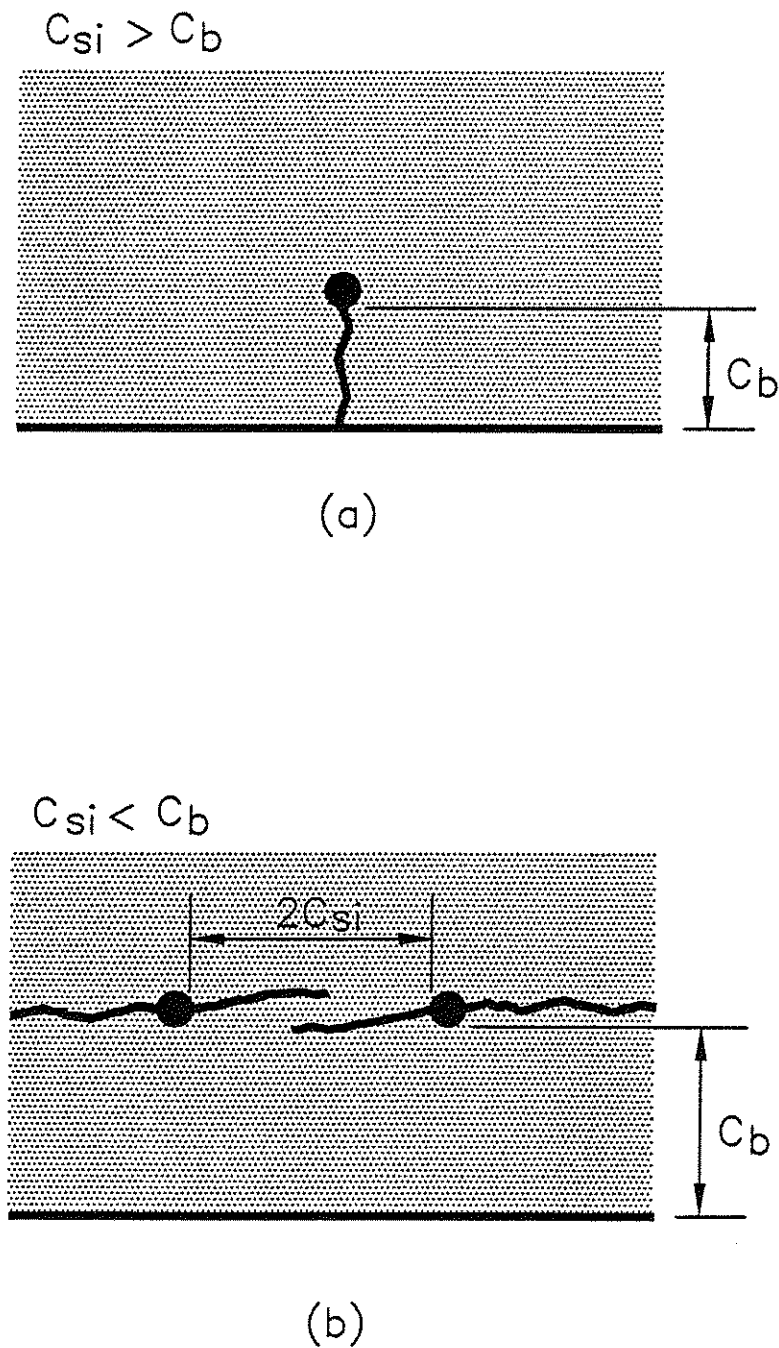


Fig. 5.1 Bond cracks: (a) $c_{si} > c_b$, (b) $c_{si} < c_b$ (Darwin et al. 1995a, 1996a)

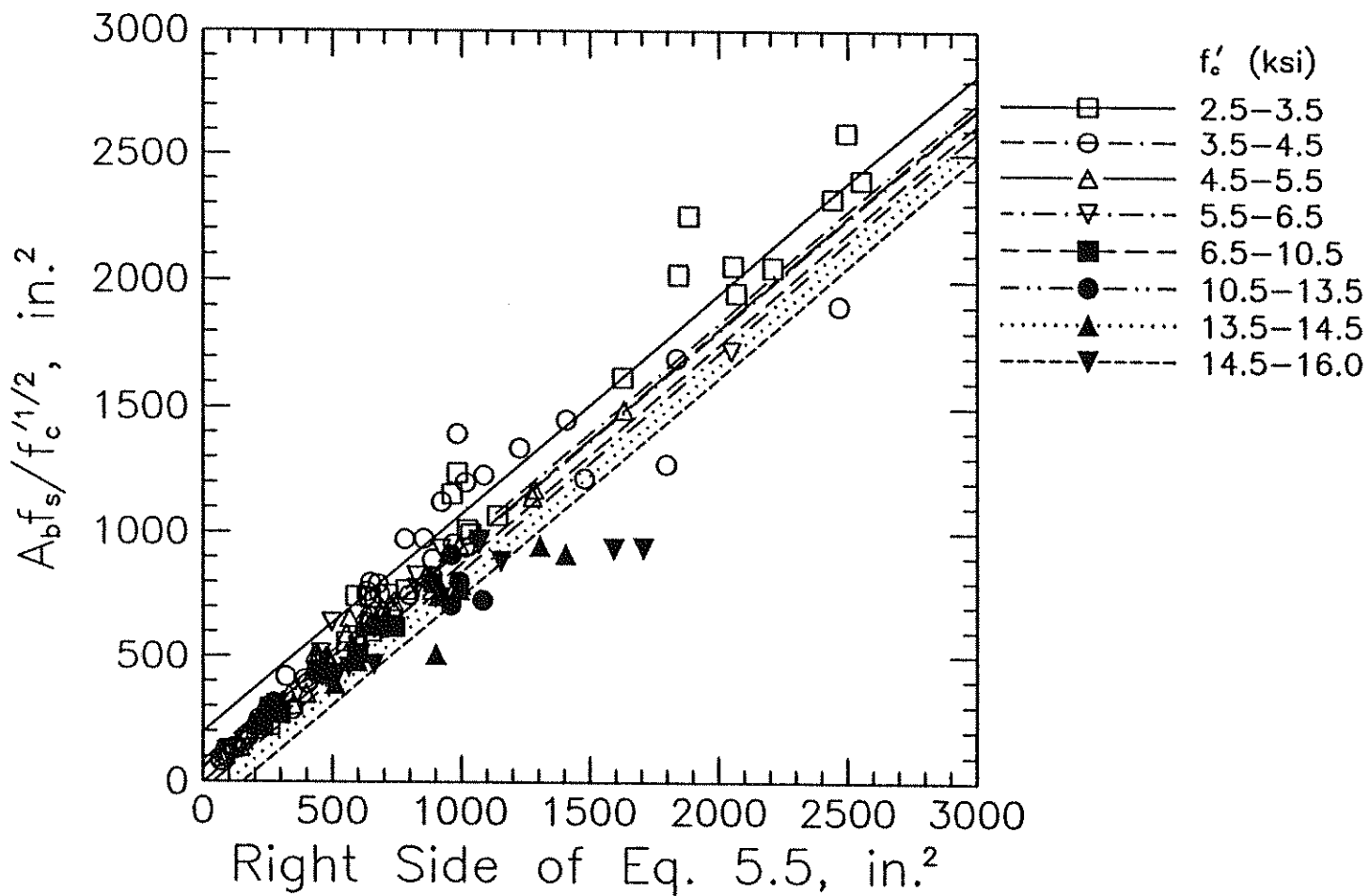


Fig. 5.2 Experimental bond force, $T_c = A_b f_s$, normalized with respect to $f_c'^{1/2}$, versus predicted bond strength determined using Eq. 5.5 as a function of concrete strength for bars without confining transverse reinforcement

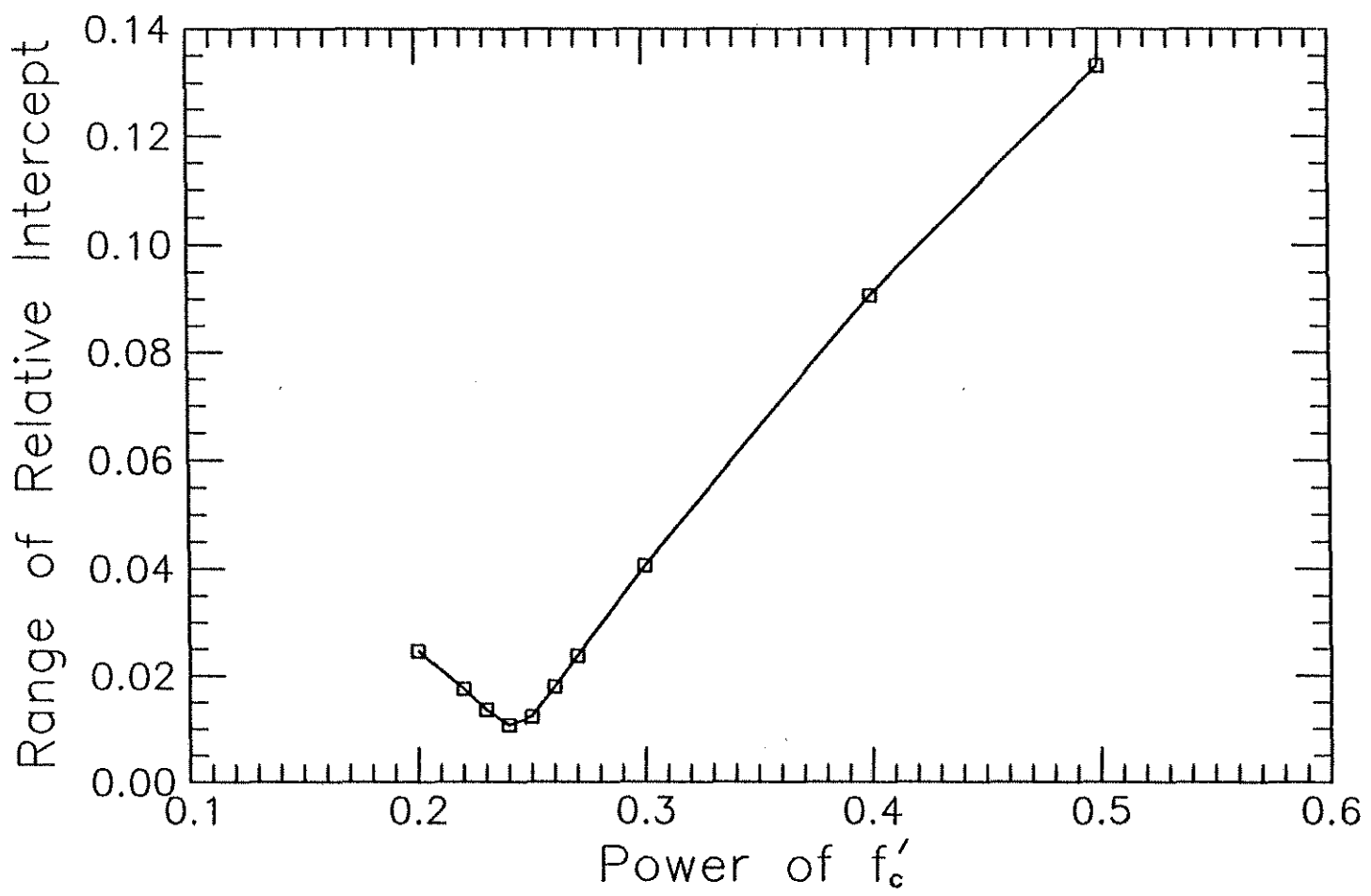


Fig. 5.3 Range of relative intercept obtained from dummy variable analyses for experimental bond force, normalized with respect to $f'_c P$ versus predicted bond strength determined using Eq. 5.3 and $c_{si} + 0.25$ in. as the effective value of c_{si} as a function of the power of f'_c for bars without confining transverse reinforcement

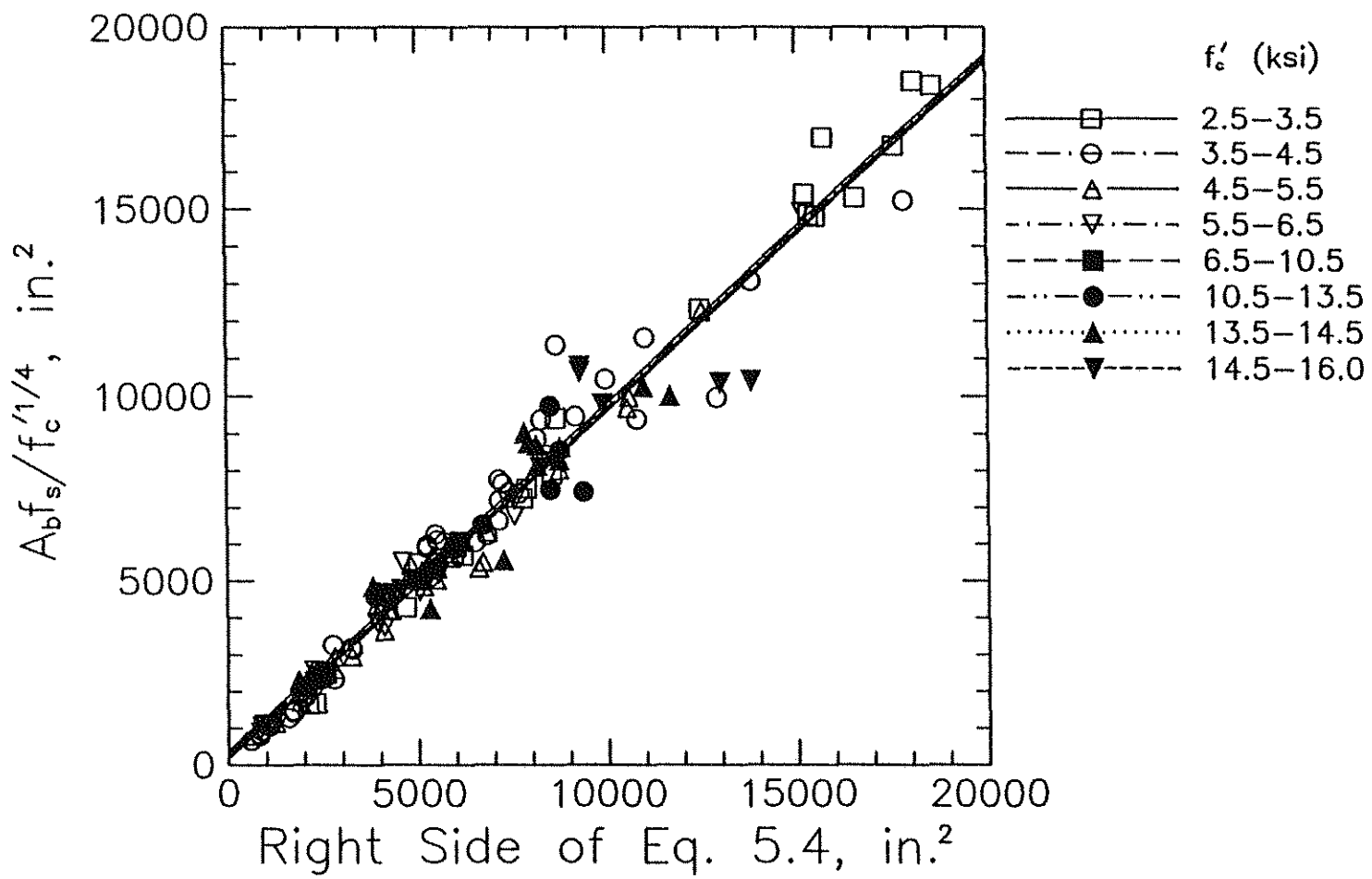


Fig. 5.4 Experimental bond force, $T_c = A_b f_s$, normalized with respect to $f_c'^{1/4}$, versus predicted bond strength determined using Eq. 5.4 as a function of concrete strength for bars without confining transverse reinforcement

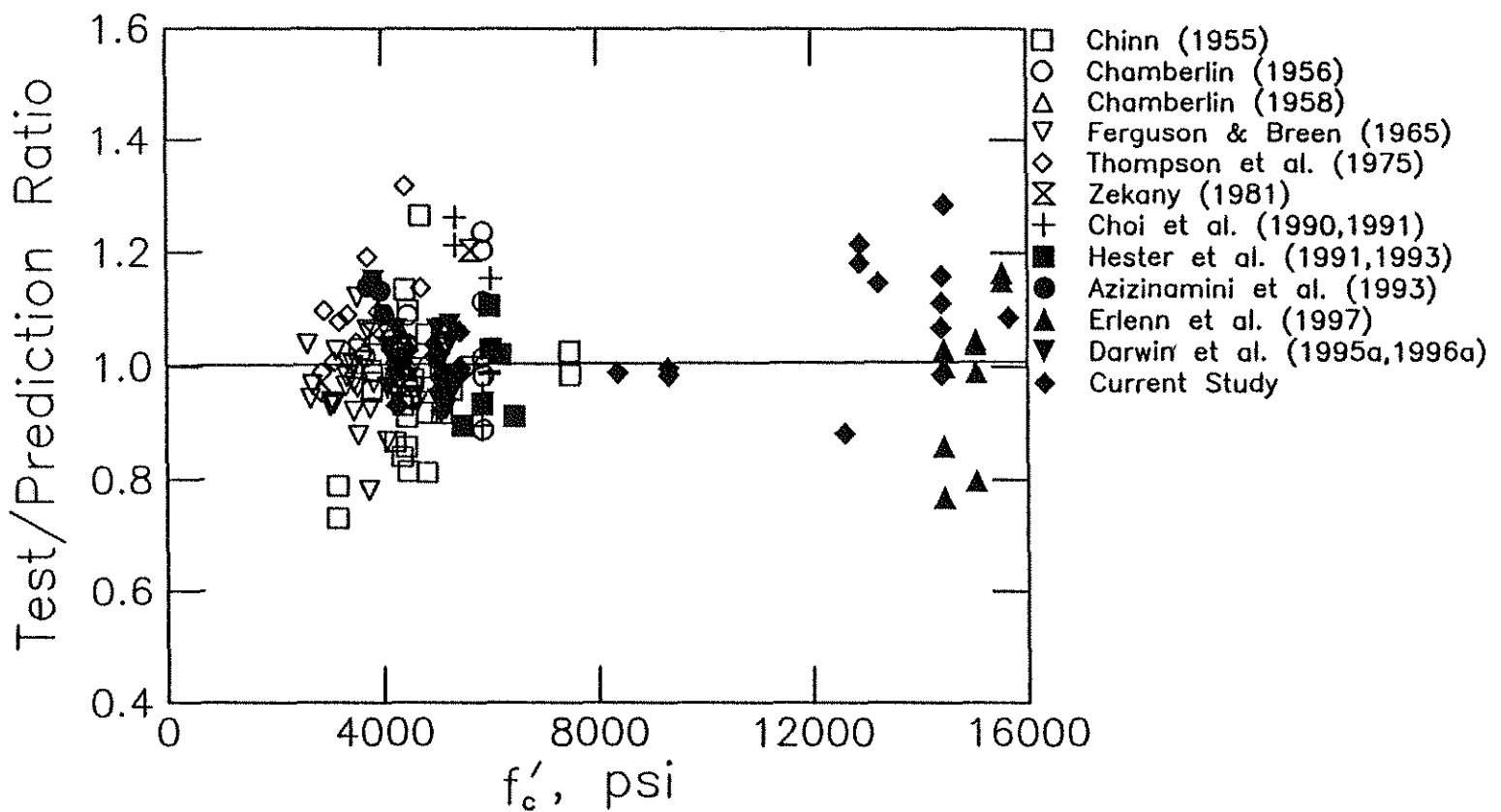


Fig. 5.5a Test/prediction ratio determined using Eq. 5.4 versus concrete compressive strength, f'_c , for bars without confining transverse reinforcement

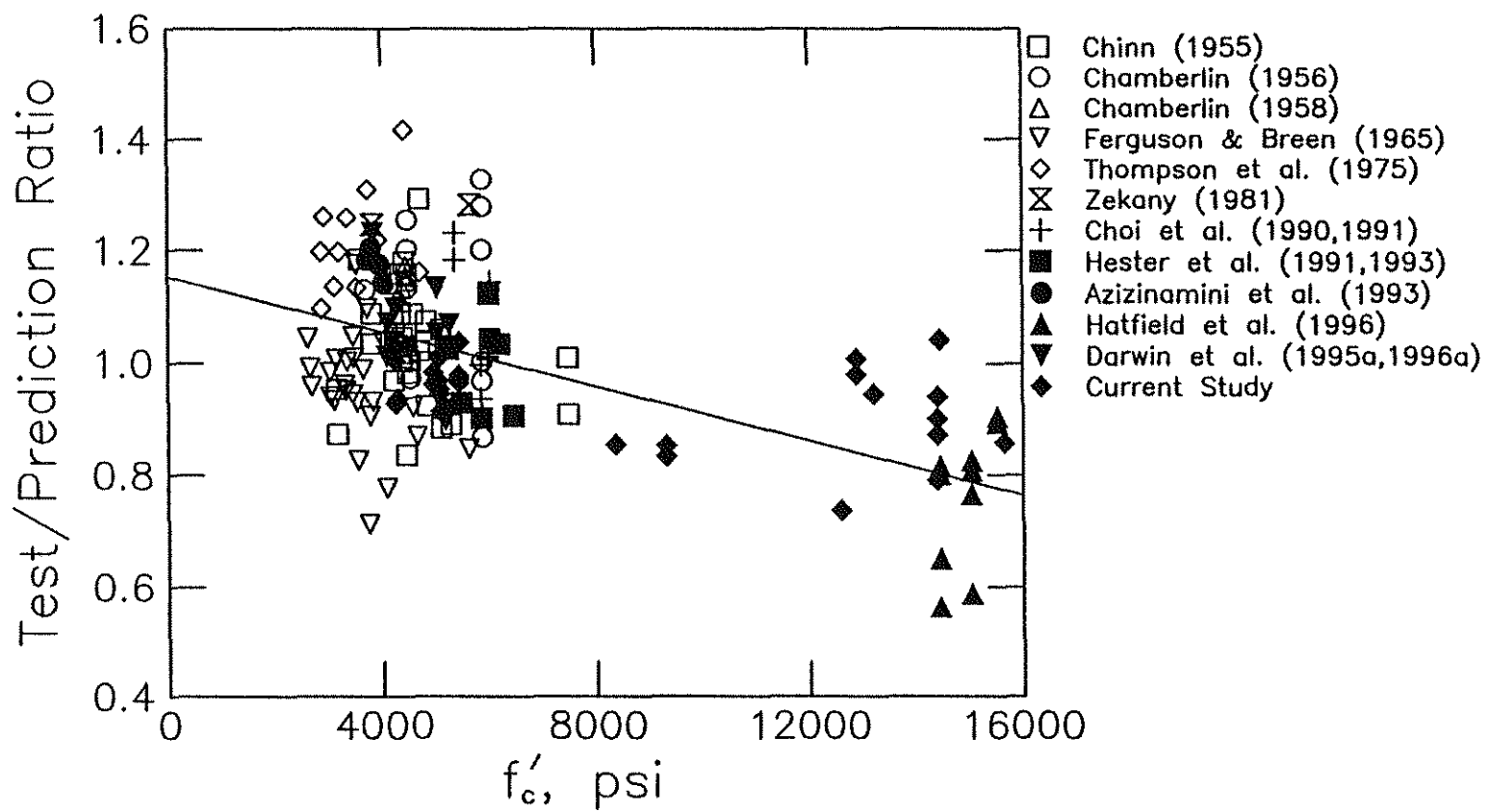


Fig. 5.5b Test/prediction ratio determined using Eq. 5.5 versus concrete compressive strength, f'_c , for bars without confining transverse reinforcement

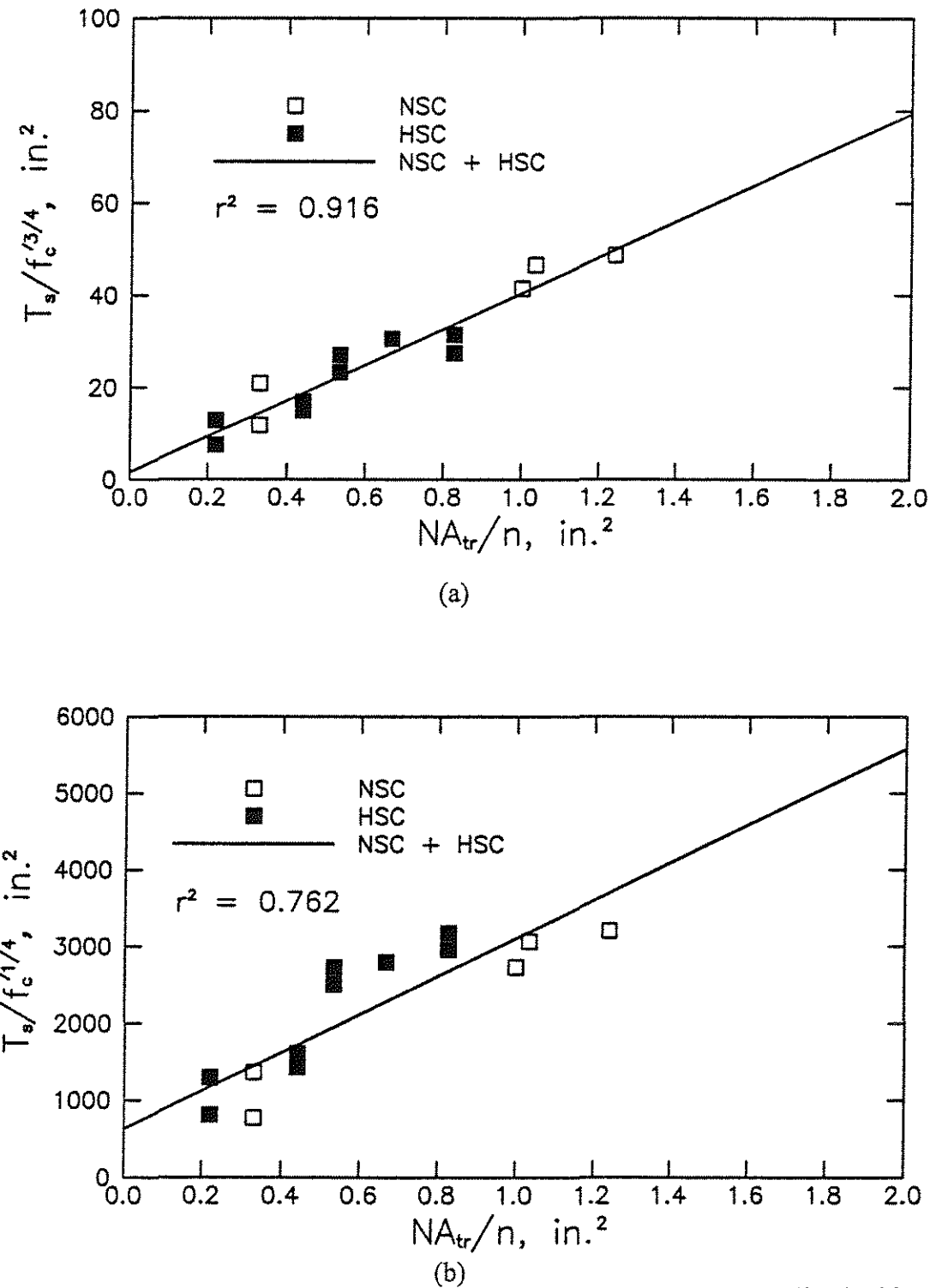


Fig. 5.6 Increase in bond force due to transverse reinforcement, T_s , normalized with respect to $f'_c P$ versus NA_{tr}/n for the 8N3 bars, (a) $p = \frac{3}{4}$, (b) $p = \frac{1}{4}$

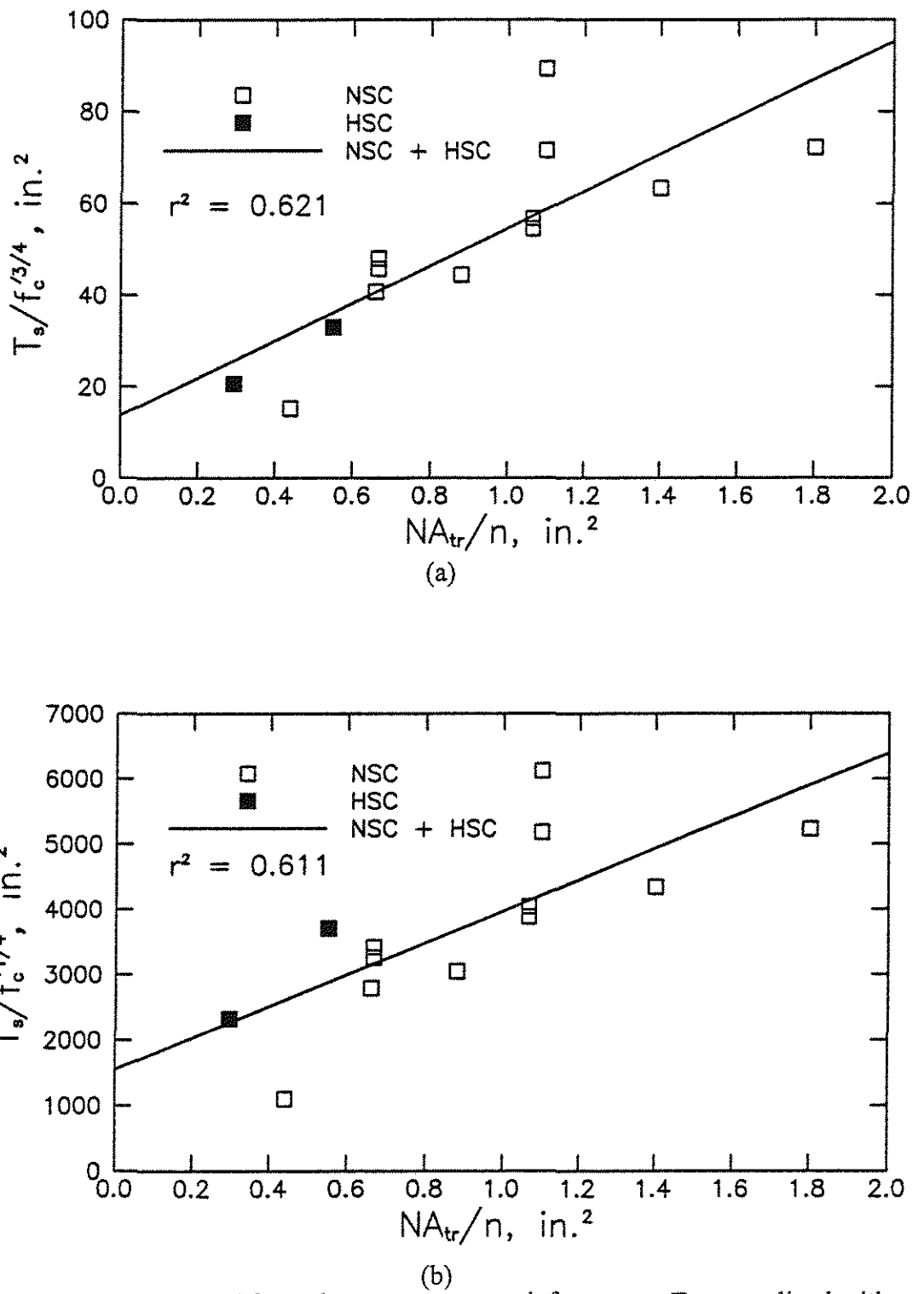
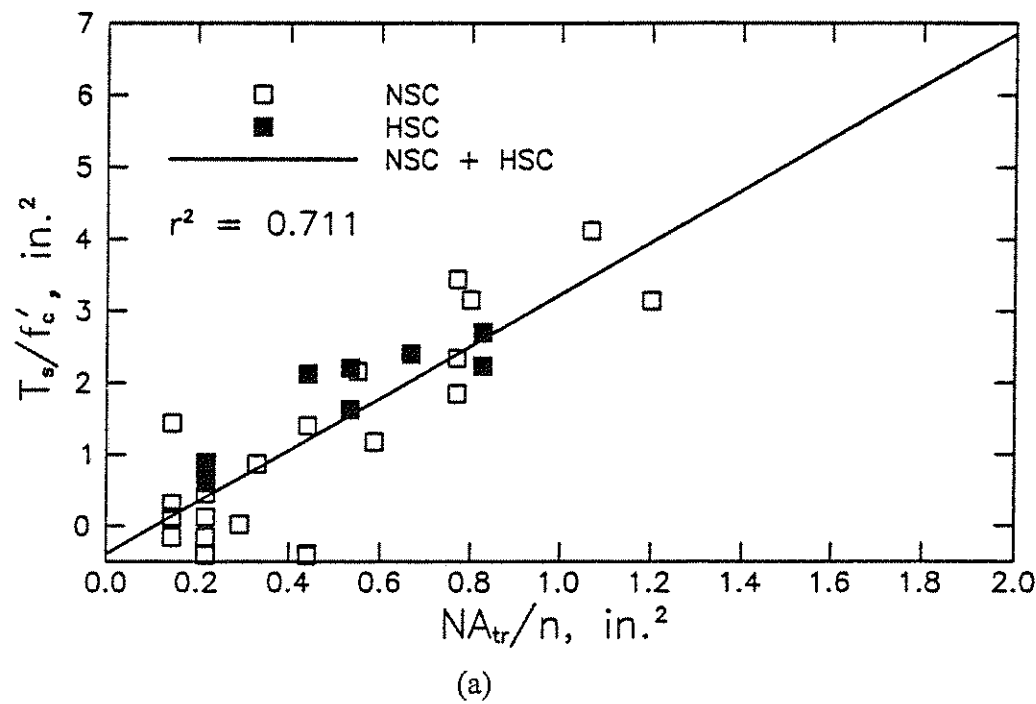
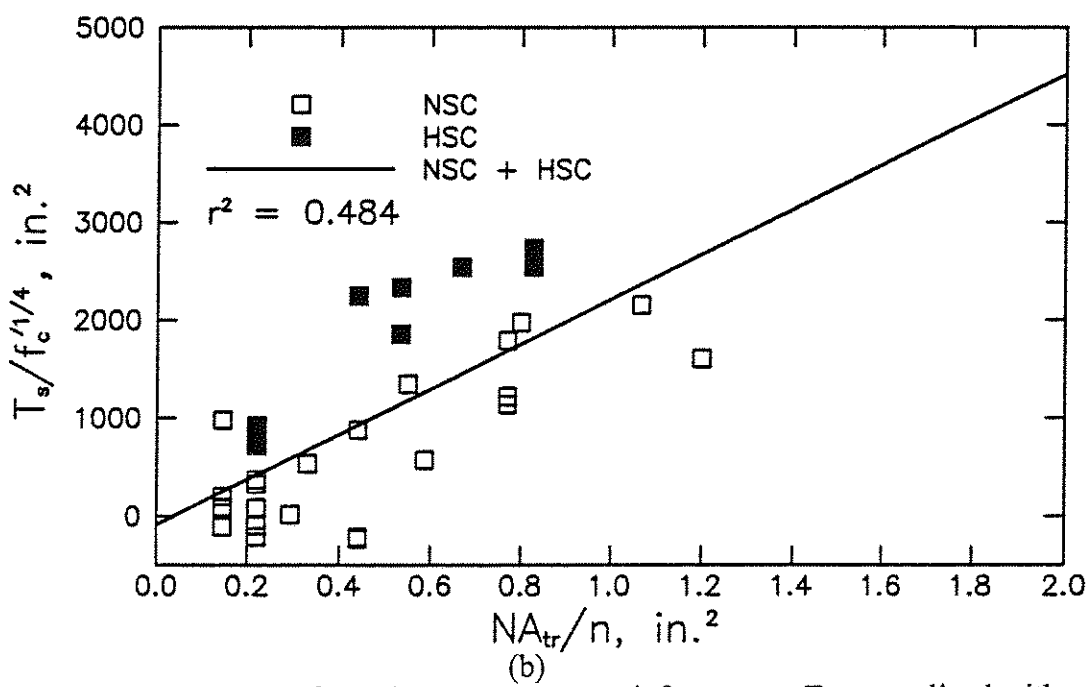


Fig. 5.7 Increase in bond force due to transverse reinforcement, T_s , normalized with respect to $f'_c{}^p$ versus NA_{tr}/n for the 11F3 bars, (a) $p = 3/4$, (b) $p = 1/4$



(a)



(b)

Fig. 5.8 Increase in bond force due to transverse reinforcement, T_s , normalized with respect to f'_c^p versus NA_{tr}/n for No. 8 conventional bars, (a) $p = 1.0$, (b) $p = 1/4$

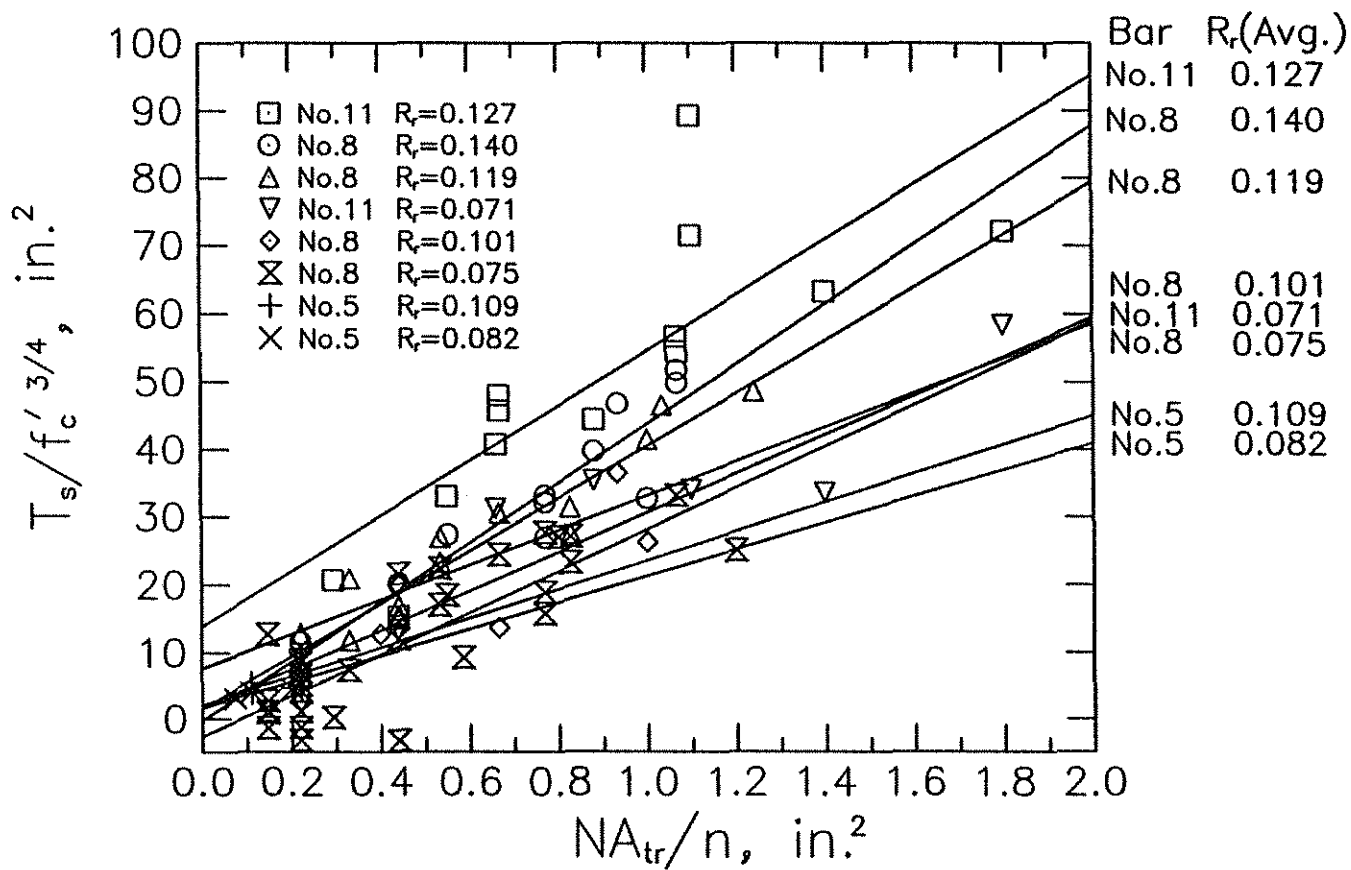


Fig. 5.9 Increase in bond force due to transverse reinforcement, T_s , normalized with respect to $f_c'^{3/4}$, versus NA_{tr}/n for bars in concrete containing limestone coarse aggregate

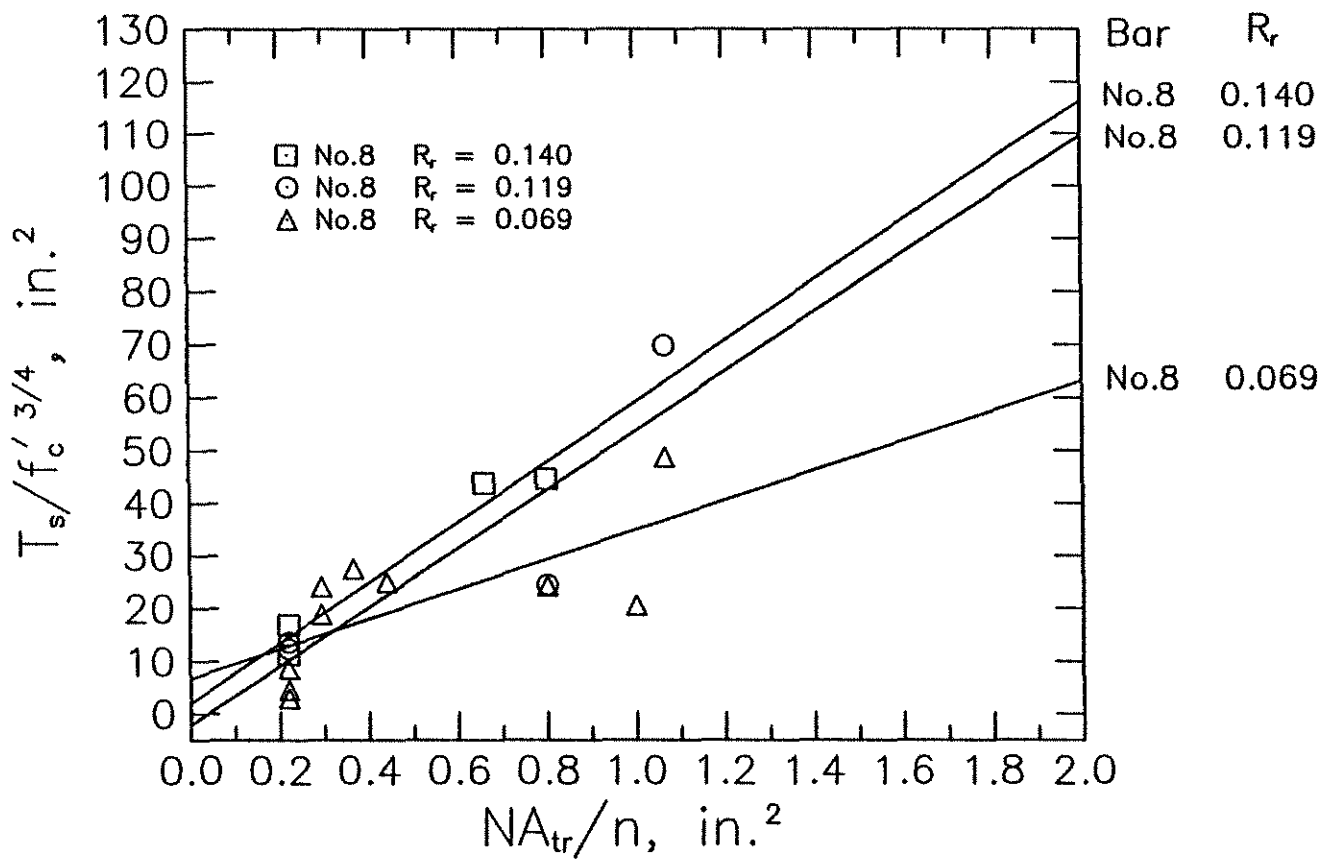


Fig. 5.10 Increase in bond force due to transverse reinforcement, T_s , normalized with respect to $f'_c{}^{3/4}$, versus NA_{tr}/n for bars in concrete containing basalt coarse aggregate

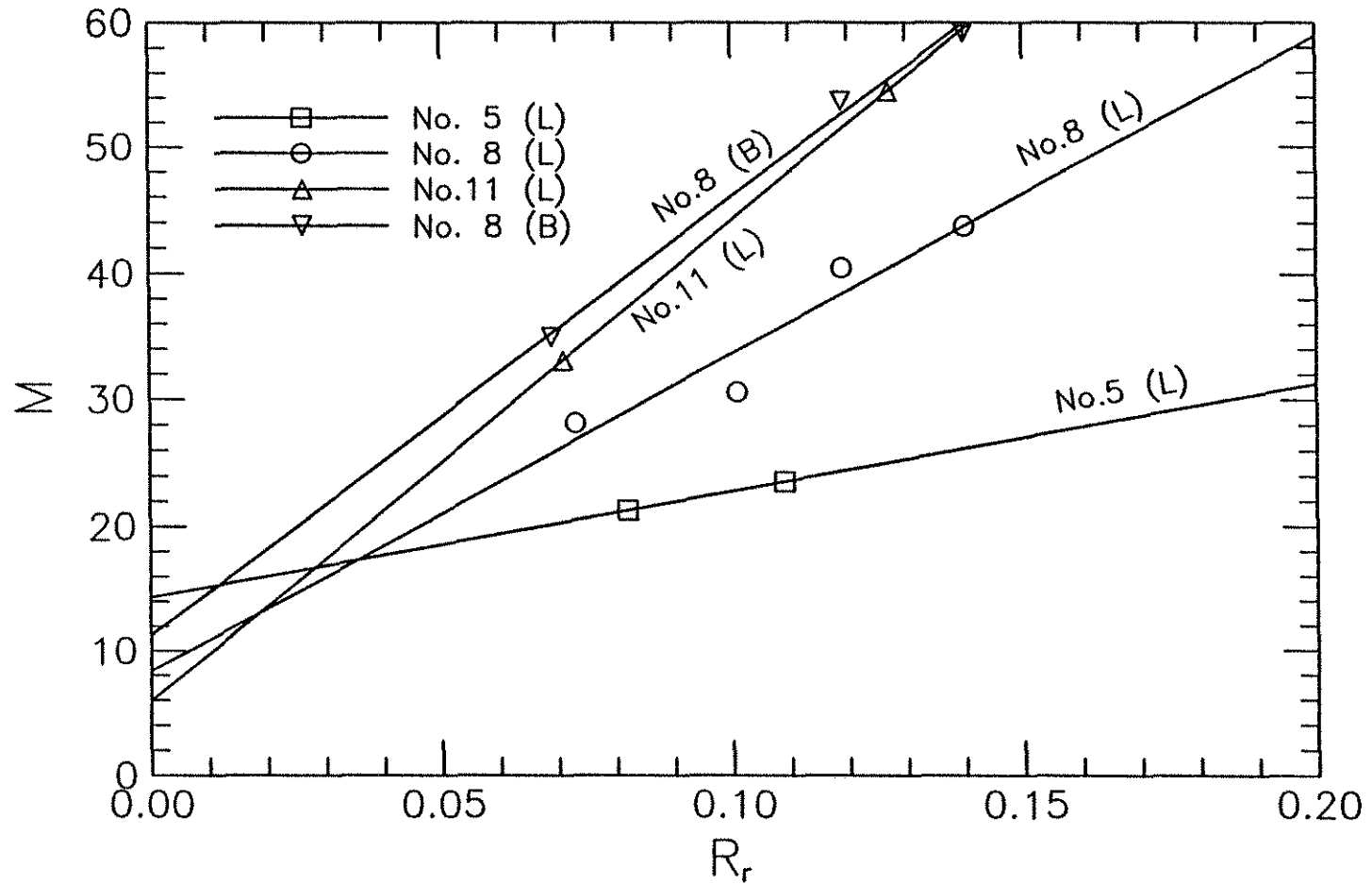


Fig. 5.11 Mean slope from Eq. 5.7, M , for $p = 3/4$ versus relative rib area, R_r , for No. 5, No. 8, and No. 11 bars cast in concrete containing limestone coarse aggregate and No. 8 bars cast in concrete containing basalt coarse aggregate

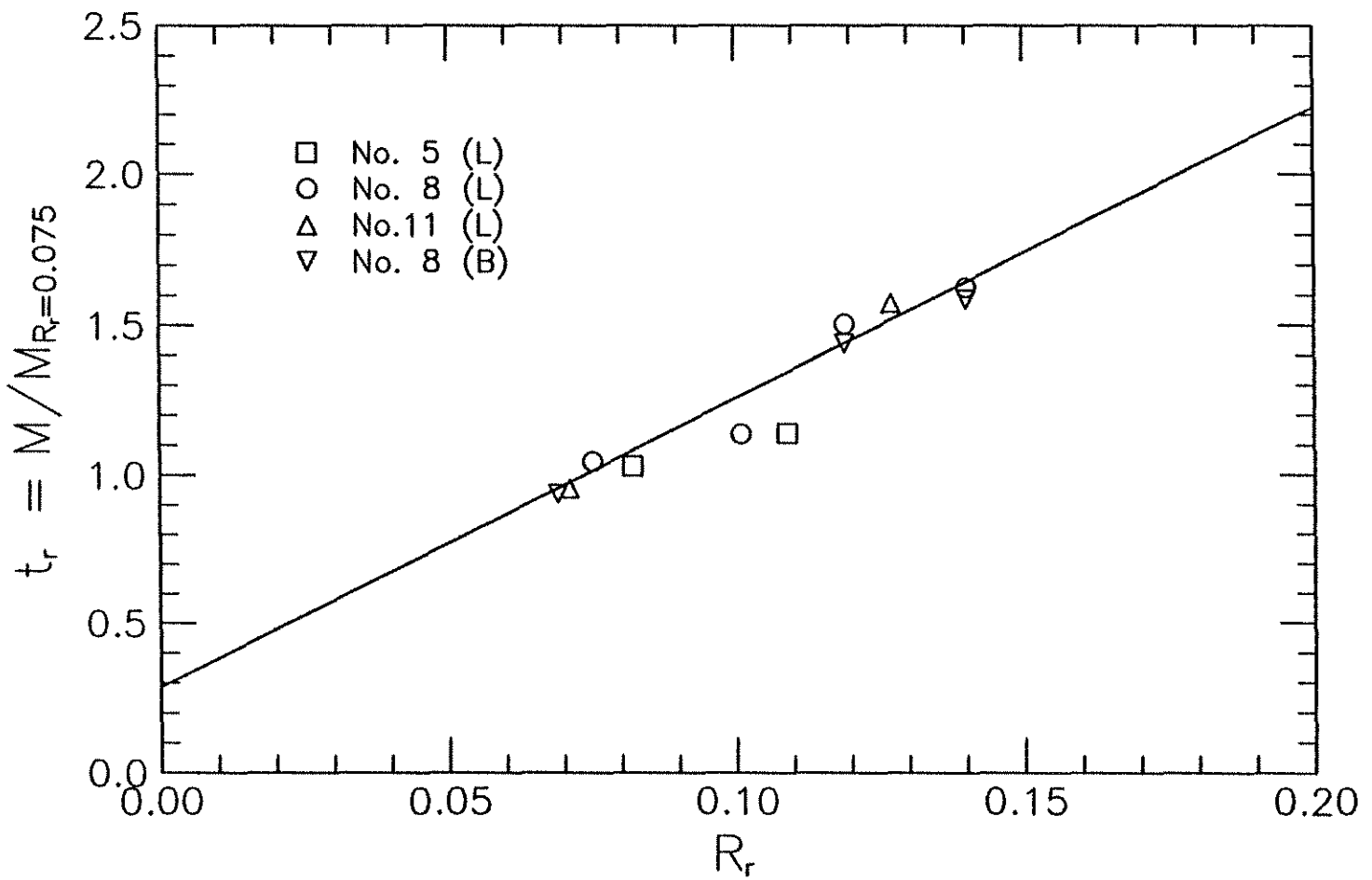


Fig. 5.12 Factor representing effect of relative rib area on increase in bond strength due to transverse reinforcement, $M/M_{R_f}=0.075$, versus relative rib area, R_r

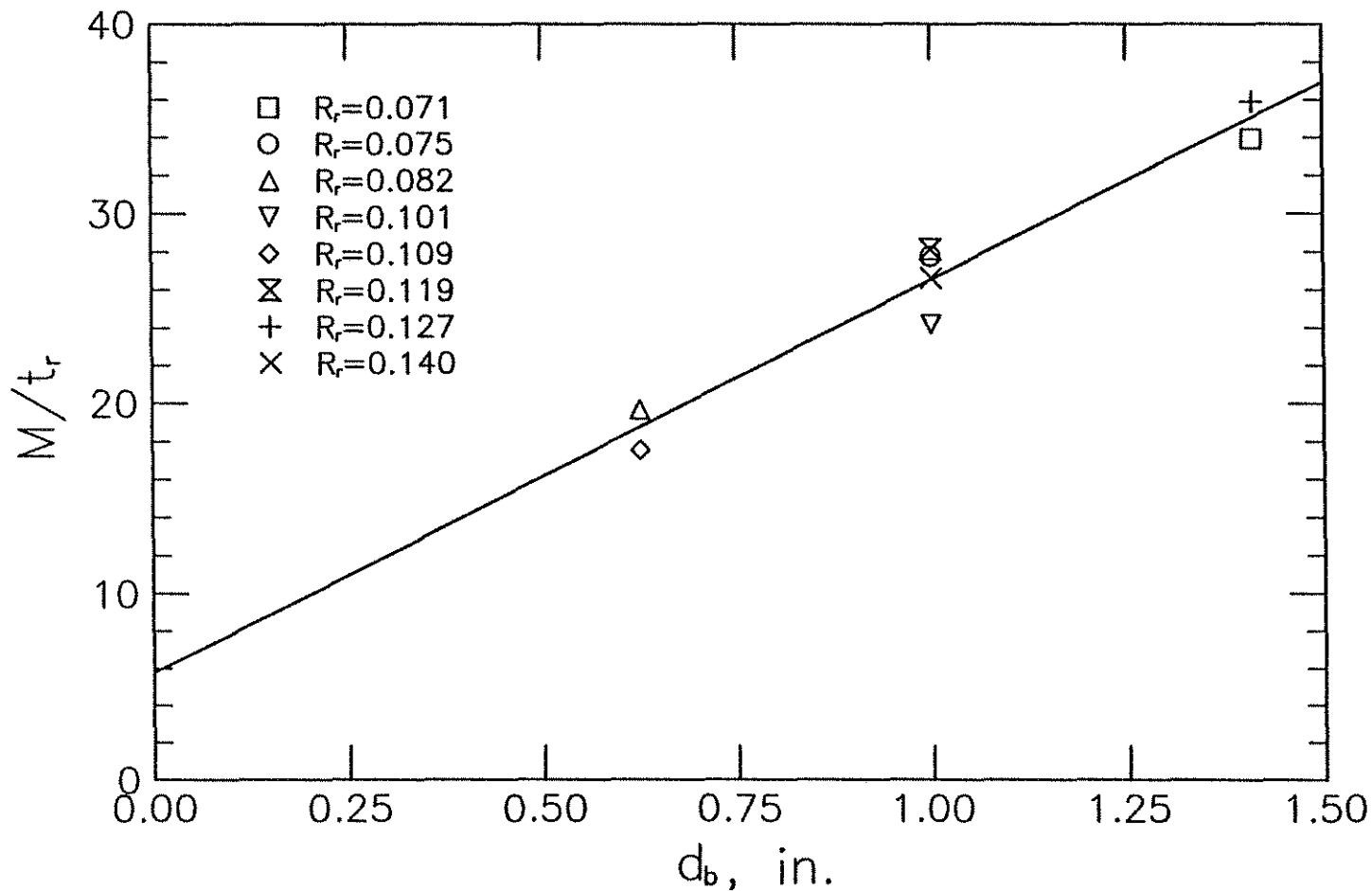


Fig. 5.13 Mean slope from Eq. 5.7, M , normalized with respect to $t_r = 9.6 R_r + 0.28$ versus nominal bar diameter, d_b

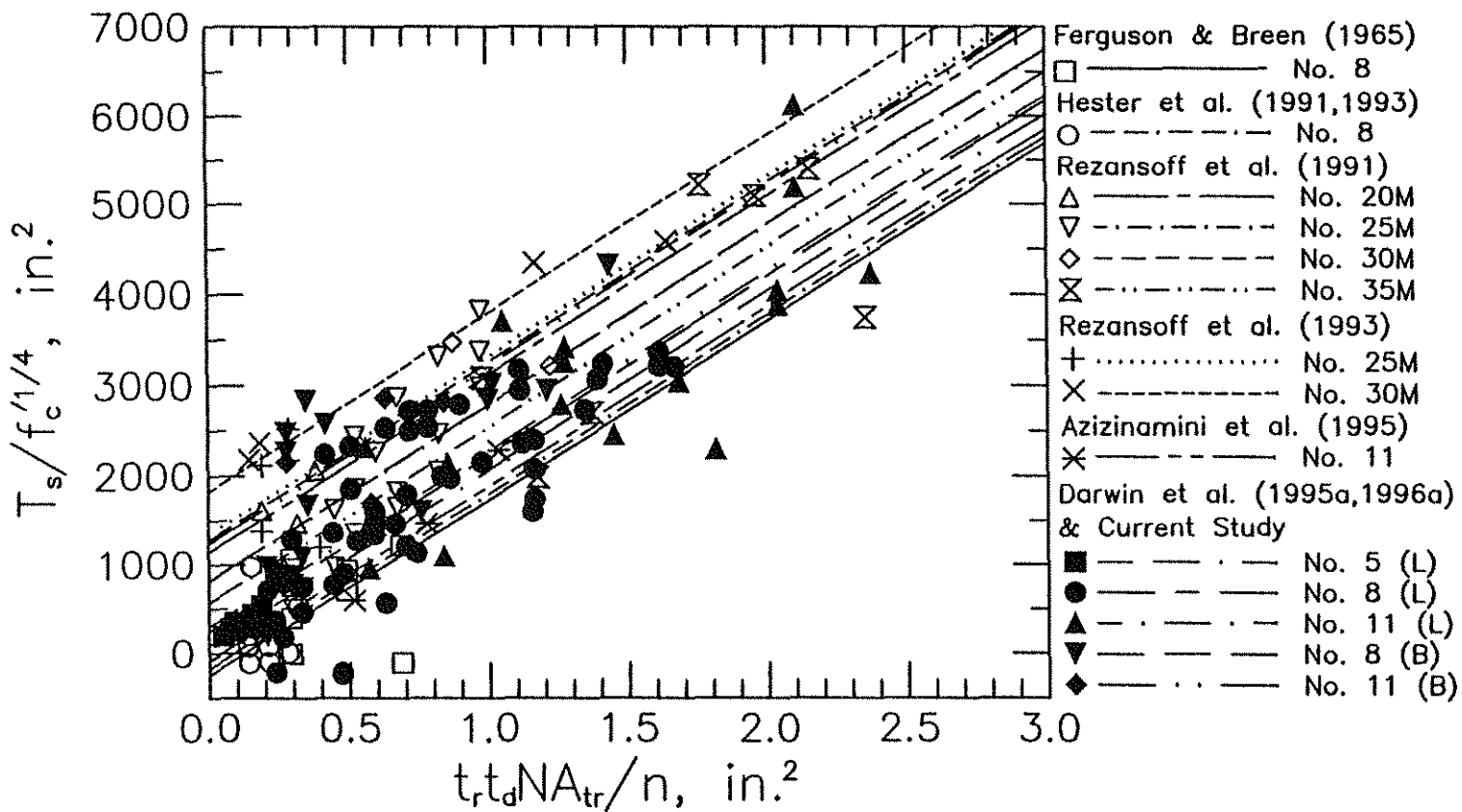


Fig. 5.14a Increase in bond force due to transverse reinforcement, T_s , normalized with respect to $f'_c^{1/4}$, versus $(t_r t_d N A_{tr}/n)^{p=1/4}$ for 163 specimens with $l_d/d_b \geq 16$ and $(c + K_{tr})/d_b \leq 4$, [in this case, $K_{tr} = 35.3 t_r t_d N A_{tr}/n$, $t_r = 9.6 R_r + 0.28$, and $t_d = 0.72 d_b + 0.28$, as developed by Darwin et al. (1995b, 1996b)]

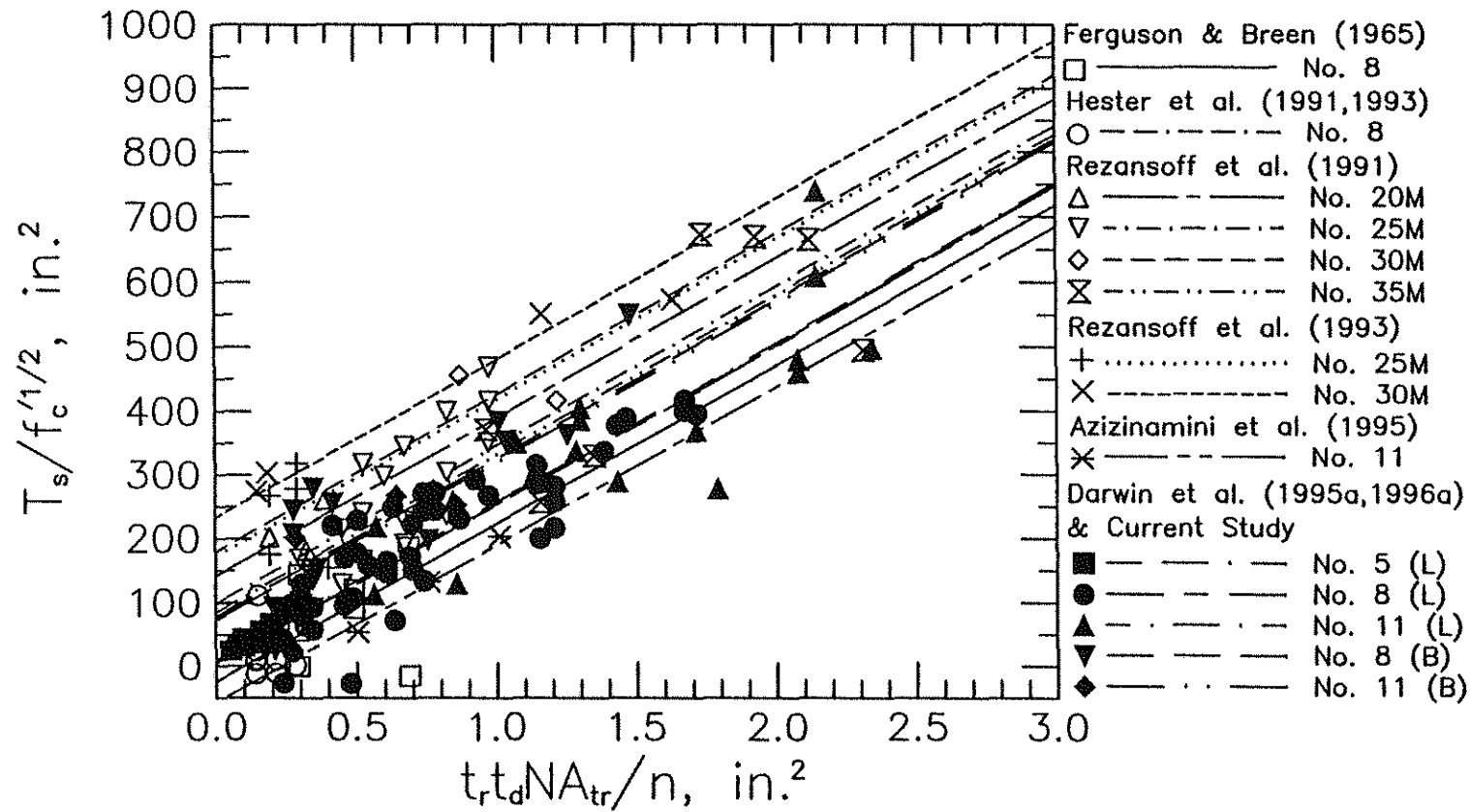


Fig. 5.14b Increase in bond force due to transverse reinforcement, T_s , normalized with respect to $f'_c^{1/4}$, versus $(t_r t_d N A_{tr}/n)^{1/2}$ for 163 specimens with $l_d/d_b \geq 16$ and $(c + K_{tr})/d_b \leq 4$, [in this case, $K_{tr} = 35.3 t_r t_d N A_{tr}/n$, $t_r = 9.6 R_r + 0.28$, and $t_d = 0.72 d_b + 0.28$, as developed by Darwin et al. (1995b, 1996b)]

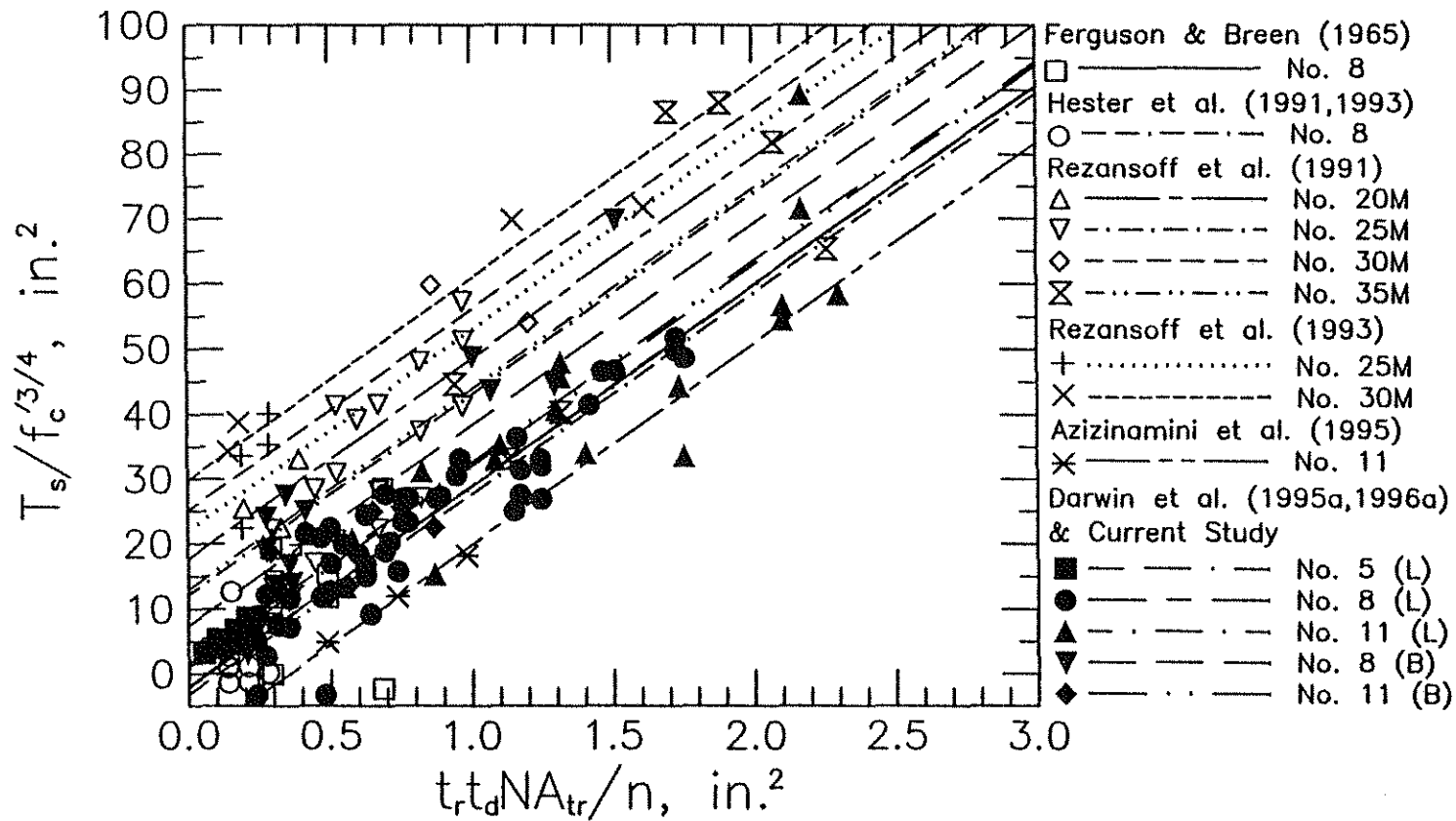


Fig. 5.14c Increase in bond force due to transverse reinforcement, T_s , normalized with respect to $f_c'^{3/4}$, versus $(t_r t_d N A_{tr} / n)^{3/4}$ for 163 specimens with $l_d/d_b \geq 16$ and $(c + K_{tr})/d_b \leq 4$, [in this case, $K_{tr} = 35.3 t_r t_d N A_{tr} / n$, $t_r = 9.6 R_r + 0.28$, and $t_d = 0.72 d_b + 0.28$, as developed by Darwin et al. (1995b, 1996b)]

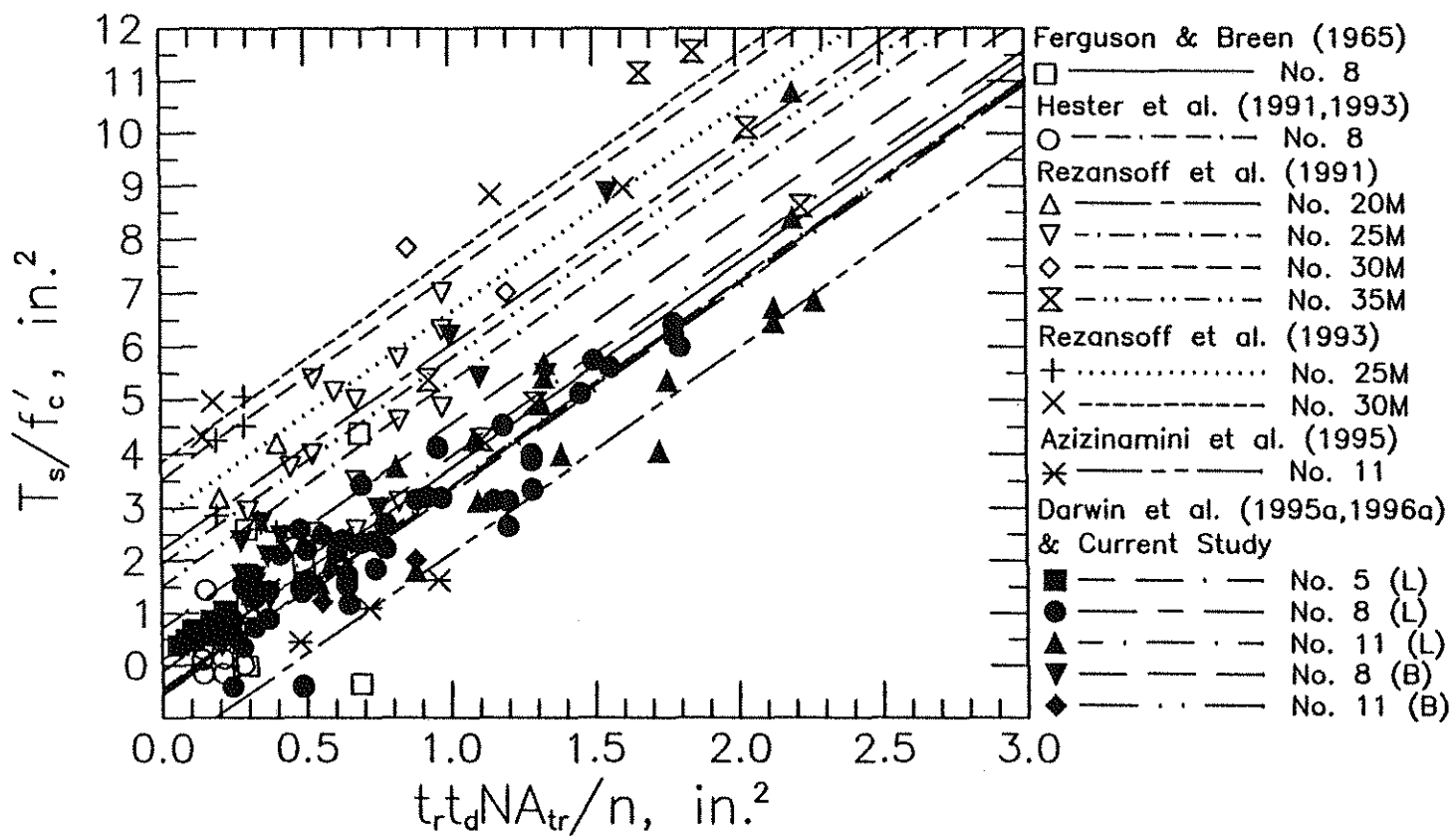


Fig. 5.14d Increase in bond force due to transverse reinforcement, T_s , normalized with respect to $f'_c^{1/4}$, versus $(t_r t_d N A_{tr}/n)_{p=1}$ for 163 specimens with $l_d/d_b \geq 16$ and $(c + K_{tr})/d_b \leq 4$, [in this case, $K_{tr} = 35.3 t_r t_d N A_{tr}/n$, $t_r = 9.6 R_f + 0.28$, and $t_d = 0.72 d_b + 0.28$, as developed by Darwin et al. (1995b, 1996b)]

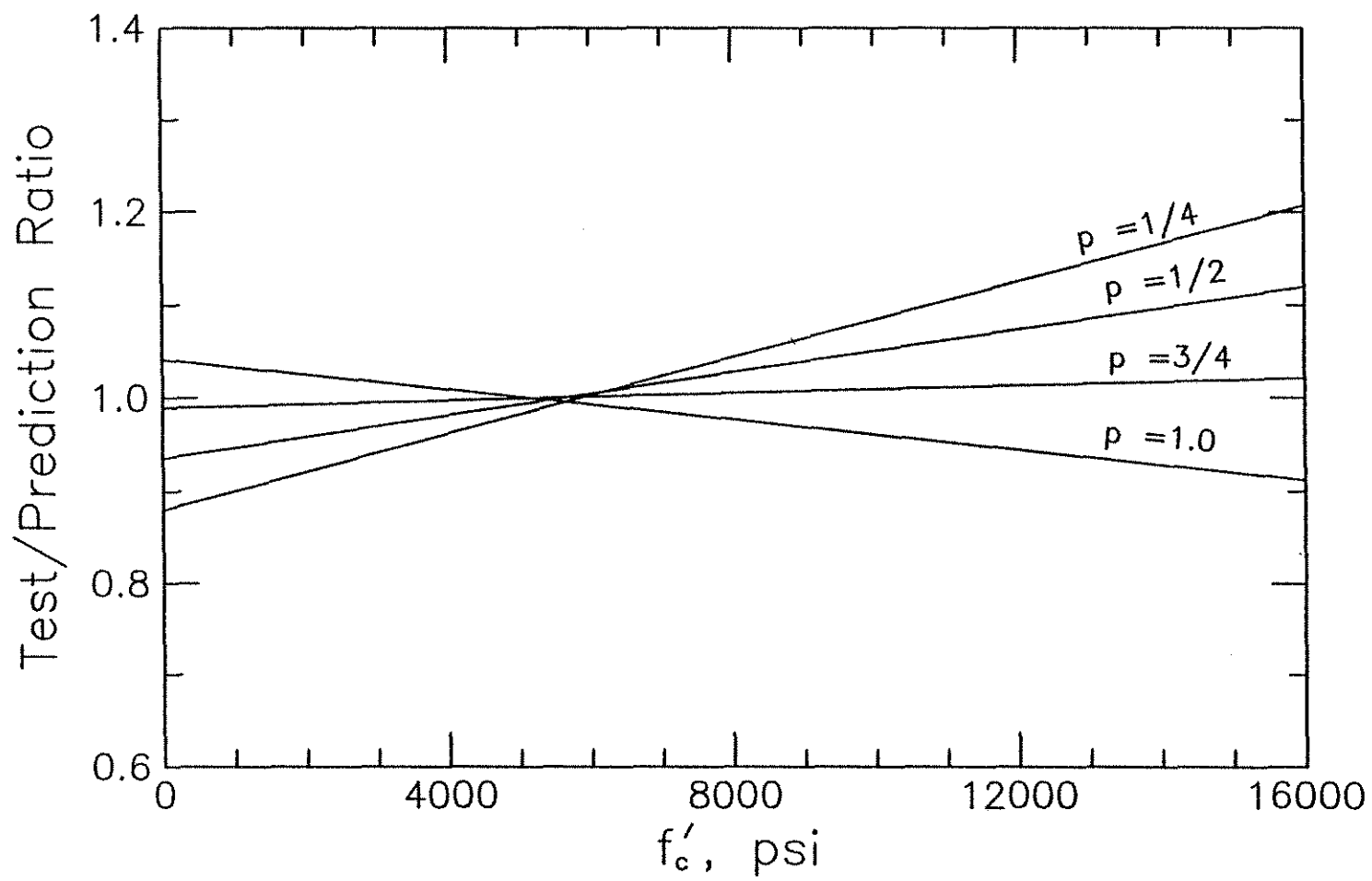


Fig. 5.15 Test/prediction ratios determined using Eqs. 5.13a - 5.13d corresponding to the powers of f'_c , $p = 1/4, 1/2, 3/4$, and 1.0, respectively, versus concrete compressive strength, f'_c , for 163 specimens

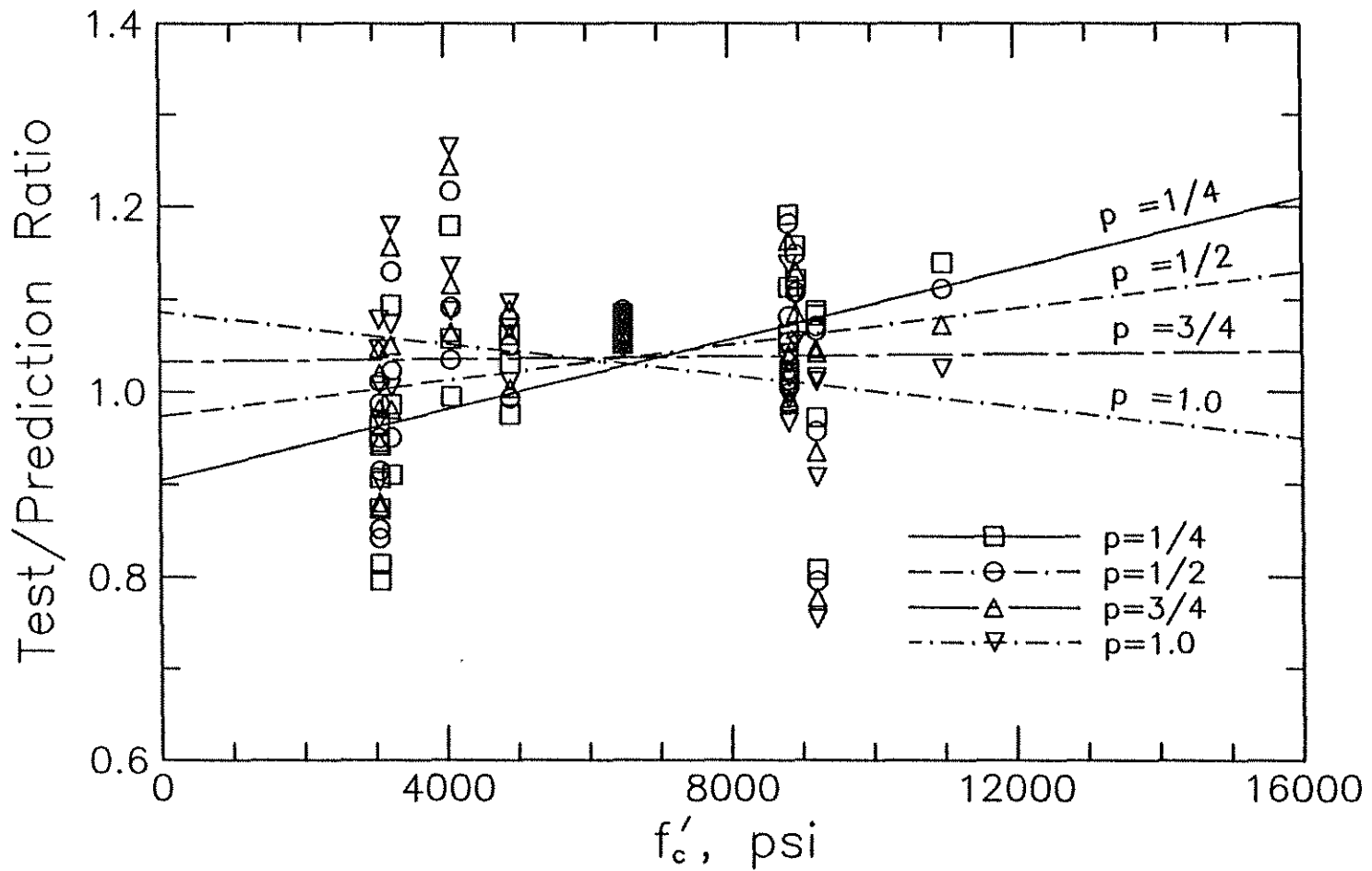


Fig. 5.16 Test/prediction ratios determined using Eqs. 5.13a - 5.13d corresponding to the powers of f'_c , $p = 1/4, 1/2, 3/4$, and 1.0, respectively, versus concrete compressive strength, f'_c , for specimens tested by Kadoriku (1994)

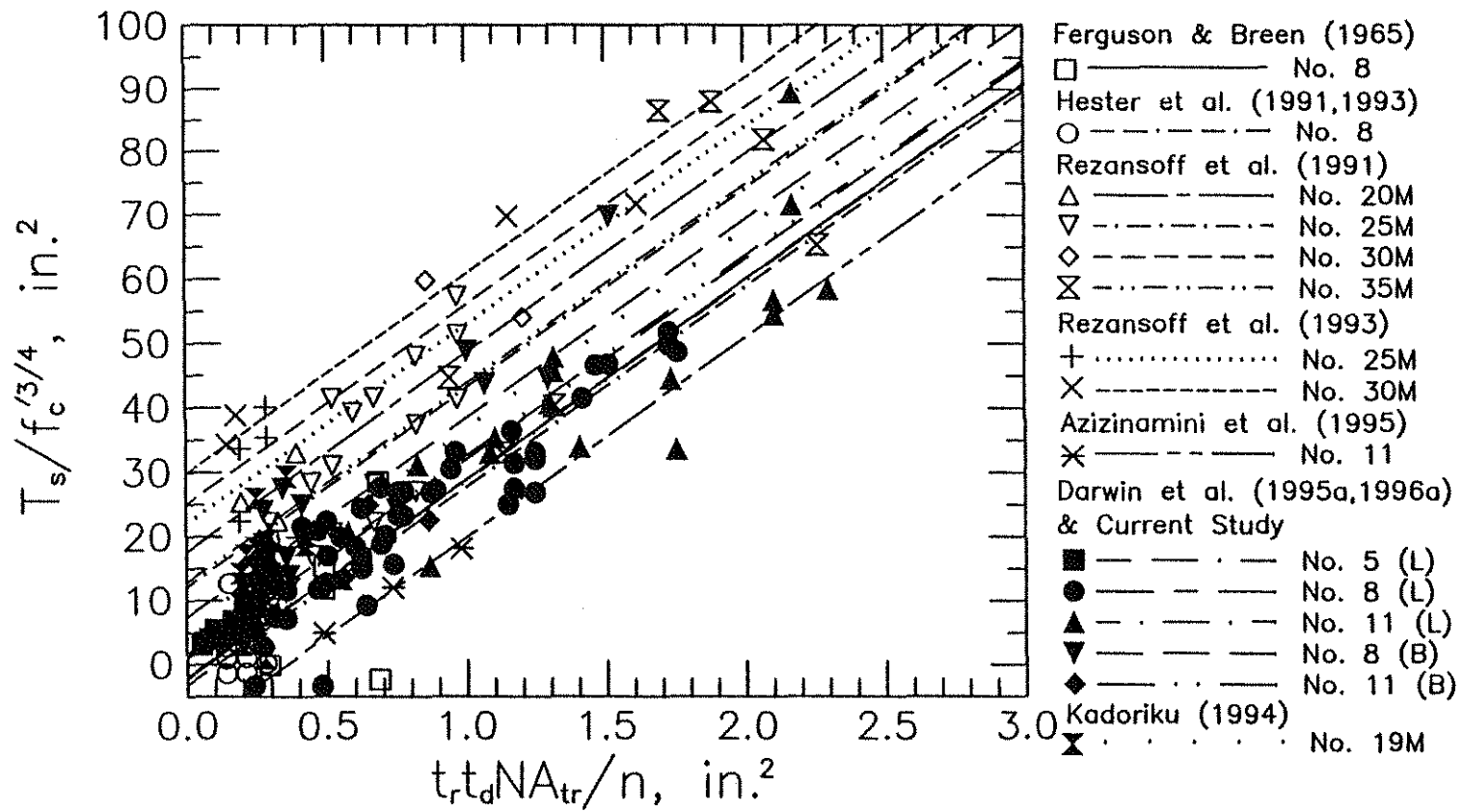


Fig. 5.17 Increase in bond force due to transverse reinforcement, T_s , normalized with respect to $f'_c^{3/4}$, versus $(t_r t_d N A_{tr}/n)^{3/4}$ for 196 specimens with $l_d/d_b \geq 16$ and $(c + K_{tr})/d_b \leq 4$, [in this case, $K_{tr} = 35.3 t_r t_d N A_{tr}/n$, $t_r = 9.6 R_r + 0.28$, and $t_d = 0.72 d_b + 0.28$ as developed by Darwin et al. (1995b, 1996b)]

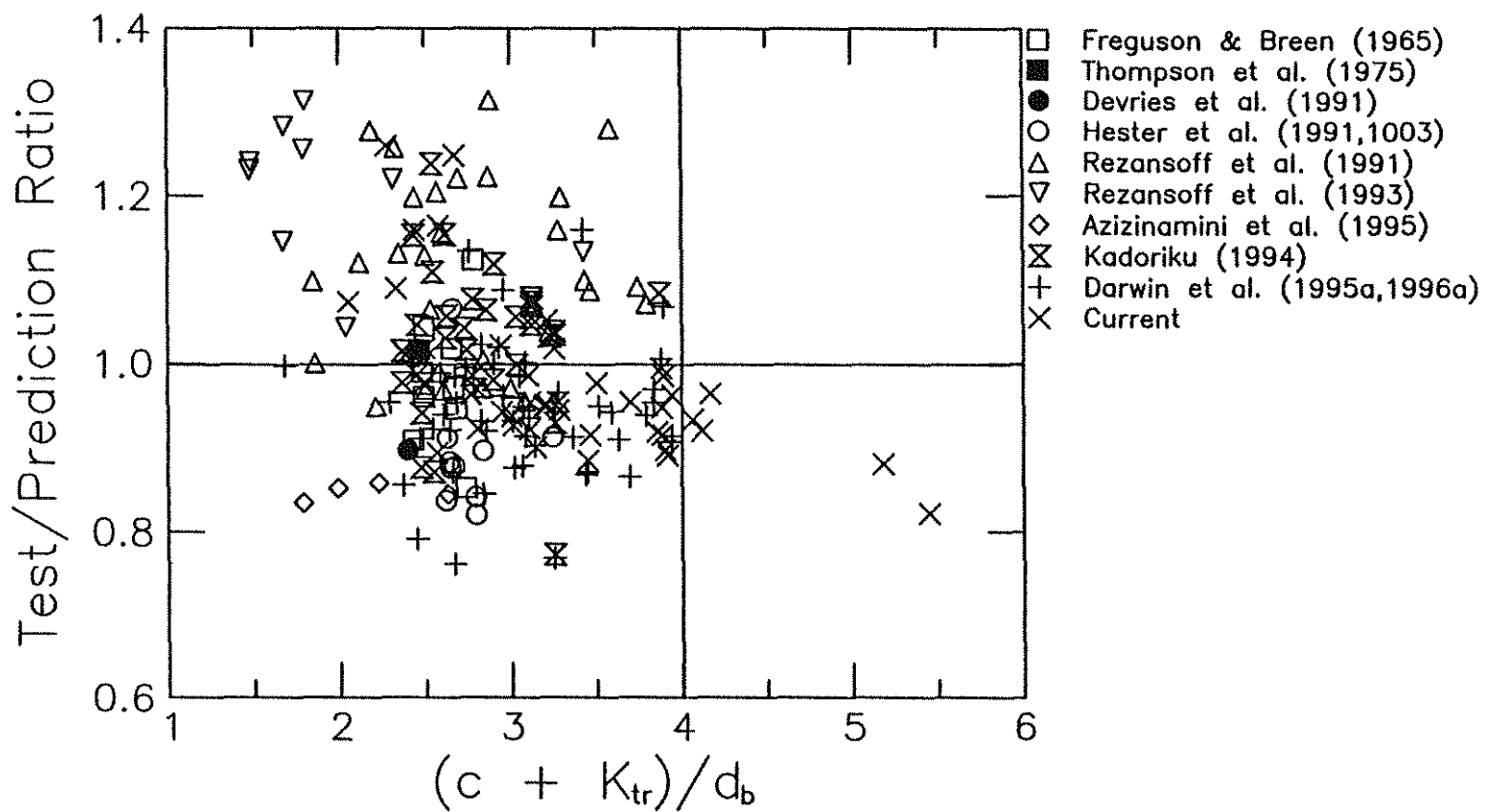


Fig. 5.18 Test/prediction ratio versus $(c + K_{tr})/d_b$ for 196 specimens [$K_{tr} = (0.518 t_f t_d A_{tr}/sn) f'_c^{1/2}$, $t_f = 9.6 R_f + 0.28$, $t_d = 0.78 d_b + 0.22$]

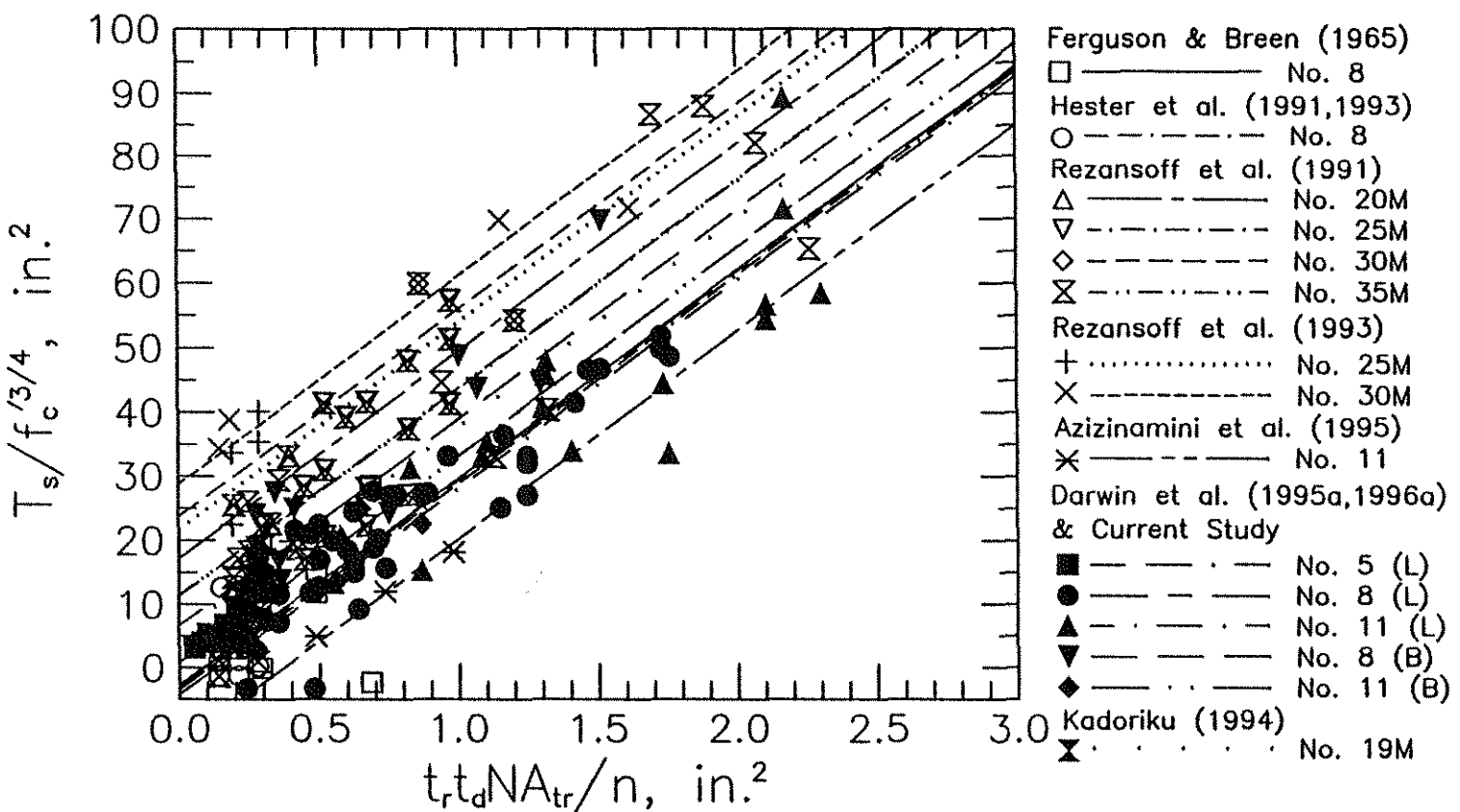


Fig. 5.19 Increase in bond force due to transverse reinforcement, T_s , normalized with respect to $f_c'^{3/4}$ versus $t_r t_d N A_{tr} / n$ for 191 specimens with $l_d/d_b \geq 16$ and $(c + K_{tr})/d_b \leq 4$, [in this case, $K_{tr} = (0.52 t_r t_d N A_{tr} / n) f_c'^{3/2}$, $t_r = 9.6 R_r + 0.28$, and $t_d = 0.78 d_b + 0.22$]

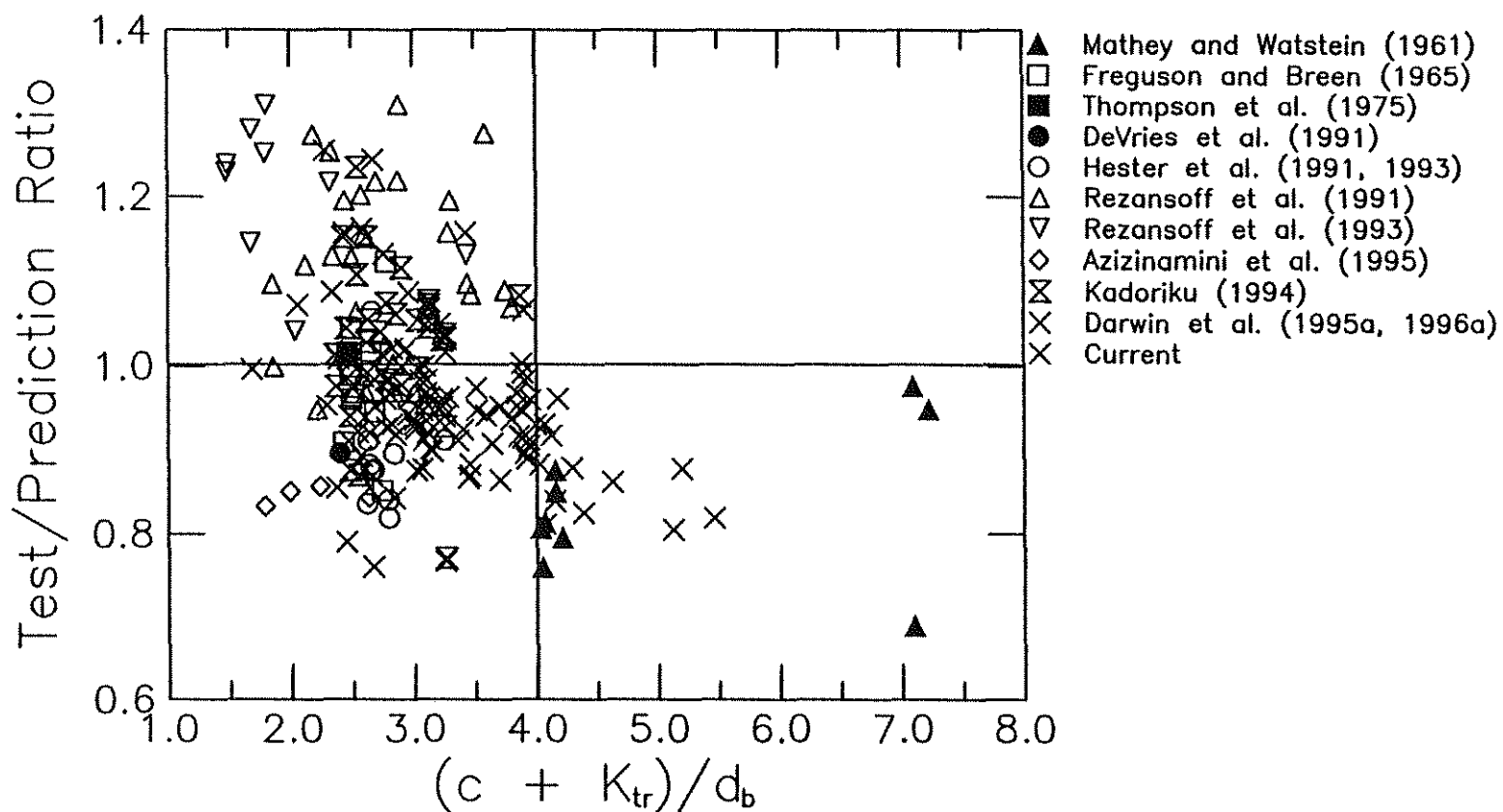


Fig. 5.20 Test/prediction ratio using Eq. 5.18 versus $(c + K_{tr})/d_b$ for 213 specimens with $l_d/d_b \geq 16$ [$K_{tr} = (0.52 t_r t_d A_{tr}/sn) f'_c^{1/2}$, $t_r = 9.6 R_r + 0.28$, $t_d = 0.78 d_b + 0.22$]

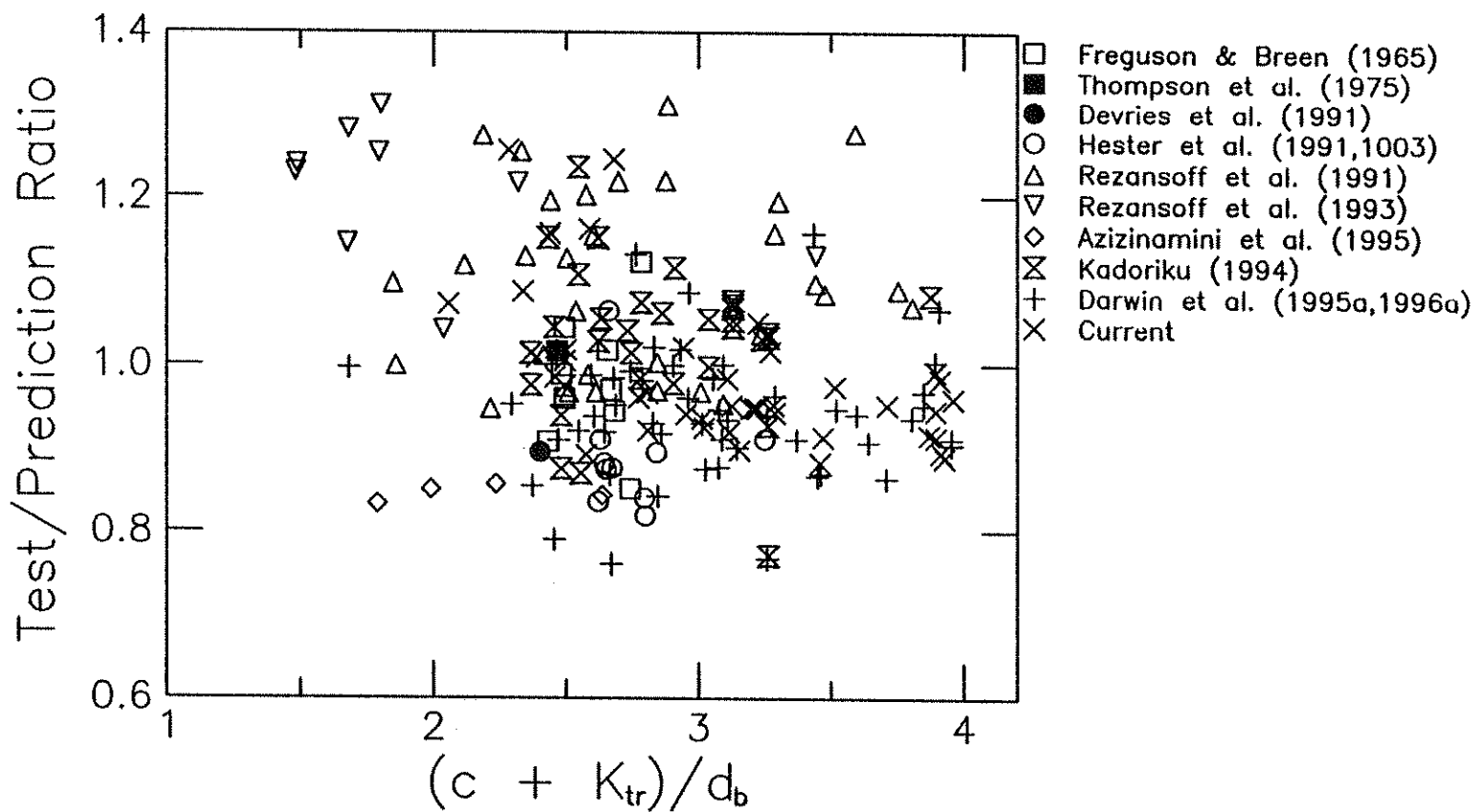


Fig. 5.21 Test/prediction ratio using Eq. 5.18 versus $(c + K_{tr})/d_b$ for 191 specimens with $l_d/d_b \geq 16$ and $(c + K_{tr})/d_b \leq 4$
 $[K_{tr} = (0.52t_r t_d A_{tr}/sn)f'_c{}^{1/2}, t_r = 9.6 R_r + 0.28, t_d = 0.78 d_b + 0.22]$

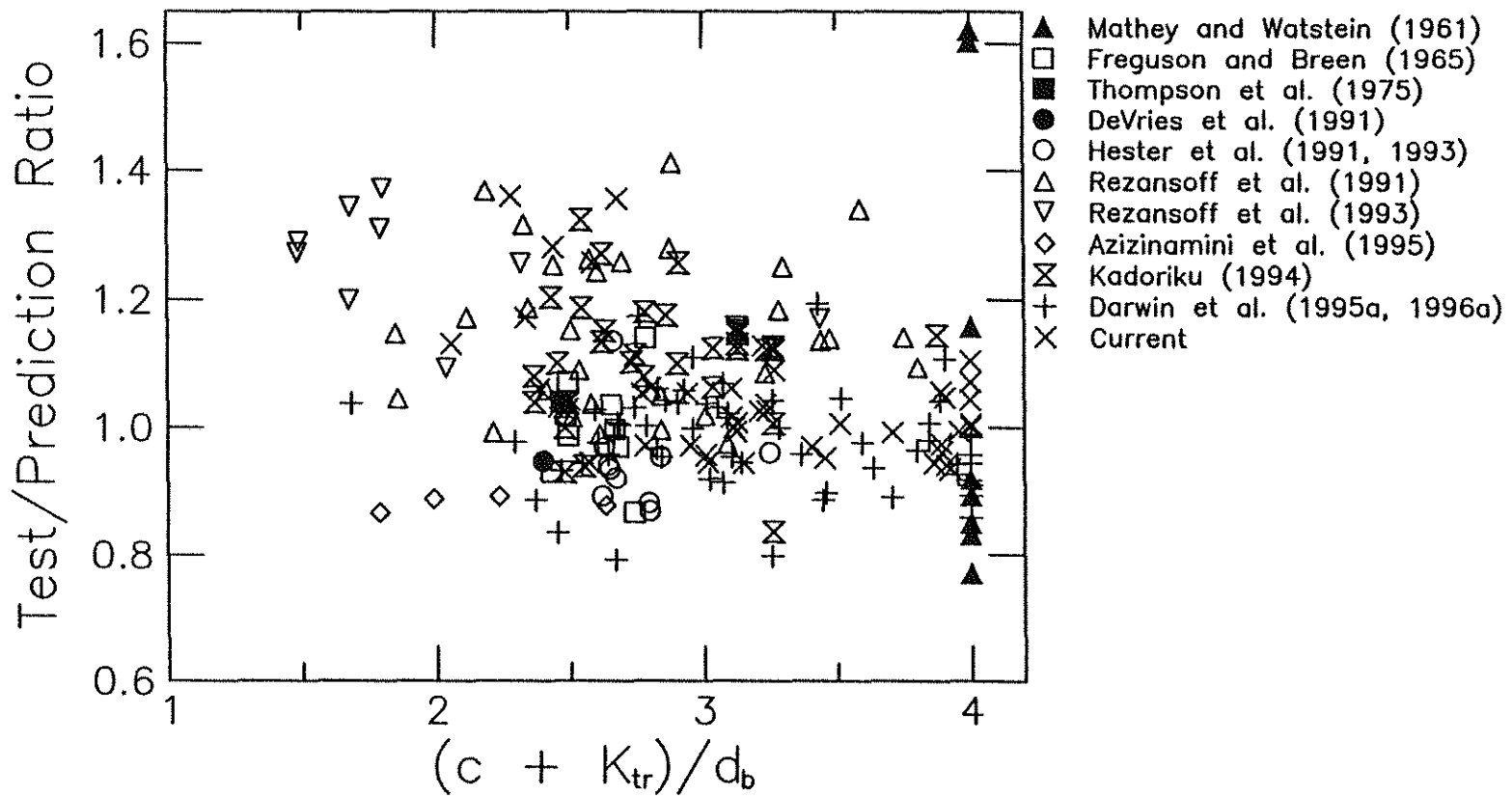


Fig. 5.22 Test/prediction ratio using Eq. 5.20 versus $(c + K_{tr})/d_b$ for 213 specimens with $l_d/d_b \geq 16$ and setting $(c + K_{tr})/d_b \leq 4$
 $[K_{tr} = (0.52t_r t_d A_{tr}/sn)f'_c^{1/2}, t_r = 9.6 R_r + 0.28, t_d = 0.78 d_b + 0.22]$

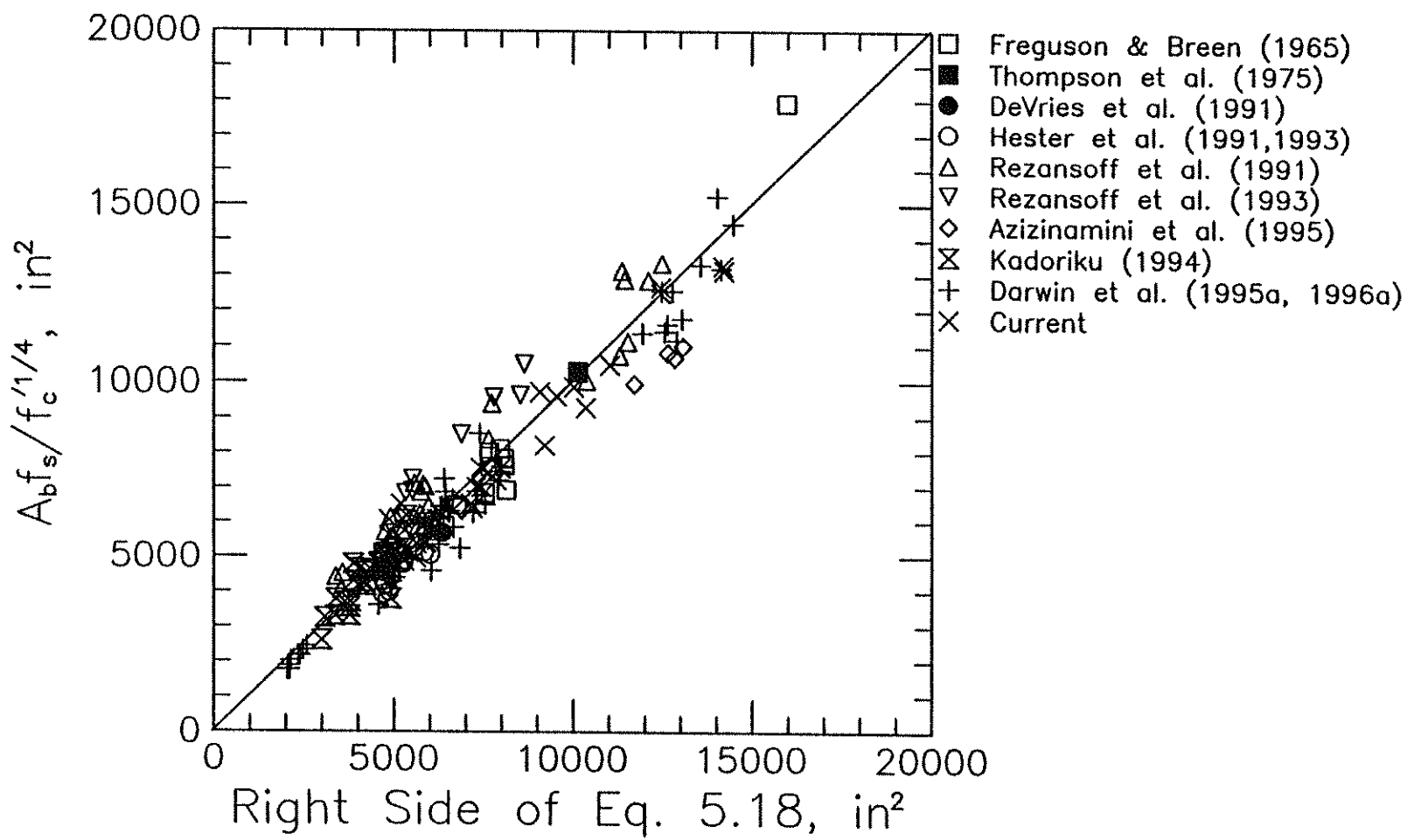


Fig. 5.23 Experimental bond force, $T_b = A_b f_s$, normalized with respect to $f_c'^{1/4}$ versus predicted bond strength determined using Eq. 5.18 for 191 specimens containing bars confined by transverse reinforcement with $l_d/d_b \geq 16$ and $(c + K_{tr})/d_b \leq 4$ [$K_{tr} = (0.52 t_i t_d A_{tr}/s_n) f_c'^{1/2}$, $t_r = 9.6 R_r + 0.28$, $t_d = 0.78 d_b + 0.22$]

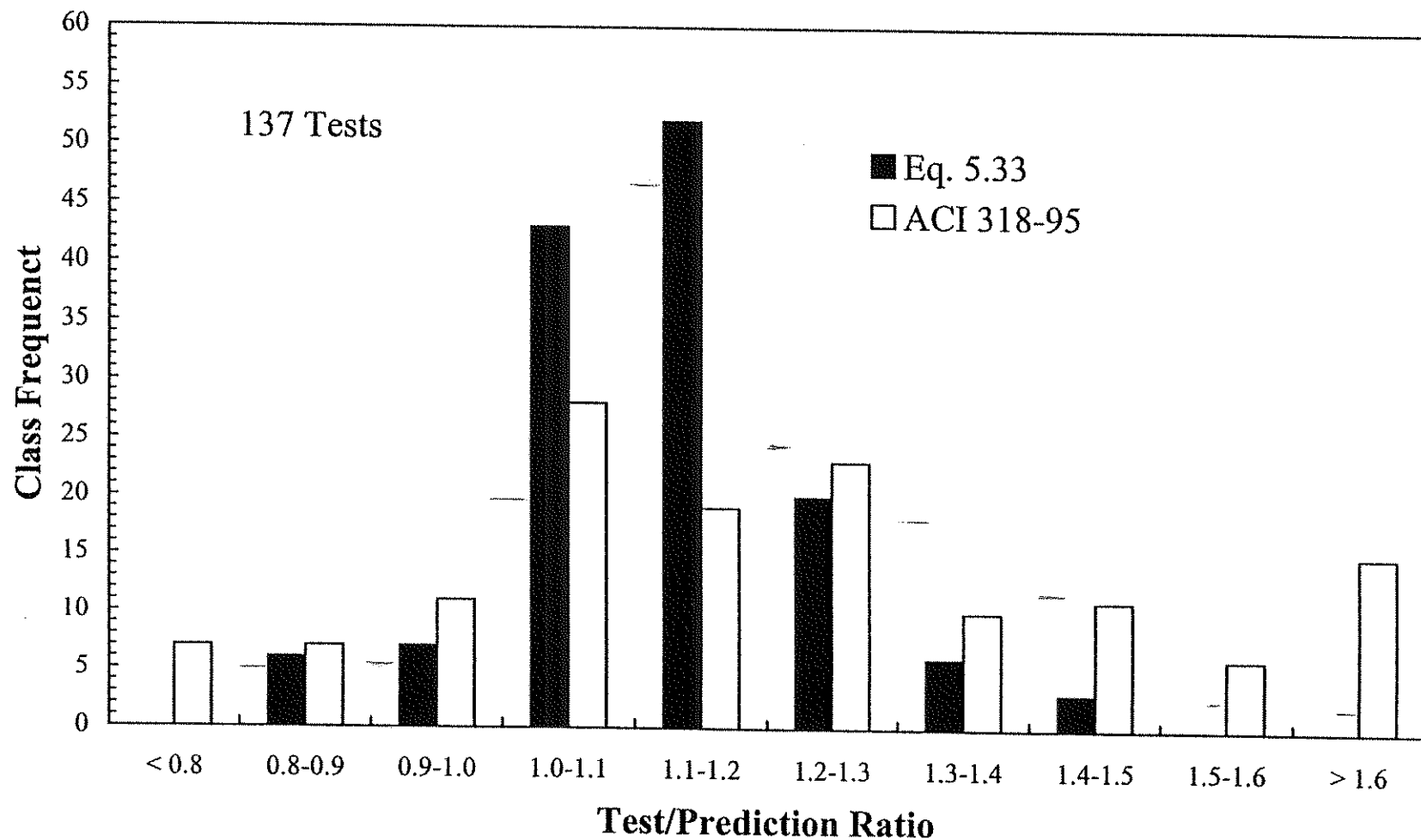


Fig. 5.24 Comparison of test/prediction ratio distribution using Eq. 5.33 and ACI 318-95 for specimens containing bars without confining transverse reinforcement

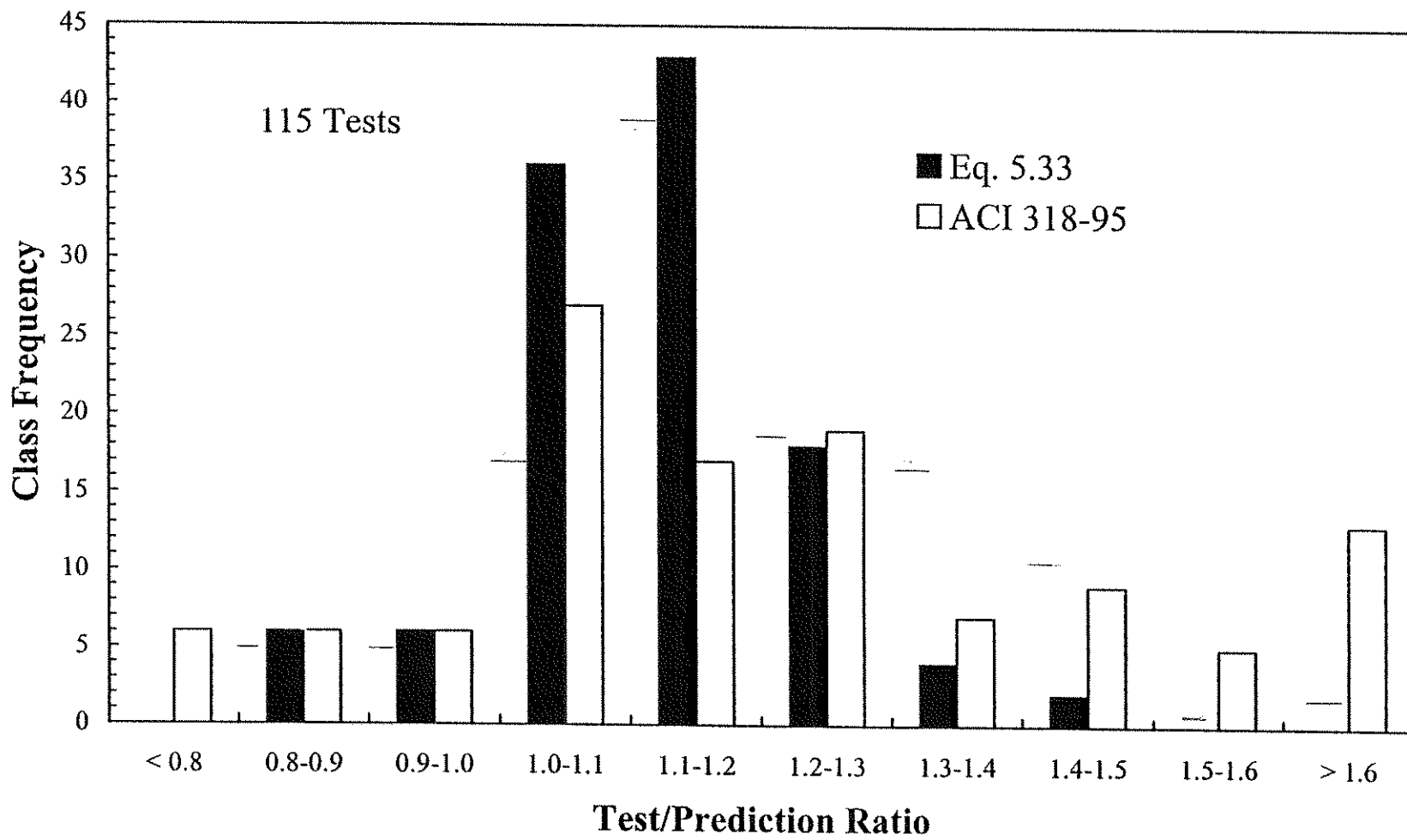


Fig. 5.25 Comparison of test/prediction ratio distribution using Eq. 5.33 and ACI 318-95 for specimens containing No. 7 and larger bars without confining transverse reinforcement

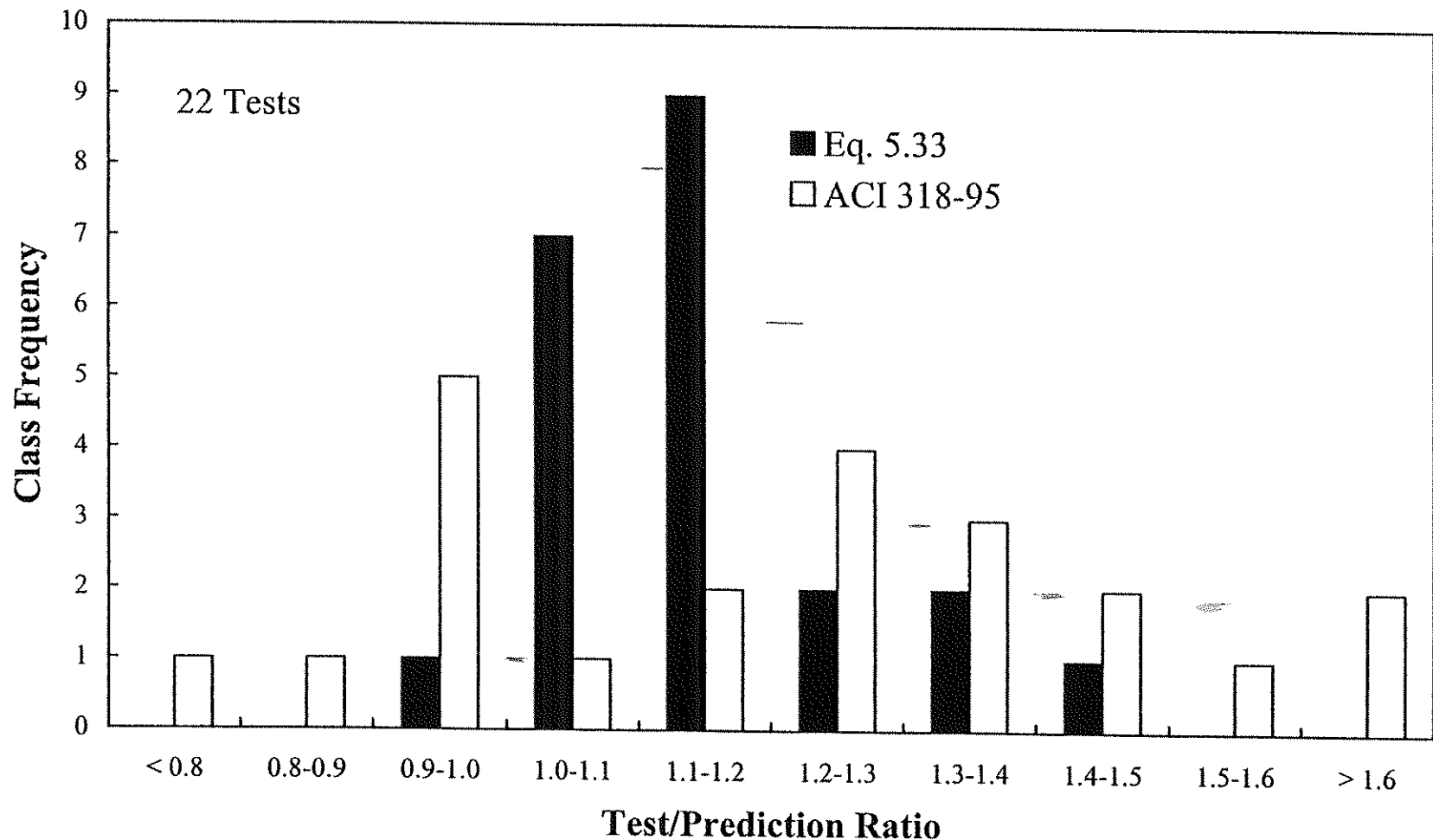


Fig. 5.26 Comparison of test/prediction ratio distribution using Eq. 5.33 and ACI 318-95 for specimens containing No. 6 and smaller bars without confining transverse reinforcement

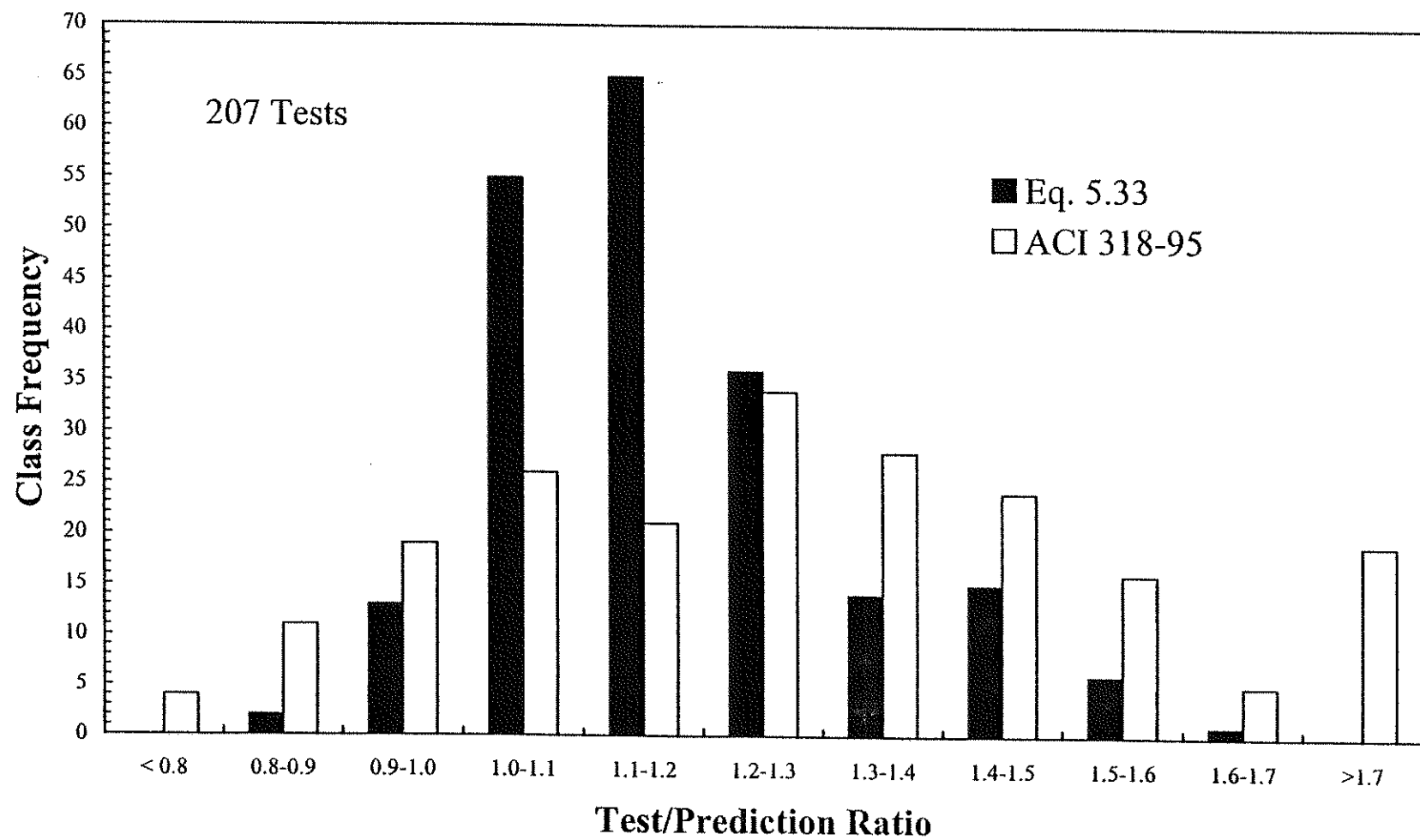
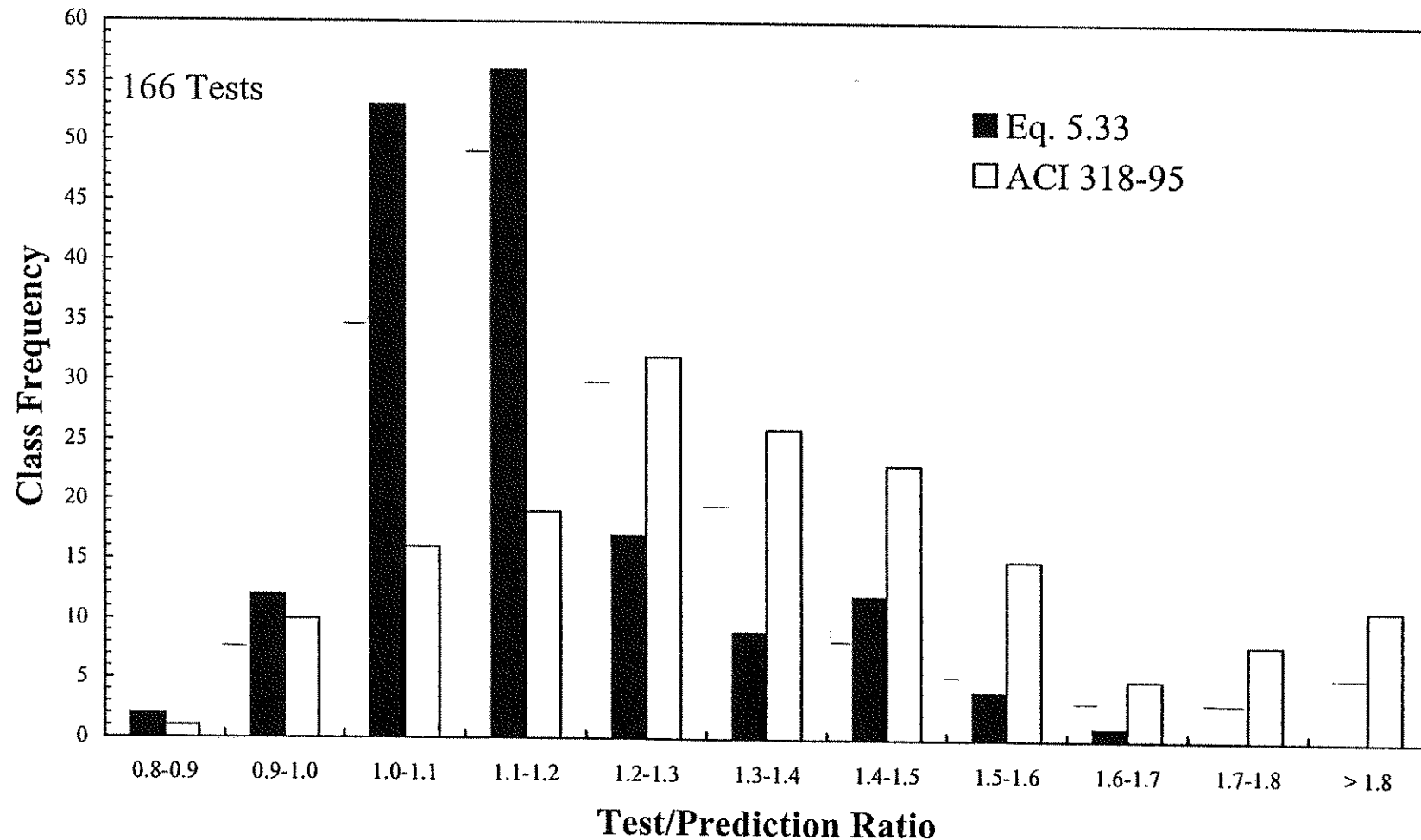


Fig. 5.27 Comparison of test/prediction ratio distribution using Eq. 5.33 and ACI 318-95 for specimens containing bars with confining transverse reinforcement



284

Fig. 5.28 Comparison of test/prediction ratio distribution using Eq. 5.33 and ACI 318-95 for specimens containing No. 7 and larger bars with confining transverse reinforcement

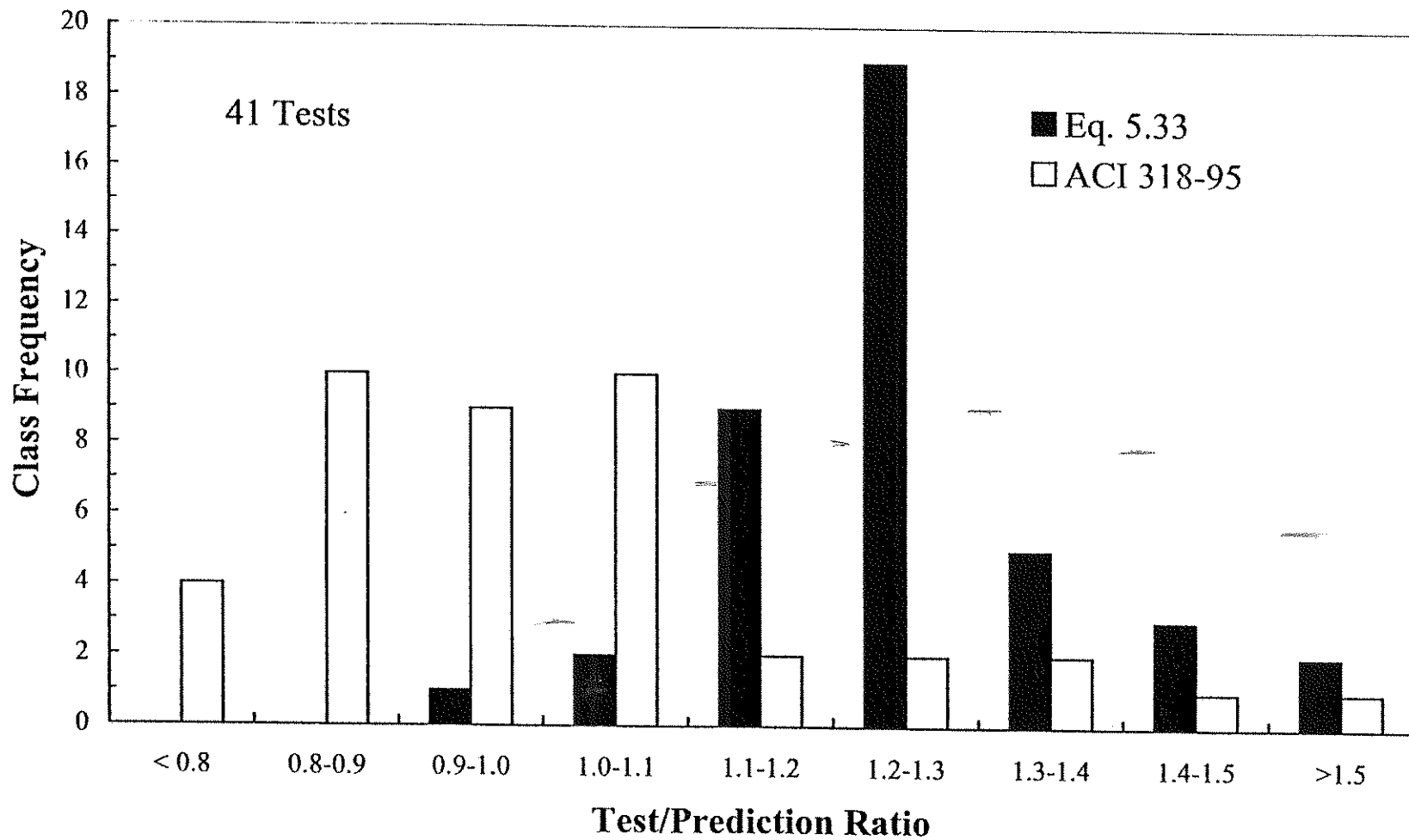


Fig. 5.29 Comparison of test/prediction ratio distribution using Eq. 5.33 and ACI 318-95 for specimens containing No. 6 and smaller bars with confining transverse reinforcement

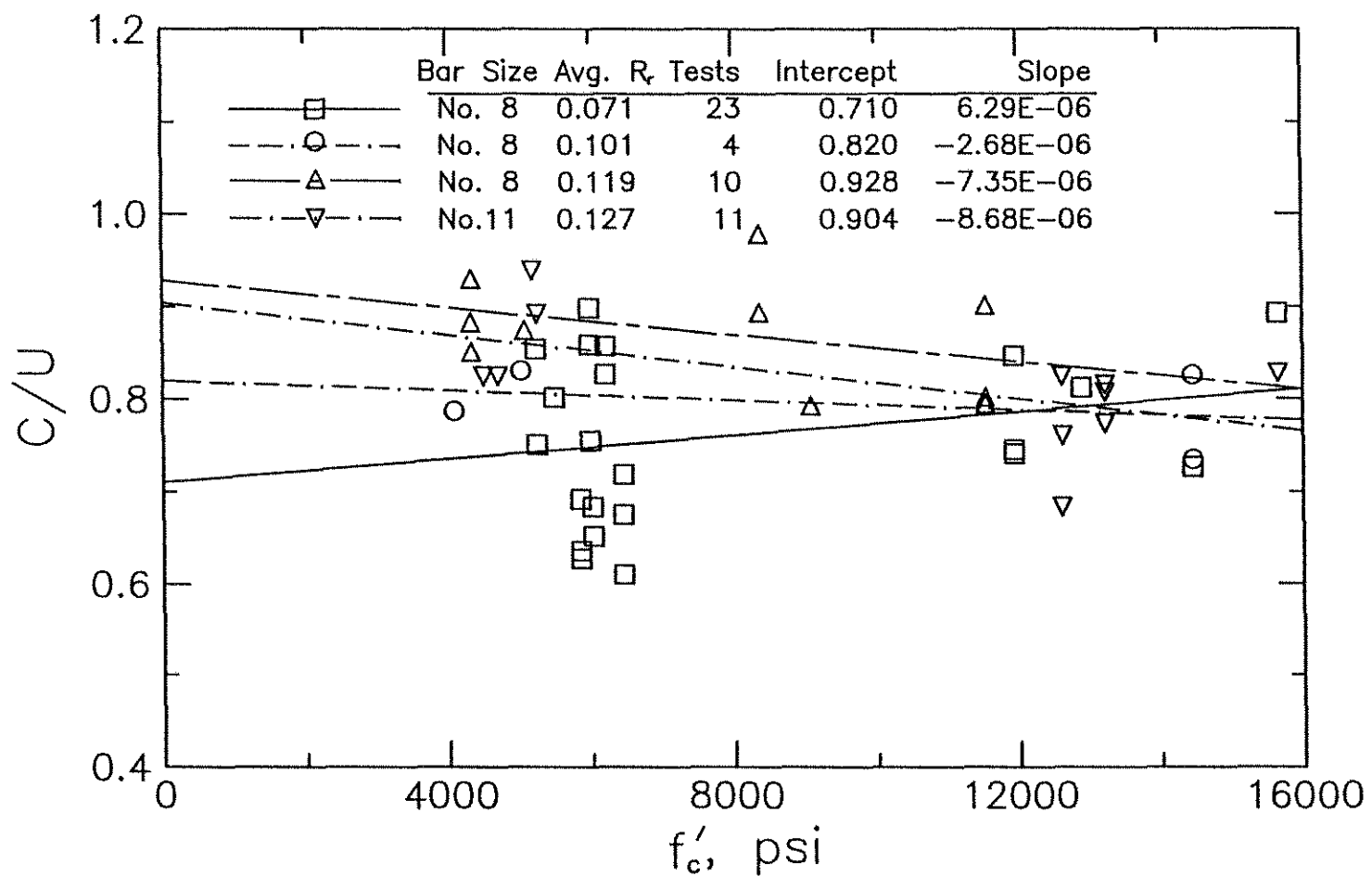


Fig. 6.1 Normalized relative splice strength ratio, C/U , versus concrete compressive strength, f'_c , for matched pairs of specimens containing epoxy-coated and uncoated No. 8 conventional bars and No. 8 and No. 11 high relative rib area, R_r , bars

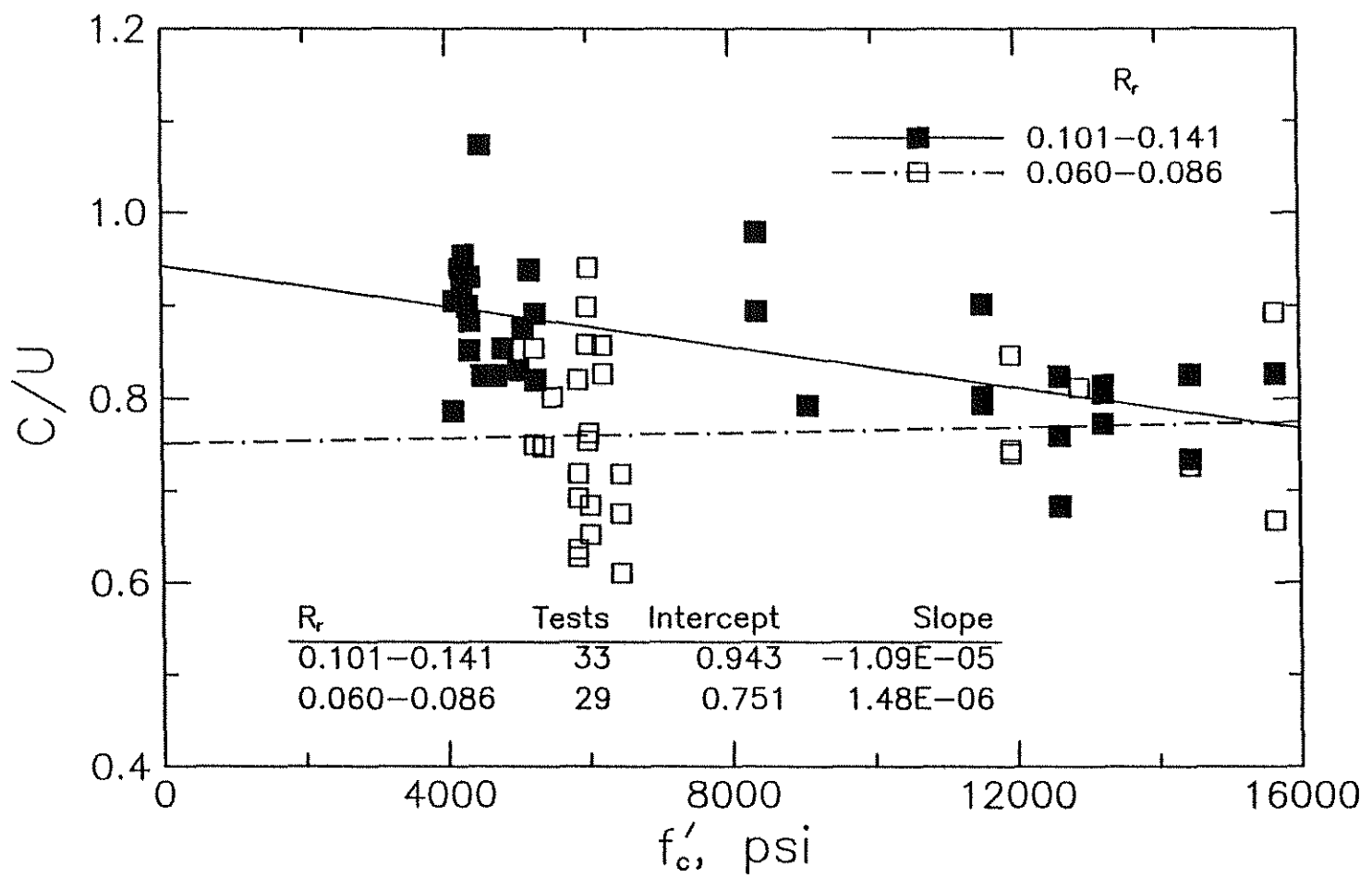


Fig. 6.2 Normalized relative splice strength ratio, C/U , versus concrete compressive strength, f'_c , for 62 matched pairs of splice specimens containing epoxy-coated and uncoated bars

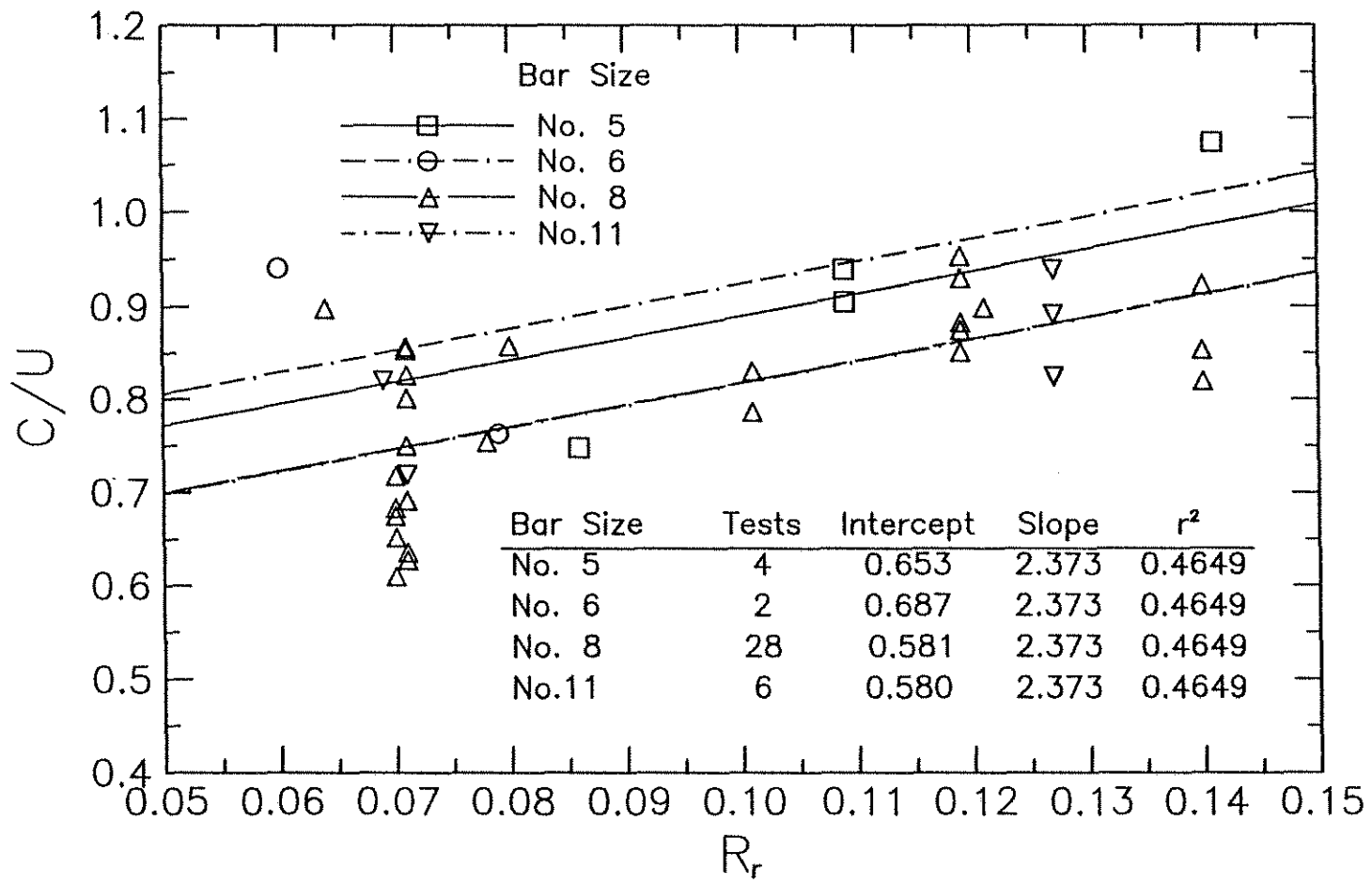


Fig. 6.3 Normalized relative splice strength ratio, C/U , versus relative rib area, R_r , for matched pairs of specimens cast with normal-strength concrete containing epoxy-coated and uncoated bars

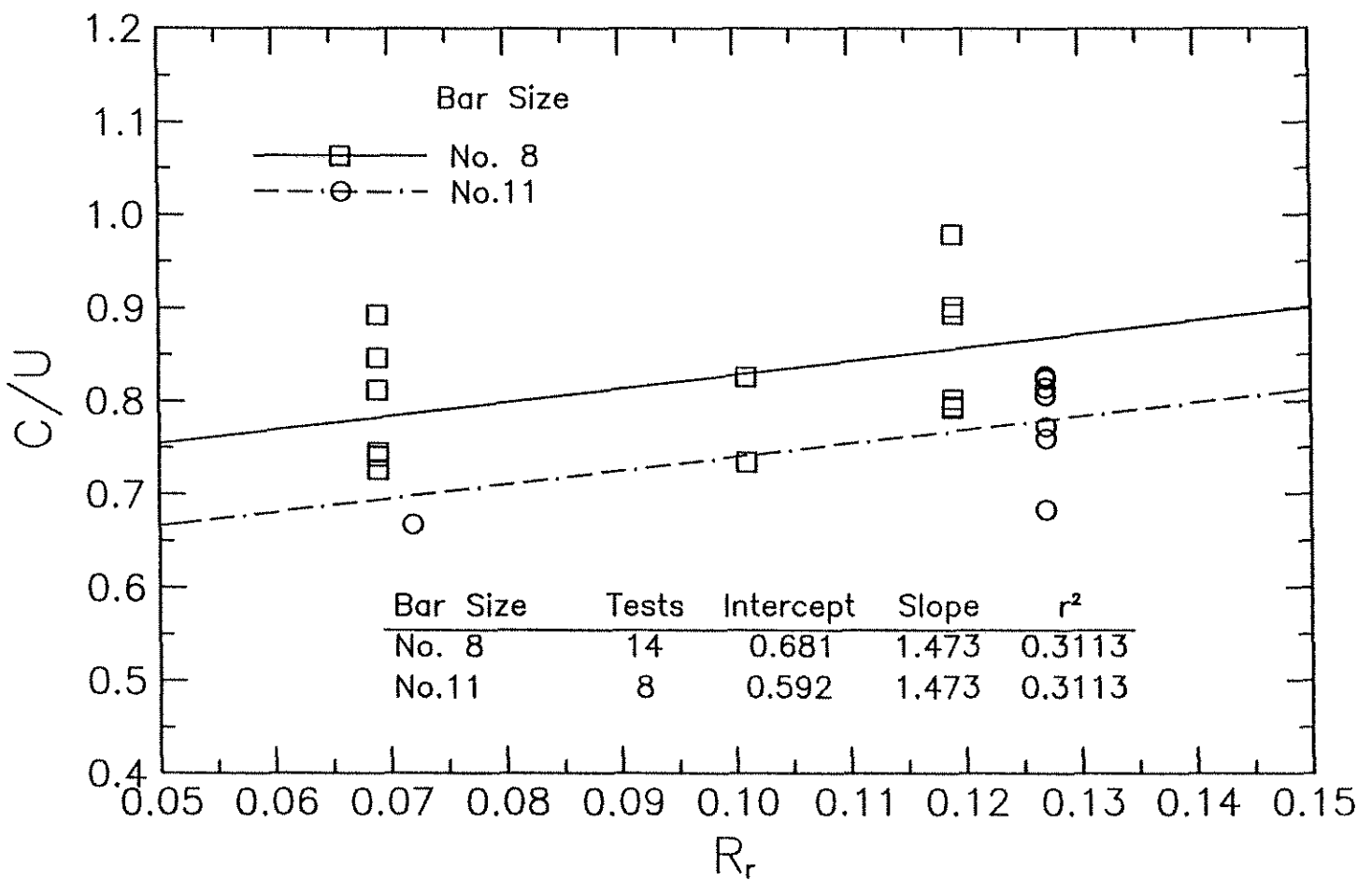
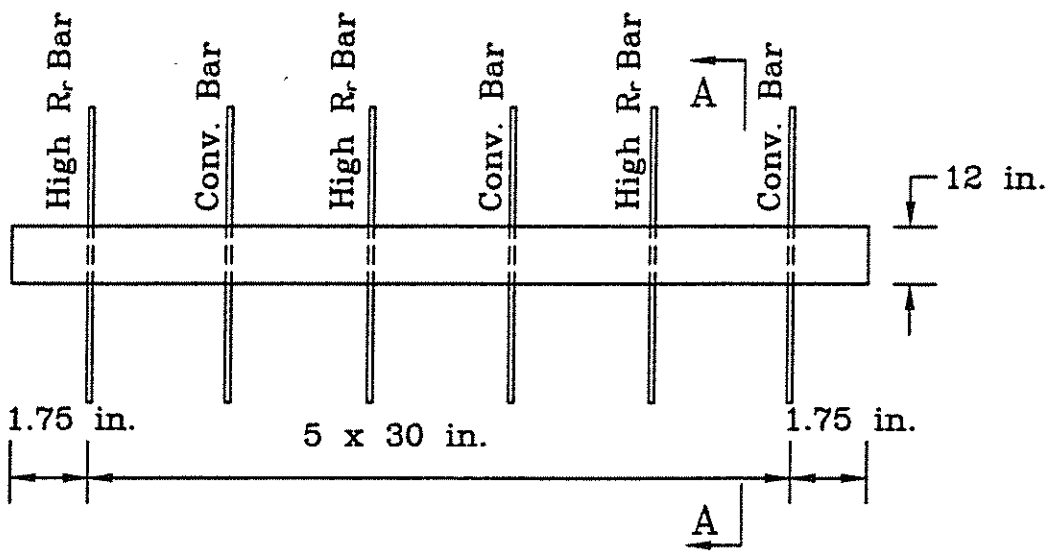
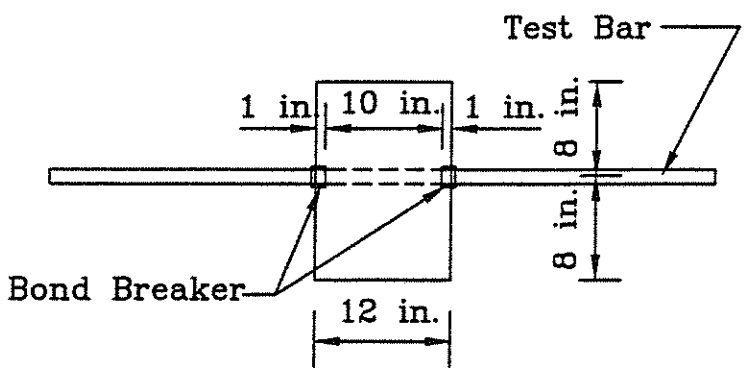


Fig. 6.4 Normalized relative splice strength ratio, C/U , versus relative rib area, R_r , for matched pairs of specimens cast with high-strength concrete containing epoxy-coated and uncoated bars

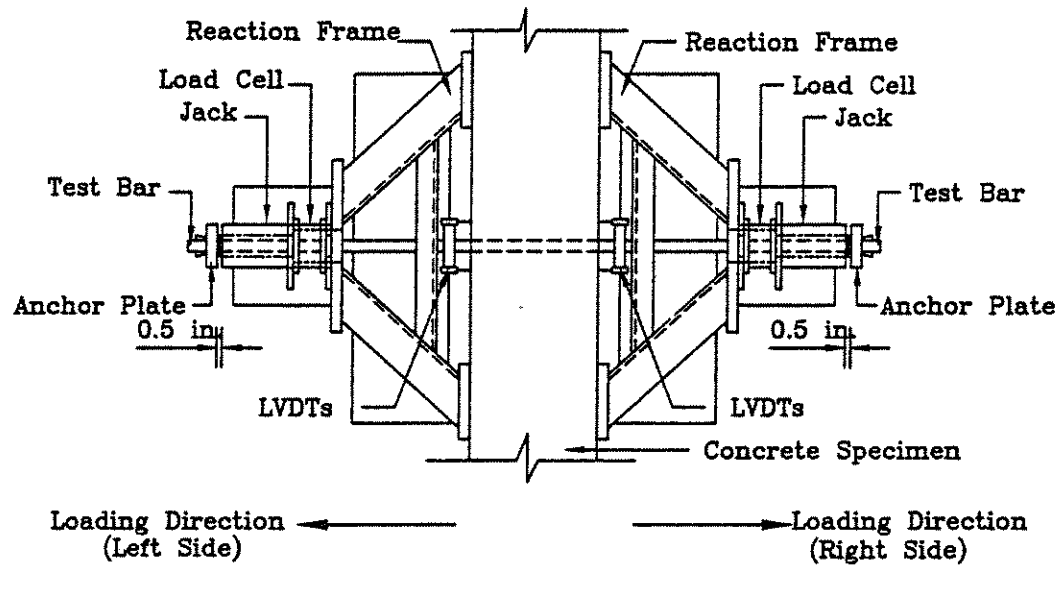


PLAN VIEW

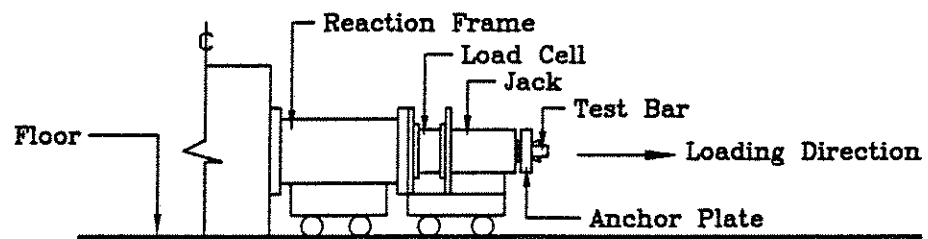


SECTION A-A

Fig. 7.1 Schematic of reversed cyclic loading specimen



PLAN VIEW



SIDE VIEW

Fig. 7.2 Schematic of reversed cyclic loading test setup

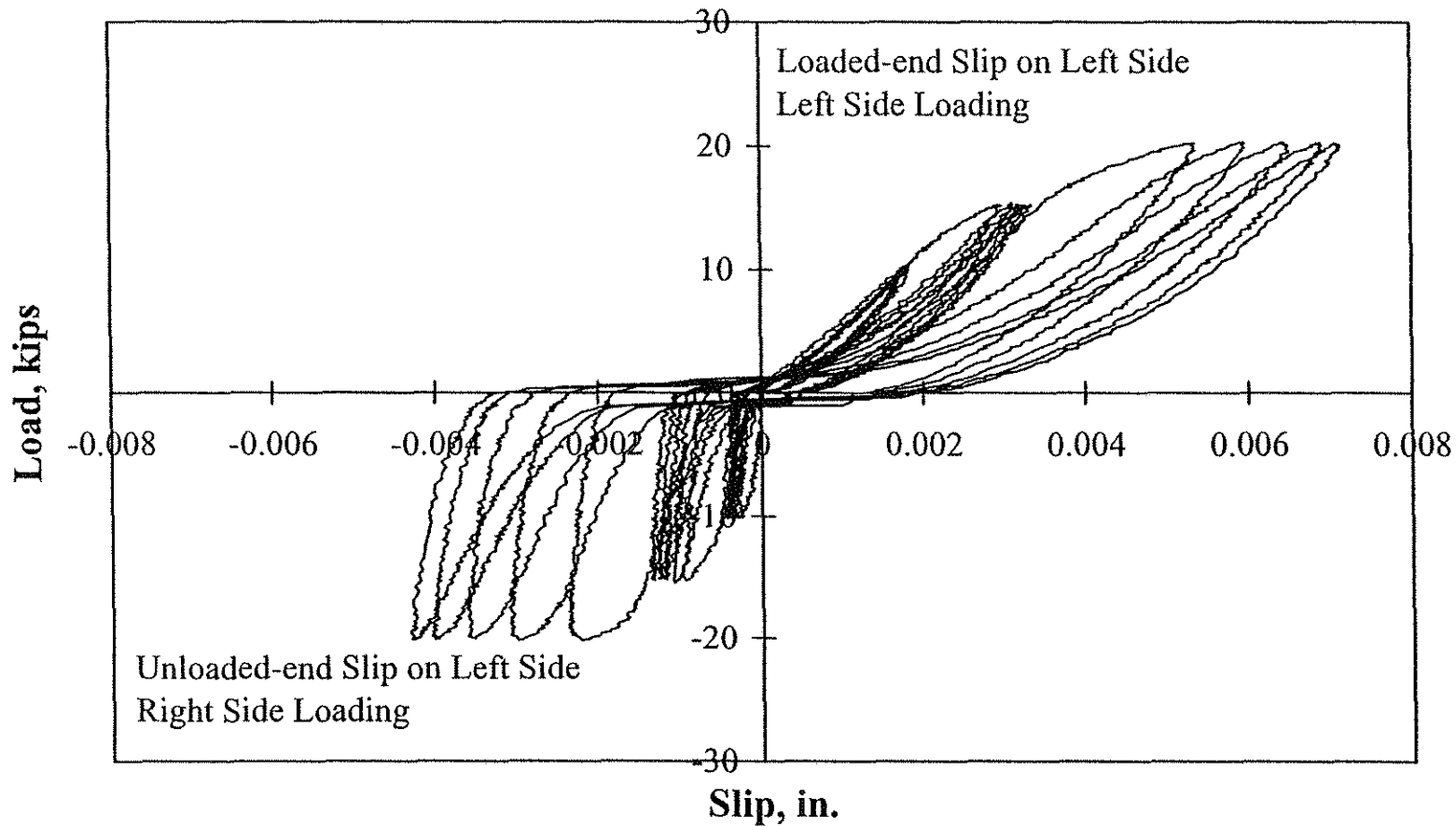


Fig. 7.3a Load versus loaded end and unloaded end slips for bar 8C0A-3 on the left side of the specimen

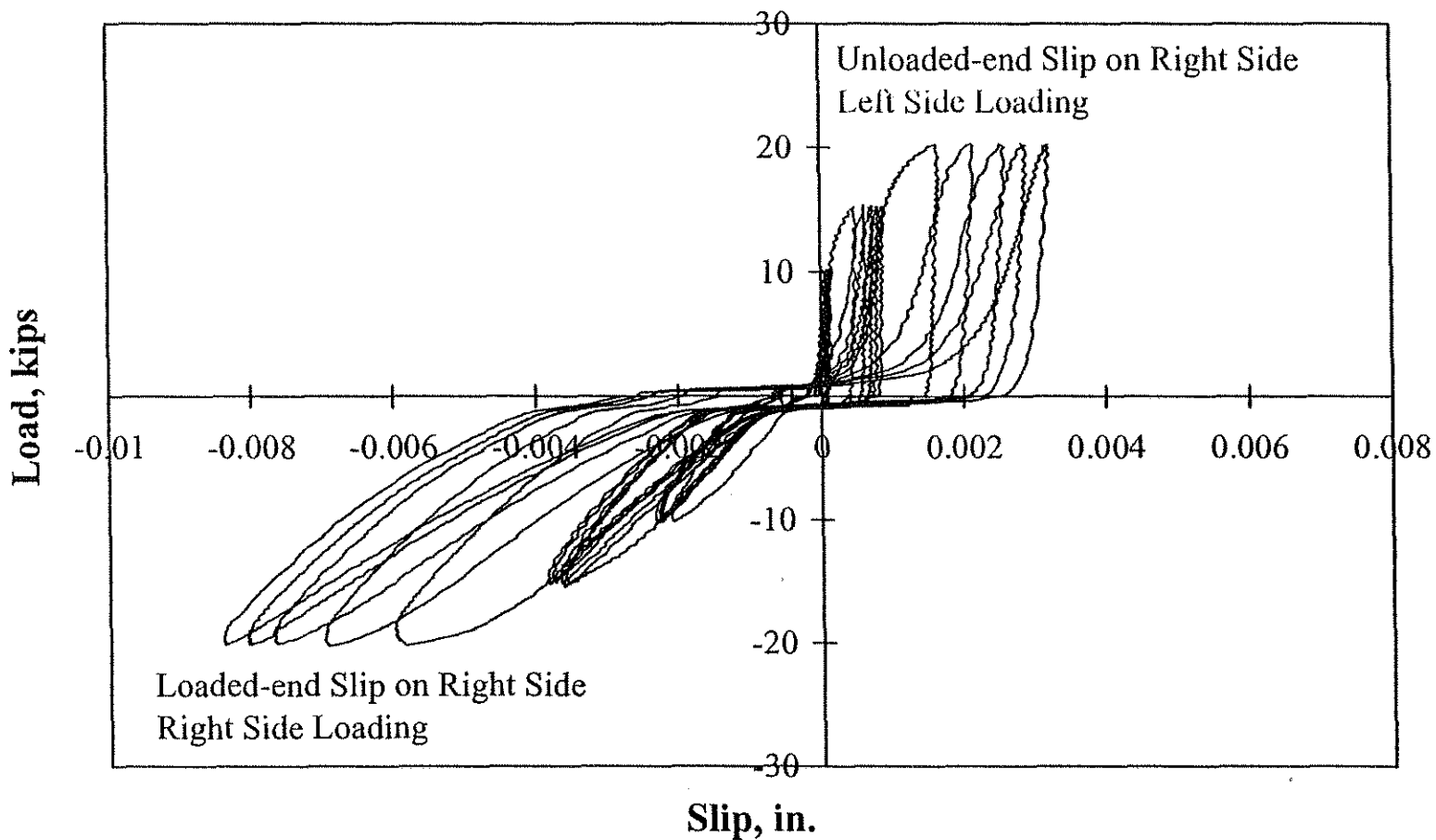


Fig. 7.3b Load versus loaded end and unloaded end slips for bar 8C0A-3 on the right side of the specimen

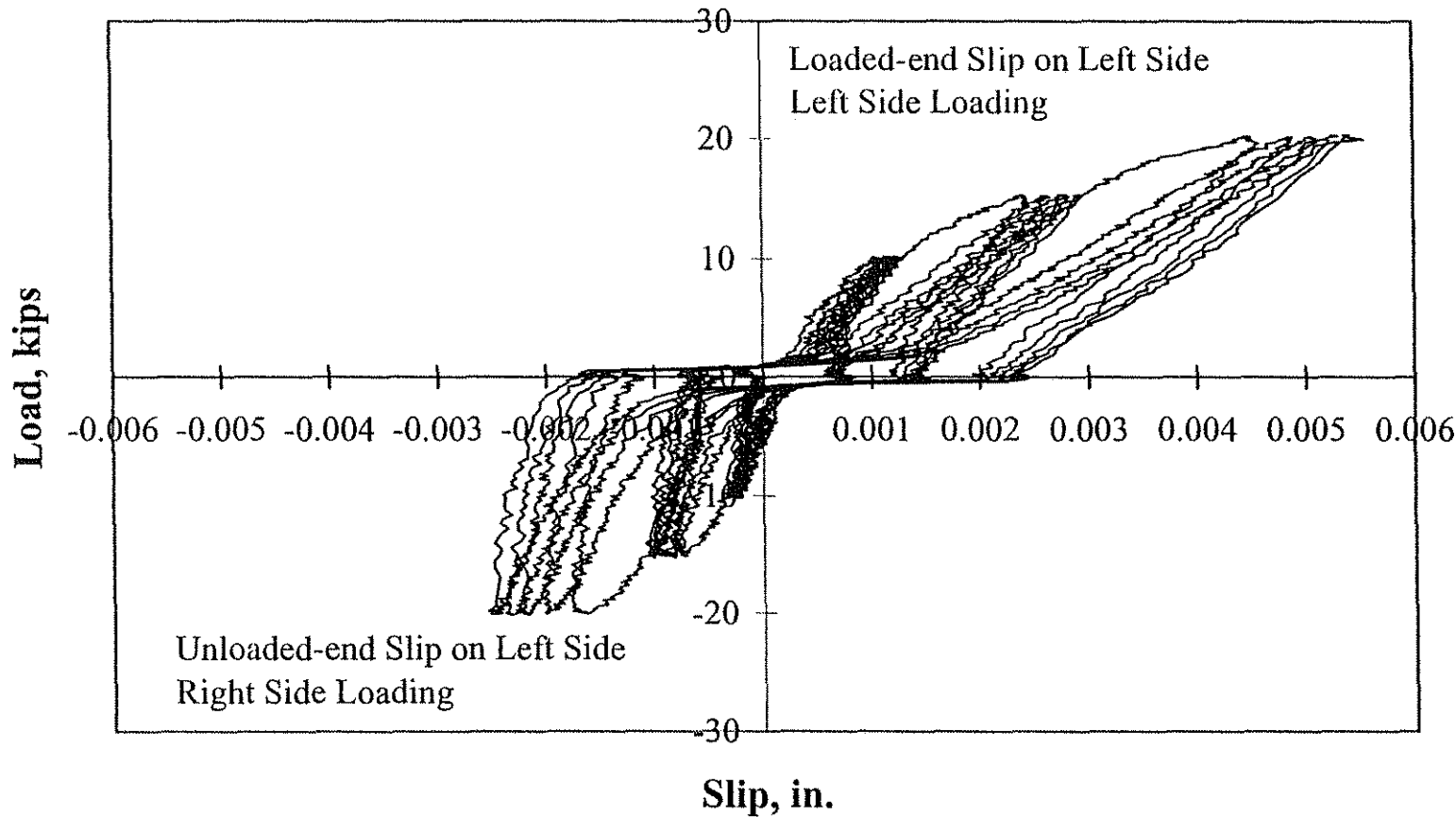


Fig. 7.3c Load versus loaded end and unloaded end slips for bar 8C0A-5 on the left side of the specimen

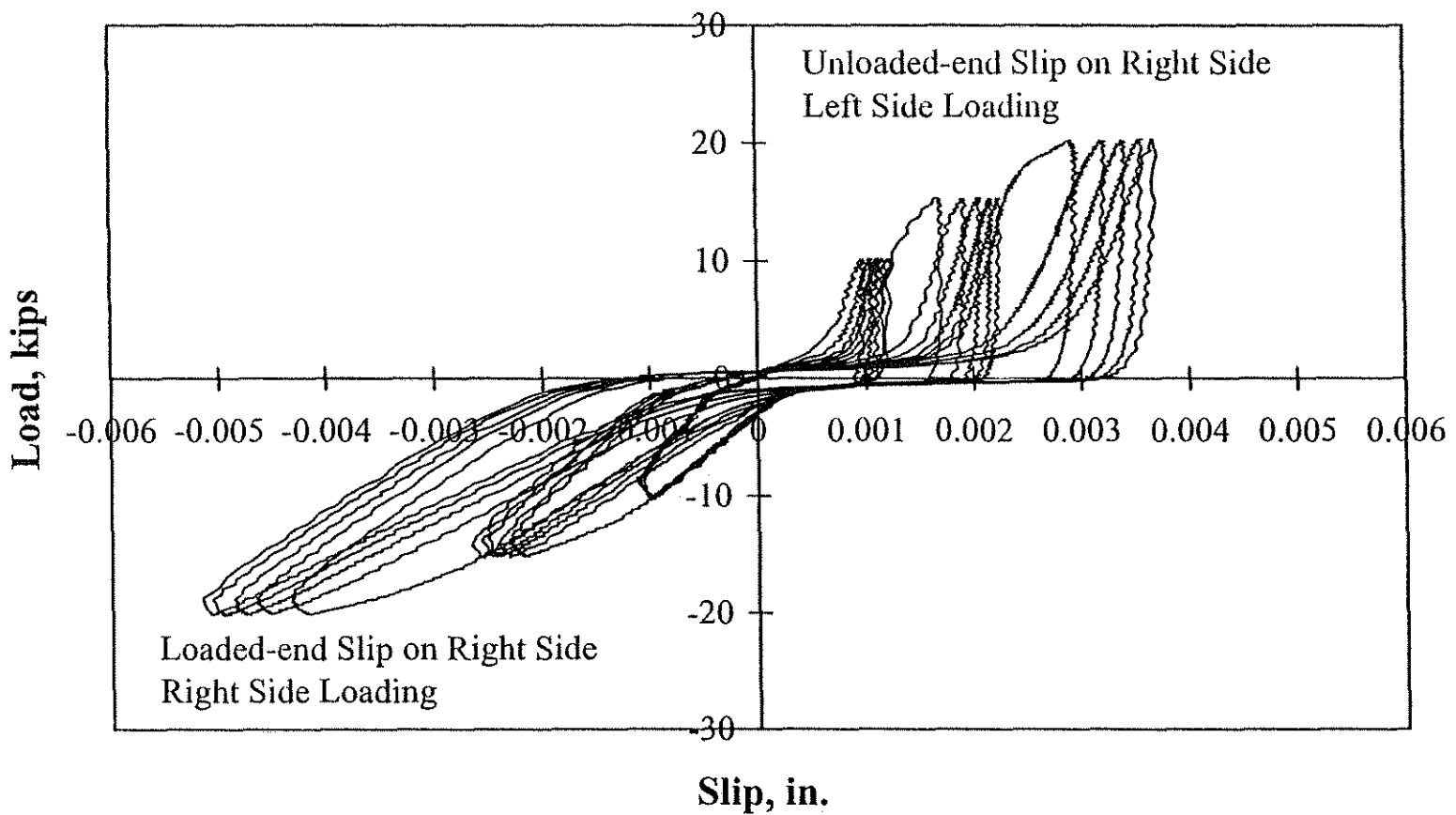


Fig. 7.3d Load versus loaded end and unloaded end slips for bar 8C0A-5 on the right side of the specimen

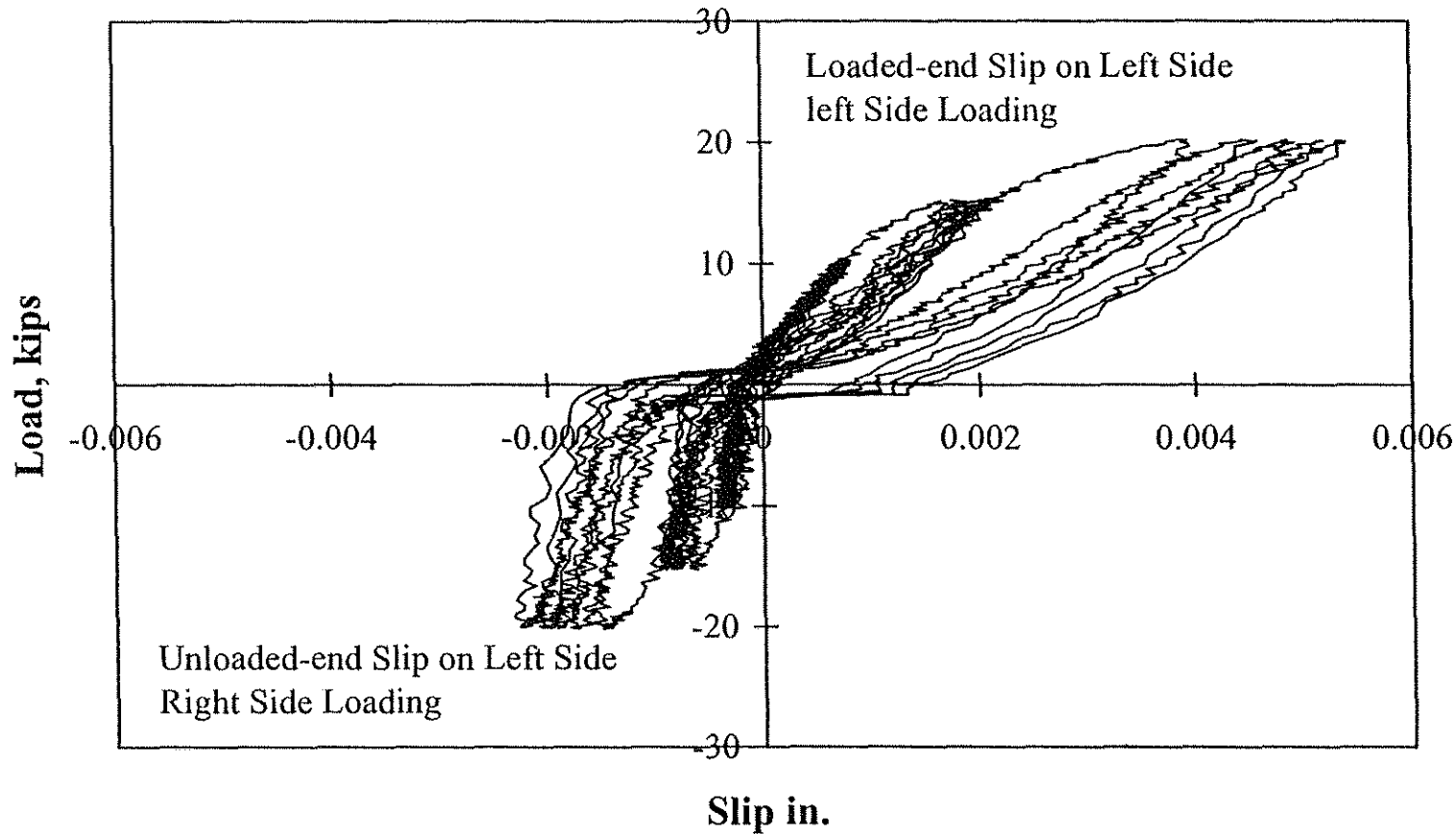


Fig. 7.3e Load versus loaded end and unloaded end slips for bar 8C0A-7 on the left side of the specimen

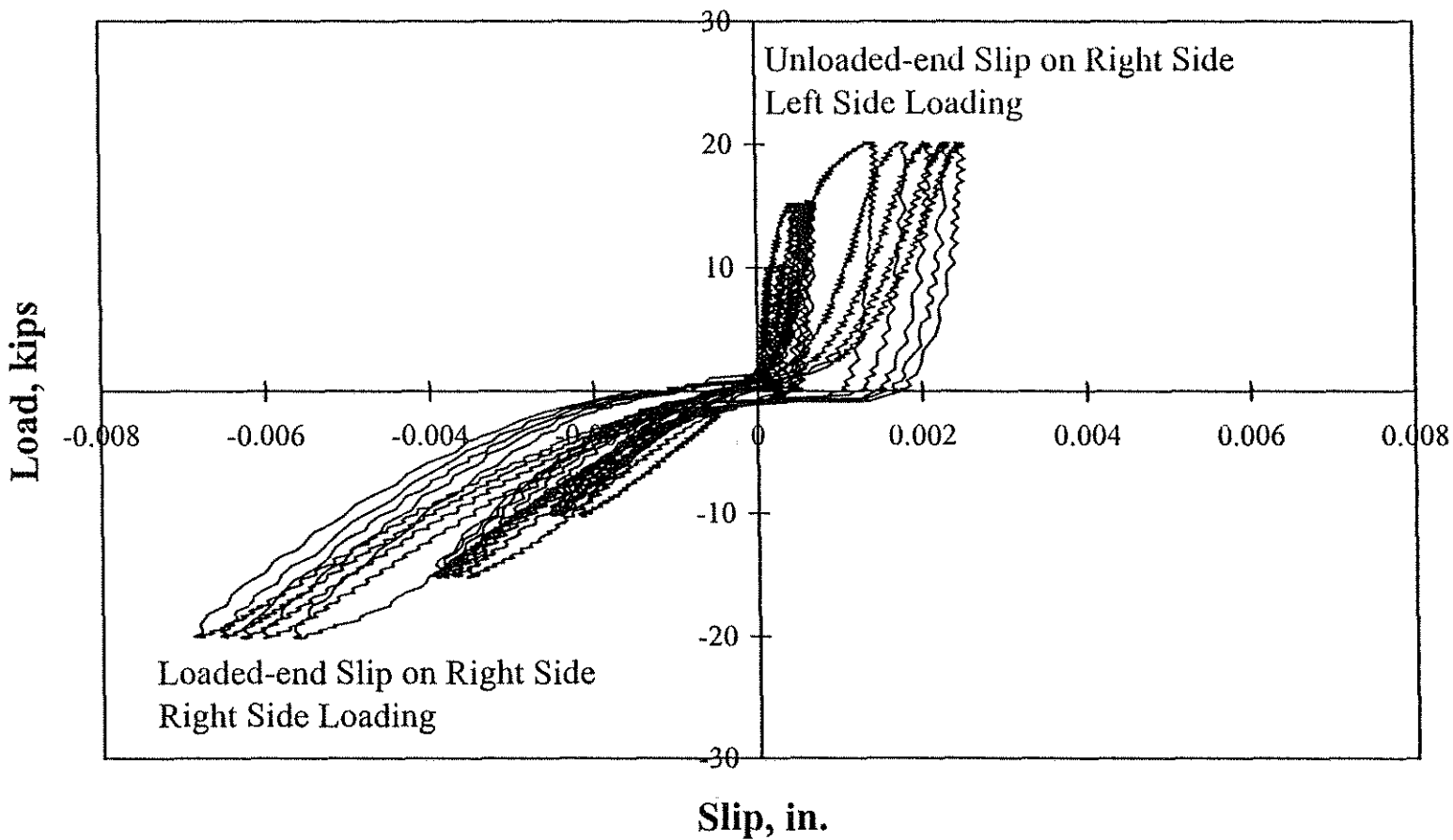


Fig. 7.3f Load versus loaded end and unloaded end slips for bar 8C0A-7 on the right side of the specimen

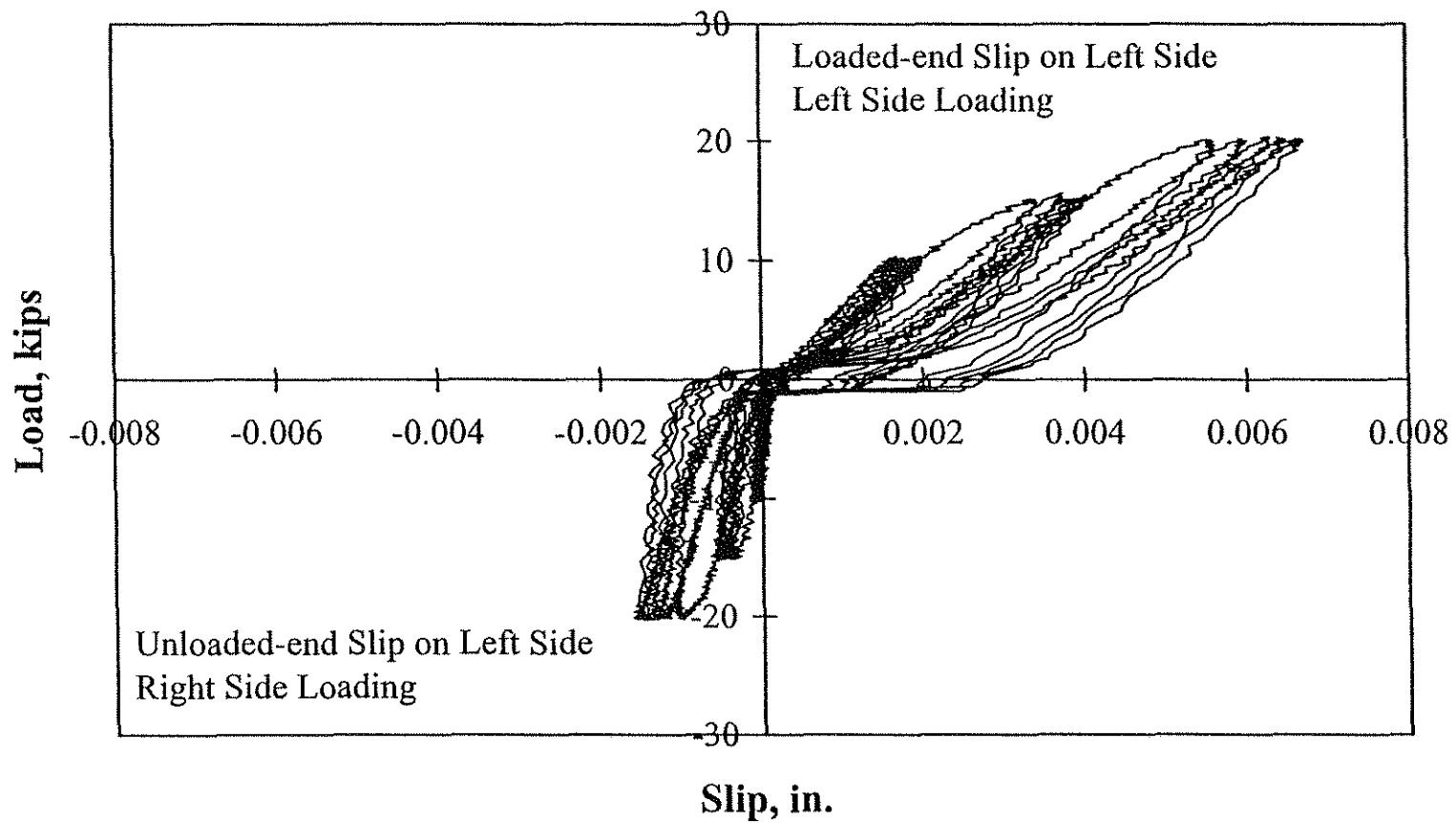


Fig. 7.3g Load versus loaded end and unloaded end slips for bar 8C0A-9 on the left side of the specimen

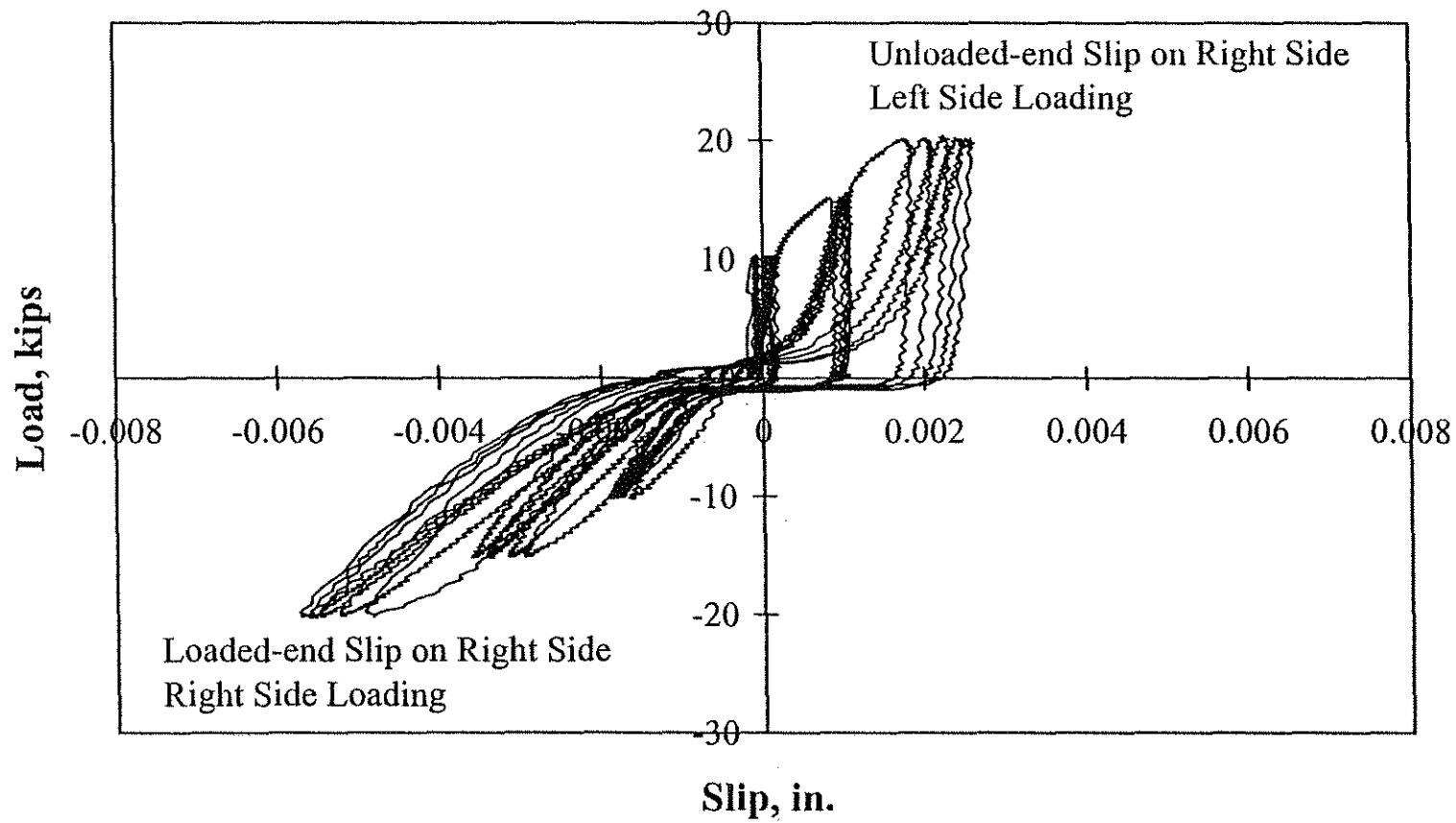


Fig. 7.3h Load versus loaded end and unloaded end slips for bar 8C0A-9 on the right side of the specimen

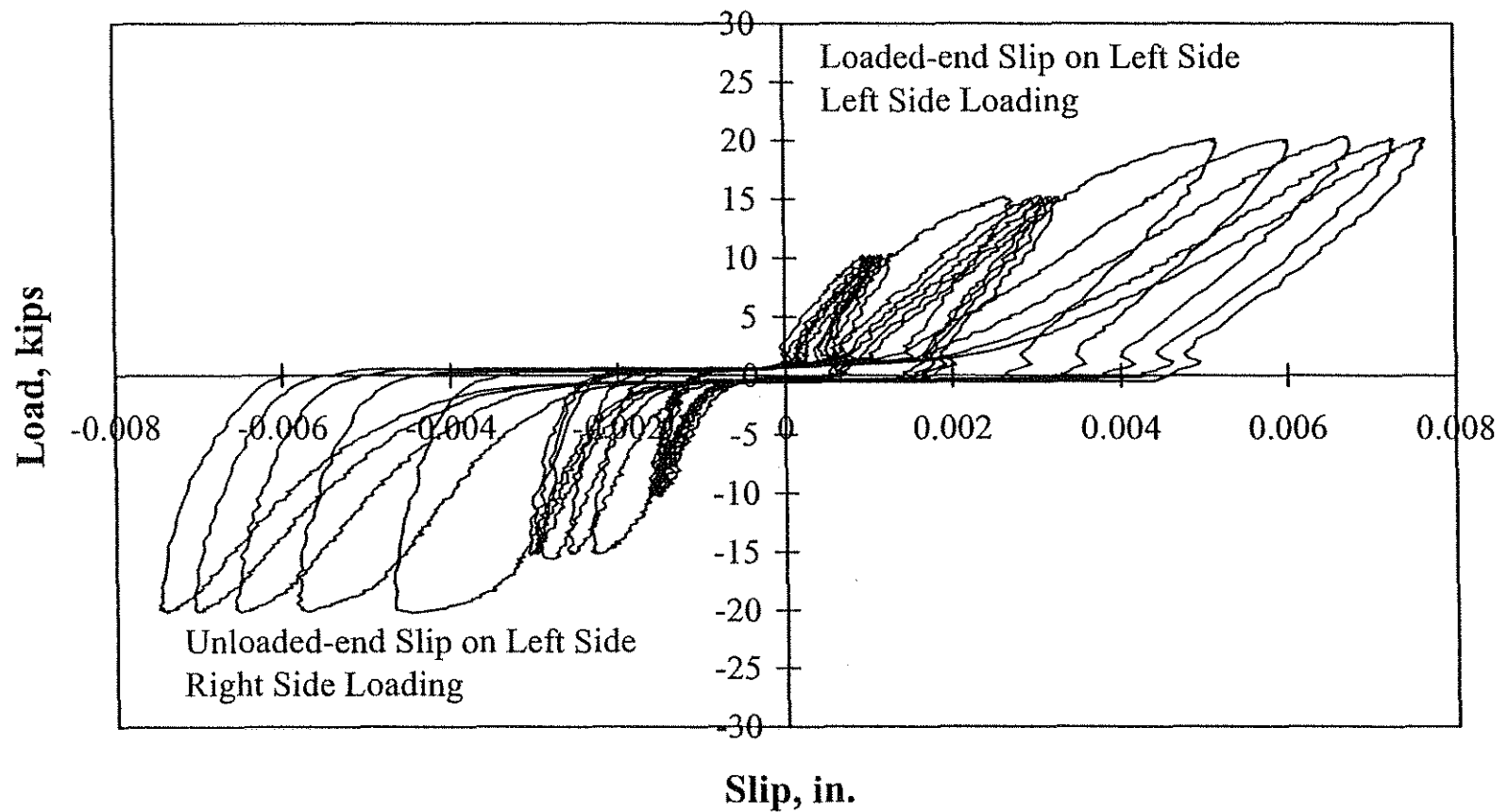


Fig. 7.3i Load versus loaded end and unloaded end slips for bar 8C0A-11 on the left side of the specimen

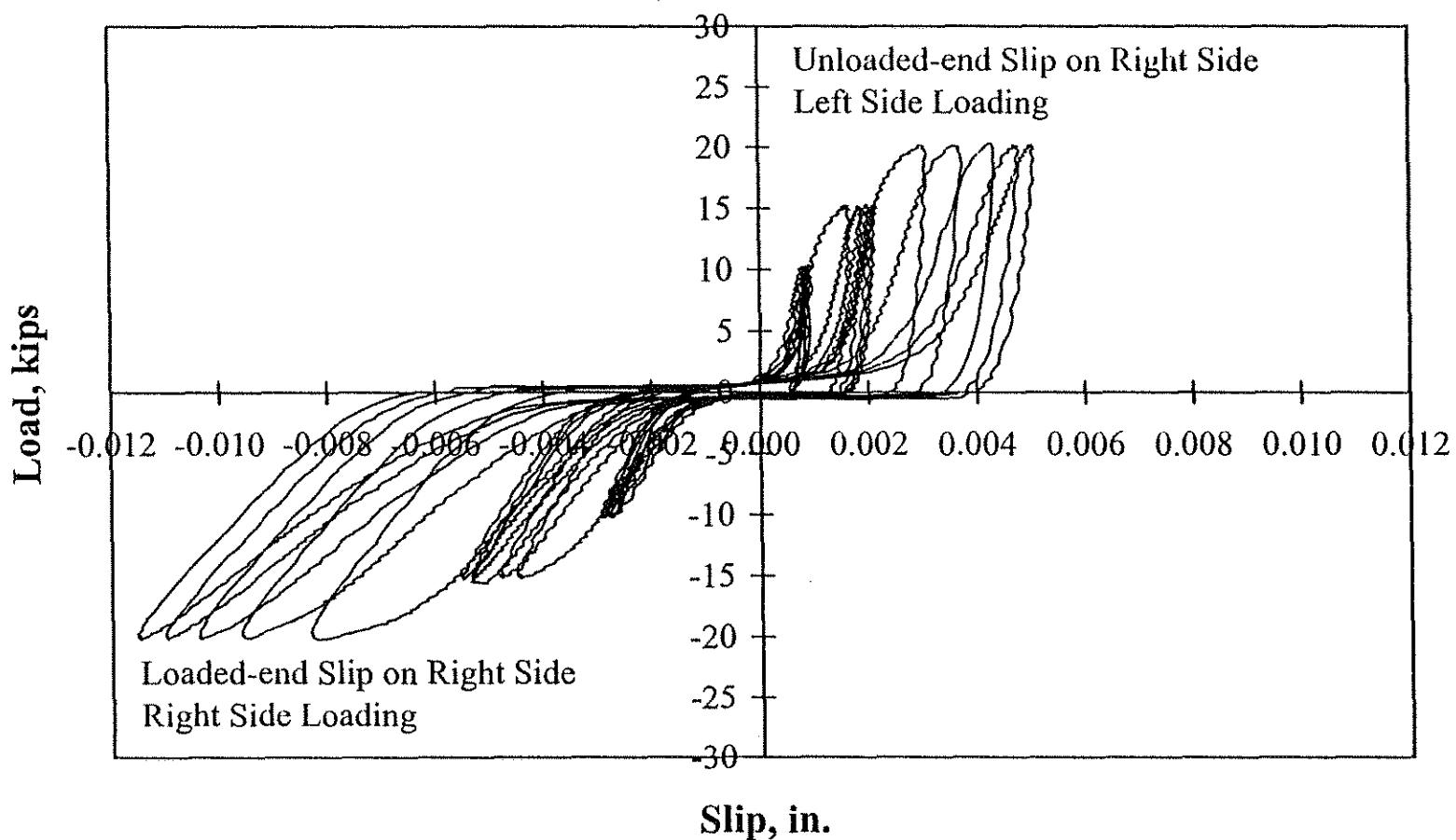


Fig. 7.3j Load versus loaded end and unloaded end slips for bar 8C0A-11 on the right side of the specimen

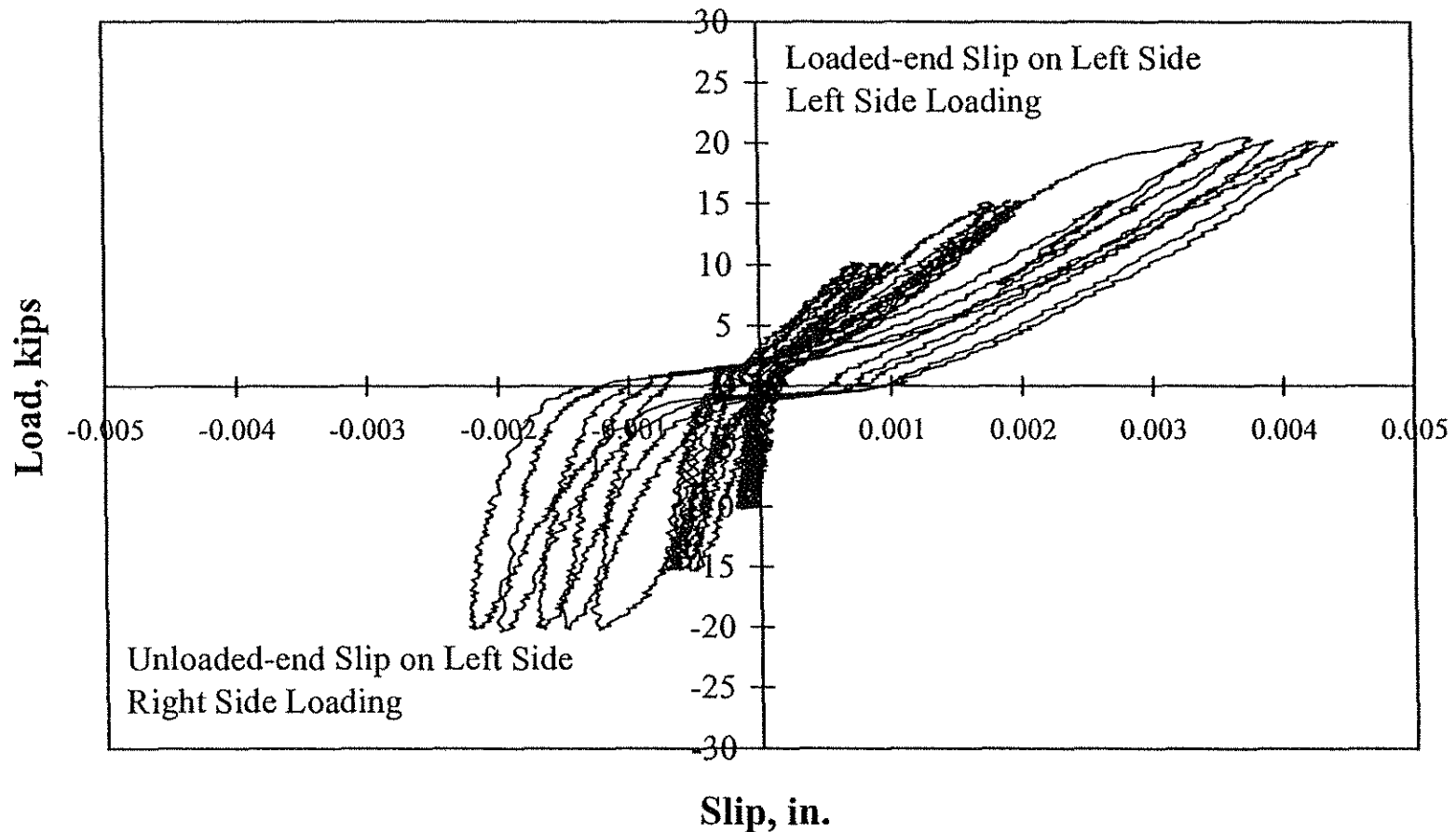


Fig. 7.3k Load versus loaded end and unloaded end slips for bar 8N3-4 on the left side of the specimen

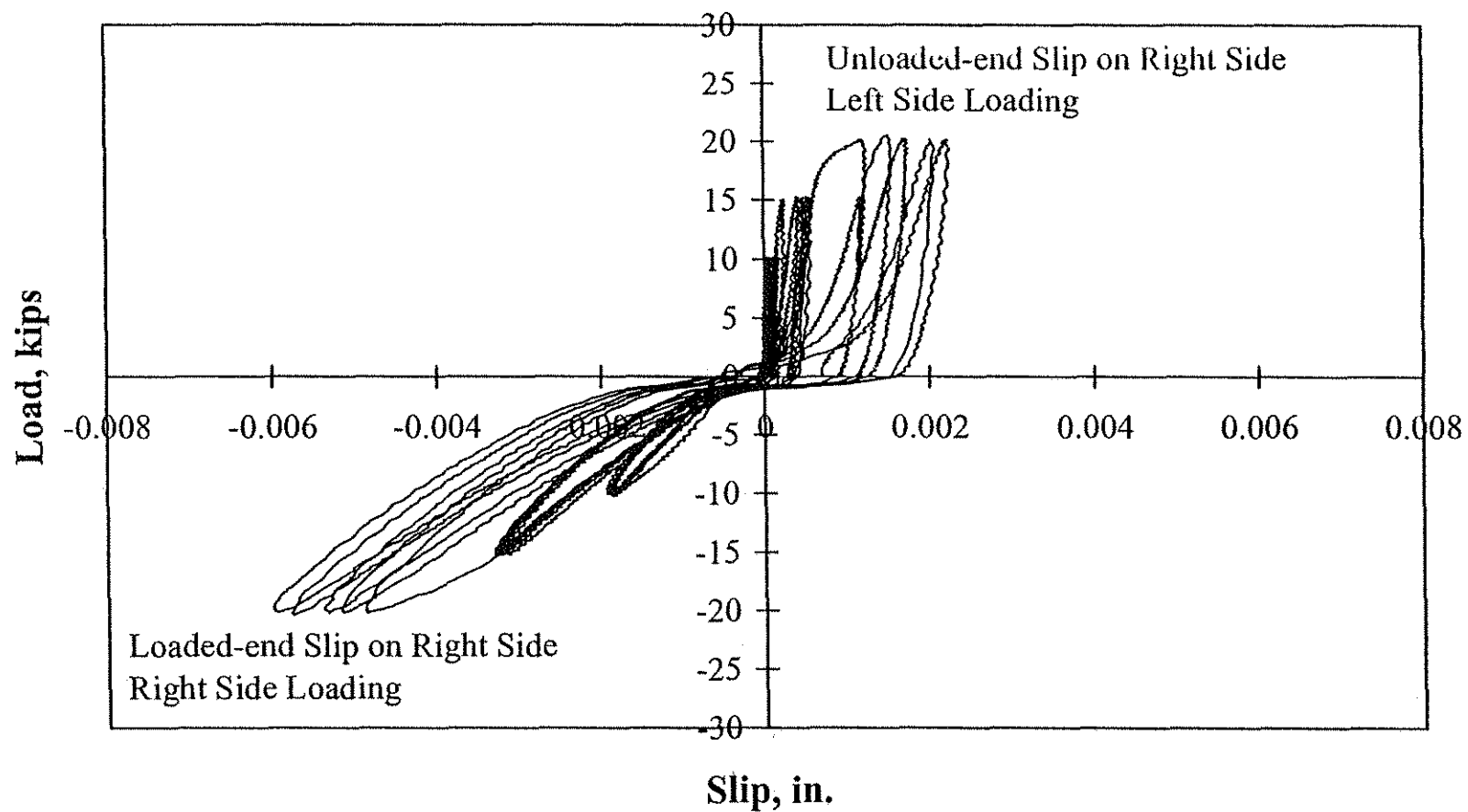


Fig. 7.31 Load versus loaded end and unloaded end slips for bar 8N3-4 on the right side of the specimen

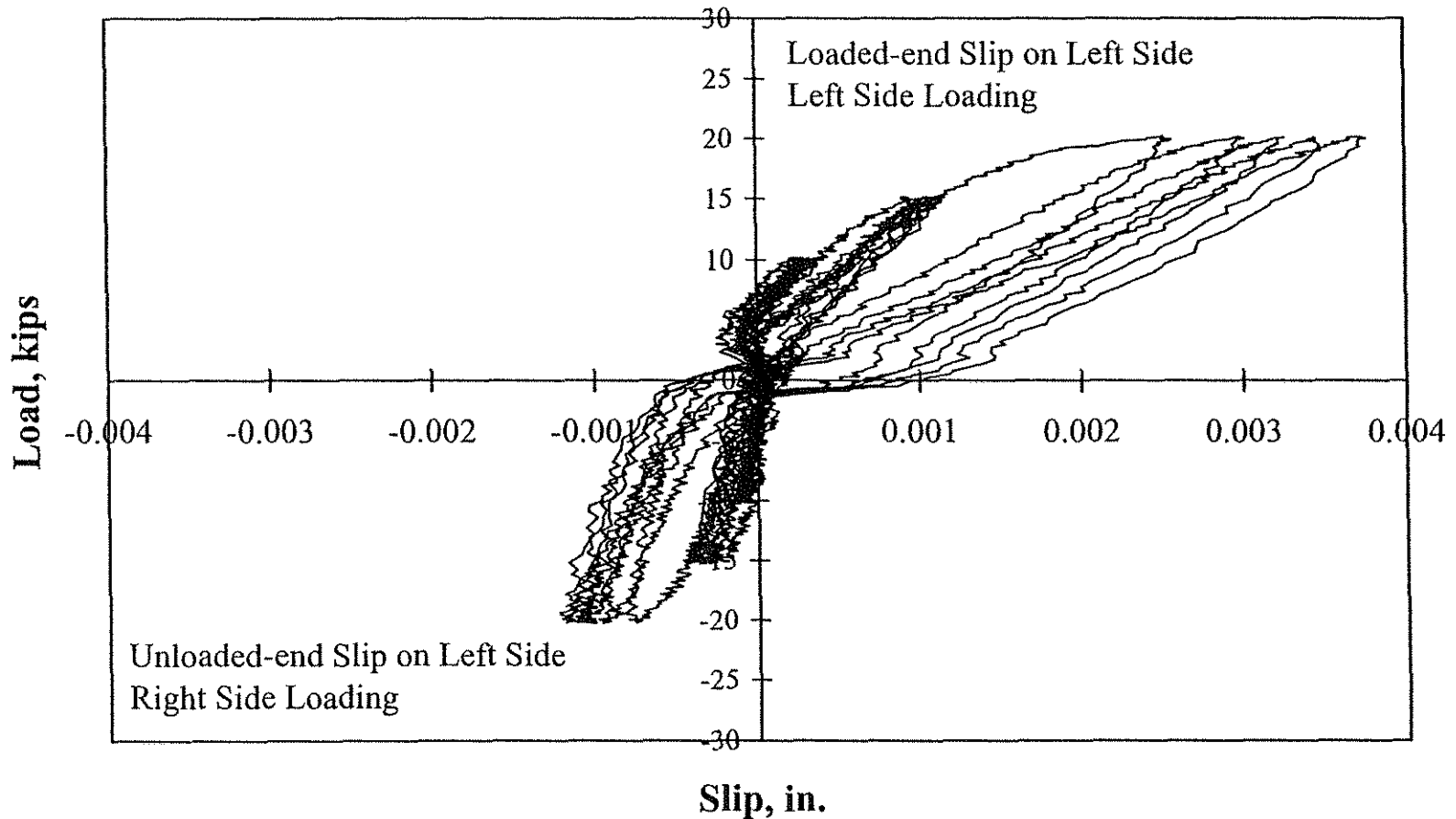


Fig. 7.3m Load versus loaded end and unloaded end slips for bar 8N3-6 on the left side of the specimen

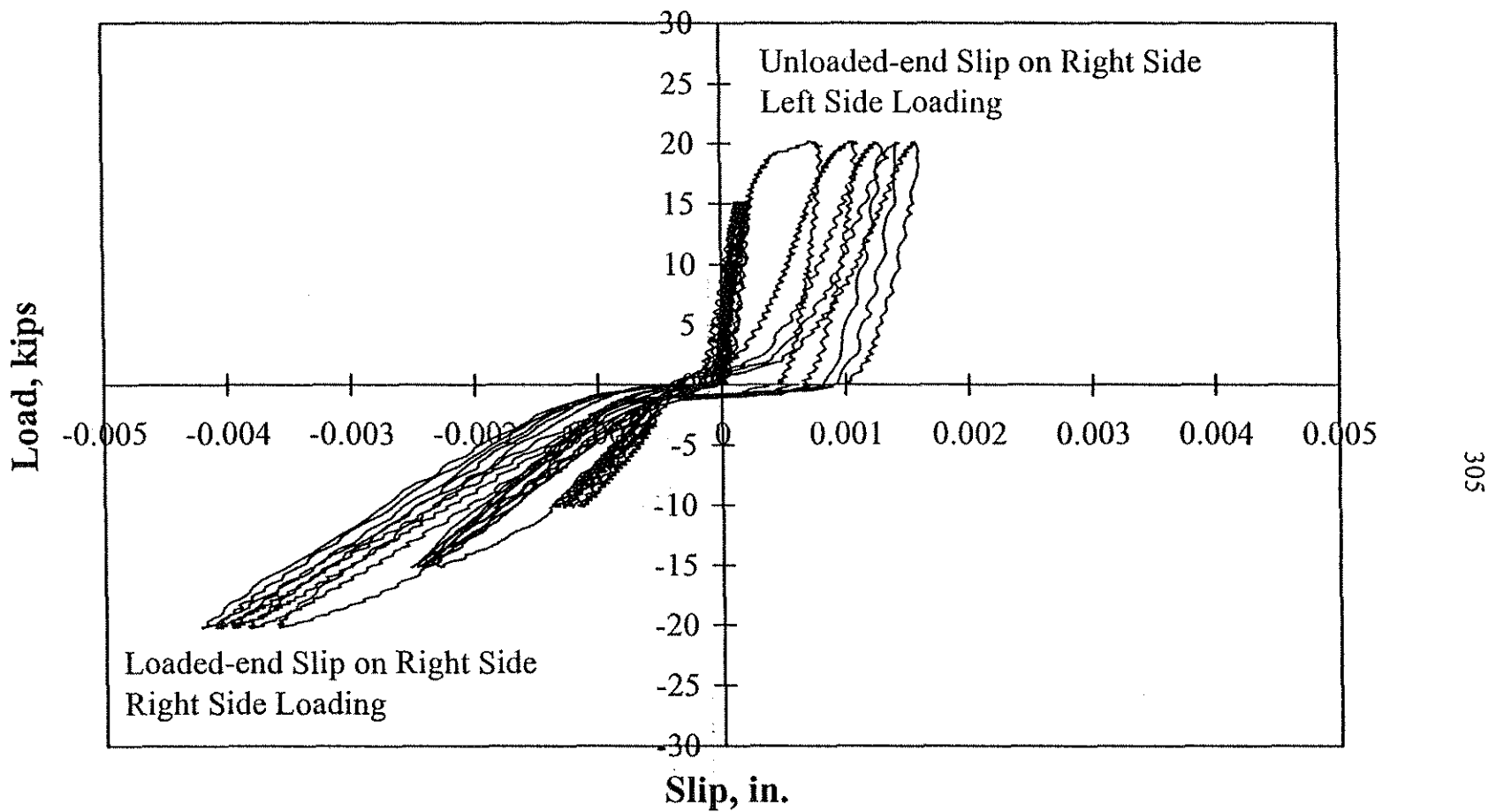


Fig. 7.3n Load versus loaded end and unloaded end slips for bar 8N3-6 on the right side of the specimen

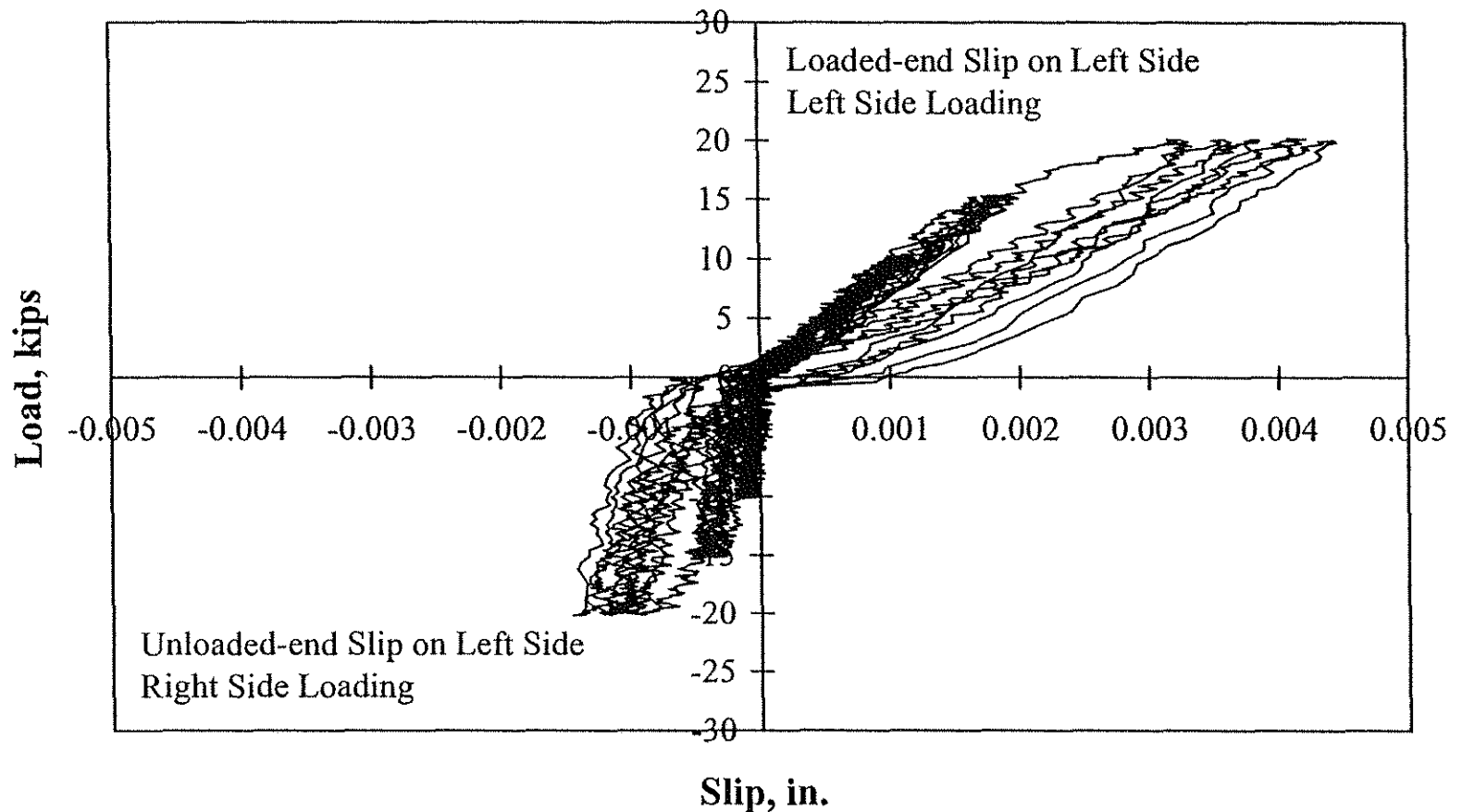


Fig. 7.3o Load versus loaded end and unloaded end slips for bar 8N3-8 on the left side of the specimen

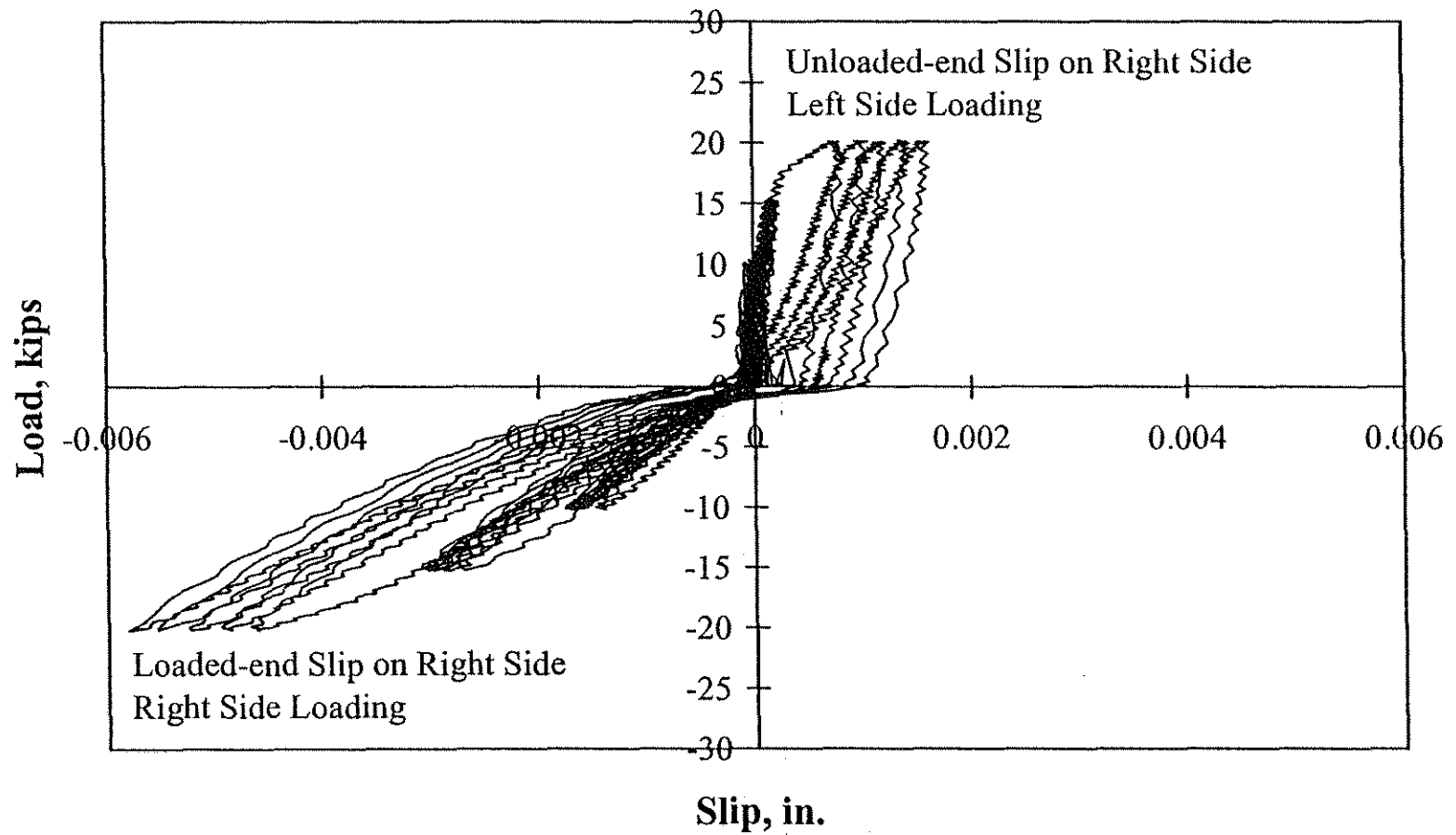


Fig. 7.3p Load versus loaded end and unloaded end slips for bar 8N3-8 on the right side of the specimen

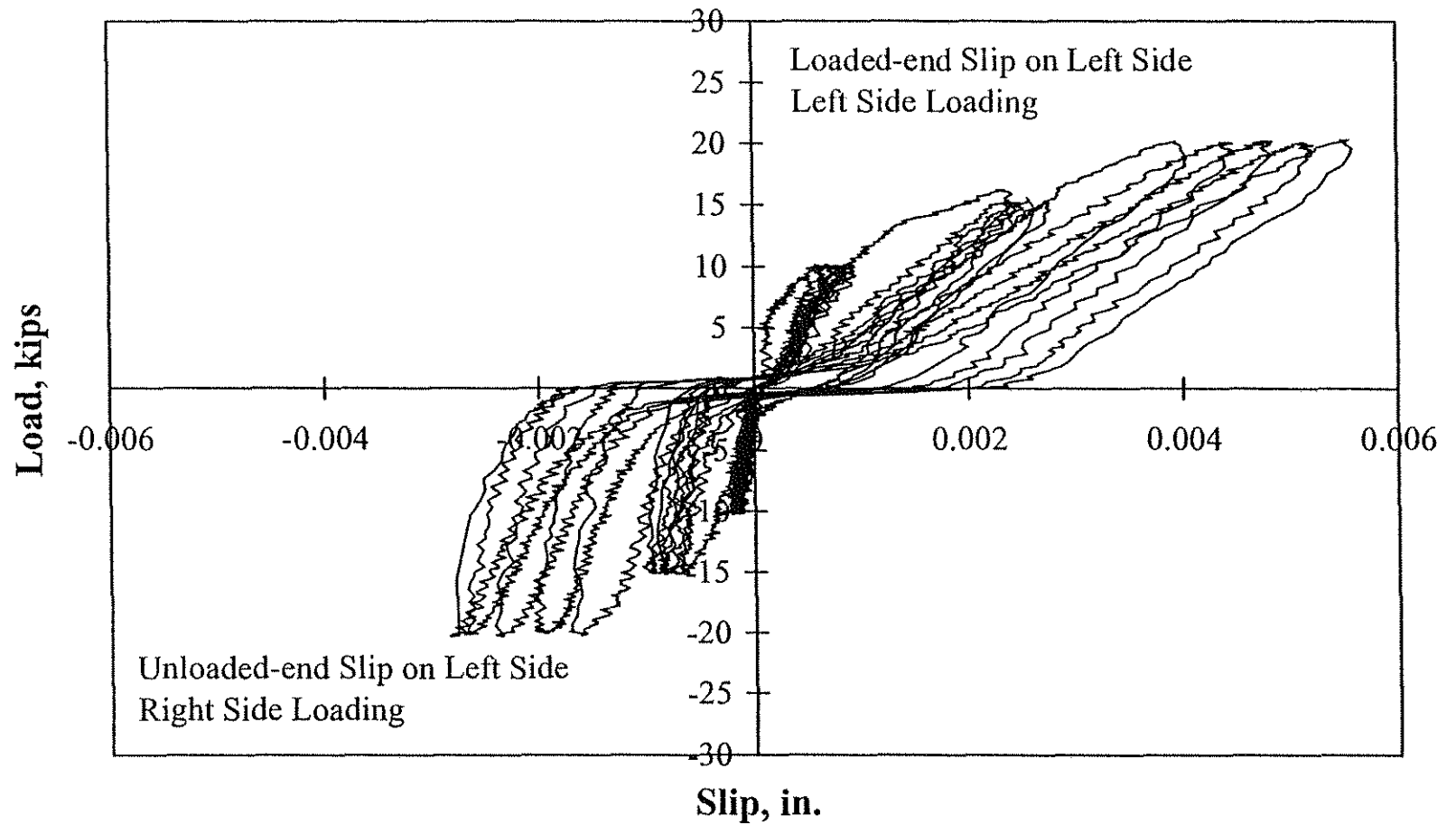


Fig. 7.3q Load versus loaded end and unloaded end slips for bar 8N3-10 on the left side of the specimen

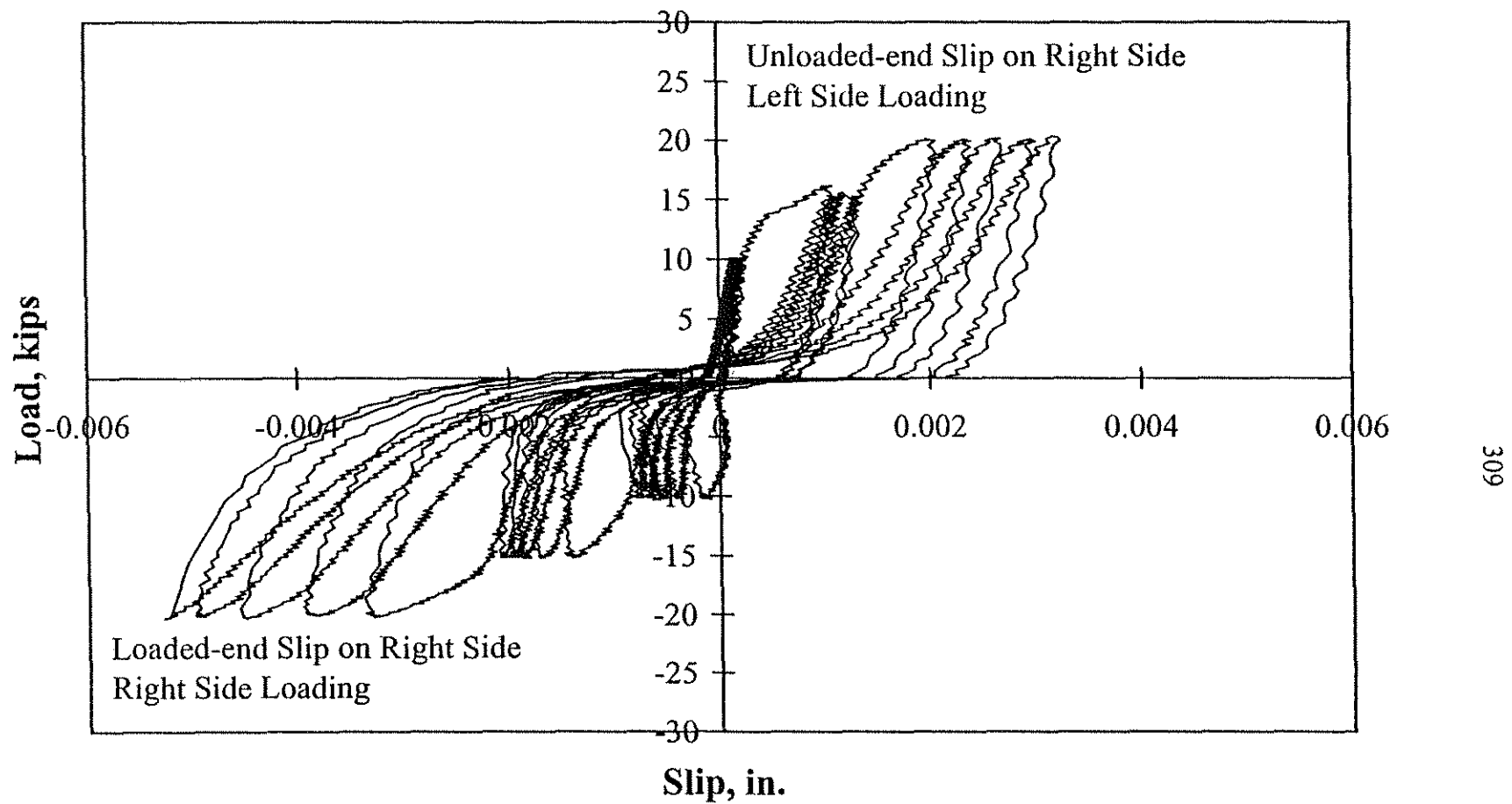


Fig. 7.3r Load versus loaded end and unloaded end slips for bar 8N3-10 on the right side of the specimen

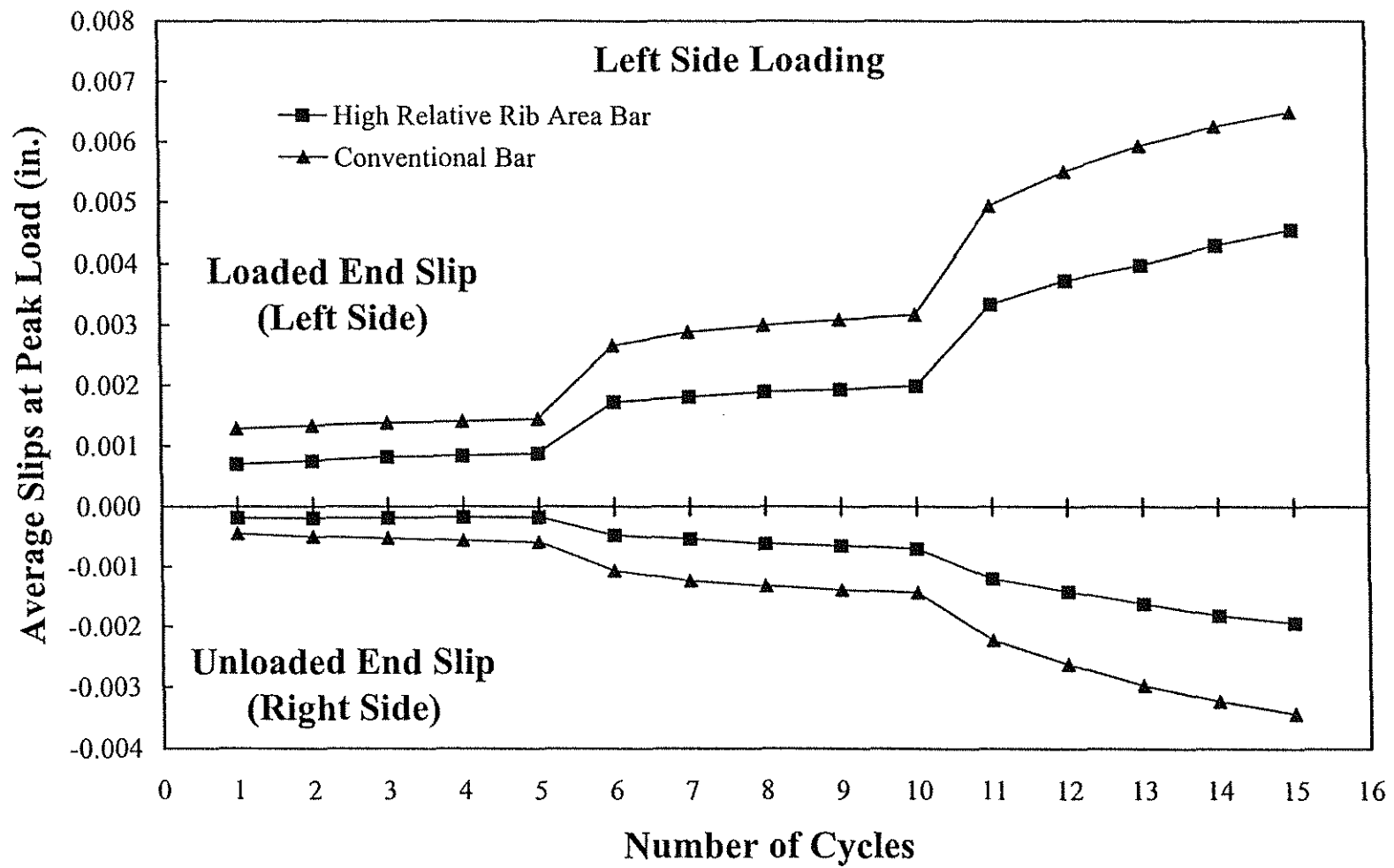


Fig. 7.4 Average slips of conventional bars 3, 5, 7, 9, and 11 and high relative rib area bars 4, 6, 8, and 10 at peak loads versus number of loading cycles for left side loading

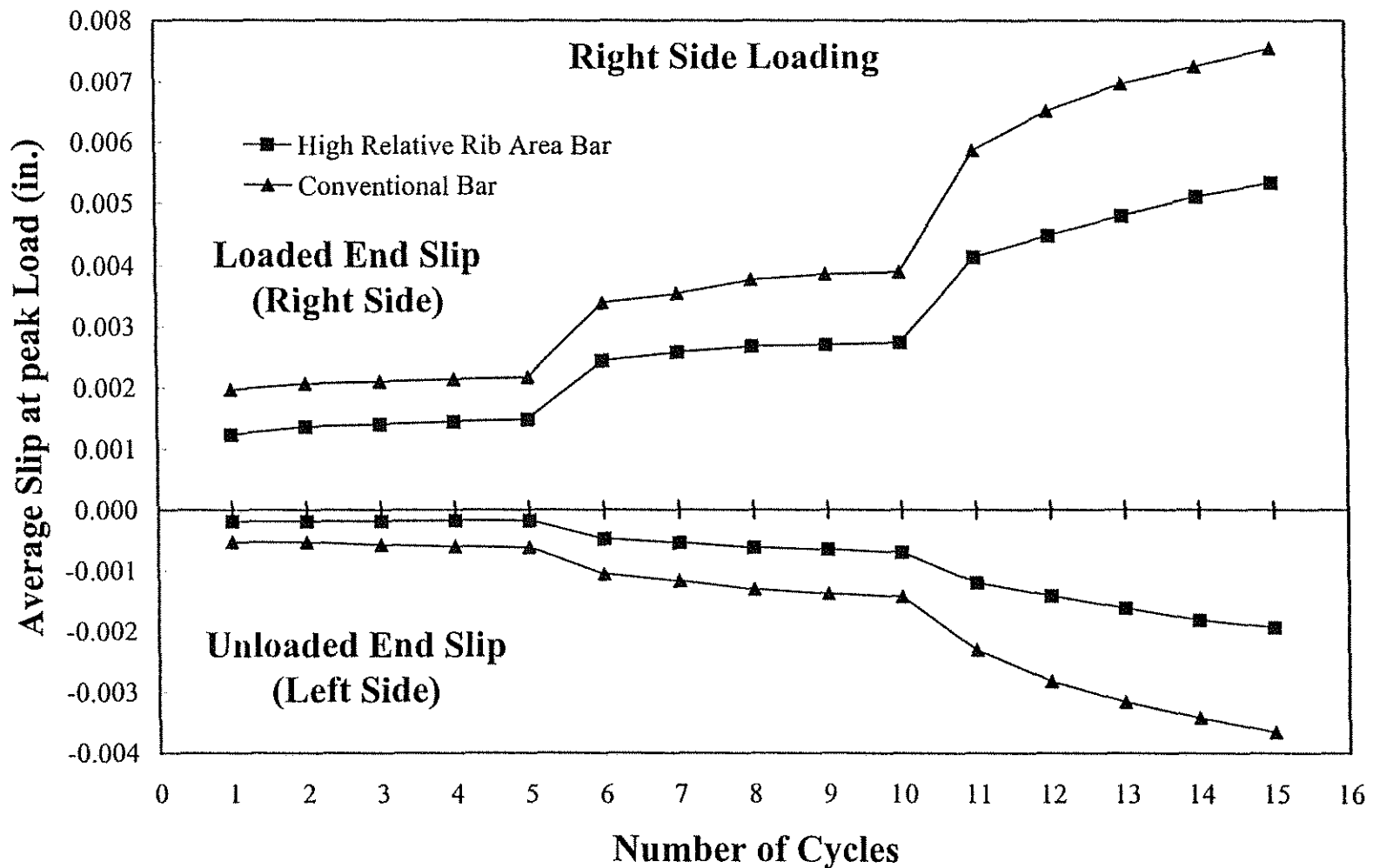


Fig. 7.5 Average slips of conventional bars 3, 5, 7, 9, and 11 and high relative rib area bars 4, 6, 8, and 10 at peak loads versus number of loading cycles for right side loading

APPENDIX A: CALCULATION OF FLEXURAL STRESS OF DEVELOPED AND SPLICED BARS

General

The working stress method has often been used in studies to determine the experimental bar stresses at failure for developed and spliced bars. In this appendix, the calculations of bar stresses using three methods, the working stress method, the ultimate strength method, and the moment-curvature method, are described. The data base for the calculations includes 439 development/splice specimens. The stresses calculated using the working stress method and the ultimate stress method are compared with those calculated using the moment-curvature method to study the relative values of bar stresses obtained using the different methods. The comparisons show that, for beams in which the bars did not yield, the working stress method, in general, overestimates the bar stresses for beams made with high-strength concrete and underestimates the bar stresses for beams made with normal-strength concrete when compared to the moment-curvature method. This is especially true for concrete strengths lower than 3000 psi (20.7 MPa). For beams in which the bars did not yield, the ultimate strength method overestimates bar stresses when compared to the moment-curvature method. For beams cast with high strength concrete with bars that yielded, the working stress method overestimates bar stresses, while the ultimate strength method underestimates bar stresses. The comparisons described in this appendix are used to choose the methods for calculating bar stresses in this study.

Test Data

Four hundred thirty nine beams containing developed/spliced bars are used in this analysis, including 299 specimens tested in previous studies (Chinn et al. 1955,

Chamberlin 1956, 1958, Mathey and Watstein 1961, Ferguson and Thompson 1965, Ferguson and Breen 1965, Thompson et al. 1975, Zekany et al. 1981, Choi et al. 1990, 1991, DeVries et al. 1991, Hester et al. 1991, 1993, Rezanoff et al. 1991, 1993, Azizinamini et al. 1993, 1995, Darwin et al. 1995a, 1996a) and 140 specimens tested in this study. The specimens include 63 beams in which the bars yielded prior to failure and 376 beams in which the bars did not yield. Concrete strengths ranged from 1000 to 16100 psi (6.9 to 111.0 MPa). The yield strengths of bars ranged from 50.0 to 114.7 ksi (398 to 791 MPa). Specimen properties are summarized in Table A.1. More complete information about the specimens is presented in Tables 5.5 and 5.10.

Calculation Methods

For the calculations in this study, the expression in ACI 318-95 is used to determine the modulus of elasticity of concrete.

$$E_c = 57,000\sqrt{f'_c} \quad (\text{A.1})$$

in which f'_c , the concrete compressive strength, and $\sqrt{f'_c}$ are expressed in psi. A modulus of elasticity (E_s) of 29,000 ksi (200,000 MPa) is used for steel bars. For all three methods, concrete is treated as a no-tension material and the area of steel, A_s , is taken as the area of the bars assuming that they are continuous rather than spliced.

Working stress method

The basic assumption of the working stress method is that strains vary linearly over the depth of the member and that stress is a linear function of strain ($\sigma = E\varepsilon$). The stress in the concrete and steel bars can be determined based on static equilibrium and compatibility of strain using a transformed section by replacing the

area of steel with an equivalent area of concrete, nA_s , in which $n = E_s/E_c$ and A_s = total steel area.

Ultimate strength method

An average concrete compressive stress of $0.85f'_c$ is assumed to be uniformly distributed over a stress block of a depth $a = \beta_1 c$, in which β_1 is equal to 0.85 for $f'_c \leq 4000$ psi (27.6 MPa) and $0.85 - 0.05f'_c \geq 0.65$ for $f'_c > 4000$ psi (27.6 MPa), and c is the distance from the extreme concrete compressive fiber to the neutral axis (ACI 318-95). The bar stress can be calculated based on these assumptions.

Moment-curvature method

The moment-curvature method is based on flexural theory and an assumed nonlinear stress distribution in the concrete. The applied moment can be expressed as a function of beam curvature which is related to concrete strain. A parabolic equation (Hognestad 1951) is used for the relationship between concrete stress, f_c , and strain, ε_c .

$$f_c = f'_c \left[\frac{2\varepsilon_c}{\varepsilon_o} - \left(\frac{\varepsilon_c}{\varepsilon_o} \right)^2 \right] \quad (\text{A.2})$$

where ε_o is concrete strain at maximum concrete stress. The concrete stress-strain curves (Fig. A.1) shown by Nilson (1997) are used to obtain the values of ε_o for f'_c of 3000, 4000, 5000, 6000, 8000, 10,000, and 12,000 psi (20.7, 27.6, 34.5, 41.4, 55.2, 69.0, and 82.7 MPa). For this data, ε_o is nearly a linear function of f'_c for high strength concrete [$f'_c \geq 8000$ psi (55.2 MPa)]. Therefore, values of ε_o for $f'_c > 12,000$ psi (82.7 MPa) are obtained by extrapolation of the best-fit line for f'_c of 8000, 10,000, and 12,000 psi (55.2, 69.0, and 82.7 MPa). For concrete compressive

strength less than 3000 psi (20.7 MPa), the values of ε_o are determined using Eq. A.3 (Bashur and Darwin 1976, 1978).

$$\varepsilon_o = \frac{f'_c}{363000 + 400f'_c} \quad (\text{A.3})$$

The curve of ε_o versus f'_c used in this study is shown in Fig. A.2.

Due to a lack of information about the stress-strain curves of the bars in the specimens, the stress-strain curves (Fig. A.3) adopted by Nilson (1997) are used in the current study as a basis for establishing stress-strain curves for use in the moment-curvature calculations. A modulus of elasticity of 29,000 ksi (200,000 MPa) is used before bars yield. The steel strain at the initiation of strain hardening (ε_{sh}) is 0.0086 for grade 60 steel and 0.0035 for grade 75 and above. There is no flat portion in the stress-strain curve for $f_y \geq 101.5$ ksi (700 MPa). The modulus of elasticity for hardening (E_h) is 614 ksi (4244 MPa) (0.021E_s) for $f_y = 60$ ksi (414 MPa), 713 ksi (4916 MPa) (0.025E_s) for $f_y = 75$ ksi (517 MPa), and 1212 ksi (8357 MPa) (0.042E_s) for $f_y \geq 90$ ksi (620 MPa). The values of ε_{sh} and E_h for f_y between 60 and 90 ksi (411 and 620 MPa) are obtained using linear interpolation. The steel stress-strain curves used in the current study are shown in Fig. A.4.

Calculation Results

Bar stresses calculated using the three methods are given in Table A.1. The applied moments for 18 specimens with bars that yielded are greater than the moment capacities calculated using the moment-curvature method, preventing the calculation of bar stresses using this method. This can happen as the results of variability in yield strengths of bars.

Comparisons

The moment-curvature method is believed, in general, to be better than the other two methods to calculate bar stresses since it considers the nonlinear stress-strain behavior of the concrete. Therefore, the bar stresses calculated using the working stress method, f_{sw} , and the ultimate strength method, f_{su} , are compared to those calculated using the moment-curvature method, f_{sc} , to study the relative values of the stresses obtained using the three methods.

Fig. A.5 shows the ratio of f_{sw} to f_{sc} as a function of $\varepsilon_{ct}/\varepsilon_0$ for the bars with $f_{sc} < f_y$, in which ε_{ct} is the strain at the extreme concrete compressive fiber at failure based on the moment-curvature method. The figure shows that f_{sw}/f_{sc} decreases with an increase in $\varepsilon_{ct}/\varepsilon_0$. f_{sw} is within 1% of f_{sc} for $\varepsilon_{ct}/\varepsilon_0 < 0.4$. More than 50 percent of the beams with $f_{sc} < f_y$ have $\varepsilon_{ct}/\varepsilon_0 > 0.4$. Fig. A.6 shows that, compared to the moment-curvature method, the working stress method overestimates bar stresses for high strength concrete, and underestimates bar stresses for normal strength, especially for $f'_c < 3000$ psi (20.6 MPa). The values of f_{sw}/f_{sc} range from 0.940 to 1.002 for normal strength concrete and from 0.996 to 1.010 for high strength concrete.

The ratios of f_{su} to f_{sc} are plotted versus $\varepsilon_{ct}/\varepsilon_0$ in Fig. A.7 for beams with $f_{sc} < f_y$. The figure shows that, in general, f_{su}/f_{sc} increases with an increase in $\varepsilon_{ct}/\varepsilon_0$, especially when $\varepsilon_{ct}/\varepsilon_0$ is greater than 0.4. Fig. A.8 shows the plot of f_{su}/f_{sc} versus f'_c . As expected, for beams with $f_{sc} < f_y$, the ultimate strength method underestimates bar stresses, compared to the moment-curvature method. The values of f_{su}/f_{sc} range from 0.909 to 1.025 for normal strength concrete and from 0.919 to 0.960 for high strength concrete. f_{su}/f_{sc} is below 1.0 for more than 98% of the beams.

The values of f_{sw}/f_{sc} are plotted versus $\varepsilon_{ct}/\varepsilon_0$ and f'_c in Figs. A.9 and A.10, respectively, for beams with $f_{sc} \geq f_y$. The figures show that the working stress method

consistently overestimates the bar stresses for high-strength concrete, compared to the moment-curvature method. The values of f_{sw}/f_{sc} range from 0.970 to 1.040 for normal-strength concrete and from 1.007 to 1.056 for high-strength concrete. f_{sw}/f_{sc} is greater than 1.0 for bars with $f_{sc} \geq f_y$ in all cases for beams made with high-strength concrete and in 55 percent of the beams made with normal-strength concrete. As can be observed in Figs. A.9 and A.10, the ratio f_{sw}/f_{sc} exhibits significant scatter.

Figs. A.11 and A.12 compare f_{su}/f_{sc} versus $\varepsilon_{cr}/\varepsilon_o$ and f'_c , respectively, for beams with $f_{sc} \geq f_y$. Contrary to the results for the working stress method (Figs. A.9 and A.10), the ultimate strength method underestimates the bar stresses for high-strength concrete, as well as many specimens cast with normal-strength concrete. The values of f_{su}/f_{sc} range from 0.956 to 1.021 for normal-strength concrete and from 0.949 to 0.997 for high-strength concrete. f_{su}/f_{sc} is less than 1.0 for all of the beams made with high-strength concrete and 41 percent of the beams made with normal-strength concrete. For the beams with $f_{sc} \geq f_y$, the ultimate strength method produces a more conservative prediction of bond strength than the working strength method.

Table A.1
Data and bar stress for specimens containing developed and spliced bars

Study	Specimen	b	d	A _s ***	M _u	f _c	f _y	ϵ_{cr}/ϵ_0 **	f _{sc+}	f _{sw++}	f _{su+++}
	No.	(in.)	(in.)	(in. ²)	(in-kips)	(psi)	(ksi)		(ksi)	(ksi)	(ksi)
China (1955)	D31	3.69	6.50	0.110	40.01	4700	79.00	0.286	60.70	60.35	57.65
	D36	3.69	6.50	0.110	32.42	4410	79.00	0.240	49.21	48.95	46.48
	D10	3.62	6.50	0.440	64.83	4370	57.00	0.304	26.41	26.27	24.13
	D20	3.75	6.50	0.440	66.58	4230	57.00	0.313	27.12	26.95	24.83
	D22	3.69	6.50	0.440	59.06	4480	57.00	0.265	23.97	23.89	21.80
	D13	7.31	6.50	0.440	125.63	4820	57.00	0.347	49.14	48.93	46.36
	D14	3.69	6.50	0.440	80.84	4820	57.00	0.351	32.82	32.63	30.32
	D15	7.25	6.50	0.440	108.11	4290	57.00	0.325	42.45	42.24	39.83
	D21	7.31	6.50	0.440	111.11	4480	57.00	0.322	43.53	43.35	40.88
	D29	3.69	6.50	0.440	111.87	7480	57.00	0.345	44.62	44.60	41.61
	D3	9.00	6.50	0.880	184.17	4350	57.00	0.381	37.15	36.86	34.64
	D32	7.25	6.50	0.440	118.12	4700	57.00	0.333	46.24	46.05	43.51
	D38	4.62	6.50	0.440	69.82	3160	57.00	0.361	28.50	28.16	26.30
	D39	3.69	6.50	0.440	67.57	3160	57.00	0.416	28.05	27.62	25.92
	D5	5.50	6.50	0.440	111.86	4180	57.00	0.422	44.76	44.34	42.19
	D6	7.25	6.50	0.880	163.68	4340	57.00	0.395	33.48	33.17	31.06
	D7	3.62	6.50	0.440	83.57	4450	57.00	0.396	34.15	33.85	31.71
	D8	7.25	6.50	0.880	177.67	4570	57.00	0.414	36.28	35.95	33.81
	D9	3.62	6.50	0.440	86.32	4380	57.00	0.417	35.33	34.98	32.90
	D34	3.62	6.50	0.440	90.58	3800	57.00	0.501	37.46	36.86	35.27
	D12	3.75	6.50	0.440	113.12	4530	57.00	0.538	46.37	45.70	44.12
	D17	3.69	6.50	0.440	97.60	3580	57.00	0.571	40.56	39.74	38.62
	D19	7.31	6.50	0.440	153.39	4230	57.00	1.118	57.60	59.93	57.96
	D23	3.62	6.50	0.440	96.86	4450	57.00	0.469	39.70	39.23	37.31
	D24	7.25	6.50	0.440	110.62	4450	57.00	0.324	43.37	43.18	40.72
	D30	3.69	6.50	0.440	132.63	7480	57.00	0.417	53.04	52.88	49.98
	D4	9.00	6.50	0.880	234.21	4470	57.00	0.490	47.40	46.84	44.94
	D40	7.38	6.50	0.440	130.12	5280	57.00	0.332	50.69	50.55	47.84
	D25	3.62	6.50	0.440	144.40	5100	57.00	1.111	57.00	58.25	57.66
	D26	3.69	6.50	0.440	138.64	5100	57.00	0.624	56.82	55.87	54.84
	D35	3.62	6.50	0.440	135.13	3800	57.00	0.836	56.91	54.99	56.49
	D33	6.80	6.50	1.560	237.77	4830	57.00	0.483	28.60	28.20	26.46
Chamberlin (1956)	SIII15	6.00	4.75	0.200	29.76	4470	50.00	0.212	34.55	34.52	32.29
	SIII16	6.00	4.75	0.200	32.85	4470	50.00	0.236	38.17	38.11	35.76
	SIII31	6.00	4.75	0.200	34.38	5870	50.00	0.200	39.60	39.66	37.16
	SIII32	6.00	4.75	0.200	40.20	5870	50.00	0.236	46.33	46.37	43.66
	SIII33	6.00	4.75	0.200	42.00	5870	50.00	0.247	48.43	48.45	45.68
	SIII11	6.00	4.75	0.200	35.34	3680	50.00	0.296	41.39	41.17	38.90
	SIII27	6.00	4.75	0.200	40.25	5870	50.00	0.236	46.40	46.43	43.72
	SIII28	6.00	4.75	0.200	42.76	5870	50.00	0.252	49.30	49.32	46.53
	SIII29	6.00	4.75	0.200	42.76	5870	50.00	0.252	49.30	49.32	46.53
	SIV53	6.00	4.75	0.400	78.31	4540	50.00	0.461	47.43	46.95	44.88
	SII23	9.00	7.63	0.440	128.02	4470	50.00	0.246	41.93	41.89	39.47
Chamberlin (1958)	3a	6.00	4.75	0.400	54.64	4450	50.00	0.314	32.94	32.78	30.48
	3b	6.00	4.75	0.400	55.01	4450	50.00	0.316	33.16	33.00	30.70
	3c	6.00	4.75	0.400	55.81	4450	50.00	0.321	33.65	33.48	31.18
	4a	6.00	4.75	0.200	36.74	4370	50.00	0.270	42.75	42.64	40.20
	4b	6.00	4.75	0.200	37.82	4370	50.00	0.279	44.02	43.89	41.43
	4c	6.00	4.75	0.200	37.33	4370	50.00	0.275	43.44	43.32	40.87
Ferguson and Breen (1965)	8R18a	17.03	12.72	1.580	748.08	3470	99.00	0.319	41.60	41.32	39.11
	8R24a	17.12	12.86	1.580	1078.94	3530	99.00	0.462	59.53	58.88	56.98
	8F30a	17.09	12.94	1.580	969.99	3030	74.00	0.460	53.48	52.78	51.06
	8F36a	17.16	13.09	1.580	1291.05	4650	63.50	0.953	66.22	68.74	66.34
	8F36b	16.94	13.13	1.580	1149.08	3770	74.00	0.455	61.90	61.30	59.29
	8F36k	9.69	13.21	1.580	1000.92	3460	74.00	0.638	55.84	54.65	54.10
	8F39a*	17.06	13.06	1.580	1378.95	3650	63.50	-	74.00	72.90	
	8F42a*	17.19	13.09	1.580	1223.98	2660	63.50	-	-	65.98	65.93
	8F42b*	17.16	13.08	1.580	1398.97	3830	63.50	-	-	74.86	73.54
	8R42a	17.19	12.94	1.580	1308.01	3310	99.00	0.602	72.21	71.01	70.20
	8R48a	17.03	13.02	1.580	1347.93	3040	99.00	0.671	74.43	72.88	72.84
	8R64a	17.09	12.98	1.580	1659.99	3550	99.00	0.759	91.70	89.71	90.64
	8R80a	17.03	13.03	1.580	1792.95	3740	99.00	0.794	98.61	96.41	97.80
	IIIR24a	24.09	15.72	3.120	2279.93	3720	93.00	0.420	52.30	51.81	49.70
	IIIR30a	24.09	16.08	3.120	2640.93	4030	93.00	0.445	59.03	58.50	56.38
	IIIF36a	24.09	15.79	3.120	2849.99	4570	73.00	0.452	64.66	64.16	61.90

Table A.1
Data and bar stress for specimens containing developed and spliced bars (continued)

Study	Specimen No.	b (in.)	d (in.)	A _s *** (in. ²)	M _u (in-kips)	f _c (psi)	f _y (ksi)	$\epsilon_{cr}/\epsilon_0^{**}$	f _{sc+} (ksi)	f _{sw++} (ksi)	f _{su+++} (ksi)
	11F36b	24.03	15.83	3.120	2617.43	3350	65.00	0.532	60.09	59.20	57.81
	11F42a	24.00	15.82	3.120	2813.87	3530	65.00	0.555	64.57	63.61	62.33
	11F48a	24.16	15.80	3.120	3255.90	3140	73.00	1.059	73.91	73.88	74.56
	11F48b*	24.15	15.93	3.120	3218.86	3330	65.00	-	-	72.32	72.24
	11R48a	24.16	15.83	3.120	3679.14	5620	93.00	0.504	82.31	82.22	79.95
	11R48b	24.22	15.43	3.120	3070.00	3100	93.00	0.727	73.20	71.43	71.98
	11F60a*	23.97	15.83	3.120	3530.06	2610	73.00	-	-	80.34	84.80
	11F60b*	24.00	15.92	3.120	3520.20	4090	65.00	-	-	78.78	78.02
	11R60a	24.00	16.01	3.120	3320.20	2690	93.00	0.866	77.19	74.61	77.00
	11R60b	24.00	15.58	3.120	3820.44	3460	93.00	0.862	90.35	87.80	90.11
	8F36c	17.09	13.00	1.580	1130.00	2740	74.00	0.594	62.56	61.33	60.63
	8F36d	17.06	12.97	1.580	1390.00	3580	74.00	0.800	74.74	74.31	74.31
	8F36e	17.12	12.94	1.580	1460.00	4170	74.00	0.944	77.28	77.44	77.44
	8F36f	17.06	13.04	1.580	1471.00	3780	74.00	1.071	77.64	79.01	78.15
	8F36g	17.03	12.94	1.580	1388.00	3070	74.00	1.003	75.34	75.51	75.78
	8F36h	17.03	13.00	1.580	1023.00	1910	74.00	0.743	57.88	56.02	56.93
	8F36j	17.12	13.03	1.580	1172.00	1820	74.00	0.939	66.98	64.09	67.30
	8F30b	17.04	13.03	1.580	1060.00	2610	74.00	0.573	58.62	57.47	56.63
	11R36a	24.06	15.33	3.120	3512.00	3020	93.00	0.918	85.26	82.35	85.46
Thompson et al. (1975)	6-12-4/2/2-6/6	33.00	10.63	2.640	1451.40	3730	61.70	0.443	57.96	57.40	55.36
	8-18-4/3/2-6/6	36.00	9.50	4.740	2227.64	4710	59.30	0.546	57.00	56.26	54.64
	8-18-4/3/2.5-4/6	36.00	9.50	4.740	1927.54	2920	59.30	0.723	50.86	49.33	49.70
	8-24-4/2/2-6/6	36.00	10.50	4.740	2203.18	3105	59.30	0.649	51.89	50.64	50.27
	11-25-6/2/3-5/5	44.06	10.30	7.800	3068.58	3920	66.30	0.567	45.00	44.19	42.95
	11-30-4/2/2-6/6	40.88	10.30	9.360	3085.99	2865	60.50	0.795	39.56	37.99	38.93
	11-30-4/2/4-6/6	44.88	10.30	9.360	3645.28	3350	63.40	0.764	45.90	44.39	45.02
	11-30-4/2/2.7-4/6	44.88	10.30	6.240	3253.77	4420	63.30	0.583	58.48	57.59	56.32
	11-45-4/1/2-6/6	40.88	11.30	9.360	4085.46	3520	60.50	0.746	46.72	45.28	45.70
	14-60-4/2/2-5/5	37.50	13.30	11.250	5696.83	2865	57.70	1.070	48.13	45.23	49.36
	14-60-4/2/4-5/5*	41.50	13.15	11.250	7119.12	3200	57.70	-	-	56.64	63.31
	11-30-4/2/2-6/6-S5	40.88	10.30	9.360	3780.98	3063	65.00	1.003	49.06	46.47	49.85
	11-20-4/2/2-6/6-SP	40.88	10.30	9.360	3461.63	3620	67.30	0.719	43.61	42.32	42.43
	11-20-4/2/2-6/6-S5	40.88	10.30	9.360	3315.19	3400	67.30	0.726	41.92	40.61	40.81
	8-15-4/2/2-6/6-S5	36.00	10.50	4.740	2501.69	3507	61.10	0.677	58.66	57.31	57.13
Mathey and Watstein (1961)	4-7-2	8.00	16.00	0.200	269.84	4210	114.70	0.248	88.71	88.60	85.94
	4-7-1	8.00	16.00	0.200	280.54	4265	114.70	0.256	92.21	92.10	89.39
	4-10.5-3	8.00	16.00	0.200	344.51	3675	114.70	0.355	113.71	113.30	110.73
	4-10.5-2	8.00	16.00	0.200	350.09	4055	114.70	0.339	115.26	115.00	112.26
	4-14-2	8.00	16.00	0.200	305.32	3710	114.70	0.310	100.69	100.40	97.78
	8-21-1	8.00	16.00	0.790	711.86	4235	97.00	0.382	62.16	61.80	59.34
	8-28-1	8.00	16.00	0.790	890.29	4485	97.00	0.468	77.79	77.20	74.99
	8-28-2	8.00	16.00	0.790	824.72	3700	97.00	0.503	72.59	71.80	70.06
	8-34-1	8.00	16.00	0.790	1058.16	3745	97.00	0.671	93.63	92.10	91.90
	8-14-1	8.00	16.00	0.790	383.39	3585	97.00	0.223	33.51	33.40	31.32
	8-34-2	8.00	16.00	0.790	1030.70	3765	97.00	0.646	91.10	89.70	89.22
	8-14-2	8.00	16.00	0.790	489.11	4055	97.00	0.263	42.63	42.50	40.14
	8-7-1	8.00	16.00	0.790	329.06	4005	97.00	0.175	28.63	28.60	26.68
	8-21-2	8.00	16.00	0.790	610.33	3495	97.00	0.376	53.62	53.20	50.99
Hester et al. (1991, 1993)	1-8N3160U	16.00	13.50	2.370	1432.92	5990	63.80	0.333	50.13	50.03	47.18
	2-8C3160U	16.00	13.99	2.370	1375.87	6200	69.00	0.291	46.25	46.24	43.39
	3-8S3160U	16.09	13.69	2.370	1360.99	6020	71.10	0.305	46.86	46.81	43.98
	4-8S3160U	16.08	13.62	2.370	1228.12	6450	71.10	0.261	42.36	42.40	39.59
	5-8C3160U	16.09	13.72	2.370	1157.87	5490	69.00	0.275	39.86	39.82	37.20
	6-8C3220U	16.06	13.54	2.370	1489.08	5850	69.00	0.352	51.99	51.85	49.04
	7-8C3160U	16.03	13.58	1.580	885.07	5240	69.00	0.257	45.40	45.37	42.74
	7-8C3-16-3-U	16.00	13.77	1.580	1019.02	5240	69.00	0.2917	51.57	51.49	48.75
	4-8S3-16-2-U	16.09	13.82	2.370	1384.10	6450	71.10	0.2890	47.05	47.06	44.15
	4-8S3-16-3-U	16.09	13.68	2.370	1456.14	6450	71.10	0.3108	50.06	50.04	47.09
	5-8C3-16-2-U	16.10	13.86	2.370	1366.90	5490	69.00	0.3232	46.62	46.51	43.80
	6-8C3-22 3/4-3-U	16.06	13.53	2.370	1619.93	5850	69.00	0.3866	56.66	56.45	53.68
	1-8N3-16-2-U	16.00	13.50	2.370	1603.91	5990	63.80	0.3773	56.18	56.00	53.18
	6-8C3-22 3/4-4-U	16.03	13.51	2.370	1594.93	5850	69.00	0.3815	55.87	55.67	52.89
	5-8C3-16-3-U	16.09	13.56	2.370	1243.96	5490	69.00	0.3035	43.39	43.31	40.63
	3-8S3-16-2-U	16.06	13.66	2.370	1347.88	6020	71.10	0.3034	46.51	46.47	43.65
	2-8C3-16-2-U	16.00	13.95	2.370	1305.00	6200	69.00	0.2765	43.98	43.99	41.18

Table A.1
Data and bar stress for specimens containing developed and spliced bars (continued)

Study	Specimen No.	b (in.)	d (in.)	A _s *** (in. ²)	M _u (in-kips)	f _c (psi)	f _y (ksi)	ϵ_{cr}/ϵ_o **	$\epsilon_{sc}+$ (ksi)	f _{sw++} (ksi)	f _{su+++} (ksi)
Choi et al. (1990, 1991)	1-SN0120U	10.50	14.69	0.620	521.00	5360	63.80	0.244	61.51	61.51	58.73
	1-SN0120U	15.75	14.69	0.930	813.00	5360	63.80	0.267	64.00	63.99	61.16
	2-6C0120U	11.00	14.63	0.880	610.04	6010	70.90	0.223	51.34	51.40	48.65
	2-6S0120U	11.00	14.63	0.880	542.98	6010	63.80	0.197	45.67	45.75	43.17
	3-8N0160U	12.00	14.00	1.580	857.93	5980	63.80	0.257	43.00	43.02	40.29
	3-8S0160U	12.00	14.00	1.580	854.00	5980	67.00	0.256	42.84	42.82	40.09
	4-11C0240U	13.65	13.30	3.120	1371.99	5850	63.10	0.337	37.93	37.82	35.21
	4-11S0240U	13.65	13.30	3.120	1459.06	5850	64.60	0.360	40.37	40.22	37.61
	20-6-2	11.02	11.61	0.930	685.32	4277.43	72.50	0.486	70.77	70.12	68.11
	20-6-3	11.02	11.61	0.930	747.92	3885.94	72.50	0.997	75.23	76.69	75.55
Rezansoff et al. (1991)	20-6-1	11.02	11.61	0.930	777.26	4045.43	72.50	1.238	77.86	79.62	78.50
	20-8-11*	11.02	11.50	1.550	1175.34	4465.93	65.54	-	-	74.60	75.00
	20-8-9	11.02	11.00	1.550	901.43	4204.93	65.54	0.616	61.10	60.05	59.12
	20-8-10	11.02	11.00	1.550	962.37	4407.93	65.54	0.639	65.16	64.03	63.28
	20-8-1*	11.02	11.50	1.550	1142.44	5219.91	65.54	-	-	72.22	71.05
	20-8-12	11.02	11.00	1.550	964.59	4349.93	65.54	0.649	65.38	64.20	63.56
	20-8-2	11.02	11.50	1.550	1028.11	5741.9	65.54	0.497	65.36	64.84	62.59
	20-8-3	11.02	11.50	1.550	1014.06	5509.91	65.54	0.507	64.59	64.02	61.89
	20-8-6*	11.02	11.50	1.550	1190.75	4770.42	65.54	-	-	75.45	75.37
	20-8-7	11.02	11.00	1.550	922.57	4494.93	65.54	0.595	62.30	61.35	60.17
	20-8-8	11.02	11.00	1.550	895.18	4349.93	65.54	0.592	60.52	59.58	58.40
	20-8-5*	11.02	11.50	1.550	1199.55	4770.42	65.54	-	-	76.01	76.01
	20-8-4*	11.02	11.50	1.550	1129.23	4335.43	65.54	-	-	71.73	71.94
	20-8-21	11.02	11.00	1.550	682.87	3378.44	60.90	0.539	46.58	45.76	44.45
	20-8-13	11.02	11.50	1.550	801.86	3508.94	64.38	0.577	52.17	51.22	50.14
	20-8-14	11.02	11.50	1.550	832.56	3276.95	64.38	0.645	54.51	53.28	52.84
	20-8-15	11.02	11.50	1.550	856.77	3624.94	64.38	0.607	55.74	54.68	53.81
	20-8-16	11.02	11.50	1.550	856.73	3291.45	60.90	0.666	56.14	54.82	54.57
	20-8-18	11.02	11.50	1.550	856.82	3349.44	60.90	0.655	56.07	54.80	54.43
	20-8-19	11.02	11.00	1.550	664.08	3218.95	60.90	0.545	45.41	44.56	43.34
	20-8-17	11.02	11.50	1.550	951.31	3479.94	60.90	0.930	60.90	60.78	61.08
	20-8-20	11.02	11.00	1.550	670.31	3291.45	60.90	0.540	45.78	44.95	43.67
Rezansoff et al. (1993)	20-9-1	12.99	17.91	2.170	2033.65	3537.94	67.28	0.552	59.66	58.74	57.44
	20-9-2	12.99	17.91	2.170	2241.59	3378.44	67.28	0.648	66.15	64.82	64.42
	20-11-4	12.99	17.79	3.100	2303.03	4349.93	66.12	0.469	48.03	47.51	45.52
	20-11-2	12.99	17.00	3.100	3232.23	4335.43	69.02	1.380	69.92	69.95	70.91
	20-11-1	12.99	17.00	3.100	3177.35	4770.42	69.02	0.793	69.02	68.59	68.39
	20-11-3	12.99	17.79	3.100	2540.41	4465.93	66.12	0.514	53.02	52.37	50.59
	20-11-8	12.99	18.30	3.100	3042.67	3349.44	66.12	0.801	63.30	61.36	62.61
	20-11-5	12.99	17.30	3.100	2988.49	3624.94	66.12	0.819	65.82	63.81	65.26
	20-11-6	12.99	17.30	3.100	2554.34	3624.94	66.12	0.665	55.80	54.54	54.21
	20-11-7	12.99	18.30	3.100	2546.56	3291.45	66.12	0.646	52.59	51.38	50.94
	2a	13.58	10.49	2.325	1238.53	3958	64.52	0.772	60.24	58.56	59.31
	2b	13.58	10.49	2.325	1238.54	3799	64.52	0.807	60.48	58.63	59.83
	5a	15.43	17.40	3.255	2801.17	4031	68.87	0.565	56.96	56.08	54.76
	5b	15.43	17.40	3.255	3281.36	3726	68.87	0.743	67.50	65.83	66.37
Zekany et al. (1981)	6	11.61	10.49	2.325	1060.92	3624.94	64.52	0.801	52.50	50.77	51.83
	1b*	8.66	10.49	1.550	925.63	3798.94	64.52	-	-	65.91	69.82
	1a*	8.66	10.49	1.550	977.75	3958.43	64.52	-	-	69.54	74.05
	7	11.61	10.49	2.325	973.78	3624.94	64.52	0.713	47.93	46.60	46.68
	3a*	11.61	10.49	2.325	1364.48	3958.43	64.52	-	-	65.12	69.76
	3b	11.61	10.49	2.325	1235.27	3798.94	64.52	0.950	61.57	59.03	62.03
	8	13.58	10.49	2.325	718.18	3624.94	64.52	0.431	34.50	34.05	32.20
	4b	12.99	17.40	3.255	3341.38	3726.44	68.87	1.209	68.87	67.65	70.17
	9*	12.99	17.40	3.255	3607.50	3885.94	68.87	-	-	72.95	76.40
	10*	12.99	17.40	3.255	3430.35	4088.93	68.87	-	-	69.27	70.99
	4a	12.99	17.40	3.255	3023.47	4030.93	68.87	0.720	62.56	61.08	61.25
	9-53-B-N	27.25	13.44	5.000	2826.03	5650	62.80	0.382	47.77	47.56	44.92
	N-N-80B	27.25	13.30	6.240	2720.75	3825	60.10	0.485	38.53	37.96	36.27
	9-53-B	27.25	13.44	5.000	3408.05	5700	62.80	0.469	57.79	57.36	54.99
	11-40-B-A	27.25	13.30	6.240	3252.13	5425	60.10	0.435	45.28	44.94	42.59
	2-4-5-80-B	27.25	13.30	6.240	3056.12	4200	60.10	0.510	43.16	42.54	40.87
	2-5-40-B(4)	27.25	13.30	6.240	2980.31	3850	60.10	0.537	42.31	41.59	40.17
	3-5-53-B	27.25	13.30	6.240	2824.61	3775	60.10	0.513	40.09	39.44	37.90
	2-4-5-53-B	27.25	13.30	6.240	3015.75	4125	60.10	0.511	42.62	42.00	40.35

Table A.1
Data and bar stress for specimens containing developed and spliced bars (continued)

Study	Specimen No.	b (in.)	d (in.)	A,*** (in. ²)	M _a (in-kips)	f _c (psi)	f _y (ksi)	ϵ_{cr}/ϵ_o **	f _{sc+} (ksi)	f _{sw++} (ksi)	f _{su+++} (ksi)
DeVries et al. (1991)	11-53-B	27.25	13.30	6.240	3036.56	4025	60.10	0.527	43.00	42.32	40.79
	11-40-B	27.25	13.30	6.240	3291.82	5050	60.10	0.471	46.03	45.58	43.47
	11-53-B-D	27.25	13.30	6.240	2433.42	4125	60.10	0.399	34.23	33.89	31.82
	3-5-40-B	27.25	13.30	6.240	2735.99	3750	60.10	0.497	38.82	38.21	36.60
	8G-9B-P6	11.00	14.50	0.880	833.43	8850	76.63	0.234	70.16	70.39	66.96
	8N-9B-P6	11.10	14.38	0.880	663.07	8300	76.63	0.195	56.34	56.55	53.54
	8G-22B-P9	11.00	14.31	2.000	1349.42	7460	66.40	0.326	52.74	52.76	49.61
	8N-18B-P9	11.10	13.94	2.000	1286.89	7660	70.35	0.316	51.63	51.68	48.51
	8G-16B-P9	11.00	14.37	2.000	1090.40	7460	66.40	0.257	42.34	42.44	39.49
	8G-18B-P9	11.00	14.19	2.000	1331.99	8610	70.35	0.291	52.25	52.38	49.05
Azizinamini et al. (1993)	10N-12B-P9	11.00	14.25	2.000	964.14	9780	70.35	0.188	37.33	37.63	34.76
	10G-12B-P9	11.00	14.19	2.000	959.02	9680	70.35	0.190	37.32	37.61	34.74
	15G-12B-P9	11.10	14.25	2.000	1272.15	16100	70.35	0.166	48.65	49.09	45.60
	15N-12B-P9	11.10	14.19	2.000	1304.68	13440	70.35	0.197	50.42	50.77	47.22
	BB-8-5-23	9.00	12.50	1.580	818.35	5290	77.85	0.406	47.30	47.01	44.53
	AB83-8-15-41	9.00	12.50	1.580	1304.64	15120	77.85	0.280	72.67	73.07	68.63
	BB-11-5-24	12.00	13.89	3.120	1116.04	5080	70.80	0.308	29.82	29.73	27.39
	BB-11-5-40	12.00	13.89	3.120	1615.17	5080	70.80	0.466	43.44	43.03	40.91
	BB-11-12-24	12.00	13.89	3.120	1721.04	12730	70.80	0.228	44.40	44.72	41.20
	B-11-12-40	12.00	13.89	3.120	2263.17	13000	70.80	0.300	58.47	58.78	54.78
Azizinamini et al. (1995)	BB-11-11-45	18.00	15.89	4.680	3238.39	10900	70.80	0.261	48.63	48.90	45.38
	BB-11-15-36	18.00	15.89	4.680	3823.83	14550	70.80	0.245	56.95	57.34	53.32
	BB-11-5-36	18.00	15.89	4.680	3050.83	6170	73.72	0.394	46.93	46.75	44.07
	BB-11-13-40	18.00	15.89	4.680	3841.90	13600	73.72	0.260	57.34	57.70	53.72
	BB-11-15-13	12.00	13.89	3.120	1160.08	14330	73.72	0.137	29.76	30.06	27.35
	AB83-11-15-57.5	12.00	13.89	3.120	2763.53	13870	73.72	0.353	71.39	71.66	67.40
	AB89-11-15-80	12.00	13.89	3.120	2923.22	15120	73.72	0.426	73.88	75.64	71.17
	AB83-11-15-57.5S-50	12.00	13.89	3.120	3046.01	15120	73.70	0.544	75.96	78.82	74.34
	ABS-11-15-45S-60	18.00	15.89	4.680	4725.79	14890	70.50	0.301	70.48	70.83	66.42
	ABS-11-15-45S-100	18.00	15.89	4.680	5375.79	14850	70.50	0.713	76.59	80.57	76.06
Darwin et al. (1995a, 1996a)	ABS-11-15-40S-150	18.00	15.89	4.680	5575.79	15760	70.50	0.788	79.06	83.46	78.79
	1.1	16.08	13.76	1.580	1021.00	5020	67.69	0.302	51.78	51.66	48.97
	1.2	24.06	13.79	3.160	1746.00	5020	67.69	0.309	44.77	44.65	42.04
	1.3	16.07	13.75	2.370	1310.00	5020	67.69	0.337	45.22	45.05	42.47
	2.4	12.13	13.79	1.580	1058.95	5250	75.42	0.366	54.29	54.08	51.40
	2.5	12.13	13.67	1.580	1138.37	5250	75.42	0.403	58.97	58.67	56.06
	4.5	12.12	13.79	1.580	993.89	4090	67.69	0.420	51.50	51.06	48.86
	6.5	12.10	13.63	1.580	1031.15	4220	75.42	0.437	54.06	53.59	51.41
	8.3	12.11	13.53	1.580	1171.00	3830	77.96	0.527	62.38	58.64	57.08
	10.2	12.13	13.78	1.580	1190.93	4250	80.57	0.500	61.84	61.47	60.13
	13.4	12.19	13.92	0.930	710.33	4110	61.83	0.350	60.26	59.96	57.46
	14.3	12.14	13.89	0.930	742.98	4200	61.83	0.485	61.83	62.84	60.33
	15.5	18.05	13.47	3.120	2013.00	5250	77.77	0.450	54.51	54.10	51.75
	16.2	18.07	13.64	3.120	1974.32	5180	77.77	0.435	52.75	52.38	49.98
	12.1	12.07	13.90	1.240	707.52	4120	66.39	0.312	45.63	45.42	43.00
	12.3	12.14	13.88	0.930	573.02	4120	66.39	0.279	48.67	48.52	46.06
	13.2	12.11	13.86	0.930	661.45	4110	66.39	0.328	56.35	56.10	53.59
	12.2	12.12	13.94	1.240	710.72	4120	61.83	0.311	45.68	45.48	43.06
	12.4	12.12	13.96	0.930	618.00	4120	61.83	0.300	52.21	52.02	49.53
	13.1	12.18	13.88	0.930	659.29	4110	61.83	0.325	56.06	55.82	53.31
	14.5	12.13	13.91	0.620	481.90	4200	66.39	0.271	60.29	60.15	57.58
	14.6	12.05	13.89	0.620	507.47	4200	61.83	0.484	61.83	63.45	60.85
	1.5	16.07	13.74	2.370	1517.96	5020	67.69	0.397	52.54	52.24	49.72
	1.6	16.05	13.74	2.370	1511.00	5020	67.69	0.396	52.30	52.00	49.48
	2.1	12.12	13.70	1.580	1214.06	5250	64.52	0.432	62.81	62.43	59.91
	2.2	12.12	13.58	1.580	1526.04	5250	75.42	0.848	77.78	79.20	77.60
	2.3	12.11	13.56	1.580	1413.04	5250	75.42	0.524	74.12	73.45	71.46
	3.4	12.14	13.73	1.580	1087.02	5110	64.72	0.388	56.07	55.80	53.20
	3.5	12.17	13.74	2.370	1479.14	3810	64.72	0.612	53.05	52.02	51.15
	4.1	12.16	13.72	1.580	1211.07	4090	64.52	0.531	63.33	62.54	60.92
	4.2	12.17	13.74	1.580	1403.04	4090	75.42	0.631	73.54	72.34	71.59
	4.4	12.15	13.73	1.580	1141.02	4090	67.67	0.495	59.55	58.88	57.03
	5.1	18.22	13.79	2.370	1888.06	4190	65.70	0.539	65.43	64.62	63.03
	5.2	18.16	13.73	2.370	1902.13	4190	75.00	0.550	66.26	65.41	63.90
	5.3	12.11	13.68	1.580	1310.97	4190	75.00	0.576	68.83	67.88	66.59

Table A.1
Data and bar stress for specimens containing developed and spliced bars (continued)

Study	Specimen No.	b (in.)	d (in.)	A _s *** (in. ²)	M _u (in.-kips)	f _c (psi)	f _y (ksi)	$\varepsilon_{cv}/\varepsilon_o^{**}$	f _{sc+} (ksi)	f _{sw++} (ksi)	f _{su+++} (ksi)
	5.4	12.12	13.68	1.580	1137.00	4190	64.52	0.487	59.50	58.87	56.94
	5.5	12.12	13.67	1.580	896.05	4190	64.72	0.373	46.74	46.43	44.09
	5.6	12.11	13.84	1.580	1296.93	4190	75.42	0.556	67.22	66.34	64.88
	6.1	12.18	13.69	2.370	1796.97	4220	65.70	0.713	64.71	63.26	63.33
	6.2	12.11	13.62	2.370	2114.91	4220	75.42	1.190	76.21	74.88	77.57
	6.3	12.13	13.63	1.580	886.95	4220	75.42	0.368	46.39	46.09	43.73
	6.4	12.11	13.58	1.580	703.09	4220	64.72	0.288	36.83	36.68	34.35
	7.1	12.00	13.77	1.580	907.97	4160	75.42	0.378	47.05	46.72	44.40
	7.2	12.06	13.72	1.580	1080.95	4160	67.69	0.462	56.37	55.82	53.77
	7.5	11.97	13.64	2.370	2067.67	4160	75.42	0.932	75.42	73.17	75.73
	7.6	12.01	13.77	1.580	861.75	4160	67.69	0.357	44.62	44.34	41.99
	8.1	12.13	13.76	2.370	1983.97	3830	77.96	0.900	72.14	69.67	72.21
	8.2*	12.16	13.69	2.370	2246.95	3830	80.57	-	-	79.32	85.08
	8.4	12.10	13.91	1.580	958.93	3830	80.57	0.420	49.37	48.90	46.79
	9.1	12.14	13.70	1.580	1226.75	4230	80.57	0.526	64.16	63.40	61.70
	9.2	12.10	13.84	1.580	1350.36	4230	75.42	0.579	70.02	69.06	67.78
	9.3	12.19	13.78	1.580	1075.81	4230	77.96	0.445	55.75	55.25	53.10
	9.4	12.11	13.72	1.580	1259.48	4230	75.42	0.542	65.82	65.00	63.42
	10.3	12.11	13.77	1.580	1144.80	4250	77.96	0.479	59.45	58.85	56.86
	10.4	12.07	13.75	1.580	1203.66	4250	77.96	0.511	62.68	61.98	60.18
	11.1	12.20	13.68	2.370	1902.14	4380	75.42	0.740	68.52	66.94	67.31
	11.2	12.19	13.72	1.580	1201.57	4380	77.96	0.495	62.58	61.94	60.00
	11.3	12.13	13.60	1.580	1199.89	4380	80.57	0.504	63.11	62.44	60.56
	11.4	12.15	13.77	1.580	1216.68	4380	75.42	0.500	63.15	62.49	60.58
	14.1	12.12	13.86	2.370	1724.85	4200	67.69	0.665	61.19	59.96	59.51
	14.2	12.19	13.72	2.370	1788.25	4200	67.69	0.708	64.24	62.81	62.83
	15.1	12.11	13.46	3.120	2449.40	5250	77.77	0.802	69.11	67.33	68.34
	15.2	12.11	13.46	3.120	2287.15	5250	65.54	0.731	64.28	62.87	62.96
	15.3	12.04	13.63	3.120	2287.46	5250	65.54	0.714	63.40	62.07	61.97
	15.4	12.08	13.50	3.120	2807.04	5250	77.77	1.338	78.90	76.93	80.55
	16.3	18.03	13.62	3.120	2311.21	5180	77.77	0.524	62.06	61.42	59.50
	16.4	18.06	13.45	3.120	2272.56	5180	66.69	0.525	61.84	61.19	59.28
	17.3	18.03	13.48	3.120	2556.52	4710	77.77	0.660	70.06	68.85	68.26
	17.4	18.07	13.52	3.120	2451.93	4710	66.69	0.636	66.69	65.82	64.83
	17.5	18.09	13.48	3.120	2175.18	4710	66.69	0.540	59.30	58.57	56.89
	17.6	18.07	13.54	3.120	2571.40	4710	77.77	0.657	70.12	68.92	68.30
	18.1	18.05	13.52	3.120	3006.64	4700	77.77	1.342	80.90	80.72	82.05
	18.3	18.05	13.43	3.120	2564.31	4700	77.77	0.668	70.58	69.33	68.83
	18.4	18.08	13.62	3.120	2490.09	4700	66.69	0.689	66.69	66.33	65.38
Current Study	19.1	18.14	13.66	2.370	2094.88	4250	80.57	0.616	73.51	72.39	71.46
	19.2	18.06	13.66	2.370	1936.99	4250	80.57	0.563	67.85	66.96	65.54
	19.3	18.10	13.62	2.370	2030.72	4250	80.57	0.598	71.43	70.39	69.28
	19.4	18.13	13.63	2.370	2193.87	4250	80.57	0.655	77.28	75.98	75.45
	20.1	18.05	13.61	4.680	3805.41	5080	77.77	0.856	71.08	69.00	70.78
	20.2	18.05	13.56	4.680	3823.67	5080	77.77	0.871	71.81	69.64	71.63
	20.3	18.07	13.58	4.680	3668.18	5080	77.77	0.816	68.52	66.66	67.88
	20.4	18.10	13.64	4.680	3642.81	5080	77.77	0.798	67.65	65.88	66.86
	20.5	12.03	13.85	2.370	1419.06	5080	80.57	0.445	49.53	49.14	46.85
	20.6	12.08	13.76	2.370	1621.05	5080	80.57	0.525	57.15	56.51	54.65
	21.1	12.05	13.65	2.370	2032.63	4330	80.57	0.834	73.88	71.79	73.40
	21.2	12.13	13.76	2.370	1918.42	4330	80.57	0.751	68.77	67.14	67.65
	21.3	12.10	13.65	2.370	2095.80	4330	80.57	0.866	76.25	73.97	76.04
	21.4	12.06	13.78	2.370	1929.46	4330	80.57	0.758	69.10	67.43	68.03
	21.5	12.14	13.58	1.580	1460.33	4330	80.57	0.645	77.35	76.11	75.45
	21.6	12.14	13.59	1.580	1234.56	4330	80.57	0.527	65.08	64.33	62.61
	22.1	12.11	13.53	3.120	2161.45	6300	77.77	0.563	59.46	58.80	57.00
	22.2	12.10	13.49	3.120	2569.05	6300	77.77	0.702	71.35	70.10	69.72
	22.3	11.98	13.49	3.120	2577.14	6300	77.77	0.711	71.66	70.36	70.10
	22.4	12.06	13.51	3.120	2496.85	6300	77.77	0.676	69.15	68.02	67.34
	22.5	17.86	12.58	4.700	3148.81	6300	77.77	0.639	62.41	61.46	60.37
	22.6	17.87	13.00	4.700	3536.22	6700	77.77	0.649	67.55	66.57	65.52
	23a.1	18.28	13.62	2.370	2325.92	9080	80.57	0.378	78.87	79.24	75.57
	23a.2	18.28	13.69	2.370	1856.66	9080	80.57	0.293	62.48	62.89	59.37
	23a.3	18.18	13.66	2.370	2398.85	9080	80.57	0.425	80.57	81.48	77.83
	23a.4	18.13	13.69	2.370	2346.13	9080	80.57	0.380	79.15	79.51	75.85

Table A.1
Data and bar stress for specimens containing developed and spliced bars (continued)

Study	Specimen No.	b (in.)	d (in.)	A _s *** (in. ²)	M _u (in-kips)	f _c (psi)	f _y (ksi)	$\varepsilon_{cr}/\varepsilon_o$ **	f _{sc+} (ksi)	f _{sw++} (ksi)	f _{su+++} (ksi)
	23a.5	18.19	13.63	1.580	1247.93	9320	80.57	0.227	62.34	62.71	59.37
	23a.6	12.24	13.67	1.580	1492.52	9320	80.57	0.352	75.47	75.90	72.18
	23b.1	12.15	13.73	2.370	2281.34	8370	80.57	0.500	79.04	78.69	75.88
	23b.2	12.10	13.67	2.370	2029.48	8370	80.57	0.442	70.51	70.34	67.21
	23b.3	18.23	12.72	1.580	1328.07	8370	80.57	0.282	71.64	71.80	68.29
	23b.4	18.18	12.53	1.580	1281.69	8370	80.57	0.279	70.24	70.40	66.91
	23b.5	12.03	13.56	3.120	1954.35	4500	77.77	0.691	54.80	53.57	53.30
	23b.6	12.04	13.44	3.120	1605.17	4500	77.77	0.550	45.10	44.40	42.91
	24.1	12.14	13.69	1.580	1184.90	4300	79.07	0.498	61.91	61.25	59.35
	24.2	12.15	13.77	1.580	1067.27	4300	79.07	0.437	55.32	54.85	52.65
	24.3	12.08	13.52	1.580	1131.78	4300	79.07	0.486	59.93	59.32	57.35
	24.4	12.07	13.42	1.580	1038.88	4300	79.07	0.447	55.38	54.88	52.72
	25.1	12.19	14.37	0.930	808.01	4490	62.98	0.679	63.72	65.86	63.23
	25.2	12.16	14.25	0.930	854.21	4490	62.98	0.949	67.58	70.25	67.67
	25.3	12.12	14.28	0.930	811.24	4490	62.98	0.727	64.33	66.59	63.98
	25.4	12.28	14.28	0.930	772.05	4490	62.98	0.382	62.98	63.33	60.68
	26.1	12.03	13.77	2.370	1823.88	4960	79.07	0.620	64.59	63.59	62.53
	26.2	12.08	13.64	2.370	1556.60	4960	79.07	0.520	55.43	54.81	52.95
	26.3	12.11	13.78	2.370	1769.37	4960	79.07	0.593	62.51	61.62	60.32
	26.4	12.03	13.50	2.370	1684.55	4960	79.07	0.585	60.83	59.98	58.61
	26.5	12.15	13.75	2.370	1816.40	4960	77.96	0.613	64.35	63.38	62.26
	26.6	12.06	13.69	2.370	1757.71	4960	77.96	0.597	62.53	61.63	60.36
	27.1	12.22	13.61	2.370	2356.61	10810	79.07	0.516	79.98	81.48	77.75
	27.2	12.12	13.71	2.370	2235.69	10810	77.96	0.490	78.52	79.84	76.07
	27.3	12.06	13.53	2.370	2303.27	10810	79.07	0.471	79.21	80.16	76.42
	27.4	12.15	13.54	2.370	2221.80	10810	77.96	0.399	77.21	77.29	73.49
	27.5	18.16	13.66	2.370	2283.52	10810	79.07	0.308	77.07	77.31	73.34
	27.6	18.12	13.65	2.370	2352.52	10810	77.96	0.377	78.42	79.69	75.69
	28.1	11.71	13.42	3.120	2646.19	12610	77.77	0.395	71.23	71.36	67.39
	28.2	12.13	13.52	3.120	2037.94	12610	77.77	0.286	54.17	54.46	50.50
	28.3	18.10	13.45	4.680	3751.70	12610	77.77	0.362	67.03	67.21	63.20
	28.4	18.09	13.52	4.680	2577.20	12610	77.77	0.239	45.62	45.92	42.34
	28.5	18.09	13.45	3.120	1944.03	12610	77.77	0.210	50.89	51.23	47.68
	28.6	18.11	13.52	3.120	1605.27	12610	77.77	0.170	41.76	42.07	38.95
	29.1	12.06	13.68	2.370	2409.70	10620	79.07	0.589	80.98	82.99	79.36
	29.2	12.14	13.60	2.370	2507.67	10620	77.96	0.809	83.65	86.86	83.35
	29.3	12.13	13.64	2.370	2267.34	10620	79.07	0.409	78.23	78.27	74.54
	29.4	12.17	13.66	2.370	2284.36	10620	77.96	0.453	77.96	78.75	75.02
	29.5	18.10	13.66	2.370	2244.00	10620	79.07	0.307	75.79	76.02	72.09
	29.6	18.17	13.71	2.370	2310.82	10620	77.96	0.314	77.72	77.96	74.00
	30.1	12.19	13.51	3.120	2484.77	13220	77.77	0.340	66.07	66.32	62.19
	30.2	12.07	13.54	3.120	1925.92	13220	77.77	0.259	51.00	51.31	47.49
	30.3	18.02	13.47	4.680	3755.66	13220	77.77	0.348	66.88	67.11	62.98
	30.4	18.04	13.49	4.680	3048.65	13220	77.77	0.277	54.09	54.39	50.48
	30.5	18.12	13.44	3.120	2554.85	13220	77.77	0.270	66.95	67.30	63.19
	30.6	18.14	13.26	3.120	2052.36	13220	77.77	0.219	54.47	54.82	51.10
	31.1	12.12	13.43	1.580	1332.79	12890	79.07	0.238	68.25	68.61	64.64
	31.2	12.20	13.52	1.580	1120.76	12890	79.07	0.195	56.94	57.30	53.72
	31.3	12.15	13.52	1.580	1282.40	12890	77.96	0.225	65.21	65.58	61.70
	31.4	12.08	13.70	1.580	1051.88	12890	77.96	0.180	52.72	53.06	49.66
	31.5	12.26	13.56	2.370	1787.42	12890	79.07	0.268	61.43	61.76	57.77
	31.6	12.17	13.44	2.370	1826.94	12890	69.50	0.280	63.42	63.75	59.70
	32.1	12.17	13.52	3.120	2390.41	14400	77.77	0.303	63.33	63.65	59.41
	32.2	12.14	13.51	3.120	2319.28	14400	66.69	0.294	61.49	61.82	57.62
	32.3	18.14	13.45	3.120	2322.63	14400	77.77	0.227	60.64	61.02	57.04
	32.4	18.20	13.50	3.120	2345.68	14400	66.69	0.227	61.01	61.39	57.40
	33.1	12.16	13.55	2.370	1714.32	5360	79.07	0.547	61.32	60.62	58.85
	33.2	12.10	13.66	2.370	1731.68	5360	69.50	0.547	61.42	60.72	58.95
	33.3	18.14	13.63	2.370	1664.60	5360	79.07	0.388	57.60	57.34	54.67
	33.4	18.12	13.64	2.370	1686.66	5360	69.50	0.393	58.32	58.05	55.39
	33.5	12.14	13.87	1.580	1107.51	5230	79.07	0.382	56.46	56.21	53.56
	33.6	12.17	13.82	1.580	1131.60	5230	69.50	0.393	57.94	57.66	55.03
	34.1	18.13	13.66	2.370	1676.71	5440	79.07	0.385	57.88	57.64	54.93
	34.2	18.17	13.61	2.370	1786.85	5440	79.07	0.416	61.97	61.65	59.03
	34.3	18.12	13.49	2.370	1685.25	5440	69.50	0.396	58.94	58.67	56.00

Table A.1
Data and bar stress for specimens containing developed and spliced bars (continued)

Study	Specimen	b	d	A _s ***	M _a	f _c	f _y	ϵ_{c}/ϵ_0 **	f _{sc} +	f _{sw} ++	f _{su} +++
No.		(in.)	(in.)	(in. ²)	(in-kips)	(psi)	(ksi)		(ksi)	(ksi)	(ksi)
34.4		18.21	13.53	2.370	1678.59	5440	69.50	0.391	58.49	58.23	55.54
35.1		12.08	13.69	1.580	1320.85	5330	75.42	0.471	68.44	67.96	65.60
35.2		12.25	13.54	1.580	1076.02	5330	75.42	0.378	56.21	55.98	53.30
35.3		12.08	13.60	1.580	1185.68	5330	69.50	0.422	61.77	61.43	58.86
35.4		12.16	13.75	1.580	1081.80	5330	69.50	0.372	55.61	55.40	52.70
36.1		12.16	13.55	2.370	2137.29	5060	79.07	0.762	77.39	75.70	76.29
36.2		12.13	13.56	2.370	1882.60	5060	79.07	0.648	67.75	66.63	65.84
36.3		18.17	13.55	2.370	1796.33	5060	69.50	0.448	62.78	62.34	59.96
36.4		18.14	13.56	2.370	1724.14	5060	69.50	0.427	60.17	59.79	57.32
37.1		12.11	12.70	3.160	1793.61	4800	69.50	0.650	59.97	58.63	60.88
37.2		12.14	12.60	3.160	1818.37	4800	69.50	0.671	61.40	59.95	62.35
37.3		12.11	13.48	2.370	1735.81	4800	75.42	0.625	62.92	61.90	60.93
37.4		12.07	13.47	2.370	2018.69	4800	75.42	0.762	73.78	72.10	72.70
38.1		18.25	13.75	2.370	1578.10	5080	69.50	0.375	54.18	53.93	51.31
38.2		18.17	13.51	2.370	1727.78	5080	69.50	0.429	60.51	60.13	57.66
38.3		12.08	13.47	2.370	1900.09	5080	79.07	0.665	68.93	67.74	67.13
38.4		12.13	13.53	2.370	1700.11	5080	79.07	0.573	61.12	60.31	58.81
38.5		12.16	13.65	1.580	1302.30	5080	79.07	0.483	67.83	67.28	65.06
38.6		12.17	13.64	1.580	1093.89	5080	79.07	0.397	56.86	56.56	53.99
39.1		12.16	13.51	2.370	1674.51	14450	67.69	0.230	57.61	57.98	54.02
39.2		12.18	13.49	2.370	2103.24	14450	67.69	0.522	69.74	72.93	68.55
39.3		12.17	13.45	2.370	2256.55	14450	77.96	0.327	77.96	78.48	74.01
39.4		12.09	13.47	2.370	1641.38	14450	77.96	0.228	56.64	57.01	53.08
39.5		12.15	13.47	2.370	1437.77	14450	67.69	0.197	49.56	49.93	46.30
39.6		12.19	13.59	2.370	1969.08	14450	67.69	0.270	67.38	67.76	63.49
40.1		12.16	13.26	3.120	2470.52	15650	77.77	0.304	66.60	67.00	62.57
40.2		12.16	13.28	3.120	2053.49	15650	77.77	0.249	55.16	55.58	51.47
40.3		12.15	13.31	3.120	1467.31	15650	65.54	0.174	39.25	39.63	36.28
40.4		12.09	13.33	3.120	2197.11	13650	65.54	0.267	58.83	59.25	55.02
40.5		12.11	13.67	1.580	1315.94	15650	77.96	0.196	65.81	66.28	62.32
40.6		12.26	13.88	1.580	1190.21	15650	77.96	0.171	58.53	58.97	55.32
41.1		12.14	13.49	1.580	1289.49	10180	80.57	0.275	66.16	66.40	62.68
41.2		12.16	13.38	2.370	2413.64	10180	80.57	0.653	83.02	85.12	81.76
41.3		12.11	13.56	2.370	2280.88	10180	80.57	0.432	79.35	79.31	75.75
41.4		12.20	13.40	2.370	2194.43	10180	77.96	0.421	77.27	77.26	73.66
41.5		18.32	13.51	2.370	1935.31	10500	69.50	0.267	66.01	66.28	62.53
41.6		18.22	13.63	2.370	1934.31	10500	69.50	0.264	65.38	65.65	61.92
42.1		12.11	13.50	1.580	1260.15	11930	77.96	0.237	64.32	64.66	60.85
42.2		12.09	13.64	1.580	944.33	11930	77.96	0.172	47.64	47.95	44.78
42.3		12.11	13.64	2.370	1531.38	11930	77.96	0.243	52.45	52.75	49.10
42.4		12.17	13.74	2.370	2075.90	11930	77.96	0.331	70.70	70.94	66.89
42.5		12.18	13.62	2.370	2265.96	11930	77.96	0.369	77.92	78.10	74.04
42.6		12.15	13.53	2.370	1906.13	11930	77.96	0.310	65.90	66.16	62.17
43.1		12.15	13.63	1.580	1028.57	11530	80.57	0.193	51.96	52.27	48.93
43.2		12.06	13.68	1.580	1288.47	11530	80.57	0.244	64.95	65.27	61.48
43.3		12.22	13.83	2.370	2326.36	11530	80.57	0.380	78.81	78.95	74.97
43.4		12.09	13.58	2.370	1844.42	11530	80.57	0.307	63.63	63.88	59.97
43.5		12.07	13.54	2.370	2149.92	11530	80.57	0.365	74.50	74.67	70.69
43.6		12.07	13.62	2.370	2458.31	11530	80.57	0.567	82.73	84.86	80.99

* Experimental moment was greater than the moment capacity calculated using the moment-curvature method

** Ratio of strain at concrete extreme compressive fiber to the concrete strain at maximum stress in concrete stress-strain curve

*** Total area of steel bars

+ Bar stress calculated using the moment-curvature method

++ Bar stress calculated using the working stress method

+++ Bar stress calculated using the ultimate strength method

1 in. = 25.4 mm; 1 psi = 6.895 kPa; 1 ksi = 6.895 MPa

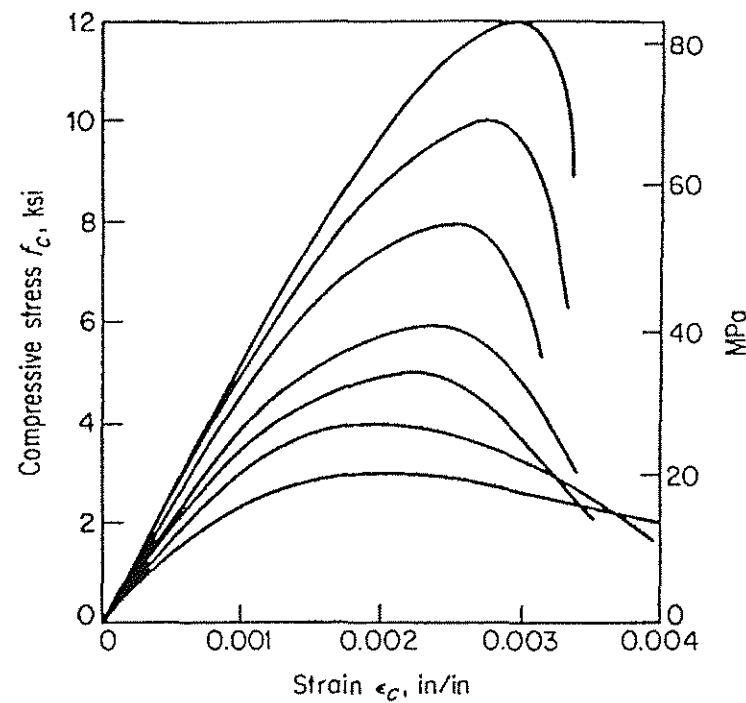


Fig. A.1 Typical compressive stress-strain curves for normal density concrete (Nilson 1997)

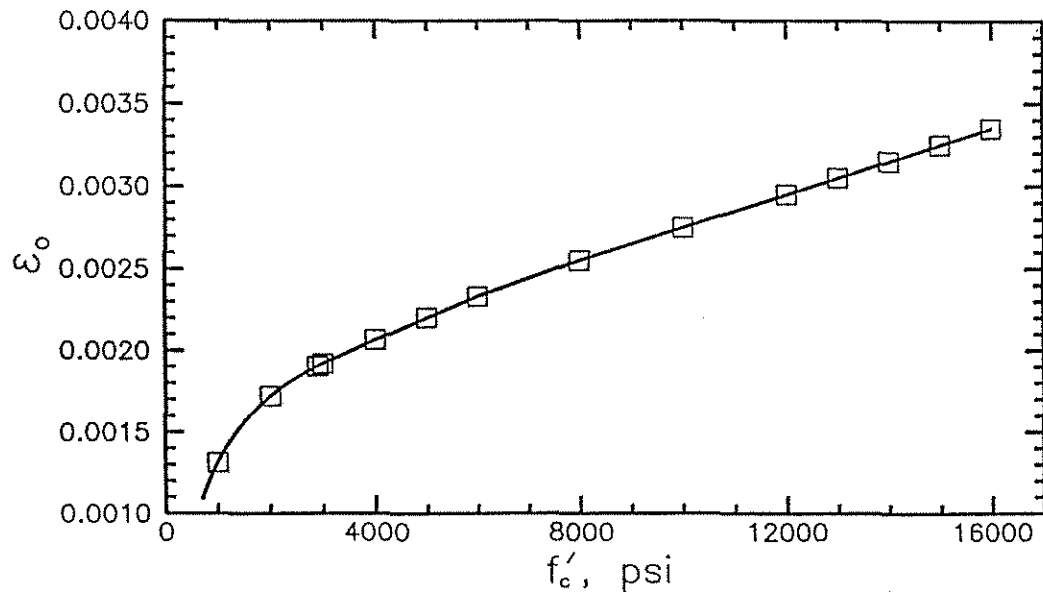


Fig. A.2 Concrete compressive strain at maximum compressive stress, ϵ_o , versus concrete compressive strength, f'_c , for normal density concrete used in the current study

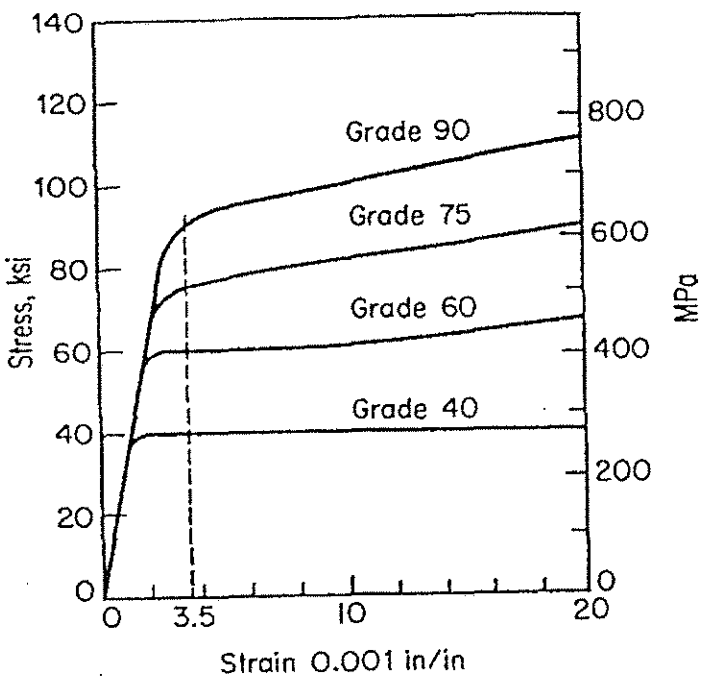


Fig. A.3 Typical stress-strain curves for reinforcing bars (Nilson 1997)

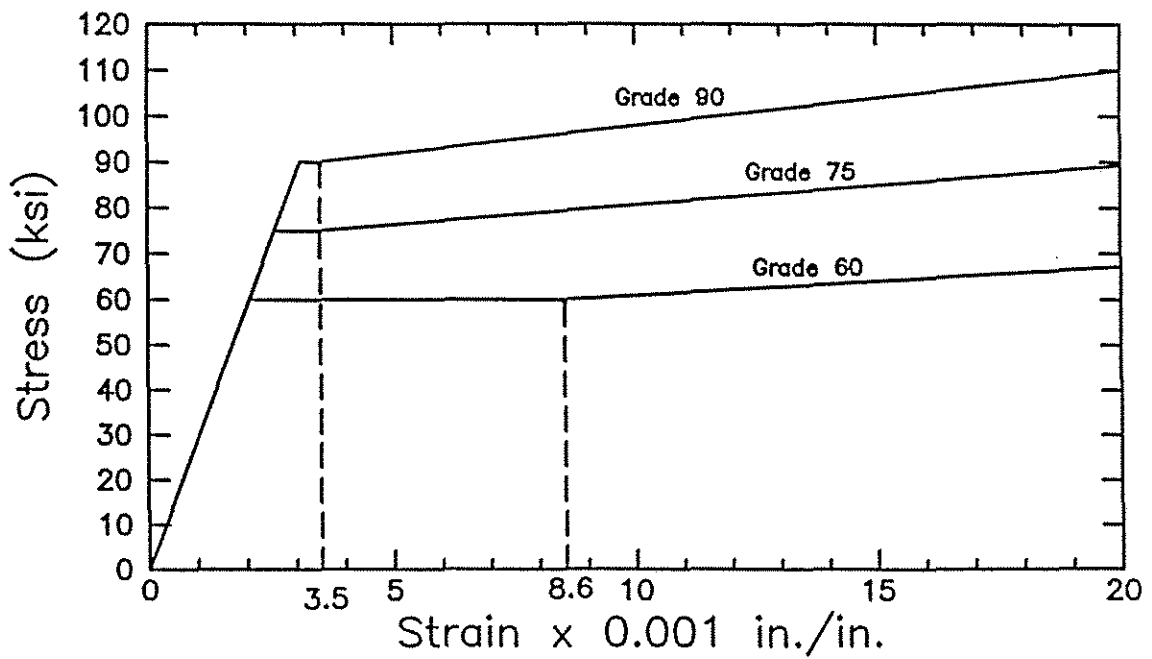


Fig. A.4 Ideal stress-strain curves for reinforcing bars used in the current study

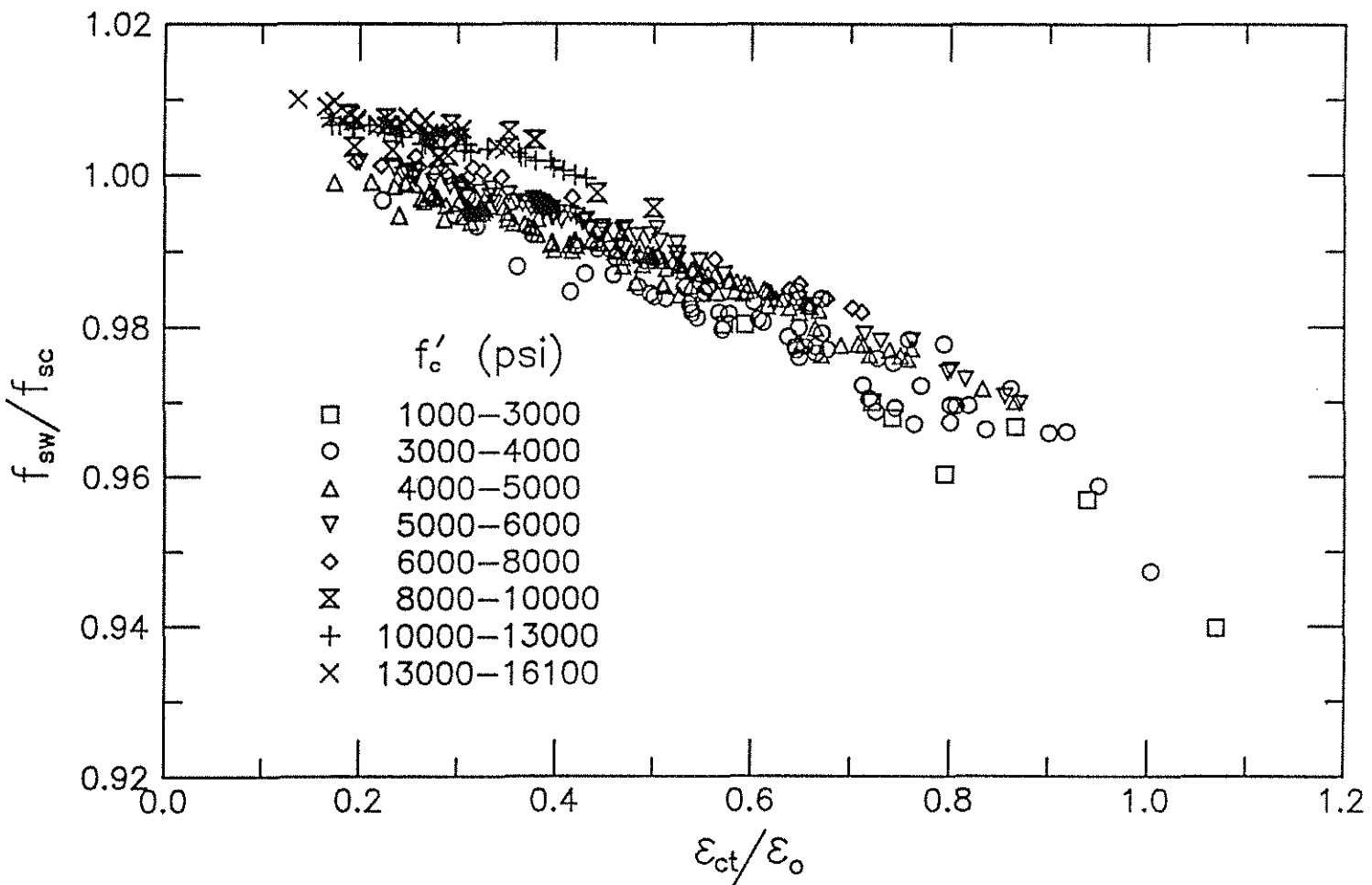


Fig. A.5 Ratio of bar stress calculated using the working stress method, f_{sw} , to bar stress calculated using the moment-curvature method, f_{sc} , versus ratio of concrete strain at extreme compressive fiber to concrete strain at maximum stress from concrete stress-strain curve for bars with $f_{sc} < f_y$

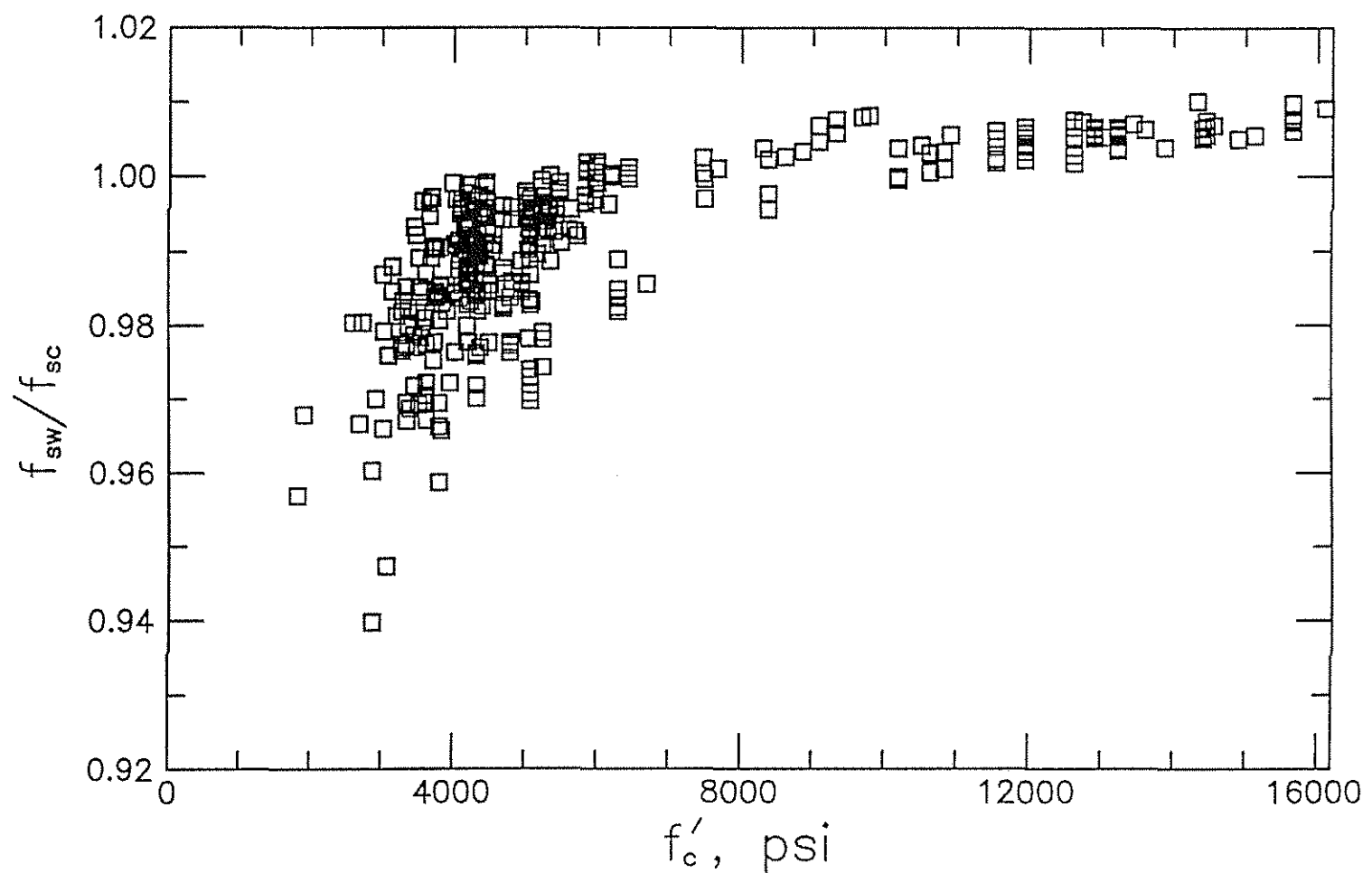


Fig. A.6 Ratio of bar stress calculated using the working stress method, f_{sw} , to bar stress calculated using the moment-curvature method, f_{sc} , versus concrete compressive strength, f'_c , for bars with $f_{sc} < f_y$

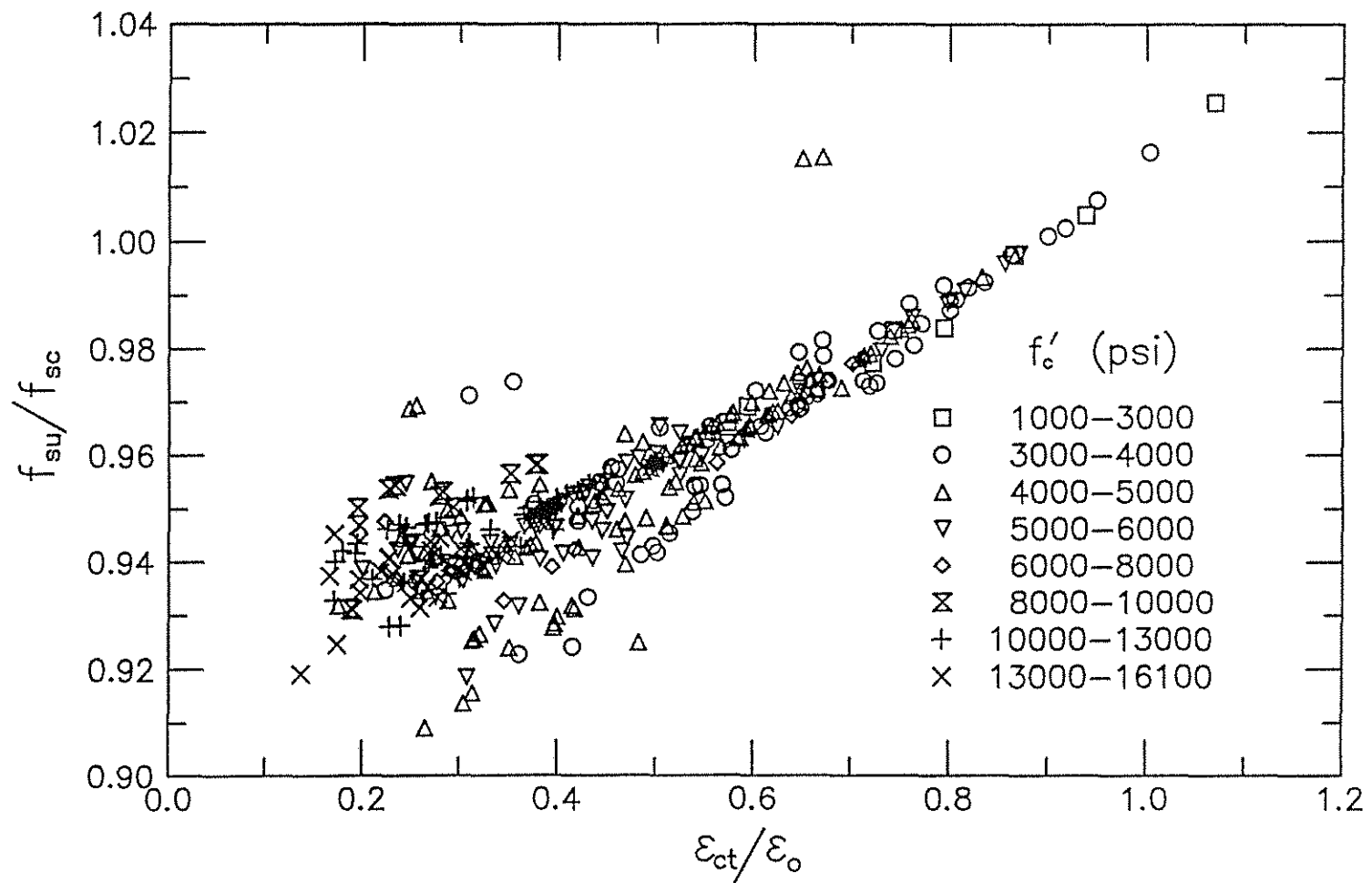


Fig. A.7 Ratio of bar stress calculated using the ultimate strength method, f_{su} , to bar stress calculated using the moment-curvature method, f_{sc} , versus ratio of concrete strain at extreme compressive fiber to concrete strain at maximum stress from concrete stress-strain curve for bars with $f_{sc} < f_y$

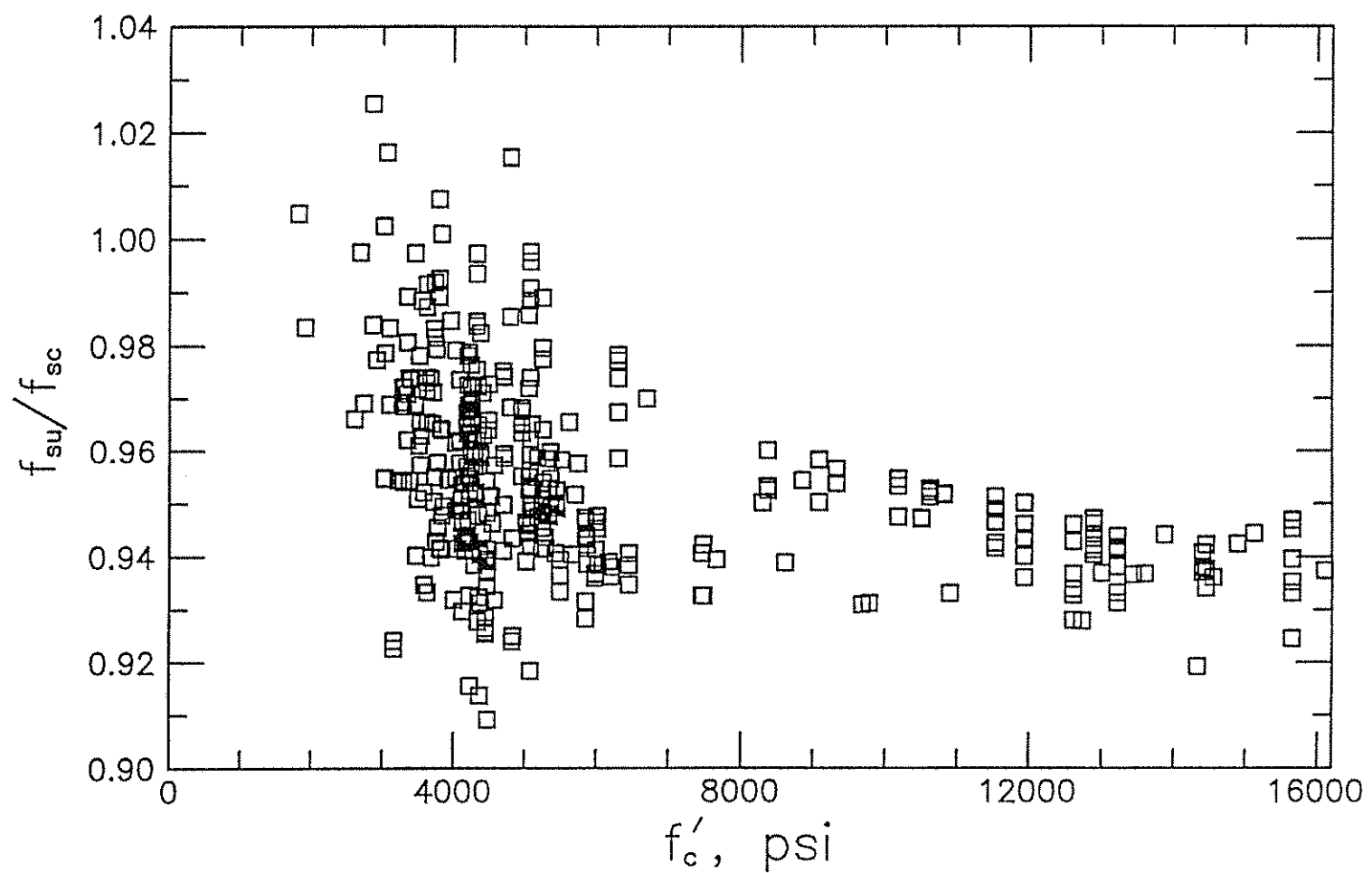


Fig. A.8 Ratio of bar stress calculated using the ultimate strength method, f_{su} , to bar stress calculated using the moment-curvature method, f_{sc} , versus concrete compressive strength, f'_c , for bars with $f_{sc} < f_y$

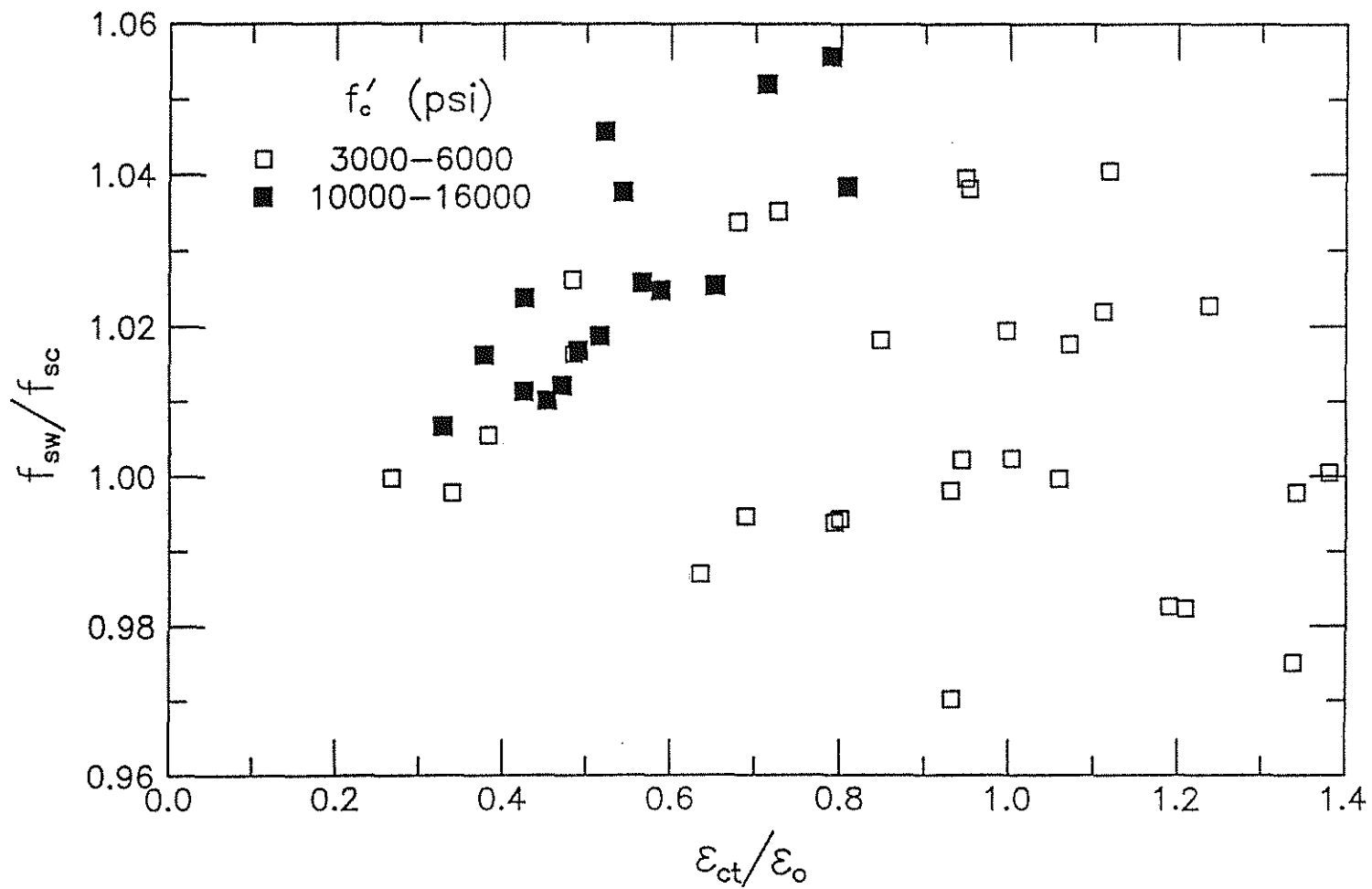


Fig. A.9 Ratio of bar stress calculated using the working stress method, f_{sw} , to bar stress calculated using the moment-curvature method, f_{sc} , versus ratio of concrete strain at extreme compressive fiber to concrete strain at maximum stress from concrete stress-strain curve for bars with $f_{sc} \geq f_y$

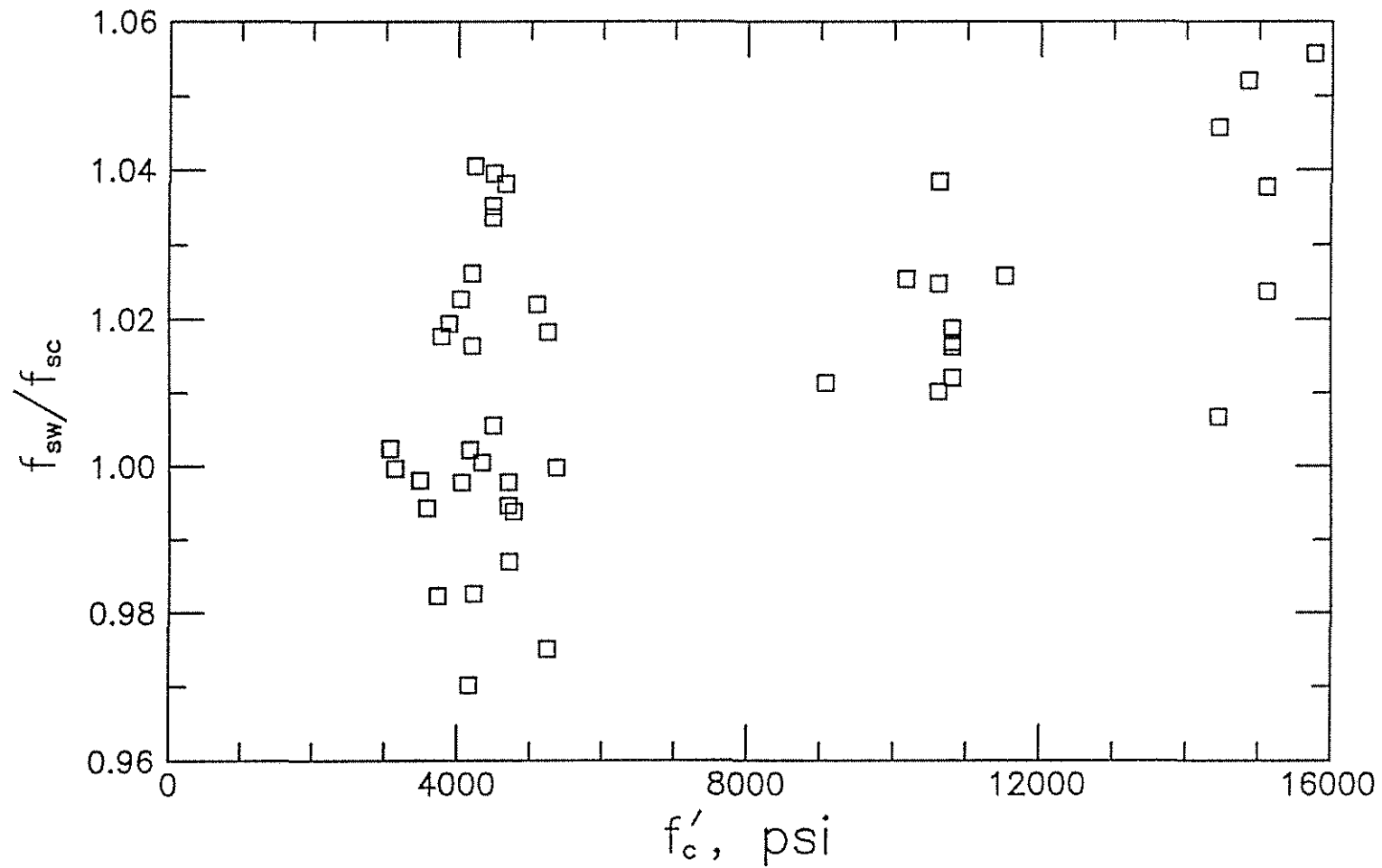


Fig. A.10 Ratio of bar stress calculated using the working stress method, f_{sw} , to bar stress calculated using the moment-curvature method, f_{sc} , versus concrete compressive strength, f'_c , for bars with $f_{sc} \geq f_y$

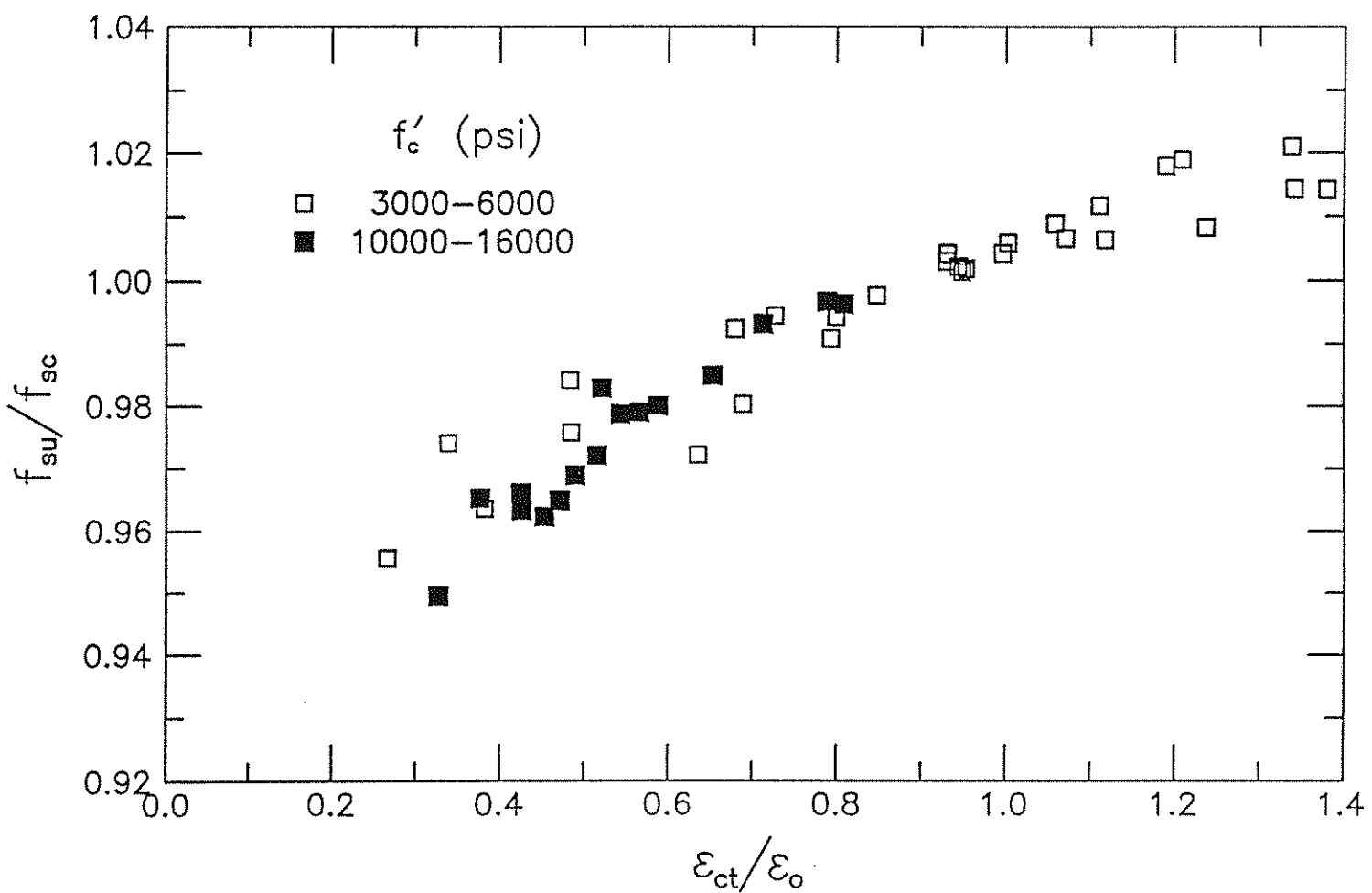


Fig. A.11 Ratio of bar stress calculated using the ultimate strength method, f_{su} , to bar stress calculated using the moment-curvature method, f_{sc} , versus ratio of concrete strain at extreme compressive fiber to concrete strain at maximum stress from concrete stress-strain curve for bars with $f_{sc} \geq f_y$

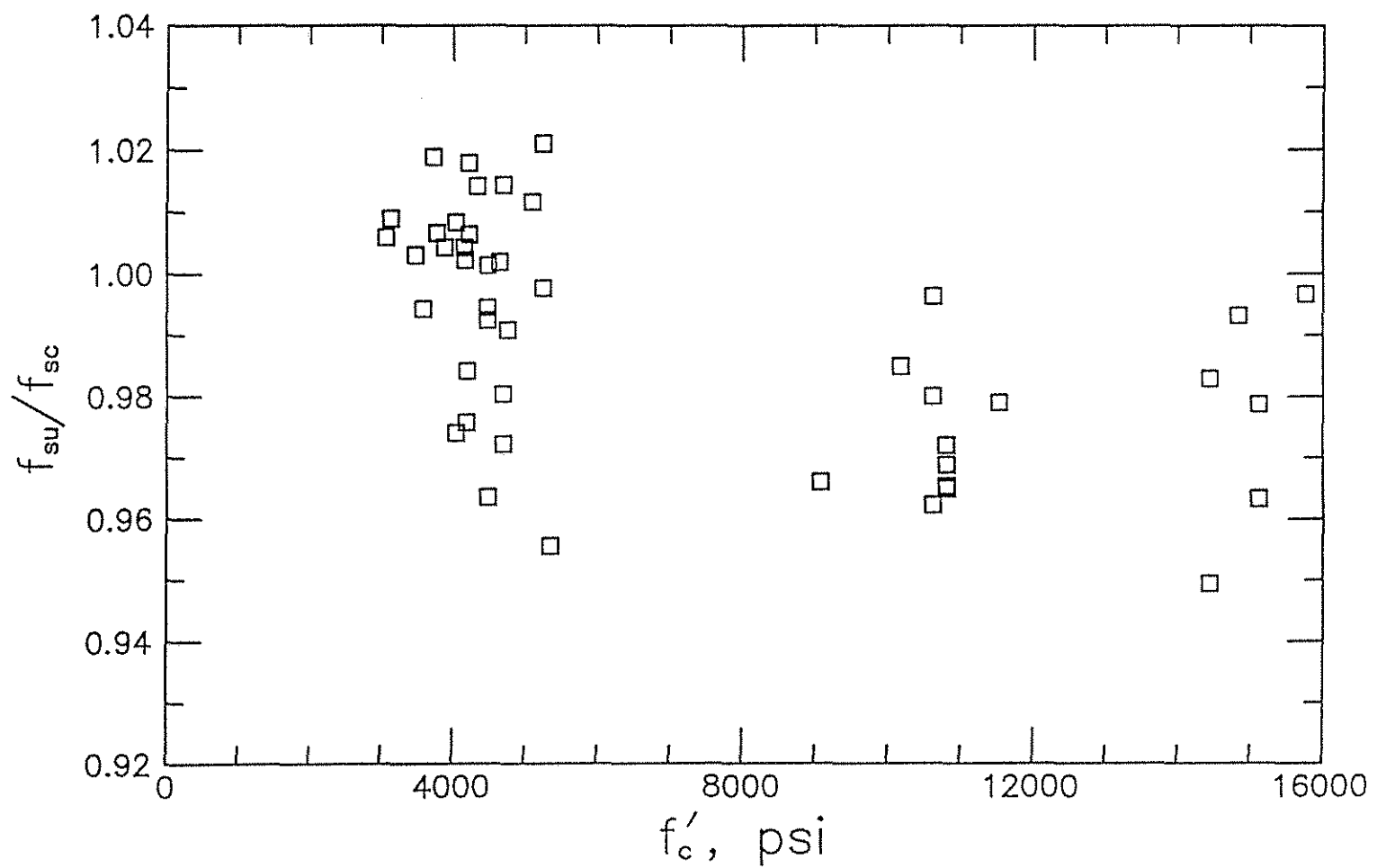


Fig. A.12 Ratio of bar stress calculated using the ultimate strength method, f_{su} , to bar stress calculated using the moment-curvature method, f_{sc} , versus concrete compressive strength, f'_c , for bars with $f_{sc} \geq f_y$

APPENDIX B: DATA FOR DEVELOPING DEVELOPMENT/SPLICE LENGTH CRITERIA IN CHAPTER 5

Table B.1 gives the coefficients obtained in the derivation of Eq. 5.3 for different powers of f'_c , p , and different effective values of c_{si} . Table B.2 shows test/prediction ratios for 171 specimens containing bars not confined by transverse reinforcement using Eq. 5.3 for different powers of powers of f'_c , p , and different effective values of c_{si} . Table B.3 shows test/prediction ratios for 163 specimens containing bars confined by transverse reinforcement, with $l_d/d_b \geq 16$ and $(c + K_{tr})/d_b \leq 4$ [in this case, $K_{tr} = 35.3t_r t_d N A_{tr}/n$, $t_r = 9.6 R_r + 0.28$, and $t_d = 0.72 d_b + 0.28$, as developed by Darwin et al (1995b, 1996b)], using Eq. 5.13a -5.13d corresponding to the powers of f'_c , p , equal to 1/4, 1/2, 3/4, and 1.0, respectively.

Table B.2
Test/Predication ratios using Eq. 5.3 for different powers of f_c
and definitions of effective value c_{si}

$f_c^{0.22}$	Test/Predication Ratio								
	$c_{si}+0.25$	1.7 c_{si}	1.6 c_{si}	1.5 c_{si}	1.4 c_{si}	1.3 c_{si}	1.2 c_{si}	1.1 c_{si}	1.0 c_{si}
Total 171 tests									
Max.	1.3027	1.3065	1.3128	1.3165	1.3169	1.3121	1.3010	1.3042	1.3137
Min.	0.7142	0.7224	0.7215	0.7205	0.7196	0.7182	0.7161	0.7140	0.7103
Mean	0.9989	0.9989	0.9990	0.9990	0.9990	0.9991	0.9991	0.9990	0.9992
St. Dev.	0.1052	0.1034	0.1035	0.1037	0.1040	0.1046	0.1053	0.1065	0.1081
COV	0.1053	0.1036	0.1036	0.1038	0.1041	0.1047	0.1054	0.1066	0.1082
$f_c < 6000$ psi, 131 tests									
Max.	1.3008	1.2853	1.2833	1.2812	1.2789	1.2827	1.2929	1.3042	1.3137
Min.	0.7142	0.7224	0.7215	0.7205	0.7196	0.7182	0.7161	0.7140	0.7103
Mean	0.9918	0.9913	0.9912	0.9910	0.9910	0.9912	0.9914	0.9915	0.9924
St. Dev.	0.0980	0.0959	0.0954	0.0952	0.0954	0.0965	0.0982	0.1008	0.1043
COV	0.0988	0.0967	0.0962	0.0961	0.0963	0.0974	0.0991	0.1017	0.1051
$f_c = 6000-10000$ psi, 11 tests									
Max.	1.1417	1.1622	1.1582	1.1535	1.1482	1.1416	1.1337	1.1250	1.1153
Min.	0.9098	0.8823	0.8812	0.8802	0.8792	0.8850	0.9034	0.9203	0.9331
Mean	1.0131	1.0143	1.0128	1.0113	1.0097	1.0093	1.0116	1.0147	1.0181
St. Dev.	0.0534	0.0643	0.0635	0.0625	0.0614	0.0583	0.0524	0.0482	0.0467
COV	0.0527	0.0634	0.0627	0.0618	0.0608	0.0578	0.0518	0.0475	0.0459
$f_c = 10000-15600$ psi, 29 tests									
Max.	1.3027	1.3065	1.3128	1.3165	1.3169	1.3121	1.3010	1.2832	1.2590
Min.	0.7816	0.7799	0.7807	0.7818	0.7831	0.7850	0.7873	0.7904	0.7813
Mean	1.0257	1.0277	1.0290	1.0301	1.0308	1.0307	1.0292	1.0270	1.0224
St. Dev.	0.1430	0.1399	0.1416	0.1429	0.1437	0.1437	0.1425	0.1401	0.1370
COV	0.1394	0.1362	0.1376	0.1387	0.1394	0.1394	0.1385	0.1364	0.1340

$f_c^{0.23}$	Test/Predication Ratio								
	$c_{si}+0.25$	1.7 c_{si}	1.6 c_{si}	1.5 c_{si}	1.4 c_{si}	1.3 c_{si}	1.2 c_{si}	1.1 c_{si}	1.0 c_{si}
Total 171 tests									
Max.	1.3060	1.2979	1.3042	1.3081	1.3088	1.3042	1.2978	1.3092	1.3189
Min.	0.7199	0.7284	0.7273	0.7263	0.7254	0.7240	0.7217	0.7195	0.7158
Mean	1.0000	0.9999	0.9999	0.9999	1.0000	1.0001	1.0001	1.0001	1.0001
St. Dev.	0.1047	0.1030	0.1030	0.1032	0.1035	0.1041	0.1048	0.1060	0.1076
COV	0.1047	0.1030	0.1030	0.1032	0.1035	0.1041	0.1048	0.1059	0.1076
$f_c < 6000$ psi, 131 tests									
Max.	1.3060	1.2902	1.2880	1.2859	1.2837	1.2876	1.2978	1.3092	1.3189
Min.	0.7199	0.7284	0.7273	0.7263	0.7254	0.7240	0.7217	0.7195	0.7158
Mean	0.9950	0.9943	0.9942	0.9941	0.9942	0.9944	0.9945	0.9948	0.9955
St. Dev.	0.0982	0.0961	0.0956	0.0954	0.0956	0.0966	0.0983	0.1009	0.1043
COV	0.0987	0.0967	0.0962	0.0960	0.0962	0.0972	0.0989	0.1014	0.1048
$f_c = 6000-10000$ psi, 11 tests									
Max.	1.1439	1.1642	1.1601	1.1555	1.1504	1.1438	1.1358	1.1271	1.1170
Min.	0.9105	0.8828	0.8817	0.8807	0.8797	0.8854	0.9040	0.9211	0.9340
Mean	1.0124	1.0135	1.0119	1.0104	1.0088	1.0084	1.0107	1.0139	1.0172
St. Dev.	0.0541	0.0649	0.0640	0.0630	0.0619	0.0588	0.0529	0.0489	0.0470
COV	0.0535	0.0640	0.0633	0.0623	0.0613	0.0583	0.0524	0.0482	0.0463
$f_c = 10000-15600$ psi, 29 tests									
Max.	1.2945	1.2979	1.3042	1.3081	1.3088	1.3042	1.2933	1.2759	1.2510
Min.	0.7723	0.7707	0.7714	0.7725	0.7738	0.7757	0.7779	0.7809	0.7794
Mean	1.0177	1.0198	1.0210	1.0221	1.0229	1.0228	1.0211	1.0190	1.0143
St. Dev.	0.1425	0.1393	0.1410	0.1423	0.1432	0.1432	0.1420	0.1397	0.1363
COV	0.1400	0.1366	0.1381	0.1393	0.1400	0.1400	0.1391	0.1371	0.1344

Table B.2 (continued)
Test/Prediction ratios using Eq. 5.3 for different powers of f_c
and definitions of effective value of c_{si}

$f_c^{0.24}$	Test/Prediction Ratio								
	$c_{si}+0.25$	1.7 c_{si}	1.6 c_{si}	1.5 c_{si}	1.4 c_{si}	1.3 c_{si}	1.2 c_{si}	1.1 c_{si}	1.0 c_{si}
Total 171 tests									
Max.	1.3104	1.2939	1.2941	1.2978	1.2982	1.2935	1.3020	1.3137	1.3236
Min.	0.7254	0.7340	0.7330	0.7319	0.7308	0.7294	0.7271	0.7249	0.7211
Mean	0.9999	0.9998	0.9999	0.9998	0.9998	0.9999	1.0001	1.0001	1.0000
St. Dev.	0.1044	0.1027	0.1027	0.1028	0.1031	0.1037	0.1044	0.1056	0.1073
COV	0.1044	0.1028	0.1027	0.1028	0.1031	0.1037	0.1044	0.1056	0.1073
$f_c < 6000$ psi, 131 tests									
Max.	1.3104	1.2939	1.2919	1.2896	1.2872	1.2913	1.3020	1.3137	1.3236
Min.	0.7254	0.7340	0.7330	0.7319	0.7308	0.7294	0.7271	0.7249	0.7211
Mean	0.9970	0.9962	0.9962	0.9960	0.9960	0.9962	0.9966	0.9968	0.9975
St. Dev.	0.0984	0.0964	0.0959	0.0956	0.0958	0.0968	0.0985	0.1010	0.1044
COV	0.0987	0.0968	0.0962	0.0960	0.0962	0.0972	0.0988	0.1013	0.1047
$f_c = 6000-10000$ psi, 11 tests									
Max.	1.1439	1.1643	1.1603	1.1556	1.1503	1.1438	1.1360	1.1273	1.1171
Min.	0.9107	0.8829	0.8818	0.8807	0.8796	0.8854	0.9041	0.9213	0.9342
Mean	1.0108	1.0119	1.0105	1.0089	1.0071	1.0067	1.0092	1.0123	1.0156
St. Dev.	0.0547	0.0652	0.0643	0.0633	0.0621	0.0590	0.0533	0.0494	0.0474
COV	0.0541	0.0644	0.0637	0.0627	0.0616	0.0586	0.0528	0.0488	0.0467
$f_c = 10000-15600$ psi, 29 tests									
Max.	1.2841	1.2877	1.2941	1.2978	1.2982	1.2935	1.2827	1.2653	1.2403
Min.	0.7628	0.7614	0.7621	0.7631	0.7642	0.7661	0.7683	0.7713	0.7734
Mean	1.0092	1.0114	1.0126	1.0136	1.0142	1.0141	1.0125	1.0103	1.0057
St. Dev.	0.1416	0.1385	0.1401	0.1415	0.1423	0.1422	0.1411	0.1387	0.1353
COV	0.1403	0.1369	0.1384	0.1396	0.1403	0.1403	0.1393	0.1373	0.1346

$f_c^{0.25}$	Test/Prediction Ratio								
	$c_{si}+0.25$	1.7 c_{si}	1.6 c_{si}	1.5 c_{si}	1.4 c_{si}	1.3 c_{si}	1.2 c_{si}	1.1 c_{si}	1.0 c_{si}
Total 171 tests									
Max.	1.3150	1.2977	1.2956	1.2933	1.2911	1.2952	1.3062	1.3182	1.3323
Min.	0.7310	0.7397	0.7386	0.7375	0.7365	0.7349	0.7326	0.7303	0.7286
Mean	1.0000	0.9999	0.9999	0.9998	1.0000	0.9999	1.0001	1.0001	1.0029
St. Dev.	0.1043	0.1027	0.1026	0.1027	0.1030	0.1035	0.1042	0.1054	0.1075
COV	0.1043	0.1027	0.1026	0.1027	0.1030	0.1035	0.1042	0.1054	0.1072
$f_c < 6000$ psi, 131 tests									
Max.	1.3150	1.2977	1.2956	1.2933	1.2911	1.2952	1.3062	1.3182	1.3323
Min.	0.7310	0.7397	0.7386	0.7375	0.7365	0.7349	0.7326	0.7303	0.7286
Mean	0.9991	0.9982	0.9981	0.9980	0.9982	0.9982	0.9986	0.9988	1.0023
St. Dev.	0.0986	0.0967	0.0962	0.0959	0.0961	0.0971	0.0987	0.1012	0.1049
COV	0.0987	0.0969	0.0963	0.0961	0.0963	0.0972	0.0988	0.1013	0.1046
$f_c = 6000-10000$ psi, 11 tests									
Max.	1.1441	1.1644	1.1604	1.1557	1.1507	1.1440	1.1362	1.1275	1.1203
Min.	0.9109	0.8831	0.8819	0.8808	0.8797	0.8854	0.9043	0.9215	0.9371
Mean	1.0093	1.0105	1.0089	1.0073	1.0057	1.0051	1.0076	1.0107	1.0169
St. Dev.	0.0554	0.0657	0.0647	0.0637	0.0625	0.0594	0.0538	0.0500	0.0481
COV	0.0549	0.0650	0.0642	0.0632	0.0621	0.0590	0.0534	0.0495	0.0473
$f_c = 10000-15600$ psi, 29 tests									
Max.	1.2741	1.2777	1.2839	1.2875	1.2881	1.2831	1.2723	1.2548	1.2330
Min.	0.7536	0.7522	0.7528	0.7538	0.7550	0.7567	0.7589	0.7619	0.7662
Mean	1.0009	1.0031	1.0043	1.0052	1.0059	1.0056	1.0040	1.0018	1.0000
St. Dev.	0.1407	0.1377	0.1393	0.1406	0.1415	0.1414	0.1402	0.1377	0.1346
COV	0.1406	0.1372	0.1387	0.1399	0.1406	0.1406	0.1396	0.1375	0.1346

Table B.2 (continued)
Test/Prediction ratios using Eq. 5.3 for different powers of f_c
and definitions of effective value of c_{si}

$f_c^{0.26}$	Test/Predication Ratio								
	$c_{si}+0.25$	1.7 c_{si}	1.6 c_{si}	1.5 c_{si}	1.4 c_{si}	1.3 c_{si}	1.2 c_{si}	1.1 c_{si}	1.0 c_{si}
Total 171 tests									
Max.	1.3195	1.3014	1.2993	1.2972	1.2947	1.2989	1.3102	1.3226	1.3331
Min.	0.7365	0.7430	0.7436	0.7433	0.7421	0.7404	0.7381	0.7358	0.7318
Mean	1.0000	0.9998	0.9998	0.9999	0.9999	0.9998	1.0000	1.0001	1.0000
St. Dev.	0.1044	0.1028	0.1027	0.1027	0.1030	0.1035	0.1042	0.1054	0.1072
COV	0.1044	0.1028	0.1027	0.1027	0.1030	0.1035	0.1042	0.1054	0.1072
$f_c < 6000$ psi, 131 tests									
Max.	1.3195	1.3014	1.2993	1.2972	1.2947	1.2989	1.3102	1.3226	1.3331
Min.	0.7365	0.7454	0.7443	0.7433	0.7421	0.7404	0.7381	0.7358	0.7318
Mean	1.0010	1.0001	1.0001	1.0001	1.0001	1.0001	1.0005	1.0008	1.0016
St. Dev.	0.0989	0.0971	0.0966	0.0963	0.0964	0.0974	0.0990	0.1014	0.1047
COV	0.0988	0.0971	0.0965	0.0963	0.0964	0.0974	0.0989	0.1013	0.1046
$f_c = 6000-10000$ psi, 11 tests									
Max.	1.1442	1.1644	1.1605	1.1560	1.1508	1.1441	1.1362	1.1277	1.1174
Min.	0.9111	0.8831	0.8819	0.8809	0.8797	0.8854	0.9042	0.9216	0.9346
Mean	1.0077	1.0089	1.0073	1.0058	1.0041	1.0034	1.0059	1.0091	1.0124
St. Dev.	0.0562	0.0662	0.0653	0.0642	0.0630	0.0598	0.0544	0.0509	0.0487
COV	0.0558	0.0657	0.0648	0.0638	0.0627	0.0596	0.0541	0.0504	0.0481
$f_c = 10000-15600$ psi, 29 tests									
Max.	1.2639	1.2677	1.2738	1.2775	1.2778	1.2727	1.2619	1.2444	1.2195
Min.	0.7443	0.7430	0.7436	0.7446	0.7457	0.7474	0.7495	0.7525	0.7545
Mean	0.9925	0.9948	0.9959	0.9970	0.9976	0.9971	0.9955	0.9933	0.9885
St. Dev.	0.1398	0.1369	0.1385	0.1398	0.1406	0.1405	0.1393	0.1368	0.1334
COV	0.1409	0.1376	0.1391	0.1402	0.1410	0.1409	0.1399	0.1377	0.1349

$f_c^{0.27}$	Test/Predication Ratio								
	$c_{si}+0.25$	1.7 c_{si}	1.6 c_{si}	1.5 c_{si}	1.4 c_{si}	1.3 c_{si}	1.2 c_{si}	1.1 c_{si}	1.0 c_{si}
Total 171 tests									
Max.	1.3239	1.3051	1.3030	1.3007	1.2983	1.3029	1.3144	1.3270	1.3377
Min.	0.7352	0.7339	0.7345	0.7354	0.7365	0.7383	0.7403	0.7412	0.7371
Mean	1.0000	0.9998	0.9998	0.9998	0.9998	1.0000	1.0000	1.0000	1.0000
St. Dev.	0.1047	0.1031	0.1030	0.1030	0.1032	0.1037	0.1044	0.1057	0.1074
COV	0.1047	0.1032	0.1030	0.1030	0.1032	0.1038	0.1045	0.1057	0.1074
$f_c < 6000$ psi, 131 tests									
Max.	1.3239	1.3051	1.3030	1.3007	1.2983	1.3029	1.3144	1.3270	1.3377
Min.	0.7420	0.7511	0.7500	0.7489	0.7477	0.7461	0.7436	0.7412	0.7371
Mean	1.0030	1.0020	1.0020	1.0019	1.0020	1.0023	1.0025	1.0027	1.0036
St. Dev.	0.0993	0.0976	0.0970	0.0967	0.0968	0.0978	0.0993	0.1017	0.1050
COV	0.0990	0.0974	0.0968	0.0965	0.0967	0.0975	0.0991	0.1014	0.1046
$f_c = 6000-10000$ psi, 11 tests									
Max.	1.1443	1.1645	1.1606	1.1559	1.1509	1.1444	1.1364	1.1277	1.1171
Min.	0.9112	0.8832	0.8820	0.8808	0.8796	0.8855	0.9043	0.9217	0.9345
Mean	1.0062	1.0073	1.0057	1.0041	1.0024	1.0020	1.0043	1.0074	1.0107
St. Dev.	0.0572	0.0669	0.0660	0.0648	0.0636	0.0605	0.0552	0.0518	0.0494
COV	0.0568	0.0664	0.0656	0.0646	0.0634	0.0604	0.0550	0.0515	0.0489
$f_c = 10000-15600$ psi, 29 tests									
Max.	1.2538	1.2577	1.2638	1.2672	1.2675	1.2627	1.2516	1.2340	1.2084
Min.	0.7352	0.7339	0.7345	0.7354	0.7365	0.7383	0.7403	0.7432	0.7456
Mean	0.9842	0.9866	0.9877	0.9886	0.9891	0.9889	0.9871	0.9847	0.9799
St. Dev.	0.1390	0.1361	0.1377	0.1390	0.1398	0.1397	0.1384	0.1359	0.1323
COV	0.1413	0.1380	0.1394	0.1406	0.1413	0.1413	0.1402	0.1380	0.1350

Table B.2 (continued)
Test/Predication ratios using Eq. 5.3 for different powers of f_c'
and definitions of effective value of c_{si}

$f_c'^{0.5}$	Test/Predication Ratio								
	$c_{si}+0.25$	1.7 c_{si}	1.6 c_{si}	1.5 c_{si}	1.4 c_{si}	1.3 c_{si}	1.2 c_{si}	1.1 c_{si}	1.0 c_{si}
Total 171 tests									
Max.	1.4162	1.3806	1.3779	1.3753	1.3721	1.3801	1.3989	1.4186	1.4354
Min.	0.5491	0.5490	0.5491	0.5494	0.5498	0.5508	0.5523	0.5545	0.5561
Mean	0.9990	0.9987	0.9987	0.9988	0.9987	0.9989	0.9990	0.9990	0.9992
St. Dev.	0.1522	0.1521	0.1515	0.1509	0.1506	0.1505	0.1506	0.1513	0.1524
COV	0.1523	0.1523	0.1517	0.1511	0.1508	0.1507	0.1508	0.1514	0.1525
$f_c'<6000$ psi, 131 tests									
Max.	1.4162	1.3806	1.3779	1.3753	1.3721	1.3801	1.3989	1.4186	1.4354
Min.	0.7090	0.7008	0.7017	0.7028	0.7040	0.7067	0.7112	0.7167	0.7233
Mean	1.0448	1.0435	1.0436	1.0437	1.0439	1.0443	1.0448	1.0452	1.0463
St. Dev.	0.1246	0.1265	0.1254	0.1244	0.1236	0.1232	0.1229	0.1235	0.1241
COV	0.1193	0.1213	0.1201	0.1192	0.1184	0.1180	0.1177	0.1182	0.1186
$f_c'=6000-10000$ psi, 11 tests									
Max.	1.1401	1.1608	1.1572	1.1532	1.1484	1.1421	1.1339	1.1248	1.1138
Min.	0.8339	0.8362	0.8359	0.8359	0.8359	0.8366	0.8376	0.8395	0.8576
Mean	0.9644	0.9658	0.9638	0.9619	0.9596	0.9588	0.9616	0.9649	0.9683
St. Dev.	0.0984	0.1024	0.1014	0.1002	0.0987	0.0966	0.0948	0.0948	0.0917
COV	0.1020	0.1061	0.1052	0.1041	0.1029	0.1007	0.0986	0.0982	0.0947
$f_c'=10000-15600$ psi, 29 tests									
Max.	1.0385	1.0435	1.0486	1.0516	1.0516	1.0470	1.0362	1.0195	0.9958
Min.	0.5491	0.5490	0.5491	0.5494	0.5498	0.5508	0.5523	0.5545	0.5561
Mean	0.8049	0.8090	0.8094	0.8098	0.8096	0.8086	0.8063	0.8033	0.7981
St. Dev.	0.1252	0.1239	0.1252	0.1262	0.1267	0.1263	0.1245	0.1215	0.1174
COV	0.1555	0.1532	0.1547	0.1558	0.1565	0.1561	0.1544	0.1512	0.1471

$f_c'^{0.25}$	Test/Predication Ratio								
	$c_{si}+0.24$	$c_{si}+0.26$	$c_{si}+0.28$	$c_{si}+0.30$	$c_{si}+0.32$	$c_{si}+0.34$	$c_{si}+0.36$	$c_{si}+0.38$	$c_{si}+0.40$
Total 171 tests									
Max.	1.3150	1.3146	1.3140	1.3133	1.3129	1.3123	1.3117	1.3112	1.3110
Min.	0.7310	0.7312	0.7317	0.7321	0.7327	0.7332	0.7337	0.7342	0.7349
Mean	1.0000	1.0000	1.0000	1.0000	1.0000	1.0000	0.9999	0.9998	1.0000
St. Dev.	0.1043	0.1042	0.1041	0.1039	0.1038	0.1037	0.1035	0.1034	0.1034
COV	0.1043	0.1042	0.1041	0.1039	0.1038	0.1037	0.1035	0.1035	0.1034
$f_c'<6000$ psi, 131 tests									
Max.	1.3150	1.3146	1.3140	1.3133	1.3129	1.3123	1.3117	1.3112	1.3110
Min.	0.7310	0.7312	0.7317	0.7321	0.7327	0.7332	0.7337	0.7342	0.7349
Mean	0.9991	0.9990	0.9991	0.9990	0.9991	0.9991	0.9990	0.9990	0.9991
St. Dev.	0.0986	0.0985	0.0983	0.0982	0.0980	0.0980	0.0979	0.0979	0.0979
COV	0.0987	0.0986	0.0984	0.0983	0.0981	0.0981	0.0980	0.0980	0.0980
$f_c'=6000-10000$ psi, 11 tests									
Max.	1.1441	1.1451	1.1470	1.1489	1.1508	1.1526	1.1541	1.1558	1.1576
Min.	0.9109	0.9098	0.9075	0.9051	0.9028	0.9005	0.8980	0.8955	0.8933
Mean	1.0093	1.0092	1.0090	1.0088	1.0086	1.0084	1.0084	1.0084	1.0086
St. Dev.	0.0554	0.0558	0.0566	0.0574	0.0583	0.0592	0.0600	0.0609	0.0618
COV	0.0549	0.0552	0.0561	0.0569	0.0578	0.0587	0.0595	0.0604	0.0613
$f_c'=10000-15600$ psi, 29 tests									
Max.	1.2741	1.2738	1.2730	1.2717	1.2702	1.2683	1.2659	1.2633	1.2608
Min.	0.7536	0.7532	0.7527	0.7523	0.7519	0.7515	0.7511	0.7508	0.7507
Mean	1.0009	1.0008	1.0009	1.0008	1.0009	1.0008	1.0007	1.0006	1.0007
St. Dev.	0.1407	0.1406	0.1404	0.1401	0.1397	0.1393	0.1387	0.1382	0.1376
COV	0.1406	0.1405	0.1403	0.1399	0.1396	0.1391	0.1386	0.1381	0.1376

Table B.3
**Test/prediction strength ratios, using Eqs. 5.13a - 5.13d,
for 163 specimens**

Specimen No.*	f_c (psi)	$p = 1/4^{**}$	Test/Prediction Strength Ratio+		
			$p = 1/2$	$p = 3/4$	$p = 1.0$
Ferguson and Breen (1965)					
8F36c	2740	0.868	0.892	0.911	0.925
8F36d	3580	0.914	0.933	0.949	0.961
8F36e	4170	0.965	0.981	0.993	1.001
8F36f	3780	0.942	0.960	0.974	0.985
8F36g	3070	1.004	1.029	1.048	1.063
8F36h	1910	0.783	0.822	0.854	0.879
8F36j	1820	0.932	0.981	1.021	1.052
8F30b	2610	0.910	0.940	0.963	0.980
11R36a	3020	1.073	1.101	1.126	1.149
Thompson et al. (1975)					
11-30-4/2/2-6/6-S5	3063	0.968	0.995	1.019	1.039
DeVries et al. (1991)					
8G-22B-P9	7460	0.927	0.916	0.902	0.883
Hester et al. (1991, 1993)					
1.2	5990	1.047	1.062	1.072	1.078
2.2	6200	0.822	0.834	0.842	0.846
3.2	6020	0.866	0.879	0.888	0.894
4.2	6450	0.863	0.873	0.881	0.884
4.3	6450	0.890	0.897	0.901	0.901
5.2	5490	0.889	0.905	0.916	0.924
5.3	5490	0.804	0.816	0.824	0.830
6.2	5850	0.866	0.875	0.881	0.884
6.3	5850	0.835	0.841	0.845	0.846
7.2	5240	0.897	0.909	0.917	0.921
Rezansoff et al. (1991)					
20-6-2	4277	1.107	1.141	1.165	1.182
20-6-3	3886	1.240	1.287	1.323	1.350
20-6-1	4045	1.210	1.252	1.284	1.307
20-8-11	4466	1.256	1.274	1.286	1.295
20-8-9	4205	1.007	1.028	1.044	1.056
20-8-1	5220	1.103	1.101	1.094	1.084
20-8-12	4350	1.066	1.084	1.098	1.108
20-8-2	5742	0.995	0.987	0.976	0.961
20-8-3	5510	0.978	0.978	0.974	0.967
20-8-6	4770	1.183	1.196	1.204	1.208
20-8-7	4495	0.985	1.004	1.017	1.027
20-8-8	4350	0.977	0.995	1.009	1.019
20-8-5	4770	1.212	1.222	1.228	1.230
20-8-4	4335	1.170	1.189	1.204	1.215
20-8-13	3509	0.953	0.982	1.005	1.023
20-8-14	3277	1.053	1.094	1.126	1.153
20-8-15	3625	1.072	1.108	1.138	1.162
20-8-16	3291	1.042	1.077	1.104	1.125
20-8-18	3349	1.124	1.171	1.210	1.244
20-8-19	3219	0.895	0.928	0.953	0.973
20-8-17	3480	1.183	1.226	1.262	1.292
20-8-20	3291	0.927	0.964	0.994	1.019
20-9-1	3538	1.043	1.075	1.104	1.131
20-9-2	3378	1.159	1.194	1.224	1.251
20-11-2	4335	1.053	1.064	1.076	1.086
20-11-1	4770	1.057	1.063	1.068	1.072

Table B.3 (continued)
Test/prediction strength ratios, using Eqs. 5.13a - 5.13d,
for 163 specimens

Specimen No.*	f_c (psi)	Test/Prediction Strength Ratio ⁺			
		$p = 1/4^{**}$	$p = 1/2$	$p = 3/4$	$p = 1.0$
20-11-3	4466	0.955	0.965	0.974	0.982
20-11-8	3349	1.063	1.098	1.133	1.166
20-11-5	3625	1.107	1.135	1.163	1.189
20-11-6	3625	0.934	0.953	0.971	0.987
20-11-7	3291	0.888	0.923	0.958	0.992
Rezansoff et al. (1993)					
6	3625	0.991	1.023	1.048	1.068
1b	3799	1.203	1.234	1.259	1.277
1a	3958	1.262	1.293	1.317	1.335
3a	3958	1.232	1.264	1.287	1.305
3b	3799	1.099	1.128	1.151	1.167
4b	3726	1.193	1.216	1.233	1.246
9	3886	1.178	1.201	1.223	1.241
10	4089	1.101	1.120	1.138	1.154
4a	4031	1.202	1.226	1.243	1.256
Azizinamini et al. (1995 at CTL)					
AB83-11-15-57.5S-50	15120	0.880	0.861	0.837	0.806
Azizinamini et al. (1995 at UNL)					
ABS-11-15-45S-60	14890	0.918	0.890	0.855	0.812
ABS-11-15-45S-100	14850	0.954	0.911	0.861	0.803
ABS-11-15-40S-150	15760	0.980	0.918	0.848	0.769
Darwin et al. (1995a, 1995b)					
12.1	4120	0.798	0.845	0.880	0.906
12.2	4120	0.782	0.823	0.854	0.875
12.3	4120	0.839	0.890	0.929	0.959
12.4	4120	0.873	0.922	0.958	0.985
13.1	4110	0.847	0.890	0.922	0.945
13.2	4110	0.861	0.906	0.940	0.966
14.5	4200	0.879	0.920	0.950	0.972
14.6	4200	0.894	0.931	0.958	0.976
1.6	5020	0.906	0.914	0.917	0.916
2.1	5250	0.881	0.883	0.882	0.879
2.2	5250	0.953	0.936	0.917	0.897
2.3	5250	0.957	0.953	0.946	0.936
3.4	5110	0.763	0.769	0.771	0.772
3.5	3810	0.825	0.844	0.859	0.872
4.1	4090	0.846	0.861	0.874	0.885
4.4	4090	0.962	0.980	0.993	1.003
5.1	4190	0.991	1.011	1.027	1.040
5.2	4190	0.865	0.868	0.869	0.869
5.3	4190	0.909	0.912	0.913	0.913
5.4	4190	0.902	0.921	0.935	0.947
5.5	4190	0.741	0.754	0.765	0.773
6.1	4220	0.964	0.983	0.999	1.011
6.2	4220	0.964	0.962	0.958	0.954
6.3	4220	0.926	0.945	0.958	0.967
6.4	4220	0.761	0.780	0.795	0.806
7.1	4160	0.877	0.894	0.906	0.915
7.5	4160	0.945	0.944	0.942	0.940
7.6	4160	0.846	0.866	0.880	0.891
8.1	3830	1.085	1.114	1.139	1.161
8.2	3830	1.137	1.152	1.165	1.176

Table B.3 (continued)
Test/prediction strength ratios, using Eqs. 5.13a - 5.13d,
for 163 specimens

Specimen No.*	f_c (psi)	Test/Prediction Strength Ratio+			
		p = 1/4**	p = 1/2	p = 3/4	p = 1.0
8.4	3830	0.947	0.971	0.989	1.003
9.1	4230	0.976	0.992	1.004	1.012
9.2	4230	1.065	1.071	1.073	1.074
9.3	4230	0.891	0.910	0.924	0.934
9.4	4230	0.997	1.013	1.023	1.031
10.3	4250	0.911	0.929	0.943	0.953
11.1	4380	1.016	1.015	1.010	1.005
11.2	4380	0.946	0.961	0.973	0.982
11.4	4380	0.943	0.956	0.965	0.971
14.1	4200	0.969	0.988	1.001	1.011
14.2	4200	0.953	0.962	0.969	0.974
15.2	5250	0.928	0.918	0.909	0.900
15.3	5250	0.931	0.928	0.925	0.920
15.4	5250	1.041	1.022	1.005	0.987
16.3	5180	0.918	0.916	0.913	0.909
16.4	5180	0.948	0.953	0.956	0.958
17.3	4710	0.947	0.942	0.938	0.933
17.4	4710	0.978	0.983	0.987	0.991
17.5	4710	0.865	0.867	0.870	0.872
18.1	4700	1.110	1.100	1.092	1.084
18.3	4700	0.988	0.987	0.984	0.982
18.4	4700	0.999	1.006	1.011	1.015
Current Study					
19.3	4250	0.926	0.937	0.945	0.951
19.4	4250	1.004	1.017	1.025	1.031
21.1	4330	0.929	0.926	0.922	0.918
21.3	4330	0.982	0.982	0.980	0.978
21.5	4330	0.952	0.952	0.951	0.949
23a.1	9080	0.970	0.936	0.895	0.848
23a.3	9080	0.997	0.962	0.920	0.871
23a.4	9080	0.977	0.943	0.901	0.854
23b.1	8370	1.095	1.035	0.969	0.900
27.2	10810	1.188	1.147	1.098	1.039
27.4	10810	1.162	1.098	1.026	0.946
27.6	10810	1.168	1.119	1.060	0.993
29.2	10620	1.353	1.315	1.267	1.209
29.4	10620	1.273	1.228	1.173	1.108
29.6	10620	1.324	1.295	1.257	1.209
31.3	12890	1.025	1.002	0.971	0.931
33.2	5360	0.969	0.964	0.955	0.943
33.4	5360	0.913	0.918	0.919	0.917
33.6	5230	0.907	0.918	0.926	0.931
35.1	5330	0.984	0.973	0.958	0.942
35.3	5330	0.953	0.956	0.954	0.949
37.4	4800	0.999	0.984	0.966	0.949
39.2	14450	1.116	1.054	0.978	0.890
39.3	14450	1.291	1.237	1.170	1.089
41.1	10180	1.051	1.026	0.992	0.951
41.2	10180	1.086	0.988	0.886	0.783
41.3	10180	1.158	1.084	1.001	0.912
41.4	10180	1.136	1.067	0.992	0.910
41.5	10500	0.999	0.983	0.960	0.931

Table B.3 (continued)
Test/prediction strength ratios, using Eqs. 5.13a - 5.13d,
for 163 specimens

Specimen No.*	f_c (psi)	Test/Prediction Strength Ratio+			
		p = 1/4**	p = 1/2	p = 3/4	p = 1.0
41.6	10500	0.989	0.973	0.951	0.922
42.1	11930	0.969	0.952	0.928	0.898
42.4	11930	1.080	1.024	0.958	0.884
42.5	11930	1.100	1.017	0.926	0.829
43.2	11530	0.956	0.927	0.890	0.845
43.3	11530	1.117	1.033	0.939	0.839
43.6	11530	1.050	0.940	0.827	0.715
20.1	5080	0.956	0.942	0.929	0.916
20.2	5080	0.968	0.953	0.940	0.927
20.3	5080	1.036	1.029	1.022	1.013
20.4	5080	1.023	1.016	1.009	1.001
28.1	12610	1.126	1.046	0.958	0.863
28.3	12610	1.083	1.041	0.991	0.932
30.1	13220	1.138	1.082	1.015	0.939
30.3	13220	1.133	1.110	1.079	1.041
40.1	15650	1.082	0.999	0.904	0.800
40.4	15650	1.012	0.960	0.899	0.827
		Max	1.353	1.315	1.323
		Min	0.741	0.754	0.765
		Mean	1.000	1.002	0.999
		St.Dev.	0.122	0.117	0.120
		COV	0.122	0.116	0.120
					0.132

* Data of the specimens are given in Table 5.11.

** Power used to characterize T_s

+ Predicted strength = Eq. 5.13a for p = 1/4
 = Eq. 5.13b for p = 1/2
 = Eq. 5.13c for p = 3/4
 = Eq. 5.13d for p = 1.0

1 psi = 6.895 kPa

**APPENDIX C: DATA OF FLEXURAL CRACK AND DENSITY FOR THE
MATCHED PAIRS OF SPECIMENS CONTAINING
EPOXY-COATED AND UNCOATED BARS**

Table C.1 and C.2 compare flexural crack density and flexural crack width at a bar stress of 20 and 30 ksi (137.9 and 206.9 MPa), respectively, between beams containing epoxy-coated and uncoated bars in matched pairs of specimens.

Table C.1
**Comparison of flexural crack density and flexural crack width at a bar stress
of 20 ksi between beams containing coated and uncoated bars
in matched pairs of specimens**

Specimen No.	Surface [†] Condition	Bar Designation	Length outside of Splice Region (ft)	Total No. [‡] of Cracks	Avg. Max. ⁺⁺⁺ Crack Width (in.)	Crack* Density (in./ft)	Sum of** Crack Widths (in.)	Ratios of C/U***		
								Max. Crack Width	Crack Density	Sum of Crack Widths
28.1	U	11F3	3.92	8	0.0035	2.043	0.024			
28.2	C	11F3	3.92	6	0.0030	1.532	0.017	0.857	0.750	0.708
28.3	U	11F3	3.67	8	0.0030	2.182	0.022			
28.4	C	11F3	3.67	6	0.0045	1.636	0.020	1.500	0.750	0.909
28.5	U	11F3	3.50	6	0.0030	1.714	0.016			
28.6	C	11F3	5.75	5	0.0040	0.870	0.017	1.333	0.507	1.063
30.1	U	11F3	3.92	7	0.0025	1.787	0.015			
30.2	C	11F3	3.92	5	0.0030	1.277	0.013	1.200	0.714	0.867
30.3	U	11F3	3.67	9	0.0020	2.455	0.012			
30.4	C	11F3	3.67	6	0.0020	1.636	0.010	1.000	0.667	0.833
30.5	U	11F3	3.50	4	0.0030	1.143	0.010			
30.6	C	11F3	3.50	4	0.0020	1.143	0.008	0.667	1.000	0.800
31.1	U	8N1	4.67	4	0.0020	0.857	0.008			
31.2	C	8N1	4.67	4	0.0025	0.857	0.009	1.250	1.000	1.125
31.3	U	8N0	4.67	5	0.0020	1.071	0.010			
31.4	C	8N0	4.67	4	0.0025	0.857	0.009	1.250	0.800	0.900
37.4	U	8F1	4.25	8	0.0030	1.882	0.018			
37.3	C	8F1	4.25	10	0.0025	2.353	0.019	0.833	1.250	1.056
39.2	U	8N1	4.67	8	0.0030	1.714	-			
39.1	C	8N1	4.67	7	0.0030	1.500	-	1.000	0.875	-
39.3	U	8N0	4.67	6	0.0030	1.286	-			
39.4	C	8N0	4.67	5	0.0030	1.071	-	1.000	0.833	-
39.6	U	8C1	4.67	8	0.0030	1.714	-			
39.5	C	8C1	4.67	6	0.0040	1.286	-	1.333	0.750	-
40.1	U	11F3	4.08	7	0.0040	1.714	-			
40.2	C	11F3	4.08	6	0.0045	1.469	-	1.125	0.857	-
40.4	U	11N0	4.08	9	0.0030	2.204	-			
40.3	C	11N0	4.08	5	0.0060	1.224	-	2.000	0.556	-
40.5	U	8N0	4.58	-	-	-	-			
40.6	C	8N0	4.58	5	0.0040	1.091	-			
42.1	U	8N0	4.67	-	-	-	-			
42.2	C	8N0	4.67	-	-	-	-			
42.4	U	8N0	4.67	-	-	-	-			
42.3	C	8N0	4.67	-	-	-	-			
42.5	U	8N0	4.67	-	-	-	-			
42.6	C	8N0	4.67	-	-	-	-			
43.2	U	8N3	4.67	6	0.0035	1.286	-			
43.1	C	8N3	4.67	7	0.0035	1.500	-	1.000	1.167	-
43.3	U	8N3	4.67	9	0.0025	1.929	-			
43.4	C	8N3	4.67	7	0.0050	1.500	-	2.000	0.778	-
43.6	U	8N3	4.67	9	0.0025	1.929	-			
43.5	C	8N3	4.67	8	0.0030	1.714	-	1.200	0.889	-

Table C.2 (continued)
Comparison of flexural crack density and flexural crack width at a bar stress
of 30 ksi between beams containing coated and uncoated bars
in matched pairs of specimens

Specimen No.	Surface Condition	Bar Designation	Length outside of Splice Region (ft)	Total No. ⁺⁺ of Cracks	Avg. Max. ⁺⁺⁺ Crack Width (in.)	Crack* Density (in./ft)	Sum of** Crack Widths (in.)	Ratios of C/U***		
								Max. Crack Width	Crack Density	Sum of Crack Widths
								Max	1.714	1.000
								Min.	1.000	0.507
								Average	1.316	0.851
								Max.	1.500	1.143
								Min.	1.059	0.700
								Average	1.244	0.900
								Max.	1.714	1.143
								Min.	1.000	0.507
								Average	1.284	0.859

+ U = Uncoated, C = Coated

++ Total number of flexural cracks in the constant moment region outside of the splice region

+++ Average maximum flexural crack width on the west and east sides of splices in the constant moment region

* Number of flexural cracks in unit foot length

** Sum of flexural crack widths cross the centerline of the beam on the east and west sides of splices in the constant moment region outside of the splice region

*** Ratios for crack density or maximum crack width or sum of crack widths of beams with coated bars to beams with uncoated bars

1 in. = 25.4 mm, 1 ft = 305 mm, 1 ksi = 6.895 MPa

